Neural bases of space representation by functional magnetic resonance imaging (fMRI)

Justine Cléry

N°d'ordre NNT : 2017LYSE1102

THESE de DOCTORAT DE L'UNIVERSITE DE LYON
opérée au sein de
l'Université Claude Bernard Lyon 1

Ecole Doctorale : ED 476 – NSCo
Neurosciences et Cognition

Spécialité de doctorat :
Neurosciences

Soutenue publiquement le 20/06/2017, par :

Justine Cléry

BASES NEURALES DE LA REPRESENTATION SPATIALE GRACE A L'IMAGERIE PAR RESONANCE MAGNETIQUE FONCTIONNELLE (IRMF)

/

NEURAL BASES OF SPACE REPRESENTATION BY FUNCTIONAL MAGNETIC RESONANCE IMAGING (FMRI)

Directrice de thèse : **Dr Suliann Ben Hamed**

Devant le jury composé de :

Noppeney Uta,	Pr, Univ Bermingham, UK	*Rapporteure*
Coello Yann,	P.U, Univ Lille, Lille	*Rapporteur*
Macaluso Emiliano,	P.U, CRNL-UCBL, Lyon	*Examinateur*
Ben Hamed Suliann,	D.R., ISCMJ, Lyon	*Examinatrice*

UNIVERSITE CLAUDE BERNARD - LYON 1

Président de l'Université	**M. le Professeur Frédéric FLEURY**
Président du Conseil Académique	M. le Professeur Hamda BEN HADID
Vice-président du Conseil d'Administration	M. le Professeur Didier REVEL
Vice-président du Conseil Formation et Vie Universitaire	M. le Professeur Philippe CHEVALIER
Vice-président de la Commission Recherche	M. Fabrice VALLÉE
Directrice Générale des Services	Mme Dominique MARCHAND

COMPOSANTES SANTE

Faculté de Médecine Lyon Est – Claude Bernard	Directeur : M. le Professeur G. RODE
Faculté de Médecine et de Maïeutique Lyon Sud – Charles Mérieux	Directeur : Mme la Professeure C. BURILLON
Faculté d'Odontologie	Directeur : M. le Professeur D. BOURGEOIS
Institut des Sciences Pharmaceutiques et Biologiques	Directeur : Mme la Professeure C. VINCIGUERRA
Institut des Sciences et Techniques de la Réadaptation	Directeur : M. X. PERROT
Département de formation et Centre de Recherche en Biologie Humaine	Directeur : Mme la Professeure A-M. SCHOTT

COMPOSANTES ET DEPARTEMENTS DE SCIENCES ET TECHNOLOGIE

Faculté des Sciences et Technologies	Directeur : M. F. DE MARCHI
Département Biologie	Directeur : M. le Professeur F. THEVENARD
Département Chimie Biochimie	Directeur : Mme C. FELIX
Département GEP	Directeur : M. Hassan HAMMOURI
Département Informatique	Directeur : M. le Professeur S. AKKOUCHE
Département Mathématiques	Directeur : M. le Professeur G. TOMANOV
Département Mécanique	Directeur : M. le Professeur H. BEN HADID
Département Physique	Directeur : M. le Professeur J-C PLENET
UFR Sciences et Techniques des Activités Physiques et Sportives	Directeur : M. Y. VANPOULLE
Observatoire des Sciences de l'Univers de Lyon	Directeur : M. B. GUIDERDONI
Polytech Lyon	Directeur : M. le Professeur E. PERRIN
Ecole Supérieure de Chimie Physique Electronique	Directeur : M. G. PIGNAULT
Institut Universitaire de Technologie de Lyon 1	Directeur : M. le Professeur C. VITON
Ecole Supérieure du Professorat et de l'Education	Directeur : M. le Professeur A. MOUGNIOTTE
Institut de Science Financière et d'Assurances	Directeur : M. N. LEBOISNE

À ma famille pour son soutien et sa confiance continus,

À mon mari qui m'apporte tant chaque jour,

À mon père parti trop tôt...

REMERCIEMENTS

I would like to extend my gratitude and sincere appreciation to Uta Noppeney and Yann Coello for accepting to examine the present thesis. Your expert opinion is an invaluable asset for the evaluation of my work. I would like to thank Emiliano Macaluso for accepting to be present for my thesis defense.

Suliann, je ne te remercierais jamais assez pour toute la confiance que tu m'as accordée tout au long de ces quatre années ! Tes précieux conseils, tes encouragements, ton sourire et surtout ta bonne humeur m'ont permis de donner le meilleur de moi-même et d'essayer de me surpasser à chaque fois. À tes côtés, j'ai appris beaucoup de choses que ce soit en terme de travail ou bien sur moi-même, et qui vont m'être utiles pour mes futures années de recherches. Merci pour tout ! Olivier, merci de m'avoir initié à l'analyse des données d'imagerie et pour tous tes précieux conseils pendant mon stage, surtout les petites astuces qui permettent de gagner un temps fou pour les analyses ! Claire, merci pour tes conseils et retours, que ce soit pour les animaux, les analyses, lors des colloques ou bien pour les articles.

Merci à Soline de m'avoir initié à l'entrainement des animaux, je n'oublierais pas la période passée à se casser la tête pour savoir comment construire nos cubes compatibles IRM. Un grand merci à Pauline pour tout ce que tu m'as apporté, ta complicité, ta bonne humeur et ta tarte à la gomme resteront inoubliables. Tes connaissances et tes recherches constantes sur le bien-être animal ont permis d'améliorer pas mal de choses ! Julie, tu as su apprendre vite et être autonome tout en cherchant à améliorer tout ce qui pouvait l'être. Ton aide ces derniers mois m'a été précieuse et surtout merci de m'avoir soutenu pendant les moments de stress et de doutes ! Mathilda, transmettre son savoir n'est pas toujours chose aisée et pourtant tu as toujours été à l'écoute, su poser les bonnes questions et mettre en pratique intelligemment mes conseils.

Merci pour ton soutien, tes nombreuses relectures et corrections des derniers mois. Et n'oublie pas, même de l'autre côté de la planète tu pourras compter sur mon aide ! Un merci particulier à Franck pour toute l'aide que tu m'as apportée depuis l'installation de Primage malgré tous les obstacles et problèmes rencontrés ! Ton optimisme et ton investissement permanents ont été un vrai atout, surtout dans cette dernière ligne droite ! Merci également Nathalie pour ton aide sur certaines analyses.

Je tiens également à remercier Jean-Luc, Fabrice et Jonathan pour votre aide et pour votre travail quotidien à l'animalerie, ainsi que Sylvain et Johan pour les bugs informatiques. Je remercie les membres de l'équipe, passés et présents pour tout ce que l'on a partagé au cours de ces années : Sameh, Elaine, Serge, Fabio, Slimane, Corentin, Yann, Célia, Bassem, Mégane, Lou… Un grand merci aux membres du laboratoire, étudiants, post-doctorants, ingénieurs ou chercheurs, pour les rencontres, les repas partagés et les retours constructifs.

Merci à ma famille et en particulier mes parents pour m'avoir toujours soutenue et encouragée dans mes projets malgré les épreuves à surmonter. Un merci à ma petite sœur Marjolaine qui est venue partager mon quotidien au travail pendant un mois et qui suit un peu plus mes pas chaque jour. Merci à ma sœur Aurélia et mon frère Romain pour tous nos moments complices passés et présents. Merci à mes amies Iris, Marion et Mélanie pour leur soutien et leurs amitiés sincères depuis toutes ces années. Et enfin, merci à toi Michaël de partager ma vie, de me soutenir, de m'aider et me permettre de donner le meilleur de moi-même chaque jour. Merci pour tout…

Et enfin, je n'oublie pas de remercier mes petits loulous : Zira, Toumai, Elak, Samouraï et mon petit Scooby sans qui cette recherche n'aurait pu aboutir et pour tous les moments de complicité partagés. Vos personnalités, bien propres à chacun d'entre vous me manqueront…

Table of contents

Résumé

Bases neurales de la représentation spatiale grâce à l'imagerie par résonance magnétique fonctionnelle (IRMf).

La construction de la représentation de soi est basée sur l'intégration des informations que l'on reçoit des différentes modalités sensorielles telles que les informations visuelles, auditives, tactiles ou proprioceptives. L'interaction entre les actions et les mouvements, et plus récemment les interactions sociales et l'espace ont été étudiées essentiellement au niveau comportemental, moins au niveau fonctionnel et beaucoup reste encore à élucider. En particulier, il est important et essentiel de comprendre exactement quels processus sont impliqués dans la construction d'une représentation spatiale et comment ces processus sont mis en œuvre, non seulement au niveau local par l'activité de neurones spécifiques, dans une zone corticale spécifique, mais aussi à l'échelle du réseau dans son ensemble ainsi qu'à l'échelle du cerveau entier.

Le premier axe de ma thèse s'intéresse à l'espace peripersonnel, qui est l'espace le plus proche de nous et qui représente l'un des sous-espaces fonctionnels de la représentation spatiale. Nous faisons l'hypothèse que ce sont les mêmes régions qui contribuent à la convergence multisensorielle, à la prédiction des conséquences sur le traitement tactile d'une stimulation visuelle approchant le corps et à la construction de l'espace peripersonnel. Pour tester cette hypothèse, nous avons étudié l'effet des aspects prédictifs temporels et spatiaux d'un stimulus visuel dynamique sur la détection du stimulus tactile chez l'Homme (étude comportementale) et le primate non humain (étude en IRM fonctionnelle) ainsi que les bases neuronales de la représentation de l'espace proche et de la représentation de l'espace lointain, chez le primate non humain (étude en IRM fonctionnelle). Nous mettons en évidence l'implication d'un réseau parieto-frontal, essentiellement composé par l'aire intrapariétale ventrale VIP et l'aire

prémotrice F4 qui sont activées par ces trois mécanismes différents. Nous proposons que ce réseau traite non seulement la trajectoire de l'objet approchant vis-à-vis du corps, mais qu'il anticipe également ses conséquences sur le corps et prépare des actions de protection en réponse à ce stimulus approchant.

Le deuxième axe de ma thèse porte sur la caractérisation de l'étendue de la plasticité dans la représentation visuelle dans le cerveau adulte (par opposition aux premiers stades de plasticité observées autour des périodes critiques du développement) et en particulier, sur des développements méthodologiques permettant de mesurer les changements fins dans le cortex visuel induits par une telle plasticité. Plus précisément, nous avons développé un ensemble de méthodes d'IRM à haute résolution : imagerie fonctionnelle (cartographie visuelle à haute résolution, IRM au repos), pharmacologique (imagerie spectroscopique du GABA) et structurelle (IRM anatomique, DTI basée sur la diffusion des molécules d'eau), afin de définir des mesures de référence pour évaluer les changements induits par la plasticité à différents moments après son induction, à travers une étude longitudinale réalisée chez les mêmes animaux. Certaines de ces méthodes nécessitent encore quelques raffinements et ajustements mais, dans l'ensemble, elles montrent leur potentiel prometteur pour étudier la plasticité chez les primates non humains.

Dans l'ensemble, ce travail de thèse a permis de créer un lien fonctionnel entre les études d'IRMf effectuées chez l'Homme et les études d'enregistrement d'électrophysiologies chez le primate non humain. De plus, il entraine de nouvelles stratégies et pistes d'explorations à étudier dans le domaine de la représentation spatiale, à la fois chez l'Homme et le primate non humain.

Mots clés : Représentation spatiale, intégration multisensorielle, espace péripersonnel, réseau parieto-frontal, plasticité visuel, primate non humain, IRMf

Summary

Neural bases of space representation by functional magnetic resonance imaging (fMRI)

The construction of the representation of self is based on the integration of information received by our different sensory modalities such as visual, auditory, tactile or proprioceptive information. The interaction between actions and movements and more recently social interactions and space are being explored at the behavioral level, but less so at the functional level and much more remains to be elucidated. In particular, it is important and fundamental to understand exactly which processes are involved in space representation and how, not only from a partial view focusing on specific cortical areas and single neuron processes but at the scale of the whole brain and the functional networks.

The first axis of my thesis focuses on peripersonal space, that is the space that is closest to us, and represents one of the functional subspaces of spatial representation. We assume that it is the same regions that contribute to multisensory convergence, to the prediction of the consequences of a looming visual stimulus onto tactile processing and to the construction of peripersonal space. To test this hypothesis, we investigated the effect of the temporal and spatial predictive aspects of a dynamical looming visual stimulus onto tactile stimulus detection in humans (behavioral study) and non-human primates (fMRI study); the neural bases of near space and far space representations, in non-human primate (fMRI study). We highlight the involvement of a parieto-frontal network, essentially composed by the ventral intraparietal area VIP, the premotor area F4 as well as striate and extra-striate cortical regions, which are activated by these three different mechanisms. We propose that this network not only processes the trajectory of the looming object with respect to the body, but also anticipates its consequences onto the body and prepares protective actions in response to the looming stimulus.

The second axis of my thesis focuses on characterizing the extent of plasticity in the visual representation of the adult brain (as opposed to the early stages around the critical developmental periods) and in particular, how the associated fine-grained changes in the visual cortex can be precisely quantified along multiple dimensions (anatomical, functional, pharmacological). Specifically, we have developed a set of high-resolution MRI methods to assess functional (high-resolution visual mapping fMRI, rs-MRI), pharmacological (GABA spectroscopy imaging) and structural (anatomical MRI, DTI) imaging to define reference measures against which to evaluate the changes induced by plasticity at different times after its induction, through a longitudinal study performed in the same animals. Some of these methods need to be more refined but they show that they are really promising to study plasticity in non-human primate.

On the whole, this present doctoral research allows to make a functional link between human fMRI studies and monkey single cell recording studies and provides new strategies and explorations to perform on the spatial representation field both in humans and non-human primates.

Keywords: Space representation, multisensory integration, peripersonal space, functional parieto-frontal network, visual plasticity, non-human primate, fMRI

Abbreviations

Cortical areas

FEF	Frontal Eye Field
F2	Premotor area F2
F4	Premotor area F4
F5	Premotor area F5
LIP	Lateral intraparietal area
MIP	Medial intraparietal area
MST	Medial superior area
MT	Middle temporal area
PMZ	Paramotor zone
SII	Secondary somatosensory cortex
TO	Temporoparietal associated area
VIP	Ventral intraparietal area
V1	Visual area V1
V2	Visual area V2
V3	Visual area V3
V4	Visual area V4
1	somatosensory area 1
3b	somatosensory area 3B
45A	Orbitofrontal area
7	Parietal area
7op	Parietal operculum area 7op

Cortical sulci

CAS	Calcarine sulcus
CIS	Cingulate sulcus
CS	Central sulcus
HS	Hippocampal sulcus
IOS	Inferior occipital sulcus
IPS	Intraparietal Sulci
LUS	Lunate sulcus
OTS	Occipitotemporal sulcus

POS	Parieto-occipital sulcus
PS	Principal sulcus
STS	Superior temporal sulcus

Imagery

fMRI	functional Magnetic Resonance Imaging
BOLD	Blood Oxygenation level-dependent
MION	Monocrystalline Iron Oxide Nanoparticle
MR	Magnetic Resonance
MRS	Magnetic Resonance Spectroscopy
SNR	Signal-to-Noise Ratio
TR	Repetition Time
TI	Inversion Time
TE	Echo TIme
FA	Fractional anisotropy
DTI	Diffusion Tensor Imaging
MPRAGE	Magnetization-Prepared Rapid Gradient-Echo
FOV	Field of View
EPI	Echo Planar Imaging

Others

BCI	Basal Causal Inference
CSF	Cerebro-Spinal Fluid
E/I	Balance between Excitation and Inhibition
GABA	*gamma*-Aminobutyric acid
ICA	Independent Component Analysis
MD	Monocular Deprivation
PD	Parkinson Disease
RF	Receptive Field
ROI	Region of Interest
RT	Reaction Time
Run	Functional time series

« Pour progresser, il ne suffit pas de vouloir agir,

il faut d'abord savoir dans quel sens agir. »

Gustave Le Bon

Manuscript Organization

This PhD manuscript is composed of the research that I have conducted or contributed to during the past three and a half years as a doctorate student. It is organized in the form of published articles, submitted articles, articles in preparation and preliminary data. This amounts to a total of 5 articles, including two review articles (see publications list, p 19)

The manuscript is divided along two axes. The first axis focuses on the representation of the peripersonal space. It is composed of an introduction in which Part I gives an overview of the field of multisensory convergence, multisensory integration, impact prediction (introducing Chapter 1 and 2) and peripersonal space (introducing Chapter 3 and 4), Part II is a review article of literature about the link between these multisensory modalities and peripersonal space. This introduction is followed by the section "Impact prediction" presenting a human psychophysical study that demonstrates that tactile detection is enhanced by visual predictive cues (article published in *The Journal of Neuroscience 2015,* Chapter 1) and investigating the neural bases subserving this enhancement, with a fMRI study in monkeys (article submitted in *The Journal of Neuroscience 2017,* Chapter 2). The next section "Peripersonal space" describes the neural bases involved in the peripersonal space (article submitted in *Cerebral Cortex*, Chapter 3) and the dynamics and plasticity of this space (review article published in *Neuropsychologia 2015*, Chapter 4). These two sections are wrapped up by a discussion.

The second axis focuses on the visual representation plasticity. It is composed of an introduction giving an overview of some fundamental points of brain plasticity. The methodology section describes how we have implemented functional magnetic resonance imaging on a 3T scanner and developed MRI sequences to study visual plasticity (Chapter 5); and how we have implemented a semi-invasive animal model to study different ways of inducing plasticity and its consequences (Chapter 6). The results section presents the

preliminary (behavioral and functional) data obtained for this axis (Chapter 7) and is followed by a discussion

The two axes are merged around a general discussion, conclusions and perspectives section.

During my thesis, I was also involved in other projects within my team but also in collaborations with others laboratories. I have analyzed part of the data concerning whole brain mapping of visual and tactile convergence in the macaque monkey study. This study where I am second author was published in *NeuroImage 2015* (Appendix 1). I currently work in collaboration with Emmanuel Procyk and Céline Amiez of the team "Neurobiology of executive functions" on a study where we examine the cingulate cortex activations observed through various MRI studies performed by our team (reward, tactile stimulation, eyes movement). I will be the first author of this article (Appendix 2).

I have spent a lot of time training monkeys for my projects but also for others projects of my team. I have participated in a project about the neural bases of proactive inhibition and attentional orientation (analyses still in progress), on a project about the influence of Atomoxetine on non-selective and selective spatial attention in the non-human primate (Appendixe 3). I helped to develop DTI acquisition performed in monkey *in vivo*. (Appendix 4).

All the work performed during my doctoral years will lead to a total of 6 articles as first author, one article as second author and three others articles.

Publications list

Articles on doctoral research axes

Cléry J, Ben Hamed S (in prep). Frontier of self and impact prediction.

Introduction Part II, pp. 45-80

Cléry J*, Guipponi O*, Wardak C, Ben Hamed S (2015). Impact prediction by looming visual stimuli enhances tactile detection. ***J. Neuroscience***. 35 (10): 4179–4189.

Chapter 1, pp. 86-97

Cléry J, Guipponi O, Odouard S, Pinède S, Wardak C, Ben Hamed S (submitted). The prediction of impact of a looming stimulus onto the body is subserved by multisensory integration mechanisms.

Chapter 2, pp. 98-147

Cléry J, Guipponi O, Odouard S, Pinède S, Wardak C, Ben Hamed S (submitted). Cortical networks for encoding near and far space in the non-human primate.

Chapter 3, pp. 152-190

Cléry J, Guipponi O, Wardak C, Ben Hamed S (2015). Neuronal bases of peripersonal and extrapersonal spaces, their plasticity and their dynamics: Knowns and unknowns. ***Neuropsychologia*** 70 (2015) 313–326.

Chapter 4, pp. 191-205

Appendices

Guipponi O, **Cléry** J, Odouard S, Wardak C, Ben Hamed S (2015). Whole brain mapping of visual and tactile convergence in the macaque monkey. ***NeuroImage***, 117 (2015) 93–102.

Cléry J, Amiez C, Guipponi O, Wardak C, Procyk E, Ben Hamed S (article in preparation). Somatosensory, reward, and eye fields organization within the monkey cingulate motor areas.

Froesel M, Reynaud AJ, Guedj C, Ben Hadj Hassen S, **Cléry** J, Meunier M, Ben Hamed S, Hadj-Bouziane F (article in preparation). Noradrenaline differentially affects attention-related evidence accumulation and decision thresholds

Tounekti S, Bihan-Poudec Y, Troalen T, **Cléry** J, Froesel M, Lamberton F, Ben Hamed S, Hiba B (article in preparation). In-vivo High-Resolution DTI of Macaque Monkey Brain at 3T.

General

Introduction

Each of us builds an internal representation of space, integrating information received by our different sensory modalities. In other words, our representation of space is constructed on the basis of incoming visual information, but also auditory, proprioceptive and tactile information. This spatial representation therefore involves many senses such as vision, touch, hearing and relies essentially on multisensory interactions that are implemented at the neuronal level through multisensory integration.

Numerous studies in the last decades have brought a lot of information on this space representation from different perspectives: navigation and spatial memory (for review, see Grieves and Jeffery, 2017), the contribution of the visual and dorsal streams (for review, see Medendorp et al., 2016), spatial attention (for review, see Jerde and Curtis, 2013), eye movements and saccades (for review, see Lappi, 2016; Zimmermann and Lappe, 2016). The interaction between actions and movements and more recently social interactions and space are being explored at the behavioral level, but less so at the functional level and much more remains to be elucidated. In particular, it is important and fundamental to understand exactly which processes are involved in space representation and how, not only with a partial view focusing on specific cortical areas but at the scale of the whole brain.

From a clinical perspective, a deficit in any of the sensory modalities can have significant consequences on our representation of space and consequently on our daily life, it is thus important to understand the neural basis of this representation in order to identify ways to compensate for it, improve it in the case of injuries, deficits or diseases. During this doctoral research work, I worked along two main axes:

1) The representation of the peripersonal space. Spatial representation is often approached as a notion of unitary space, however there is now ample evidence that this space is actually divided into several functional spaces. The first axis of my thesis focuses on one of these functional subspaces, namely peripersonal space, that is, the space that is closest to us.

We have investigated the interaction between the body (as assessed by touch and somatosensory stimulations) and this space (as assessed by dynamic visual stimuli), both in humans and non-human primates, through several studies investigating the following issues: the effect of the temporal and spatial predictive aspects of a dynamical looming visual stimulus onto tactile stimulus detection in humans (behavioral study) and non-human primates (functional Magnetic Resonance Imaging study: fMRI); the neural bases of near space and far space representations, in non-human primate (fMRI study).

2) Plasticity of the adult visual representation. The visual skills can evolve, for example, when playing tennis, training will make it possible to incorporate the racket into the field of vision. This change co-occurs with changes in motor control that extend action beyond the hand, incorporating the racket as a tool. The second axis of my thesis has therefore focused on characterizing the extent of plasticity in visual representation in the adult brain (as opposed to the early stages around the critical developmental periods) and in particular, on the development of methods and technics to study such fine-grained changes in the visual cortex as induced by plasticity.

The majority of these studies are performed in non-human primates. In fact, the rhesus macaque (macaca mulatta) is a dominant model for cognitive neuroscience since this species, among the different animal models that dominate the neurosciences, has the following characteristics:

- This species is able to learn complex behavioral tasks used to study human cognitive functions. This distinguishes it from rat and mouse models and makes it more suitable for the study of high-level cortical functions.

- Because of its phylogenetic proximity to the human species, much of the fine observations made in this species (by targeted cell recordings or by anatomical studies) can be transposed directly to humans (whose study of cortical functions is dominated by fMRI).

Our choice to work with macaques using fMRI, a discipline still emerging, is based on the desire to evaluate in more details the conditions and limits of the transposition of knowledge between non-human primates and humans, concerning the cortical functions, as a missing functional link between human fMRI studies and monkey single cell recording studies. The use of this fMRI technique has another important advantage. It makes it possible to identify and locate the activations of certain voxels and thus precisely guide electrophysiological unitary or population activity recordings in well-characterized cortical regions.

References

Grieves RM, Jeffery KJ (2017) The representation of space in the brain. Behavioural Processes 135:113–131.

Jerde TA, Curtis CE (2013) Maps of space in human frontoparietal cortex. Journal of Physiology-Paris 107:510–516.

Lappi O (2016) Eye movements in the wild: Oculomotor control, gaze behavior & frames of reference. Neurosci Biobehav Rev 69:49–68.

Medendorp WP, de Brouwer AJ, Smeets JBJ (2016) Dynamic representations of visual space for perception and action. Cortex. DOI: 10.1016/j.cortex.2016.11.013.

Zimmermann E, Lappe M (2016) Visual Space Constructed by Saccade Motor Maps. Front Hum Neurosci 10. DOI: 10.3389/fnhum.2016.00225.

Axis I:

Representation of the peripersonal space

Introduction: Part I

The construction of the representation of self is based on the brain's association of all the sensory information (visual, auditory, tactile and proprioceptive, **Figure 1**) that comes to us continuously and that translates the relative state of our body in respect to our environment (Duhamel et al., 1997; Longo et al., 2010; Azañón et al., 2010). This phenomenon is called multisensory integration. A disruption of the integration between visual, tactile and proprioceptive information generates a feeling of excorporation or evanescence of the body that is found in certain pathologies such as autism or schizophrenia.

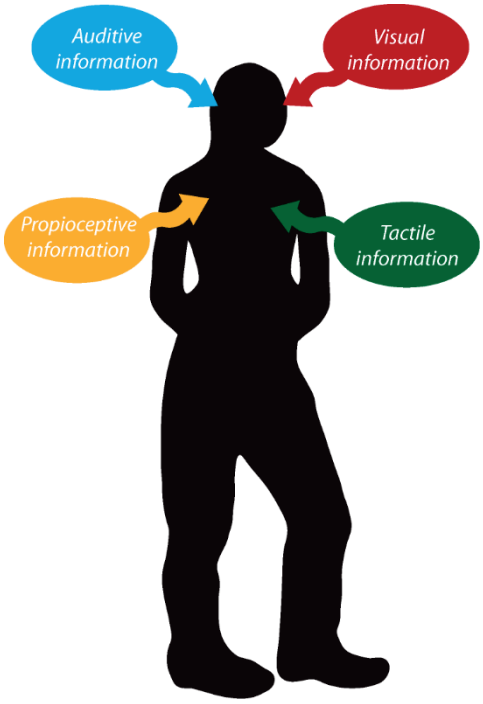

Figure 1: Sensory information arriving continuously allow the multisensory integration and the construction of the self representation.

This process of multisensory integration recruits visuo-tactile multisensory cortical regions that are considered to be at the heart of the sense of belonging of the body, i.e. the feeling that our body is effectively ours (Petkova et al., 2011). Interestingly, these same visuo-

tactile multisensory cortical areas are also involved in the coding of peripersonal space, that is, the part of the space closest to the subject that surrounds the defined somatosensory boundaries of the body by the skin (Brozzoli et al., 2012; Macaluso and Maravita, 2010).

1. Multisensory convergence

A multisensory convergence area corresponds to a brain region which receives afferent connections of different sensory modalities (Pandya and Kuypers, 1969; Jones and Powell, 1970; Meredith, 2002). That is to say that these regions can be activated by visual stimulations but also by tactile simulations or even three or more different sensory modalities. For example, several studies have shown that the temporal superior sulcus receives afferent connections from the primary visual cortex, the primary auditory cortex and somatosensory areas (Jones and Powell, 1970; Seltzer and Pandya, 1980; Schroeder and Foxe, 2005; for review, see Beauchamp, 2005a). Multisensory convergence has been described in many species including rodents (Toldi et al., 1986; Di et al., 1994; Barth et al., 1995; Brett-Green et al., 2003, 2004), cats (Berman and Cynader, 1972; Minciacchi et al., 1987; Wallace et al., 1992; Yaka et al., 2002), monkeys (Pandya and Kuypers, 1969; Jones and Powell, 1970; Hyvärinen and Poranen, 1974; Seltzer and Pandya, 1980; Maunsell and van Essen, 1983; Ungerleider and Desimone, 1986; Lewis and Van Essen, 2000; Duhamel et al., 1998; Avillac et al., 2005; Guipponi et al., 2013, 2015) and humans (Downar et al., 2000; Bremmer et al., 2001; Calvert, 2001; Wright et al., 2003; Beauchamp et al., 2004; Stein and Stanford, 2008).

The parietal cortex has long been known as a place of multisensory convergence (Pandya and Kuypers, 1969; Jones and Powell, 1970; Hyvärinen and Poranen, 1974; Seltzer and Pandya, 1980; Duhamel et al., 1998; Avillac et al., 2005), hence its qualification of associative cortex. In particular, the ventral intraparietal area (VIP) has been shown to be a place of visual,

proprioceptive, vestibular, auditory and tactile convergence (Colby et al., 1993; Duhamel et al., 1998; Bremmer et al., 2002b; Schlack et al., 2002, 2005; Schroeder and Foxe, 2005).

A recent study (Guipponi et al., 2013) shows that while visual and tactile modalities are strongly represented and activate mostly non-overlapping sectors within the intraparietal sulcus (IPS), a specific sector within VIP area is involved in the processing of the movement component of the environment with respect to the subject, independently of the sensory modality by which this movement is perceived (**Figure 2**).

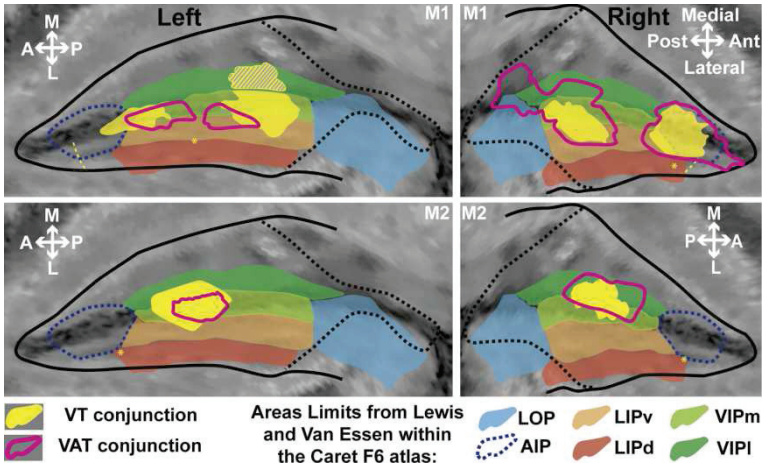

Figure 2: Projection of the VT (visuo-tactile) and VAT (visuo-audio-tactile) conjunction results onto the F6 Caret atlas. Only the activations at the fundus of the IPS (Guipponi et al., 2013).

This amodal representation of movement is proposed to be a key component in the construction of peripersonal space (Cléry et al., 2015b). It is important to note that multisensory convergence is not specific to the parietal cortex, but involves a parieto-frontal network (Guipponi et al., 2015) the description of which has only marginally evolved since the early work by Gross and Graziano (for reviews, see Gross and Graziano, 1995; Graziano and Cooke, 2006). Besides, and quite unexpectedly, this amodal representation of space also recruits primary sensory areas, in particular the visual areas and the primary somatosensory areas (Guipponi et al., 2015).

2. Multisensory integration

Multisensory integration is a neural process by which the neuronal response (in spikes per second) to two sensory stimuli of different modalities (e.g. visual and tactile) presented simultaneously, is different from the sum of neuronal responses produced by this same neuron in response to each sensory stimulus presented independently (Avillac et al., 2007, **Figure 3**).

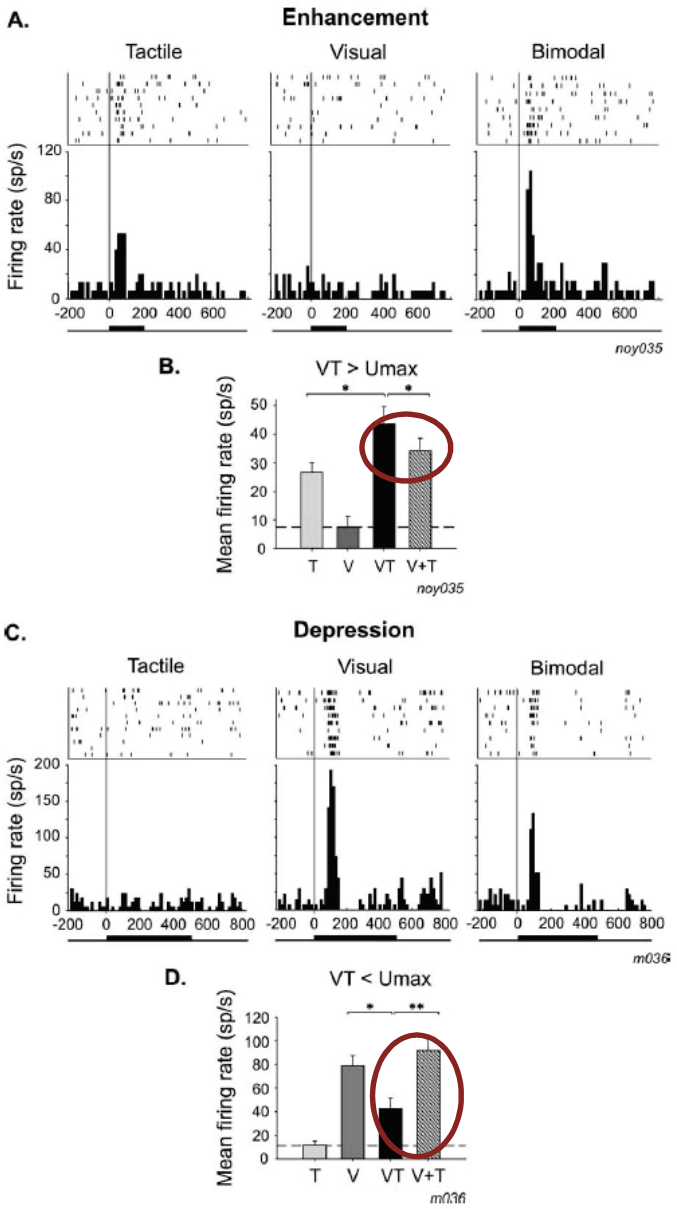

Figure 3: Single-cell examples of multisensory integration in unimodal neurons. A, B, Single-cell examples of enhancement responses. C, D, Single-cell examples of depression responses (Avillac et al., 2007). The red circles emphasize the difference in response of a neuron to a bimodal stimulation or to the sum of two independent unimodal stimulations.

From a behavioral point of view, this corresponds to the fact that a light tactile stimulus alone will be difficult to detect, whereas if it is very strong, the stimulus will be sufficient in itself to be detected. The addition of a coherent low salience visual stimulus will improve the detection of the weak tactile stimulus (**Figure 4**).

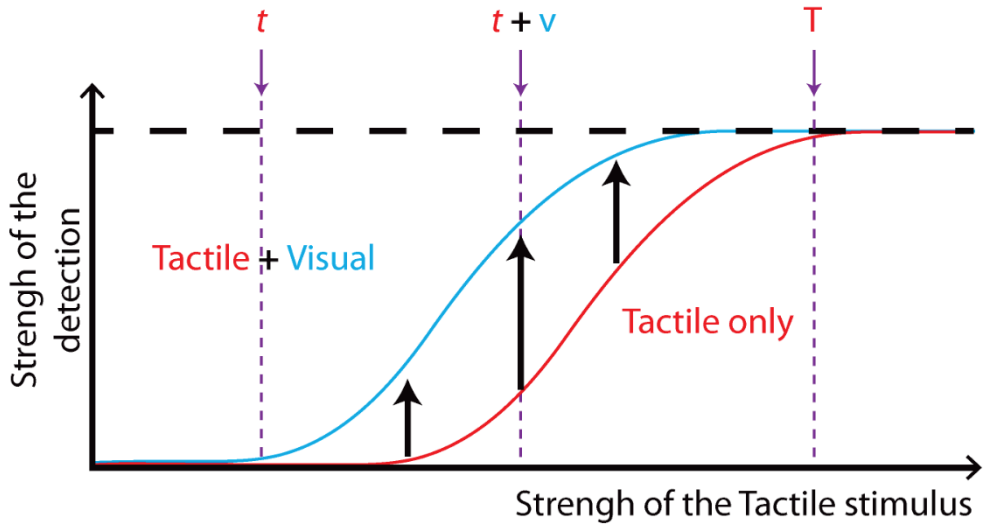

Figure 4 : Multisensory integration from a behavioral point of view.

It is assumed that the maximum of multisensory integration is observed when two stimuli of the different modalities presented are spatially and temporally congruent. The spatial congruency corresponds to the fact that the information comes from the same spatial source. For example, if one touches the hand of a monkey, or when one approaches the hand of this zone of the body evoking a visual response, this will lead in both cases to a response by the same neuron if this neuron has multisensory visuo-tactile characteristic. This is due in particular to the spatial overlap of the visual and the tactile receptive fields of these visuo-tactile bimodal neurons (Duhamel et al., 1998; Avillac et al., 2005). The temporal congruency corresponds to the simultaneity of the stimuli, i.e. they are presented in the same temporal window (Avillac et al., 2007; for review, see Wallace and Stevenson, 2014).

3. Impact prediction to the body

The general framework of multisensory integration assumes that multimodal sensory inputs have a common source (Sugita and Suzuki, 2003). This framework has been specifically extended in the case of dynamic multimodal sources, particularly in the context of visual-auditory integration, demonstrating that auditory stimuli that are spatially and temporally congruent improve the perception of both static (McDonald et al., 2000) and dynamic (Maier et al., 2004; Cappe et al., 2009; Leo et al., 2011; Parise et al., 2012) visual stimuli. This is understandable from an ecological point of view, since a visual information source can simultaneously be a source of auditory information (for example, seeing the lips move at the same time as hearing the words being pronounced).

In the context of visuo-tactile integration, this is less clear. Indeed, the impact of a stimulus on the face is rarely simultaneous with the first visual information about it. We rarely simultaneously experience seeing and being touched by a mosquito on the face whereas a more common situation is to see (or hear) the approach of the mosquito and then to feel its bite on the skin. Hyvärinen et Poranen (1974) described very early on the visual response of parietal neurons as an "anticipated activation" that appears before the neuron's tactile receptive field is touched. As a result, visual objects approaching the body have a high potential impact on this body and are therefore predictive of tactile activation and especially, harmful tactile activations.

Consequently, it would be more pertinent to be able to predict the impact time of the stimulus on the face rather than the simultaneity between visual and tactile information. Indeed, a dynamic approaching stimulus may have delayed consequences on a second sensory modality. The heteromodal somatosensory consequences of such a stimulus can be fully predicted by its spatiotemporal dynamics.

In addition, recent studies have shown that approaching auditory (Canzoneri et al., 2012) or looming visual stimuli (Kandula et al., 2015; De Paepe et al., 2016) predictively accelerate tactile processing and enhance tactile sensitivity (Cléry et al., 2015a, see Chapter 1). Indeed, when the approaching stimulus predicts correctly (spatially and / or temporally) the tactile stimulation, the reaction times of the subjects are shorter (**Figure 5)**.

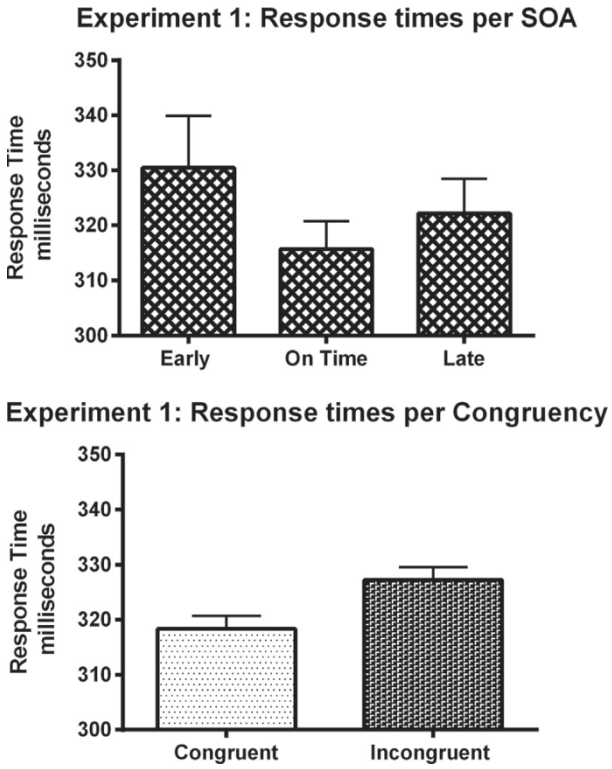

Figure 5 : Average response time from when the tactile stimulus is delivered. The top graph shows the mean response times plotted per Stimulus Onset Asynchrony (SOA). The response times for "On Time" are shorter than for the "Early" (before the visual impact) and "Late" (after the visual impact). The bottom graph shows that response times are shorter when the tactile stimulus is delivered on the same side as the impacting stimulus (congruent condition), from Kandula et al., 2015.

4. Evaluate multisensory integration using fMRI technique

Functional magnetic resonance imaging (fMRI) is a technique measuring brain activity. This technique is based on variations in blood oxygenation and flow in response to neural activity, called BOLD signal (Blood Oxygenation level-dependent). Indeed, when a brain area is more active, it consumes more oxygen and to meet this demand the blood flow increases in

this area. This technique allows us to see which parts of the brain are involved in specific cognitive processes such as learning or perception by producing an activation map.

While electrophysiological recordings show the activity of a neuron or a population of neurons, the BOLD signal reflects the indirect activity of thousands of neurons for each voxel. Therefore, with the first studies on multisensory integration using the fMRI technique, the question of how to compare fMRI results with electrophysiological records has arisen. Indeed, electrophysiology makes it possible to determine whether the recorded neuron is unimodal, bimodal or multimodal, whereas in fMRI, these different types of neurons can compose the same voxel and it is not possible to discriminate them (Benevento et al., 1977; Bruce et al., 1981; Meredith and Stein, 1983, 1986; Hikosaka et al., 1988; Barraclough et al., 2005; Allman and Meredith, 2007; Allman et al., 2008; Stein and Stanford, 2008).

This is why different criteria have been established in recent years to evaluate multisensory integration using this fMRI technique. These criteria are based on the statistical analyzes carried out on the magnetic resonance (MR) time series (Beauchamp, 2005b; Werner and Noppeney, 2011; Gentile et al., 2011; Love et al., 2011; Tyll et al., 2013). There are three main criteria (**Figure 6**) :

- ***Super/supra-additive criterion***: the multisensory response is larger than the sum of the unisensory responses (the most stringent criterion).
- ***Maxi-criterion***: the multisensory response is larger than the maximum of the unisensory responses.
- ***Mean-criterion***: the multisensory response is larger than the mean of unisensory responses (the least stringent criterion).

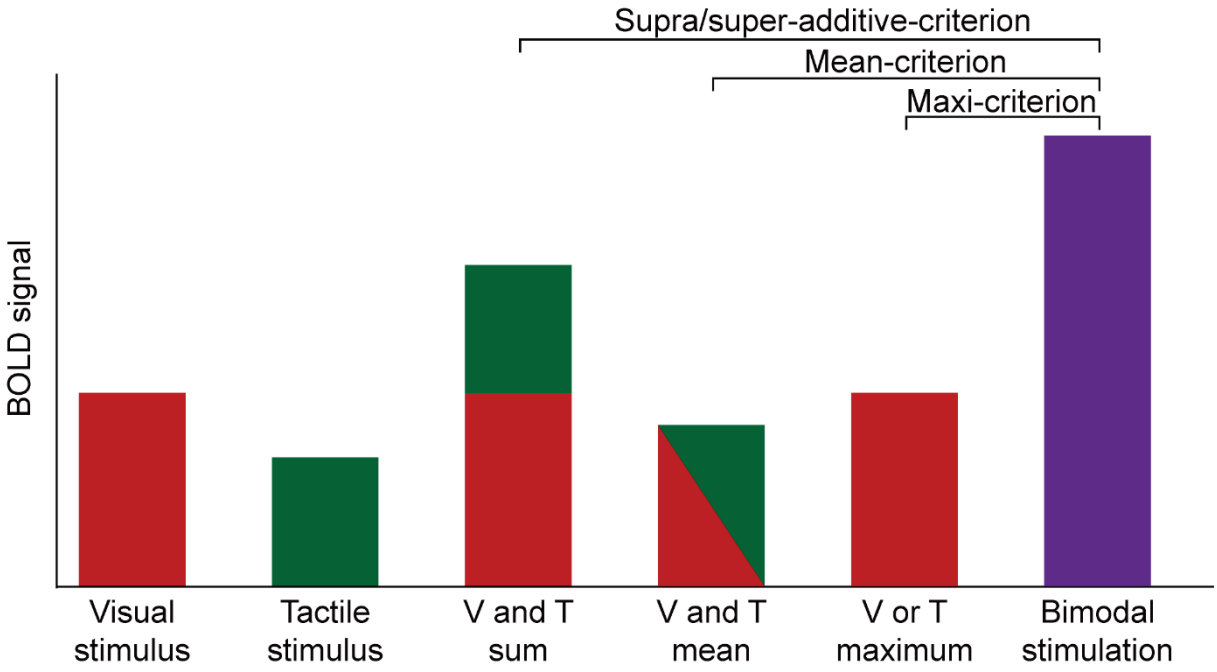

Figure 6 : Illustration of multisensory integration criteria in fMRI.

5. Bayesian Causal Inference

Most models of multisensory integration impose forced fusion between the sensory modalities, assuming a common source of sensory signals (Landy et al., 1995; Jacobs, 1999; Ernst and Banks, 2002; van Beers et al., 2002; Knill and Saunders, 2003; Alais and Burr, 2004; Hillis et al., 2004). However, to adequately reflect the world, the brain needs to integrate multisensory information that is associated to the same source while at the same time segregating multisensory information from different sources. Alternative models have thus been developed to account for this ecological ambiguity in the processing of concomitant multisensory information incoming to the brain. Bayesian Causal Inference framework (BCI) that probabilistically associates diverse sensory outcomes with a set of potential sources and that explicitly models the potential external situations that could have generated the observed sensory signals, appears as a very powerful computational framework in this respect (Körding

et al., 2007; Shams and Beierholm, 2010; Parise et al., 2012). Under the common source hypothesis, the sensory signals are integrated weighted by their reliability into the most reliable unbiased estimate (Ernst and Banks, 2002; Alais and Burr, 2004). Under the hypothesis of separate sources, signals are processed independently. Crucially, the brain does not know what causal structure best accounts for the sensory evidence: fusion or segregation. It thus needs to infer it from the available spatial, temporal and structural information, and prior knowledge on the environment (Slutsky and Recanzone, 2001; Lewald and Guski, 2003; Wallace et al., 2004; Gepshtein et al., 2005). The Bayesian Causal Inference model computes a final estimate of the actual structure of the incoming sensory evidence by averaging the spatial estimates under forced-fusion (common sources) and full-segregation (independent sources) assumptions weighted by the posterior probabilities of each causal structure (Körding et al., 2007). Using decisional strategies such as model averaging, model selection or probability matching, to combine the estimates under the various causal structures allows to obtain a final estimate of a physical property (Wozny et al., 2010).

In humans, Rohe and Noppeney (2015a, 2015b, 2016) demonstrate that BCI is performed by a neural hierarchy of multisensory processes. First, in primary sensory areas (such as visual or auditory cortices), sensory signals are segregated on the basis that two signals are generated by independent sources. Secondly, in the posterior intraparietal sulcus, sensory signals are fused, on the basis that two signals are from a common source. Finally, in anterior intraparietal sulcus, the uncertainty about the world's causal structure is taken into account and sensory signals are combined as predicted by Bayesian Causal Inference. Indeed, only parietal cortices integrate signals weighted by their bottom-up sensory reliabilities and top-down task relevance into multisensory spatial priority maps (Rohe and Noppeney, 2016). The generalization of this framework to dynamic stimuli is an important current concern in the field.

6. Space representation

Perceived space is a construct whose aim is to capture the environment to perform a specific action, perceptual, gestural, locomotory... (Jeannerod, 1987). Farnè et al. (2005a, 2005b) propose that space derives from the "perceptual space" and that this space is composed by different neuronal representations, each built in relation to the behavior we can perform in the environment. Space can be separated in different ways: corporeal/extracorporeal space; near/far space and perceived/represented space.

Among friends, we have close contacts, we can whisper in the ear of the other, or even kiss or hug. When we are dealing with a stranger, we keep our distance, ready to flee or attack, until we get to know this person better. This space around our body changes according to our mood or our environment, it is dynamic. The brain thus has a representation of the modular space, some cortical regions will be involved in the processing of *extrapersonal space* (or *far space*) while other cortical regions will participate in the processing of *peripersonal space* (or *near space*).

The far (extrapersonal) space corresponds to the space of action of the whole body (displacement) and of view, it is a space of projection (Pizzamiglio et al., 1989). It is the space far away from us on which we cannot act directly with our bodies. The near space (peripersonal) corresponds to the visuo-motor action space of the hand and the mouth, it is the manipulative space enabling us to delimit a space of security around our body, in direct connection with the consciousness that we have of the limits of this body. It is therefore the space that surrounds us and which we can directly interact with, **Figure 7** (for reviews, see Cléry et al., 2015b; de Vignemont and Iannetti, 2015). It is proposed that these two spaces be coded by different cerebral areas and neural mechanisms. Thus, in monkeys, neurons encoding far space are essentially visual whereas neurons encoding near space are mostly bimodal (Jeannerod, 2003).

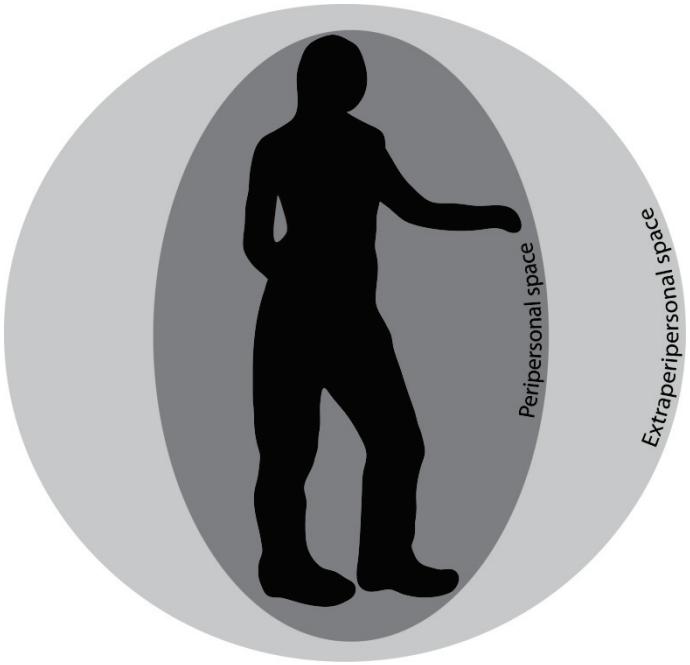

Figure 7 : Spaces around the body.The peripersonal space is the space that directly surrounds us and with which we can directly interact whereas the extrapersonal space is the space that is far away from the subject and that cannot be directly acted upon by the body (Cléry et al., 2015).

The construction and representation of self as an independent individual autonomously acting on its environment deeply relies on somatosensation (i.e. the primary processing of somatosensory cortical inputs) and somatoperception (i.e. the process of perceiving the body itself, and particularly of ensuring somatic perceptual constancy –Longo et al., 2010). It also deeply relies on the continuous interaction of the body with its environment, including remapping information from the body surface into an egocentric reference frame (Duhamel et al., 1997) as well as remapping information from the external world through their contact with the body (Azañón et al., 2010; Longo et al., 2010). These processes recruit multisensory cortical regions which are thought to be at the core of body ownership, i.e. the feeling that our body is indeed our own (Petkova et al., 2011). Interestingly, multisensory visuo-tactile cortical areas are also involved in the coding of peripersonal space, that is the portion of space that surrounds the body somatosensory limits and is closest to it (for reviews, see Macaluso and Maravita, 2010; Brozzoli et al., 2012; Cléry et al., 2015b; de Vignemont and Iannetti, 2015). This space

is characterized by a high degree of multisensory integration between visual, tactile and auditory information, which differs from farther regions of space (Cardinali et al., 2009, see also section Axis I, Introduction: Part II).

Hemispatial neglect

Early studies have shown that, in non-human primates, the ablation in the prearcuate sulcus of area 8 (Rizzolatti et al., 1983), corresponding to the Frontal Eye Field (FEF), results in an inattention to the contralateral objects, and this is more pronounced for the far objects than for the near objects, but also a decrease in the control of the movements of the eyes (Wardak et al., 2006) leading in a deficit of the visual process of objects in this part of the visual field. On the contrary, the ablation, in the postarcuate sulcus, of the frontal area 6 produces a severe inattention to the contralateral objects, but this time more pronounced for the near objects than for the far objects (Rizzolatti et al., 1983).

This inattention to the contralateral objects corresponds to a pathology called *hemispatial neglect*. It is characterized by an inability to detect, orientate towards, or respond to, meaningful stimuli when presented in the contralesional hemi-space (Heilman et al., 2000). In 1991, Halligan et Marshall provided the first neuropsychological evidence of left hemispatial neglect in the near space but not in the far space after a unilateral lesion of the right hemisphere. Since then, numerous studies in humans have described cases of hemispatial neglect specific to the near space (Berti and Frassinetti, 2000; Beschin and Robertson, 1997; Bisiach et al., 1986; Guariglia and Antonucci, 1992; Halligan et al., 2003; Halligan and Marshall, 1991; Ortigue et al., 2006) or specific to the far space (Coslett et al., 1993; Cowey et al., 1994, 1999; Vuilleumier et al., 1998; Ackroyd et al., 2002; Ortigue et al., 2006) suggesting that near space and far space can be coded separately by the brain.

It is important to determine the neural bases involved in these representations of space in order to better understand the dysfunctions observed in certain pathologies such as hemispatial neglect, and to try to find solutions to compensate for these deficits but also to understand the neural mechanisms through which our projected actions onto the far and near space are integrated and modulated by emotional and social components.

References

Ackroyd K, Riddoch MJ, Humphreys GW, Nightingale S, Townsend S (2002) Widening the sphere of influence: using a tool to extend extrapersonal visual space in a patient with severe neglect. Neurocase 8:1–12.

Alais D, Burr D (2004) The ventriloquist effect results from near-optimal bimodal integration. Curr Biol 14:257–262.

Allman BL, Keniston LP, Meredith MA (2008) Subthreshold auditory inputs to extrastriate visual neurons are responsive to parametric changes in stimulus quality: sensory-specific versus non-specific coding. Brain Res 1242:95–101.

Allman BL, Meredith MA (2007) Multisensory processing in "unimodal" neurons: cross-modal subthreshold auditory effects in cat extrastriate visual cortex. J Neurophysiol 98:545–549.

Avillac M, Denève S, Olivier E, Pouget A, Duhamel J-R (2005) Reference frames for representing visual and tactile locations in parietal cortex. Nat Neurosci 8:941–949.

Avillac M, Hamed SB, Duhamel J-R (2007) Multisensory Integration in the Ventral Intraparietal Area of the Macaque Monkey. J Neurosci 27:1922–1932.

Azañón E, Longo MR, Soto-Faraco S, Haggard P (2010) The Posterior Parietal Cortex Remaps Touch into External Space. Current Biology 20:1304–1309.

Barraclough NE, Xiao D, Baker CI, Oram MW, Perrett DI (2005) Integration of visual and auditory information by superior temporal sulcus neurons responsive to the sight of actions. J Cogn Neurosci 17:377–391.

Barth DS, Goldberg N, Brett B, Di S (1995) The spatiotemporal organization of auditory, visual, and auditory-visual evoked potentials in rat cortex. Brain Res 678:177–190.

Beauchamp MS (2005a) See me, hear me, touch me: multisensory integration in lateral occipital-temporal cortex. Current Opinion in Neurobiology 15:145–153.

Beauchamp MS (2005b) Statistical Criteria in fMRI Studies of Multisensory Integration. Neuroinformatics 3:93–113.

Beauchamp MS, Lee KE, Argall BD, Martin A (2004) Integration of Auditory and Visual Information about Objects in Superior Temporal Sulcus. Neuron 41:809–823.

Benevento LA, Fallon J, Davis BJ, Rezak M (1977) Auditory--visual interaction in single cells in the cortex of the superior temporal sulcus and the orbital frontal cortex of the macaque monkey. Exp Neurol 57:849–872.

Berman N, Cynader M (1972) Comparison of receptive-field organization of the superior colliculus in Siamese and normal cats. J Physiol (Lond) 224:363–389.

Berti A, Frassinetti F (2000) When far becomes near: remapping of space by tool use. J Cogn Neurosci 12:415–420.

Beschin N, Robertson IH (1997) Personal versus extrapersonal neglect: a group study of their dissociation using a reliable clinical test. Cortex 33:379–384.

Bisiach E, Perani D, Vallar G, Berti A (1986) Unilateral neglect: personal and extra-personal. Neuropsychologia 24:759–767.

Bremmer F, Klam F, Duhamel J-R, Ben Hamed S, Graf W (2002) Visual–vestibular interactive responses in the macaque ventral intraparietal area (VIP). European Journal of Neuroscience 16:1569–1586.

Bremmer F, Schlack A, Shah NJ, Zafiris O, Kubischik M, Hoffmann K, Zilles K, Fink GR (2001) Polymodal motion processing in posterior parietal and premotor cortex: a human fMRI study strongly implies equivalencies between humans and monkeys. Neuron 29:287–296.

Brett-Green B, Fifková E, Larue DT, Winer JA, Barth DS (2003) A multisensory zone in rat parietotemporal cortex: intra- and extracellular physiology and thalamocortical connections. J Comp Neurol 460:223–237.

Brett-Green B, Paulsen M, Staba RJ, Fifková E, Barth DS (2004) Two distinct regions of secondary somatosensory cortex in the rat: topographical organization and multisensory responses. J Neurophysiol 91:1327–1336.

Brozzoli C, Makin TR, Cardinali L, Holmes NP, Farnè A (2012) Peripersonal Space: A Multisensory Interface for Body–Object Interactions. In: The Neural Bases of Multisensory Processes (Murray MM, Wallace MT, eds) Frontiers in Neuroscience. Boca Raton (FL): CRC Press/Taylor & Francis.

Bruce C, Desimone R, Gross CG (1981) Visual properties of neurons in a polysensory area in superior temporal sulcus of the macaque. J Neurophysiol 46:369–384.

Calvert GA (2001) Crossmodal Processing in the Human Brain: Insights from Functional Neuroimaging Studies. Cereb Cortex 11:1110–1123.

Canzoneri E, Magosso E, Serino A (2012) Dynamic Sounds Capture the Boundaries of Peripersonal Space Representation in Humans. PLoS ONE 7:e44306.

Cappe C, Thut G, Romei V, Murray MM (2009) Selective integration of auditory-visual looming cues by humans. Neuropsychologia 47:1045–1052.

Cardinali L, Brozzoli C, Farnè A (2009) Peripersonal space and body schema: two labels for the same concept? Brain Topogr 21:252–260.

Cléry J, Guipponi O, Odouard S, Wardak C, Ben Hamed S (2015a) Impact prediction by looming visual stimuli enhances tactile detection. J Neurosci 35:4179–4189.

Cléry J, Guipponi O, Wardak C, Ben Hamed S (2015b) Neuronal bases of peripersonal and extrapersonal spaces, their plasticity and their dynamics: Knowns and unknowns. Neuropsychologia 70:313–326.

Colby CL, Duhamel JR, Goldberg ME (1993) Ventral intraparietal area of the macaque: anatomic location and visual response properties. Journal of Neurophysiology 69:902–914.

Coslett HB, Schwartz MF, Goldberg G, Haas D, Perkins J (1993) Multi-modal hemispatial deficits after left hemisphere stroke. A disorder of attention? Brain 116 (Pt 3):527–554.

Cowey A, Small M, Ellis S (1994) Left visuo-spatial neglect can be worse in far than in near space. Neuropsychologia 32:1059–1066.

Cowey A, Small M, Ellis S (1999) No abrupt change in visual hemineglect from near to far space. Neuropsychologia 37:1–6.

De Paepe AL, Crombez G, Legrain V (2016) What's Coming Near? The Influence of Dynamical Visual Stimuli on Nociceptive Processing. PLOS ONE 11:e0155864.

de Vignemont F, Iannetti GD (2015) How many peripersonal spaces? Neuropsychologia 70:327–334.

Di S, Brett B, Barth DS (1994) Polysensory evoked potentials in rat parietotemporal cortex: combined auditory and somatosensory responses. Brain Res 642:267–280.

Downar J, Crawley AP, Mikulis DJ, Davis KD (2000) A multimodal cortical network for the detection of changes in the sensory environment. Nat Neurosci 3:277–283.

Duhamel J-R, Bremmer F, BenHamed S, Graf W (1997) Spatial invariance of visual receptive fields in parietal cortex neurons. Nature 389:845–848.

Duhamel J-R, Colby CL, Goldberg ME (1998) Ventral Intraparietal Area of the Macaque: Congruent Visual and Somatic Response Properties. Journal of Neurophysiology 79:126–136.

Ernst MO, Banks MS (2002) Humans integrate visual and haptic information in a statistically optimal fashion. Nature 415:429–433.

Farnè A, Demattè ML, Làdavas E (2005a) Neuropsychological evidence of modular organization of the near peripersonal space. Neurology 65:1754–1758.

Farnè A, Iriki A, Làdavas E (2005b) Shaping multisensory action–space with tools: evidence from patients with cross-modal extinction. Neuropsychologia 43:238–248.

Gentile G, Petkova VI, Ehrsson HH (2011) Integration of Visual and Tactile Signals From the Hand in the Human Brain: An fMRI Study. Journal of Neurophysiology 105:910–922.

Gepshtein S, Burge J, Ernst MO, Banks MS (2005) The combination of vision and touch depends on spatial proximity. J Vis 5:1013–1023.

Graziano MSA, Cooke DF (2006) Parieto-frontal interactions, personal space, and defensive behavior. Neuropsychologia 44:845–859.

Gross CG, Graziano MSA (1995) REVIEW: Multiple Representations of Space in the Brain. Neuroscientist 1:43–50.

Guariglia C, Antonucci G (1992) Personal and extrapersonal space: a case of neglect dissociation. Neuropsychologia 30:1001–1009.

Guipponi O, Cléry J, Odouard S, Wardak C, Ben Hamed S (2015) Whole brain mapping of visual and tactile convergence in the macaque monkey. NeuroImage 117:93–102.

Guipponi O, Wardak C, Ibarrola D, Comte J-C, Sappey-Marinier D, Pinède S, Hamed SB (2013) Multimodal Convergence within the Intraparietal Sulcus of the Macaque Monkey. J Neurosci 33:4128–4139.

Halligan PW, Fink GR, Marshall JC, Vallar G (2003) Spatial cognition: evidence from visual neglect. Trends Cogn Sci (Regul Ed) 7:125–133.

Halligan PW, Marshall JC (1991) Left neglect for near but not far space in man. Nature 350:498–500.

Heilman KM, Valenstein E, Watson RT (2000) Neglect and related disorders. Semin Neurol 20:463–470.

Hikosaka K, Iwai E, Saito H, Tanaka K (1988) Polysensory properties of neurons in the anterior bank of the caudal superior temporal sulcus of the macaque monkey. J Neurophysiol 60:1615–1637.

Hillis JM, Watt SJ, Landy MS, Banks MS (2004) Slant from texture and disparity cues: optimal cue combination. J Vis 4:967–992.

Hyvärinen J, Poranen A (1974) Function of the parietal associative area 7 as revealed from cellular discharges in alert monkeys. Brain 97:673–692.

Jacobs RA (1999) Optimal integration of texture and motion cues to depth. Vision Res 39:3621–3629.

Jeannerod M (1987) Neurophysiological and Neuropsychological Aspects of Spatial Neglect, Volume 45 - 1st Edition, Advances in Psychology.

Jeannerod M (2003) The mechanism of self-recognition in humans. Behav Brain Res 142:1–15.

Jones EG, Powell TP (1970) Connexions of the somatic sensory cortex of the rhesus monkey. 3. Thalamic connexions. Brain 93:37–56.

Kandula M, Hofman D, Dijkerman HC (2015) Visuo-tactile interactions are dependent on the predictive value of the visual stimulus. Neuropsychologia 70:358–366.

Knill DC, Saunders JA (2003) Do humans optimally integrate stereo and texture information for judgments of surface slant? Vision Res 43:2539–2558.

Körding KP, Beierholm U, Ma WJ, Quartz S, Tenenbaum JB, Shams L (2007) Causal Inference in Multisensory Perception. PLoS ONE 2:e943.

Landy MS, Maloney LT, Johnston EB, Young M (1995) Measurement and modeling of depth cue combination: in defense of weak fusion. Vision Res 35:389–412.

Leo F, Romei V, Freeman E, Ladavas E, Driver J (2011) Looming sounds enhance orientation sensitivity for visual stimuli on the same side as such sounds. Exp Brain Res 213:193–201.

Lewald J, Guski R (2003) Cross-modal perceptual integration of spatially and temporally disparate auditory and visual stimuli. Brain Res Cogn Brain Res 16:468–478.

Lewis JW, Van Essen DC (2000) Corticocortical connections of visual, sensorimotor, and multimodal processing areas in the parietal lobe of the macaque monkey. J Comp Neurol 428:112–137.

Longo MR, Azañón E, Haggard P (2010) More than skin deep: Body representation beyond primary somatosensory cortex. Neuropsychologia 48:655–668.

Love SA, Pollick FE, Latinus M (2011) Cerebral Correlates and Statistical Criteria of Cross-Modal Face and Voice Integration. Seeing and Perceiving 24:351–367.

Macaluso E, Maravita A (2010) The representation of space near the body through touch and vision. Neuropsychologia 48:782–795.

Maier JX, Neuhoff JG, Logothetis NK, Ghazanfar AA (2004) Multisensory Integration of Looming Signals by Rhesus Monkeys. Neuron 43:177–181.

Maunsell JH, van Essen DC (1983) The connections of the middle temporal visual area (MT) and their relationship to a cortical hierarchy in the macaque monkey. J Neurosci 3:2563–2586.

McDonald JJ, Teder-Sälejärvi WA, Hillyard SA (2000) Involuntary orienting to sound improves visual perception. Nature 407:906–908.

Meredith MA (2002) On the neuronal basis for multisensory convergence: a brief overview. Brain Res Cogn Brain Res 14:31–40.

Meredith MA, Stein BE (1983) Interactions among converging sensory inputs in the superior colliculus. Science 221:389–391.

Meredith MA, Stein BE (1986) Visual, auditory, and somatosensory convergence on cells in superior colliculus results in multisensory integration. J Neurophysiol 56:640–662.

Minciacchi D, Tassinari G, Antonini A (1987) Visual and somatosensory integration in the anterior ectosylvian cortex of the cat. Brain Res 410:21–31.

Ortigue S, Mégevand P, Perren F, Landis T, Blanke O (2006) Double dissociation between representational personal and extrapersonal neglect. Neurology 66:1414–1417.

Pandya DN, Kuypers HG (1969) Cortico-cortical connections in the rhesus monkey. Brain Res 13:13–36.

Parise CV, Spence C, Ernst MO (2012) When correlation implies causation in multisensory integration. Curr Biol 22:46–49.

Petkova VI, Khoshnevis M, Ehrsson HH (2011) The perspective matters! Multisensory integration in ego-centric reference frames determines full-body ownership. Front Psychology 2:35.

Pizzamiglio L, Cappa S, Vallar G, Zoccolotti P, Bottini G, Ciurli P, Guariglia C, Antonucci G (1989) Visual neglect for far and near extra-personal space in humans. Cortex 25:471–477.

Rizzolatti G, Matelli M, Pavesi G (1983) Deficits in attention and movement following the removal of postarcuate (area 6) and prearcuate (area 8) cortex in macaque monkeys. Brain 106 (Pt 3):655–673.

Rohe T, Noppeney U (2015a) Cortical Hierarchies Perform Bayesian Causal Inference in Multisensory Perception. PLoS Biol 13:e1002073.

Rohe T, Noppeney U (2015b) Sensory reliability shapes perceptual inference via two mechanisms. Journal of Vision 15:22.

Rohe T, Noppeney U (2016) Distinct Computational Principles Govern Multisensory Integration in Primary Sensory and Association Cortices. Curr Biol 26:509–514.

Schlack A, Hoffmann K-P, Bremmer F (2002) Interaction of linear vestibular and visual stimulation in the macaque ventral intraparietal area (VIP). Eur J Neurosci 16:1877–1886.

Schlack A, Sterbing-D'Angelo SJ, Hartung K, Hoffmann K-P, Bremmer F (2005) Multisensory space representations in the macaque ventral intraparietal area. J Neurosci 25:4616–4625.

Schroeder CE, Foxe J (2005) Multisensory contributions to low-level, "unisensory" processing. Curr Opin Neurobiol 15:454–458.

Seltzer B, Pandya DN (1980) Converging visual and somatic sensory cortical input to the intraparietal sulcus of the rhesus monkey. Brain Res 192:339–351.

Shams L, Beierholm UR (2010) Causal inference in perception. Trends in Cognitive Sciences 14:425–432.

Slutsky DA, Recanzone GH (2001) Temporal and spatial dependency of the ventriloquism effect. Neuroreport 12:7–10.

Stein BE, Stanford TR (2008) Multisensory integration: current issues from the perspective of the single neuron. Nat Rev Neurosci 9:255–266.

Sugita Y, Suzuki Y (2003) Audiovisual perception: Implicit estimation of sound-arrival time. Nature 421:911–911.

Toldi J, Fehér O, Wolff JR (1986) Sensory interactive zones in the rat cerebral cortex. Neuroscience 18:461–465.

Tyll S, Bonath B, Schoenfeld MA, Heinze H-J, Ohl FW, Noesselt T (2013) Neural basis of multisensory looming signals. NeuroImage 65:13–22.

Ungerleider LG, Desimone R (1986) Cortical connections of visual area MT in the macaque. J Comp Neurol 248:190–222.

van Beers RJ, Wolpert DM, Haggard P (2002) When feeling is more important than seeing in sensorimotor adaptation. Curr Biol 12:834–837.

Vuilleumier P, Valenza N, Mayer E, Reverdin A, Landis T (1998) Near and far visual space in unilateral neglect. Ann Neurol 43:406–410.

Wallace MT, Meredith MA, Stein BE (1992) Integration of multiple sensory modalities in cat cortex. Exp Brain Res 91:484–488.

Wallace MT, Roberson GE, Hairston WD, Stein BE, Vaughan JW, Schirillo JA (2004) Unifying multisensory signals across time and space. Exp Brain Res 158:252–258.

Wallace MT, Stevenson RA (2014) The construct of the multisensory temporal binding window and its dysregulation in developmental disabilities. Neuropsychologia 64C:105–123.

Wardak C, Ibos G, Duhamel J-R, Olivier E (2006) Contribution of the monkey frontal eye field to covert visual attention. J Neurosci 26:4228–4235.

Werner S, Noppeney U (2011) The Contributions of Transient and Sustained Response Codes to Audiovisual Integration. Cereb Cortex 21:920–931.

Wozny DR, Beierholm UR, Shams L (2010) Probability matching as a computational strategy used in perception. PLoS Comput Biol 6.

Wright TM, Pelphrey KA, Allison T, McKeown MJ, McCarthy G (2003) Polysensory interactions along lateral temporal regions evoked by audiovisual speech. Cereb Cortex 13:1034–1043.

Yaka R, Notkin N, Yinon U, Wollberg Z (2002) Visual, auditory and bimodal activity in the banks of the lateral suprasylvian sulcus in the cat. Neurosci Behav Physiol 32:103–108.

Introduction: Part II

Frontier of self and impact prediction

Review in prepration

Frontier of self and impact prediction

Justine Cléry and Suliann Ben Hamed

Institut des Sciences Cognitives Marc Jeannerod, UMR5229, CNRS-Université Claude Bernard Lyon I, 67 Boulevard Pinel, 69675 Bron, France

Corresponding author: Suliann Ben Hamed, benhamed@isc.cnrs.fr

Keywords: visual, tactile, looming stimuli, prediction, multisensory integration, peripersonal space.

Abstract:

The construction of a coherent representation of our body and the mapping of the space immediately surrounding it is of the highest ecological importance. Indeed, this space has at least several specificities: it is a space where proximal actions are planned in order to interact with our environment; it is a space that contributes to the experience of self and self-boundaries, through tactile perception; last, it is a space that contributes to the experience of body integrity against external events. In last decades, numerous studies have been interested in this peripersonal space (PPS), defined as the space directly surrounding us and which we can interact with (for reviews, see Cléry et al., 2015b; de Vignemont and Iannetti, 2015; di Pellegrino and Làdavas, 2015). These studies have contributed to the understanding of how this space is constructed, encoded and modulated. The majority of these studies focused on subparts of this PPS (the hand, the face or the trunk) and very few of them investigated the interaction between PPS subparts. In the present review, we summarize the latest advances on this research and we discuss the news perspectives that are set forth for futures investigations on this topic. We describe the most recent methods used to estimate the PPS boundaries by the means of dynamic stimuli. We then highlight how impact prediction and approaching stimuli modulate this space by social, emotional and action-related components involving principally a parieto-frontal network. In a next step, we review evidence that there is not a unique representation of peripersonal space but at least three sub-sections (hand, face and trunk PPS). Last, we discuss how these subspaces interact, and we question whether and how bodily self-consciousness (BSC) is functionally and behaviorally linked to PPS.

1 PERIPERSONAL SPACE

In everyday life, we are solicited by multiple stimuli in our environment. The space around us is filled with conspecifics, animals and objects, often animated by their own goals. Most of the time, this implies interacting with these elements of the environment along a very rich and complex repertoire that depends on the context and the very nature of this environment. This required the construction of a coherent representation of our body and the mapping of the space immediately surrounding it, the so-called peripersonal space (PPS), both in order to estimate the consequences of the environment and the consequences of our own actions onto our body. Interestingly, this PPS is subserved in the brain by specific neuronal mechanisms embedded in a well identified cortical network that specifically processes visual or auditory information occurring in the space that directly surrounds us and in which we can interact as well as the tactile information occurring right at the frontier of our body.

Visuo-tactile neurons as a possible substrate for PPS encoding in the cortex. Research in non-human primates has shown that multisensory cues, in particular those involving the body, are processed and integrated by a specialized neural system mapping the peripersonal space (**Figure 1A**). Specific populations of multisensory neurons integrate tactile information on the body (arm, face or trunk) with visual or auditory stimuli occurring in peripersonal space, i.e. close to the body. These multisensory neurons are described in the fronto-parietal network of the macaque brain involving the ventral premotor cortex (vPM; F4, G. Rizzolatti et al., 1981a, 1981b; or polysensory zone PZ, Graziano et al., 1994; M. S. A. Graziano et al., 1997; Graziano et al., 1999; Fogassi et al., 1996; Graziano and Cooke, 2006), the ventral intraparietal area on the fundus of the intraparietal sulcus (VIP, J. Hyvärinen and Poranen, 1974; Duhamel et al., 1997, 1998; Avillac et al., 2005; Schlack et al., 2005; Graziano and Cooke, 2006), in the parietal areas 7b as well as in subcortical regions such as the putamen (Graziano and Gross, 1993). Though the response properties of these neurons are modulated by eye position their visual receptive fields are anchored to specific body

parts. This suggests that the representation of multisensory of PPS they hold is body-part centered (Duhamel et al., 1997; Avillac et al., 2005; Graziano and Cooke, 2006; Graziano et al., 2000).

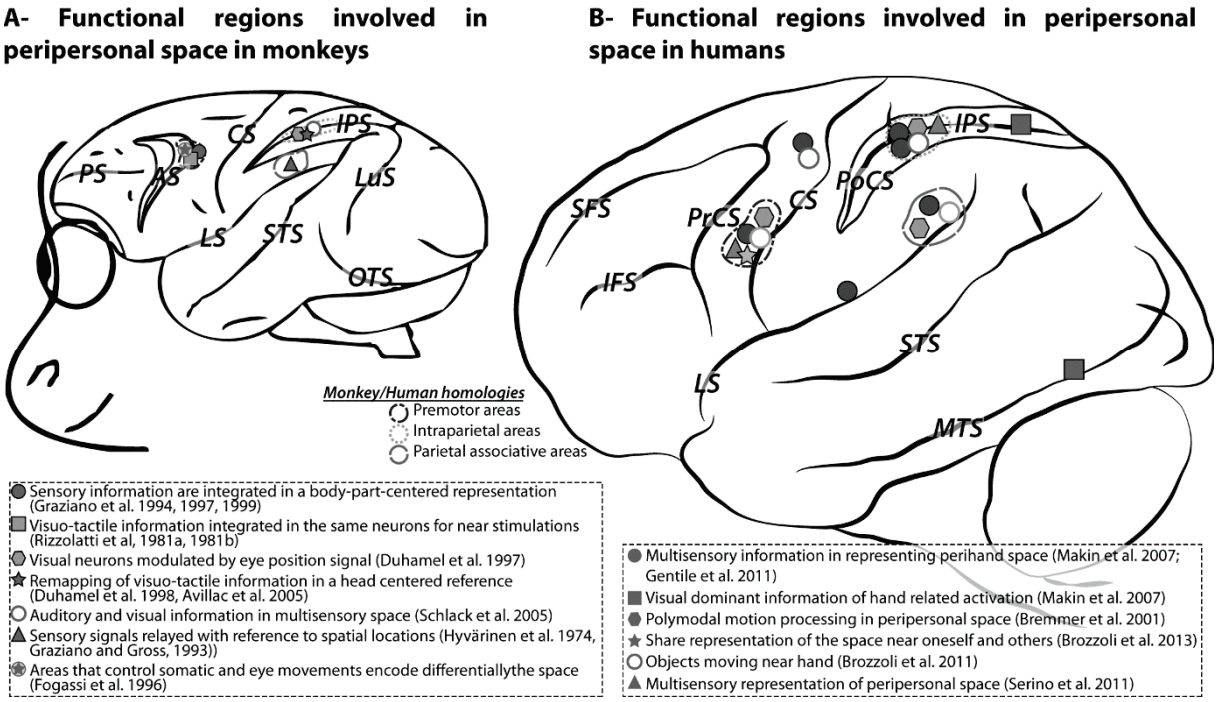

Figure 1: Functional regions involved in peripersonal space in monkeys (A) and in humans (B). Three homologous regions coding peripersonal space representation have been found in monkeys and humans: premotor, intraparietal and parietal associative areas. *Cortical sulci: AS, arcuate sulcus; CS, central sulcus; IFS, inferior frontal sulcus; IPS, intraparietal sulcus; LS, lateral sulcus; LuS, luneate sulcus; MTS, middle temporal sulcus; PoCS, postcentral sulcus; PrCS, precentral sulcus; PS, principal sulcus; SFS, superior frontal sulcus; STS, superior temporal sulcus; OTS, occipito-temporal sulcus.*

Clinical evidence for visuo-tactile interactions in PPS. Extinction is a neurological condition whereby patients fail to detect contralesional stimuli only when challenged in the sensory processing they are required to perform by the presentation of a double (ipsilesional and contralesional) simultaneous stimulation (Bender, 1952; Mattingley et al., 1997; Làdavas and Serino, 2008). This condition is observed both when the concurrent stimuli are from the same sensory modality (e.g. both visual, unimodal extinction) and when the concurrent stimuli are from

two different modalities (e.g. one is visual and the other is tactile, cross-modal extinction). Indeed, in right brain-damaged patients with tactile extinction, visual or auditory stimulations on the ipsilesional side exacerbate contralesional tactile extinction. In contrast, if the visual and tactile stimuli are both presented on the same contralesional side, then, the clinical deficit is reduced (Làdavas et al., 1998a). Therefore, cross-modal extinction can be modulated as a function of the spatial arrangement of the stimuli with respect to the patient's body (Farnè et al., 2005a, 2005b; for review, see Làdavas, 2002). Importantly, this modulation is most consistently obvious when visuo-tactile interactions occur in the space close to the patients' body, as compared to in far space (di Pellegrino et al., 1997; Làdavas et al., 1998a, 2000). This finding is taken as evidence for the existence of a peripersonal space in the human brain, relying on the integration of visual and tactile information in the space close to the body, in a way very similar to that described in monkeys (Làdavas, 2002). Most of these studies place the bimodal stimuli close to the hand. Subsequent studies confirmed that this visuo-tactile integration was not specific of the PPS around the hand but could also be reported around other body parts, such as the face (Farnè et al., 2005a; Farnè and Làdavas, 2002; Làdavas et al., 1998b). From a neuroanatomical point of view, studies have shown that brain lesions in frontal, temporal and parietal cortex in the right hemisphere are the most common regions leading to extinction (Driver and Vuilleumier, 2001; Farnè et al., 2005b; Kamtchum-Tatuene et al., 2017; Mattingley et al., 1997; Vossel et al., 2011), at locations considered as the human homologues of the monkey cortical regions involved in PPS processing and described above. In particular, this neurological disorder appears most often in patients with focal parietal lesions and specifically within the temporo-parietal junction, a region crucially involved in self-processing (Blanke, 2012; Blanke et al., 2002)

Behavioral evidence for the existence of PPS. The above clinical evidence in favor of the existence of a PPS system in the human brain is corroborated by behavioral studies in healthy participants (Spence et al., 2004; Macaluso and Maravita, 2010; Occelli et al., 2011). These studies

showed that the modulation of tactile perception by visual or auditory stimuli is more pronounced when these are presented close, as compared to far, from the body. Neuroimaging studies using EEG (Sambo and Forster, 2008), TMS (Serino et al., 2011) and fMRI (Bremmer et al., 2001; Makin et al., 2007; Gentile et al., 2011; Brozzoli et al., 2011, 2013) demonstrated that multisensory representation of PPS occurs in both in parietal and prefrontal areas (**Figure 1B**) where PPS neurons have been identified in the homologous macaque regions (for reviews, see Cléry et al., 2015b; di Pellegrino and Làdavas, 2015).

There is no physically separation between the PPS (near space) and the extrapersonal space (far space) in the real world, however the brain does represent a boundary between these two spaces. That is to say between what is close to our bodies, which can potentially impact, interact with or attack us, and what is further away, at a distance in which we cannot act upon except by a full displacement of the body. More importantly, this boundary is not fixed and can vary within and across individuals (Cléry et al., 2015b; de Vignemont and Iannetti, 2015; Farnè et al., 2005a, 2005b; Maravita and Iriki, 2004). Indeed, the limits between PPS and far space can be very different from one subject to the other, as well as the sharpness of the representational gradient between these two spaces (**Figure 2**). Likewise, with a given subject, these limits can vary as a function of the sensory, cognitive or social context, and appears to be reliably skewed under certain psychiatric conditions (see for review Cléry et al., 2015b).

Possible PPS functions. Objects approaching us or a predator may pose a threat, and signal the need to initiate defensive behavior. As a result looming stimuli often indicate an intrusion in our peripersonal space, that correlates with an enhanced tactile processing as assessed both by d'-sensitivity measures and reaction time measures (Canzoneri et al., 2012; Cléry et al., 2015a; De Paepe et al., 2016; Kandula et al., 2015). As a result, the PPS has been proposed to define a safety boundary around the body (Cléry et al., 2015a, 2015b; de Vignemont and Iannetti, 2015; Graziano and Cooke, 2006; Sambo and Iannetti, 2013, Chapter 2 and 3). However, peripersonal space is also,

by definition, the space that is closed to our body, or self. Accordingly, recent studies and reviews highlight the link between peripersonal space and body self-consciousness. For example, Grivaz et al. (2017) propose a meta-analysis of human studies, comparing the cortical bases of peripersonal space and body self-consciousness, with a specific focus on their overlap and their respective specificities.

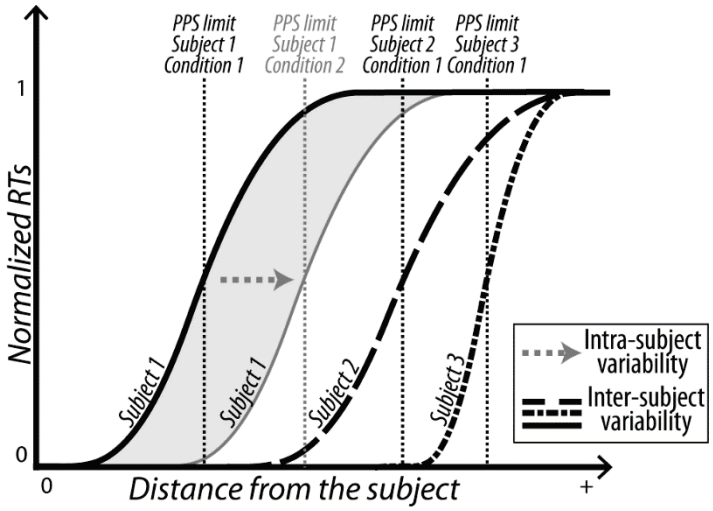

Figure 2: Intra and inter-individual variabilities for peripersonal space boundary. The limits between peripersonal space, closest to us, and far space, can vary within individuals as a function of sensory, cognitive or social context. These limits can also vary across individuals as a function of their own experiences and feelings (phobia, relationships, …).

In the following, we will first review the different methods developed to measure PPS (sections 2), the role of impact prediction in the definition of PPS (section 3), evidence for modulations of PPS (section 4), a discussion on the modular nature of PPS (section 5) and last, the functional link between peripersonal space and body self-consciousness (section 6).

2 MEASUREMENTS OF PERIPERSONAL SPACE

Both in the human brain and in the monkey brain, the neurons that represent PPS are more strongly driven by dynamic stimuli approaching the body than by static stimuli. This for example the case for the bimodal and trimodal neurons that can be recorded both from the ventral

intraparietal area (Colby et al., 1993a; Duhamel et al., 1997) and the premotor cortex (Fogassi et al., 1996; Graziano et al., 1994; M. S. A. Graziano et al., 1997; Graziano et al., 1999). The firing rate of some of these neurons increase as function of the velocity of the looming stimulus, suggesting that these neurons might be computing the time to impact on the body (Fogassi et al., 1996).

Based on these findings, Serino's group has developed a method to estimate the boundary of the PPS using dynamic stimuli. Indeed, these stimuli have a higher ecological relevance than static stimuli when it comes to studying PPS. Besides, this approach is more similar (though not identical) to the experimental conditions used in monkey neurophysiology, thus allowing a more direct comparison across species (Canzoneri et al., 2012).

The idea behind this paradigm is to measure the behavioral responses in humans that are expected to reflect the properties and putative function of the receptive fields (RFs) of the PPS primate neurons. The paradigm relies on using a dynamic multisensory (audio-tactile or visuo-tactile) interaction task in order to assess the limits of PPS (defined as the inflection point where a notable increase in multisensory integration can be observed) and is considered as a functionally and ecologically more relevant paradigm than previous designs. Specifically, participants have to respond as fast as possible to tactile stimuli presented somewhere on their body, while task-irrelevant heteromodal cues (auditory or visual stimuli) looming toward or receding from the body part stimulated by the tactile stimulus are presented (Canzoneri et al., 2016, 2013a, 2013b, 2012; Galli et al., 2015; Noel et al., 2015a, 2015b; Teneggi et al., 2013). On each trial, tactile stimuli are presented at different timing with respect to the trajectory of the sound/visual dynamic stimuli. In other words, the tactile stimulus was delivered when the sound or visual dynamic stimulus was perceived at a variable distance from the body of the subject. PPS limits is inferred from the function associating the measured reaction time (RTs) to the tactile stimulus at the body part of interest (the hand, the face or the trunk), to the distance at which the visual or auditory dynamic stimulus was

presented.

RTs to tactile stimuli progressively decrease as a function of the distance at which the sound/visual looming stimulus is presented; and conversely, RTs progressively increase as a function of the distance at which the sound/visual receding stimulus is presented. The authors propose that this function describes the relationship between tactile processing and the position of auditory or visual stimuli in space and allows to estimate the critical distance at which an external stimulus starts to affect tactile processing. This distance, along a spatial continuum between far space and the external surface of the body, allows to approximate the boundary of PPS representation in humans.

This new paradigm was first developed and used in the context of a dynamic audio-tactile interaction task to investigate hand-related PPS thanks to tactile stimulations presented on the hand, (Canzoneri et al., 2013a, 2013b, 2012). This paradigm was also used to investigate the effect of social variables onto face-anchored PPS, using a dynamic audio-tactile interaction task with tactile stimulations delivered onto the face (Teneggi et al., 2013). Recently this paradigm was also adapted to studies investigating the full body illusion (Noel et al., 2015a, 2015b; Serino et al., 2015b). In a recent study, we also adapt this paradigm to subliminal stimulation conditions to demonstrate that PPS is not only characterized by a speeding of RTs but also by an enhancement of multisensory integration processes as assessed by d' measures (Cléry et al., 2015a).

Overall, this paradigm opens new perspectives in the study peripersonal space and how it is modulated by the context (top-down information, bottom-up evidence, social cues etc.), experience (learning, priors etc.) and action.

3 Looming stimuli and Touch or Impact prediction to the Body

The ecological significance between stable stimuli close to our body (e.g. a wall, a desk) and dynamic stimuli looming towards us (e.g. a mosquito, a ball) are different. Looming stimuli are

potentially more dangerous than other visual stimuli, including dynamic stimuli with no predicted impact to the body. A predator, a dominant conspecific, or a mere branch coming up at high speed are dangerous if one does not detect them fast enough to produce the appropriate escape motor repertoire. Such looming stimuli are known to trigger stereotyped defense responses (in monkeys: Schiff et al., 1962; in human infant: Ball and Tronick, 1971). Interestingly, threatening looming stimuli are perceived as having a shorter time-to-impact latency as compared to non-threatening objects moving at the same objective speed (Vagnoni et al., 2012).

Temporal prediction. In a visuo-auditory context, looming visual stimuli have shown to trigger pronounced orienting behavior toward simultaneous congruent auditory cues compared with receding stimuli, both in non-human primates (Maier et al., 2004) and in 5-month-old human infants (Walker-Andrews and Lennon 1985). Looming structured sounds can specifically benefit visual orientation sensitivity (Romei et al., 2009, Leo, et al 2011). In a recent study (Cléry et al., 2015a), we show that subjects have an enhanced tactile sensitivity in the presence of looming visual stimuli as compared to receding visual stimuli, confirming the idea that looming stimuli are more relevant than receding stimuli to the body. Indeed, while both size and depth cues most probably contribute to the modulation of tactile sensitivity on the face, this study indicates that the movement vector cue (away from or toward the subject) is actually the dominant cue affecting tactile detection, as slower looming stimuli result in a delayed predicted time of impact on the face, and hence a delayed time at which tactile sensitivity is maximally enhanced (Cléry et al., 2015a). In other words, the trajectory and speed of the looming visual stimuli fully account for the temporal and dynamic predictive cues that are exploited by the brain to anticipate touch or impact to the body. Likewise, other auditory or visuo-tactile integration studies (Canzoneri et al., 2012; Kandula et al., 2015) have shown that reaction times are shorter when the tactile stimulus is delivered at the impact time of the looming stimulus and suggest that looming stimuli predictively speed up tactile processing. Specifically, the speed of the looming stimulus seems to guide the nervous system in defining a

high touch/impact probability window not unlike the multisensory temporal binding window described during the physiological and perceptual binding of two stimuli into the representation of a same and unique external source and defining the degree of temporal tolerance of the brain in this binding process (for review, see Wallace and Stevenson, 2014).

Spatial prediction. Besides, we found in our psychophysics study that tactile sensitivity is also enhanced not only at the predicted time but also at the predicted location of impact of a looming visual stimulus to the face (Cléry et al., 2015a), fully reflecting the expected subjective consequences of the visual stimulus onto the tactile modality. Importantly, this enhancement is also observed for stimuli trajectories that do not predict a direct impact to the face but rather brush past it, suggesting that PPS is incorporates in the body schema and the prediction of intrusion of a visual stimulus into the space triggers the same tactile enhancement mechanisms whether a direct touch/impact on the body is actually expected or not.

Possible neural mechanisms. In addition to a baseline multisensory enhancement, tactile sensitivity thus appears to be further enhanced by the predictive components of the heteromodal visual or auditory stimuli. By definition, this process involves cross-modal influences, and it was suggested that the cortical regions responsible for this multisensory touch/impact prediction highly overlap with the corresponding multisensory convergence and integration functional network. While this has never been explicitly investigated in these terms, early observations are in full agreement with this hypothesis. First, the visual response observed in parietal tactile neurons (and more generally in bimodal visuo-tactile neurons) was initially interpreted as an "anticipatory activation", predictive of touch in the corresponding skin (Juhani Hyvärinen and Poranen, 1974). Second, some neurons in the ventral intraparietal area (VIP) integrate vestibular proprioceptive self-motions and visual motion cues to encode relative self-motion with respect to the environment (Bremmer et al., 2002a, 2002b, 2000, 1997; Duhamel et al., 1997). These neurons have been shown to respond to both visual and tactile stimuli (Duhamel et al., 1997; Guipponi et al., 2015, 2013) and

perform nonlinear sub-, super-, or additive multisensory integration operations (Avillac et al., 2007, 2004). Recently, an fMRI study in the non-human primate confirms that this area VIP is involved in impact prediction to the face in a visuo-tactile context (Cléry et al., 2015b, Chapter 2). As a result, this area appears to process both the consequences of ones' own whole-body movements onto the environment as well as the consequences of movement of objects within the environment, relative to the body. Last, premotor area F4, an area highly connected with parietal area VIP, is also robustly activated, bilaterally by impact prediction (Cléry et al., 2015b). Most importantly, in both parietal area VIP and premotor area F4, these activations are systematically significantly higher when the looming stimulus is spatially and temporally predictive of the tactile stimulus than when these two stimuli are presented simultaneously, strongly suggesting that these two areas are indeed, at the neuronal level predictively processing temporal and spatial cues, possibly via non-linear integrative neuronal mechanisms (Cléry et al., 2015b, Chapter 2).

As seen in section 1, the area VIP and F4 are proposed to play a key role in the definition of peripersonal space. A recent study in fMRI performed in monkeys to assess the neural bases encoding near and far space during naturalistic 3D moving objects, highlights the involvement both of VIP and F4 for peripersonal space encoding (Chapter 3). This confirms the prior observations from single neuron studies in monkeys (Colby et al., 1993; Bremmer et al., 2002a, 2002b; Rizzolatti et al., 1981; Graziano et al., 1997). However, two important observations need to be highlighted at this point. First, our fMRI data highlight that within an area VIP anatomically defined as the fundal IPS region, the voxels in which we identify visual and tactile convergence (Guipponi et al., 2013) are also the very same voxels in which we identify prediction of touch/impact to the body (Chapter 2) as well as a selectivity for near space encoding (Chapter 3), suggesting that these different functions are possibly implemented unique neuronal computations (see Cléry et al., 2015b, for discussion). Second, this same fMRI set of studies allows to identify the larger cortical network involved in touch/impact prediction to the body and near space processing, encompassing, in

addition to subsectors of the classically defined VIP, a subsector of premotor area F4 as well as the fundus of superior temporal sulcus FST and early striate and extra-striate areas. This extremely strong overlap between the touch/impact prediction to the body network and the near space processing network provides strong support to the idea that functionally, PPS includes the skin as a frontier of self, or alternatively, that the frontier of self is defined not only by the skin but also by the PPS (these two views being functionally speaking completely equivalent).

A putative defense PPS. A visual stimulus intruding into peripersonal space close to one's cheek enhances tactile processing on the close by cheek, at the predicted time of impact, more than a visual stimulus predicting an impact to the other cheek (Cléry et al., 2015b, Chapter 2). This suggests that intrusion into PPS predicts touch or impact to the close by body surface. Yet in another study, Canzoneri et al. demonstrate (2012) that tactile processing on the hand is speeded by the presence of a looming sound, predicting an impact on the hand or within a well-defined distance from the hand, i.e. within a hand-referenced PPS. In monkeys, the electrical microstimulation of the neurons of these two regions induces a behavioral defense and avoidance repertoire of whole body movements, suggesting their involvement in the coding of a defense peripersonal space (Cooke and Graziano, 2004; Graziano et al., 2002; Graziano and Cooke, 2006). All this taken together suggests the existence of a security margin around the face and the body and all of the single neuron, the microstimulation and the fMRI monkey data suggest that this function is subserved by the occipito-parieto-frontal network described above (for reviews, see Cléry et al., 2015b; di Pellegrino and Làdavas, 2015).

Some studies performed in humans were interested not just in tactile stimuli but more precisely in nociceptive stimuli. In two studies, De Paepe et al. used temporal order judgment tasks, to assess whether the perception of nociceptive stimuli and their localization was influenced by proximal visual stimuli thus contributing to the construction of an integrated representation of PPS as has been described for touch (De Paepe et al., 2015, 2014). Participants were requested to judge

which of two nociceptive stimuli was presented first, each stimulus being presented on one hand – the two hand being thus stimulated. Each dual nociceptive stimulation was preceded by visual cues presented either unilaterally or bilaterally, and either close to the subject's body, or far from it. The authors further requested the participants to either cross their hands over their body's midline or not. They found that the unilateral visual cue prioritized the perception of nociceptive stimuli delivered on the hand adjacent to the unilateral visual cue. This effect increased when the cue was presented close to the participant's hand (De Paepe et al., 2014), irrespective of posture. This demonstrates the visuo-nociceptive interaction revealed by these studies occur in a predominantly hand-anchored frame of reference and not in a body-anchored frame of reference (De Paepe et al., 2015). In a third study (De Paepe et al., 2016), participants were asked to respond as fast as possible indicating the side on which they perceived a nociceptive stimulus on their hand while a visual stimulus with different temporal onset synchronies was either approaching or receding with respect to the participant's left or right hand. De Paepe et al. report that reaction times are fastest when the visual stimulus appears close to the stimulated hand and that this effect is more pronounced for visual looming stimuli. Taken together, these three studies confirm an interaction between the coding of nociceptive information and a peripersonal frame of reference bringing additional support to the proposal that PPS may contribute to the definition of a safety margin representation around the body that is designed to protect it from potential physical threat.

A recent review (Van der Stoep et al., 2015) suggests that, depending on their distance to the body, different combinations of sensory information might be more or less relevant . For example, touch and vision interactions are expected to dominate in peripersonal space, as they correlate with an interaction between the body and the environment (e.g., for grasping or defence). In contrast, auditory and visual information may be more relevant in extrapersonal space away from the subject's body as they provide information about far away objects, and contribute to spatial orienting, navigation and interaction with others (e.g. during conversation). As tactile stimuli can

only be perceived when applied to the body, visuotactile and audiotactile interactions (e.g. in the case of touch or impact to the body) inherently occur near the body and the peripersonal space boundary can therefore be explained by spatial alignment of different stimulus modalities with respect to the body. A more recent review from the same group (Van der Stoep et al., 2016) focuses on whether multisensory integration operates according to the same rules throughout the whole of 3-D space. Their meta-analysis highlights the fact that not only the space around us is divided into distinct functional regions, defined by the body part there are mostly related to (e.g., the hand, the face or the trunck), but it also suggests that multisensory interactions are modulated by the region of space in which stimuli happen to be presented, e.g. the distance to the body. Therefore, futures studies on peripersonal space and notably on impact prediction onto the body need to take into account the several spatial constraints that are expected to influence multisensory integration processing: the spatial and temporal dynamics of the stimuli, the distance from the different body parts, the ongoing movement of the subject as well as the social, valence and sensory nature of the environment and its organization with respect to the subject.

4 MODULATIONS OF PERIPERSONAL SPACE

Peripersonal space appears to have a singular function in our representation of space, associated, as described above, with and enhanced processing of sensory information as assessed behaviourally (reaction times, sensitivity) or functionally (single cell recordings, fMRI). In the last years, there has been a growing interest on the flexibility and plasticity of this peripersonal space (for review, see Cléry et al., 2015b; de Vignemont and Iannetti, 2015).

Early evidence for a tool-induced reorganization of PPS. Several studies show that using a tool to reach objects in far space can extend the boundaries of PPS representation. In monkeys, Iriki et al. (1996) showed that, after a training period of using a rake to access food placed at a distance beyond arm reach, hand-centered visual RFs of neurons located in the intraparietal sulcus extended so as to encompass the rake. In humans, neuropsychological (Farnè and Làdavas, 2000; Maravita

et al., 2001) and psychophysical (Holmes et al., 2004; Maravita and Iriki, 2004; Serino et al., 2007; Galli et al., 2015) studies demonstrated that, after using a tool, crossmodal interactions between visual or auditory stimuli presented in the far space and tactile stimuli at the hand increase. This is all the more pronounced at the location where the tool has been used. Taken together, these findings bring support to the idea that the extent of PPS representation is dynamically reshaped by repeated experience and learning, allowing for an extension of the domain of action of the body beyond its structural limits (Maravita and Iriki, 2004; Gallese and Sinigaglia, 2010; Costantini et al., 2011). Early studies on this topic suggest that an active use of the tool is necessary for extending PPS representation. Since then, studies have shown that neither a physical, nor a functional interaction between near and far space is actually necessary to extend PPS representation (Bassolino et al., 2010; Goldenberg and Iriki, 2007; Serino et al., 2015a).

Sensory synchrony as a possible trigger of tool-induced reorganization of PPS. In this last study, Serino et al. (2015a) bring support to an alternative hypothesis, generated by a neural network model, that PPS representation plasticity following tool-use arises neither from the function of the tool nor on the actions performed when using it, but is rather triggered by the experienced sensory feedback, i.e. the synchronous tactile stimulation of the hand when holding the tool and heteromodal (auditory or visual) stimulation in the far space where the tool is being manipulated (for a review on tool-use, see Martel et al., 2016). In other words, temporal synchrony between sensory input in far space and tactile input arising from object manipulation by the hand is proposed to play a key role in the functional definition of PPS from an action driven perspective.

Non-motor driven reorganization of PPS. Several studies show that tool can remap the peripersonal space. This define peripersonal space from the point of view of a "goal-directed action" perspective in which we want to reach for somethings and grasp it (for review, see de Vignemont and Iannetti, 2015). However, recent evidence show that other cognitive factors than action can remap this space such as fear, anxiety, social engagement and contribute to a "protective and

defensive" view of peripersonal space.

a- Bottom-up driven reorganization of PPS.

It is now well established that certain categories of bottom-up signals drive an instantaneous resizing of PPS. This is the case of threatening stimuli. For example, tactile processing is facilitated when physically threatening pictures (for instance a snake or a knife) are presented in the PPS, leading to faster responses than when such pictures are presented further away (for instance near a different body part) (Poliakoff et al., 2007; Van Damme et al., 2009). Likewise, sounds that elicited a negative emotion (e.g. screaming woman) or sounds that have a negative ecological connotation (e.g. barking dog), induce faster reactions times when they appear close to the subject as compared to neutral or positive valence sounds (Taffou and Viaud-Delmon, 2014; Ferri et al., 2015). In addition, the distance a visual stimulus to the body has a stronger influence on reaction times to a tactile stimulus on the skin if it is perceived as threatening. This indicates that not only is PPS resized by a threatening object, but the information relative to its distance from the body is enhanced relative to that of a non-threatening one (de Haan et al., 2016).

Importantly, whatever the estimated level of threat represented by a visual object, the observed expansion of peripersonal space was reduced when the threatening part of dangerous objects was oriented towards participants, as compared to when oriented away (Coello et al., 2012). This suggests that the interpretation of the higher order context in reference with the body is crucial in affecting the boundary of peripersonal space. In other words, the resizing of PPS is due both to bottom-up and top-down factors. All taken together, these different studies show that the emotional aspects and characteristics of the threat in relation to the body influence the defensive peripersonal space and the safety body margin.

b- Top-down driven reorganization of PPS: social factors.

Top-down factors are also shown to resize PPS. For example, the presence of an observer

and the nature of the interaction with her/him reshape the peripersonal space representation (Teneggi et al., 2013). Indeed, peripersonal space boundaries shrink when a neutral observer is standing in far space. This is not observed when the observer is replaced by a mannequin. This thus suggests that one's peripersonal space resizes in the presence of others. Importantly, this resizing depends on the nature of the social interaction with these observers. For example, peripersonal space boundaries between self and an observer merge after an economic game with this person, but only if she/he behaved cooperatively (Teneggi et al., 2013). Peripersonal space is thus shaped by our valuation of other people's behaviour and is modulated by social interactions. This thus reflects a modulation of low-level 3D visual information processing by high-level cognitive variables.

However, the expansion and contraction of our PPS representation may not be the only change induced by the presence of others. Indeed, some studies suggest that we remap observed sensory and motor experiences of others onto our own bodily representations, thanks to a so-called "mirror system" that has been described both in the monkey and human brain. This system is activated both when we are touched ourselves, when we view another person being touched, as well as when events occur in the space near the other's body (Blakemore et al., 2005; Keysers and Gazzola, 2009; Serino et al., 2008; Cardini et al., 2010). Ishida et al. (2009), using single cell recordings in non-human primates, show that bimodal parietal neurons which encode sensory events occurring in the space around the monkey's own hand also respond to events occurring in the space around another monkey's hand. Similar functional activations are observed in premotor cortex in humans (Brozzoli et al., 2013; Holt et al., 2014).

A review by Ishida et al. (2015) based on monkey neurophysiology as well as human fMRI studies, reports shared self-other body representation coding in multiple brain areas including visuotactile neurons in parietal cortex (Ishida et al., 2009), secondary somatosensory cortex (Keysers et al., 2004, 2010; Blakemore et al., 2005; Ebisch et al., 2008; Keysers and Gazzola, 2009) and in insular cortex (Fitzgibbon et al., 2010, 2012; Lamm and Singer, 2010; Krahé et al., 2013)

associated with affective touch and interoception. Importantly, Maister et al. (2015) show that increased multisensory integration in the PPS of another person involves remapping of our own peripersonal space onto that of the other person without however a fusion between the two PPS, that is to say without including the space between the two subjects.

c- Interactions between an action-based peripersonal space and interpersonal space.

Recent studies were interested in investigating the link between peripersonal space for action and interpersonal space, defined as the space in which we maintain a distance around our bodies and in which any intrusion by others may cause discomfort. As seen above, this space can be modified by emotional and socially relevant interactions, including complex social information such as perceived morality of another person, age and gender (Iachini et al., 2015, 2016). Peripersonal space for acting and interpersonal space share a common motor nature and are sensitive, at different degrees, to social modulation. Hence the proposal that social processing might be embodied and grounded in the body acting in space (Iachini et al., 2014). This evidence in this respect is mitigated. Indeed, in the hands of Patané et al., tool-use remaps the action-related PPS, measured by a reaching-distance toward a confederate, but does not affect the social-related interpersonal space measured by a comfort-distance task suggesting that these two space representations have no full functional overlap between them (Patané et al., 2016). In the hands of Quesque et al. (2016), using a different paradigm in which participants observed a point-light walker approaching them from different directions and passing near them at different distances from their right or left shoulder, comfortable, interpersonal distance, is found to be linked to the representation of peripersonal space. This indicates that increasing peripersonal space through tool use has the immediate consequence that comfortable interpersonal distance from another person also increases, corroborating the hypothesis that interpersonal-comfort space and peripersonal-reaching space share a common motor nature (Iachini et al., 2014, 2016; Coello and Fischer, 2015).

d- Interaction between PPS and personality traits.

PPS size can be related to some key personality traits. The study of defensive reflex responses is instrumental to address this question. Indeed, these defensive reflex responses can be finely modulated by the position of the stimulus within peripersonal space. An important aspect of this modulation in that it is specific to the body part for which the reflex response provides protection (Sambo et al., 2012a, 2012b). For example, subcortical defensive responses like hand-blink reflex (HBR) are enhanced when a threat is brought close to the face by one's own stimulated hand, by another person's hand and when the hand of the participant enters in the PPS of another individual. Importantly, the interaction between these defensive reflexes vary from one individual to another, as a function of several personality traits. For example, the enhancement of the HBR is larger in participants with a strong empathic tendency when observing another individual from a third person perspective, suggesting that interpersonal interactions shape perception of threat and defensive responses and more so in empathic participants (Fossataro et al., 2016). Along the same lines, the size of an individual's peripersonal space is correlated with trait anxiety, with a larger peripersonal space in more anxious individuals (Sambo and Iannetti, 2013; for review, see de Vignemont and Iannetti, 2015). Likewise, PPS size in claustrophobic subjects is different from that of non-claustrophobic subjects. Claustrophobia is a situational phobia characterized by intense anxiety in relation to enclosed spaces and physically restrictive situations (American Psychiatric Association, 2000). Lourenco et al. (2011) investigated whether the size of near space relates to individual differences in claustrophobic fear, as measured by reported anxiety in enclosed spaces and physically restrictive situations and show that claustrophobic fear is associated with increased size of the near space immediately surrounding the body. Vagnoni et al. (2012) show the same results and extend them by showing that emotions not only alter the perception of space as a static entity, but it also affects the perception of dynamically moving objects, such as those on a collision course with the observer. Importantly, claustrophobia is not only associated with an increased PPS

relative to non–claustrophobic subjects, but it is also characterized by a less flexible PPS. Indeed, when using a stick during a line bisection task, whereas individuals low in claustrophobic fear demonstrate the expected expansion of peripersonal space individuals high in claustrophobic fear show less expansion following tool-use (Hunley et al., 2017).

In summary, peripersonal space is not a fixed space but a dynamic space which is continuously modulated by our environment (social, emotional, functional). The dynamic adjustment of this "boundary" of self may be related to an optimization of the behavioural outcome and repertoire (protective, pro-active) to the outside environment, based on online estimation of bottom-up information (visual, tactile, auditory, proprioceptive…) as well as of top-down cognitive information (context, emotion, social interactions …) (Cléry et al., 2015b; de Vignemont and Iannetti, 2015). One prediction of PPS as the output computation of the integration of multiple sources of information predicts that the properties and specificities of the PPS will depend on the body part it is referring to.

5 Different representations of body-related PPS

The majority of studies on peripersonal space focused on the hand and to a lesser extent on the face. We have seen that this "boundary" of peripersonal space representation is modulated both by action (for example after tool-use) and emotional/social context (fear, anxiety, cooperation). Besides, these modulations can vary within individuals between contexts and situation, and also between individuals. The question we are addressing here is whether the representation of peripersonal space follow the same constraints and rules the same for all body parts or not?

Measuring the influence of looming stimuli presented at different distances from a given body part on the reaction times to a tactile stimulus (Canzoneri et al., 2012, 2013a, 2013b; Teneggi et al., 2013; Galli et al., 2015; Noel et al., 2015a, 2015b), Serino et al. (2015b) characterize PPS

from a body-referenced perspective. In a first experiment, they test the effect of looming and receding auditory stimuli in relation to the trunk on tactile detection on this body part. As previously described for the hand and the face, they show that looming sounds modulated tactile processing as a function of the distance of the sound from the body and that this effect is selective for looming sounds. The majority of experiments on peripersonal space are done only in the front space of the subject. Therefore, in second experiment, the authors also introduce looming and receding auditory stimuli from the front or back of peri-trunk. They confirm that only sounds looming towards the trunk are mapped into the representation of the trunk-PPS. No notable difference can be observed between a frontal trunk-PPS and a hind trunk-PPS. In third experiment, the authors test the effect of looming and receding auditory stimuli from the hand-PPS. They show that sounds modulate tactile processing as a function of the distance of the sound from the hand. This effect is observed not only for the looming sounds but also for the receding sounds, though the speeding of tactile detection on the hand is more pronounced for looming stimuli than for receding stimuli. Importantly, the distance at which the sounds started to have a significant effect onto tactile processing is shorter for the hand-PPS than for trunk-PPS, indicating that trunk-PPS is larger than the hand-PPS. The authors then directly compare the representations of the hand-PPS and trunk-PPS. For this, while using looming and receding sounds from the body part stimulated, they apply tactile stimulations either to the trunk or to the hand placed close to the trunk (experiment 4) or to the hand placed far from the trunk (experiment 5). The authors show that when the hand is close to the trunk, the trunk-PPS and its properties dominate onto the hand-PPS, while this is not the case when the hand is far away from the trunk. In summary, two different PPS representations can be distinguished, one anchored to the hand and that is sensitive to both looming and receding stimuli at close distance and another one, anchored to the trunk and sensitive only for looming stimuli and encompassing more peripersonal space (in terms of distance to the body) than hand-PPS. Importantly, these two representations are not independent. To further investigate the nature of the

interaction between the sub-PPSs, the authors further test the effect of looming and receding stimuli (auditory or visual) from the trunk or the face PPS while tactile stimuli are presented either to the face or the trunk. Tactile processing on the trunk gets enhanced by looming stimuli both towards the face or the trunk, indicating that the trunk-PPS encompasses the face-PPS. The reverse is however not true, as tactile processing on the face is not enhanced by stimuli looming toward the trunk.

To summarize this exhaustive study, Serino et al. show that the size of PPS representation varies according to the stimulated body part, being progressively bigger for the hand, the face and largest for the trunk (**Figure 3A**). Tactile processing is modulated in a space-dependant manner by looming stimuli for these different body parts but also by receding stimuli for the hand, though the reported effect remains smaller than that observed for looming stimuli. Most importantly, while the size of PPS representation around the trunk is relatively constant, the PPS representation around the hand or the face vary according to their position with respect to the rest of the body and with respect to the trajectory of the stimulus with respect to the body (**Figure 3B**). These findings are compatible with the function of a peripersonal space as a multisensory-motor interface for body-object interaction (Brozzoli et al., 2012b).

Overall, there is thus not a unique representation of body peripersonal space but at least three body-part specific PPS representations, with different extension and direction tuning, and referenced to the common reference frame of the trunk. For future studies, research needs to take these new characteristics of PPS representation into account when designing the experiments. This first extensive mapping of humans PPS representation opens new perspectives in peripersonal space research. For example, how do these three body-part specific PPS representations be incorporated in a “goal-directed action” or a “protective/defensive” view of PPS?

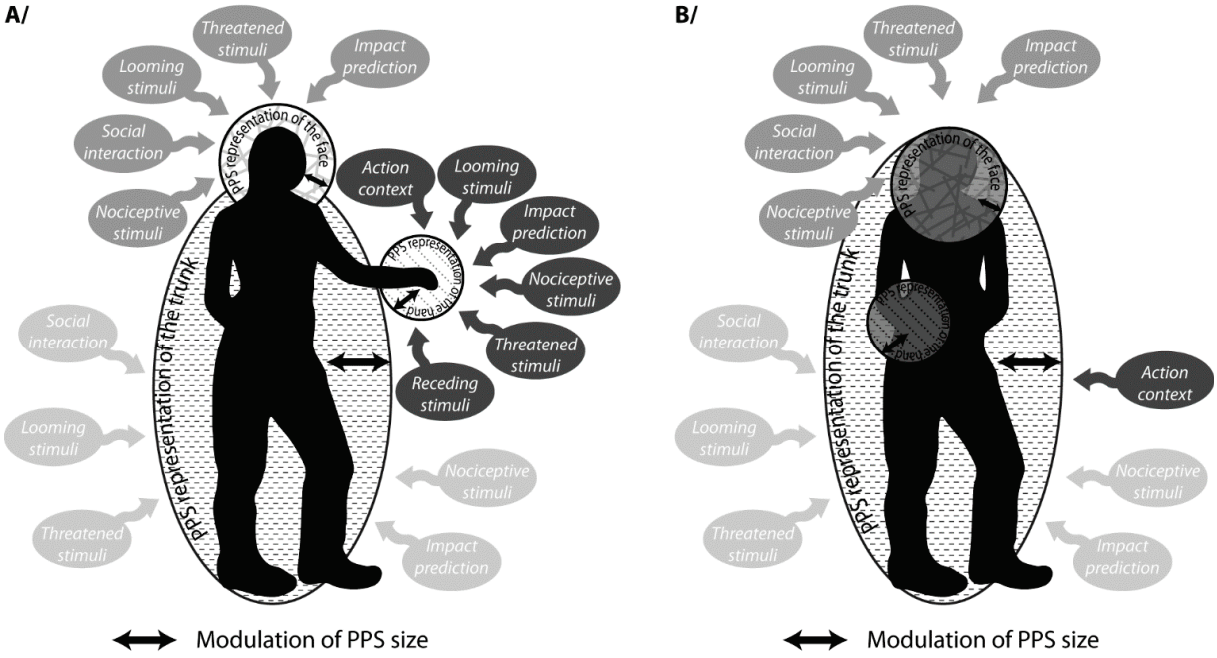

Figure 3: Peripersonal space representation is modulated by numerous factor as much by impact prediction or approaching stimuli as by social, emotional and action components. A/ There are at least three sub-representations of the PPS: the trunk, the face and the hand. B/ These representations can be merge following their relative distance from the trunk.

6 PERIPERSONAL SPACE AND BODILY SELF-CONSCIOUSNESS

The trunk-PPS representation integrates both body-related signals (proprioceptive, tactile) but also information related to stimuli from the outside world (visual and auditory) that can potentially interact with the body, in a global, egocentric frame of reference. This representation may thus constitute a basic neural representation that is relevant for the self, self-consciousness and self-consciousness in relation with the outside world (Blanke and Metzinger, 2009; Blanke, 2012; Blanke et al., 2015; Tsakiris et al., 2007; Tsakiris, 2010; Serino et al., 2015b). In the follow we will shortly review the growing evidence providing a possible link between PPS and self-consciousness.

Bodily self-consciousness (BSC), that is the feeling that the physical body and its parts is ours, is argued to be one of the cardinal features of subjective experience, i.e. binding whatever external or internal experience to self (Gallagher, 2000; Blanke and Metzinger, 2009). In the last

years, multisensory bodily illusion paradigms have been developed to study BSC in the laboratory, describing the detailed behavioural mechanisms underlying the sensation of ownership for the hand using the rubber hand illusion (Botvinick and Cohen, 1998), for the face using the enfacement illusion (Tsakiris, 2008; Sforza et al., 2010), or for the entire body using the full-body illusion, the out-of-body illusion or the body-swap illusion (Ehrsson et al., 2007; Lenggenhager et al., 2007; Petkova and Ehrsson, 2008). These illusions are based on the application of visuo-tactile stimuli between the body (or body part) of the participant and a virtual body (or fake body part). By manipulating multisensory cues, it is possible to induce ownership over fake or virtual body parts or whole bodies. These studies, have led to a growing consensus that ownership over hands, faces, and bodies crucially relies on the integration of multiple bodily signals in the brain, including tactile, proprioceptive, visual and auditory signals (Blanke, 2012; Blanke et al., 2015; Ehrsson et al., 2004; Ehrsson, 2012; Makin et al., 2008; Serino et al., 2013; Tsakiris, 2010). As a result, there seems to be a direct link between the neural mechanism underlying multisensory PPS processing and BSC. However, to this date, most of the studies investigated separately the brain mechanism underlying PPS on the one hand and BSC on the other hand. In a recent study, Grivaz et al., (2017), conduct an extensive meta-analysis of functional neuroimaging studies to determine the key neural structures for PPS, for BSC and identify their potential functional overlaps in humans. The authors thus performed a systematic quantitative coordinate-based meta-analysis on human functional neuroimagining studies (Eickhoff et al., 2009, 2012; Turkeltaub et al., 2002). They selected 35 PET or fMRI studies: 18 studies assessing brain regions involved in the encoding of unisensory and multisensory stimuli within the PPS (whether the hand, the face or the trunk PPS); 17 studies assessing brain regions involved in the BSC of a body or a part of the body. They identified a bilateral PPS network including superior parietal, temporo-parietal and ventral premotor regions. These regions play a key role in sensory-motor processes, mediating interactions between the individual and the immediate environment, integrating sensory information and driving potential

motor responses. (Graziano and Cooke, 2006; Làdavas and Serino, 2008; Cléry et al., 2015b; Grivaz et al., 2017). On the other hand, the BSC network includes the posterior parietal cortex (IPS bilaterally), the superior parietal lobule (SPL), the right ventral premotor cortex, and the left anterior insula. These regions are involved in multisensory integration, attention and awareness. In particular, the insula plays a key role in integration of exteroceptive body-related cues and interoceptive signals that have been considered important for generating subjective experience (Craig, 2009; Damasio and Meyer, 2009; Park and Tallon-Baudry, 2014; Seth, 2013; Seth and Friston, 2016; Tsakiris, 2010). Although BSC and PPS representations are not associated to the exactly the same functions, they do activate common fronto-parietal regions. Indeed, the conjunction analysis performed by Grivaz et al. shows that PPS and BSC tasks anatomically overlap in only two clusters located in the left parietal cortex (dorsally at the intersection between the SPL, the IPS and area 2 and ventrally between area 2 and IPS). The activations of this dorsal SPL/IPS supports the hypothesis that multisensory integration of bodily cues contribute both to the construction of PPS and BSC (Brozzoli et al., 2012a; Gentile et al., 2013; Grivaz et al., 2017). In spite of the fact that they are not activated in PPS studies, the premotor and insular clusters involved in BSC are systematically co-activated with the parietal clusters involved in PPS processing during several cognitive tasks suggesting that these regions are functionally interconnected. This suggests a clear functional distinction between these two cognitive processes. This is further confirmed by the fact that the fronto-parietal areas involved in PPS are located more proximal to the central sulcus than those that are associated with BSC, which appear more distal. Thus, overall, PPS and BSC are subserved by only partially overlapping functional networks supporting the idea that they correspond to two distinct functions, whereby PPS possibly implements a multisensory-motor interface for body-objects interaction and BSC is related with bodily awareness and self-consciousness.

7 CONCLUSION

In conclusion, peripersonal space representation is a complex psychological and functional construct that can be subdivided on multiple entities referenced to different body parts and whose exact configuration depend on multiple factors. This complex PPS representation continuously changes as a function of the incoming bottom-up sensory information, motor experience for example during tool use, or top-down factors, including experience, social interactions, personality or psychiatric traits (**Figure 3**). This PPS representation is subserved by a well-identified parieto-frontal network that has some degree of overlap with the body self-consciousness network and one may predict that impairments in PPS representation or self-consciousness might have consequences on the other process. This opens new research way for the future years.

References

American Psychiatric Association, 2000. Diagnostic and statistical manual of mental disorders. (4th ed., text rev.). Washington DC.

Avillac, M., Denève, S., Olivier, E., Pouget, A., Duhamel, J.-R., 2005. Reference frames for representing visual and tactile locations in parietal cortex. Nat Neurosci 8, 941–949. doi:10.1038/nn1480

Avillac, M., Hamed, S.B., Duhamel, J.-R., 2007. Multisensory Integration in the Ventral Intraparietal Area of the Macaque Monkey. J. Neurosci. 27, 1922–1932. doi:10.1523/JNEUROSCI.2646-06.2007

Avillac, M., Olivier, E., Denève, S., Ben Hamed, S., Duhamel, J.-R., 2004. Multisensory integration in multiple reference frames in the posterior parietal cortex. Cognitive Processing 5, 159–166. doi:10.1007/s10339-004-0021-3

Ball, W., Tronick, E., 1971. Infant responses to impending collision: optical and real. Science 171, 818–820.

Bassolino, M., Serino, A., Ubaldi, S., Làdavas, E., 2010. Everyday use of the computer mouse extends peripersonal space representation. Neuropsychologia 48, 803–811. doi:10.1016/j.neuropsychologia.2009.11.009

Bender, M.., 1952. Disorders of perception. Springfield, IL: Charles C. Thomas.

Blakemore, S.-J., Bristow, D., Bird, G., Frith, C., Ward, J., 2005. Somatosensory activations during the observation of touch and a case of vision–touch synaesthesia. Brain 128, 1571–1583. doi:10.1093/brain/awh500

Blanke, O., 2012. Multisensory brain mechanisms of bodily self-consciousness. Nat Rev Neurosci 13, 556–571. doi:10.1038/nrn3292

Blanke, O., Metzinger, T., 2009. Full-body illusions and minimal phenomenal selfhood. Trends Cogn. Sci. (Regul. Ed.) 13, 7–13. doi:10.1016/j.tics.2008.10.003

Blanke, O., Ortigue, S., Landis, T., Seeck, M., 2002. Stimulating illusory own-body perceptions. Nature 419, 269–270. doi:10.1038/419269a

Blanke, O., Slater, M., Serino, A., 2015. Behavioral, Neural, and Computational Principles of Bodily Self-Consciousness. Neuron 88, 145–166. doi:10.1016/j.neuron.2015.09.029

Botvinick, M., Cohen, J., 1998. Rubber hands “feel” touch that eyes see. Nature 391, 756–756. doi:10.1038/35784

Bremmer, F., Duhamel, J.-R., Ben Hamed, S., Graf, W., 2002a. Heading encoding in the macaque ventral intraparietal area (VIP). European Journal of Neuroscience 16, 1554–1568. doi:10.1046/j.1460-9568.2002.02207.x

Bremmer, F., Duhamel, J.R., Ben Hamed, S., Graf, W., 2000. Stages of self-motion processing in primate posterior parietal cortex. Int. Rev. Neurobiol. 44, 173–198.

Bremmer, F., Duhamel, J.-R., Ben Hamed, S., Graf, W., 1997. The representation of movement in near extra-personal space in the macaque ventral intraparietal area (VIP)., in: Thier, P., Karnath, H.-O. (Eds.), Parietal Lobe Contributions to Orientation in 3D Space, Experimental Brain Research Series, Vol 25. Springer, pp. 619–630.

Bremmer, F., Klam, F., Duhamel, J.-R., Ben Hamed, S., Graf, W., 2002b. Visual–vestibular interactive responses in the macaque ventral intraparietal area (VIP). European Journal of Neuroscience 16, 1569–1586. doi:10.1046/j.1460-9568.2002.02206.x

Bremmer, F., Schlack, A., Kaminiarz, A., Hoffmann, K.-P., 2013. Encoding of movement in near extrapersonal space in primate area VIP. Front Behav Neurosci 7, 8. doi:10.3389/fnbeh.2013.00008

Bremmer, F., Schlack, A., Shah, N.J., Zafiris, O., Kubischik, M., Hoffmann, K., Zilles, K., Fink, G.R., 2001. Polymodal motion processing in posterior parietal and premotor cortex: a human fMRI study strongly implies equivalencies between humans and monkeys. Neuron 29, 287–296.

Brozzoli, C., Gentile, G., Bergouignan, L., Ehrsson, H.H., 2013. A Shared Representation of the Space Near Oneself and Others in the Human Premotor Cortex. Current Biology 23, 1764–1768. doi:10.1016/j.cub.2013.07.004

Brozzoli, C., Gentile, G., Ehrsson, H.H., 2012a. That's near my hand! Parietal and premotor coding of hand-centered space contributes to localization and self-attribution of the hand. J. Neurosci. 32, 14573–14582. doi:10.1523/JNEUROSCI.2660-12.2012

Brozzoli, C., Gentile, G., Petkova, V.I., Ehrsson, H.H., 2011. fMRI Adaptation Reveals a Cortical Mechanism for the Coding of Space Near the Hand. J. Neurosci. 31, 9023–9031. doi:10.1523/JNEUROSCI.1172-11.2011

Brozzoli, C., Makin, T.R., Cardinali, L., Holmes, N.P., Farnè, A., 2012b. Peripersonal Space: A Multisensory Interface for Body–Object Interactions, in: Murray, M.M., Wallace, M.T. (Eds.), The Neural Bases of Multisensory Processes, Frontiers in Neuroscience. CRC Press/Taylor & Francis, Boca Raton (FL).

Canzoneri, E., di Pellegrino, G., Herbelin, B., Blanke, O., Serino, A., 2016. Conceptual processing is referenced to the experienced location of the self, not to the location of the physical body. Cognition 154, 182–192. doi:10.1016/j.cognition.2016.05.016

Canzoneri, E., Magosso, E., Serino, A., 2012. Dynamic Sounds Capture the Boundaries of Peripersonal Space Representation in Humans. PLoS ONE 7, e44306. doi:10.1371/journal.pone.0044306

Canzoneri, E., Marzolla, M., Amoresano, A., Verni, G., Serino, A., 2013a. Amputation and prosthesis implantation shape body and peripersonal space representations. Scientific Reports 3, 2844. doi:10.1038/srep02844

Canzoneri, E., Ubaldi, S., Rastelli, V., Finisguerra, A., Bassolino, M., Serino, A., 2013b. Tool-use reshapes the boundaries of body and peripersonal space representations. Exp Brain Res 228, 25–42. doi:10.1007/s00221-013-3532-2

Cardini, F., Costantini, M., Galati, G., Romani, G.L., Làdavas, E., Serino, A., 2010. Viewing One's Own Face Being Touched Modulates Tactile Perception: An fMRI Study. Journal of Cognitive Neuroscience 23, 503–513. doi:10.1162/jocn.2010.21484

Cléry, J., Guipponi, O., Odouard, S., Wardak, C., Ben Hamed, S., 2015a. Impact prediction by looming visual stimuli enhances tactile detection. J. Neurosci. 35, 4179–4189. doi:10.1523/JNEUROSCI.3031-14.2015

Cléry, J., Guipponi, O., Wardak, C., Ben Hamed, S., 2015b. Neuronal bases of peripersonal and extrapersonal spaces, their plasticity and their dynamics: Knowns and unknowns. Neuropsychologia 70, 313–326. doi:10.1016/j.neuropsychologia.2014.10.022

Coello, Y., Bourgeois, J., Iachini, T., 2012. Embodied perception of reachable space: how do we manage threatening objects? Cogn Process 13, 131–135. doi:10.1007/s10339-012-0470-z

Coello, Y., Fischer, M.H., 2015. Perceptual and Emotional Embodiment: Foundations of Embodied Cognition. Routledge.

Colby, C.L., Duhamel, J.R., Goldberg, M.E., 1993a. Ventral intraparietal area of the macaque: anatomic location and visual response properties. Journal of Neurophysiology 69, 902–914.

Colby, C.L., Duhamel, J.R., Goldberg, M.E., 1993b. Ventral intraparietal area of the macaque: anatomic location and visual response properties. Journal of Neurophysiology 69, 902–914.

Cooke, D.F., Graziano, M.S.A., 2004. Sensorimotor Integration in the Precentral Gyrus: Polysensory Neurons and Defensive Movements. Journal of Neurophysiology 91, 1648–1660. doi:10.1152/jn.00955.2003

Costantini, M., Ambrosini, E., Sinigaglia, C., Gallese, V., 2011. Tool-use observation makes far objects ready-to-hand. Neuropsychologia 49, 2658–2663. doi:10.1016/j.neuropsychologia.2011.05.013

Craig, A.D., 2009. How do you feel — now? The anterior insula and human awareness. Nat Rev Neurosci 10, 59–70. doi:10.1038/nrn2555

Damasio, A., Meyer, K., 2009. CHAPTER 1 - Consciousness: An Overview of the Phenomenon and of Its Possible Neural Basis1, in: The Neurology of Consciousness. Academic Press, San Diego, pp. 3–14. doi:10.1016/B978-0-12-374168-4.00001-0

de Haan, A.M., Smit, M., Stigchel, S.V. der, Dijkerman, H.C., 2016. Approaching threat modulates visuotactile interactions in peripersonal space. Exp Brain Res 234, 1875–1884. doi:10.1007/s00221-016-4571-2

De Paepe, A.L., Crombez, G., Legrain, V., 2016. What's Coming Near? The Influence of Dynamical Visual Stimuli on Nociceptive Processing. PLOS ONE 11, e0155864. doi:10.1371/journal.pone.0155864
De Paepe, A.L., Crombez, G., Legrain, V., 2015. From a Somatotopic to a Spatiotopic Frame of Reference for the Localization of Nociceptive Stimuli. PLoS ONE 10, e0137120. doi:10.1371/journal.pone.0137120
De Paepe, A.L., Crombez, G., Spence, C., Legrain, V., 2014. Mapping nociceptive stimuli in a peripersonal frame of reference: evidence from a temporal order judgment task. Neuropsychologia 56, 219–228. doi:10.1016/j.neuropsychologia.2014.01.016
de Vignemont, F., Iannetti, G.D., 2015. How many peripersonal spaces? Neuropsychologia 70, 327–334. doi:10.1016/j.neuropsychologia.2014.11.018
di Pellegrino, G., Làdavas, E., 2015. Peripersonal space in the brain. Neuropsychologia 66, 126–133. doi:10.1016/j.neuropsychologia.2014.11.011
di Pellegrino, G., Làdavas, E., Farné, A., 1997. Seeing where your hands are. Nature 388, 730–730. doi:10.1038/41921
Driver, J., Vuilleumier, P., 2001. Perceptual awareness and its loss in unilateral neglect and extinction. Cognition, The Cognitive Neuroscience of Consciousness 79, 39–88. doi:10.1016/S0010-0277(00)00124-4
Duhamel, J.-R., Bremmer, F., BenHamed, S., Graf, W., 1997. Spatial invariance of visual receptive fields in parietal cortex neurons. Nature 389, 845–848. doi:10.1038/39865
Duhamel, J.-R., Colby, C.L., Goldberg, M.E., 1998. Ventral Intraparietal Area of the Macaque: Congruent Visual and Somatic Response Properties. Journal of Neurophysiology 79, 126–136.
Ebisch, S.J.H., Perrucci, M.G., Ferretti, A., Del Gratta, C., Romani, G.L., Gallese, V., 2008. The Sense of Touch: Embodied Simulation in a Visuotactile Mirroring Mechanism for Observed Animate or Inanimate Touch. Journal of Cognitive Neuroscience 20, 1611–1623. doi:10.1162/jocn.2008.20111
Ehrsson, H.H., 2012. The concept of body ownership and its relation to multisensory integration. Stein—The New Handbook of Multisensory Processes. MIT Press.
Ehrsson, H.H., Spence, C., Passingham, R.E., 2004. That's my hand! Activity in premotor cortex reflects feeling of ownership of a limb. Science 305, 875–877. doi:10.1126/science.1097011
Ehrsson, H.H., Wiech, K., Weiskopf, N., Dolan, R.J., Passingham, R.E., 2007. Threatening a rubber hand that you feel is yours elicits a cortical anxiety response. PNAS 104, 9828–9833. doi:10.1073/pnas.0610011104
Eickhoff, S.B., Bzdok, D., Laird, A.R., Kurth, F., Fox, P.T., 2012. Activation likelihood estimation meta-analysis revisited. NeuroImage 59, 2349–2361. doi:10.1016/j.neuroimage.2011.09.017
Eickhoff, S.B., Laird, A.R., Grefkes, C., Wang, L.E., Zilles, K., Fox, P.T., 2009. Coordinate-based activation likelihood estimation meta-analysis of neuroimaging data: A random-effects approach based on empirical estimates of spatial uncertainty. Hum. Brain Mapp. 30, 2907–2926. doi:10.1002/hbm.20718
Farnè, A., Demattè, M.L., Làdavas, E., 2005a. Neuropsychological evidence of modular organization of the near peripersonal space. Neurology 65, 1754–1758. doi:10.1212/01.wnl.0000187121.30480.09
Farnè, A., Iriki, A., Làdavas, E., 2005b. Shaping multisensory action–space with tools: evidence from patients with cross-modal extinction. Neuropsychologia, Movement, Action and Consciousness: Toward a Physiology of Intentionality A Special Issue in Honour of Marc Jeannerod 43, 238–248. doi:10.1016/j.neuropsychologia.2004.11.010
Farnè, A., Làdavas, E., 2002. Auditory peripersonal space in humans. J Cogn Neurosci 14, 1030–1043. doi:10.1162/089892902320474481
Farnè, A., Làdavas, E., 2000. Dynamic size-change of hand peripersonal space following tool use. Neuroreport 11, 1645–1649.

Ferri, F., Tajadura-Jiménez, A., Väljamäe, A., Vastano, R., Costantini, M., 2015. Emotion-inducing approaching sounds shape the boundaries of multisensory peripersonal space. Neuropsychologia 70, 468–475. doi:10.1016/j.neuropsychologia.2015.03.001

Fitzgibbon, B.M., Enticott, P.G., Rich, A.N., Giummarra, M.J., Georgiou-Karistianis, N., Bradshaw, J.L., 2012. Mirror-sensory synaesthesia: Exploring "shared" sensory experiences as synaesthesia. Neuroscience & Biobehavioral Reviews 36, 645–657. doi:10.1016/j.neubiorev.2011.09.006

Fitzgibbon, B.M., Giummarra, M.J., Georgiou-Karistianis, N., Enticott, P.G., Bradshaw, J.L., 2010. Shared pain: From empathy to synaesthesia. Neuroscience & Biobehavioral Reviews 34, 500–512. doi:10.1016/j.neubiorev.2009.10.007

Fogassi, L., Gallese, V., Fadiga, L., Luppino, G., Matelli, M., Rizzolatti, G., 1996. Coding of peripersonal space in inferior premotor cortex (area F4). J. Neurophysiol. 76, 141–157.

Fossataro, C., Sambo, C.F., Garbarini, F., Iannetti, G.D., 2016. Interpersonal interactions and empathy modulate perception of threat and defensive responses. Scientific Reports 6, 19353. doi:10.1038/srep19353

Gallagher, S., 2000. Philosophical conceptions of the self: implications for cognitive science. Trends in Cognitive Sciences 4, 14–21. doi:10.1016/S1364-6613(99)01417-5

Gallese, V., Sinigaglia, C., 2010. The bodily self as power for action. Neuropsychologia, The Sense of Body 48, 746–755. doi:10.1016/j.neuropsychologia.2009.09.038

Galli, G., Noel, J.P., Canzoneri, E., Blanke, O., Serino, A., 2015. The wheelchair as a full-body tool extending the peripersonal space. Front. Psychol. 6. doi:10.3389/fpsyg.2015.00639

Gentile, G., Guterstam, A., Brozzoli, C., Ehrsson, H.H., 2013. Disintegration of multisensory signals from the real hand reduces default limb self-attribution: an fMRI study. J. Neurosci. 33, 13350–13366. doi:10.1523/JNEUROSCI.1363-13.2013

Gentile, G., Petkova, V.I., Ehrsson, H.H., 2011. Integration of Visual and Tactile Signals From the Hand in the Human Brain: An fMRI Study. Journal of Neurophysiology 105, 910–922. doi:10.1152/jn.00840.2010

Goldenberg, G., Iriki, A., 2007. From sticks to coffee-maker: mastery of tools and technology by human and non-human primates. Cortex 43, 285–288.

Graziano, M.S., Gross, C.G., 1993. A bimodal map of space: somatosensory receptive fields in the macaque putamen with corresponding visual receptive fields. Exp Brain Res 97, 96–109.

Graziano, M.S., Hu, X.T., Gross, C.G., 1997. Visuospatial properties of ventral premotor cortex. J. Neurophysiol. 77, 2268–2292.

Graziano, M.S., Yap, G.S., Gross, C.G., 1994. Coding of visual space by premotor neurons. Science 266, 1054–1057.

Graziano, M.S.A., Cooke, D.F., 2006. Parieto-frontal interactions, personal space, and defensive behavior. Neuropsychologia 44, 845–859. doi:10.1016/j.neuropsychologia.2005.09.009

Graziano, M.S.A., Cooke, D.F., Taylor, C.S.R., 2000. Coding the Location of the Arm by Sight. Science 290, 1782–1786. doi:10.1126/science.290.5497.1782

Graziano, M.S.A., Hu, X.T., Gross, C.G., 1997. Visuospatial Properties of Ventral Premotor Cortex. Journal of Neurophysiology 77, 2268–2292.

Graziano, M.S.A., Reiss, L.A.J., Gross, C.G., 1999. A neuronal representation of the location of nearby sounds. Nature 397, 428–430. doi:10.1038/17115

Graziano, M.S.A., Taylor, C.S.R., Moore, T., 2002. Complex Movements Evoked by Microstimulation of Precentral Cortex. Neuron 34, 841–851. doi:10.1016/S0896-6273(02)00698-0

Grivaz, P., Blanke, O., Serino, A., 2017. Common and distinct brain regions processing multisensory bodily signals for peripersonal space and body ownership. NeuroImage 147, 602–618. doi:10.1016/j.neuroimage.2016.12.052

Guipponi, O., Cléry, J., Odouard, S., Wardak, C., Ben Hamed, S., 2015. Whole brain mapping of visual and tactile convergence in the macaque monkey. NeuroImage 117, 93–102. doi:10.1016/j.neuroimage.2015.05.022

Guipponi, O., Wardak, C., Ibarrola, D., Comte, J.-C., Sappey-Marinier, D., Pinède, S., Hamed, S.B., 2013. Multimodal Convergence within the Intraparietal Sulcus of the Macaque Monkey. J. Neurosci. 33, 4128–4139. doi:10.1523/JNEUROSCI.1421-12.2013

Holmes, N.P., Calvert, G.A., Spence, C., 2004. Extending or projecting peripersonal space with tools? Multisensory interactions highlight only the distal and proximal ends of tools. Neuroscience Letters 372, 62–67. doi:10.1016/j.neulet.2004.09.024

Holt, D.J., Cassidy, B.S., Yue, X., Rauch, S.L., Boeke, E.A., Nasr, S., Tootell, R.B.H., Coombs, G., 2014. Neural Correlates of Personal Space Intrusion. J. Neurosci. 34, 4123–4134. doi:10.1523/JNEUROSCI.0686-13.2014

Hunley, S.B., Marker, A.M., Lourenco, S.F., 2017. Individual Differences in the Flexibility of Peripersonal Space. Experimental Psychology 64, 49–55. doi:10.1027/1618-3169/a000350

Hyvärinen, J., Poranen, A., 1974. Function of the parietal associative area 7 as revealed from cellular discharges in alert monkeys. Brain 97, 673–692.

Hyvärinen, J., Poranen, A., 1974. Function of the Parietal Associative Area 7 as Revealed from Cellular Discharges in Alert Monkeys. Brain 97, 673–692. doi:10.1093/brain/97.1.673

Iachini, T., Coello, Y., Frassinetti, F., Ruggiero, G., 2014. Body Space in Social Interactions: A Comparison of Reaching and Comfort Distance in Immersive Virtual Reality. PLoS ONE 9. doi:10.1371/journal.pone.0111511

Iachini, T., Coello, Y., Frassinetti, F., Senese, V.P., Galante, F., Ruggiero, G., 2016. Peripersonal and interpersonal space in virtual and real environments: Effects of gender and age. Journal of Environmental Psychology 45, 154–164. doi:10.1016/j.jenvp.2016.01.004

Iachini, T., Pagliaro, S., Ruggiero, G., 2015. Near or far? It depends on my impression: moral information and spatial behavior in virtual interactions. Acta Psychol (Amst) 161, 131–136. doi:10.1016/j.actpsy.2015.09.003

Iriki, A., Tanaka, M., Iwamura, Y., 1996. Coding of modified body schema during tool use by macaque postcentral neurones. Neuroreport 7, 2325–2330.

Ishida, H., Nakajima, K., Inase, M., Murata, A., 2009. Shared Mapping of Own and Others' Bodies in Visuotactile Bimodal Area of Monkey Parietal Cortex. Journal of Cognitive Neuroscience 22, 83–96. doi:10.1162/jocn.2009.21185

Ishida, H., Suzuki, K., Grandi, L.C., 2015. Predictive coding accounts of shared representations in parieto-insular networks. Neuropsychologia 70, 442–454. doi:10.1016/j.neuropsychologia.2014.10.020

Kamtchum-Tatuene, J., Allali, G., Saj, A., Bernati, T., Sztajzel, R., Pollak, P., Momjian-Mayor, I., Kleinschmidt, A., 2017. An exploratory cohort study of sensory extinction in acute stroke: prevalence, risk factors, and time course. J Neural Transm (Vienna) 124, 483–494. doi:10.1007/s00702-016-1663-x

Kandula, M., Hofman, D., Dijkerman, H.C., 2015. Visuo-tactile interactions are dependent on the predictive value of the visual stimulus. Neuropsychologia 70, 358–366. doi:10.1016/j.neuropsychologia.2014.12.008

Keysers, C., Gazzola, V., 2009. Expanding the mirror: vicarious activity for actions, emotions, and sensations. Current Opinion in Neurobiology, Motor systems • Neurology of behaviour 19, 666–671. doi:10.1016/j.conb.2009.10.006

Keysers, C., Kaas, J.H., Gazzola, V., 2010. Somatosensation in social perception. Nat Rev Neurosci 11, 417–428. doi:10.1038/nrn2833

Keysers, C., Wicker, B., Gazzola, V., Anton, J.-L., Fogassi, L., Gallese, V., 2004. A Touching Sight: SII/PV Activation during the Observation and Experience of Touch. Neuron 42, 335–346. doi:10.1016/S0896-6273(04)00156-4

Krahé, C., Springer, A., Weinman, J.A., Fotopoulou, A. (Katerina), 2013. The Social Modulation of Pain: Others as Predictive Signals of Salience – a Systematic Review. Front. Hum. Neurosci. 7. doi:10.3389/fnhum.2013.00386

Làdavas, E., 2002. Functional and dynamic properties of visual peripersonal space. Trends in Cognitive Sciences 6, 17–22. doi:10.1016/S1364-6613(00)01814-3
Làdavas, E., di Pellegrino, G., Farnè, A., Zeloni, G., 1998a. Neuropsychological evidence of an integrated visuotactile representation of peripersonal space in humans. J Cogn Neurosci 10, 581–589.
Làdavas, E., Farnè, A., Zeloni, G., Pellegrino, G. di, 2000. Seeing or not seeing where your hands are. Exp Brain Res 131, 458–467. doi:10.1007/s002219900264
Làdavas, E., Serino, A., 2008. Action-dependent plasticity in peripersonal space representations. Cogn Neuropsychol 25, 1099–1113.
Làdavas, E., Zeloni, G., Farnè, A., 1998b. Visual peripersonal space centred on the face in humans. Brain 121 (Pt 12), 2317–2326.
Lamm, C., Singer, T., 2010. The role of anterior insular cortex in social emotions. Brain Struct Funct 214, 579–591. doi:10.1007/s00429-010-0251-3
Lenggenhager, B., Tadi, T., Metzinger, T., Blanke, O., 2007. Video ergo sum: manipulating bodily self-consciousness. Science 317, 1096–1099. doi:10.1126/science.1143439
Lourenco, S.F., Longo, M.R., Pathman, T., 2011. Near space and its relation to claustrophobic fear. Cognition 119, 448–453. doi:10.1016/j.cognition.2011.02.009
Macaluso, E., Maravita, A., 2010. The representation of space near the body through touch and vision. Neuropsychologia, The Sense of Body 48, 782–795. doi:10.1016/j.neuropsychologia.2009.10.010
Maister, L., Cardini, F., Zamariola, G., Serino, A., Tsakiris, M., 2015. Your place or mine: Shared sensory experiences elicit a remapping of peripersonal space. Neuropsychologia 70, 455–461. doi:10.1016/j.neuropsychologia.2014.10.027
Makin, T.R., Holmes, N.P., Ehrsson, H.H., 2008. On the other hand: Dummy hands and peripersonal space. Behavioural Brain Research 191, 1–10. doi:10.1016/j.bbr.2008.02.041
Makin, T.R., Holmes, N.P., Zohary, E., 2007. Is That Near My Hand? Multisensory Representation of Peripersonal Space in Human Intraparietal Sulcus. J. Neurosci. 27, 731–740. doi:10.1523/JNEUROSCI.3653-06.2007
Maravita, A., Husain, M., Clarke, K., Driver, J., 2001. Reaching with a tool extends visual–tactile interactions into far space: evidence from cross-modal extinction. Neuropsychologia 39, 580–585. doi:10.1016/S0028-3932(00)00150-0
Maravita, A., Iriki, A., 2004. Tools for the body (schema). Trends in Cognitive Sciences 8, 79–86. doi:10.1016/j.tics.2003.12.008
Martel, M., Cardinali, L., Roy, A.C., Farnè, A., 2016. Tool-use: An open window into body representation and its plasticity. Cognitive Neuropsychology 33, 82–101. doi:10.1080/02643294.2016.1167678
Mattingley, J.B., Driver, J., Beschin, N., Robertson, I.H., 1997. Attentional competition between modalities: extinction between touch and vision after right hemisphere damage. Neuropsychologia 35, 867–880. doi:10.1016/S0028-3932(97)00008-0
Noel, J.-P., Grivaz, P., Marmaroli, P., Lissek, H., Blanke, O., Serino, A., 2015a. Full body action remapping of peripersonal space: The case of walking. Neuropsychologia 70, 375–384. doi:10.1016/j.neuropsychologia.2014.08.030
Noel, J.-P., Pfeiffer, C., Blanke, O., Serino, A., 2015b. Peripersonal space as the space of the bodily self. Cognition 144, 49–57. doi:10.1016/j.cognition.2015.07.012
Occelli, V., Spence, C., Zampini, M., 2011. Audiotactile interactions in front and rear space. Neuroscience & Biobehavioral Reviews 35, 589–598. doi:10.1016/j.neubiorev.2010.07.004
Park, H.-D., Tallon-Baudry, C., 2014. The neural subjective frame: from bodily signals to perceptual consciousness. Philos. Trans. R. Soc. Lond., B, Biol. Sci. 369, 20130208. doi:10.1098/rstb.2013.0208
Patané, I., Iachini, T., Farnè, A., Frassinetti, F., 2016. Disentangling Action from Social Space: Tool-Use Differently Shapes the Space around Us. PLoS ONE 11. doi:10.1371/journal.pone.0154247

Petkova, V.I., Ehrsson, H.H., 2008. If I Were You: Perceptual Illusion of Body Swapping. PLOS ONE 3, e3832. doi:10.1371/journal.pone.0003832
Poliakoff, E., Miles, E., Li, X., Blanchette, I., 2007. The effect of visual threat on spatial attention to touch. Cognition 102, 405–414. doi:10.1016/j.cognition.2006.01.006
Quesque, F., Ruggiero, G., Mouta, S., Santos, J., Iachini, T., Coello, Y., 2016. Keeping you at arm's length: modifying peripersonal space influences interpersonal distance. Psychological Research 1–12. doi:10.1007/s00426-016-0782-1
Rizzolatti, G., Scandolara, C., Matelli, M., Gentilucci, M., 1981a. Afferent properties of periarcuate neurons in macaque monkeys. I. Somatosensory responses. Behav. Brain Res. 2, 125–146.
Rizzolatti, G., Scandolara, C., Matelli, M., Gentilucci, M., 1981b. Afferent properties of periarcuate neurons in macaque monkeys. II. Visual responses. Behav. Brain Res. 2, 147–163.
Rizzolatti, G., Scandolara, C., Matelli, M., Gentilucci, M., 1981. Afferent properties of periarcuate neurons in macaque monkeys. II. Visual responses. Behav. Brain Res. 2, 147–163.
Sambo, C.F., Forster, B., 2008. An ERP Investigation on Visuotactile Interactions in Peripersonal and Extrapersonal Space: Evidence for the Spatial Rule. Journal of Cognitive Neuroscience 21, 1550–1559. doi:10.1162/jocn.2009.21109
Sambo, C.F., Forster, B., Williams, S.C., Iannetti, G.D., 2012a. To blink or not to blink: fine cognitive tuning of the defensive peripersonal space. J. Neurosci. 32, 12921–12927. doi:10.1523/JNEUROSCI.0607-12.2012
Sambo, C.F., Iannetti, G.D., 2013. Better Safe Than Sorry? The Safety Margin Surrounding the Body Is Increased by Anxiety. J. Neurosci. 33, 14225–14230. doi:10.1523/JNEUROSCI.0706-13.2013
Sambo, C.F., Liang, M., Cruccu, G., Iannetti, G.D., 2012b. Defensive peripersonal space: the blink reflex evoked by hand stimulation is increased when the hand is near the face. J. Neurophysiol. 107, 880–889. doi:10.1152/jn.00731.2011
Schiff, W., Caviness, J.A., Gibson, J.J., 1962. Persistent fear responses in rhesus monkeys to the optical stimulus of "looming." Science 136, 982–983.
Schlack, A., Sterbing-D'Angelo, S.J., Hartung, K., Hoffmann, K.-P., Bremmer, F., 2005. Multisensory space representations in the macaque ventral intraparietal area. J. Neurosci. 25, 4616–4625. doi:10.1523/JNEUROSCI.0455-05.2005
Serino, A., Alsmith, A., Costantini, M., Mandrigin, A., Tajadura-Jimenez, A., Lopez, C., 2013. Bodily ownership and self-location: Components of bodily self-consciousness. Consciousness and Cognition 22, 1239–1252. doi:10.1016/j.concog.2013.08.013
Serino, A., Bassolino, M., Farnè, A., Làdavas, E., 2007. Extended Multisensory Space in Blind Cane Users. Psychological Science 18, 642–648. doi:10.1111/j.1467-9280.2007.01952.x
Serino, A., Canzoneri, E., Avenanti, A., 2011. Fronto-parietal Areas Necessary for a Multisensory Representation of Peripersonal Space in Humans: An rTMS Study. Journal of Cognitive Neuroscience 23, 2956–2967. doi:10.1162/jocn_a_00006
Serino, A., Canzoneri, E., Marzolla, M., di Pellegrino, G., Magosso, E., 2015a. Extending peripersonal space representation without tool-use: evidence from a combined behavioral-computational approach. Front. Behav. Neurosci. 9. doi:10.3389/fnbeh.2015.00004
Serino, A., Noel, J.-P., Galli, G., Canzoneri, E., Marmaroli, P., Lissek, H., Blanke, O., 2015b. Body part-centered and full body-centered peripersonal space representations. Scientific Reports 5. doi:10.1038/srep18603
Serino, A., Pizzoferrato, F., Làdavas, E., 2008. Viewing a Face (Especially One's Own Face) Being Touched Enhances Tactile Perception on the Face. Psychological Science 19, 434–438. doi:10.1111/j.1467-9280.2008.02105.x
Seth, A.K., 2013. Interoceptive inference, emotion, and the embodied self. Trends in Cognitive Sciences 17, 565–573. doi:10.1016/j.tics.2013.09.007
Seth, A.K., Friston, K.J., 2016. Active interoceptive inference and the emotional brain. Phil. Trans. R. Soc. B 371, 20160007. doi:10.1098/rstb.2016.0007

Sforza, A., Bufalari, I., Haggard, P., Aglioti, S.M., 2010. My face in yours: Visuo-tactile facial stimulation influences sense of identity. Soc Neurosci 5, 148–162. doi:10.1080/17470910903205503

Spence, C., Pavani, F., Maravita, A., Holmes, N., 2004. Multisensory contributions to the 3-D representation of visuotactile peripersonal space in humans: evidence from the crossmodal congruency task. Journal of Physiology-Paris, Representation of 3-D Space Using Different Senses In Different Species 98, 171–189. doi:10.1016/j.jphysparis.2004.03.008

Taffou, M., Viaud-Delmon, I., 2014. Cynophobic Fear Adaptively Extends Peri-Personal Space. Front. Psychiatry 5. doi:10.3389/fpsyt.2014.00122

Teneggi, C., Canzoneri, E., di Pellegrino, G., Serino, A., 2013. Social modulation of peripersonal space boundaries. Curr. Biol. 23, 406–411. doi:10.1016/j.cub.2013.01.043

Tsakiris, M., 2010. My body in the brain: A neurocognitive model of body-ownership. Neuropsychologia, The Sense of Body 48, 703–712. doi:10.1016/j.neuropsychologia.2009.09.034

Tsakiris, M., 2008. Looking for myself: current multisensory input alters self-face recognition. PLoS ONE 3, e4040. doi:10.1371/journal.pone.0004040

Tsakiris, M., Schütz-Bosbach, S., Gallagher, S., 2007. On agency and body-ownership: Phenomenological and neurocognitive reflections. Consciousness and Cognition, Subjectivity and the Body 16, 645–660. doi:10.1016/j.concog.2007.05.012

Turkeltaub, P.E., Eden, G.F., Jones, K.M., Zeffiro, T.A., 2002. Meta-Analysis of the Functional Neuroanatomy of Single-Word Reading: Method and Validation. NeuroImage 16, 765–780. doi:10.1006/nimg.2002.1131

Vagnoni, E., Lourenco, S.F., Longo, M.R., 2012. Threat modulates perception of looming visual stimuli. Current Biology 22, R826–R827. doi:10.1016/j.cub.2012.07.053

Van Damme, S., Gallace, A., Spence, C., Crombez, G., Moseley, G.L., 2009. Does the sight of physical threat induce a tactile processing bias?: Modality-specific attentional facilitation induced by viewing threatening pictures. Brain Research 1253, 100–106. doi:10.1016/j.brainres.2008.11.072

Van der Stoep, N., Nijboer, T.C.W., Van der Stigchel, S., Spence, C., 2015. Multisensory interactions in the depth plane in front and rear space: A review. Neuropsychologia 70, 335–349. doi:10.1016/j.neuropsychologia.2014.12.007

Van der Stoep, N., Serino, A., Di Luca, M., Spence, C., 2016. Depth: the Forgotten Dimension in Multisensory Research. Multisensory research. doi:10.1163/22134808-00002525

Vossel, S., Eschenbeck, P., Weiss, P.H., Weidner, R., Saliger, J., Karbe, H., Fink, G.R., 2011. Visual extinction in relation to visuospatial neglect after right-hemispheric stroke: quantitative assessment and statistical lesion-symptom mapping. Journal of Neurology, Neurosurgery & Psychiatry 82, 862–868. doi:10.1136/jnnp.2010.224261

Wallace, M.T., Stevenson, R.A., 2014. The construct of the multisensory temporal binding window and its dysregulation in developmental disabilities. Neuropsychologia 64C, 105–123. doi:10.1016/j.neuropsychologia.2014.08.005

Axis I Objectives

The first objective of this first axis is to confirm the hypothesis according to which, in a context of visual objects approaching the face, multisensory integration is maximized not by temporal simultaneity, but rather by the predictive nature of the visual stimulus on the tactile stimulation. For this, a behavioral study was conducted in humans to describe the perceptual correlates of this hypothesis (Chapter 1). Using the same stimuli, we carried out another study in the non-human primate to describe the neural bases underlying this hypothesis using the fMRI technique. This study is presented in Chapter 2. These two studies are discussed in the context of multisensory integration and spatial, temporal prediction and Bayesian causal inference.

The second objective of this first axis is to propose a precise mapping of the cortical networks involved in the treatment of the near space with respect to the far space and to measure their degree of overlap with the predictive network highlighted in Chapter 2. For this purpose, a study was carried out in the non-human primate using fMRI to describe the neuronal bases underlying the respective encoding of near space and far space (Chapter 3).

The accumulated knowledge on the understanding of the neural bases involved in the processes of near and far space has grown in recent years. A majority of studies are developed in relation to a theoretical framework centered on the fact that it is the actions and specifically the arm and the actions linked to the hand that shape the cortical representation of the peripersonal space. We have written a review (Chapter 4) in which we propose to extend this framework by including other variables that have the potential to shape this space: low-level sensory signals, oculomotor signals, parietal and premotor functional properties, object use, emotional and social contexts.

Impact prediction

Summary of publications on Impact prediction

The ecological significance of stable stimuli close to our body (e.g. a wall, a desk) and dynamic stimuli looming towards us (e.g. a mosquito, a ball) are different. Looming stimuli are potentially more dangerous than other visual stimuli, including dynamic stimuli with no predicted impact on the body. Objects approaching us or a predator may pose a threat, and signal the need to initiate a defensive behavior. These potential impacts suggest an intrusion in our peripersonal space, which contributes to the enhancement of the system to make it more efficient in order to face the potential threat (Canzoneri et al., 2012; Cléry et al., 2015a; Kandula et al., 2015; De Paepe et al., 2016).

Chapter 1: Impact Prediction by Looming Visual Stimuli Enhances Tactile Detection (Published in "*The Journal of Neuroscience*", March 11th 2015 • 35(10):4179–4189).

A dynamic looming stimulus can have delayed consequences for a second sensory modality which can be fully predicted by its spatiotemporal dynamics. Dynamic looming stimuli have been shown to speed up tactile processing (Canzoneri et al., 2012; Kandula et al., 2015; De Paepe et al., 2016). In this psychophysical study, we tested whether or not visual stimuli looming toward the face predictively enhance heteromodal tactile sensitivity around the expected time of impact and at its expected location on the body.

In this study, we used visual and tactile stimulations. Visual stimuli consisted of a dynamic visual stimulus which mimicked an impact onto the face (rapidly approaching the subject). Tactile stimuli corresponded to air puffs directed to the left or right cheek of the

subjects. Subjects had to fixate on a central point throughout the trial. A visual stimulus, a tactile stimulus, or a combination of both visual and tactile stimuli was presented. At the end of the trial, subjects were requested to report if they had detected a tactile stimulus. We measured the d' which quantifies the sensitivity of each subject to tactile stimulations as a function of the stimulation context.

The results show that temporal impact prediction maximizes the d' within a temporal prediction window with the maximum tactile enhancement observed when the tactile stimulus is applied at the estimated time of impact. This temporal window is modulated by the speed of the looming visual stimulus. The spatial impact prediction maximizes the d'. The predictive cues contained in the looming cone trajectories are crucially contributing to enhanced tactile detection at the predicted impact location at the expected time of impact. We additionally show that a looming stimulus that brushes past the face also enhances tactile sensitivity on the nearby cheek, suggesting that the space close to the face is incorporated into the subjects' body schema.

The results clearly show that visual stimuli looming toward the face provide the nervous system with predictive cues that selectively enhance tactile sensitivity at the expected impact location of the visual stimulus, using three predictive dimensions: the estimated time of impact, the estimated position of impact and dynamic depth cues.

Chapter 2: The prediction of impact of a looming stimulus onto the body is subserved by multisensory integration mechanisms (Submitted in "*The Journal of Neuroscience*", March 6th 2017, JN-RM-0610-17).

Recent studies show that looming stimuli enhance tactile processing at the predicted time of impact and at the expected location of impact, both as measured by enhanced tactile

sensitivity (Cléry et al., 2015a) and shorter reaction times (Canzoneri et al., 2012; Kandula et al., 2015), including when specifically probing nociceptive perception (De Paepe et al., 2016). However, the neurophysiological mechanisms by which the dynamic information provided by one sensory modality predictively enhances the processing of another sensory modality remain unknown. Is the enhancement of the tactile detection that we have observed in our psychophysical study, reflected by the hyperactivation of the cortical networks under the same conditions?

Therefore, we used functional magnetic resonance imaging in the non-human primate, to investigate the neural bases of the prediction of an impact to the body by a looming stimulus, i.e. the neural bases of the interaction between a dynamic visual stimulus approaching the body and its expected consequences onto an independent sensory modality, namely, touch.

In this study, we used the same visual and tactile stimulations as in our psychophysical study (Chapter 1). The monkeys were required to fixate on a central point during all the acquisition and during the presentation of stimuli. Monkeys were rewarded for maintaining this fixation as long as possible. We manipulated the spatial and temporal relationships between the visual and the tactile stimulations so as to isolate the specific contribution of either temporal prediction or spatial prediction cues on the cortical activations.

We show that looming visual stimuli towards the body enhance the tactile information processing within a temporal window and at a spatial location that coincide with the prediction of impact on the body. Indeed, spatial and temporal prediction enhances functional activations, as compared to the activations observed for spatially or temporally incongruent tactile and dynamic visual cues. The activated network is essentially composed of occipital (striate and extrastriate areas), parietal (e.g. intraparietal ventral area), premotor and prefrontal areas (e.g. F4 area). These activations reflect both an active integration of visual and tactile information and of spatial and temporal prediction information. The identified cortical network coincides

with a well-described multisensory visuo-tactile convergence and integration network suggested to play a key role in the definition of peripersonal space (Rizzolatti et al., 1997; Graziano and Cooke, 2006; Guipponi et al., 2013, 2015).

References

Canzoneri E, Magosso E, Serino A (2012) Dynamic Sounds Capture the Boundaries of Peripersonal Space Representation in Humans. PLoS ONE 7:e44306.

Cléry J, Guipponi O, Odouard S, Wardak C, Ben Hamed S (2015) Impact prediction by looming visual stimuli enhances tactile detection. J Neurosci 35:4179–4189.

De Paepe AL, Crombez G, Legrain V (2016) What's Coming Near? The Influence of Dynamical Visual Stimuli on Nociceptive Processing. PLOS ONE 11:e0155864.

Graziano MSA, Cooke DF (2006) Parieto-frontal interactions, personal space, and defensive behavior. Neuropsychologia 44:845–859.

Guipponi O, Cléry J, Odouard S, Wardak C, Ben Hamed S (2015) Whole brain mapping of visual and tactile convergence in the macaque monkey. NeuroImage 117:93–102.

Guipponi O, Wardak C, Ibarrola D, Comte J-C, Sappey-Marinier D, Pinède S, Hamed SB (2013) Multimodal Convergence within the Intraparietal Sulcus of the Macaque Monkey. J Neurosci 33:4128–4139.

Kandula M, Hofman D, Dijkerman HC (2015) Visuo-tactile interactions are dependent on the predictive value of the visual stimulus. Neuropsychologia 70:358–366.

Rizzolatti G, Fadiga L, Fogassi L, Gallese V (1997) The space around us. Science 277:190–191.

Chapter 1 :

Impact Prediction by Looming Visual Stimuli Enhances Tactile Detection

Published in "*The Journal of Neuroscience*", March 11th 2015 • 35(10):4179–4189

Behavioral/Cognitive

Impact Prediction by Looming Visual Stimuli Enhances Tactile Detection

Justine Cléry,* Olivier Guipponi,* Soline Odouard, Claire Wardak, and Suliann Ben Hamed
Centre de Neuroscience Cognitive, CNRS UMR 5229, Université Claude Bernard Lyon I, 69675 Bron cedex, France

From an ecological point of view, approaching objects are potentially more harmful than receding objects. A predator, a dominant conspecific, or a mere branch coming up at high speed can all be dangerous if one does not detect them and produce the appropriate escape behavior fast enough. And indeed, looming stimuli trigger stereotyped defensive responses in both monkeys and human infants. However, while the heteromodal somatosensory consequences of visual looming stimuli can be fully predicted by their spatiotemporal dynamics, few studies if any have explored whether visual stimuli looming toward the face predictively enhance heteromodal tactile sensitivity around the expected time of impact and at its expected location on the body. In the present study, we report that, in addition to triggering a defensive motor repertoire, looming stimuli toward the face provide the nervous system with predictive cues that enhance tactile sensitivity on the face. Specifically, we describe an enhancement of tactile processes at the expected time and location of impact of the stimulus on the face. We additionally show that a looming stimulus that brushes past the face also enhances tactile sensitivity on the nearby cheek, suggesting that the space close to the face is incorporated into the subjects' body schema. We propose that this cross-modal predictive facilitation involves multisensory convergence areas subserving the representation of a peripersonal space and a safety boundary of self.

Key words: **body limit; looming visual stimuli; multisensory integration; prediction of impact; predictive coding**

Introduction

From an ecological point of view, approaching objects are potentially harmful. A predator, a dominant conspecific, or a mere branch coming up at high speed are dangerous if one does not detect them fast enough to produce the appropriate escape motor repertoire. And indeed, looming stimuli trigger stereotyped defensive responses in both monkeys (Schiff et al., 1962) and human infants (Ball and Tronick, 1971); the estimated time of impact to the body of threatening looming stimuli is shorter than that of neutral looming stimuli (Vagnoni et al., 2012), and looming visual stimuli trigger pronounced orienting behavior toward simultaneous congruent auditory cues compared with receding stimuli, both in nonhuman primates (Maier et al., 2004) and in 5-month-old human infants (Walker-Andrews and Lennon, 1985). This suggests that the dynamics of visual stimuli with respect to the subject exerts cross-modal influences and possibly recruits multisensory integration processes. These observations are in agreement with the general multisensory integration framework, which assumes a common source for multimodal sensory inputs (Sugita and Suzuki, 2003). They specifically extend this framework to the case of dynamical multimodal sources, demonstrating that spatially and temporally congruent auditory stimuli enhance the perception of both static (McDonald et al., 2000) and dynamic visual stimuli (Maier et al., 2004; Cappe et al., 2009; Leo et al., 2011; Parise et al., 2012). Such bimodal dynamic stimuli are frequent in everyday life (visuoauditory: a car passing a pedestrian; visuotactile: a mosquito walking on one's forearm). The neural substrates that result in the integration of this dynamic sensory information are increasingly understood both in humans (Cappe et al., 2012; Tyll et al., 2013) and in nonhuman primates (Maier and Ghazanfar, 2007; Maier et al., 2008). Overall, these studies derive multisensory integration principals for looming multisensory stimuli under the assumption of a causal common source.

However, a dynamic looming stimulus can also have delayed consequences for a second sensory modality. For example, an object approaching the face will induce a tactile stimulation at the moment of its impact on the body. The heteromodal somatosensory consequences of such a stimulus can be fully predicted by its spatiotemporal dynamics. Accordingly, approaching auditory (Canzoneri et al., 2012) or visual (Kandula et al., 2014) looming stimuli predictively speeds up tactile processing. In the following, we test whether visual stimuli looming toward the face predictively enhance heteromodal tactile sensitivity around the expected time of impact and at its expected location on the body. We discuss our observations in relationship with neurophysiological and behavioral evidence suggesting the existence of a defense peripersonal space defining a safety margin around the body (Gentilucci et al., 1988; Rizzolatti et al., 1988; Colby et al.,

Received July 23, 2014; revised Jan. 22, 2015; accepted Jan. 28, 2015.

Author contributions: C.W. and S.B.H. designed research; J.C., O.G., and S.O. performed research; S.B.H. contributed unpublished reagents/analytic tools; J.C. and O.G. analyzed data; J.C., O.G., C.W., and S.B.H. wrote the paper.

We thank Karen Reilley for her help with the EMG recordings and Serge Pinède for his technical assistance in preparing the experiments.

*J.C. and O.G. contributed equally to this work.

The authors declare no competing financial interests.

Correspondence should be addressed to Suliann Ben Hamed, Centre de Neuroscience Cognitive, CNRS UMR 5229, Université Claude Bernard Lyon I, 67 Boulevard Pinel, 69675 Bron Cedex, France. E-mail: benhamed@isc.cnrs.fr.

DOI:10.1523/JNEUROSCI.3031-14.2015

 0270-6474/15/354179-11$15.00/0

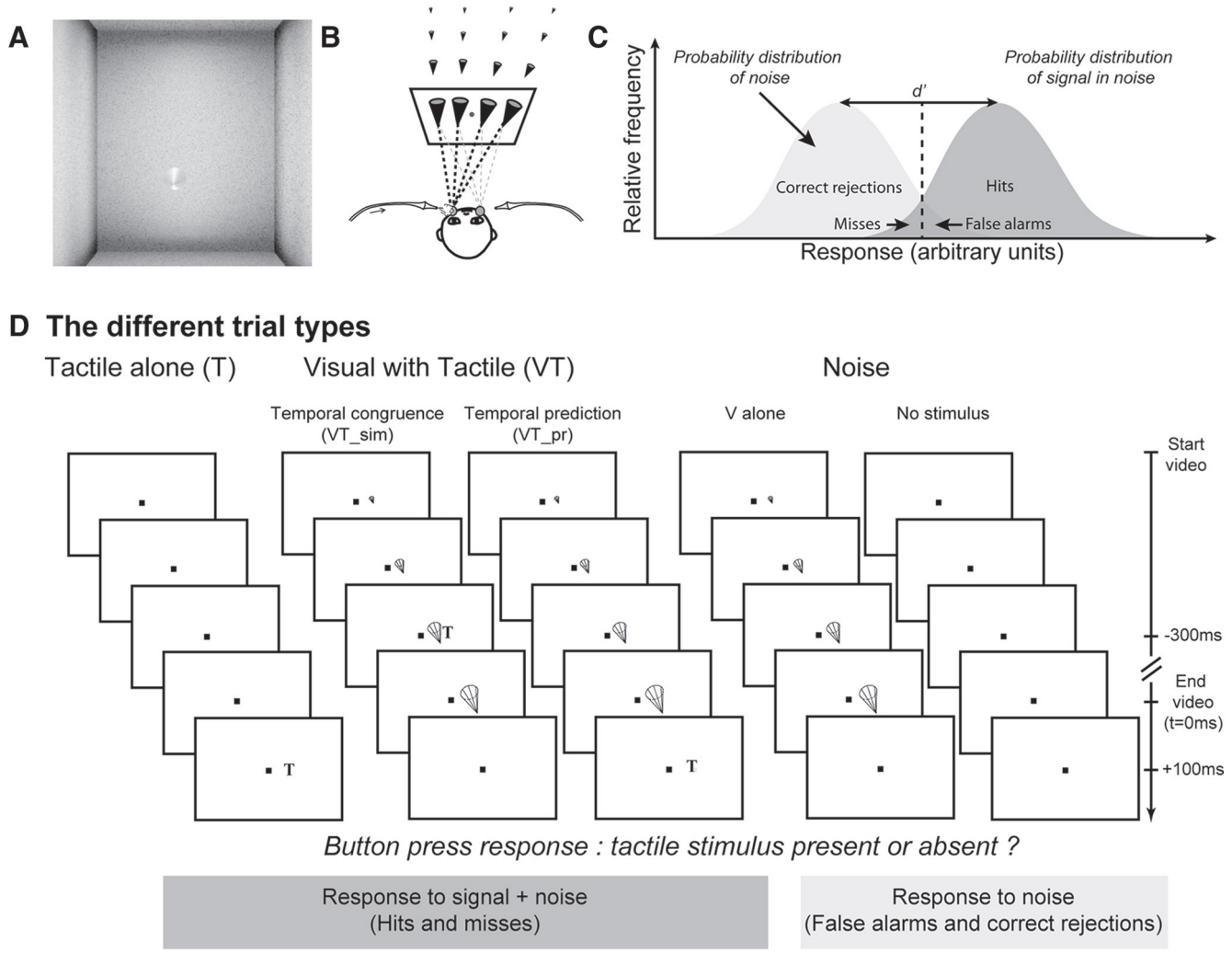

Figure 1. Experimental protocol. ***A***, Visual stimulus: video sequence of a cone in a 3D environment, looming toward the subject's face. ***B***, Experimental setup, air-puff delivery, and possible apparent looming cone trajectories. ***C***, Signal detection theory and *d'* measure estimation. ***D***, Possible variants of signal trials (tactile alone or visual with tactile) and noise trials (visual alone trials or no stimulus trials); example of a temporal prediction bloc–Experiment 1.

1993; Graziano et al., 1994, 2002; Gross and Graziano, 1995; Fogassi et al., 1996; Duhamel et al., 1998, Cooke and Graziano, 2004; Graziano and Cooke, 2006).

Materials and Methods

The experimental protocol was approved by the local ethics committee in biomedical research (Comité de protection des personnes sud-est IV, N CPP 11/025) and all participants gave their written informed consent.

Experimental set-up

Subjects sat in a chair at 50 cm from a 23 inch computer monitor. Their heads were restrained by a chin rest. Their arms were placed on a table and they held a gamepad with their two hands. Vertical and horizontal eye positions were monitored using a video eye tracker (EyeLink; sampling at 120 Hz, spatial resolution $<1°$). Data acquisition, eye monitoring, and visual presentation were controlled by a PC running Presentation (Neurobehavioral Systems).

Visual stimuli. The fixation point was a $0.06° \times 0.06°$ yellow square (0.67 cd $/m^2$). The screen background was set to a structured 3D environment with visual depth cues (Fig. 1*A*). Visual stimuli consisted of eight possible video sequences of a cone, pointing toward the subject, moving within this 3D environment, originating away from and rapidly approaching the subject. For Experiments 1–4, the cone could originate from eight possible locations around the fixation point: ($-6.8°$, $-1.0°$), ($-3.2°$, $-1.0°$), ($-2.8°$, $-1.0°$), ($-1.1°$, $-1.0°$), ($1.1°$, $-1.0°$), ($2.8°$, $-1.0°$), ($3.2°$, $-1.0°$) and ($6.8°$, $-1.0°$). The cone moved along trajectories that intersected the subject's face at two possible locations, on the left or right cheeks, close to the nostrils (Fig. 1*B*). For Experiment 5, the cone origins were slightly modified to achieve the desired percept: ($-5.8°$, $-1.0°$), ($-2.8°$, $-1.0°$), ($-1.1°$, $-1.0°$), ($-0.2°$, $-1.0°$), ($0.2°$, $-1.0°$), ($1.1°$, $-1.0°$), ($2.8°$, $-1.0°$), ($5.8°$, $-1.0°$). In this experiment, the cone trajectory could either intersect the face on the left or right cheek or move past the face on the left or on the right. Each video sequence consisted of 24 images played for a total duration of 800 ms. The 3D environment and different cone trajectories were all constructed with the Blender software (http://www.blender.org/).

Tactile stimuli. Tactile stimuli consisted of air puffs directed to the left or right cheek of the subjects, at locations coinciding with the two possible visual cone trajectory endpoints (Fig. 1*B*), through tubes placed at 2–4 mm from each cheek and rigidly fixed to the chin rest. The relative position between the screen and the air-puff tubing was maintained constant throughout the experiments and across subjects. The intensity of the left and right air puffs was adjusted independently, and for each subject, to achieve a 50% detection rate as estimated over a short block of 20 trials (one block for the left air puff and one block for the right air puff). The air-puff delivery system was placed in an independent room, separated from the experimental room, so that the subjects could not predict air-puff delivery from the sound produced by the delivery system. Air puffs were delivered to the subjects through long tubing connecting

the air-puff delivery system to a rigid connector fixed on the chin rest. The latency of air-puff outlet at the tubing end following the opening of the solenoid air pressure valve was measured as a function of air-puff intensity, using a silicon on-chip signal-conditioned pressure sensor (MPX5700 Series; Freescale). Detection thresholds were achieved with air pressures varying between 0.05 and 0.1 bars, corresponding to average air-puff latencies of 220 ms. Throughout this manuscript, air-puff timings are corrected to reflect the actual time at which the air puffs hit the face.

Experimental procedure

Subjects had to fixate on a central yellow point throughout the trial. The fixation was monitored to remain within an eye-tolerance window of 2° (controlled by a video eye tracker) around the fixation stimulus. One to three seconds following trial start, a visual stimulus, a tactile stimulus, or a combination of both visual and tactile stimuli was presented. No-stimulation trials were also presented. The precise ratios of trial types are detailed below for each experiment. At the end of the trial, subjects were requested to report the detection of a tactile stimulus by a "Yes" button press (right-hand gamepad button) and respond by a "No" button press otherwise (left-hand gamepad button). To maximize multisensory integration, we used very weak tactile stimuli to the face, specifically directed to the left or right cheeks (see above, Tactile stimuli).The main measure reported in the present study is a d' measure quantifying the sensitivity of each subject to tactile stimulations as a function of the stimulation context (no stimulation, tactile stimulation alone, or tactile stimulation associated with visual stimulation of specific spatial and temporal properties; Fig. 1*C*,*D*). This measure is based on a reliable estimate of false reports of tactile stimuli in noise (False alarms) and correct reports of tactile stimuli (Hits). Each d' is calculated by collecting the subject's response to a minimum of 75 trials per stimulation context. The d' measures were estimated for the different stimulation conditions in five different experiments as follows.

Experiment 1: influence of a visual looming stimulus on tactile d′, temporal prediction. Ten subjects participated in this study (27.2 ± 5.3 years, five males and five females; Fig. 3*A*). All subjects were naive to the purpose of the experiment except one (S.B.H.). All participants had normal or corrected-to-normal vision. Five possible trial types were presented to the subjects. Noise trials allowed the estimation of their false alarm rate. The trials could either be no-stimulus trials (1/6 of all trials) or visual stimulation-only trials (1/3 of all trials). Signal trials allowed the estimation of their Hit rate as a function of the stimulation condition. The trials could be (1) tactile stimulation-only trials (1/6 of all trials, allowing estimation of d' for pure tactile stimuli), (2) visual stimulation + tactile stimulation presented midway through the visual video trials (1/6 of all trials, 300 ms before video offset, allowing the estimation of d' for tactile stimuli in the presence of a visual stimulus), and (3) visual stimulation + tactile stimulation presented when the visual cone is expected to impact the face on the cheek predicted by the cone trajectory trials (1/6 of all trials, 100 ms after video offset, allowing the estimation of d' for tactile stimuli, which are spatially and temporally predicted by a dynamical visual looming stimulus). Trials were presented pseudorandomly. Subjects were allowed to rest whenever they needed by closing their eyes. During these rest periods, they were instructed not to move their head in the rest chin so as not to change the distance of the air-puff tubing to their face or to change eye calibration and 450 trials were collected in all.

Experiment 2: influence of a visual looming stimulus on tactile d′, temporal prediction window. Ten subjects participated in this study (26.5 ± 4.0 years, four males and six females; Fig. 3*B*). All subjects were naive to the purpose of the experiment. All participants had normal or corrected-to-normal vision. Seven possible trial types were presented to the subjects. Noise trials were composed of no-stimulus trials (1/10 of all trials) and of visual stimulus-only trials (4/10 of all trials). Signal trials were as follows: (1) tactile stimulation-only trials (1/10 of all trials, allowing estimation of d' to pure tactile stimuli) and (2) visual stimulation + tactile stimulation trials in which the tactile stimulus could be presented at four possible timings with respect to the visual stimuli (1/10 of all trials for each possible timing: −300 ms, −100 ms, 100 ms, or 300 ms from the end of the video, allowing the estimation of d' for tactile stimuli in each condition). Trials were presented pseudorandomly. Subjects were allowed to rest whenever they needed by closing their eyes. Rest periods were arranged as in Experiment 1 and 450 total trials were collected.

Experiment 3: influence of the speed of a visual looming stimulus on the temporal prediction window, as assessed from the enhancement of tactile d′. Ten subjects participated in this study (28.0 ± 5.4 years, two males and eight females; Fig. 3*C*). All subjects were naive to the purpose of the experiment, except two (J.C. and S.B.H.). Importantly, the looming stimuli approached the subjects' face and aimed for the cheek at half the speed of those used in Experiments 1, 2, 4, 5, and 6 (the exact same video sequences were used for all experiments, except in Experiment 3, each image of the video sequence stayed twice as long on the screen, compared with the images presented in Experiments 1, 2, 4, 5, and 6). Five possible trial types were presented to the subjects. Noise trials were composed of no-stimulus trials (1/6 of all trials) and of visual stimulus-only trials (2/6 of all trials). Signal trials were as follows: (1) tactile stimulation-only trials (1/6 of all trials, allowing estimation of d' to pure tactile stimuli) and (2) visual stimulation + tactile stimulation trials in which the tactile stimulus could be presented at two possible timings with respect to the visual stimuli (1/6 of all trials for each possible timing: 100 ms or 250 ms from the end of the video, allowing the estimation of d' for tactile stimuli in each condition). Trials were presented pseudorandomly. Subjects were allowed to rest whenever they needed by closing their eyes. Rest periods were arranged as in Experiment 1 and 500 total trials were collected.

Experiment 4: influence of a visual looming stimulus on tactile d′, spatial prediction. Ten subjects participated in this study (24.3 ± 2.4 years, four males and six females; Fig. 4*A*). All subjects were naive to the purpose of the experiment, except one (J.C.). All participants had normal or corrected-to-normal vision. Five possible trial types were presented to the subjects. Noise trials were as in Experiment 1. Signal trials were as follows: (1) tactile stimulation-only trials (1/6 of all trials, allowing estimation of d' for pure tactile stimuli), (2) visual stimulation + tactile stimulation presented when the visual cone is expected to impact the face on the cheek predicted by the cone trajectory trials (1/6 of all trials, 100 ms after video offset, allowing estimation of d' for tactile stimuli, which are spatially and temporally predicted by a dynamical visual stimulus), and (3) trials with visual stimulation + tactile stimulation presented at the time at which the visual cone is expected to impact the face but on the opposite cheek from the one predicted by the cone trajectory (1/6 of all trials, 100 ms after video offset, allowing the estimation of d' to tactile stimuli, which is temporally predicted by a dynamical visual stimulus but spatially incongruent to it). Trials were presented pseudorandomly. Subjects were allowed to rest whenever they needed by closing their eyes. Rest periods were arranged as in Experiment 1 and 450 total trials were collected.

Experiment 5: influence of visual stimulus impact on tactile detection. Ten subjects participated in this study (27.8 ± 5.8 years, three males and seven females; Fig. 4*B*). All subjects were naive to the purpose of the experiment, except two (J.C. and S.B.H.). All trial types were as in Experiment 1, except that in half of the video sequences the cone trajectories did not cross the subjects' face but continued to the right or to the left of the face. Rest periods were arranged as in Experiment 1 and 450 total trials were collected.

Experiment 6: influence of a visual receding stimulus on tactile d′. Ten subjects participated in this study (27.8 ± 5.8 years, three males and seven females; Fig. 4*C*). All subjects were naive to the purpose of the experiment, except one (J.C.). All trial types were as in Experiment 1, except that the visual video sequences were played in reverse order such that the cones appeared to move away from the subjects rather than toward their face. Rest periods were arranged as in Experiment 1 and 450 total trials were collected.

Analysis

Data analysis was performed in MATLAB (The MathWorks). For each experiment, we extracted, for each signal trial type (i.e., each trial type in which a tactile stimulus was effectively presented), and for each subject, the d' quantifying the subject's sensitivity at detecting tactile stimuli (Table 1). For all experiments, we also quantified the response criterion for each such subject within a given experiment and confirmed that this

Table 1. Average raw *d′* values, per experiment and per experimental condition, quantifying the subjects' sensitivity at detecting tactile stimuli

Experiment	# subject	Experimental condition				
1, Figure 3*A*	10	*d′* (tactile only) 1.45	*d′* (V predicting T) 1.89	*d′* (V during T) 1.69		
2, Figure 3*B*	10	*d′* (tactile only) 1.37	*d′* (−300 ms) 2.06	*d′* (−100 ms) 1.79	*d′* (100 ms) 2.37	*d′* (300 ms) 2.01
3, Figure 3*C*	10	*d′* (tactile only) 0.66	*d′* (100 ms) 1.45	*d′* (250 ms) 1.75		
4, Figure 4*A*	10	*d′* (tactile only) 2.20	*d′* (V and T spatially congruent) 2.66		*d′* (V and T spatially incongruent) 2.40	
5, Figure 4*B*	10	*d′* (tactile only) 1.72	*d′* (V toward face) 2.72	*d′* (V past face) 2.47		
6, Figure 4*C*	10	*d′* (tactile only) 1.92	*d′* (V predicting T) 2.03	*d′* (V during T) 2.27		

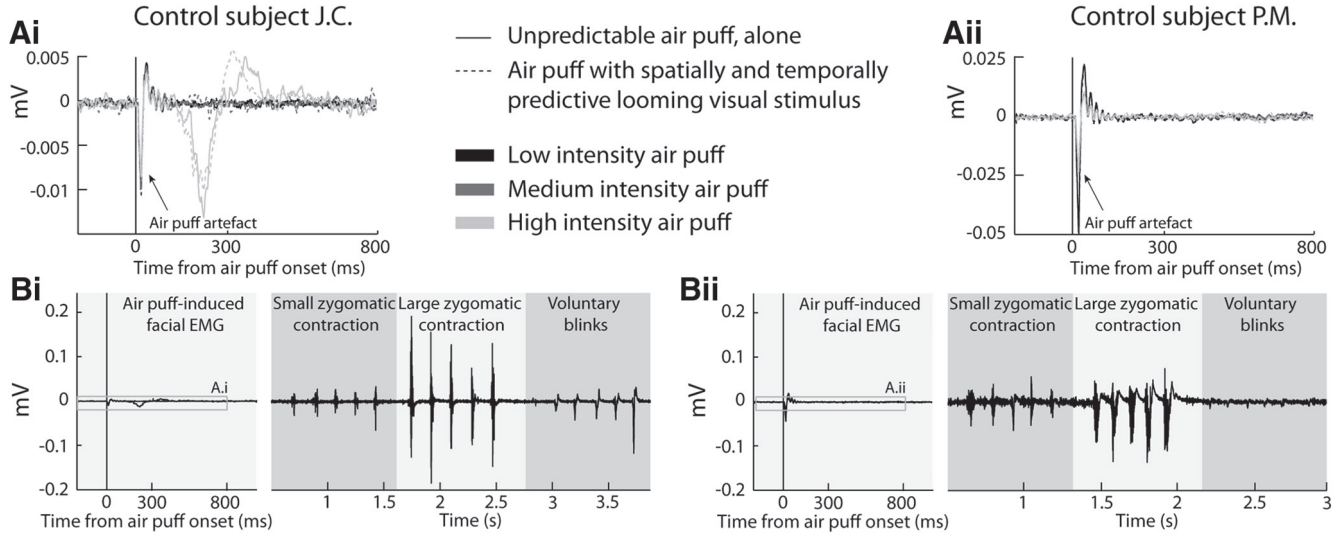

Figure 2. Low-intensity air puffs, whether unpredicted or fully predictable, do not produce anticipatory facial contractions that could account for changes in tactile sensitivity. ***A***, Average facial EMG aligned on air-puff delivery, as a function of whether the air puff is unpredictable (continuous lines) or fully predictable (dashed lines), for low air-puff intensities (black; subject J.C.: 55% detections for predictable air puffs and 85% for unpredictable air puffs; subject P.M.: 60% detections for predictable air puffs and 60% for unpredictable air puffs), medium air-puff intensities (medium gray; just above threshold air puff, 0.05 bars), and high air-puff intensities (light gray; reported as aversive by subjects, 0.5 bars). ***B***, For comparison, same data as in ***A*** reproduced with the same *y*-scale as facial EMG recordings during five small zygomatic contractions, five large zygomatic contractions, or five voluntary eye blinks. Data for control subject J.C. are presented on the left (plots ***Ai*** and ***Bi***) and data for control subject P.M. are presented on the right (plots ***Aii*** and ***Bii***).

criterion was independent of trial type (data not shown). Statistical effects were first assessed using a repeated-measure one-way ANOVA, followed by *post hoc* paired *t* tests for which the appropriate Bonferroni correction was applied (* symbol on all figures), unless otherwise specified (filled circle symbol on all figures). For the ANOVA tests, the *F*-values and *p* values are reported as well as the corresponding partial η squared. For the *t* tests, the *t* statistics (*t* statistics), the degree of freedom (df), and the Cohen's *d* are indicated to allow for a direct assessment of the effect size.

Control for the absence of facial muscle contraction induced by air-puff delivery

Our main prediction in the present work is that visual and temporal predictive cues will result in an enhancement in tactile sensitivity due to sensory processes (namely multisensory integration). However, predictive cues could also result in subjects unconsciously contracting their facial muscles around the air-puff impact point, in anticipation of air-puff delivery. This could result in a local change in tactile sensitivity. We thus measured, on two representative control subjects (Fig. 2; J.C., left plots, P.M. right plots), the facial EMG (Fig. 2; zygomatic minor, in a tendon-belly configuration, reference behind the ear for subject J.C. and on the forehead for subject P.M., naive subject; Biopac Systems, EMG100C amplification module, gain 2000, acquisition frequency 1 kHz, low-pass filter 500 Hz, high pass filter 10 Hz, 50 Hz band cut filter), while the subjects were submitted to temporally unpredictable (Fig. 2*Ai*,*Aii*, continuous lines) or fully predictive (Fig. 2*Ai*,*Aii*, dashed lines), low-intensity (Fig. 2*Ai*,*Aii*, black; subject J.C.: 85% detections for predictable air puffs and 55% for unpredictable air puffs; subject P.M.: 60% detections for predictable air puffs and 60% for unpredictable air puffs), medium-intensity (Fig. 2*Ai*,*Aii*, medium gray; just above threshold air puff, 0.05 bars), or high-intensity (Fig. 2*Ai*,*Aii*, light gray; reported as aversive by subjects, 0.5 bars) air puffs. The air puffs were located as in the main experiments, and the EMG recording electrodes were placed on the same side as the air-puff delivery tubing, one just above the lip commissure and the other on the other side of the nasolabial fold, above the first one, such that the air puff impacted bare skin. Apart from the electric artifact induced by the air-puff trigger, no modulation of the facial EMG could be observed, neither at the low air-puff intensities used in the main experiments, nor at higher intensities (Fig. 2*Aii*; except for blinks evoked at the highest aversive intensities for subject J.C.). To allow for a proper interpretation of this absence of effect, the facial EMGs recorded during small zygomatic contractions, large zygomatic contractions, or voluntary eye blinks are also shown, on the same *y*-scale (Fig. 2*Bi*,*ii*). This allows for the proper attribution of the modulation of J.C.'s facial EMG by high-intensity air puffs to blinks and not to a zygomatic minor muscle contraction, the EMG signature of which is different from that of a blink. The EMG modulation evoked by these nonvoluntary blinks is smaller than that observed following voluntary blinks, corroborating the fact that the underlying neural bases of voluntary and spontaneous or reflexive blinks are different (Guipponi et al., 2014).

Results

The main experimental measures reported below are tactile *d′* sensitivity measures. This measure is based on the analysis of how often subjects report the presence of a tactile stimulus when none was actually presented (i.e., responses to noise, also referred to as false alarms) and how often they correctly report the presence of tactile stimuli when a stimulus was indeed presented (i.e., responses to signal, also referred to as hits or correct detections).

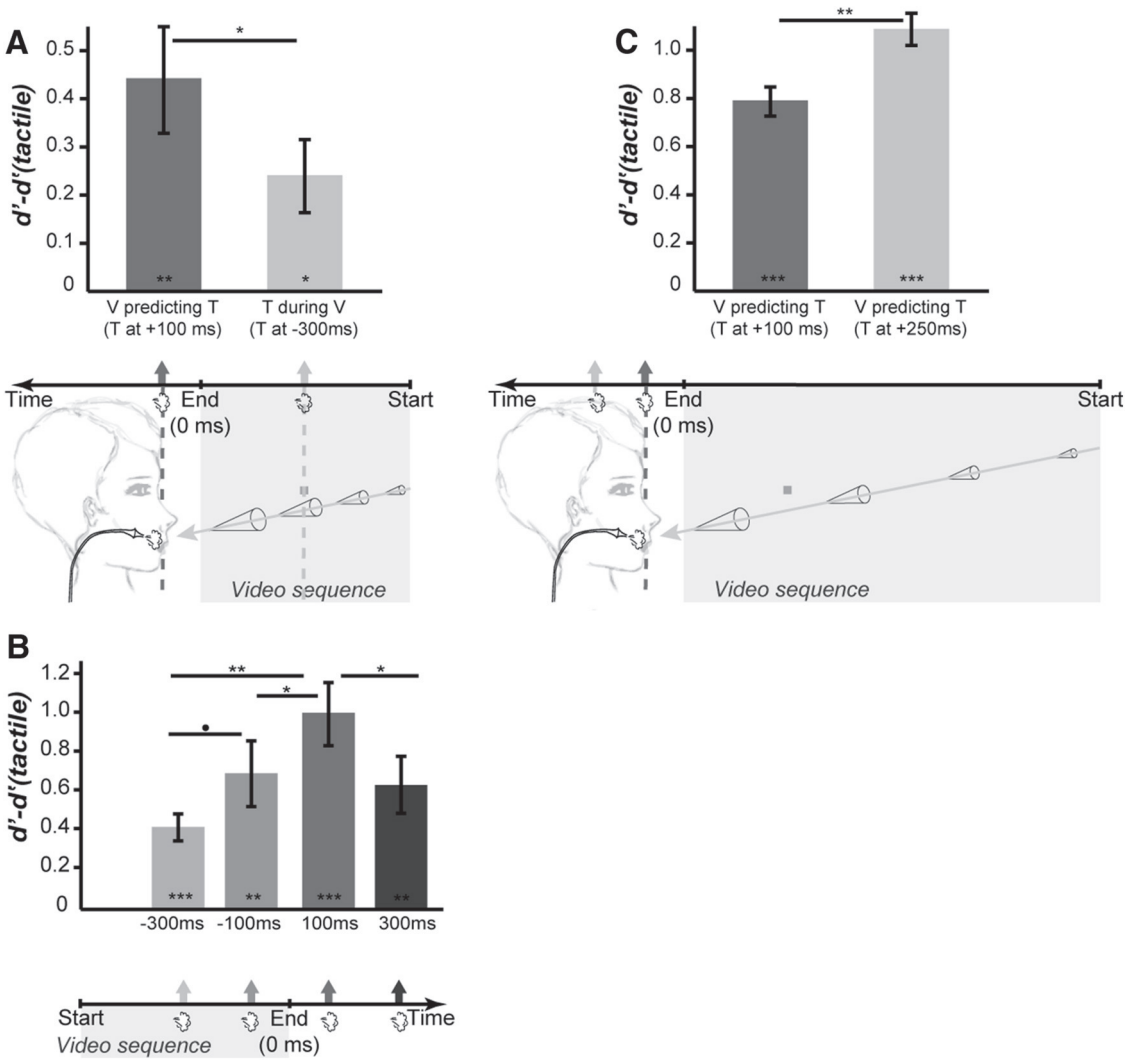

Figure 3. Temporal prediction. ***A***, Temporal prediction versus temporal simultaneity. Bar plots represent the mean (±SE) of the difference between the baseline tactile *d′* [*d′* (tactile)] and the *d′* obtained when the tactile stimulus is applied during the visual video sequence (T during V) or at the predicted time of impact of the looming cone onto the subject's face (V predicting T). ***B***, Temporal prediction window. Bar plots represent the mean (±SE) of the difference between the baseline tactile *d′* (tactile) and the *d′* obtained when the tactile stimulus is applied at different temporal asynchronies from the end of the visual video sequence. ***C***, Temporal prediction window is modulated by the speed of the looming visual stimulus. Bar plots represent the mean (±SE) of the difference between the baseline tactile *d′* (tactile) and the *d′* obtained when the tactile stimulus is applied at +100 ms or +250 ms from the end of the visual video sequence of looming stimuli played at half the speed of those used in ***A*** and ***B***. Significant statistical differences between each test condition and the *d′* (tactile) baseline are indicated by symbols inside the bars. Statistical differences across the test conditions are indicated by symbols above the bar plots. *$p < 0.05$, Bonferroni corrected; **$p < 0.01$, Bonferroni corrected; ***$p < 0.001$, Bonferroni corrected; ˙$p < 0.05$, no correction for multiple comparisons.

The *d′*s are high when stimuli can unambiguously be detected and low when they are difficult to discriminate against noise (Fig. 1*C*). As a result, they reflect the sensitivity of the subject to the stimulus of interest. In the following, we analyze how the sensitivity to a tactile stimulus is affected by the simultaneous presentation of a dynamical looming visual stimulus, as a function of its spatial and temporal characteristics relative to the tactile stimulus.

Temporal prediction versus temporal simultaneity

The classical multisensory integration framework assumes that maximum cross-modal enhancement is obtained for spatially and temporally colocalized sensory sources. In a first experiment (Fig. 3*A*, Table 1), we question whether tactile detection is indeed maximized by the simultaneous presentation of a dynamic visual stimulus approaching the face (specifically the cheeks) or whether maximum tactile processing enhancement is obtained at the predicted time of impact of the looming stimulus on the face. We measured the tactile *d′* of subjects when the tactile stimulus was applied to one of their cheeks as follows: (1) in the absence of any visual stimulation [*d′* (Tactile), serving as a baseline], (2) midway through the video sequence of a cone looming toward their face and predicting an impact at the very location of the tactile stimulus (T during V, 300 ms before the end of the video sequence), or (3) following the video sequence of a cone looming toward their face at its predicted time and location of impact to the skin (V predicting T, 100 ms following the end of the video sequence). There was a significant effect of the experimental conditions onto the subjects' tactile *d′*, as assessed from a repeated-measure one-way ANOVA ($F_{(2,18)} = 11.89$, $p < 0.0005$, partial η squared = 57%). Specifically, and as expected from previous studies, *d′* (Tactile) was significantly smaller than *d′* (T during V) (Table 1, one-tailed *t* test, $p = 0.0053$, *t* statistics = 3.2, df = 9, Cohen's $d = 0.45$, Bonferroni corrected $p < 0.05$; Fig. 3*A*, dark

gray bar) and d' (V predicting T) (Table 1, one-tailed t test, $p = 0.0018$, t statistics = 3.9, df = 9, Cohen's $d = 0.89$, Bonferroni corrected $p < 0.01$; Fig. 3*A*, light gray bar). Most interestingly, d' (T during V) was also significantly smaller than d' (V predicting T) (Table 1, one-tailed t test, $p = 0.0165$, t statistics = 2.5, df = 9, Cohen's $d = 0.41$, Bonferroni corrected $p < 0.05$; Fig. 3*A*). Thus maximum tactile detection is achieved when the tactile stimulus is temporally predicted by a visual stimulus looming toward the location of the tactile stimulation compared to when visual and tactile stimuli are presented simultaneously. This effect did not depend on the tactile stimulation side (left or right cheeks), nor on the origin of the looming visual stimulus (left or right visual field, periphery or center of the visual field). All the statistically significant comparisons performed above still hold when two-tailed t tests are performed instead of one-tailed t tests. This can directly be assessed from the t statistics and p values described above, because the t statistics are symmetric at about zero. It is, however, important to note that one-tailed t tests are fully appropriate here, because we have a strong a priori hypothesis on the directionality of the effects, due to the expected impact of multisensory integration and predictive coding on the subjects' overt responses.

Temporal prediction window

In Experiment 2, we manipulate the temporal asynchrony between the dynamic visual stimulus and the tactile stimulus to identify the temporal window of tactile sensitivity enhancement around the end of the looming stimulus video sequence. There was a significant effect of the time at which the air puffs were delivered relative to the end of the visual stimulus onto the subjects' tactile d', as assessed from a repeated-measure one-way ANOVA ($F_{(4,36)} = 17.74$, $p < 0.00001$, partial η squared = 66%). Specifically, all visuotactile conditions were associated with significantly higher d' than the d' (Tactile) baseline condition (Table 1, Fig. 3*B*; one-tailed t test, all ps < 0.0014, t statistics ranging from 4.1 to 6.1, df = 9, Cohen's d ranging from 0.67 to 1.40, Bonferroni corrected $p < 0.01$ or better). Maximum tactile enhancement is obtained when the tactile stimulus is applied at the estimated time of impact of the looming cone on the face (100 ms, same timing as that used in Experiment 1; Fig. 3*B*). This d' is significantly higher than that obtained for a tactile stimulus presented 300 ms before the end of the video sequence (Table 1, Fig. 3*B*; $p = 0.000515$, t statistics = 4.8, df = 9, Cohen's $d = 0.81$, Bonferroni corrected $p < 0.01$), 100 ms before the end of the video sequence; Table 1, Fig. 3*B*; $p = 0.0039$, t statistics = 3.4, df = 9, Cohen's $d = 0.40$, Bonferroni corrected $p < 0.015$), or 300 ms following the end of the video sequence (Table 1, Fig. 3*B*; $p = 0.0093$, t statistics = 2.9, df = 9, Cohen's $d = 0.45$, Bonferroni corrected $p < 0.05$). All the statistically significant comparisons performed above still hold when two-tailed t tests are performed instead of one-tailed t tests, except for the very last test, as can directly be assessed from the t statistics and p values provided. Here again, it is, however, important to note that one-tailed t tests are fully appropriate here, under the prediction that maximum tactile enhancement is obtained at the expected time of impact.

The temporal prediction window depends on the speed of the looming stimulus

In Experiment 2, maximum tactile enhancement is obtained at 100 ms following the end of the video sequence of the looming objects. To test whether the time of maximum tactile enhancement depends on the predicted time of impact to the face and thus on the speed of the looming object, in Experiment 3, we used dynamic visual stimuli looming at half the speed of those used in all other experiments, and we probed tactile sensitivity at 100 and 250 ms following the end of the video sequence. There was a significant effect of the time at which the air puffs were delivered relative to the end of the visual stimulus onto the subjects' tactile d', as assessed from a repeated-measure one-way ANOVA ($F_{(4,36)} = 52.7$, $p < 0.00001$, partial η squared = 85%). Specifically, all visuotactile conditions were associated with significantly higher d' than the d' (tactile) baseline condition (Table 1, Fig. 3*B*; one-tailed t test, all ps < 0.00001, t statistics ranging from 6.7 to 8.3, df = 9, Cohen's d ranging from 1.0 to 1.48, Bonferroni corrected $p < 0.00001$ or better). Importantly, maximum tactile enhancement is obtained when the tactile stimulus is applied at the estimated time of impact of the looming cone on the face (Fig. 3*C*; 250 ms, compared with 100 ms, the timing revealing maximum enhancement in tactile sensitivity in Experiment 2, $p = 0.0013$, t statistics = 4.1, df = 9, Cohen's $d = 0.5$, Bonferroni corrected $p < 0.01$). In other words, for a high-speed looming stimulus (Experiment 2), tactile sensitivity is higher at 100 ms (predicted time of impact) following the end of the stimulus than later (300 ms), while for a low-speed stimulus (Experiment 3), tactile sensitivity is lower at 100 ms following the end of the stimulus than later (250 ms, predicted time of impact, between-subject one-tailed unpaired t test, t statistics = 4.53, df = 18, $p = 0.00012$, Cohen's $d = 2.03$). All the statistically significant comparisons performed above still hold when two-tailed t tests are performed instead of one-tailed t tests, as can directly be assessed from the t statistics and p values provided.

Spatial prediction

In Experiments 1 and 2, the tactile stimulus is always presented at the expected impact location. In Experiment 3, we test whether spatial prediction also contributes to tactile processing enhancement. We measured the tactile d' of subjects when the tactile stimulus was applied to one of their cheeks (1) in the absence of any visual stimulation [d' (Tactile)], (2) following the video sequence of a cone looming toward their face at the time and location predicted by the dynamic visual stimulus [d' (V and T spatially congruent)], or (3) following the video sequence of a cone looming toward their face at the time predicted by this visual stimulus but at the opposite location [d' (V and T spatially incongruent)]. Here again, there was a significant effect of the experimental conditions onto the subjects' tactile d', as assessed from a repeated-measure one-way ANOVA ($F_{(2,18)} = 14.45$, $p < 0.0002$, partial η squared = 62%). Specifically, we find that tactile sensitivity was significantly increased with respect to the baseline d' (Tactile) when V and T were spatially congruent (Table 1, Fig. 4*A*, dark gray bar; one-tailed t test, $p = 0.00048$, t statistics = 4.8, df = 9, Cohen's $d = 0.73$, Bonferroni corrected $p < 0.01$). When V and T were spatially incongruent, a similar trend could be observed at an uncorrected level (Table 1, Fig. 4*A*, light gray bar; one-tailed t test, $p = 0.029$, t statistics = 2.2, df = 9, Cohen's d = 0.36). Most interestingly, d' (V and T spatially incongruent) was also significantly smaller than d' (V and T spatially congruent) (Table 1, Fig. 4*A*; one-tailed t test, $p = 0.0015$, t statistics = 4.0, df = 9, Cohen's $d = 0.47$, Bonferroni corrected $p < 0.01$). This crucial observation still holds true when two-tailed t tests are used, as can directly be assessed from the t statistics and p values provided. Thus maximum tactile detection is achieved when the tactile stimulus is both temporally and spatially predicted by a visual stimulus looming compared to when the visual stimulus is only temporally predictive of the tactile stimulus. Again, this effect did not depend on the tactile stimulation side (left or right

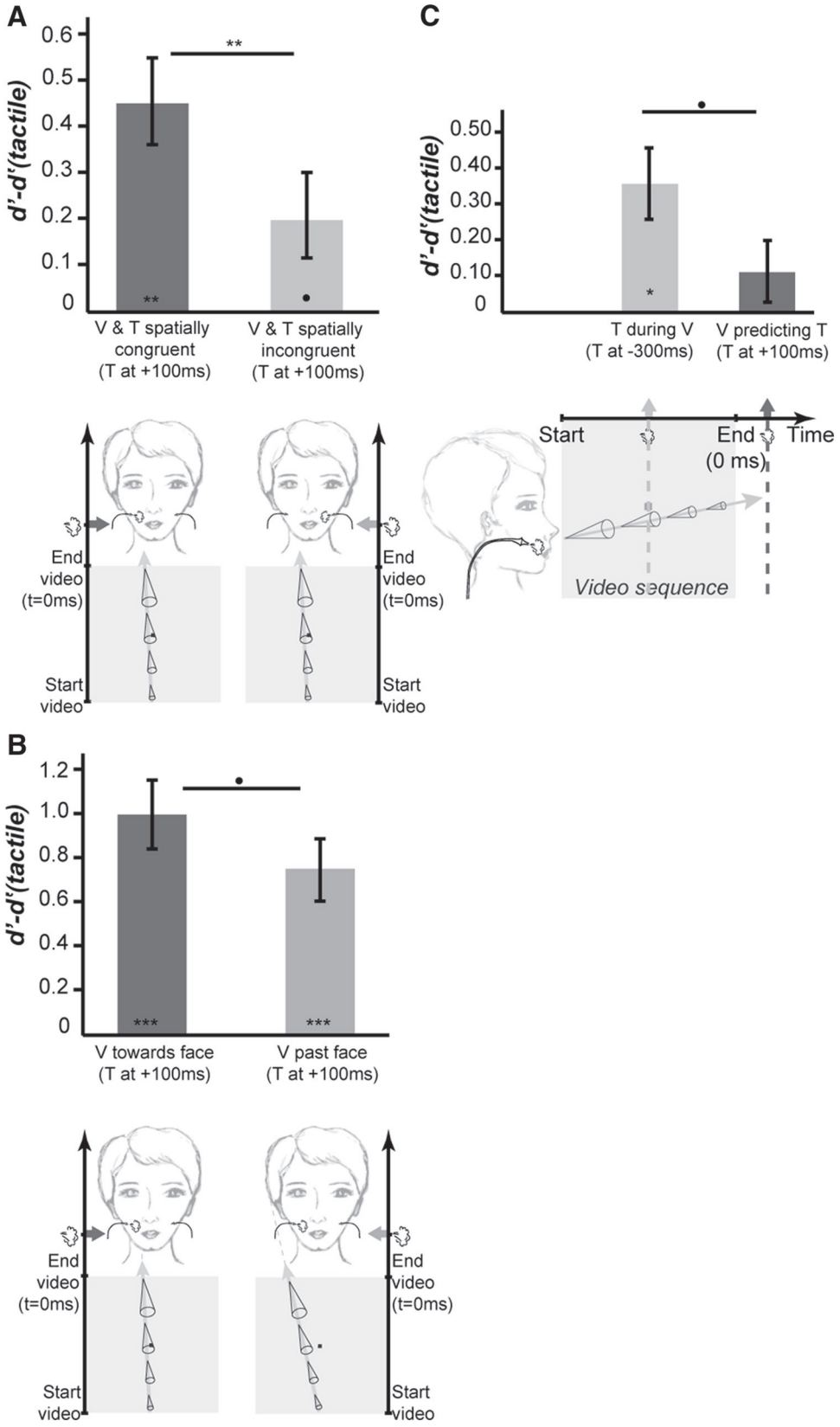

Figure 4. Spatial prediction. ***A***, Spatial congruence. Bar plots represent the mean (±SE) of the difference between the baseline tactile *d'* (tactile) and the *d'* obtained when the tactile stimulus is applied following the offset of the looming cone onto the subject's face, at its predicted impact time, at the location predicted by the cone trajectory (V and T spatially congruent) or on the opposite cheek (V and T spatially incongruent). ***B***, Body limits. Bar plots represent the mean (±SE) of the difference between the baseline tactile *d'* (tactile) and the *d'* obtained when the tactile stimulus is applied at the end of looming cone video sequence, at its predicted impact time, when the cone trajectory predicts an impact to the face (V toward face) or not (V past face). ***C***, Looming versus receding stimuli. Bar plots represent the mean (±SE) of the difference between the baseline tactile *d'* (tactile) and the *d'* obtained when the tactile stimulus is applied during the visual video sequence of a cone receding away from the subject's face (T during V) or at the end of the video sequence (V predicting T). All else as in Figure 3.

cheek) or on the origin of the looming visual stimulus (left or right visual field, periphery, or center of the visual field). These observations, together with those reported in the first two experiments, indicate that both temporal and spatial predictions contribute to enhanced target detection.

Body limit

In the above experiment, we show that the enhancement of tactile sensitivity is highest on the cheek to be impacted by a looming stimulus compared with the opposite cheek on which no impact is predicted. In Experiment 4, we test whether a looming stimulus with a trajectory brushing past the face but predicting no impact to the skin also contributes to tactile processing enhancement. We measured the tactile d' of subjects when the tactile stimulus was applied to one of their cheeks (1) in the absence of any visual stimulation [d'(Tactile)], (2) following the video sequence of a cone looming toward their face at the time and location predicted by the dynamic visual stimulus [d'(V toward face)], or (3) following the video sequence of a cone looming past their face and predicting no impact to the skin [d'(V past face)]. There was a significant effect of the experimental conditions onto the subjects' tactile d', as assessed from a repeated-measure one-way ANOVA ($F_{(2,18)} = 26.37$, $p < 0.00001$, partial η squared = 75%). Specifically, we find that tactile sensitivity was significantly increased with respect to the baseline d'(Tactile) both when the visual trajectory pointed toward the face (Table 1, Fig. 4*B*, dark gray bar; one-tailed t test, $p = 0.000059$, t statistics = 6.4, df = 9, Cohen's $d = 1.67$, Bonferroni corrected $p < 0.001$) or past it (Table 1, Fig. 4*B*, light gray bar; one-tailed t test, $p = 0.00027$, t statistics = 5.2, df = 9, Cohen's $d = 1.27$, Bonferroni corrected $p < 0.001$). Both these observations still hold true when two-tailed t tests are used, as can directly be assessed from the t statistics and p values provided. Importantly, d'(V toward face) was on average higher than d'(V past face) although this trend failed to reach significance at Bonferroni corrected level (Table 1, Fig. 4*B*; one-tailed t test, t statistics = 1.9, df = 9, Cohen's $d = 0.39$, $p = 0.0445$). As a result, tactile processing enhancement is only marginally reduced by a nonimpacting ipsilateral looming stimulus compared with what we describe in Experiment 3 for a looming visual impacting the contralateral cheek. This effect holds independently of the side of tactile stimulation (left or right cheek) or of the origin of the looming visual stimulus (left or right visual field, periphery, or center of the visual field).

Looming versus receding stimuli

In the previous experiments, the dynamical visual stimulus was a looming cone approaching the face. The spatial and temporal prediction enhancement of tactile detection described above could be fully due to the predictive cues provided by the stimulus trajectory. Alternatively, the reported effect could reflect an attentional spatiotemporal enhancement of tactile processing at the predicted location, independent of the fact that the trajectory of the cone is predictive of an impact on the face. To test for this effect, we repeated the first experiment, but this time with inverted video sequences, i.e., with dynamical visual stimuli receding away from the subject's face. A significant effect of the experimental conditions onto the subjects' tactile d', as assessed from a repeated-measure one-way ANOVA, was also observed ($F_{(2,18)} = 5.91$, $p < 0.01$, partial η squared = 40%). Specifically, we find that with a receding cone, the baseline d'(Tactile) is statistically smaller than d'(T during V) (Table 1, Fig. 4*C*, light gray bar; one-tailed t test, $p = 0.0077$, t statistics = 3.0, df = 9, Cohen's $d = 0.67$, Bonferroni corrected $p < 0.05$) but statistically undistinguishable from d'(V predicting T) (Table 1, Fig. 4*C*, dark gray bar; one-tailed t test, $p = 0.1121$, t statistics = 1.3, df = 9, Cohen's $d = 0.22$). In contrast with what was observed in the first experiment, d'(V predicting T) had a statistically nonsignificant trend to be smaller than d'(T during V) (Table 1, Fig. 4*C*; one-tailed t test, $p = 0.028$, t statistics = 2.2, df = 9, Cohen's $d = 0.495$, $p < 0.05$ uncorrected). This effect did not depend on the tactile stimulation side (left or right cheek) or on the origin of the looming visual stimulus (left or right visual field, periphery, or center of the visual field). Importantly, the change between the baseline d'(Tactile) and the d' obtained during the looming condition (from Experiment 1) is significantly different from the change between the baseline d'(Tactile) and the d' obtained the receding condition (from Experiment 5), as assessed from a between-subject one-tailed unpaired t test (t statistics = 2.4, df = 18, $p = 0.0136$, Cohen's $d = 1.06$, this observation still holds true when a two-tailed t test is used).

Overall, these observations indicate that the effects reported in the previous experiments cannot be accounted for by general attentional perceptual enhancement effects but rather that the predictive cues contained in the looming cone trajectories are crucially contributing to enhanced tactile detection at the predicted impact location at the expected time of impact.

Discussion

This study demonstrates that visual stimuli looming toward the face provide the nervous system with predictive cues that selectively enhance tactile sensitivity at the expected impact location of the visual stimulus. In the following, we discuss these observations in the context of multisensory integration, peripersonal space, and a defense boundary of self.

Predictive cues

Three predictive dimensions of the visual looming stimulus contribute to enhancing tactile sensitivity on the face.

The estimated time of impact

With high-speed looming stimuli, maximum tactile sensitivity is observed at 100 ms following the disappearance of the looming stimulus, at the subjective time of their impact to the face (Experiments 1 and 2; Fig. 3*A*,*B*). Importantly, with low-speed looming stimuli, maximum enhancement of tactile sensitivity is observed later, indicating that the enhancement of tactile sensitivity adjusts to the speed of the looming stimuli and to the time of their predicted impact on the face (Experiment 3; Fig. 3*C*). Several studies demonstrate that the temporal coincidence (Sugita and Suzuki, 2003) and temporal correlation (Parise et al., 2012) between a looming visual stimulus and a sound maximize audiovisual integration. The phenomenon we report here is completely different in that, in the presence of dynamic looming visual stimuli, maximum enhancement of tactile processing is achieved at the predicted time of impact, reflecting the expected subjective consequence of the visual stimulus onto the tactile modality. Interestingly, the perceptual and physiological binding of two stimuli into the representation of a unique external source is subjected to some degree of temporal tolerance, resulting in the description of a multisensory temporal binding window (for review, see Wallace and Stevenson, 2014). The bell-shaped pattern of enhanced tactile sensitivity around the predicted time of impact, as described by our Experiment 2 (Fig. 3*B*), suggests that a similar probabilistic temporal window of predicted impact may be at play when processing the consequences of a looming stimulus

onto our body, and possibly points toward common neuronal bases.

The estimated position of impact
Maximal tactile sensitivity enhancement is observed when the tactile stimulus is presented at the expected location of impact of the looming stimulus on the face compared with an impact on the opposite side of the face (Experiment 4; Fig. 4*A*). This nicely matches the spatial multisensory integration rule as initially formulated (Stein and Meredith, 1993), most probably because of the crucial importance of spatial information when predicting an impact to the body (see Spence, 2013 and; Stein and Stanford, 2008, for a discussion of the task dependence of multisensory integration processes).

Dynamic depth cues
Maximum tactile sensitivity enhancement is selectively observed for a looming stimulus while a receding stimulus hardly has any effect on tactile sensitivity (Experiment 6; Fig. 4*C*). This effect is similar to what is observed for orienting biases due to looming stimuli (Maier et al., 2004), except for the major difference that we probe tactile sensitivity after the looming visual stimulus has disappeared. While both size and depth cues most probably contribute to the modulation of tactile sensitivity on the face, we propose that the movement vector cue (away from or toward the subject) is actually the dominant cue affecting tactile detection. Indeed, the spatial, temporal, and dynamic predictive cues are fully accounted for by the trajectory and speed of the looming visual stimuli. This is confirmed by the fact that slower looming stimuli result in a delayed predicted time of impact on the face, and hence a delayed time at which tactile sensitivity is maximally enhanced (Experiment 3; Fig. 3*C*).

Impact prediction and multisensory integration
Multisensory integration and causal inference
Multisensory integration is a neuronal process by which the response of a neuron in spikes per second to two sensory stimuli of different modalities (say visual and tactile), presented simultaneously, is different from the sum of the spikes per second produced by this same neuron in response to each sensory stimulus presented independently (Avillac et al., 2007). Multisensory integration is maximized when the two sensory stimuli are presented at the same location (spatial congruence) and at the same time (temporal congruence) and are low-energy stimuli (inverse effectiveness; Stein and Meredith, 1993), though recent evidence indicates that these factors are highly interdependent (Carriere et al., 2008; Royal et al., 2009; Ghose and Wallace, 2014; for review, see Wallace and Stevenson, 2014) and task dependent (Doehrmann and Naumer, 2008; Spence, 2013; van Atteveldt et al., 2014). This leads to the notion of causal inference: a visual and an auditory signal originating at the same spatial location at the same time share a unique underlying cause (Körding et al., 2007; Shams and Beierholm, 2010; Parise et al., 2012).

Baseline multisensory enhancement
The mere presence of a looming visual stimulus around tactile stimulation enhances tactile sensitivity, including when the tactile stimulus is presented during the looming phase (Experiments 1–3) or when the looming stimulus predicts an impact away from the tactile stimulation location (Experiments 4 and 5). This baseline effect could be due to an alerting effect of the visual stimulus, though it needs to be noted that this alerting effect is present only for looming stimuli, as receding stimuli do not induce an increase in tactile sensitivity (Experiment 6). This nonspecific enhancement of tactile sensitivity most probably builds on the classical multisensory integration mechanisms described above.

Impact prediction
On top of a baseline multisensory enhancement, tactile sensitivity is further enhanced by the predictive components of the heteromodal visual stimulus. This situation is encountered in everyday life. For example, anticipating the impact of an obstacle onto the body is of vital importance. Because this process involves crossmodal influences, we propose that the cortical regions responsible for this multisensory impact prediction highly overlap with the multisensory convergence and integration functional network. Very early on, Hyvärinen and Poranen (1974) (cited in Brozzoli et al., 2012) described the visual response of parietal neurons "as an anticipatory activation" that appears before the neuron's tactile receptive field is touched. The ventral intraparietal area (VIP) is an ideal candidate for impact prediction. Indeed, its neurons integrate vestibular proprioceptive self-motions and visual motion cues to encode relative self-motion with respect to the environment (Bremmer et al., 1997, 1999, 2000, 2002a, b; Duhamel et al., 1997). This region encodes both large field visual movements mimicking the consequences of the displacement of a subject within its environment (Bremmer et al., 1999, 2000, 2002a, b) and the movement of visual objects within the near peripersonal space (Bremmer et al., 1997, 2013). Importantly, VIP neurons respond to both visual and tactile stimuli (Duhamel et al., 1998; Guipponi et al., 2013) and perform nonlinear sub-, super-, or additive multisensory integration operations (Avillac et al., 2004, 2007). Most interestingly, this cortical region has been proposed to play a key role in the definition of a defense peripersonal space.

Impact prediction and peripersonal space
Our observations indicate that, quite surprisingly, a visual stimulus intruding into peripersonal space close to one's cheek has a higher impact prediction effect on our cheek than a visual stimulus predicting an impact to the other cheek. This enhancement is smaller than that observed for spatially congruent looming stimuli, but this difference does not reach significance at the corrected level. This suggests the existence of a security margin around the face, looming stimuli approaching too close to the face alerting our nervous system of a potentially harmful impact to the body. Our observations parallel a recent study by Canzoneri et al. (2012), which demonstrates that tactile processing on the hand is speeded by the presence of a looming sound, predicting an impact on the hand or within a well defined distance from the hand. A parietal–prefrontal cortical network composed of the VIP and premotor area F4 is suggested to play a crucial role in the definition of a defense peripersonal space. The neurons of both these regions have bimodal visuotactile receptive fields representing close peripersonal space and the corresponding skin surface (Gentilucci et al., 1988; Rizzolatti et al., 1988; Colby et al., 1993; Graziano et al., 1994; Gross and Graziano, 1995; Fogassi et al., 1996; Duhamel et al., 1998). The electrical microstimulation of both regions induces a behavioral defense repertoire of whole-body movements, suggesting their involvement in the coding of a defense peripersonal space (Graziano et al., 2002; Cooke and Graziano, 2004; Graziano and Cooke, 2006). We predict that this cortical network subserving a defense peripersonal space plays a key role in the prediction of an impact onto the body. Preliminary nonhuman primate functional-imaging data from our research group corroborate this prediction (Cléry et al., 2014).

Predictive coding and multisensory integration

Dynamic visual stimuli are not necessarily predictive of impact (e.g., a mosquito approaching our face for a blood dinner), but can be coincident with tactile stimulation (e.g., a mosquito moving on one's arm). The Bayesian framework has proven extremely successful in accounting for the behavioral (Fetsch et al., 2010) and single-cell recording (Gu et al., 2008) manifestations of multisensory integration. In addition, divisive normalization operated by local neuronal populations has been shown to account for inverse effectiveness and spatial congruence rules (Ohshiro et al., 2011; Fetsch et al., 2013) as well as for flexible adaptation to cue reliability (Morgan et al., 2008). On the other hand, the general predictive coding framework relying on internal generative models (or priors) constructed through experience (Friston and Kiebel, 2009; Friston, 2010) has been successfully applied to speech comprehension, in which visual cues are predictive of auditory speech information (van Wassenhove et al., 2005; van Wassenhove, 2013; Altieri, 2014; Lee and Noppeney, 2014). So how does a given functional multisensory integration network perform either coincident or predictive context- or task-dependent computations? Context-dependent time-varying priors could account for the reported behavioral effects. Alternatively, phase resetting of ongoing neuronal oscillations by a given sensory input (looming visual), predictively preparing neurons to respond to a second sensory input (tactile) with a particular timing relationship with the first sensory input, has been proposed as a general model for predictive neuronal processing (Lakatos et al., 2005, 2007; Kayser et al., 2008; van Atteveldt et al., 2014). This mechanism could be at the origin of enhanced tactile sensitivity during impact prediction. The local and global neuronal mechanisms by which the speed, distance, and trajectory characteristics of a looming stimulus with respect to the subject are integrated to estimate time to impact, the specific cortical regions that process this information, and how it is used for phase resetting remain to be unveiled.

References

Altieri N (2014) Multisensory integration, learning, and the predictive coding hypothesis. Front Psychol 5:257. CrossRef Medline

Avillac M, Olivier E, Denève S, Ben Hamed S, Duhamel J-R (2004) Multisensory integration in multiple reference frames in the posterior parietal cortex. Cogn Process 5:159–166. CrossRef

Avillac M, Ben Hamed S, Duhamel JR (2007) Multisensory integration in the ventral intraparietal area of the macaque monkey. J Neurosci 27:1922–1932. CrossRef Medline

Ball W, Tronick E (1971) Infant responses to impending collision: optical and real. Science 171:818–820. CrossRef Medline

Bremmer F, Duhamel J-R, Ben Hamed S, Graf W (1997) The representation of movement in near extra-personal space in the macaque ventral intraparietal area (VIP). In: Parietal lobe contributions to orientation in 3D space, Vol 25, Experimental brain research series (Thier P, Karnath H-O, eds), pp 619–630. Heidelberg: Springer.

Bremmer F, Graf W, Ben Hamed S, Duhamel JR (1999) Eye position encoding in the macaque ventral intraparietal area (VIP). Neuroreport 10:873–878. CrossRef Medline

Bremmer F, Duhamel JR, Ben Hamed S, Graf W (2000) Stages of self-motion processing in primate posterior parietal cortex. Int Rev Neurobiol 44:173–198. CrossRef Medline

Bremmer F, Duhamel JR, Ben Hamed S, Graf W (2002a) Heading encoding in the macaque ventral intraparietal area (VIP). Eur J Neurosci 16:1554–1568. CrossRef Medline

Bremmer F, Klam F, Duhamel JR, Ben Hamed S, Graf W (2002b) Visual-vestibular interactive responses in the macaque ventral intraparietal area (VIP). Eur J Neurosci 16:1569–1586. CrossRef Medline

Bremmer F, Schlack A, Kaminiarz A, Hoffmann KP (2013) Encoding of movement in near extrapersonal space in primate area VIP. Front Behav Neurosci 7:8. CrossRef Medline

Brozzoli C, Makin TR, Cardinali L, Holmes NP, Farnè A (2012) Peripersonal space: a multisensory interface for body–object interactions. In: The neural bases of multisensory processes, Frontiers in neuroscience (Murray MM, Wallace MT, eds). Boca Raton, FL: CRC.

Canzoneri E, Magosso E, Serino A (2012) Dynamic sounds capture the boundaries of peripersonal space representation in humans. PLoS One 7:e44306. CrossRef Medline

Cappe C, Thut G, Romei V, Murray MM (2009) Selective integration of auditory-visual looming cues by humans. Neuropsychologia 47:1045–1052. CrossRef Medline

Cappe C, Thelen A, Romei V, Thut G, Murray MM (2012) Looming signals reveal synergistic principles of multisensory integration. J Neurosci 32:1171–1182. CrossRef Medline

Carriere BN, Royal DW, Wallace MT (2008) Spatial heterogeneity of cortical receptive fields and its impact on multisensory interactions. J Neurophysiol 99:2357–2368. CrossRef Medline

Cléry J, Guipponi O, Wardak C, Ben Hamed S (2014) Neuronal bases of peripersonal and extrapersonal spaces, their plasticity and their dynamics: knowns and unknowns. Neuropsychologia.pii:S0028-3932(14)00382-0. CrossRef Medline

Colby CL, Duhamel JR, Goldberg ME (1993) Ventral intraparietal area of the macaque: anatomic location and visual response properties. J Neurophysiol 69:902–914. Medline

Cooke DF, Graziano MS (2004) Sensorimotor integration in the precentral gyrus: polysensory neurons and defensive movements. J Neurophysiol 91:1648–1660. CrossRef Medline

Doehrmann O, Naumer MJ (2008) Semantics and the multisensory brain: how meaning modulates processes of audio-visual integration. Brain Res 1242:136–150. CrossRef Medline

Duhamel JR, Bremmer F, Ben Hamed S, Graf W (1997) Spatial invariance of visual receptive fields in parietal cortex neurons. Nature 389:845–848. CrossRef Medline

Duhamel JR, Colby CL, Goldberg ME (1998) Ventral intraparietal area of the macaque: congruent visual and somatic response properties. J Neurophysiol 79:126–136. Medline

Fetsch CR, Deangelis GC, Angelaki DE (2010) Visual–vestibular cue integration for heading perception: applications of optimal cue integration theory. Eur J Neurosci 31:1721–1729. CrossRef Medline

Fetsch CR, DeAngelis GC, Angelaki DE (2013) Bridging the gap between theories of sensory cue integration and the physiology of multisensory neurons. Nat Rev Neurosci 14:429–442. CrossRef Medline

Fogassi L, Gallese V, Fadiga L, Luppino G, Matelli M, Rizzolatti G (1996) Coding of peripersonal space in inferior premotor cortex (area F4). J Neurophysiol 76:141–157. Medline

Friston K (2010) The free-energy principle: a unified brain theory? Nat Rev Neurosci 11:127–138. CrossRef Medline

Friston K, Kiebel S (2009) Predictive coding under the free-energy principle. Philos Trans R Soc Lond B Biol Sci 364:1211–1221. CrossRef Medline

Gentilucci M, Fogassi L, Luppino G, Matelli M, Camarda R, Rizzolatti G (1988) Functional organization of inferior area 6 in the macaque monkey. I. Somatotopy and the control of proximal movements. Exp Brain Res 71:475–490. CrossRef Medline

Ghose D, Wallace MT (2014) Heterogeneity in the spatial receptive field architecture of multisensory neurons of the superior colliculus and its effects on multisensory integration. Neuroscience 256:147–162. CrossRef Medline

Graziano MS, Cooke DF (2006) Parieto-frontal interactions, personal space, and defensive behavior. Neuropsychologia 44:2621–2635. CrossRef Medline

Graziano MS, Yap GS, Gross CG (1994) Coding of visual space by premotor neurons. Science 266:1054–1057. CrossRef Medline

Graziano MS, Taylor CS, Moore T (2002) Complex movements evoked by microstimulation of precentral cortex. Neuron 34:841–851. CrossRef Medline

Gross CG, Graziano MSA (1995) Review: multiple representations of space in the brain. Neuroscientist 1:43–50. CrossRef

Gu Y, Angelaki DE, Deangelis GC (2008) Neural correlates of multisensory cue integration in macaque MSTd. Nat Neurosci 11:1201–1210. CrossRef Medline

Guipponi O, Wardak C, Ibarrola D, Comte JC, Sappey-Marinier D, Pinède S, Ben Hamed S (2013) Multimodal convergence within the intraparietal sulcus of the macaque monkey. J Neurosci 33:4128–4139. CrossRef Medline

Guipponi O, Odouard S, Pinède S, Wardak C, Ben Hamed S (2014) fMRI

cortical correlates of spontaneous eye blinks in the nonhuman primate. Cereb Cortex. Advance online publication. doi:10.1093/cercor/bhu038. CrossRef Medline

Hyvärinen J, Poranen A (1974) Function of the parietal associative area 7 as revealed from cellular discharges in alert monkeys. Brain 97:673–692. CrossRef Medline

Kandula M, Hofman D, Chris Dijkerman H (2014) Visuo-tactile interactions are dependent on the predictive value of the visual stimulus. Neuropsychologia Available at: http://www.sciencedirect.com/science/article/pii/S002839321400462X. Accessed December 10, 2014. doi:10.1016/j.neuropsychologia.2014.12.008.

Kayser C, Petkov CI, Logothetis NK (2008) Visual modulation of neurons in auditory cortex. Cereb Cortex 18:1560–1574. CrossRef Medline

Körding KP, Beierholm U, Ma WJ, Quartz S, Tenenbaum JB, Shams L (2007) Causal inference in multisensory perception. PLoS One 2:e943. CrossRef Medline

Lakatos P, Shah AS, Knuth KH, Ulbert I, Karmos G, Schroeder CE (2005) An oscillatory hierarchy controlling neuronal excitability and stimulus processing in the auditory cortex. J Neurophysiol 94:1904–1911. CrossRef Medline

Lakatos P, Chen CM, O'Connell MN, Mills A, Schroeder CE (2007) Neuronal oscillations and multisensory interaction in primary auditory cortex. Neuron 53:279–292. CrossRef Medline

Lee H, Noppeney U (2014) Temporal prediction errors in visual and auditory cortices. Curr Biol 24:R309–R310. CrossRef Medline

Leo F, Romei V, Freeman E, Ladavas E, Driver J (2011) Looming sounds enhance orientation sensitivity for visual stimuli on the same side as such sounds. Exp Brain Res 213:193–201. CrossRef Medline

Maier JX, Ghazanfar AA (2007) Looming biases in monkey auditory cortex. J Neurosci 27:4093–4100. CrossRef Medline

Maier JX, Neuhoff JG, Logothetis NK, Ghazanfar AA (2004) Multisensory integration of looming signals by rhesus monkeys. Neuron 43:177–181. CrossRef Medline

Maier JX, Chandrasekaran C, Ghazanfar AA (2008) Integration of bimodal looming signals through neuronal coherence in the temporal lobe. Curr Biol 18:963–968. CrossRef Medline

McDonald JJ, Teder-Sälejärvi WA, Hillyard SA (2000) Involuntary orienting to sound improves visual perception. Nature 407:906–908. CrossRef Medline

Morgan ML, Deangelis GC, Angelaki DE (2008) Multisensory integration in macaque visual cortex depends on cue reliability. Neuron 59:662–673. CrossRef Medline

Ohshiro T, Angelaki DE, DeAngelis GC (2011) A normalization model of multisensory integration. Nat Neurosci 14:775–782. CrossRef Medline

Parise CV, Spence C, Ernst MO (2012) When correlation implies causation in multisensory integration. Curr Biol 22:46–49. CrossRef Medline

Rizzolatti G, Camarda R, Fogassi L, Gentilucci M, Luppino G, Matelli M (1988) Functional organization of inferior area 6 in the macaque monkey. II. Area F5 and the control of distal movements. Exp Brain Res 71:491–507. CrossRef Medline

Royal DW, Carriere BN, Wallace MT (2009) Spatiotemporal architecture of cortical receptive fields and its impact on multisensory interactions. Exp Brain Res 198:127–136. CrossRef Medline

Schiff W, Caviness JA, Gibson JJ (1962) Persistent fear responses in rhesus monkeys to the optical stimulus of "looming." Science 136:982–983. CrossRef Medline

Shams L, Beierholm UR (2010) Causal inference in perception. Trends Cogn Sci 14:425–432. CrossRef Medline

Spence C (2013) Just how important is spatial coincidence to multisensory integration? Evaluating the spatial rule. Ann N Y Acad Sci 1296:31–49. CrossRef Medline

Stein BE, Meredith MA (1993) The merging of the senses. Cambridge, MA: MIT.

Stein BE, Stanford TR (2008) Multisensory integration: current issues from the perspective of the single neuron. Nat Rev Neurosci 9:255–266. CrossRef Medline

Sugita Y, Suzuki Y (2003) Audiovisual perception: implicit estimation of sound-arrival time. Nature 421:911. CrossRef Medline

Tyll S, Bonath B, Schoenfeld MA, Heinze HJ, Ohl FW, Noesselt T (2013) Neural basis of multisensory looming signals. Neuroimage 65:13–22. CrossRef Medline

Vagnoni E, Lourenco SF, Longo MR (2012) Threat modulates perception of looming visual stimuli. Curr Biol 22:R826–R827. CrossRef Medline

van Atteveldt N, Murray MM, Thut G, Schroeder CE (2014) Multisensory integration: flexible use of general operations. Neuron 81:1240–1253. CrossRef Medline

van Wassenhove V (2013) Speech through ears and eyes: interfacing the senses with the supramodal brain. Front Psychol 4:388. CrossRef Medline

van Wassenhove V, Grant KW, Poeppel D (2005) Visual speech speeds up the neural processing of auditory speech. Proc Natl Acad Sci U S A 102:1181–1186. CrossRef Medline

Walker-Andrews AS, Lennon EM (1985) Auditory-visual perception of changing distance by human infants. Child Dev 56:544–548. CrossRef Medline

Wallace MT, Stevenson RA (2014) The construct of the multisensory temporal binding window and its dysregulation in developmental disabilities. Neuropsychologia 64C:105–123. CrossRef Medline

Chapter 2 :

The prediction of impact of a looming stimulus onto the body is subserved by multisensory integration mechanisms

Submitted in "*The Journal of Neuroscience*", March 6th 2017, JN-RM-0610-17.

The prediction of impact of a looming stimulus onto the body is subserved by multisensory integration mechanisms

Justine Cléry, Olivier Guipponi, Soline Odouard, Serge Pinède, Claire Wardak and Suliann Ben Hamed

Institut des Sciences Cognitives Marc Jeannerod, UMR5229, CNRS-Université Claude Bernard Lyon I*, 67 Boulevard Pinel, 69675 Bron, France*

Corresponding author: Suliann Ben Hamed, benhamed@isc.cnrs.fr

Keywords: visual, tactile, looming stimuli, prediction, fMRI, macaque monkey, multisensory integration.

Running title: Neural bases of prediction of impact to the body.

Abstract:

In the jungle, survival is highly correlated with the ability to detect and distinguish between an approaching predator and a putative prey. From an ecological perspective, a predator rapidly approaching its prey is a stronger cue for flight than a slowly moving predator. In the present study, we use functional magnetic resonance imaging (fMRI) in the non-human primate, to investigate the neural bases of the prediction of an impact to the body by a looming stimulus, i.e. the neural bases of the interaction between a dynamic visual stimulus approaching the body and its expected consequences onto an independent sensory modality, namely, touch. We identify a core cortical network of occipital, parietal, premotor and prefrontal areas maximally activated by tactile stimulations presented at the predicted time and location of impact of the looming stimulus on the face, as compared to the activations observed for spatially or temporally incongruent tactile and dynamic visual cues. These activations reflect both an active integration of visual and tactile information and of spatial and temporal prediction information. The identified cortical network coincides with a well described multisensory visuo-tactile convergence and integration network suggested to play a key role in the definition of peripersonal space. These observations are discussed in the context of multisensory integration and spatial, temporal prediction and causal Bayesian inference.

Significance statement:

Looming stimuli have a particular ecological relevance as they are expected to come into contact with the body, evoking touch or pain sensations and possibly triggering an approach or escape behaviour depending on their identity. Here, we identify the non-human primate functional network that is maximally activated by tactile stimulations presented at the predicted time and location of impact of the looming stimulus. Our findings suggest that the integration of spatial and temporal predictive cues possibly rely on the same neural mechanisms that are involved in multisensory integration.

INTRODUCTION

In the jungle, survival is highly correlated with the ability to detect and distinguish between a predator and a putative prey. From an ecological perspective, a predator rapidly approaching its prey is a stronger cue for flight than a slowly moving predator. Experimentally, such a situation can be modeled as a looming stimulus moving towards the subject of the experiment. In such a context, looming stimuli have been described to elicit stereotyped defensive behavior both in monkeys (Schiff et al., 1962) and in human infants (Ball and Tronick, 1971). These observations suggest that subjects predict the possible consequences of these stimuli onto their body and anticipate these consequences by producing an escape motor repertoire. These predictive mechanisms are expected to be hetero-modal by essence: the sensory consequences of looming stimuli, be they visual or auditory, are mostly predicted onto the tactile modality, as an impact to the body. And indeed, recent studies show that looming stimuli enhance tactile processing at the predicted time of impact and at the expected location of impact, both as measured by enhanced tactile sensitivity (Cléry et al., 2015a) and shorter reaction times (Canzoneri et al., 2012; Kandula et al., 2015), including when specifically probing nociceptive perception (De Paepe et al., 2016). Likewise, looming auditory-visual multisensory stimuli increase behavioral orienting indices (Maier et al., 2004; Cappe et al., 2009c). Threatening visual looming stimuli, such as spiders as compared to butterflies, further shortened the reaction times to tactile probes presented on the skin (de Haan et al., 2016). These several lines of behavioral evidence strongly suggest that the predictive mechanisms at play in estimating the consequences of looming stimuli on the skin pertain to more general processes involved in the defense of body integrity.

However, the neurophysiological mechanisms by which the dynamic information provided by one sensory modality predictively enhances the processing of another sensory modality remain

unknown. A parsimonious hypothesis is that these processes involve cortical regions receiving neuronal information from both sensory modalities and optimally combining these multisensory signals. In the specific context of visual looming stimuli predicting an impact to the face, this parsimonious view predicts the contribution of a well characterized visuo-tactile convergence network of post-arcuate premotor (specifically premotor zone PMz, a subsector of area F4), intraparietal (specifically ventral intraparietal area VIP) and striate and extrastriate visual areas (Guipponi et al., 2013, 2015). Consolidating this parsimonious prediction, the parietal and the premotor components of this functional network have been involved in the representation of a defense peripersonal space (PPS -see for reviews Graziano and Cooke, 2006; Cléry et al., 2015b) as well as in approaching behavior (Rizzolatti et al., 1997).

Here, we used functional magnetic resonance imaging (fMRI) in the non-human primate to test this hypothesis and to specifically identify the neural bases of the prediction of an impact of a looming visual stimulus onto the body. While the monkeys were maintaining their gaze onto a central point, we presented them with a visual looming stimulus coming towards the face or/and a tactile stimulation (airpuff) on the face. These visual and tactile stimuli were either presented in isolation in independent blocks or played together in the same blocks. When played together, we manipulated the spatial and temporal relationships between the visual and the tactile stimulations so as to isolate the specific contribution of either temporal prediction or spatial prediction cues on the cortical activations. Our observations confirm the parsimonious hypothesis outlined above, that impact prediction (i.e. the anticipation of touch) onto the face activates a core post-arcuate, intraparietal striate and extrastriate cortical network previously associated with multisensory convergence and multisensory integration. Importantly, we show that the activity of this network is highly dependent upon the spatial and temporal predictive information held by the looming visual stimulus. These observations are discussed in the context of multisensory integration and spatial,

temporal prediction and causal Bayesian inference.

MATERIALS AND METHODS

All procedures were in compliance with the guidelines of the European Community on animal care (European Community Council, Directive 2010/63/UE). All the protocols used in this experiment were approved by the local animal care committee (agreement # C2EA42-12-10-0401-002). The animals' welfare and the steps taken to reduce suffering were in accordance with the recommendations of the Weatherall report, "The use of non-human primates in research".

Subjects and Materials

Two rhesus monkeys (female M1, male M2, 10-8 years old, 6-7 kg) participated in the study. The animals were implanted with a plastic magnetic resonance imaging (MRI) compatible headset covered by dental acrylic. The anesthesia during surgery was induced by Zoletil (Tiletamine-Zolazepam, Virbac, 5mg/kg) and followed by Isoflurane (Belamont, 1-2%). Postsurgery analgesia was ensured thanks to Temgesic (buprenorphine, 0.3mg/ml, 0.01 mg/kg). During recovery, proper analgesic and antibiotic coverage was provided. The surgical procedures conformed to European and National Institutes of Health guidelines for the care and use of laboratory animals.

During the scanning sessions, monkeys sat in a sphinx position in a plastic monkey chair positioned within a horizontal magnet (1.5-T MR scanner Sonata; Siemens, Erlangen, Germany) facing a translucent screen placed 90cm from the eyes. Their head was restrained and equipped with MRI-compatible headphones customized for monkeys (MR Confon GmbH, Magdeburg, Germany). A radial receive-only surface coil (10 cm diameter) was positioned above the head. Eye position was monitored at 120 Hz during scanning using a pupil-corneal reflection tracking system (Iscan®, Cambridge, MA). Animals were rewarded with liquid dispensed by a computer-controlled reward delivery system (Crist®) thanks to a plastic tube coming to their mouth. The task, all the

behavioral parameters, and the sensory stimulations were monitored by two computers running with Matlab® and Presentation® (Neurobehavioural systems, Albany, Canada). Visual stimulations were projected onto the screen with a Canon XEED SX60 projector. Tactile stimulations were delivered through Teflon tubing and 2 articulated plastic arms connected to distant air pressure electro-valves. Monkeys were trained in a mock scan environment approaching to the best the actual MRI scanner setup.

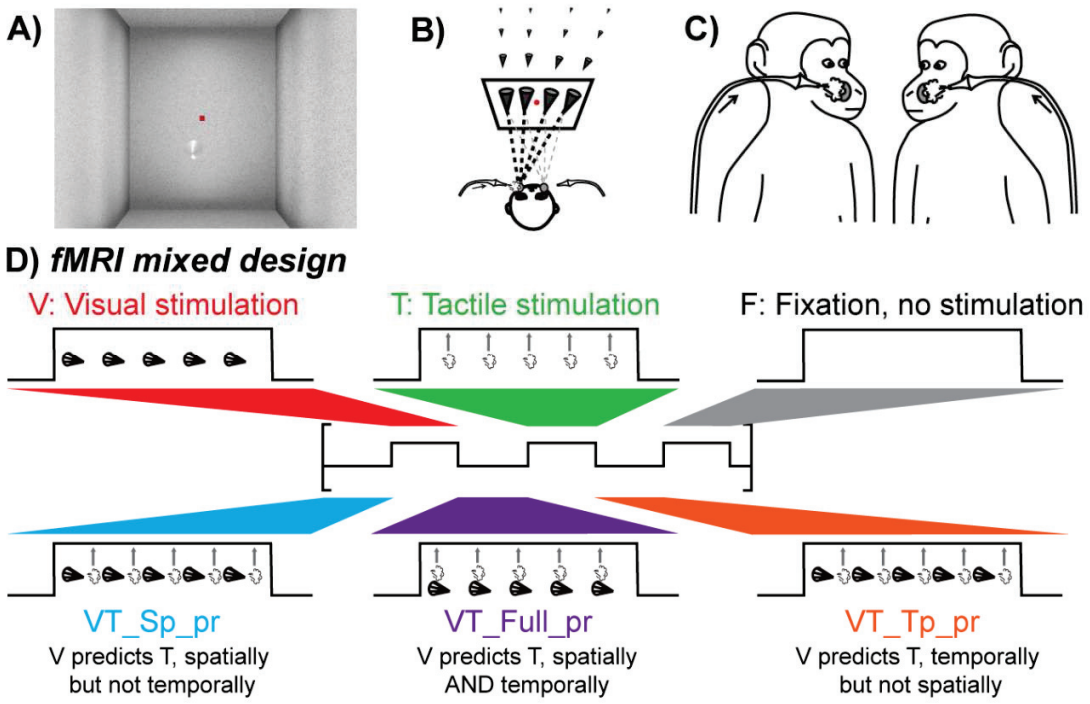

Figure 1: **Methods.** A) Visual stimuli consisted in a video sequence of a cone placed in a 3D environment and looming towards the animal's face. The red dot corresponds to the spatial location the monkey was required to fixate in order to be rewarded. B) The trajectory of the looming cone could start from four different points in the back of the visual scene, two ipsilateral and two contralateral to the predicted impact location with respect to the monkey's face. C) Tactile stimulations were directed to the center of the face thanks to airpuffs directed to the left or right cheek, coinciding with the predicted impact of the looming visual stimulus on the monkey's face. D) We used a mixed fMRI design. Each run was thus composed of five conditions organized in blocks (15 pulses per condition), during which visual (looming cone)

and tactile (50 ms airpuff) events were organized as follows: a unimodal visual stimulation condition (V), a unimodal tactile stimulation condition (T), a bimodal condition in which the visual stimulus is spatially and temporally predictive of the tactile stimulus (VT_Full_pr), a bimodal condition in which the visual stimulus is spatially but not temporally predictive of the tactile stimulus (VT_Sp_pr) and a bimodal condition in which the visual stimulus is temporally but not spatially predictive of the tactile stimulus (VT_Tp_pr).

Task and Stimuli

The animals were trained to maintain fixation on a red central spot (0.24°x0.24°) while stimulations (visual and/or tactile) were delivered. The monkeys were rewarded for staying within a 2°x2° tolerance window centered on the fixation spot. The reward delivery was scheduled to encourage long fixation without breaks (i.e. the interval between successive deliveries was decreased and their amount was increased, up to a fixed limit, as long as the eyes did not leave the window). The fixation spot was placed in the center of a background representing a 3D environment with visual depth cues and was present all throughout the runs (Figure 1A). The 3D environment and different cone trajectories, at eye level, were all constructed with the Blender software (http://www.blender.org/). Visual and/or tactile stimuli were presented to the monkeys as follows.

Visual stimuli consisted in a low contrast dynamic 3D cone-shaped stimulus, pointing towards the monkey, moving within this 3D environment, originating away from and rapidly approaching the monkey (Figure 1A). The trajectory of this looming stimulus was adjusted so as to induce the percept of a potential impact on the monkey's face at two possible locations, on the left or right cheeks, close to the snout. For each impact location, the cone trajectory could originate from eight possible locations around the fixation point: four in the left hemifield and four in the right hemifield at +/- 0.32°, +/- 1.27°, +/- 3.16° and +/- 4.11°. As a result, half of the cone trajectories crossed the mid-sagittal plane and induced a predicted impact to the face on the

contralateral cheek with respect to the spatial origin of the cone (Figure 1B).

Tactile stimuli consisted in air puffs delivered at two possible locations on the monkey's face, on the left or right cheeks, at the two possible impact locations predicted by the cone trajectory, close to the nose and the mouth (Figure 1C). These puffs were delivered, with a pressure intensity set at 0.3 bars, thanks to tubes the extremities of which were at 2-4 mm from each cheek of the monkeys. This barely perceivable airpuff intensity was chosen so as to maximize the multisensory integration processes expected to take place when combined with a visual stimulus. Indeed, at the single neuron level, multisensory integration processes have been shown to be inversely proportional to the strength of each unimodal stimulus, the lower their intensity, the higher the deviation of the neuron's multisensory response from their unimodal response (Stein and Meredith, 1993; Avillac et al., 2004, 2007). Airpuff duration was set to 50ms (as measured with a silicon pressure on chip signal conditioned sensor, MPX5700 Series, Freescale™) and successive airpuffs were separated by a random time interval ranging from 1500 to 2800ms.

The visual and tactile sensory modalities were tested in the same runs, either in separate blocks (unimodal stimulations) or in same blocks (bimodal stimulations) (Figure 1D). In the visual unimodal blocks, the movement of the visual cone had a duration of 550 ms and two looming stimuli were separated by a random timing ranging from 1300 to 2800 ms. In the tactile unimodal blocks, airpuff duration was set to 50 ms and successive airpuffs were separated by a random time interval ranging from 1300 to 2800 ms. For the bimodal conditions, we defined three different types of stimulation blocks: 1) *Temporally simultaneous and spatially congruent bimodal blocks* (VT spatially predictive, VT_Sp_pr), in which the tactile stimulus was presented while the visual stimulus was approaching the face of the monkey (mid-course of the visual stimulus, airpuff latency as measured with the pressure sensor), at the location at which the visual stimulus was expected to impact the face; 2) *Temporally and spatially predictive bimodal blocks* (VT fully predictive,

VT_Full_pr), in which the tactile stimulus was presented at the moment when the visual stimulus was expected to impact the face (airpuff latency as measured with the pressure sensor), at the spatial location of the expected impact; 3) *Temporally predictive but spatially incongruent bimodal blocks* (VT temporally predictive, VT_Tp_pr), in which the tactile stimulus was presented at the moment when the visual stimulus was expected to impact the face, but at a location symmetrical to where the visual stimulus was expected to impact the face. In all these bimodal blocks, visual stimuli were presented with the same temporal dynamics as in the unimodal visual blocks. It is crucial to note that the visual and tactile stimuli were designed to have a low salience so as to maximize the multisensory integration, as discussed above (Stein and Meredith, 1993).

Functional time series (runs) were organized as follows: 15-volume blocks of unimodal and bimodal stimulation blocks were followed by a 15-volume block of pure fixation baseline (Figure 1D); this sequence was played twice, resulting in a 180-volume run. The 6 types of blocks were presented in 10 counterbalanced possible orders.

Scanning

Before each scanning session, a contrast agent, composed of monocrystalline iron oxide nanoparticles (Feraheme®, Vanduffel et al., 2001), was injected into the animal's femoral/saphenous vein (4-10 mg/kg). Brain activations produce increased BOLD signal changes. In contrast, when using MION contrast agents, brain activations produce decreased signal changes signal (Kolster et al., 2014). For the sake of clarity, the polarity of the contrast agent MR signal changes was inverted. We acquired gradient-echo echoplanar (EPI) images covering the whole brain (1.5 T; repetition time (TR) 2.08s; echo time (TE) 27 ms; 32 sagittal slices; 2x2x2 mm voxels). A total of 135 (132) runs was acquired for M1 (/M2).

Analysis

A total of 98 runs for monkey 1 and 92 runs for monkey 2 was selected based on the quality of the monkey's fixation throughout each run (>85% within the eye fixation tolerance window). Runs were analyzed using SPM8 (Wellcome Department of Cognitive Neurology, London, United Kingdom). For spatial preprocessing, functional volumes were first realigned and rigidly coregistered with the anatomy of each individual monkey (T1-weighted MPRAGE 3D 0.6x0.6x0.6 mm or 0.5x0.5x0.5 mm voxel acquired at 1.5T) in stereotactic space. The JIP program (Mandeville et al., 2011) was used to perform a non-rigid coregistration (warping) of mean functional image onto the individual anatomies.

Fixed effect individual analyses were performed for each monkey, with a level of significance set at $P < 0.05$ corrected for multiple comparisons (FWE, *t*-scores>4.89) and $P < 0.001$ (uncorrected level, *t*-scores>3.1). In all analyses, realignment parameters, as well as eye movement traces, were included as covariates of no interest to remove eye movement and brain motion artifacts. When coordinates are provided, they are expressed with respect to the anterior commissure. Results are displayed on coronal sections or flattened maps obtained with Caret (van Essen et al., 2001; http://www.nitrc.org/projects/caret/).

Assigning the activations to a specific cortical area was performed on each individual monkey brain using the monkey brain atlases made available on http://scalablebrainatlas.incf.org. These atlases allow mapping specific anatomical coronal sections with several cytoarchitetonic parcellation studies. We used the Lewis and Van Essen (2000) and the Paxinos Rhesus Monkey (2000) parcellations. For some areas, we additionally referred to more recent works (e.g. Petrides et al., 2005; or Belmalih et al., 2009). We further checked that the group activations faithfully reflected, in their localization and their assignment, the individual activations identified in each

monkey.

Events related analysis. For each condition, we extracted visual times (in mid-course of the visual stimulus) and tactile times of presentation. For baseline referencing, we arbitrarily defined fixation events within each unimodal and each bimodal condition, assigned at intermediate timings between two successive stimuli sequences. For bimodal conditions, we performed two types of analyses, one based on the timings of the visual stimuli and one based on the timings of the tactile stimuli. In figure 3, color contours correspond to the activations obtained relative to the looming visual stimuli time onset and black contours correspond to the activations obtained relative to tactile stimuli time onset (*t*-scores >3.1). In all of the three bimodal conditions, the spatial extent of the observed functional activations is only marginally affected by whether the analyses are performed relative to the visual or to the tactile stimuli. Thus, unless stated otherwise, the communication of the results and their discussion refer to the analysis timed on the visual stimuli.

Regions of interest. We performed regions of interest (ROI) analyses using MarsBar toolbox (Brett et al., 2002), based on the fixed effects individual analyses results. The ROIs were defined using the activations obtained at FWE-corrected level (*t*-scores>4.8) or at uncorrected level (*t*-scores>3.1) when the activations failed to reach the corrected level with the contrast fully predictive bimodal VT condition (VT_Full_pr) versus Fixation. The percent of signal change (PSC) are extracted for each ROI for all the runs using SPM8 and the MarsBar toolbox. The significance of these PSCs across all runs was assessed using paired t-tests, in Matlab™ (The MathWorks Inc., Natick, MA, USA).

Potential covariates. In all analyses, realignment parameters, as well as eye movement traces, were included as covariates of no interest to remove eye movement and brain motion artifacts. However, some of the stimulations might have induced a specific behavioral pattern

biasing our analysis, not fully accounted for by the above regressors. For example, air-puffs to the face might have evoked facial mimics (see Guipponi et al., 2014 for an analysis of blink related activations) inducing some degree of variability in the point of impact of the air puffs. While we cannot completely rule out this possibility, our experimental set-up allows us to minimize its impact. First, monkeys worked head-restrained (to maintain the brain at the optimal position within the scanner, to minimize movement artifacts on the fMRI signal and to allow for a precise monitoring of their eye movements). As a result, the tactile stimulations to the face were stable in a given session. When drinking the liquid reward, small lip movements occurred. These movements thus correlated with reward timing. The air puffs were placed on the cheeks on each side of the monkey's nose at a location that was not affected by the lip movements. Air-puffs are often suspected to activate the auditory system. In the present study, the air-puff delivery system was placed outside the MRI scanner room and the monkeys were wearing headphones to protect their hearing from the high intensity sound produced by the scanner. By placing a microphone inside the headphones, we confirm that no air-puff triggered sound could be recorded, whether in the absence or presence of a weak MRI scanner noise (Guipponi et al., 2015). Second, monkeys were required to maintain their gaze on a small fixation point, within a tolerance window of 2°x2°. This was controlled online and was used to motivate the animal to maximize fixation rates (as fixation disruptions, such as saccades or drifts, affected the reward schedule). Eye traces were also analyzed offline for the selection of the runs to include in the analysis (good fixation for 85% of the run duration, with no major fixation interruptions).

Pupil size analysis. During the scanning sessions, pupil size (eye pupil horizontal diameter, in pixels) was recorded together with eye position signals. The variations of pupil size were analyzed as a function of block condition, in order to identify possible autonomic markers that the monkeys were interpreting differently each stimulation block, based on the predictive information

provided by each block (figure 2). Specifically, changes in pupil size in time were normalized with respect to the pupil size average of each session. The main pupil size analysis describes the average deviation of pupil size in each block condition with respect to the overall session average, per monkey.

RESULTS

Monkeys were exposed, in the same time series, to six different types of stimulation blocks, in a mixed fMRI design (Figure 1D), while required to fixate a central red point all throughout. These six conditions were: 1) pure fixation blocks; 2) visual only blocks, with looming visual stimuli evolving in a virtual 3D environment (Figure 1A), running along several possible trajectories predicting an impact to the face at two possible locations (Figure 1B); 3) tactile only blocks with tactile stimulations at two possible facial locations coinciding with the two possible endpoints of the looming visual stimuli (Figure 1C); 4-6) three possible bimodal visuo-tactile stimulations (Figure 1D) with the visual stimulus spatially and temporally predicting the tactile stimulus (VT_Full_pr), the visual stimulus predicting the tactile stimulus spatially but not temporally (VT_Sp_pr) or the visual stimulus predicting the tactile stimulus temporally but not spatially (VT_Tp_pr). In the following, we describe the behavioral and functional correlates of the spatial and temporal prediction information held by the visual looming stimulus onto the processing of the tactile stimulus.

Changes in pupil size reveal an implicit processing of predictive signals

The monkeys were required to fixate the central red spot as long as possible in order to maximize their reward schedule, irrespectively of the type of stimulation they were presented with. They thus didn't produce any overt indicator that they processed the distinct stimulation blocks. This was done on purpose so as to probe the prediction of impact of looming of visual stimuli onto tactile perception in the absence of any active cognitive task to be operated on any of the two sensory inputs, as this would necessarily have interfered with low level multisensory integrative processes. However, if the perception of tactile or the visual stimuli is influenced by their co-

occurrence (due to multisensory integration) and how they are perceived is further differentially modulated by the temporal and spatial contingencies between these two stimuli (due to spatial and temporal prediction), one can expect block structure to modulate autonomic parameters such as pupil size. Indeed, pupil diameter adjusts as a function of the overall illumination (photomotor reflex) and reflects a phasic response of LC neurons (Aston-Jones and Cohen, 2005; Koss, 1986; Samuels and Szabadi, 2008; Murphy et al., 2011; Laeng et al., 2012; Eldar et al., 2013). However, under constant illumination conditions, pupil size can also vary. An increase in pupil diameter has been associated with arousal (Bradshaw, 1967), alertness (Yoss et al., 1970) and decision making (Simpson and Hale, 1969). Pupil size changes have been shown to index behavioral and attentional performance (Gilzenrat et al., 2010, Eldar et al., 2013; Kihara et al., 2015; for review, see Laeng et al., 2012), surprise and updating (Nassar et al., 2012; O'Reilly et al., 2013), increased uncertainty in the environment, changes in uncertainty, learning (Preuschoff et al., 2011) and emotional content of the stimulation (Bradley et al., 2008). In contrast, pupil constriction has been associated with information updating (O'Reilly et al., 2013). These variations rely on two major neuromodulation systems, the noradrenergic locus coeruleus system (Rajkowski et al., 1994, Aston-Jones and Cohen, 2005; Jepma and Nieuwenhuis, 2010; Bouret and Sara, 2005; Yu and Dayan, 2005; Sara, 2009) and the cholinergic basal forebrain system (Yu, 2012). Accordingly, the analysis of how pupil size varied as a function of the different stimulation blocks is expected to provide an implicit indicator of a selective processing of predictive sensory stimulations as compared to non-predictive sensory stimulations (Figure 2).

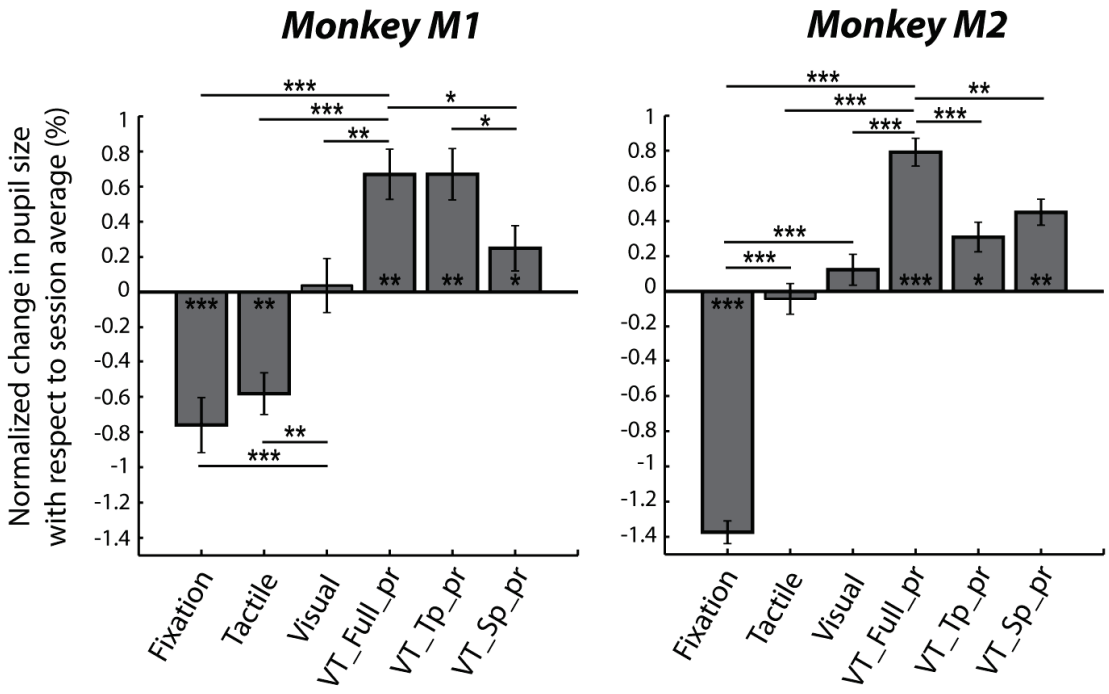

Figure 2. **Pupil size changes as a function of the predictive structure of the stimulation blocks.** Average normalized changes in pupil size with respect to session average (in %), for each of monkeys M1 and M2, for the unimodal visual stimulation condition (Visual), the unimodal tactile stimulation condition (Tactile), the bimodal condition in which the visual stimulus is spatially and temporally predictive of the tactile stimulus (VT_Full_pr), the bimodal condition in which the visual stimulus is spatially but not temporally predictive of the tactile stimulus (VT_Sp_pr) and the bimodal condition in which the visual stimulus is temporally but not spatially predictive of the tactile stimulus (VT_Tp_pr). The statistical significance of paired t-tests is represented as follows: *, P<0.05; **, P<0.01; ***, P<0.001.

Specifically, in both monkeys, pupil size was consistently smaller on fixation blocks than the corresponding average pupil size in each functional run (paired t-test, $p<0.001$, for both monkeys). Pupil size was also larger on unimodal visual blocks than the corresponding average pupil size observed on fixation blocks (paired t-test, $p<0.001$, for both monkeys). This result is the opposite from what could have been predicted from the photomotor reflex: the additional presence

of the looming visual stimuli is expected to induce, if anything, a phasic reduction in pupil size, resulting in a decrease in the average pupil size on visual blocks relative to fixation blocks. We actually observe the opposite, suggesting that the looming visual stimuli evoke in both monkeys an increased arousal/expectation state associated with relatively enlarged pupils. A similar increase in pupil size as compared to fixation can also be observed in the unimodal tactile block, for monkey M2 (paired t-test, $p<0.001$). Crucially, pupil size was statistically larger on the three bimodal predictive conditions as compared to the fixation blocks (paired t-test, $p<0.01$, for both monkeys) but also as compared to the unimodal visual blocks (paired t-test, $p<0.01$, for both monkeys). It is to be noted that in all these three conditions, the visual stimuli that could have induced phasic changes in pupil size are actually identical to those presented during the unimodal visual blocks. The fact that the bimodal conditions correlated with larger pupil size than in the unimodal visual condition is an indication that the tactile stimulus was processed by the monkey.

In the bimodal conditions, for monkey M2, pupil size changes are maximal in blocks in which the visual stimuli both spatially and temporally predict the tactile stimulation (paired t-test, $p<0.01$, when compared to the spatially but not temporally predictive condition, $p<0.001$, when compared to the temporally but not spatially predictive condition). Monkey M1, appears to mostly rely on the temporal predictive cues (paired t-test, $p<0.05$, when comparing the fully predictive blocks to the spatially but not temporally predictive condition, $p>0.05$, when comparing the fully predictive blocks to the temporally but not spatially predictive condition). Overall, these observations indicate that pupil size changes can serve as an implicit autonomous marker that the monkeys are distinctly processing the predictive signals provided by each block, correlating with the functional observations that will now be described.

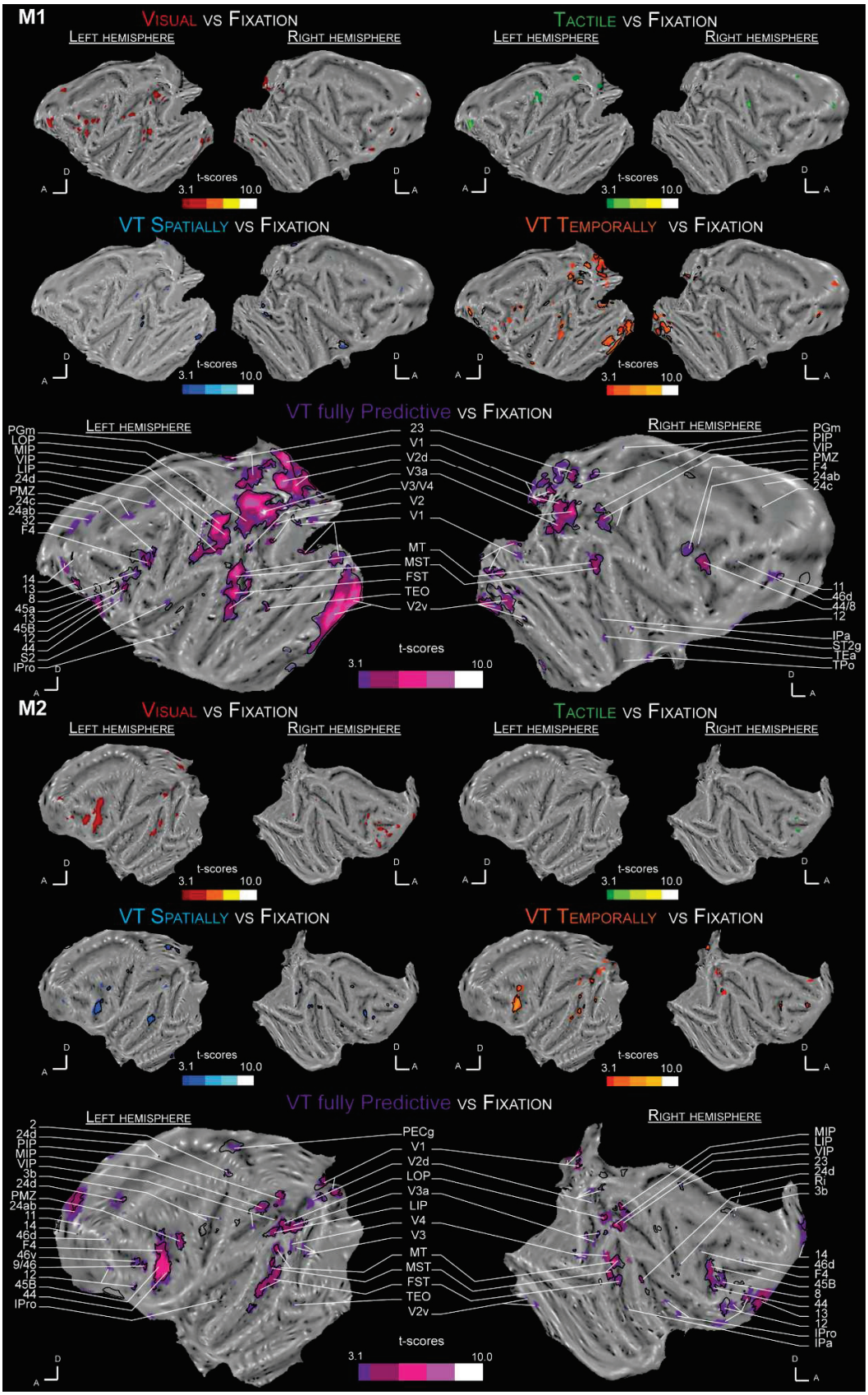
M1
VISUAL VS FIXATION
LEFT HEMISPHERE
RIGHT HEMISPHERE
TACTILE VS FIXATION
VT SPATIALLY VS FIXATION
VT TEMPORALLY VS FIXATION
t-scores
3.1
10.0
VT fully Predictive VS FIXATION
PGm
LOP
MIP
VIP
LIP
24d
PMZ
24c
24ab
32
F4
14
13
8
45a
13
45B
12
44
S2
IPro
23
V1
V2d
V3a
V3/V4
V2
MT
MST
FST
TEO
V2v
PIP
F4
11
46d
44/8
IPa
ST2g
TEa
TPo
M2
2
24d
PIP
MIP
VIP
3b
24d
PMZ
24ab
11
14
46d
F4
46v
9/46
12
45B
44
IPro
PECg
V1
V2d
LOP
V3a
LIP
V4
V3
MT
MST
FST
TEO
V2v
MIP
LIP
VIP
23
24d
Ri
3b
14
46d
F4
45B
8
44
13
12
IPro
IPa

Figure 3: **Whole Brain activation maps for the Visual (Red), Tactile (Green), VT spatially predictive (Blue), VT temporally predictive (Orange) and VT fully predictive (Purple) conditions.** Each contrast is performed with a level of significance set at P<0.001 uncorrected level, t-scores>3.1 for each monkey (M1 and M2). Dark lines represent VT bimodal cortical activations when the time reference is based on the tactile stimulus time rather than on the end of the visual looming sequence, as in the main analysis. Abbreviations : 2 somatosensory area 2; 3b somatosensory area 3b; 8 area 8; 9/46 area 9/4611 area 11; 12 area 12; 13 orbitofrontal area 13; 14 area 14; 23 area 23; 24ab area 24ab; 24c area 24c; 24d area 24d; 32 area 32; 44 area 44; 45 area 45; 46v ventral area 46; 46d posterior subdivision of area 46; F4 frontal area F4; FST floor of superior temporal sulcus; IPa intraparietal sulcus associated area; IPro insular proisocortex; LIP lateral intraparietal area; LOP lateral occipital parietal cortex; MIP medial intraparietal area; MST medial superior temporal area; MT middle temporal area; PECg parietal area PE, cingulate part; PGm parietal area PG, medial part; PIP posterior intraparietal area; PMZ premotor zone; Ri retroinsular area; S2 secondary somatosensory cortex; ST2g superior temporal sulcus area 2, gyral part; TEa temporal area TEa; TEO temporal area TE, occipital part; TPo temporal parietooccipital associated area in sts; V1 visual area 1; V2 visual area 2; V2v ventral visual area 2; V2d dorsal visual area 2; V3a visual area 3a; V3 visual area 3; V4 visual area 4; VIP ventral intraparietal area.

Unimodal stimulations evoke very weak cortical functional activations

The visual and tactile stimulations were specifically designed to have a low salience (low contrast looming cone onto the 3D visual background, low intensity tactile stimuli) so as to maximize the expected neuronal integration processes (Stein and Meredith, 1993; Avillac et al., 2004, 2007) . Confirming that these stimuli were indeed low salience stimuli, both evoke very weak cortical functional activations when presented each on their own, as can be seen on their individual functional whole brain flat-map (figure 3). Specifically, in both monkeys, the visual looming stimuli sparsely activate very low striate or extrastriate cortical region, the intraparietal cortex as well as the peri-arcuate premotor cortex (Figure 3, red activations, *t*-scores >3.1). Tactile stimulations evoke even weaker cortical activations, mostly in somatosensory related cortices, in

monkey M1, and around the post-central sulcus in the right hemisphere of monkey M2 (Figure 3, green activations, *t*-scores >3.1). These tactile maps can be confronted with those obtained in with stronger tactile stimuli (figure 2 in Guipponi et al., 2015; Wardak et al., 2016).

An occipito-parieto-temporo-premotor network is strongly activated by a tactile stimulus presented at the predicted time of impact of a looming visual stimulus on the face

Figure 3 also presents the whole brain functional activation flat maps for the three bimodal visuo-tactile stimulation blocks: for the spatially predictive bimodal condition (VT_Sp_pr, blue activations, *t*-scores >3.1), the temporally predictive bimodal condition (VT_Tp_pr, orange activations, *t*-scores >3.1) and the fully predictive bimodal condition (VT_Full_pr, purple activations, *t*-scores >3.1). Color contours correspond to the activations obtained relative to the looming visual stimuli time onset. Black contours correspond to the activations obtained relative to tactile stimuli time onset (*t*-scores >3.1). Crucial to the interpretation of the present data, in all of the three bimodal conditions, the observed functional activations are only marginally affected by whether the analyses are performed relative to the visual or to the tactile stimuli. Only activations identified at least in three hemispheres out of four are discussed below.

In blocks in which visual stimuli are spatially AND temporally predictive of tactile stimuli (VT_Full_pr), the activations are strikingly more widespread and stronger than those observed during unimodal visual or tactile stimulations (Figure 3, purple activations, *t*-scores >3.1). Specifically, these include large portions of the striate and extrastriate cortex in areas V1, V2, V3, V3a and V4, temporal sulcus activations including areas MT, MST, FST and TEO, parietal activations including areas LOP, VIP and MIP, insular activations (area IPro), cingular activations (area 24c-d) and prefrontal/premotor activations including premotor zone PMZ, premotor area F4, area 44, area 45b and area 46.

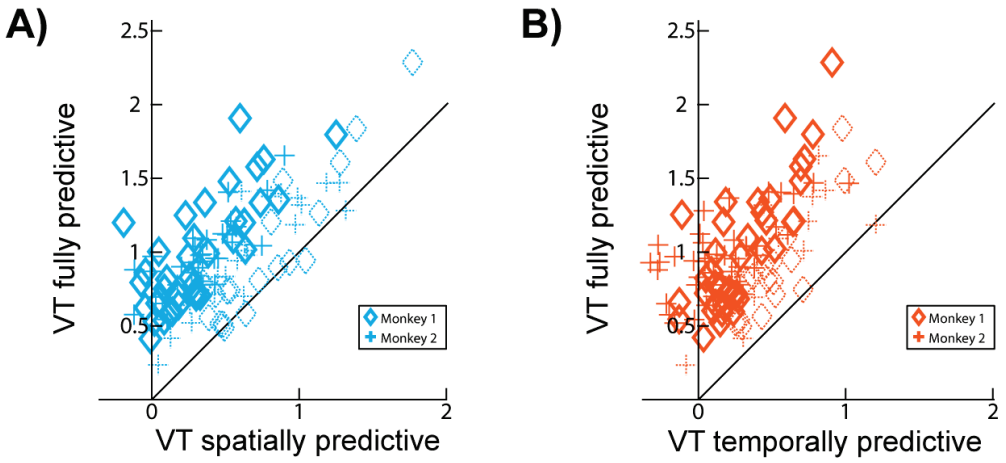

Figure 4: **Temporal and spatial prediction maximizes cortical activations.** ROIs are defined from the VT fully predictive based on end of visual looming sequence vs fixation contrast in the two monkeys (M1: 57 ROIs; M2: 55 ROIs). A, Percent Signal Change in the VT fully predictive condition as a function of the Percent Signal Change in the VT spatially predictive condition (paired-ttest, M1: p = 0, M2: p = 0). B, Percent Signal Change in the VT fully predictive condition as a function of the Percent Signal Change in the VT temporally predictive condition (paired-ttest M1: p = 0, M2: p = 0).

Both spatial and temporal prediction cues of impact to the face are crucial to the observed activations

In striking contrast to what is observed when the visual looming stimulus predicts the tactile stimulus both in time and space, in blocks in which visual stimuli are temporally but not spatially predictive of tactile stimuli (i.e. when the tactile stimulus is presented at the expected impact time of the looming visual stimulus, but on the opposite cheek on the face, VT_Tp_pr, figure 3, orange maps), functional activations are overall weaker and smaller. This is even more pronounced for blocks in which visual stimuli are spatially but not temporally predictive of tactile stimuli (i.e. when the tactile stimulus is presented at the expected impact location of the looming visual stimulus on the face, but while the visual stimulus is still halfway through its trajectory, VT_Sp_pr, figure 3,

blue maps). Specifically, in the majority of regions of interest identified in the fully predictive condition (figure 3, purple maps), the percentage of signal change (PSC) is statistically higher in the fully predictive bimodal condition than in the bimodal spatially predictive condition (figure 4a; M1: paired *t*-test: $p < 10^{-16}$, VTpr > VTsp ($p<0.05$): 35/57 ROIs = 61%, VTpr > VTsp ($0.05<p<0.07$): 2/57 ROIs = 4%, VTpr ≈ VTsp: 20/57 ROIs = 35% ; M2: paired *t*-test: $p < 10^{-23}$, VTpr > VTsp ($p<0.05$): 27/55 ROIs = 49%, VTpr > VTsp ($0.05<p<0.07$): 7/55 ROIs = 13%, VTpr ≈ VTsp: 21/55 ROIs = 38%). Because visual stimuli could originate from 8 different locations in the far visual field (4 locations ipsilateral to the impact point and 4 contralateral) but predict only two possible impact locations to the face (left or right cheek), the spatial effects reported here cannot be accounted for by other aspects of the stimulus. Similarly, in the majority of regions of interest, the PSCs are statistically higher in the fully predictive bimodal condition than in the bimodal temporally predictive condition (figure 4b; M1: paired *t*-test: $p < 10^{-21}$, VTpr > VTtp ($p<0.05$): 40/57 ROIs = 70%, VTpr > VTtp ($0.05<p<0.07$): 4/57 ROIs = 7%, VTpr ≈ VTtp: 13/57 ROIs = 23%; M2: paired *t*-test: $p < 10^{-25}$, VTpr > VTtp ($p<0.05$): 42/55 ROIs = 76%, VTpr > VTsp ($0.05<p<0.07$): 7/55 ROIs = 13%, VTpr ≈ VTtp: 6/55 ROIs = 11%).

Thus, maximal enhancement is observed in the identified functional network, when the tactile stimulus is presented in a time window and at a location compatible with the prediction of impact of the visual dynamic stimulus onto the face. This is further exemplified on a subset of ROIs, selected in key extrastriate (MST), parietal (VIP) and premotor (areas PMZ or F4) cortices of both hemispheres of both monkeys. For all these ROIs, there is a significant stimulation block effect (one-way ANOVA, $p<0.05$, except for right F4 region of monkey 2). Specifically, as can be seen in figure 5, the bimodal fully predictive condition (purple) is in most cases statistically different from both the visual (red) and the tactile (green) conditions. This bimodal fully predictive

condition is also statistically different from both the bimodal spatially predictive (blue) or/and the bimodal temporally predictive (orange) conditions in extrastriate visual area MST and posterior parietal area VIP (except in the left hemisphere of monkey M2 where the spatially predictive condition is not statistically different from the fully predictive condition). In premotor areas PMZ and F4 (figure 5), the difference in the PCS between the fully predictive condition and the two partially predictive conditions is less marked, more so for the spatially predictive condition (statistical difference reached for only one ROI) than for the temporally predictive condition (statistical difference reached for 2/4 ROIs).

This predictive heteromodal functional enhancement results from a multisensory integration process of visual and tactile information

Several statistical criteria can be applied to demonstrate multisensory integrative processes on hemodynamic activations (Beauchamp, 2005; Werner and Noppeney, 2011; Gentile et al., 2011; Love et al., 2011; Tyll et al., 2013). A first criterion is the *mean-criterion*, requiring that the integrated response be larger than the mean of unisensory responses. This is the least stringent criterion. A second criterion is the *super-additive-criterion*, requiring that the integrated response be larger than the sum of the unisensory responses. This criterion is very stringent when all PSCs are positive. A last criterion is the *max-criterion*, requiring that the integrated response be larger than the maximum of the unisensory responses. This criterion can be considered as an intermediate criterion. Tables 1 and 2 summarize how, for each of the identified ROIs, the PSCs in the different blocks statistically fulfill each of the three possible multisensory integration criteria. When focusing on the areas activated by the predictive condition in at least three hemispheres out of four (Tables 1 and 2, bold fonts), all of them fulfill the mean-criterion except two (M1: 40/42 ROIs = 95%, M2: 46 ROIs = 100%), and from half to three quarters fulfill either the super-additive criterion

(M1: 22/42 ROIs = 52%, M2: 34/46 = 74%) or the max-criterion (M1: 30/42 ROIs = 71%, 4 ROIs at (0.05<p<0.07) = 10%, M2: 36/46 = 78%, 3 ROIs at (0.05<p<0.07) = 10%). Table 3 summarizes how many of the three criteria are fulfilled for each of these ROIs. Striate and extrastriate visual areas V1, V2d/v V3A, V3/V4 and MST achieve from two to three criteria in all activated hemispheres, to the exception of area MT. Parietal area VIP_{post} (as opposed to a more anterior ventral intraparietal activation named VIP_{ant}), the polysensory motor zone PMZ on the convexity of F4 as well as orbitofrontal area 12 maximize the three multisensory integration criteria in virtually all the activated hemispheres. Prefrontal area 44, cingulate area 23 and insular area IPro also maximize from two to three of these criteria in all identified ROIs. This possibly singles out these areas in the prediction of the impact of a looming stimulus to the body, as will be discussed below.

Figure 5: **Impact prediction activates a parieto-frontal network.** Histograms represent the percent signal change for Visual (Red), Tactile (Green), VT fully predictive (Purple), VT temporally predictive (Orange) and VT spatially predictive (Blue) conditions for monkey 1 and 2, for selected ROIs in the extrastriate cortex (MST), the parietal cortex (area VIP, posterior ROI) and the premotor cortex (areas PMZ or F4). The contrast used to extract percent signal change is the VT predictive versus fixation contrast (P <0.05, FWE-corrected level (FWE) or P<0.001, uncorrected level (unc). For each ROI, block effect is assessed by a repeated measure one-way ANOVA; significance of PSCs difference with respect to baseline and amongst themselves is assessed using paired t-tests, *P<0.05; **P<0.01; ***P<0.001, °0.05<P<0.07).

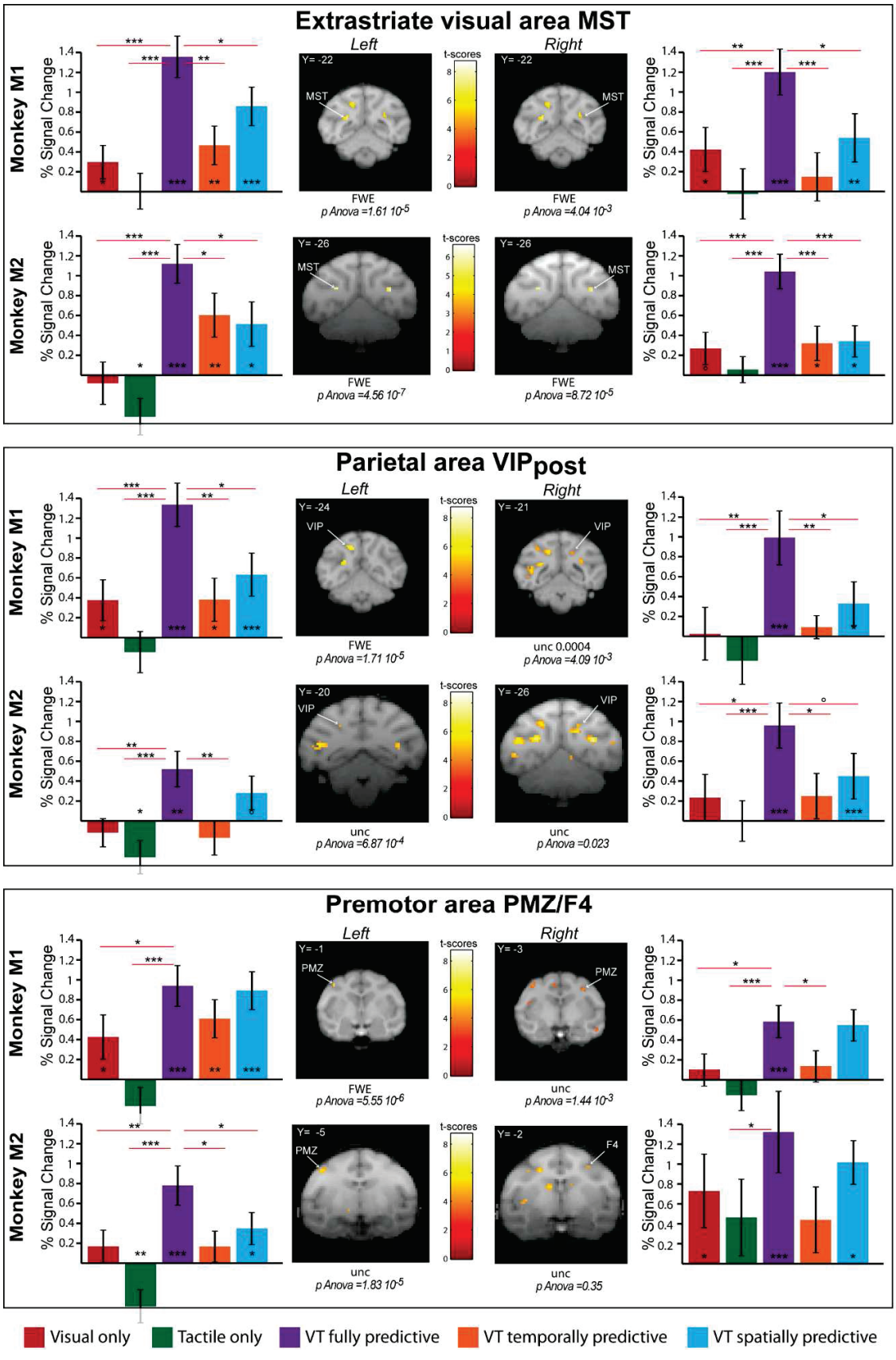
Extrastriate visual area MST
Left
Right
Monkey M1
Monkey M2
% Signal Change
t-scores
Y= -22
MST
FWE
p Anova =1.61 10-5
p Anova =4.04 10-3
Y= -26
p Anova =4.56 10-7
p Anova =8.72 10-5
Parietal area VIPpost
Y= -24
VIP
Y= -21
unc 0.0004
p Anova =4.09 10-3
Y= -20
unc
p Anova =6.87 10-4
p Anova =0.023
Premotor area PMZ/F4
Y= -1
PMZ
p Anova =5.55 10-6
p Anova =1.44 10-3
Y= -5
p Anova =1.83 10-5
Y= -2
F4
p Anova =0.35
Visual only
Tactile only
VT fully predictive
VT temporally predictive
VT spatially predictive

Spatial and temporal cues are actively integrated towards impact prediction

The above analysis demonstrates that a majority of ROIs within the identified network actively integrate visual and tactile information during the fully predictive condition. Here, we seek to understand whether spatial and temporal cues are also actively integrated during the fully predictive condition. To this effect we assess how the PSCs measured during the fully predictive condition compare to those obtained during the spatially predictive condition and the temporally predictive condition and meet the *mean-criterion*, the *super-additive-criterion*, and the *max-criterion* (Tables 1 and 2). The *super-additive-criterion*, the most stringent criterion, is rarely met (M1: 3/42 ROIs = 7%, 3 ROIs ($0.05<p<0.07$) = 7%, M2: 7/46 ROIs = 15%, 1 ROI ($0.05<p<0.07$) = 2%). In contrast, a higher proportion of ROIs meet the *max-criterion* (M1: 22/42 ROIs = 52%, 3 ROIs ($0.05<p<0.07$) = 7%, M2: 19/46 ROIs = 41%, 12 ROIs ($0.05<p<0.07$) = 26%), and more so the *mean-criterion* (M1: 27/42 ROIs = 64%, 4 ROIs ($0.05<p<0.07$) = 10%, M2: 39/46 ROIs = 85%, 3 ROIs ($0.05<p<0.07$) = 7%). Table 3 recapitulates how many of the three criteria are fulfilled for each of the identified ROIs. Striate and extrastriate visual areas V3A, V3/V4 and MST achieve from two to three criteria in all activated hemispheres, MT achieve from two to three criteria in three activated hemispheres, to the exception of areas V1, V2d/v. Parietal area VIP_{ant} (as opposed to a more posterior ventral intraparietal activation named VIP_{post}), lateral occipital parietal area LOP and the cingulate area 24ab maximize from two to three temporally and spatially predictive integration criteria in virtually all the activated hemispheres. This strongly suggests that spatial and temporal predictive information is actively integrated at the neuronal level and possibly highlights a cortical network specifically involved in the integration of these predictive cues. Single cell recordings in key regions of this cortical network will allow to test whether this results from optimal cue combination and directly predicts behavior as demonstrated in other instances (e.g. visuo-

vestibular integration in parietal area VIP, Fetsch et al., 2012; Pitkow et al., 2015).

A similar predictive multisensory integration process is also at play in the pulvinar

The pulvinar is the largest thalamic nucleus and it is proposed to be part of a major thalamo-cortical pathway for multisensory and sensorimotor integration (Cappe et al., 2009b, 2012; Tyll et al., 2011; Henschke et al., 2015). In the fully predictive bimodal condition, we observe activations at uncorrected level ($p<0.001$), within this subcortical nucleus, in both hemispheres of both monkeys (Figure 6, t-scores, M1: left hemisphere: $t=3.69$, right hemisphere: $t=3.15$; M2: left hemisphere: $t=3.56$; right hemisphere: $t=4.0$). For 3/4 of the ROIs defined in the pulvinar, there is a significant stimulation block effect (one-way ANOVA, $p<0.05$ or better). Specifically, the bimodal fully predictive condition (figure 6, purple) is in most cases statistically different from both the visual (red) and the tactile (green) conditions. This bimodal fully predictive condition is also statistically different from the bimodal temporally predictive (orange) condition in 3/4 ROIS and from the bimodal spatially predictive (blue) condition in 1/4 ROI. All three multisensory integration criteria reach statistical significance in the left hemisphere of M1 and the right hemisphere of M2. For the other two hemispheres, only the mean-criterion reaches statistical significance. A higher field MRI study is needed to provide both a higher spatial resolution and more resolved description of the neural correlates of predictive hetero-modal sensory integration in this key subcortical nucleus.

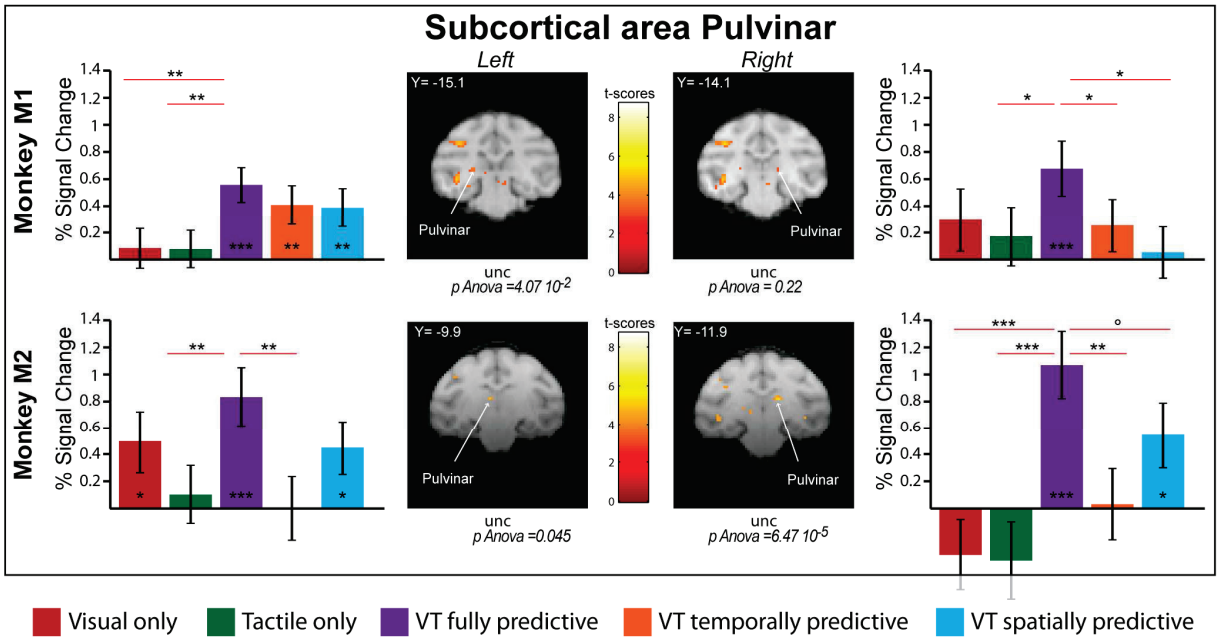

Figure 6: **Temporal and spatial prediction enhances thalamic pulvinar activations in both monkeys.** All as in figure 5.

DISCUSSION

Overall, this study demonstrates that looming visual stimuli towards the body enhance the tactile information processing within a temporal window and at a spatial location that coincide with the prediction of impact to the body. The activated network is essentially composed of striate and extrastriate visual areas, intraparietal and periarcuate premotor areas and pulvinar subsectors. In this network, this heteromodal enhancement appears to result from active multisensory integrative neuronal mechanisms. These results are discussed in relation with the ecological and behavioral significance of looming stimuli, PPS and the predictive coding framework.

Ecological and behavioral specificity of looming stimuli

Looming visual stimuli have been shown to generate stereotyped fear responses in monkeys (Schiff et al., 1962), in human infants (Ball and Tronick, 1971) and in adults (King and Cowey, 1992). These responses are absent when receding stimuli are used or when the looming object is perceived as passing by the observer rather than predicting an impact onto its body (see also Lewis and Neider, 2015). While in theory, the rate of optical increase in the size of the retinal image as an object approaches allows for a precise prediction of the time-to-collision, independently of object size or distance (Gibson, 1979), threatening objects are perceived as arriving earlier than non-threatening objects (Brendel et al., 2012; Vagnoni et al., 2012), including in infants (Ayzenberg et al., 2015).

Importantly, looming stimuli interfere with visually guided actions, independently of an observer's current goals (Moher et al., 2015). This has led to the formulation of the behavioral-urgency hypothesis (Franconeri and Simons, 2003) which proposes that dynamic events on specific trajectories with respect to the body capture attention when they require an immediate behavioral response because they represent a danger to the observer's safety.

Changes in pupil size as a behavioral marker of impact prediction to the body

Pupil size has been associated with two neuromodulation systems, the noradrenergic locus coeruleus (LC-NA) system (for review, see Sara, 2009) and the cholinergic basal forebrain system (Yu, 2012). Here we show that pupil size increases as a function of the strength of the spatial and temporal cues predicting an impact to the face. This could be related to an enhanced tonic LC-NA activity due to the impact predictive cues processing and their potential for harm to the body (Bradley et al., 2008).

Prediction of impact to the body and PPS

Looming stimuli enhance tactile processing by enhancing tactile sensitivity (Cléry et al., 2015a) and speeding reaction times (Canzoneri et al., 2012; Kandula et al., 2015). Because these behavioral effects are induced by visual stimuli and have consequences onto a heteromodal modality, namely touch, this strongly predicts the involvement of a visuo-tactile convergence network. The network we identify here is extremely similar to the visuo-tactile convergence network recently described in monkeys (Guipponi et al., 2013, 2015), though quite distinct from the network activated by pure tactile stimulations to the face (Wardak et al., 2016). A direct prediction of our observation is that the human homologue of these parietal areas (Beauchamp et al., 2004; Sereno and Huang, 2006) are also expected to contribute to impact prediction in human subjects.

Importantly, impact prediction to the face involves, the parieto-frontal (ventral intraparietal/post-arcuate PMZ/F4) network that has been associated with the definition of a defense PPS (Cléry et al., 2015b). These regions have bimodal visuo-tactile receptive fields representing close PPS and the corresponding skin surface (Gentilucci et al., 1988; Rizzolatti et al., 1988; Colby et al., 1993; Graziano et al., 1994; Gross and Graziano, 1995; Fogassi et al., 1996;

Duhamel et al., 1997). They are involved in a defense PPS encoding (Graziano and Cooke, 2006; Graziano et al., 2002; Cooke and Graziano, 2004). We suggest that this network not only processes the trajectory of the looming objet with respect to the body, but also anticipates its consequences on the body by modulating sensitivity to touch. It is unclear whether these predictive mechanisms precede the preparation of protective actions in response to the looming stimulus or are contemporary to these flight mechanisms. The fact that tactile sensitivity is also enhanced for looming stimuli brushing past the face (Cléry et al., 2015a) further supports the idea that this network is not only activated by the prediction of intrusion onto the body but more generally into PPS as a comfort zone (Quesque et al., 2016).

Prediction of impact and multisensory integration

In single cell studies, multisensory integration is the phenomenon by which the sum of neuronal responses to unisensory stimulations, in spikes per second, is different from the neuronal activity to bimodal stimulations (Stein and Stanford, 2008; Avillac et al., 2007; Stein et al., 2009). FMRI studies of multisensory integration pose very specific analysis issues, due to the nonlinear relationship that exists between spike generation and the corresponding change in the hemodynamic response (Boynton et al., 1996; Dale and Buckner, 1997; Heeger and Ress, 2002). In particular, the choice of the baseline is a critical factor (Binder et al., 1999; Stark and Squire, 2001; James and Stevenson, 2012) as well as the criteria for deciding that multisensory integration is indeed taking place (Calvert, 2001; Beauchamp et al., 2004; Beauchamp, 2005; Laurienti et al., 2005; Gentile et al., 2011; Love et al., 2011; Werner and Noppeney, 2011; Tyll et al., 2013). Here, we show that the less stringent criterion (*mean-criterion*) is reached for virtually all ROIs while the most stringent criterion (*super-additive criterion*) is reached for 50% to 75% of the ROIs, indicating active visuo-tactile integration in the identified network. This expands previous evidence for visuo-

tactile integration in the intraparietal cortex (Avillac et al., 2004, 2007) to the temporal prediction domain and to novel cortical territories. Quite surprisingly, multisensory integration is observed both in premotor and parietal and in lower striate and extrastriate visual areas, strongly indicating that multisensory integration processes in these regions is modulated by top-down contextual information including spatial and temporal predictive information.

A directly related question is whether this cortical network specifically integrates visual and tactile information or additionally distinctly integrates the spatial and temporal prediction cues. Again, we show that 70% of the ROIs fulfill the *mean-criterion* and up to 50% fulfill the *max-criterion* strongly suggesting that spatial and temporal prediction also relies on integrative mechanisms.

Impact prediction and the pulvinar

Thalamic neurons are suggested to perform multisensory integration, possibly before multisensory information even reaches the cortex (Tyll et al., 2011). Within the thalamus, the pulvinar is associated to visual (e.g on monkeys Bender, 1981; Benevento and Miller, 1981; Petersen et al., 1985) and non-visual processes (Avanzini et al., 1980; Gattass et al., 1978). Cappe et al. (2009a) found that the monkey pulvinar nucleus exhibits the most extensive overlap of differentially retrogradely labeled neurons after injection of these retrograde neuronal tracers in auditory, somatosensory and premotor cortex. As a result, the pulvinar is expected to play a key role in multisensory integration. We confirm this role in visuo-tactile integration in the context of impact prediction, though electrophysiological studies will be needed to provide a better description of how this region modulates or even possibly gates cortical multisensory activity.

Causal multisensory inference and impact prediction

Bayesian Causal Inference framework (BCI), that probabilistically associates diverse sensory outcomes with a set of potential sources and that explicitly models the potential external situations that could have generated the observed sensory signals appears as a very powerful computational framework to study multisensory processes (Körding et al., 2007; Shams and Beierholm, 2010; Parise et al., 2012). In the BCI framework, a final estimate of the actual structure of the incoming sensory evidence is obtained by combining the estimates under the various causal structures (fusion or segregation) and evaluating the best model using methods such as model averaging, model selection, or probability matching (Wozny et al., 2010). Recent studies (Rohe and Noppeney, 2015a, 2015b, 2016) demonstrate that BCI is performed within a hierarchically organized cortical network: early sensory areas segregate sensory information (prior = information is produced by independent sources); posterior intraparietal areas fuse sensory information (prior = information is produced by a common source); while anterior parietal areas infer the causal structure of the world (implementing predictions compatible with the BCI framework).

We would like to propose to further enrich this framework with an additional dimension beyond fusion and segregation, namely delayed consequences. This implies taking into account the temporal dimension of dynamic sensory stimuli as may occur in speech where the vision of the lips precedes and predicts the sound of the voice, or in the prediction of impact of a visual object to the body. From a neuronal perspective, while single cell recordings in monkeys show that the ventral intraparietal cortex performs multisensory source fusion (i.e. multisensory integration, Avillac et al., 2004, 2007), our study suggest that this cortical area also performs multisensory prediction, possibly thanks to gamma-band synchronization which has been described to increase during the processing of looming stimuli (Maier et al., 2008) and which has been suggested to possibly implement top-down prior inferences (van Atteveldt et al., 2014).

Acknowledgments: J.C. was funded by the Fondation pour la Recherche Médicale. O.G. was funded by the French education ministry. S.BH was funded by the French Agence nationale de la recherche (Grant #ANR-05-JCJC-0230-01).

References

Aston-Jones G, Cohen JD (2005) An integrative theory of locus coeruleus-norepinephrine function: Adaptive Gain and Optimal Performance. Annual Review of Neuroscience 28:403–450.

Avanzini G, Broggi G, Franceschetti S, Spreafico R (1980) Multisensory convergence and interaction in the pulvinar-lateralis posterior complex of the cat's thalamus. Neurosci Lett 19:27–32.

Avillac M, Ben Hamed S, Duhamel J-R (2007) Multisensory Integration in the Ventral Intraparietal Area of the Macaque Monkey. J Neurosci 27:1922–1932.

Avillac M, Olivier E, Denève S, Ben Hamed S, Duhamel J-R (2004) Multisensory integration in multiple reference frames in the posterior parietal cortex. Cognitive Processing 5:159–166.

Ayzenberg V, Longo M, Lourenco S (2015) Evolutionary-based threat modulates perception of looming visual stimuli in human infants. J Vis 15:797.

Ball W, Tronick E (1971) Infant responses to impending collision: optical and real. Science 171:818–820.

Beauchamp MS (2005) Statistical Criteria in fMRI Studies of Multisensory Integration. Neuroinformatics 3:93–113.

Beauchamp MS, Lee KE, Argall BD, Martin A (2004) Integration of Auditory and Visual Information about Objects in Superior Temporal Sulcus. Neuron 41:809–823.

Belmalih A, Borra E, Contini M, Gerbella M, Rozzi S, Luppino G (2009) Multimodal architectonic subdivision of the rostral part (area F5) of the macaque ventral premotor cortex. J Comp Neurol 512:183–217.

Bender DB (1981) Retinotopic organization of macaque pulvinar. Journal of Neurophysiology 46:672–693.

Benevento LA, Miller J (1981) Visual responses of single neurons in the caudal lateral pulvinar of the macaque monkey. J Neurosci 1:1268–1278.

Binder JR, Frost JA, Hammeke TA, Bellgowan PS, Rao SM, Cox RW (1999) Conceptual processing during the conscious resting state. A functional MRI study. J Cogn Neurosci 11:80–95.

Bouret S, Sara SJ (2005) Network reset: a simplified overarching theory of locus coeruleus noradrenaline function. Trends in Neurosciences 28:574–582.

Boynton GM, Engel SA, Glover GH, Heeger DJ (1996) Linear Systems Analysis of Functional Magnetic Resonance Imaging in Human V1. J Neurosci 16:4207–4221.

Bradley MM, Miccoli L, Escrig MA, Lang PJ (2008) The pupil as a measure of emotional arousal and autonomic activation. Psychophysiology 45:602–607.

Bradshaw J (1967) Pupil size as a measure of arousal during information processing. Nature 216:515–516.

Brendel E, DeLucia PR, Hecht H, Stacy RL, Larsen JT (2012) Threatening pictures induce shortened time-to-contact estimates. Atten Percept Psychophys 74:979–987.

Brett M, Anton J-L, Valabregue R, Poline J-B (2002) Region of interest analysis using the MarsBar toolbox for SPM 99. Presented at the 8th International Conference on Functional Mapping of the Human Brain (June 2–6, 2002, Sendai, Japan), 16:S497.

Calvert GA (2001) Crossmodal Processing in the Human Brain: Insights from Functional Neuroimaging Studies. Cereb Cortex 11:1110–1123.

Canzoneri E, Magosso E, Serino A (2012) Dynamic Sounds Capture the Boundaries of Peripersonal Space Representation in Humans. PLoS ONE 7:e44306.

Cappe C, Morel A, Barone P, Rouiller EM (2009a) The Thalamocortical Projection Systems in Primate: An Anatomical Support for Multisensory and Sensorimotor Interplay. Cereb Cortex 19:2025–2037.

Cappe C, Rouiller EM, Barone P (2009b) Multisensory anatomical pathways. Hear Res 258:28–36.

Cappe C, Thelen A, Romei V, Thut G, Murray MM (2012) Looming Signals Reveal Synergistic Principles of Multisensory Integration. J Neurosci 32:1171–1182.

Cappe C, Thut G, Romei V, Murray MM (2009c) Selective integration of auditory-visual looming cues by humans. Neuropsychologia 47:1045–1052.

Cléry J, Guipponi O, Odouard S, Wardak C, Ben Hamed S (2015a) Impact prediction by looming visual stimuli enhances tactile detection. J Neurosci 35:4179–4189.

Cléry J, Guipponi O, Wardak C, Ben Hamed S (2015b) Neuronal bases of peripersonal and extrapersonal spaces, their plasticity and their dynamics: Knowns and unknowns. Neuropsychologia 70:313–326.

Colby CL, Duhamel JR, Goldberg ME (1993) Ventral intraparietal area of the macaque: anatomic location and visual response properties. Journal of Neurophysiology 69:902–914.

Cooke DF, Graziano MSA (2004) Sensorimotor Integration in the Precentral Gyrus: Polysensory Neurons and Defensive Movements. Journal of Neurophysiology 91:1648–1660.

Dale AM, Buckner RL (1997) Selective averaging of rapidly presented individual trials using fMRI. Hum Brain Mapp 5:329–340.

de Haan AM, Smit M, Stigchel SV der, Dijkerman HC (2016) Approaching threat modulates

visuotactile interactions in peripersonal space. Exp Brain Res 234:1875–1884.

De Paepe AL, Crombez G, Legrain V (2016) What's Coming Near? The Influence of Dynamical Visual Stimuli on Nociceptive Processing. PLOS ONE 11:e0155864.

Duhamel J-R, Bremmer F, BenHamed S, Graf W (1997) Spatial invariance of visual receptive fields in parietal cortex neurons. Nature 389:845–848.

Eldar E, Cohen JD, Niv Y (2013) The effects of neural gain on attention and learning. Nat Neurosci 16:1146–1153.

Fetsch CR, Pouget A, DeAngelis GC, Angelaki DE (2012) Neural correlates of reliability-based cue weighting during multisensory integration. Nat Neurosci 15:146–154.

Fogassi L, Gallese V, Fadiga L, Luppino G, Matelli M, Rizzolatti G (1996) Coding of peripersonal space in inferior premotor cortex (area F4). J Neurophysiol 76:141–157.

Franconeri SL, Simons DJ (2003) Moving and looming stimuli capture attention. Percept Psychophys 65:999–1010.

Gattass R, Oswaldo-Cruz E, Sousa AP (1978) Visuotopic organization of the cebus pulvinar: a double representation the contralateral hemifield. Brain Res 152:1–16.

Gentile G, Petkova VI, Ehrsson HH (2011) Integration of Visual and Tactile Signals From the Hand in the Human Brain: An fMRI Study. Journal of Neurophysiology 105:910–922.

Gentilucci M, Fogassi L, Luppino G, Matelli M, Camarda R, Rizzolatti G (1988) Functional organization of inferior area 6 in the macaque monkey. I. Somatotopy and the control of proximal movements. Exp Brain Res 71:475–490.

Gibson JJ (1979) The Ecological Approach to Visual Perception. Houghton Mifflin, Boston, MA.

Gilzenrat MS, Nieuwenhuis S, Jepma M, Cohen JD (2010) Pupil diameter tracks changes in control state predicted by the adaptive gain theory of locus coeruleus function. Cogn Affect Behav Neurosci 10:252–269.

Graziano MS, Yap GS, Gross CG (1994) Coding of visual space by premotor neurons. Science 266:1054–1057.

Graziano MSA, Cooke DF (2006) Parieto-frontal interactions, personal space, and defensive behavior. Neuropsychologia 44:845–859.

Graziano MSA, Taylor CSR, Moore T (2002) Complex Movements Evoked by Microstimulation of Precentral Cortex. Neuron 34:841–851.

Gross CG, Graziano MSA (1995) REVIEW ■ : Multiple Representations of Space in the Brain. Neuroscientist 1:43–50.

Guipponi O, Cléry J, Odouard S, Wardak C, Ben Hamed S (2015) Whole brain mapping of visual

and tactile convergence in the macaque monkey. NeuroImage 117:93–102.

Guipponi O, Odouard S, Pinède S, Wardak C, Ben Hamed S (2014) fMRI Cortical Correlates of Spontaneous Eye Blinks in the Nonhuman Primate. Cereb Cortex:bhu038.

Guipponi O, Wardak C, Ibarrola D, Comte J-C, Sappey-Marinier D, Pinède S, Ben Hamed S (2013) Multimodal Convergence within the Intraparietal Sulcus of the Macaque Monkey. J Neurosci 33:4128–4139.

Heeger DJ, Ress D (2002) What does fMRI tell us about neuronal activity? Nature Reviews Neuroscience 3:142–151.

Henschke JU, Noesselt T, Scheich H, Budinger E (2015) Possible anatomical pathways for short-latency multisensory integration processes in primary sensory cortices. Brain Struct Funct 220:955–977.

James TW, Stevenson RA (2012) The Use of fMRI to Assess Multisensory Integration. In: The Neural Bases of Multisensory Processes (Murray MM, Wallace MT, eds) Frontiers in Neuroscience. Boca Raton (FL): CRC Press. Available at: http://www.ncbi.nlm.nih.gov/books/NBK92856/ [Accessed August 20, 2014].

Jepma M, Nieuwenhuis S (2010) Pupil Diameter Predicts Changes in the Exploration–Exploitation Trade-off: Evidence for the Adaptive Gain Theory. Journal of Cognitive Neuroscience 23:1587–1596.

Kandula M, Hofman D, Dijkerman HC (2015) Visuo-tactile interactions are dependent on the predictive value of the visual stimulus. Neuropsychologia 70:358–366.

Kihara K, Takeuchi T, Yoshimoto S, Kondo HM, Kawahara JI (2015) Pupillometric evidence for the locus coeruleus-noradrenaline system facilitating attentional processing of action-triggered visual stimuli. Front Psychol 6 Available at: http://www.ncbi.nlm.nih.gov/pmc/articles/PMC4466527/ [Accessed October 16, 2015].

King SM, Cowey A (1992) Defensive responses to looming visual stimuli in monkeys with unilateral striate cortex ablation. Neuropsychologia 30:1017–1024.

Kolster H, Janssens T, Orban GA, Vanduffel W (2014) The Retinotopic Organization of Macaque Occipitotemporal Cortex Anterior to V4 and Caudoventral to the Middle Temporal (MT) Cluster. J Neurosci 34:10168–10191.

Körding KP, Beierholm U, Ma WJ, Quartz S, Tenenbaum JB, Shams L (2007) Causal Inference in Multisensory Perception. PLoS ONE 2:e943.

Koss MC (1986) Pupillary dilation as an index of central nervous system alpha 2-adrenoceptor activation. J Pharmacol Methods 15:1–19.

Laeng B, Sirois S, Gredebäck G (2012) Pupillometry A Window to the Preconscious? Perspectives on Psychological Science 7:18–27.

Laurienti PJ, Perrault TJ, Stanford TR, Wallace MT, Stein BE (2005) On the use of superadditivity as a metric for characterizing multisensory integration in functional neuroimaging studies. Exp Brain Res 166:289–297.

Lewis JE, Neider MB (2015) Fixation Not Required: Characterizing Oculomotor Attention Capture for Looming Stimuli. Atten Percept Psychophys 77:2247–2259.

Lewis JW, Van Essen DC (2000) Corticocortical connections of visual, sensorimotor, and multimodal processing areas in the parietal lobe of the macaque monkey. J Comp Neurol 428:112–137.

Love SA, Pollick FE, Latinus M (2011) Cerebral Correlates and Statistical Criteria of Cross-Modal Face and Voice Integration. Seeing and Perceiving 24:351–367.

Maier JX, Chandrasekaran C, Ghazanfar AA (2008) Integration of bimodal looming signals through neuronal coherence in the temporal lobe. Curr Biol 18:963–968.

Maier JX, Neuhoff JG, Logothetis NK, Ghazanfar AA (2004) Multisensory Integration of Looming Signals by Rhesus Monkeys. Neuron 43:177–181.

Mandeville JB, Choi J-K, Jarraya B, Rosen BR, Jenkins BG, Vanduffel W (2011) fMRI of Cocaine Self-Administration in Macaques Reveals Functional Inhibition of Basal Ganglia. Neuropsychopharmacology 36:1187–1198.

Moher J, Sit J, Song J-H (2015) Goal-directed action is automatically biased towards looming motion. Vision Research 113, Part B:188–197.

Murphy PR, Robertson IH, Balsters JH, O'connell RG (2011) Pupillometry and P3 index the locus coeruleus-noradrenergic arousal function in humans. Psychophysiology 48:1532–1543.

Nassar MR, Rumsey KM, Wilson RC, Parikh K, Heasly B, Gold JI (2012) Rational regulation of learning dynamics by pupil-linked arousal systems. Nat Neurosci 15:1040–1046.

O'Reilly JX, Schüffelgen U, Cuell SF, Behrens TEJ, Mars RB, Rushworth MFS (2013) Dissociable effects of surprise and model update in parietal and anterior cingulate cortex. PNAS 110:E3660–E3669.

Parise CV, Spence C, Ernst MO (2012) When correlation implies causation in multisensory integration. Curr Biol 22:46–49.

Paxinos G, Huang X-F, Toga A (2000) The Rhesus Monkey Brain in Stereotaxic Coordinates. Faculty of Health and Behavioural Sciences - Papers (Archive) Available at: http://ro.uow.edu.au/hbspapers/3613.

Petersen SE, Robinson DL, Keys W (1985) Pulvinar nuclei of the behaving rhesus monkey: visual responses and their modulation. Journal of Neurophysiology 54:867–886.

Petrides M, Cadoret G, Mackey S (2005) Orofacial somatomotor responses in the macaque monkey homologue of Broca's area. Nature 435:1235–1238.

Pitkow X, Liu S, Angelaki DE, DeAngelis GC, Pouget A (2015) How Can Single Sensory Neurons Predict Behavior? Neuron 87:411–423.

Preuschoff K, 't Hart BM, Einhauser W (2011) Pupil dilation signals surprise: evidence for noradrenaline's role in decision making. Front Neurosci 5:115.

Quesque F, Ruggiero G, Mouta S, Santos J, Iachini T, Coello Y (2016) Keeping you at arm's length: modifying peripersonal space influences interpersonal distance. Psychological Research:1–12.

Rajkowski J, Kubiak P, Aston-Jones G (1994) Locus coeruleus activity in monkey: phasic and tonic changes are associated with altered vigilance. Brain Res Bull 35:607–616.

Rizzolatti G, Camarda R, Fogassi L, Gentilucci M, Luppino G, Matelli M (1988) Functional organization of inferior area 6 in the macaque monkey. II. Area F5 and the control of distal movements. Exp Brain Res 71:491–507.

Rizzolatti G, Fadiga L, Fogassi L, Gallese V (1997) The space around us. Science 277:190–191.

Rohe T, Noppeney U (2015a) Sensory reliability shapes perceptual inference via two mechanisms. J Vis 15:22.

Rohe T, Noppeney U (2015b) Cortical hierarchies perform Bayesian causal inference in multisensory perception. PLoS Biol 13:e1002073.

Rohe T, Noppeney U (2016) Distinct Computational Principles Govern Multisensory Integration in Primary Sensory and Association Cortices. Curr Biol 26:509–514.

Samuels ER, Szabadi E (2008) Functional neuroanatomy of the noradrenergic locus coeruleus: its roles in the regulation of arousal and autonomic function part II: physiological and pharmacological manipulations and pathological alterations of locus coeruleus activity in humans. Curr Neuropharmacol 6:254–285.

Sara SJ (2009) The locus coeruleus and noradrenergic modulation of cognition. Nat Rev Neurosci 10:211–223.

Schiff W, Caviness JA, Gibson JJ (1962) Persistent fear responses in rhesus monkeys to the optical stimulus of "looming." Science 136:982–983.

Sereno MI, Huang R-S (2006) A human parietal face area contains aligned head-centered visual and tactile maps. Nat Neurosci 9:1337–1343.

Shams L, Beierholm UR (2010) Causal inference in perception. Trends in Cognitive Sciences 14:425–432.

Simpson HM, Hale SM (1969) Pupillary changes during a decision-making task. Perceptual and

Motor Skills 29:495–498.

Stark CEL, Squire LR (2001) When zero is not zero: The problem of ambiguous baseline conditions in fMRI. PNAS 98:12760–12766.

Stein BE, Meredith MA (1993) The Merging of the Senses, Cambridge : MIT press. Cambridge : MIT press.

Stein BE, Stanford TR (2008) Multisensory integration: current issues from the perspective of the single neuron. Nat Rev Neurosci 9:255–266.

Stein BE, Stanford TR, Ramachandran R, Jr TJP, Rowland BA (2009) Challenges in quantifying multisensory integration: alternative criteria, models, and inverse effectiveness. Exp Brain Res 198:113–126.

Tyll S, Bonath B, Schoenfeld MA, Heinze H-J, Ohl FW, Noesselt T (2013) Neural basis of multisensory looming signals. NeuroImage 65:13–22.

Tyll S, Budinger E, Noesselt T (2011) Thalamic influences on multisensory integration. Commun Integr Biol 4:378–381.

Vagnoni E, Lourenco SF, Longo MR (2012) Threat modulates perception of looming visual stimuli. Current Biology 22:R826–R827.

van Essen DC, Drury HA, Dickson J, Harwell J, Hanlon D, Anderson CH (2001) An Integrated Software Suite for Surface-based Analyses of Cerebral Cortex. J Am Med Inform Assoc 8:443–459.

van Atteveldt N, Murray MM, Thut G, Schroeder CE (2014) Multisensory Integration: Flexible Use of General Operations. Neuron 81:1240–1253.

Vanduffel W, Fize D, Mandeville JB, Nelissen K, Van Hecke P, Rosen BR, Tootell RBH, Orban GA (2001) Visual Motion Processing Investigated Using Contrast Agent-Enhanced fMRI in Awake Behaving Monkeys. Neuron 32:565–577.

Wardak C, Guipponi O, Pinède S, Ben Hamed S (2016) Tactile representation of the head and shoulders assessed by fMRI in the nonhuman primate. Journal of Neurophysiology 115:80–91.

Werner S, Noppeney U (2011) The Contributions of Transient and Sustained Response Codes to Audiovisual Integration. Cereb Cortex 21:920–931.

Wozny DR, Beierholm UR, Shams L (2010) Probability matching as a computational strategy used in perception. PLoS Comput Biol 6.

Yoss RE, Moyer NJ, Hollenhorst RW (1970) Pupil size and spontaneous pupillary waves associated with alertness, drowsiness, and sleep. Neurology 20:545–554.

Yu AJ (2012) Change is in the eye of the beholder. Nat Neurosci 15:933–935.

Yu AJ, Dayan P (2005) Uncertainty, Neuromodulation, and Attention. Neuron 46:681–692.

Table and table legends:

	Areas	ROIs	Coordinates	*t*-score	ROI size	% PSC	Mean / V.T	Super / V.T	Max / V.T	Mean / Sp.Tpbi	Super / Sp.Tp	Max / Sp.Tp
M1 / Left hemisphere	*Visual areas*	**V1**	**[-14 -38 1]**	**5,50**	**2**	**1.61**	+	+	+	-	-	-
		V2d	**[-7 -38 0]**	**5.43**	**1**	**1.27**	+	-	+	+*	-	-
		V2v	**[-10 -37 -6]**	**8.23**	**130**	**2.29**	+	+	+	+	-	-
		V3A	**[-6 -31 1]**	**8.70**	**454**	**1.80**	+	+	+	+	-	+
		V3/V4	**[-14 -34 7]**	**4,71**	**49**	**1,09**	+	+	+	+	-	+
		MST	**[-12 -22 2]**	**7,22**	**39**	**1,36**	+	+	+	+	-	+
		MT	**[-20 -23 0]**	**4.78**	**8mm³**	**1.34**	+	-	-	+	+*	+
	Temporal areas	**FST**	**[-19 -20-2]**	**6,57**	**32**	**1,63**	+	+	+	+	-	+
		TEO	*[-24 -20 -9]*	*4.12*	*10*	*0.77*	+	-	+	+	-	+
	Parietal areas	**LOP**	**[-7 -30 7]**	**4.44**	**3**	**1.91**	+	-	+	+	-	+
		MIP	**[-14 -24 13]**	**4.78**	**8mm³**	**0.79**	+	-	-	-	-	-
		LIP	**[-15 -21 11]**	**4.74**	**29**	**0.93**	+	-	-	-	-	-
		PGm	*[-4 -18 5]*	*3.34*	*3*	*0.71*	+	+	+	+	-	+
		VIP_{post}	**[-8 -24 12]**	**6,61**	**56**	**1,33**	+	+	+	+	-	+
		VIP_{ant}	**[-18 -14 9]**	**5,23**	**4**	**1,09**	+	-	+*	+	-	+*
	Prefrontal and premotor areas	**PMZ**	**[-18 -1 16]**	**5,36**	**3**	**0,94**	+	+	+	-	-	-
		F4	**[-14 0 13]**	**4.17**	**1**	**0.81**	+	-	+*	-	-	-
		8	**[-15 3 7]**	**3.77**	**8mm³**	**0.52**	+	+	+	-	-	-
		44	**[-19 11 4]**	**3.45**	**5**	**0.51**	+	-	+	-	-	-
		45b	**[-15 12 6]**	**5.44**	**7**	**0.70**	+	+	+	+	-	+
		45a	*[-19 13 8]*	*3.45*	*8mm³*	*0.49*	+	+	+	-	-	-
	Orbitofrontal areas	**14**	**[-1 21 2]**	**3.66**	**6**	**0.70**	-	-	-	+	-	-
		13	*[-7 17 8]*	*4.57*	*16*	*1.20*	+	+	+	+	-	-
		12	**[-20 15 4]**	**3.51**	**4**	**0.74**	+	-	+	-	-	-
	Somato-sensory area	*S2*	*[-19 -4 5]*	*3.79*	*10*	*0.72*	+	-	-	+	-	+
	Cingulate areas	**23**	**[-5 -20 2]**	**4.50**	**8mm³**	**0.97**	+	-	+*	+	-	+
		24d	**[-6 5 18]**	**3.79**	**16**	**0.83**	+	-	+	+*	-	+
		24c	*[-4 10 11]*	*3.30*	*3*	*0.59*	+	-	-	+	-	+
		24ab	**[-3 14 10]**	**3.78**	**6**	**0.75**	+	+	+	+	-	+
	Insular areas	*32*	*[-3 14 6]*	*3.72*	*4*	*0.86*	+	+	+	+	+	+
		IPro	**[- 16 1 -6]**	**3.80**	**11**	**0.53**	+	-	+*	+	-	+
	Subcortical area	**Pulvinar**	**[-12 -15 -1)**	**3.69**	**11**	**0.56**	+	+	+	-	-	-

	Areas	ROIs	Coordinates	*t*-score	ROI size	% PSC	Mean / V.T	Super / V.T	Max / V.T	Mean / Sp.Tpbi	Super / Sp.Tp	Max / Sp.Tp
M2 / Left hemisphere	*Visual areas*	**V1**	**[-18 -36 -6]**	**4,39**	**14**	**1,40**	+	+	+	+*	-	-
		V2d	**[-9 -36 -7]**	**4,63**	**74**	**1,42**	+	+	+	+	-	+*
		V3a	**[-12 -31 4]**	**5,54**	**12**	**1,21**	+	+	+	+	-	+*
		V4	**[-19 -27 1]**	**3.96**	**7**	**1.08**	+	-	+	+	-	+
		MST	**[-11 -26 1]**	**5,59**	**4**	**1,12**	+	+	+	+	-	+
		MT	**[-19 -27 1]**	**4.79**	**1**	**1.41**	+	-	-	+	-	+
	Temporal areas	**FST**	**[-18 -17 -1]**	**5,31**	**8**	**1,47**	+	+	+*	+*	-	-
		TEO	*[-21 -25 -6]*	*4.30*	*17*	*0.98*	+	+	+	+	-	-
	Parietal areas	**LOP**	**[-6 -27 3]**	**3.31**	**8mm³**	**0.93**	+	+	+	+	+	+*
		PIP	*[-7 -31 2]*	*4.04*	*8mm³*	*0.24*	+	+	+	-	-	-
		MIP	**[-8 -27 9]**	**3.58**	**8mm³**	**0.93**	+	-	-	+	+	+
		LIP	**[-9 -27 7]**	**4.84**	**1**	**1.12**	+	+	+	+	+	+
		PECg	*[-7 -21 9]*	*3.48*	*3*	*0.64*	+	+	+	+	-	-
		VIP_{post}	**[-10 -20 7]**	**3,35**	**3**	**0,52**	+	+	+	+	-	-
		VIP_{ant}	**[-13 -18 6]**	**3,81**	**8**	**0,65**	+	-	+	+	+	+
	Prefrontal and premotor areas	**PMZ**	**[-17 -5 13]**	**4,26**	**23**	**0,78**	+	+	+	+	-	+
		F4	**[-8 5 41]**	**4.14**	**5**	**0.72**	+	-	-	+	-	-
		44/8	**[-15 2 9]**	**6,60**	**55**	**1,47**	+	+	+	+	-	-
		45b	**[-17 2 12]**	**4.39**	**8mm³**	**1.19**	+	+	-	-	-	-
		46 v	*[-13 7 11]*	*3.73*	*14*	*0.80*	+	-	-	-	-	+
		46d	**[-2 23 15]**	**3.70**	**4**	**0.94**	+	-	+	-	-	-
	Orbitofrontal areas	**11/14**	**[-4 12 7]**	**3.84**	**8**	**0.70**	+	-	+	+	-	+*
		12	**[-18 10 6]**	**4.80**	**1**	**1.65**	+	+	+	+	-	+*
	Somato-sensory areas											
		2	*[-2 -24 17]*	*3.16*	*2*	*1,05*	+	+	+	+	-	-
		3b	*[-14 -14 11]*	*3.36*	*2*	*0.84*	-	-	-	-	-	-
	Cingulate areas											
		24d	**[-5 8 15]**	**4.43**	**33**	**0,78**	+	+	+	+	-	+*
		24ab	**[-5 5 7]**	**4.73**	**40**	**0.97**	+	+	+	+	+	+
	Insular areas											
		IPro	**[-15 -1 -1]**	**3.91**	**8**	**0.96**	+	+	+	+	-	+*
	Subcortical area	**Pulvinar**	**[-3 -10 1]**	**3.56**	**4**	**0.83**	+	-	-	+	-	-

Table 1. Summary of main ROIs activated by the fully predictive bimodal stimulations, per monkey (M1/M2), for the left hemisphere.

For each ROI, the table indicates peak location (x, y and z coordinates with respect to the anterior commissure), t-score at the local maximum, ROI size in voxel unit ($8mm^3$ corresponds to the ROI created by an $8mm^3$ sphere when the actual activation is too large and merges with adjacent activations), the percent signal change corresponds to the PSC of the VT fully predictive bimodal activation with respect to fixation activations sampled in the same blocks. The table also indicates 1) whether the VT fully predictive multisensory response statistically fulfils (+) or not (-) the mean-criterion, super-additive criterion and max-criterion for multisensory integration and 2) whether the VT fully predictive multisensory response statistically fulfils (+) or not (-) the mean-criterion, super-additive criterion and max-criterion for the integration of spatial and temporal predictive cues, or has a trend towards significance (*, $0.05<p<0.07$). Bold characters code for the areas identified in 3 or more hemispheres. Italic characters code for the areas identified in 2 or less hemispheres. The areas are identified and labelled in reference to the nomenclature used in the Lewis and Van Essen atlas as available in Caret and in the Scalable brain atlas. Grey shaded cells correspond to cortical activations that are missing in the corresponding cortical hemisphere.

M1 / Right hemisphere													
	Areas	ROIs	Coordinates	*t*-score	ROI size	% PSC	Mean / V.T	Super / V.T	Max / V.T	Mean / Sp.Tpbi	Super / Sp.Tp	Max / Sp.Tp
	Visual areas	**V1**	**[5 -36 1]**	**5,14**	**6**	**1,48**	+	-	+	+	-	+
		V2d	**[7 -38 1]**	**4.86**	**2**	**1.48**	+	+	+	+*	-	-
		V2v	**[7 -30 -4]**	**5,26**	**6**	**1,84**	+	-	+	-	-	-
		V3A	**[11 -30 3]**	**5.29**	**5**	**1.58**	+	+	+	+	-	+
		V3	**[7 -27 1]**	**5,90**	**8**	**1,25**	+	+	+	+	+	+
		MST	**[11 -22 3]**	**5,43**	**10**	**1,20**	+	+	+	+	-	+
		MT	**[12 -27 7]**	**3.80**	**3**	**0.71**	+	-	-	+	-	-
	Temporal areas											
		TEa	*[21 -4 -11]*	*3.75*	*11*	*0.82*	+	-	-	+	+	+
		ST2g	*[22 0 0]*	*3.57*	*4*	*0.90*	+	-	-	-	-	-
		TPo	*[14 5 -9]*	*3.60*	*5*	*0.59*	+	+	+	+	+*	+
	Parietal areas											
		PIP	*[3 -26 10]*	*4.02*	*18*	*0.76*	+	+	+	+	-	-
		PGm	*[0 -17 9]*	*3.31*	*8mm³*	*0.65*	+	-	-	+	+	+
		VIP_{post}	**[6 -21 9]**	**4.24**	**6**	**0.99**	+	+	+	+	-	+
		VIP_{ant}	**[10 -16 9]**	**3,16**	**1**	**0,62**	+	-	-	+	+*	+
	Prefrontal and premotor areas	**PMZ**	**[13 -3 14]**	**3,96**	**11**	**0,58**	+	+	+	-	-	-
		F4	**[7 ; 0 ; 16]**	**4,38**	**15**	**0,41**	+	+	+	+	+	+
		44/8	**[11 2 9]**	**4,86**	**1**	**1,02**	+	+	+	+	-	+*
		46d	**[11 11 12]**	**3.12**	**1**	**0.74**	+	-	+	+*	-	-
	Orbitofrontal areas											
		12	**[16 16 4]**	**3.83**	**3**	**1.21**	+	+	+	+	-	+*
		11	*[9 20 9]*	*3.74*	*11*	*0.79*	+	-	+	+	-	-
	Somato-sensory area											
	Cingulate areas	**23**	**[1 -27 5]**	**3.82**	**9**	**1.00**	+	+	+	+	-	+
		24c	*[1 12 15]*	*3.20*	*1*	*1.20*	-	-	-	+	-	-
		24ab	**[0 7 10]**	**3.30**	**1**	**0.54**	-	-	-	+	+	+
	Insular areas											
		IPa	*[15 -10 2]*	*4.06*	*7*	*0.64*	+	+	+	+	+*	+
	Subcortical area	**Pulvinar**	**[6 -14 -1]**	**3.15**	**2**	**0.67**	+	-	-	+	-	+

M2 / Right hemisphere													
	Areas	ROIs	Coordinates	*t*-score	ROI size	% PSC	Mean / V.T	Super / V.T	Max / V.T	Mean / Sp.Tpbi	Super / Sp.Tp	Max / Sp.Tp
	Visual areas	**V1**	**[15-36-6]**	**3,75**	**9**	**0,87**	+	+	+	+	-	+
		V2d	**[9-36-7]**	**4,25**	**43**	**1,38**	+	+	+	+	-	-
		V2v	**[11 -29 -7]**	**3.24**	**1**	**1.41**	+	+	+	+	-	-
		V3a	**[12 -32 1]**	**4.90**	**8mm³**	**0.90**	+	-	+	+	-	+
		V4	**[22 -31 -2]**	**3.73**	**10**	**0.78**	+	+	+*	+	-	+
		MST	**[14 -26 0]**	**5,83**	**6**	**1,04**	+	+	+	+	-	+
		MT	**[19 -25 -1]**	**4.59**	**8**	**1.04**	+	+	+	+	-	+
	Temporal areas	**FST**	**[16 -20 -2]**	**3,93**	**33**	**0,89**	+	+	+	+	-	+
	Parietal areas	**LOP**	**[12 -32 1]**	**4.90**	**1**	**1.09**	+	-	+	+	-	+*
		MIP	**[4 -32 5]**	**4.23**	**8mm³**	**0.41**	+	+	+	-	-	-
		LIP	**[5 -31 5]**	**5,64**	**12**	**1,17**	+	+	+	+	-	+
		VIP_{post}	**[7 -26 4]**	**4.40**	**8mm³**	**0.96**	+	+	+	+	-	+*
	Prefrontal and premotor areas	**F4**	**[13 -2 14]**	**3.33**	**2**	**1.32**	+	-	-	+	-	-
		8	**[20 6 11]**	**3.90**	**2**	**1.32**	+	-	-	+	-	-
		44	**[16 4 9]**	**4.67**	**8mm³**	**0.70**	+	+	+	+*	-	-
		45b	**[15 1 10]**	**4,71**	**169**	**1,04**	+	+	+	+	-	+*
		46d	**[11 17 18]**	**3.29**	**1**	**1.28**	+	+	+	+	-	-
	Orbitofrontal areas	**13-14**	**[8 14 9]**	**4.49**	**105**	**0.94**	+	+	+	+	+	+
		12	**[18 10 4]**	**3.79**	**8mm³**	**1.01**	+	+	+	-	-	-
	Somato-sensory area	*3b*	*[23 -7 5]*	*3.23*	*3*	*0.88*	+	+	+	+	+	+
	Cingulate areas	**23**	**[4 -16 12]**	**3.55**	**3**	**0.58**	+	+	+*	+	+	+
		24d	**[6 -6 12]**	**3.20**	**3**	**0,54**	+	+	+	+	+*	+
	Insular areas	*Ri*	*[19 -18 5]*	*4.20*	*12*	*0.99*	+	+	+	+	-	+
		IPa	*[18 -12 -6]*	*3.34*	*2*	*0.86*	+	+	+	+	-	+
		IPro	**[17 0 -2]**	**3.72**	**4**	**0.98**	+	+	+	+	-	+
	Subcortical area	**Pulvinar**	**[7 -12 2]**	**4.00**	**10**	**1.07**	+	+	+	+	-	+*

Table 2. Summary of main ROIs activated by the fully predictive bimodal stimulations, per monkey (M1/M2), for the right hemisphere. All as in Table 1.

		Monkey 1				Monkey 2			
		Visuo-tactile multisensory integration		Integration of spatial and temporal predictive cues		Visuo-tactile multisensory integration		Integration of spatial and temporal predictive cues	
Areas	ROIs	Left Hem.	Right Hem.	Left Hem.	Right Hem.	Left Hem.	Right Hem.	Left Hem.	Right Hem.
Visual areas	**V1**	3	2	0	2	3	3	1	2
	V2d	2	3	1	1	3	3	2	1
	V2v	3	2	1	0		3		1
	V3A	3	3	2	2	3	2	2	2
	V3/V4	3	3	2	3	2	3	2	2
	MST	3	3	2	2	3	3	2	2
	MT	1	1	3	1	1	3	2	2
Temporal areas	**FST**	3		2		3	3	1	2
	TEO	2		2		3		1	
	TEa		1		3				
	ST2g		1		0				
	TPo		3		3				
Parietal areas	**LOP**	2		2		3	2	3	2
	PIP		3		1	3		0	
	MIP	1		0		1	3	3	0
	LIP	1		0		3	3	3	2
	PECg					3		1	
	PGm	3	1	2	3				
	VIP$_{post}$	3	3	2	2	3	3	1	2
	VIP$_{ant}$	2	1	2	3	2		3	
Prefrontal and premotor areas	**PMZ**	3	3	0	0	3		2	
	F4	2	3	0	3	1	1	1	1
	8	3		0		3	1	1	1
	44	2	3	0	2		3		1
	45b	3		2		2	3	0	2
	45a	3		0					
	46 v					1		1	
	46 d		2		1	2	3	0	1
Orbitofrontal areas	**14**	0		1		2	3	2	3
	13	3		1					
	12	2	3	0	2	3	3	2	0
	11		2		1				
Somato-sensory area	*S2*	1		2					
	2					3		1	
	3b					0	3	0	3
Cingulate areas	**23**	2	3	2	2		3		3
	24d	2		2		3	3	2	3
	24c	1	0	2	1				
	24ab	3	0	2	3	3		3	
Insular areas	*32*	3		3					
	Ri						3		2
	IPa		3		3		3		2
	IPro	2		2		3	3	2	2
Subcortical area	**Pulvinar**	3	1	0	2	1	3	1	2

Table 3. Summary of number functional integration criteria (mean-, max- and super-) that reach statistical significance ($p<0.05$), per ROI, per hemisphere, per monkey, for visuo-tactile multisensory integration and for the integration of spatial and temporal predictive cues. All conventions are as in Table 1.

Visuo-tactile multisensory integration	p-level	Mean-criterion	Max-criterion	Super-criterion
M1	***p<0.05***	***95%***	***71%***	***52%***
	0.05<p<0.07		*10%*	
M2	***p<0.05***	***100%***	***78%***	***74%***
	0.05<p<0.07		*10%*	
Integration of spatial and temporal predictive cues	p-level	Mean-criterion	Max-criterion	Super-criterion
M1	***p<0.05***	***64%***	***52%***	***7%***
	0.05<p<0.07	*10%*	*7%*	*7%*
M2	***p<0.05***	***85%***	***41%***	***15%***
	0.05<p<0.07	*7%*	*26%*	*2%*

Table 4. Percentage of ROIs fulfilling the different functional integration criteria for each monkey. Percentage of ROIs reaching near-significance are indicated for discussion.

Peripersonal space

Summary of publications on Peripersonal space

While extra-personal space is often erroneously considered as a unique entity, early neuropsychological studies report a dissociation between near and far space processing both in humans and in monkeys (Rizzolatti et al., 1983; Halligan and Marshall, 1991; Cowey et al., 1994, 1999; Vuilleumier et al., 1998; Keller et al., 2005; Aimola et al., 2013).

Chapter 3: Cortical networks for encoding near and far space in the non-human primate

(Submitted in "*Cerebral Cortex*", April 12th 2017, CerCor-2017-00471).

A lot of studies show the involvement of prefrontal and parietal cortical regions in the encoding of space representation both in the non-human primate and in humans (Hyvärinen and Poranen, 1974; Rizzolatti et al., 1983; Gentilucci et al., 1988; Graziano et al., 1994; Gross and Graziano, 1995; Fogassi et al., 1996; Duhamel et al., 1998; Bremmer et al., 2000, 2002a, 2002b, 2013; Quinlan and Culham, 2007; Guipponi et al., 2013). However, among these cortical regions, no study to date provides, in the non-human primate, a holistic description of the cortical networks involved in the processing of far and near space.

In this study, we use fMRI in the non-human primate immersed in a naturalistic 3D environment to provide a precise mapping of the cortical networks involved in the treatment of near space with respect to far space. To this effect, we have constructed two real 3D cubes, a small one and a big one. The 6 faces of each cube were decorated with 6 different fractal images. The monkeys were required to fixate on a central LED during all the acquisition and the presentation of stimuli. Monkeys were rewarded for maintaining this fixation as long as possible. The small cube stimulated either the near space (15cm from the monkey's face) or the

far space (150cm from the monkey's face). The big cube stimulated only the far space. The small cube placed at 15 cm from the monkey's face had the same apparent size as the large cube placed at 150 cm.

This paper describes a functional gradient going from selective near space coding, to preferential near space coding, to unselective space coding, to preferential far space coding and selective far space coding. Particularly, far space processing is found to involve occipital, temporal, parietal, posterior, cingulate as well as orbitofrontal regions, possibly subserving the processing of the shape and identity of the object. Near space processing is found to involve temporal, parietal and prefrontal regions, possibly subserving the preparation of an arm/hand mediated action towards the object used for the near space stimulation. Besides, we describe a cortical network activated by intrusion into peripersonal space. Interestingly, this network is only partially overlapping with the near space coding network. Overall, these observations argue for multiple space representations, the functional significance of which remains to be assigned.

Chapter 4: Neuronal bases of peripersonal and extrapersonal spaces, their plasticity and their dynamics: Knowns and unknowns (Published in "*Neurospsychologia*", April 2015 • 70(2015)313–326)

The accumulated knowledge on the understanding of the neural bases involved in the processes of near and far space has grown in recent years. In this review, we focus on non-human primate research and we review the single cells, areal and cortical functional network mechanisms that are proposed to underlie extrapersonal and peripersonal space representations.

A majority of studies are developed in relation with a theoretical framework centered on the fact that it is the actions and specifically the arm and the actions linked to the hand that shape the cortical representation of the peripersonal space.

In this review, we propose to extend this framework by including other variables that have the potential to shape this space: low-level sensory signals from other modalities (proprioceptive, tactile, auditory, vestibular), oculomotor signals, proximal and distal motor signals, object use, emotional and social contexts. Some of these variables involve learning, such as learning how to manipulate a given tool. Others are dynamic in that they continuously change more or less predictively, such as the trajectory of a conspecific or his/her emotional state. As a result, peripersonal space appears to be not only plastic, that is to say affected by training and repeated exposure to a given sensorimotor context, but also dynamic, that is capable of an instantaneous adjustment to the ongoing low-level (sensory and motor) and higher order (inferential, emotional, social) context.

References

Aimola L, Schindler I, Venneri A (2013) Task- and response related dissociations between neglect in near and far space: a morphometric case study. Behav Neurol 27:245–257.

Bremmer F, Duhamel JR, Ben Hamed S, Graf W (2000) Stages of self-motion processing in primate posterior parietal cortex. Int Rev Neurobiol 44:173–198.

Bremmer F, Duhamel J-R, Ben Hamed S, Graf W (2002a) Heading encoding in the macaque ventral intraparietal area (VIP). European Journal of Neuroscience 16:1554–1568.

Bremmer F, Klam F, Duhamel J-R, Ben Hamed S, Graf W (2002b) Visual–vestibular interactive responses in the macaque ventral intraparietal area (VIP). European Journal of Neuroscience 16:1569–1586.

Bremmer F, Schlack A, Kaminiarz A, Hoffmann KP (2013) Encoding of movement in near extrapersonal space in primate area VIP. Front Behav Neurosci 7:8.

Cowey A, Small M, Ellis S (1994) Left visuo-spatial neglect can be worse in far than in near space. Neuropsychologia 32:1059–1066.

Cowey A, Small M, Ellis S (1999) No abrupt change in visual hemineglect from near to far space. Neuropsychologia 37:1–6.

Duhamel J-R, Colby CL, Goldberg ME (1998) Ventral Intraparietal Area of the Macaque: Congruent Visual and Somatic Response Properties. Journal of Neurophysiology 79:126–136.

Fogassi L, Gallese V, Fadiga L, Luppino G, Matelli M, Rizzolatti G (1996) Coding of peripersonal space in inferior premotor cortex (area F4). J Neurophysiol 76:141–157.

Gentilucci M, Fogassi L, Luppino G, Matelli M, Camarda R, Rizzolatti G (1988) Functional organization of inferior area 6 in the macaque monkey. I. Somatotopy and the control of proximal movements. Exp Brain Res 71:475–490.

Graziano MS, Yap GS, Gross CG (1994) Coding of visual space by premotor neurons. Science 266:1054–1057.

Gross CG, Graziano MSA (1995) REVIEW : Multiple Representations of Space in the Brain. Neuroscientist 1:43–50.

Guipponi O, Wardak C, Ibarrola D, Comte J-C, Sappey-Marinier D, Pinède S, Hamed SB (2013) Multimodal Convergence within the Intraparietal Sulcus of the Macaque Monkey. J Neurosci 33:4128–4139.

Halligan PW, Marshall JC (1991) Left neglect for near but not far space in man. Nature 350:498–500.

Hyvärinen J, Poranen A (1974) Function of the parietal associative area 7 as revealed from cellular discharges in alert monkeys. Brain 97:673–692.

Keller I, Schindler I, Kerkhoff G, von Rosen F, Golz D (2005) Visuospatial neglect in near and far space: dissociation between line bisection and letter cancellation. Neuropsychologia 43:724–731.

Quinlan DJ, Culham JC (2007) fMRI reveals a preference for near viewing in the human parieto-occipital cortex. NeuroImage 36:167–187.

Rizzolatti G, Matelli M, Pavesi G (1983) Deficits in attention and movement following the removal of postarcuate (area 6) and prearcuate (area 8) cortex in macaque monkeys. Brain 106 (Pt 3):655–673.

Vuilleumier P, Valenza N, Mayer E, Reverdin A, Landis T (1998) Near and far visual space in unilateral neglect. Ann Neurol 43:406–410.

Chapter 3 :

Cortical networks for encoding near and far space in the non-human primate

Submitted in "*Cerebral Cortex*", April 12th 2017, CerCor-2017-00471.

Cortical networks for encoding near and far space in the non-human primate

Justine Cléry, Olivier Guipponi, Soline Odouard, Claire Wardak, Suliann Ben Hamed

Institut des Sciences Cognitives Marc Jeannerod, UMR5229, CNRS-Université Claude Bernard Lyon I*, 67 Boulevard Pinel, 69675 Bron, France*

Corresponding author: Suliann Ben Hamed, benhamed@isc.cnrs.fr

Keywords: naturalistic environment, near space, far space, macaque monkey, fMRI.

Running title: Near and Far Space processing in the Non-Human Primate.

Abstract

While extra-personal space is often erroneously considered as a unique entity, early neuropsychological studies report a dissociation between near and far space processing both in humans and in monkeys. Here, we use functional MRI in a naturalistic 3D environment to describe the non-human primate near and far space cortical networks. We describe the co-occurrence of two extended functional networks respectively dedicated to near and far space processing. Specifically, far space processing involves occipital, temporal, parietal, posterior cingulated as well as orbitofrontal regions, possibly subserving the processing of the shape and identity of objects. In contrast, near space processing involves temporal, parietal and prefrontal regions, possibly subserving the preparation of an arm/hand mediated action in this proximal space. Interestingly, this network also involves somatosensory regions, suggesting a cross-modal anticipation of touch by a nearby object. Last, we also describe cortical regions that process both far and near space with a preference for one or the other. This suggests a continuous encoding of relative distance to the body, in the form of a far-to-near or near-to-far gradient. We propose that these cortical gradients in space representation subserve the physically delineable peripersonal spaces described in numerous psychology and psychophysics studies.

INTRODUCTION

Our environment is often perceived as a unitary space, however growing evidence demonstrates that the brain contains a modular and a dynamic representation of space. Early neuropsychological reports demonstrate that the unilateral ablation of the pre-arcuate cortex to area 8, corresponding to the frontal eye fields, produces, in the non-human primate, an inattention to contralateral objects, more pronounced for far objects than for near objects (Rizzolatti et al. 1983). In contrast, the inattention to contralateral objects produced by the unilateral ablation of premotor area 6 is more pronounced for near than for far objects (Rizzolatti et al. 1983). In 1991, a single case study by Halligan and Marshall, presents the first neuropsychological evidence for a left neglect in near space but not in far space after a unilateral right hemisphere stroke in humans (Halligan and Marshall 1991). The finding of the opposite dissociation confirms that, as is the case for macaque monkeys, far and near space are separately coded by the human brain (Cowey et al. 1994, 1999; Vuilleumier et al. 1998), though a task dependence of far and near space processing deficits is reported (Keller et al. 2005; Aimola et al. 2012).

In recent years, fMRI studies show that the coding of near space involves a dorsal network including the left dorsal occipital cortex, the left intraparietal cortex and the left ventral premotor cortex, while the coding of far space involves a ventral network including the ventral occipital cortex bilaterally and the right medial temporal cortex (Weiss et al. 2000; Aimola et al. 2012). The reversible perturbation of the right angular gyrus (ANG) using transcranial magnetic stimulation (TMS) alters near space perception while that of the right supramarginal gyrus (SMG) induces a higher perception deficit in far than in near space (Bjoertomt et al. 2002, 2009). In spite of this dissociation, the network involved in perceptual and motor processes remains unaffected by whether the task is being performed in the near or in the far space (Weiss et al. 2003).

Peripersonal neurons fire both when a tactile stimulus is delivered to the animal's skin and when a visual stimulus is presented in the space near the part of the body where the tactile field is located. These have been described in several cortical regions: the prefrontal cortex (Gentilucci et al. 1988; Graziano et al. 1994; Gross and Graziano 1995; Fogassi et al. 1996), corroborating with the near space neglect observed following premotor area 6 lesions (Rizzolatti et al. 1983); in the parietal cortex where Hyvärinen and Poranen (1974) describe the visual response of parietal neurons "as an anticipatory activation" that appears before the neuron's tactile RF is touched. The multimodal ventral intraparietal area VIP stands out in this respect (Duhamel et al. 1998; Avillac et al. 2004, 2007, Guipponi et al. 2013, 2015). This region encodes both large field visual movement mimicking the consequences of the displacement of a subject within its environment (Bremmer et al. 2000; Bremmer, Duhamel, et al. 2002; Bremmer, Klam, et al. 2002) and the movement of visual objects within the near peripersonal space (Bremmer et al. 1997, 2013), this, in spite of the fact that no sensitivity to the 3-dimensional structure of static stimuli could be found in VIP (Durand et al. 2007). In comparison, human VIP shows no preference for any particular spatial range (Quinlan and Culham 2007).

Beyond these two prefrontal and parietal cortical regions, little is known about the whole brain network that is involved in far space and near space processing in the non-human primate. In particular, while several functional magnetic resonance imaging (fMRI) studies describe the cortical regions involved in the processing of 3-dimensional shape from disparity (Durand et al. 2009; Joly et al. 2009) or shading and texture (Nelissen et al. 2009), to our knowledge, no study to date provides, in this specie, a description of the cortical networks involved in the processing of far and near space. Here, we use fMRI in the non-human primate immersed in a naturalistic 3D environment to describe a functional gradient going from selective near space coding, to preferential near space coding, to unselective space coding, to preferential far space

coding and selective far space coding. We also describe a cortical network activated by intrusion into peripersonal space. Interestingly, this network is only partially overlapping with the near space coding network. Overall, these observations argue for multiple space representations the functional significance of which remains to be assigned.

MATERIAL AND METHODS

All procedures were in compliance with the guidelines of European Community on animal care (European Community Council, Directive No. 86–609, November 24, 1986). All the protocols used in this experiment were approved by the animal care committee (Department of Veterinary Services, Health & Protection of Animals, permit number 69 029 0401) and the Biology Department of the University Claude Bernard Lyon 1. The animals' welfare and the steps taken to ameliorate suffering were in accordance with the recommendations of the Weatherall report, "The use of non-human primates in research".

Subjects and experimental setup

Two rhesus monkeys (female M1, male M2, 5-7 years old, 5-7 kg) participated to the study. The animals were implanted with a plastic MRI compatible headset covered by dental acrylic. The anesthesia during surgery was induced by Zoletil (Tiletamine-Zolazepam, Virbac, 15 mg/kg) and followed by Isoflurane (Belamont, 1-2%). Post-surgery analgesia was ensured thanks to Temgesic (buprenorphine, 0.3 mg/ml, 0.01 mg/kg). During recovery, proper analgesic and antibiotic coverage were provided. The surgical procedures conformed to European and National Health guidelines for the care and use of laboratory animals.

During the scanning sessions, monkeys sat in a sphinx position in a plastic monkey chair positioned within a horizontal magnet (1.5-T MR scanner Sonata; Siemens, Erlangen, Germany). Their head was restrained and they were equipped with MRI-compatible headphones customized for monkeys (MR Confon GmbH, Magdeburg, Germany). A radial receive-only surface coil (10-cm diameter) was positioned above the head. Monkeys were required to fixate a LED placed at 83cm away from their face, at eye level, aligned with their sagittal axis. Eye position was monitored at 120 Hz during scanning using a pupil-corneal reflection tracking system (Iscan®, Cambridge, MA). The calibration procedure involved the

fixation LED and 4 additional LEDs, placed in the same coronal plane as the fixation LED. All five LEDs were sequentially switched on and off and the monkey was rewarded for orienting and maintaining its gaze towards the illuminated LED. These four additional LEDs were subsequently removed during the main task during which only the central LED was present. Monkeys were rewarded with liquid dispensed by a computer-controlled reward delivery system (Crist®) thanks to a plastic tube coming to their mouth. The reward probability and quantity increased as fixation duration increased according to a subject-specific schedule, thus positively reinforcing fixation behavior. Fixation was considered as successful when the eyes remained in a window of 1° around the fixation LED. The reward schedule was uncorrelated with the scanning schedule. The task and all the behavioral parameters were controlled by two computers running Matlab® and Presentation®. Monkeys were trained in a mock scan environment approaching to the best the actual MRI scanner setup. Actual scanning was performed once their fixation performance was maximized.

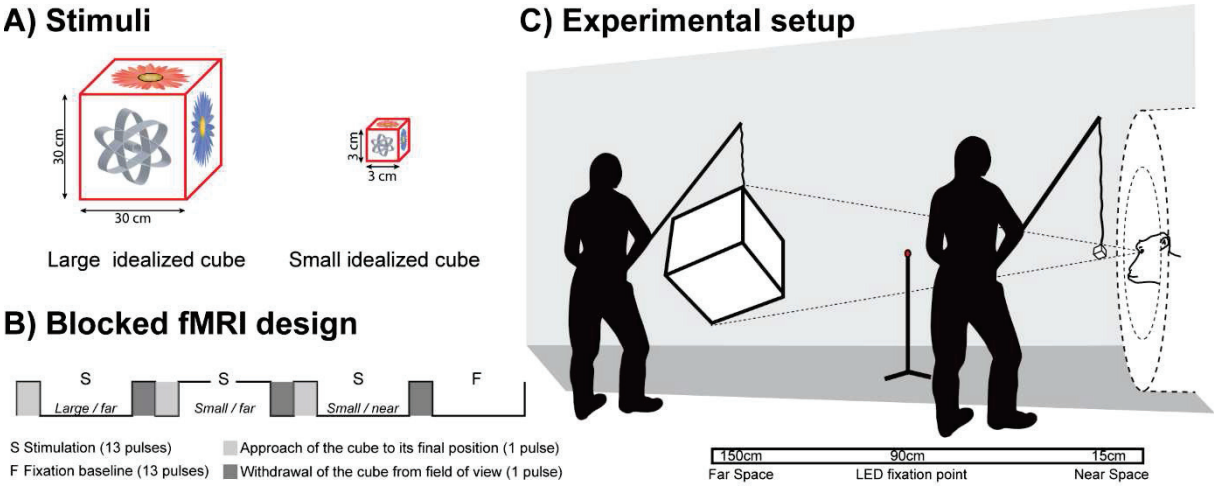

Figure 1: Figure 1: Experimental fMRI protocol. A) 3D naturalistic stimuli, a large 30x30x30 cm3 cube and an identical small 3x3x3 cm3 cube. The 6 faces of each transparent cube were decorated with 6 different fractal images. B) Block design. C) Experimental set up. Near space (15 cm from the monkey's face) and far space (150 cm from the monkey's face) were stimulated with the two types of 3D stimuli (same apparent sizes). Fixation is achieved at an intermediate position (red fixation LED, at 90cm).

Task and stimuli

The animals were trained to maintain fixation on the central LED. This allowed to control for eye vergence signals all throughout the experimental runs. An enriched stable visual scene was installed around the fMRI aperture, in front of the monkeys, so as to maximize depth cues (2m high lateral black curtains hiding the experimenters, large wooden static sticks placed along the curtains and in the back of the room, visible to the monkeys throughout the experiment). Once this behavior was stabilized, monkeys were further trained to maintain fixation while 3D objects were presented at either an average of 15 cm in front of their eyes (i.e. in the space between their head and the fixation LED, see Figure 1C) or at an average of 150 cm (i.e. in the space beyond the fixation LED, see Figure 1C), thus allowing to stimulated the space situated respectively near and far from the animals. Stimulations were achieved with either a small cube (3x3x3 cm) or a large cube (30x30x30 cm, Figure 1A), attached to a rigid holding stick. These cubes had the same apparent size when the small cube was placed at 15cm from the subject and the larger cube was placed at 150cm (Figure 1C), thus allowing to control for size effects. These cubes were constructed with transparent plastic material and the presentation of the near small object did not hide the fixation LED from the monkey. In order to maximize depth cues, the edges of the cubes were highlighted with red stripes and their transparent faces were ornamented with fractal pictures, resized for each cube such that the edges and the images occupied the same proportion in each cube (Figure 1A). Each cube was attached to a thin wooden stick by means of a transparent nylon cord. During the stimulation duration, the cube was continuously agitated by the experimenter so as to prevent neuronal habituation, but only the cube and the stick were visible to the monkeys, as the experimenters stayed hidden behind the curtains. Three conditions were tested in blocks of 13 pulses: 1) the small cube presented in the near space; 2) the small cube presented in the far space and 3) the big cube presented in the far space. Both during training and testing, the cubes were approached

(1 pulse), agitated (13 pulses) and withdrawn (1 pulse) from the target location (near or far space) by two experimenters out of the field of view (behind the black opaque curtains), one controlling the small cube and the other the large cube. The stimulation instructions (count down, type of stimulation, pulse counts etc.) were delivered to them on a computer screen placed next to them and coupled to the experimental control system.

Functional time series (runs) were organized as follows (Figure 1B): a 13-volume block of stimulation category 1 was followed by a 13-volume block of stimulation category 2, a 13-volume block of stimulation category 3, and a 13-volume block of pure fixation (baseline). Before the beginning (resp. after the end) of each block of stimulation, 1 pulse was dedicated to the approach (resp. withdrawal) of the appropriate cube towards (resp. away from) the target space. Approaching or withdrawing the cubes involved only a minimal displacement of the curtains, thanks to two vertical slits in the curtains, placed respectively close to the magnet bore or at 150cm from the monkey. These slits were firmly closed back during the main stimulation blocks. A given sequence was played three times, resulting in a 174-volume run. The blocks for the 3 categories were presented in 6 counterbalanced possible orders.

Scanning

Before each scanning session, a contrast agent, monocrystalline iron oxide nanoparticle (Feraheme®, Vanduffel et al. 2001), was injected into the animal's femoral/saphenous vein (4-10 mg/kg). Brain activations produce increased BOLD signal changes. In contrast, when using MION contrast agents, brain activations produce decreased signal changes signal (Kolster et al. 2014). For the sake of clarity, the polarity of the contrast agent MR signal changes, which corresponds essentially to a cerebral blood volume (CBV) measurement, was inverted. We acquired gradient-echo echoplanar (EPI) images covering the whole brain (1.5 T; repetition

time (TR) 2.08 s; echo time (TE) 27 ms; 32 sagittal slices; 2x2x2-mm voxels). A total of 34 (22) runs was acquired for M1 (/M2).

Analysis

A total of 20 (15) runs were selected based on the quality of the monkeys' fixation throughout each run (>80% within the tolerance window). Time series were analyzed using SPM8 (Wellcome Department of Cognitive Neurology, London, United Kingdom). For spatial preprocessing, functional volumes were first realigned and rigidly coregistered with the anatomy of each individual monkey (T1-weighted MPRAGE 3D 0.6x0.6x0.6 mm or 0.5x0.5x0.5 mm voxel acquired at 1.5T) in stereotactic space. The JIP program (Mandeville et al. 2011) was used to perform a non-rigid coregistration (warping) of a mean functional image onto the individual anatomies.

Fixed effect individual analyses were performed for each condition in each monkey, with a level of significance set at $p<0.05$ corrected for multiple comparisons (FWE, $t>4.8$, unless stated otherwise).

To define the ***preferential near space network***, we contrasted the cortical activations obtained by the stimulation of near space by a small object to those obtained by the stimulation of far space by a large object of the same apparent size as the small object in the near space and was additionally masked by the activations obtained by the stimulation of near space by a small object contrasted by fixation condition (inclusive 'near space stimulation vs. fixation' mask, uncorrected level, $p=0.05$). To define the ***selective near space network***, the above preferential near space network was additionally masked by the activations obtained by far space stimulations (exclusive 'far space stimulation vs. fixation' mask, uncorrected level, $p=0.05$). To define the ***preferential far space network***, we contrasted the cortical activations obtained by the stimulation of far space by a large object of the same apparent size as the small object in the

near space to those obtained by the stimulation of near space by a small object and was additionally masked by the activations obtained by the stimulation of far space by a large object contrasted by fixation condition (inclusive 'far space stimulation vs. fixation' mask, uncorrected level, p=0.05). To define the ***preferential encoding of the large cube in the far space network***, we contrasted the cortical activations obtained by the stimulation of far space by a large object to those obtained by the stimulation of far space by a small object and was additionally masked by the activations obtained by the stimulation of far space by a large object contrasted by fixation condition (inclusive 'Large far space stimulation vs. fixation' mask, uncorrected level, p=0.05). To define the ***selective encoding of the large cube in the far space network***, the above preferential encoding of the large cube in the far space network was additionally masked by the activations obtained by the stimulation of far space by a small object (exclusive 'Small far space stimulation vs. fixation' mask, uncorrected level, p=0.05). To define the ***specific looming toward near space network***, we contrasted the cortical activations obtained by the looming of a small object toward near space to those obtained by the stimulation of near space by a small object and was additionally masked by the activations obtained by the looming of a small object toward near space contrasted by fixation condition (inclusive 'looming toward near space vs. fixation' mask, uncorrected level, p=0.05) and masked by the activations obtained by near space stimulations (exclusive 'near space stimulation vs. fixation' mask, uncorrected level, p=0.05).

In all analyses, realignment parameters, as well as eye movement traces, were included as covariates of no interest to remove eye movement and brain motion artifacts. When coordinates are provided, they are expressed with respect to the anterior commissure. Results are displayed on flattened maps obtained with Caret, for each monkey (Van Essen et al. 2001; http://www.nitrc.org/projects/caret/). The results were consistent in the two animals for all the discussed cortical regions (i.e. activations observed in at least 3 out of 4 hemispheres). Thus,

figures 4, 5 and 6 correspond to a group analysis, so as to simplify the presentation of the results. In this case, fixed effect group analyses were performed for each sensory modality and for conjunction analyses with a level of significance set at $p<0.05$ ($t>4.8$) and projected onto the anatomy of monkey M2. In order to have an unbiased group analysis, we selected the 15 best runs of M1 (in term of fixation performance), so as to have the same number of runs for each monkey. The results are then displayed on the flattened and fiducial maps of M2.

Assigning the activations to a specific cortical area was performed on each individual monkey brain using the monkey brain atlases made available on http://scalablebrainatlas.incf.org. These atlases allow mapping specific anatomical coronal sections with several cytoarchitetonic parcellation studies. We used the Lewis and Van Essen (2000) and the Paxinos Rhesus Monkey (2000) atlases.

Regions of interest. We performed regions of interest (ROI) analyses using MarsBar toolbox (Brett et al. 2002), based on the fixed effects individual analyses results. We defined geometric cubic ROIs (2x2x2 mm) centered on the local maximum t-score based on the activations obtained at FWE-corrected level (*t*-scores>4.8) on the specific near space activations, the preference near activations, the unselective near-far space activations, the preference far activations and the specific far space activations. The percent of signal change (PSC) are extracted for each ROI for all the runs using SPM8 and the MarsBar toolbox. The significance of these PSCs across all runs was assessed using a paired t-test, in Matlab™ (The MathWorks Inc., Natick, MA, USA).

RESULTS

Monkeys were exposed, in the same time series, to naturalistic near or far space stimulations (Figure 1), while maintaining their gaze at an intermediate fixation location, so as to keep vergence signals constant all throughout the recording runs. This design allows us to describe the cortical networks involved in near and far space processing in naturalistic conditions. The reported activations in figures 2 and 3 are identified using an individual analysis, with a level of significance set at $p<0.05$, corrected for multiple comparisons (FWE, $t>4.8$). The reported activations in figures 4, 5 and 6 are identified using a group analysis, with a level of significance set at $p<0.05$, corrected for multiple comparisons (FWE, $t>4.8$). As a result, they reflect the activations that are common to the two monkeys involved in the study.

Naturalistic near and far space stimulations

Naturalistic near space stimulations with a small cube (Figure 2, yellow upper maps, small near vs. fixation contrast) activated a small extent of the occipital striate and extrastriate areas, the temporal cortex (superior temporal sulcus), the parietal cortex, the prefrontal cortex (arcuate sulcus and posterior and anterior parts of principal sulcus) as well as the orbitofrontal cortex. Far space stimulations with a far cube with the same apparent size as the near small cube (Figure 2, blue middle maps, big far vs. fixation contrast) also activated a widespread cortical network including the entire striate and extrastriate cortex, the temporal cortex, the parietal cortex, the prefrontal cortex along the arcuate sulcus and the principal sulcus as well as the orbitofrontal cortex. When far space was stimulated using a cube of the same real size as the small cube used for the near space stimulation (Figure 2, green lower maps, small far vs. fixation contrast), a similar though smaller cortical network was activated. In the following, we identify those cortical regions that are either preferentially or specifically involved in near space and far space processing respectively.

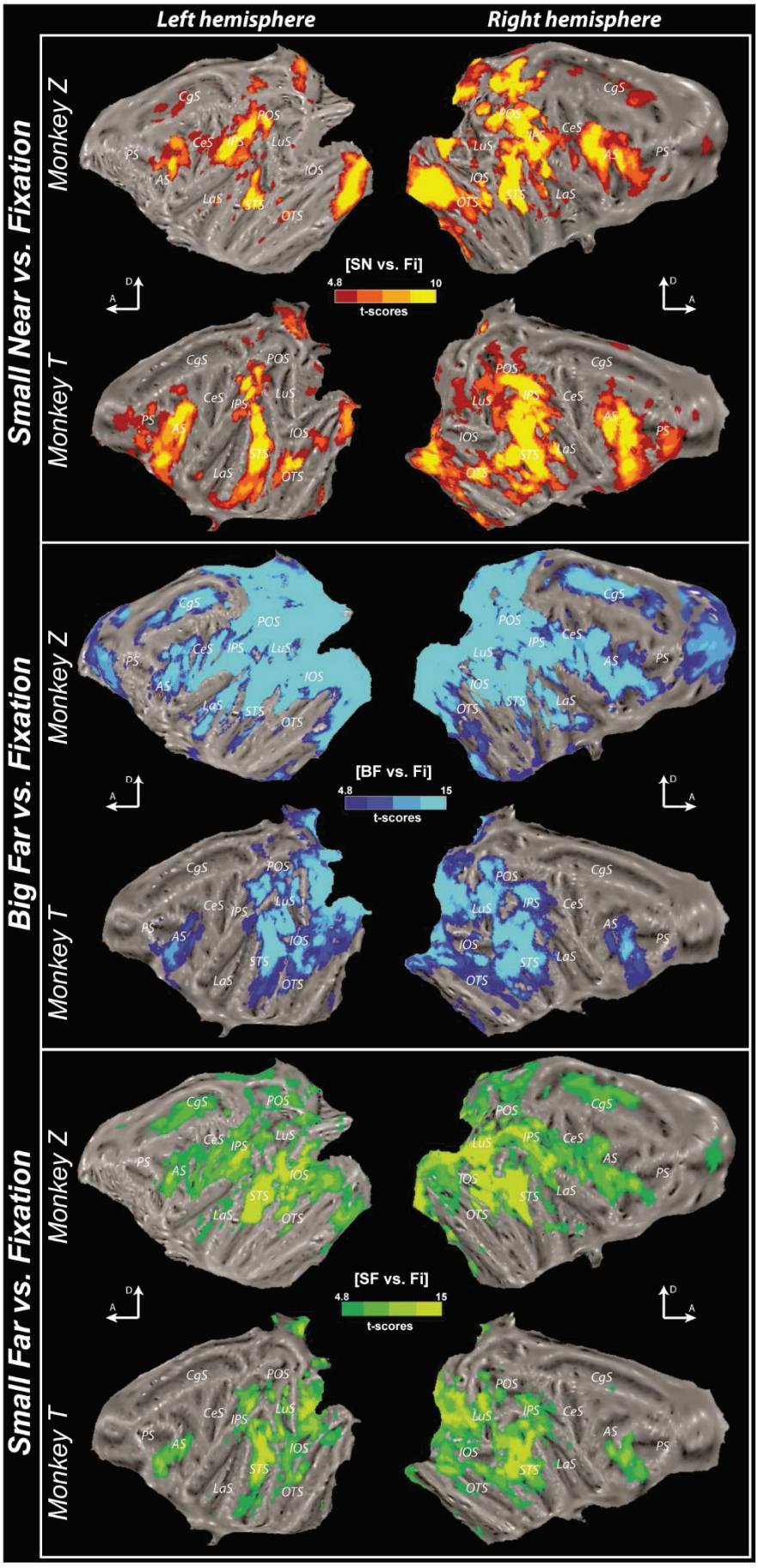
Left hemisphere
Right hemisphere
Small Near vs. Fixation
Big Far vs. Fixation
Small Far vs. Fixation
Monkey Z
Monkey T
[SN vs. Fi]
[BF vs. Fi]
[SF vs. Fi]
4.8
10
15
t-scores
CgS
POS
CeS
IPS
LuS
PS
AS
IOS
STS
LaS
OTS
D
A

Figure 2: Near space and far space individual analyses. Activations are presented on the flattened representation of the two monkey right and left hemispheres obtained with Caret. The upper part of the figure shows the near space stimulated with the small cube (SN) versus fixation contrast (t scores = 4.8 at $p<0.05$, FWE-corrected level in the red scale). Middle and lower panels present the far space respectively stimulated with the big (BF) and the small cubes (SF; t scores = 4.8 at $p<0.05$, FWE-corrected level respectively in the blue and green scales). A, Anterior; D, Dorsal; SN: small near; BF: big far; SF: small far. Cortical sulci: AS, arcuate sulcus; CgS, cingulate sulcus; CeS, central sulcus; IOS, inferior occipital sulcus; IPS, intraparietal sulcus; LaS, lateral (Sylvian) sulcus; LuS, lunate sulcus; OTS, occipital temporal sulcus; POS, parieto-occipital sulcus; PS, principal sulcus; STS, superior temporal sulcus.

Distinctions within the near space cortical network

In the following, we define three different functional near space networks: a restricted network selectively encoding near space; a larger network preferentially encoding near space with respect to far space and an even larger network encoding near space irrespectively of any coding for far space. The larger ***non-selective near space network*** corresponds to the one identified in Figure 2 (yellow upper maps, represented in the left panel of Figure 3 as a red contour) and discussed in the previous section. To define the ***preferential near space network***, we contrasted the cortical activations obtained by the stimulation of near space by a small object to those obtained by the stimulation of far space by a large object of the same apparent size as the small object in the near space and was additionally masked by the activations obtained by the stimulation of near space by a small object contrasted by fixation condition (inclusive 'near space stimulation vs. fixation' mask, uncorrected level, $p=0.05$; Figure 3: left panel, dark red, Figure 6: dark red). This contrast identifies bilateral cortical regions the contribution of which is statistically higher for near space than for far space. These include parietal areas: the posterior intraparietal sulcus (IPS: ventral intraparietal area VIP, the posterior medial intraparietal area MIP) as well as its anterior most tip (possibly anterior intraparietal area AIP), the medial parietal

cortex (area PGm) and the parietal opercular region area 7op; temporal areas: the rostral temporoparietal occipital area TPOr in the medial mid-to-anterior bank of the superior temporal sulcus, the intraparietal sulcus associated area IPa, the inferior temporal area TEAa-m, the dorsal portion of the subdivision TE1-3; insular regions: the parainsular cortex PI; somatosensory area SII within the medial bank of the lateral sulcus; prefrontal and premotor regions: dorsal premotor cortex F2, premotor area 4C or F4/F5 including premotor zone PMZ, the supplementary eye field, the frontal eye fields (area 8a as well as 8ac), prefrontal area 46p, prefrontal area 45B; frontal regions: the posterior orbitofrontal area 12.

To define the ***selective near space network***, the above preferential near space network was additionally masked by the activations obtained by far space stimulations (exclusive 'far space stimulation vs. fixation' mask, uncorrected level, p=0.05). This allows to identify a network that is exclusively involved in near space processing (Figure 3: left panel, red to yellow color scale, Figure 6: colored to yellow color scale, *t* scores = 4.8 and above, FWE-corrected level). This analysis describes discrete bilateral regions within the majority of the cortical areas highlighted by the previous contrast.

Distinctions within the far space cortical network

Likewise, we define three different functional far space networks: a restricted network selectively encoding far space; a larger network preferentially encoding far space with respect to near space and an even larger network encoding far space irrespectively of any coding for near space. The larger ***non-selective far space network*** corresponds to the one identified in Figure 2 (blue middle maps, represented in the right panel of Figure 3 as a blue contour) and discussed above. To define the ***preferential far space network***, we contrasted the cortical activations obtained by the stimulation of far space by a larger object to those obtained by the stimulation of near space by a small object of the same apparent size as the large object in the

far space was additionally masked by the activations obtained by the stimulation of far space by a large object contrasted by fixation condition (inclusive 'far space stimulation vs. fixation' mask, uncorrected level, p=0.05; Figure 3: right panel, dark blue, Figure 6: dark blue). This contrast identifies bilateral cortical regions the contribution of which is statistically higher for far space than for near space. A strong inter-individual variability can be observed, these activations being larger in Monkey Z than in monkey T. This is possibly due to the relative size between the large stimulus and the subject's body size. This will need to be further explored. In the following, only the common activations are described. These encompass the entire visual striate and extrastriate cortex: areas V1, V2, V3, V3A and V4; they also include parietal cortical regions: the posterior intraparietal area PIP, the lateral intraparietal area LIP, the medial parietal convexity (area 5v), the lateral parietal convexity (area 7a, 7ab and 7b), as well as the posterior most part of the intraparietal sulcus (caudial intraparietal area CIP, parietal reach region, PRR), these activities extending towards the parieto-occipital cortex (including areas V6A and V6); temporal cortex: medial and superior temporal area MT and MST.

When this contrast is additionally masked by the activations obtained by near space stimulations (exclusive 'near space stimulation vs. fixation' mask, uncorrected level, p=0.05), thus defining the ***selective far space network***, a network that is selectively involved in far space processing can be identified (Figure 3: right panel, dark blue to light blue color scale, Figure 6: dark blue to light blue color scale, *t* scores = 4.8 and above, FWE-corrected level). This analysis describes discrete bilateral regions essentially in occipital and temporal areas highlighted by the previous contrast and few parietal areas.

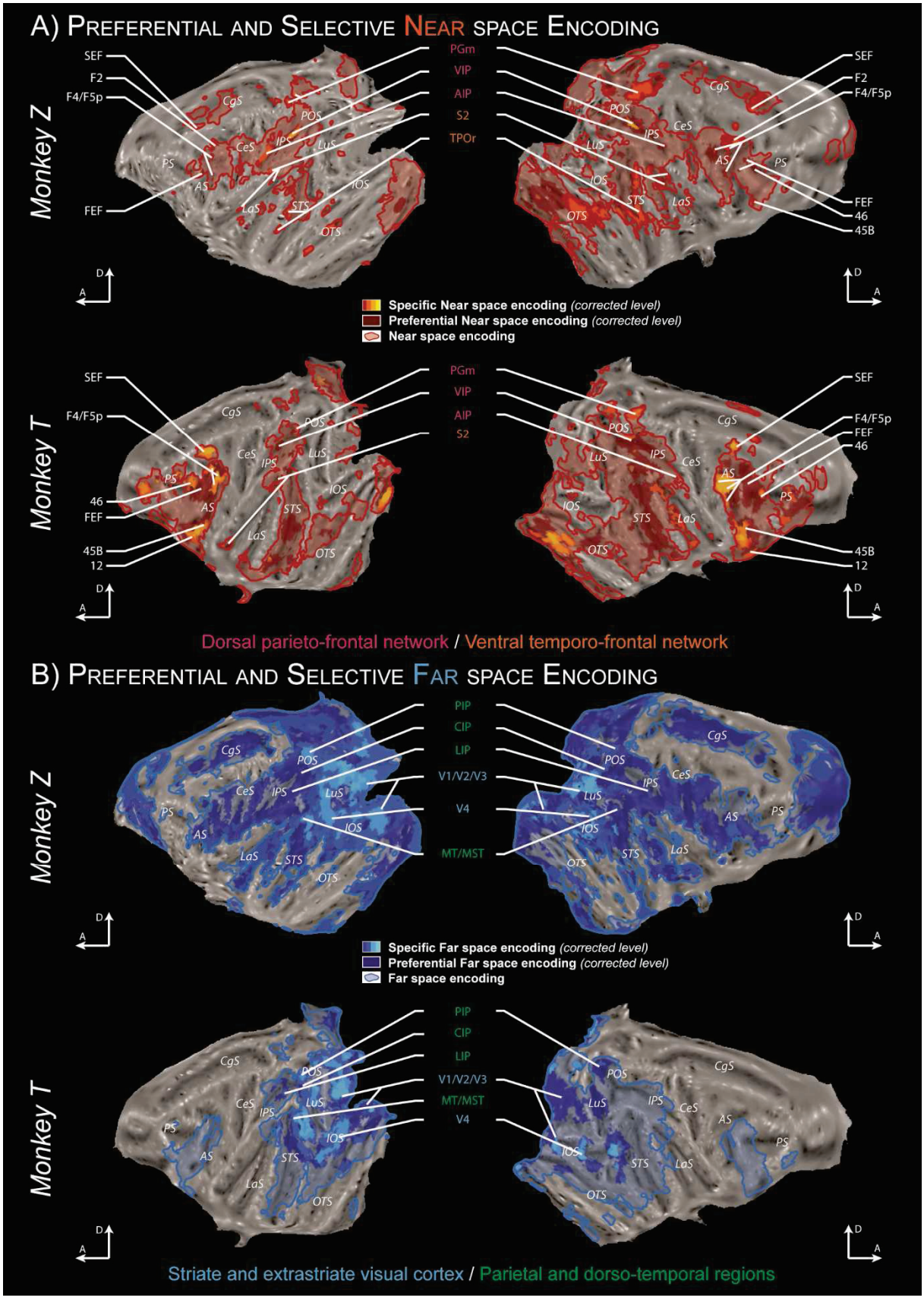

Figure 3: Non-selective, preferential and specific near and far space networks. Activations are presented on the flattened maps of individual monkeys. Only the key activations

identified in three hemispheres out of four are labelled. A) Non-selective, preferential and specific near space encoding. Preferential near space coding corresponds to the cortical regions whose activations are higher for the small cube in near space than for the large cube in far space (t scores = 4.8 at $p<0.05$, FWE-corrected level in the dark red). Specific near space encoding corresponds to the cortical regions which are activated by the small near cube but not for the large far cube (red to yellow scale, exclusive mask for far space versus fixation baseline applied at FWE-corrected level $p<0.05$). The outer red contours correspond to non-selective near space encoding (near space versus fixation, as in figure 2). B) Non-selective, preferential and specific far space encoding. Preferential far space coding corresponds to the cortical regions whose activations are higher for the large cube in far space than for the small cube in near space (t scores = 4.8 at $p<0.05$, FWE-corrected level in the dark blue). Specific far space encoding corresponds to the cortical regions which are activated by the large far cube but not for the small near cube (dark blue to light blue color scale, exclusive mask for near space versus fixation baseline applied at FWE-corrected level $p<0.05$). The outer blue contours correspond to non-selective far space encoding (far space versus fixation, as in figure 2). 12, area 12; 45B, area 45B; 46, area 46; AIP, anterior intraparietal area AIP; CIP caudial intraparietal area; F2, premotor area F2; FEF, frontal eye field; LIP, lateral intraparietal area LIP; MT/MST, medial/superior temporal areas MT/MST; F4/F5, premotor areas F4/F5; PGm, medial parietal area PGm; PIP, posterior intraparietal area PIP, S2, somatosensory area 2; SEF: supplementary eye field; TPOr, rostral temporoparietal occipital area TPOr; VIP, ventral intraparietal area VIP; V1/V2/V3/V4, visual areas V1,V2,V3 or V4. For other conventions, see Figure 2.

Far space cortical network modulation by object size

While the small cube presented in near space had the same apparent size as the far cube presented in far space, these two objects had very different physical sizes ($3x3x3cm^3$ versus $30x30x30cm^3$). As a result, part of the far or near space network specificities described above could have been due to this objective size difference (as opposed to an apparent size difference). In order to address this issue, we now compare the cortical activations obtained when stimulating far space with either a small cube or a large cube. For the sake of space, a group analysis is performed rather than a single subject analysis. This group analysis captures the

common activations already described at the single individual level in figures 2 and 3. No activations are observed with the *small object in far space* versus *large object in far space* contrast, indicating that all the cortical regions that are involved in processing the small object in far space also contribute to the processing of the large object in far space. The inverse contrast reveals a large cortical network (Figure 4, dark blue) mostly identical to that revealed by the *large cube in far space* versus *fixation* contrast (Figure 2, middle blue panels). When this contrast is additionally masked by the activations obtained by far space stimulations with the small cube (exclusive 'small cube in far space stimulation vs. fixation' mask, uncorrected level, p=0.05), a network that is selective to the large cube in far space processing as compared to the processing of smaller objects in far space (Figure 4, dark blue to light blue color scale, *t* scores = 4.8 and above, FWE-corrected level). This network includes large sectors of the visual striate and extrastriate cortex, mostly coinciding with the peripheral visual field representation (see Figure 4 in Guipponi et al., 2015 for an identification of these representations on this same group of subjects), the parieto-occipital cortex, the posterior parietal cortex, the right medial parietal cortex the anterior part of the superior temporal sulcus as well as a large extent of the prefrontal cortex, the cingulate cortex, the orbitofrontal cortex and the frontal pole.

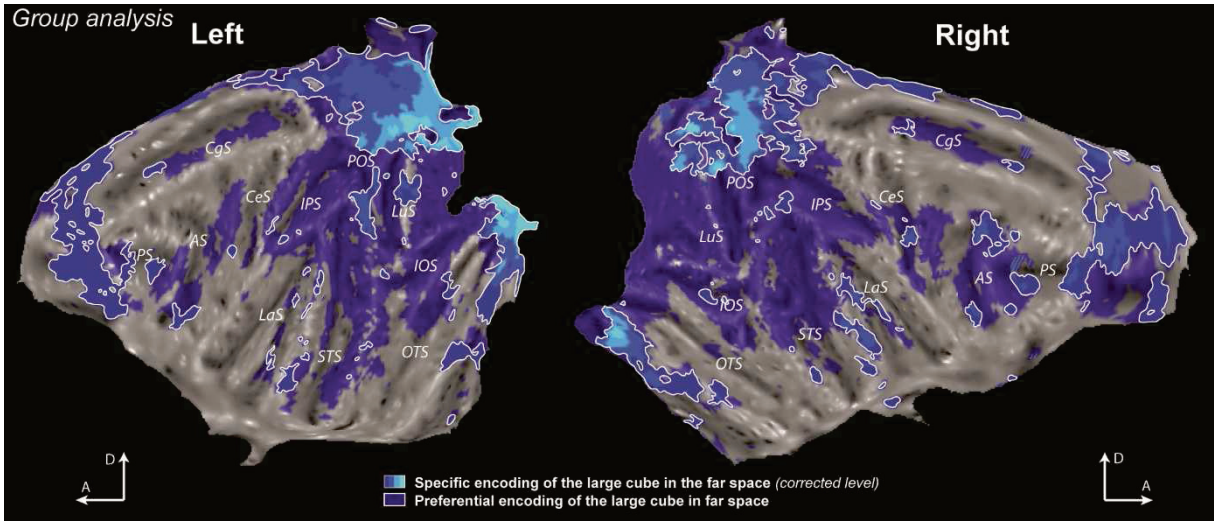

Figure 4: Preferential and specific encoding of the large cube in the far space. Activations are presented on the flattened maps of the reference monkey cortex (group analysis).

Preferential encoding of the large cube in the far space corresponds to the cortical regions whose activations are higher for the big cube in far space than for the small cube in far space (t scores = 4.8 at $p<0.05$, FWE-corrected level in the dark blue). Specific encoding of the large cube in the far space corresponds to the cortical regions which are activated by the big cube but not for the small far cube in the far space (dark blue to light blue color scale, exclusive mask for the big cube in far space versus fixation baseline applied at FWE-corrected level $p<0.05$). For other conventions, see Figure 2.

Functional activations in response to looming and recession in near and far space.

The physical approach of the cubes into far or near space and their recession back behind the curtains was controlled by the experimenters following a precise schedule indicated to them on a computer screen. The onsets of these displacements were logged together with all other task events. Here, we focus on the activations observed during these dynamic phases of the task (Figure 5). For the sake of space, a group analysis is performed rather than a single subject analysis. *The approach of the small cube into near space* produces widespread activations (Figure 6A). This network includes the orbitofrontal cortex (12, 46p), prefrontal and premotor cortex (FEF, F4, F5), parietal cortex (VIP, PIP, 7a, 7b, 7ab), temporal cortex (MT, MST, TPOr, IPa) and visual areas (V1, V2, V3). This network is mostly included in the near space network (Figure 5A, black contours, Figure 2, top panel), though a heterogeneity can be noted. Some cortical regions modulated by near space stimulations are not activated by intrusion into near space, mostly along the ventral visual stream (Figure 5A, uncolored cortex within the black contours). Other cortical regions modulated by near space stimulations are equally activated by intrusion into near space and near space stimulations (Figure 5A, colored activations within the black contours). Importantly, not all the regions that are activated by intrusion into peripersonal space are also activated by the sustained presence of a stimulus in near space (Figure 5A, white contours outside the black contours). *The approach of the big cube into far space* produced very similar activation patterns to those observed during the approach of the small cube into near

space, to the notable exception of the orbitofrontal cortex, possibly indicating an emotional component to intrusion into near space (Figure 5E). In contrast, *the approach of the small cube within far space* produced more restricted activations, mostly in the intraparietal sulcus (IPS), in the superior temporal sulcus (STS) as well as in the striate and extrastriate cortex (Figure 5C).

When the small cube recedes from near space, very few activations are observed, circumscribed to the prefrontal area 46 and the superior temporal sulcus STS (Figure 5B). A very similar activation pattern is described for *the recession of the small cube from far space* (Figure 5D). Last, activations are more widespread for *the large cube receding from far space*, quite close to those observed for the approach of this stimulus into far space (Figure 5F). This contrasts with the difference observed between the looming and recession of the small cube in near space, and support the idea that the representation of object movement vectors in the cortex differ depending on whether movement takes place in near or in far space.

Figure 5: Looming stimuli activate both Near and Far space network. Activations are presented on the flattened maps of the reference monkey cortex (group analysis). A, C and E, this presents the approach of the stimulus respectively towards near space with the small cube, towards far space with the small cube or towards far space with the big cube versus fixation contrast (t scores = 4.8 at $p<0.05$, FWE-corrected level respectively in the red, green and blue scale). B, D and F, this presents the receding of the stimulus respectively from near space with the small cube, from far space with the small cube or from far space with the big cube versus fixation contrast (t scores = 4.8 at $p<0.05$, FWE-corrected level respectively in the red, green and blue scale). On the first panel (the approach of the stimulus towards near space with the small cube), the black contours represent the near space encoding (one identified in Figure 2) and the white contours represent the specific encoding of the approach of the small cube in the near space which corresponds to the cortical regions which are activated by the approach of the small cube in the near space but not by the near space encoding (exclusive mask for the near space versus fixation baseline applied at FWE-corrected level $p<0.05$). For other conventions, see Figure 2.

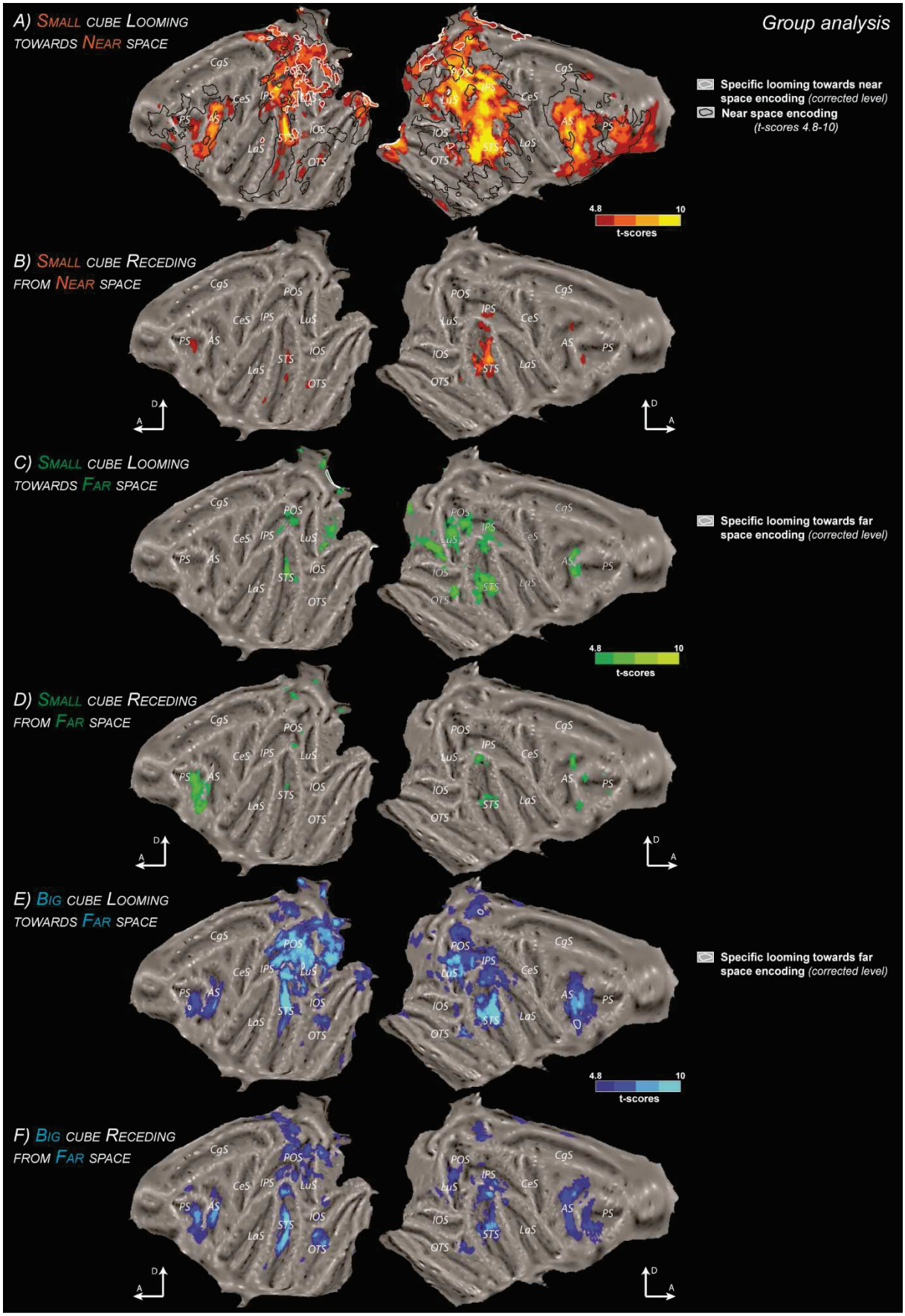
A) SMALL CUBE LOOMING TOWARDS NEAR SPACE
Group analysis
Specific looming towards near space encoding (corrected level)
Near space encoding (t-scores 4.8-10)
4.8
10
t-scores
B) SMALL CUBE RECEDING FROM NEAR SPACE
C) SMALL CUBE LOOMING TOWARDS FAR SPACE
Specific looming towards far space encoding (corrected level)
4.8
10
t-scores
D) SMALL CUBE RECEDING FROM FAR SPACE
E) BIG CUBE LOOMING TOWARDS FAR SPACE
Specific looming towards far space encoding (corrected level)
4.8
10
t-scores
F) BIG CUBE RECEDING FROM FAR SPACE
CgS
POS
CeS
IPS
LuS
PS
AS
STS
IOS
LaS
OTS
D
A

Near to far coding gradient in the arcuate (AS) and intraparietal sulcus (IPS).

Intraparietal and periarcuate regions have been shown to play a key role in space representation and space representation for action. In this section, we focus on these two regions (Figure 6). Again, for the sake of space, a group analysis is performed rather than a single subject analysis. This group analysis captures the common activations already described at the single individual level in figures 2 and 3. In the *Arcuate sulcus*, near space is specifically encoded by areas 46p, 12, F4, F5 and SEF whereas specific far space is overall represented at the inferior tip of the AS and along the gyrus posterior to the AS. In the *Intraparietal sulcus*, near space is specifically encoded by the VIP area and PGm area whereas far space is specifically encoded by the areas 5v and PIP.

Different regions of interest were defined along the AS and the IPS, and the percentage of signal change (PSC) within each of these ROIs was extracted for each contrast of specific near space, preferential near space, unselective near and far space, preferential far space and specific far space, Figure 6, histograms). Overall, this analysis confirms the existence, along the AS, bilaterally, of a progressive decrease of the PSC to near stimuli from ROIs 1 to 5, together with a progressive increase in the PSC to far stimuli. A similar progressive decrease of the PSC to near stimuli associated with a progressive increase in the PSC to far stimuli can also be observed in the IPS, bilaterally (ROIs 6 to 9). Confirming the whole brain contrast analysis, we also note deactivations or non-significant activations during the stimulation of far space by a larger object in the specific near space contrast (ROIs 1, 2 and 6, bilaterally) and the preferential near space contrast (ROIs 3 and 7, bilaterally). Likewise, the PSC during the stimulation of far space by a larger object are significantly higher than the PSC during the stimulation of near space in the specific and preference contrasts (ROIs 5 and 9, bilaterally). In the unselective near and far space contrast, the PSCs during the stimulation of near space and far space are not significantly different (ROIs 4 and 8, bilaterally).

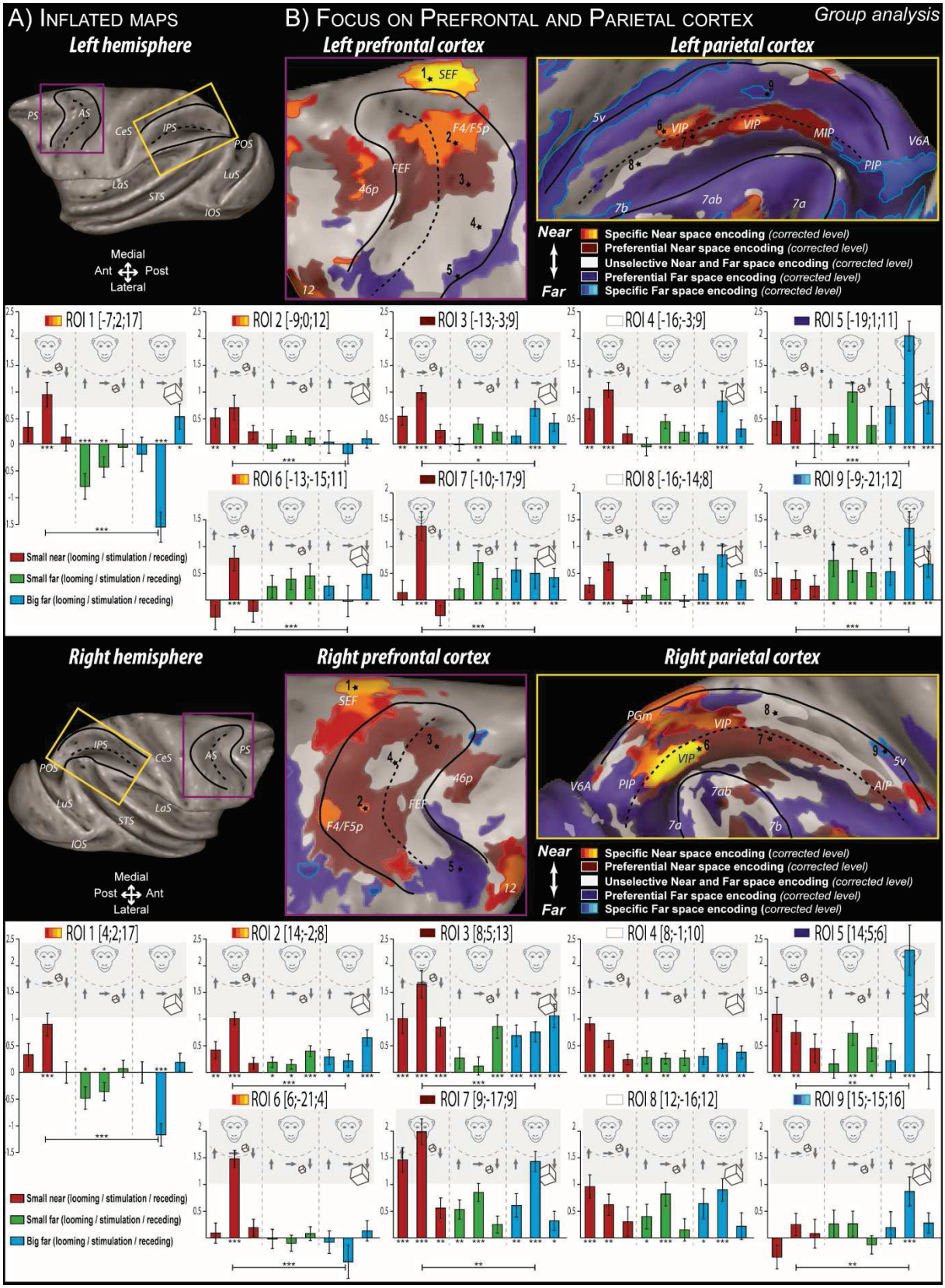

Figure 6: Near to Far coding gradient in the arcuate sulcus (AS) and the intraparietal sulcus (IPS). A) Inflated representation of the cortex, (left and right hemisphere of the reference monkey cortex). The purple inset corresponds to the AS and the yellow inset corresponds to the IPS as represented in B). Black solid lines indicate the limit between the convexity and

the banks of the IPS and AS; black dashed lines indicated the bottom of the sulcus. B) Prefrontal (purple inset) and parietal (yellow inset) activations of near and far space networks (group analysis superimposing the activations described in figure 3) on the same inflated maps, for the left and right hemispheres. Red to yellow color scale: selective near space coding; Red: preferential coding for near space; White: unselective coding for near and far space; Blue: preferential coding for far space; Dark blue to light blue color scale: selective near space coding. Gray regions correspond to regions activated neither by the large stimulus in far space nor by the small stimulus in near space. 5v, ventral area 5v; 7a,7b/7ab, areas 7a, 7b or 7ab: MIP, medial intraparietal area MIP, V6: cortical visual area V6. For other conventions, see Figure 2 and 3. Below each inflated map, the percentages of signal change (PSC) are plotted for each condition; looming of the small cube, stimulation of the small cube and receding of the small cube in the near space (red bars); looming of the small cube, stimulation of the small cube and receding of the small cube in the far space (green bars); looming of the big cube, stimulation of the big cube and receding of the big cube on the far space (red bars).

DISCUSSION

In the present study, we identify the non-human primate networks associated with either the stimulation of near or far space with naturalistic dynamic objects, in the absence of any overt task. In the following, we discuss the functional dissociation between near and far space networks in the light of the related literature.

Near space specific cortical network

The near space specific cortical network we describe in the non-human primate is surprisingly large. It involves multisensory visuo-tactile cortical regions whose neurons have already been described to encode nearby objects relative to the body, namely, the ventral premotor cortex (F4: Rizzolatti et al. 1981 and polysensory zone PZ: (Graziano et al. 1994, 1997, 1999; Fogassi et al. 1996), in agreement with the description of a near space neglect following the ablation of the postarcuate cortex, as these lesions most probably included the polysensory zone PZ -Rizzolatti et al. 1983) and ventral intraparietal area VIP, within the fundus of the intraparietal sulcus (Duhamel et al. 1997, 1998; Avillac et al. 2005; Schlack et al. 2005; Bremmer et al. 2013; Guipponi et al. 2013). It additionally involves several other cortical areas whose contribution to near space processing has been overlooked up to now. These include dorsal premotor regions, just medial to the polysensory zone PZ. This observation is in agreement with the description, in human patients with a damage in the dorsolateral prefrontal cortex, of a near space specific neglect syndrome (Aimola et al. 2012). We also describe the involvement of posterior and medial parietal areas, which together with the observed activations in the fundus of the intraparietal cortex are in perfect agreement with the description of a near space neglect in patients with posterior parietal lesions including the fundus, medial and posterior parts of the intraparietal sulcus (Halligan and Marshall 1991). Near space activations are also observed in the anterior temporal regions within the fundus of the STS and on the

inferior temporal convexity, suggesting a specific processing of the feature and identity of near objects within the ventral visual processing pathway.

Interestingly, near space specific activations can also be observed in area SII. This activation possibly reveals a general "attention-to-touch" process due to the anticipation of tactile stimulation to the body because of the vicinity of the moving stimulus to the face. Alternatively, it could actuate the strong functional link between near space processing and the somatosensory representation of self. While previous studies have mostly assumed that this link is subserved by multisensory visuo-tactile brain areas (Makin et al. 2008; Blanke 2012), the present observations suggest that low level sensory areas might also be involved in the representation of space at the frontier of self. This observation might be due to the fact that, in contrast with previous studies, the stimulus is presented extremely close (15cm) to the face of the monkeys. At this distance, the $9cm^3$moving cube can be viewed as a potentially dangerous object, all the more given that the monkeys cannot protect themselves from its presence (no escape, no goal-directed arm movements). This defensive attitude towards the near space stimulus could possibly also account for the observed orbitofrontal activations (area 12, Murray and Izquierdo 2007).

A functional circuit subserving peripersonal space representation is formed by parietal area VIP (head-centered) and premotor area F4 (arm-centered) (Matelli and Luppino 2001; Rizzolatti and Luppino 2001; Cléry, Guipponi, Wardak, et al. 2015) These two regions have anatomical connections and functional homologies and we can observed strong activations of these regions in Figure 3 and 6. This VIP-F4 network processes all the necessary information to bind together the localization of objects around our body, and specifically around the head, with actions towards these objects. It also processes the necessary visual and tactile information required to define a safety body margin contributing to the definition of self with respect to the

external world (Graziano and Cooke 2006; Brozzoli et al. 2013, 2014; Chen et al. 2014; Cléry, Guipponi, Wardak, et al. 2015).

Overall, the non-human near space specific cortical network we describe here has major specificities as compared to the analog human cortical network. Indeed, we essentially describe bilateral cortical regions, while in humans, only the left dorsal occipital cortex, the left intraparietal and the left ventral premotor appear to be involved in near space processing (Weiss et al. 2000; Aimola et al. 2012). Additionally, this near space non-human primate cortical network involves many more areas than the human network. This could be due to the fact that we stimulated near space at 15cm away from the subject's eyes while Weiss et al. (Weiss et al. 2000) for example, stimulated them at 70cm. Alternatively, this could be due to a genuine interspecies difference.

Far space specific cortical network

The far space specific cortical network we describe in the non-human primate is also very extended, involving large portions of the occipital cortex, as well as posterior temporal and superior temporal regions. This is similar to what is seen in humans as Weiss et al. (2000) describe a network involving the ventral visual stream including the ventral occipital cortex bilaterally and the right medial temporal cortex. These observations are in agreement with the description of a far space neglect following a temporal hematoma (Vuilleumier et al. 1998).

A human study (Quinlan and Culham 2007) shows a near preference coding in dPOS. There are a larger number of similarities between the human superior parieto-occipital cortex (sPOC) and the macaque parieto-occipital area which comprises areas V6 and V6A (Galletti et al. 1999, 2005). In our study, we show a clearly far space preference coding in V6A in both hemispheres. This opposite results can be explaining by the task conditions in each study. In our

task, we use naturalistic and dynamic stimuli in near or far space whereas in Quinlan and Culham (2007) study participants fixate upon points in near vs. far space with no other visual stimulation. As a result, only oculomotor signals of vergence eye position and ocular accommodation are manipulated by the task design. Last, Rizzolatti et al. describe a more pronounced hemineglect in far space than in near space following prearcuate area 8 ablations (Rizzolatti et al. 1983). This contrasts with the fact that we identify no preferential coding of far space in this region, but rather a preferential though not specific coding for near space. This discrepancy could reflect a task dependence of far and near space processing as described in humans, in active oculomotor or reaching contexts (Keller et al. 2005; Aimola et al. 2012).

Object size effects

In our hands, all the cortical regions that are involved in processing the small object in far space also contribute to the processing of the large object in far space, while the reverse is not true. At the neuronal level, this possibly suggests a multiplexing of object real-size and location in far space relative to the subject. Indeed, combing these two pieces of information could of ecological relevance, as a big object in far space is not expected to have the same valence as a small object in far space. In addition, size coding might further be normalized with respected to the actual body size of the subject big objects being possibly more dangerous for small individuals than for larger individuals (cf. difference in far space network size between monkey M1 and M2).

In humans, recent studies show that visual objects may be mapped along the ventral occipito-temporal cortex according to their real-world size. This mapping reflects the visual or functional properties associated with small versus big real-world objects (Konkle and Oliva 2012) but also abstract and conceptual size representation (Gabay et al. 2016). In these studies, a consistent medial-to lateral organization of big and small object preferences can be observed

in this ventral temporal cortex. It would be highly interesting to test different objects with real-world size well known for monkey to further characterize the functional coding interaction between real object-size and object distance from the subject.

Looming stimuli and peripersonal space

The looming of the small cube in near space results in a large activation of brain involving both the near and far space networks. Such looming stimuli have been described to trigger stereotyped defense responses and enhance reaction times or sensitivity to a second stimulus (Schiff et al. 1962; Ball and Tronick 1971; Vagnoni et al. 2012; Canzoneri et al. 2012; Kandula et al. 2015; Cléry, Guipponi, Odouard, et al. 2015) including a nociceptive stimulus (De Paepe et al. 2016). In a recent study, we also describe that this type of dynamic visual stimuli activate a parieto-frontal network highly overlapping with the one described here (Cléry, Guipponi, Wardak, et al. 2015). This functional overlap between a network encoding the presence of a stimulus within peripersonal space at the same time as intrusion into peripersonal space reinforces the view that this network encodes visual stimuli in relation with the margin of self and their possible tactile consequences on the body, whether harmful or not.

Relative encoding of near and far space as substrate for a dynamic space representation

The description of a cortical network specific for near space processing and another complementary network specific for far space processing should not have us overlook the fact that large cortical regions contribute to the processing of both far and near objects, though often favoring one over the other. This is for example the case of the lateral bank of the intraparietal sulcus and the adjacent convexity, including areas 7a, 7ab and 7b. Bimodal visuo-tactile neurons have been described in area 7b with very large receptive fields over the arm, leg, chest or even the skin of the whole body (Leinonen et al. 1979). Lesions of this region induce a

neglect in peripersonal space (Matelli et al. 1984), leading to the idea that area 7b is involved in the perception of near space and in the organization of movements towards stimuli presented in peripersonal space. The fact that we describe a privileged coding of far space in this cortical regions calls for reassessment of its functional role in relation with space processing. Indeed, while this cortical region has mostly been studied in the context of arm reach movements, highlighting its interaction with peripersonal space, this area also contains a lower body representation. As a result, it is also expected to contribute to whole body motion in the space beyond peripersonal space. This remains to be investigated.

Overall, the description of large cortical regions having either a preference for near space processing or far space processing call for reappraising far space or near space specificity. Indeed, the alternative view that we would like to put forward in the light of our observations is that of a continuous encoding of relative distance to the body, in the form of a far-to-near or near-to-far gradient. In this context, far or near space specific regions represent the extreme points of this continuum. The idea of such a continuum is supported by the fact that no abrupt change in visuo-spatial neglect can be seen between near and far space (Cowey et al. 1999). Indirect evidence for such a continuum can also be found in a recent non-human fMRI study by Joly et al. (2009), which describes disparity-related signals in far space (monkeys are fixating at 57cm) in area F5a, at a location close to the bilateral inferior periarcuate far space activation in our Figure 6. It is important to note that the existence of such a cortical far-to-near and a near-to-far gradient in space representation does not preclude the existence of a physically delineable peripersonal space, as described in numerous psychology and psychophysics study (Berti and Frassinetti 2000; Macaluso and Maravita 2010; Farnè et al. 2005; Ladavas and Serino 2008).

Overall we describe a more complex organization of near and far space processing networks than initially proposed. These results open the way to the study of the how these two

networks dynamically interact during action planning, tool use or as a function of the emotional or social contexts as some studies show that these processes are dynamics (Markman and Brendl 2005; Bassolino et al. 2010; Brozzoli et al. 2010; Lourenco and Longo 2009; Lourenco et al. 2011; Valdés-Conroy et al. 2012; Teneggi et al. 2013).

Acknowledgments: J.C. was funded by the Fondation pour la Recherche Médicale. O.G. was funded by the French education ministry. S.BH was funded by the French Agence nationale de la recherche (Grant #ANR-05-JCJC-0230-01).

Bibliography

Aimola L, Schindler I, Venneri A. 2012. Task- and response related dissociations between neglect in near and far space: A morphometric case study. Behav Neurol.

Avillac M, Denève S, Olivier E, Pouget A, Duhamel J-R. 2005. Reference frames for representing visual and tactile locations in parietal cortex. Nat Neurosci. 8:941–949.

Avillac M, Hamed SB, Duhamel J-R. 2007. Multisensory Integration in the Ventral Intraparietal Area of the Macaque Monkey. J Neurosci. 27:1922–1932.

Avillac M, Olivier E, Denève S, Ben Hamed S, Duhamel J-R. 2004. Multisensory integration in multiple reference frames in the posterior parietal cortex. Cognitive Processing. 5:159–166.

Ball W, Tronick E. 1971. Infant responses to impending collision: optical and real. Science. 171:818–820.

Bassolino M, Serino A, Ubaldi S, Làdavas E. 2010. Everyday use of the computer mouse extends peripersonal space representation. Neuropsychologia. 48:803–811.

Berti A, Frassinetti F. 2000. When far becomes near: remapping of space by tool use. J Cogn Neurosci. 12:415–420.

Bjoertomt O, Cowey A, Walsh V. 2002. Spatial neglect in near and far space investigated by repetitive transcranial magnetic stimulation. Brain. 125:2012–2022.

Bjoertomt O, Cowey A, Walsh V. 2009. Near space functioning of the human angular and supramarginal gyri. J Neuropsychol. 3:31–43.

Blanke O. 2012. Multisensory brain mechanisms of bodily self-consciousness. Nat Rev Neurosci. 13:556–571.

Bremmer F, Duhamel J-R, Ben Hamed S, Graf W. 1997. The representation of movement in near extra-personal space in the macaque ventral intraparietal area (VIP). In: Thier P,, Karnath H-O, editors. Parietal Lobe Contributions to Orientation in 3D Space. Experimental brain research Series, Vol 25. Springer. p. 619–630.

Bremmer F, Duhamel JR, Ben Hamed S, Graf W. 2000. Stages of self-motion processing in primate posterior parietal cortex. Int Rev Neurobiol. 44:173–198.

Bremmer F, Duhamel J-R, Ben Hamed S, Graf W. 2002. Heading encoding in the macaque ventral intraparietal area (VIP). European Journal of Neuroscience. 16:1554–1568.

Bremmer F, Klam F, Duhamel J-R, Ben Hamed S, Graf W. 2002. Visual–vestibular interactive responses in the macaque ventral intraparietal area (VIP). European Journal of Neuroscience. 16:1569–1586.

Bremmer F, Schlack A, Kaminiarz A, Hoffmann KP. 2013. Encoding of movement in near extrapersonal space in primate area VIP. Front Behav Neurosci. 7:8.

Brett M, Anton J-L, Valabregue R, Poline J-B. 2002. Region of interest analysis using the MarsBar toolbox for SPM 99. Presented at the 8th International Conference on Functional Mapping of the Human Brain (June 2–6, 2002, Sendai, Japan),. 16:S497.

Brozzoli C, Cardinali L, Pavani F, Farnè A. 2010. Action-specific remapping of peripersonal space. Neuropsychologia. 48:796–802.

Brozzoli C, Ehrsson HH, Farnè A. 2014. Multisensory representation of the space near the hand: from perception to action and interindividual interactions. Neuroscientist. 20:122–135.

Brozzoli C, Gentile G, Bergouignan L, Ehrsson HH. 2013. A Shared Representation of the Space Near Oneself and Others in the Human Premotor Cortex. Current Biology. 23:1764–1768.

Canzoneri E, Magosso E, Serino A. 2012. Dynamic Sounds Capture the Boundaries of Peripersonal Space Representation in Humans. PLoS ONE. 7:e44306.

Chen X, Sanayei M, Thiele A. 2014. Stimulus Roving and Flankers Affect Perceptual Learning of Contrast Discrimination in Macaca mulatta. PLoS ONE. 9:e109604.
Cléry J, Guipponi O, Odouard S, Wardak C, Ben Hamed S. 2015. Impact prediction by looming visual stimuli enhances tactile detection. J Neurosci. 35:4179–4189.
Cléry J, Guipponi O, Wardak C, Ben Hamed S. 2015. Neuronal bases of peripersonal and extrapersonal spaces, their plasticity and their dynamics: Knowns and unknowns. Neuropsychologia. 70:313–326.
Cowey A, Small M, Ellis S. 1994. Left visuo-spatial neglect can be worse in far than in near space. Neuropsychologia. 32:1059–1066.
Cowey A, Small M, Ellis S. 1999. No abrupt change in visual hemineglect from near to far space. Neuropsychologia. 37:1–6.
De Paepe AL, Crombez G, Legrain V. 2016. What's Coming Near? The Influence of Dynamical Visual Stimuli on Nociceptive Processing. PLOS ONE. 11:e0155864.
Duhamel J-R, Bremmer F, BenHamed S, Graf W. 1997. Spatial invariance of visual receptive fields in parietal cortex neurons. Nature. 389:845–848.
Duhamel J-R, Colby CL, Goldberg ME. 1998. Ventral Intraparietal Area of the Macaque: Congruent Visual and Somatic Response Properties. Journal of Neurophysiology. 79:126–136.
Durand J-B, Nelissen K, Joly O, Wardak C, Todd JT, Norman JF, Janssen P, Vanduffel W, Orban GA. 2007. Anterior regions of monkey parietal cortex process visual 3D shape. Neuron. 55:493–505.
Durand J-B, Peeters R, Norman JF, Todd JT, Orban GA. 2009. Parietal regions processing visual 3D shape extracted from disparity. NeuroImage. 46:1114–1126.
Fogassi L, Gallese V, Fadiga L, Luppino G, Matelli M, Rizzolatti G. 1996. Coding of peripersonal space in inferior premotor cortex (area F4). J Neurophysiol. 76:141–157.
Gabay S, Kalanthroff E, Henik A, Gronau N. 2016. Conceptual size representation in ventral visual cortex. Neuropsychologia. 81:198–206.
Galletti C, Fattori P, Gamberini M, Kutz DF. 1999. The cortical visual area V6: brain location and visual topography. European Journal of Neuroscience. 11:3922–3936.
Galletti C, Gamberini M, Kutz DF, Baldinotti I, Fattori P. 2005. The relationship between V6 and PO in macaque extrastriate cortex. European Journal of Neuroscience. 21:959–970.
Gentilucci M, Fogassi L, Luppino G, Matelli M, Camarda R, Rizzolatti G. 1988. Functional organization of inferior area 6 in the macaque monkey. I. Somatotopy and the control of proximal movements. Exp Brain Res. 71:475–490.
Graziano MS, Yap GS, Gross CG. 1994. Coding of visual space by premotor neurons. Science. 266:1054–1057.
Graziano MSA, Cooke DF. 2006. Parieto-frontal interactions, personal space, and defensive behavior. Neuropsychologia. 44:845–859.
Graziano MSA, Hu XT, Gross CG. 1997. Visuospatial Properties of Ventral Premotor Cortex. Journal of Neurophysiology. 77:2268–2292.
Graziano MSA, Reiss LAJ, Gross CG. 1999. A neuronal representation of the location of nearby sounds. Nature. 397:428–430.
Gross CG, Graziano MSA. 1995. REVIEW ■ : Multiple Representations of Space in the Brain. Neuroscientist. 1:43–50.
Guipponi O, Cléry J, Odouard S, Wardak C, Ben Hamed S. 2015. Whole brain mapping of visual and tactile convergence in the macaque monkey. NeuroImage. 117:93–102.
Guipponi O, Wardak C, Ibarrola D, Comte J-C, Sappey-Marinier D, Pinède S, Hamed SB. 2013. Multimodal Convergence within the Intraparietal Sulcus of the Macaque Monkey. J Neurosci. 33:4128–4139.

Halligan PW, Marshall JC. 1991. Left neglect for near but not far space in man. Nature. 350:498–500.
Hyvärinen J, Poranen A. 1974. Function of the parietal associative area 7 as revealed from cellular discharges in alert monkeys. Brain. 97:673–692.
Joly O, Vanduffel W, Orban GA. 2009. The monkey ventral premotor cortex processes 3D shape from disparity. NeuroImage. 47:262–272.
Kandula M, Hofman D, Dijkerman HC. 2015. Visuo-tactile interactions are dependent on the predictive value of the visual stimulus. Neuropsychologia. 70:358–366.
Keller I, Schindler I, Kerkhoff G, von Rosen F, Golz D. 2005. Visuospatial neglect in near and far space: dissociation between line bisection and letter cancellation. Neuropsychologia. 43:724–731.
Kolster H, Janssens T, Orban GA, Vanduffel W. 2014. The Retinotopic Organization of Macaque Occipitotemporal Cortex Anterior to V4 and Caudoventral to the Middle Temporal (MT) Cluster. J Neurosci. 34:10168–10191.
Konkle T, Oliva A. 2012. A Real-World Size Organization of Object Responses in Occipitotemporal Cortex. Neuron. 74:1114–1124.
Leinonen L, Hyvärinen J, Nyman G, Linnankoski I. 1979. I. Functional properties of neurons in lateral part of associative area 7 in awake monkeys. Exp Brain Res. 34:299–320.
Lewis JW, Van Essen DC. 2000. Corticocortical connections of visual, sensorimotor, and multimodal processing areas in the parietal lobe of the macaque monkey. J Comp Neurol. 428:112–137.
Lourenco SF, Longo MR. 2009. The plasticity of near space: evidence for contraction. Cognition. 112:451–456.
Lourenco SF, Longo MR, Pathman T. 2011. Near space and its relation to claustrophobic fear. Cognition. 119:448–453.
Macaluso E, Maravita A. 2010. The representation of space near the body through touch and vision. Neuropsychologia. 48:782–795.
Makin TR, Holmes NP, Ehrsson HH. 2008. On the other hand: dummy hands and peripersonal space. Behav Brain Res. 191:1–10.
Mandeville JB, Choi J-K, Jarraya B, Rosen BR, Jenkins BG, Vanduffel W. 2011. FMRI of cocaine self-administration in macaques reveals functional inhibition of basal ganglia. Neuropsychopharmacology. 36:1187–1198.
Markman AB, Brendl CM. 2005. Constraining theories of embodied cognition. Psychol Sci. 16:6–10.
Matelli M, Gallese V, Rizzolatti G. 1984. [Neurological deficit following a lesion in the parietal area 7b in the monkey]. Boll Soc Ital Biol Sper. 60:839–844.
Matelli M, Luppino G. 2001. Parietofrontal Circuits for Action and Space Perception in the Macaque Monkey. NeuroImage. 14:S27–S32.
Murray EA, Izquierdo A. 2007. Orbitofrontal cortex and amygdala contributions to affect and action in primates. Ann N Y Acad Sci. 1121:273–296.
Nelissen K, Joly O, Durand J-B, Todd JT, Vanduffel W, Orban GA. 2009. The Extraction of Depth Structure from Shading and Texture in the Macaque Brain. PLoS One. 4.
Paxinos G, Huang X-F, Toga A. 2000. The Rhesus Monkey Brain in Stereotaxic Coordinates. Faculty of Health and Behavioural Sciences - Papers (Archive).
Quinlan DJ, Culham JC. 2007. fMRI reveals a preference for near viewing in the human parieto-occipital cortex. NeuroImage. 36:167–187.
Rizzolatti G, Luppino G. 2001. The Cortical Motor System. Neuron. 31:889–901.
Rizzolatti G, Matelli M, Pavesi G. 1983. Deficits in attention and movement following the removal of postarcuate (area 6) and prearcuate (area 8) cortex in macaque monkeys. Brain. 106 (Pt 3):655–673.

Rizzolatti G, Scandolara C, Matelli M, Gentilucci M. 1981. Afferent properties of periarcuate neurons in macaque monkeys. II. Visual responses. Behav Brain Res. 2:147–163.
Schiff W, Caviness JA, Gibson JJ. 1962. Persistent fear responses in rhesus monkeys to the optical stimulus of "looming." Science. 136:982–983.
Schlack A, Sterbing-D'Angelo SJ, Hartung K, Hoffmann K-P, Bremmer F. 2005. Multisensory space representations in the macaque ventral intraparietal area. J Neurosci. 25:4616–4625.
Teneggi C, Canzoneri E, di Pellegrino G, Serino A. 2013. Social modulation of peripersonal space boundaries. Curr Biol. 23:406–411.
Vagnoni E, Lourenco SF, Longo MR. 2012. Threat modulates perception of looming visual stimuli. Current Biology. 22:R826–R827.
Valdés-Conroy B, Román FJ, Hinojosa JA, Shorkey SP. 2012. So far so good: emotion in the peripersonal/extrapersonal space. PLoS ONE. 7:e49162.
Van Essen DC, Drury HA, Dickson J, Harwell J, Hanlon D, Anderson CH. 2001. An integrated software suite for surface-based analyses of cerebral cortex. J Am Med Inform Assoc. 8:443–459.
Vanduffel W, Fize D, Mandeville JB, Nelissen K, Van Hecke P, Rosen BR, Tootell RBH, Orban GA. 2001. Visual Motion Processing Investigated Using Contrast Agent-Enhanced fMRI in Awake Behaving Monkeys. Neuron. 32:565–577.
Vuilleumier P, Valenza N, Mayer E, Reverdin A, Landis T. 1998. Near and far visual space in unilateral neglect. Ann Neurol. 43:406–410.
Weiss PH, Marshall JC, Wunderlich G, Tellmann L, Halligan PW, Freund HJ, Zilles K, Fink GR. 2000. Neural consequences of acting in near versus far space: a physiological basis for clinical dissociations. Brain. 123 Pt 12:2531–2541.
Weiss PH, Marshall JC, Zilles K, Fink GR. 2003. Are action and perception in near and far space additive or interactive factors? Neuroimage. 18:837–846.

Chapter 4 :

Neuronal bases of peripersonal and extrapersonal spaces, their plasticity and their dynamics: Knowns and unknowns

Published in “Neurospsychologia”, April 2015 • 70(2015)313–326

Neuropsychologia 70 (2015) 313–326

Contents lists available at ScienceDirect

Neuropsychologia

journal homepage: www.elsevier.com/locate/neuropsychologia

Research Report

Neuronal bases of peripersonal and extrapersonal spaces, their plasticity and their dynamics: Knowns and unknowns

Justine Cléry, Olivier Guipponi, Claire Wardak, Suliann Ben Hamed *

Centre de Neuroscience Cognitive, UMR5229, CNRS-Université Claude Bernard Lyon I, 67 Boulevard Pinel, 69675 Bron, France

ARTICLE INFO

Available online 24 October 2014

Keywords:
Near space
Far space
Peripersonal space
Extra-personal space
Parietal cortex
Intraparietal cortex
Prefrontal cortex
Premotor cortex
Dynamic

ABSTRACT

While space is perceived as unitary, experimental evidence indicates that the brain actually contains a modular representation of space, specific cortical regions being involved in the processing of extra-personal space, that is the space that is far away from the subject and that cannot be directly acted upon by the body, while other cortical regions process peripersonal space, that is the space that directly surrounds us and which we can act upon. In the present review, we focus on non-human primate research and we review the single cells, areal and cortical functional network mechanisms that are proposed to underlie extrapersonal and peripersonal space representations. Importantly, the current dominant framework for the study of peripersonal space is centered on the key notion that actions and specifically arm and hand-related actions, shape cortical peripersonal space representations. In the present review, we propose to enlarge this framework to include other variables that have the potential to shape peripersonal space representations, namely emotional and social information. In the initial section of the manuscript, we thus first provide an extensive up-to-date review of the low level sensory and oculomotor signals that contribute to the construction of a core cortical far and near space representation, in key parietal, premotor and prefrontal periarcuate cortical regions. We then highlight the key functional properties that are needed to encode peripersonal space and we narrow down our discussion to the specific parietal and periarcuate areas that share these properties: the parieto-premotor peripersonal space network and the parieto-premotor network for grasping. Last, we review evidence for a changing peripersonal space representation. While plastic changes in peripersonal space representation have been described during tool use and their underlying neural bases have been well characterized, the description of dynamical changes in peripersonal space representation as a function of the emotional or social context is quite novel and relies on behavioral human studies. The neural bases of such a dynamic adjustments of peripersonal space coding are yet unknown. We thus review these novel observations and we discuss their putative underlying neural bases.

1. Introduction

While our surrounding environment is often perceived as a unitary construct onto which we act and with which we interact, an ever growing body of neuropsychological evidence demonstrates that the brain actually contains a modular representation of space, some cortical regions being involved in the processing of extra-personal space, that is the space that is far away from the subject and that cannot be directly acted upon by the body, while other cortical regions appear to process peripersonal space, that is the space that directly surrounds us and which we can directly interact with (Fig. 1).

Early lesion studies in the non-human primate (Rizzolatti et al., 1983) show that the unilateral ablation of the pre-arcuate cortex to area 8, corresponding to the frontal eye-field or FEF, results in a decrease of contralateral eye movements and a neglect in the contralateral space, that is to say a deficit in the visual processing of objects in this part of the visual field (see also Wardak et al. (2006)). Interestingly, this neglect is more pronounced in the far extra-personal space and is not associated with somatosensory deficits. In contrast, post-arcuate lesions to area 6 result in a severe contralateral visual neglect, limited to peripersonal space and associated with a somatosensory neglect. This bimodal neglect in peripersonal space is also associated with a deficit in the use of the contralateral hand.

In humans, cases of neglect restricted to the near peripersonal space have been described (Berti and Frassinetti, 2000; Beschin and Robertson, 1997; Bisiach et al., 1986; Guariglia and Antonucci, 1992; Halligan et al., 2003; Halligan and Marshall, 1991; Ortigue et al., 2006), as well as cases of neglect restricted to the far extrapersonal space (Coslett et al., 1993; Cowey et al., 1994, 1999; Vuilleumier et al., 1998;

* Corresponding author.
E-mail address: benhamed@isc.cnrs.fr (S. Ben Hamed).

http://dx.doi.org/10.1016/j.neuropsychologia.2014.10.022
0028-3932/

Fig. 1. Spaces around the body. The *peripersonal space* is the space that directly surrounds us and with which we can directly interact whereas the *extrapersonal space* is the space that is far away from the subject and that cannot be directly acted upon by the body.

Ackroyd et al., 2002; Ortigue et al., 2006), though these deficits in near and far space processing appear to depend on the ongoing task being performed by the subjects (Aimola et al., 2013; Keller et al., 2005).

The reversible perturbation of the right angular gyrus (ANG) using transcranial magnetic stimulation (TMS) alters near space perception while that of the right supramarginal gyrus (SMG) induces a more marked deficit in far as compared to near space (Bjoertomt et al., 2002, 2009). Functional and lesion studies confirm the involvement of a dorsal network in the coding of near space in humans including the left dorsal occipital cortex, the left intraparietal cortex and the left ventral premotor cortex, and the complementary involvement of a ventral network in far space processing, including the ventral occipital cortex bilaterally and the right medial temporal cortex (Aimola et al., 2013; Weiss et al., 2000). Interestingly, in normal subjects, neural perceptual processes (e.g. a bisection judgment task) and motor processes (e.g. a manual bisection task) remain unaffected by whether the task is being performed in the near or the far space (Weiss et al., 2003). This is in agreement with the report of similar far and near space dissociations in patients whether performing a perceptual or a motor task (Pitzalis et al., 2001).

In the face of this accumulated knowledge, the understanding of the precise neural bases underlying near and far space processing, the construction of extrapersonal and peripersonal space representations and their relation with perception, action and body awareness is growing at a slower pace, since the seminal monkey studies issued some 15 years ago. These early studies highlight two distinct parieto-premotor networks (Jeannerod et al., 1995; Rizzolatti et al., 1998, 2014; Sakata et al., 1998; Luppino et al., 1999; Rizzolatti and Luppino, 2001; Rizzolatti and Matelli, 2003): a parieto-premotor peripersonal space network, composed of a parietal region (area VIP, see below) and a premotor region (area F4, see below), and a parieto-premotor network for grasping with the hand, composed of two parietal region (areas AIP and 7b, see below) and a premotor region (area F5, see below). The theoretical framework developed by the majority of these studies when discussing these two functional networks is an action-based perspective of space. In other words, it is centered on the key construction that actions and specifically arm and hand-related actions shape cortical peripersonal space representations. In the present review, we propose to enlarge this framework to include other variables that have the potential to shape peripersonal space representations. In the initial section of the manuscript, we thus first provide an extensive up-to-date review of the low level sensory (visual—including disparity, tactile, proprioceptive) and oculomotor (vergence) signals that contribute to the construction of a core far and near space cortical representation, in key parietal and premotor and prefrontal periarcuate cortical regions. In the next section, we highlight the key functional properties that are needed to encode peripersonal space and we narrow down our discussion to the specific parietal and periarcuate areas that share these properties. These areas coincide with the parieto-premotor peripersonal space network and the parieto-premotor network for grasping with the hand, mentioned above. Section 4 thus provides a review of seminal data on the contribution of the peripersonal space network to the definition of a defense space, as well as more recent evident evidence on its contribution to the prediction of impact to the body and to the coding of others' peripersonal space. Likewise, Section 5 provides a review of the contribution of the grasping network to goal directed hand movements in peripersonal space and to the mirroring of others' bodily movements. In all these sections, we focus on non-human primate research and we review the single cells, areal and cortical functional network mechanisms that possibly underlie the processes of interest. In the last section, we review evidence for a changing peripersonal space representation. While such changes and their underlying neural bases have been well characterized during tool use, the description of changes in peripersonal space representation as a function of the emotional or social context is quite novel, mostly relying on human studies, and their underlying neural correlates are yet unknown. We conclude with a discussion of the putative neural mechanisms that could subserve such changes.

2. Neural bases of far versus near space representation

Locating a visual object with respect to our own body involves the combination of both low level and high level cues. The high level cues are based on the cognitive interpretation of what is being perceived. For example, we can infer the distance at which a lion stands from us based on its apparent size and on the prior knowledge we have of the size of an adult lion. Low level cues include both oculomotor information such as eye vergence and visual cues such as binocular disparity information. Vergence corresponds to the conjugate eye movements that allow both eyes to focus onto a given visual object. As a result, an image of this object is projected onto each fovea, at the center of each of the right and left retinas. Vergence by providing the brain with information about where the eyes are fixating in space at the same time, carry information about the location of the object that is being fixated. However, when we are actively fixating a specific object, we are also able to simultaneously estimate the location of a visual stimulus located in front or behind this fixated object. This estimate is constructed by combining eye vergence signals with binocular disparity information. Binocular disparity corresponds to the difference in where the image of a given object falls on the left and right retina. The binocular disparity of a fixated object is thus null. The disparity of an object that is located between the eye convergence point and the face is negative, while that of an object located beyond the eye fixation point is positive. An early model suggests that the encoding of the spatial location of an object can be achieved through the modulation of the neuronal response of disparity selective neurons by eye vergence signals (Pouget and Sejnowski, 1994). And indeed, neuronal response modulation by vergence and disparity cues is documented in the several cortical

regions which have been proposed to contribute to near and far space processing.

2.1. Contribution of the parietal cortex to the coding of near peripersonal and far extrapersonal space (Fig. 2a)

Several parietal areas contribute to an enhanced representation of near space, through diverse mechanisms. In the medial parietal area V6A (Luppino et al., 2005), a significant proportion of neurons are modulated by gaze position in 3D-space as well as by vergence signals, i.e., by the location in depth of the visual object being foveated (Hadjidimitrakis et al., 2011, 2012; Breveglieri et al., 2012). Importantly, at the population level, the preferred fixation distances extend up to 30 cm from the monkey's body, i.e. within the limits of the space that can be reached by the monkey's arm. Fixations beyond 50 cm, i.e. beyond the monkey's reaching space, are also represented, but to a lesser extent. Interestingly, fixations around 45 cm from the monkey's body, at the limit of the arm's reaching distance, are the least represented. The significance of this functional limit or "gap zone" between a peripersonal reachable space and an extrapersonal unreachable space is not clear (Hadjidimitrakis et al., 2011, 2012; Breveglieri et al., 2012). A similar neuronal preference for eye fixation within the near peripersonal space is also described in other parietal areas. The majority of 7a neurons, on the cortical convexity of the inferior parietal cortex, are described to prefer fixations within 50 cm from the monkey's face (Sakata et al., 1980). The close by area 7b is dominated by the tactile modality. However, up to 30% of its face and arm related tactile neurons also have a response to visual stimuli presented close to their tactile receptive field (Hyvärinen and Shelepin, 1979; Hyvärinen, 1981). A preference for peripersonal space is additionally described in lateral intraparietal area LIP, lying on the lateral bank of the intraparietal sulcus IPS and characterized by an enhanced central visual field representation (Ben Hamed et al., 2001). Indeed, 72.5% of LIP neurons have a higher discharge rate for fixations in the near peripersonal space (Genovesio and Ferraina, 2004; Gnadt and Mays, 1995). These neurons also have higher discharge rates for disparities corresponding to visual stimuli presented between the monkey and the fixated spatial location, i.e. presented in the near peripersonal space (Genovesio and Ferraina, 2004). A similar preferential coding of the portion of space closest to the monkey can also be found on the medial bank of the IPS, in medial intraparietal area MIP or parietal reach region PRR (Bhattacharyya et al., 2009). This correlates with an alignment of disparity tuning curves and gain modulation by vergence angle during the preparation of arm reaching movement can be seen. Last, a preferential coding for moving visual stimuli in near peripersonal space is described in the ventral intraparietal area VIP, using either natural object presentations (Colby et al., 1993) or stereoscopic visual presentations allowing for a quantification of binocular disparity information during a fixed-vergence design (Yang et al., 2011; Bremmer et al., 1997, 2013) (Fig. 2a).

A recent fMRI study in the non-human primate, designed to investigated the coding of 3D visual shape, allows to capture how the intraparietal cortex encodes disparity information in the $\pm 0.6^{\circ}$ range (Durand et al., 2007). The authors show a change in the hemodynamic signals as a function of the position of the presented visual stimuli in depth in the anterior part of lateral intraparietal area LIP, in caudal intraparietal area CIP, in medial lateral area MIP/PRR, as well as in posterior parietal area PIP, matching observations from the same group in humans (Durand et al., 2009). In these parietal regions, this coding of position in depth is often associated with the coding of the 3D structure of complex objects. In contrast, in anterior parietal area AIP, the coding of 3D structure is present (Durand et al., 2007; Srivastava et al., 2009; Verhoef et al., 2010; Theys et al., 2012), in the absence of a coding of the position of visual stimuli in depth (Durand et al., 2007). Most interestingly, the majority of AIP neurons remained selective for 3D objects in the absence of disparity cues, indicating that 3D structure was partially extracted from monocular depth cues (Romero et al., 2013). A significant proportion of AIP neurons also express short latency, low visual selectivity responses to 2D object fragments containing a particular curvature (Romero et al., 2014). These responses are highly dependent upon the location of the visual stimuli within the neuron's receptive field (Romero et al., 2014). All this taken together suggests that AIP might be more interested in object fine structure rather than in its actual position in space, thus possibly challenging the contribution of this cortical region in extracting object affordances that can further be used to program and execute appropriate grip (Romero et al., 2014). Notably, in adjacent area VIP, Durand et al. (2007) do not describe any disparity-related fMRI activations, contrasting with Bremmer et al., 2013. This is most probably due to the fact that while Durand et al. (2007) manipulated disparities in the order of $\pm 0.6^{\circ}$,

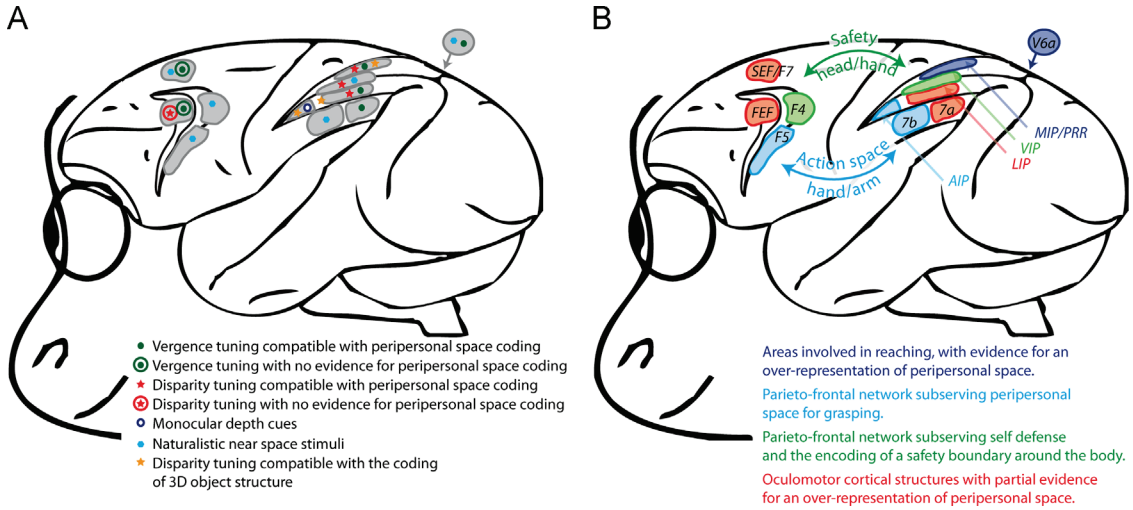

Fig. 2. (a) Meta-analysis of evidence for low level depth cues in identified intraparietal and peri-arcuate functional areas, color coded as identified in the legend. (b) Functional networks associated with an enhanced representation of peripersonal space: areas involved in reaching (dark blue), parieto-frontal network subserving peripersonal space for action (cyan), parieto-frontal network subserving self defense and the encoding of a safety boundary around the body (green), oculomotor structures with partial evidence for an over-representation of peripersonal space (red).

Bremmer et al. (2013) report that about 60% of VIP cells preferred near space disparities of -2° or below (see next paragraph).

While most of the above cited studies highlight a preferential encoding of near peripersonal space, they nonetheless often describe a simultaneous though weaker encoding of far space. In a recent monkey fMRI study (Cléry et al, ongoing work), we identify only few parietal loci representing near space to the exclusion of far space (Fig. 3, horizontal panel 1). Specifically, we use moving naturalistic cubes of identical angular (apparent) size to stimulate either the far space (1.5 m away from the monkey's face) or the near space (15 cm from the monkey's face), while the monkeys are fixating an LED placed at an intermediate location (90 cm from their face, fixation being

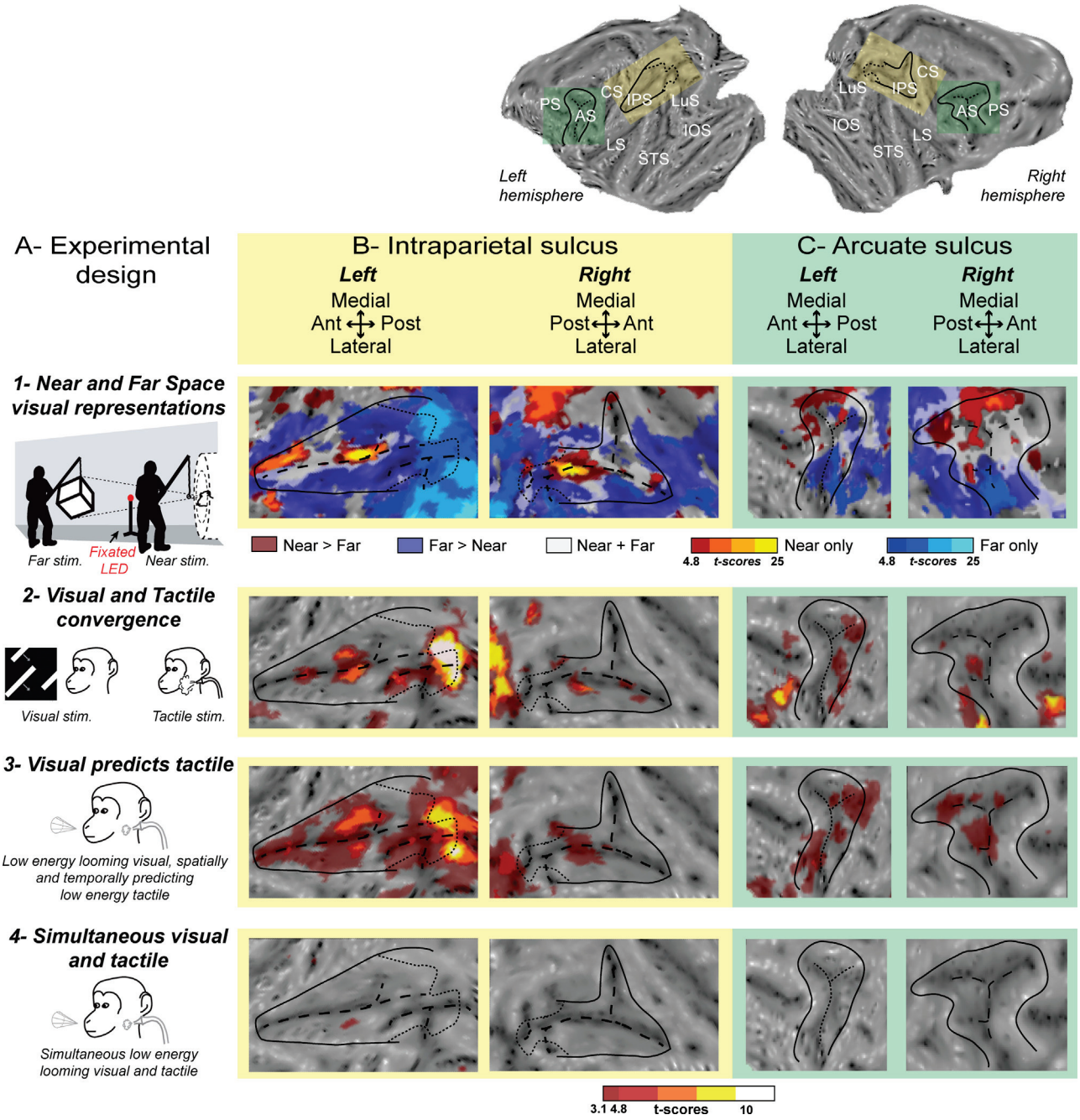

Fig. 3. fMRI mapping of the contribution of the intraparietal and periarcuate cortex to peripersonal and extrapersonal space coding, in a representative non-human primate individual. Top panel: flattened representation of the cortex, obtained with Caret (left and right hemispheres of individual monkey). The yellow inset corresponds to the IPS and the green inset corresponds to the AS, as represented in (B) and (C). Black solid lines indicates the limit between the convexity and the banks of the IPS and AS; black dashed lines indicate the bottom of the sulcus and black dotted line, the projection on the flat map of the most posterior coronal section of the IPS, just before the annectant gyrus. AS, Arcuate sulcus; CS, central sulcus; IOS, inferior occipital sulcus; IPS, intraparietal sulcus; LS, lateral sulcus; LuS, lunate sulcus; PS, principal sulcus; STS, superior temporal sulcus. (A) Experimental design for each study: 1) Neural bases of near and far space visual representations; 2) Neural bases of visual and tactile convergence; 3) Neural consequences of prediction of impact to the face by visual looming stimulus over tactile-related activation; 4) Neural consequences of simultaneous visual and tactile presentations. (B) Parietal cortical activations presented on the flattened IPS (yellow inset in the whole brain flat maps presented in the top panel). (C) Periarcuate cortical activations presented on the flattened AS (green inset in the whole brain flat maps presented in the top panel). On all maps, colors represent *t*-score scales as indicated by the legends. In study 1, all *t*-scores are at FWE-corrected level ($p < 0.05$). In studies 2–4, *t*-scores are color-coded from 3.1 uncorrected level ($p < 0.001$) to above FWE-corrected level ($p < 0.05$).

controlled with a video eye tracker, fixation window of 2°, Fig. 3a1). As a result, this study involved a larger disparity range than those manipulated in Durand et al. (2007). Posterior and medial to the intraparietal sulcus, the upper most medial portion of area V6A selectively encodes visual objects presented in the near peripersonal space (not shown). Within the intraparietal sulcus (IPS), a selective coding for near peripersonal space can be seen in ventral intraparietal area VIP (Fig. 3b1, red to yellow), matching Bremmer et al. (2013). Interestingly, this selective near space representation does not encompass the entire VIP, but nicely coincides with the VIP visuo-tactile convergence patches as identified with full strength tangential moving bars and full strength airpuff tactile stimulations to the perioral skin (Fig. 3b2, Guipponi et al., 2013a). Note that none of these two experimental contexts (Fig. 3b1, far versus near space stimulation; Fig. 3b2, visual and tactile convergence as identified from full strength sensory stimulations) lead to lateral bank LIP activations, indicating that our observations are not confounded by microsaccades, nor to medial bank activations, indicating that our observations are not confounded by blinks (Guipponi et al., 2014). In comparison, the fundal cortex surrounding these patches appears to equally represent near and far spaces (Fig. 3b1, white) and the posterior medial intraparietal bank as well as a large extent of the lateral intraparietal bank preferentially represents far space (Fig. 3b1, blue). Overall, this fMRI study captures the extent of parietal cortex dedicated to near space and far space processing. It highlights the fact that there is actually a strong overlap between the near and far space encoding networks. These overlapping representations are possibly at the origin of the construction of a unitary perceived space representation. However, how this is precisely achieved is yet unclear. A precise analysis of how vergence signals interact with disparity signals for space representation can potentially shed light of this question as well as account for the apparent partial discrepancy between these fMRI observations in the lateral and medial banks and the above cited single cell recording studies.

In humans, Quinlan and Culham (2007) show a strong over-representation of peripersonal space in the dorsal parieto-occipital sulcus (dPOS), in a region possibly corresponding to the human homolog of area V6A (Pitzalis et al., 2013). In this study, subjects viewed looming and receding moving visual stimuli presented close to their face (moving in the range of 13–17 cm from the face), at an intermediate distance from their face (moving in the range of 33–43 cm from the face) or far away (moving in the range of 73–95 cm from the face). In dPOS, BOLD contrast increased for closer stimuli. Interestingly, this was not the case in the putative hVIP, which was activated by moving stimuli irrespectively of their distance from the face. This suggests that while near space representation in dPOS strongly relies onto vergence signals, the VIP neurons might actually rely on the combination of several depth cues, including disparity, as described by Bremmer et al. (1997, 2013) and in our fMRI study on near and far space representations.

Overall, while there is clearly a growing understanding of how near and far spaces are encoded in the parietal cortex, we are still missing a systematic fine grained parametric analysis of how oculomotor vergence and sensory disparity signals interact, in a spatial range encompassing extremely close visual stimuli and far away an reachable stimuli, applied to the entire parietal cortex at the same time. Likewise, it would be interesting to further understand how higher level cues interact with vergence and disparity signals to construct a representation of space. Durand et al. (2007) have used such an approach to explore how objects are encoded in 3D. A similar approach could be extended to the analysis of space representation at large. Our ongoing Cléry et al. is an initial step in this direction. In particular, it would be of high interest to substantiate the notion of “gap zone” functionally delimiting far space from peripersonal space.

2.2. Contribution of the premotor and prefrontal cortex to the coding of near peripersonal and far extrapersonal space (Fig. 2a)

Similarly to what has been described in the parietal cortex, several premotor and prefrontal cortical regions demonstrate a preferential coding for near peripersonal space. As discussed previously, post-arcuate lesions to area 6, including areas F4 and F5, result in a severe contralateral visual neglect, limited to peripersonal space. Correlating with these observations, the neurons of area F4 essentially represent visual objects located in the peripersonal space (Rizzolatti et al., 1981; Gentilucci et al., 1988; Graziano et al., 1994; Gross and Graziano, 1995; Fogassi et al., 1996). Specifically, these neurons can be divided into pericutaneous neurons (54%), responding to visual stimuli presented in the close vicinity (a few centimeters) of the skin and distant peripersonal neurons (46%), responding to visual stimuli presented at a distance from the skin, within the animal's reaching distance (Rizzolatti et al., 1981). Interestingly, the visual receptive fields of these neurons are independent of the position of the eyes or the body and remain anchored to a specific body part. For example, a neuron responding to a visual object presented close to the right hand when the arm is stretched away from the body will continue to respond to a visual stimulus presented close to the right hand even if the arm is held close to the chest, (Graziano et al., 1994; Fogassi et al., 1996; Gentilucci et al., 1983). These neurons essentially represent the near peripersonal space around the face and the arms (for review, Rizzolatti et al., 1997, 2002). Adjacent area F5, along the inferior branch of the arcuate sulcus, contains highly overlapping movement representations of the hand and mouth, as revealed by electric stimulation studies (Rizzolatti et al., 1988; Hepp-Reymond et al., 1994). Accordingly, the neurons of this premotor cortical region respond to hand-grasping both in light and in dark and 50% of these neurons additionally presentation 3D graspable visual objects (Murata et al., 1997; Rizzolatti et al., 1988; Raos et al., 2006). These F5 neurons called “canonical” neurons have a visual selectivity that matches their motor selectivity, responding best to the object that calls for their preferred hand-grasping configuration (Murata et al., 1997; Raos et al., 2006). Following the inactivation of F5, the hand shaping that relies on the visual properties of the object to be grasped is disrupted (Fogassi et al., 2001). In relation with the scope of the present review, the visual response of F5 neurons is selective of near peripersonal space though their response mostly relies on whether the viewed object is graspable or not (operational quality) rather than on their distance from the body (Bonini et al., 2014). In the peri-arcuate cortex facing area F4, across the arcuate sulcus, the neurons of the frontal eye field (FEF, area 8) are also modulated by the distance at which a visual object is presented. Specifically, a prefrontal cortical region just anterior to the saccadic FEF is modulated by eye vergence (Gamlin and Yoon, 2000; Akao et al., 2005; Alkan et al., 2011). In addition, the FEF neurons are modulated by binocular disparity (Ferraina et al., 2000). However, none of these studies on pre-arcuate cortex functions highlight a preferential encoding of near or far extrapersonal space, in contrast with the description of a more pronounced visual neglect in the far extra-personal space following a lesion of this pre-arcuate cortex than in near peripersonal space (Rizzolatti et al., 1983) (Fig. 2a).

The same monkey fMRI study as cited above (Cléry et al., ongoing work, Fig. 3, horizontal panel 1) provides additional information on near and far space representation around the arcuate sulcus (Fig. 3c1). Within the upper branch of the arcuate sulcus, we describe stronger activations for near visual stimuli than for far visual stimuli including the premotor convexity (dorsal premotor areas F2 and F7, Fig. 3c1, red), and the prefrontal dorsal convexity (the medial portion of the FEF and area 46p, Fig. 3c1, red). A clear bilateral activation selective to the near visual space stimulation at the exclusion of the far space stimulation can be seen in area F7, at a location compatible with the

supplementary eye field SEF (not shown). The SEF is described to encode oculomotor information in a diversity of frames of references, ranging from eye- to head- to space/body (Martinez-Trujillo et al., 2004) to object-centered frame of reference (Olson and Gettner, 1995; Olson, 2003). Vergence-related activations have been described in the SEF (Alkan et al., 2011), these activation being stronger for predictive vergence than random vergence (Alvarez et al., 2010) behavior. But to our knowledge, the specific contribution of this area to near space processing has not been documented yet. A second bilateral activation specific to the disparity induced by near visual space stimulation can be seen on the posterior bank of the arcuate sulcus, across from the FEF, at a location compatible with F4 (Fig. 3c1, red). This postarcuate preferential near space representation is surrounded by cortex that equally represents near and far spaces (Fig. 3c1, white). In comparison, a preferential far space representation is observed at the tip of the lower branch of the arcuate sulcus, the inferior premotor convexity (lateral F5), as well as the prefrontal ventral convexity (Fig. 3c1, blue).

3. Multimodal peripersonal space representations

As discussed in Section 1, peripersonal space corresponds to the space that surrounds our body at the frontier with our skin. Bimodal visuo-tactile neurons responding both to tactile stimulations to the skin and to visual stimulations in the near space are suggested to be at the origin of this peripersonal space representation, as reviewed by others (Brozzoli et al., 2012; Làdavas and Farnè, 2004). A parieto-premotor network appears to play a crucial role in this peripersonal space representation. Indeed, amongst the several cortical areas discussed above as having an enhanced representation of peripersonal space, only few have neurons with these specific response properties underlined above. Peripersonal neurons firing both when a tactile stimulus is delivered to the animal's skin and when a visual stimulus is presented in the space near the part of the body where the tactile field is located can be found in two key parietal cortical areas. First, in the ventral intraparietal area VIP, which is a site of audio-visuo-tactile convergence in both humans (Bremmer et al., 2001) and non-human primates (Colby et al., 1993; Duhamel et al., 1998; Guipponi et al., 2013a), as well as a site of multisensory integration (Avillac et al., 2004, 2005, 2007). VIP neurons encode visual information in a gradient of eye- to head- frame of reference (Duhamel et al., 1997; Avillac et al., 2005), while tactile stimuli are encoded in a stable, unique head-centered frame of reference (Avillac et al., 2005). As a result, in a fraction of VIP neurons, the visual and tactile receptive fields spatially match irrespectively of eye position. For the remaining neurons, the relationship between the visual and tactile receptive fields depended on gaze direction. Visuo-tactile neurons can also be found in parietal area 7b. This area presents a coarse somatotopic organization, with a face representation on the upper inferior parietal convexity, at the border with area 7a. Lateral, along the inferior parietal convexity, and adjacent to this face representation comes an arm and hand followed by a foot representation (Hyvärinen and Shelepin, 1979; Hyvärinen, 1981; Robinson and Burton, 1980). In the face and arm region of 7b, about 33% of the cells are described as bimodal, their visual receptive fields spatially matching their tactile receptive fields (Hyvärinen and Poranen, 1974; Hyvärinen and Shelepin, 1979; Hyvärinen, 1981; Leinonen et al., 1979; Leinonen and Nyman, 1979). Peripersonal neurons can also be found in the premotor cortex, both in areas F4 and F5, in rostral area 6 (Gentilucci et al., 1988; Rizzolatti et al., 1988; Graziano et al., 1994; Gross and Graziano, 1995; Fogassi et al., 1996). This multisensory convergence in ventral premotor cortex is also observed in humans (Bremmer et al., 2001), corroborating the somatosensory neglect observed following premotor area 6 lesions (Rizzolatti et al., 1983).

In addition to their bimodal visuo-tactile response selectivities, the ventral premotor cortex F4 and F5 and the parietal areas VIP and 7b share important functional characteristics in relation with space and self-motion processing. For example, both premotor areas F4 and F5 (in humans, Bremmer et al., 2001; in monkeys, Fig. 3c2, Guipponi et al., 2013b) and parietal area VIP (in humans, Bremmer et al., 2001; in monkeys, Bremmer et al., 1999, 2000, 2002a; Guipponi et al., 2013a) are activated by large field optic flow stimulations eliciting a percept of relative motion of the subject with respect to the surrounding environment. Area VIP is activated by vestibular stimulations, contributing to the representation of the subject's displacement in its environment (Chen et al., 2011a, 2011b, 2013; Bremmer et al., 2002b; Akbarian et al., 1993). Vestibular projections to premotor cortex are also described, though they appear to be restricted, to the monkey area 6pa, coinciding with area F5 (Akbarian et al., 1993, 1994). Last, the tactile receptive fields of both cortical regions preferentially represent the face and more so the peri-oral region of the face or the arm and hand. Face representation is more marked in areas VIP (Colby et al., 1993; Duhamel et al., 1998) and F4 (Graziano et al., 1994, 1997; Fogassi et al., 1996; Gentilucci et al., 1983) while arm representation is more marked in areas 7b (Hyvärinen and Shelepin, 1979; Hyvärinen, 1981; Robinson and Burton, 1980) and F5 (Murata et al., 1997; Rizzolatti et al., 1988; Rizzolatti and Luppino, 2001; Raos et al., 2006). As a result, two distinct functional circuits subserving peripersonal space representation can be distinguished, as described below.

4. Distinct, but functionally coupled VIP head-centered and F4 arm-centered peripersonal spaces

The first peripersonal space representation circuit is formed by parietal area VIP and premotor area F4 (Fig. 2b, Rizzolatti and Luppino, 2001; Matelli and Luppino, 2001). Importantly, in spite of their strong anatomical connections and functional homologies, a key functional difference needs to be highlighted between these two cortical regions. The visual information in F4 is anchored to the limbs. As a result, both the tactile and the visual receptive fields of F4 neurons match each other, irrespectively of eye position and the location of the object in space (Graziano et al., 1994). As discussed above, in area VIP, visual and tactile information matches for a significant fraction of VIP neurons, essentially representing the near space around the face and head. For the remaining neurons, the spatial position of the VIP visual receptive fields is influenced by the gaze (Duhamel et al., 1997; Avillac et al., 2005). The tactile and visual receptive fields match is essentially described for VIP neurons representing the peripersonal space around the head (Duhamel et al., 1997). As a result, F4 visual information is anchored onto the arm/hand while in VIP, visual information is anchored to the head (Fig. 4). Interestingly, a recent study (Chen et al., 2014) describes that, under large-field, multi-patch, random-dot motion visual stimulations, virtually all VIP neurons represented visual information in an eye centered and not in a head centered frame of reference. This contrasts with the seminal Duhamel et al. (1997) observations, suggesting that the spatial reference frames of visual responses in VIP may depend on the visual stimulation conditions, i.e. on the ongoing sensory context, thus hinting towards a context-dependent, dynamic space representation

4.1. Defense, avoidance and margin of safety around the body

The VIP-F4 network thus processes all the necessary information to bind together the localization of objects around our body, and specifically around the head, with actions towards these objects. Specifically, VIP represents the relative movement between the

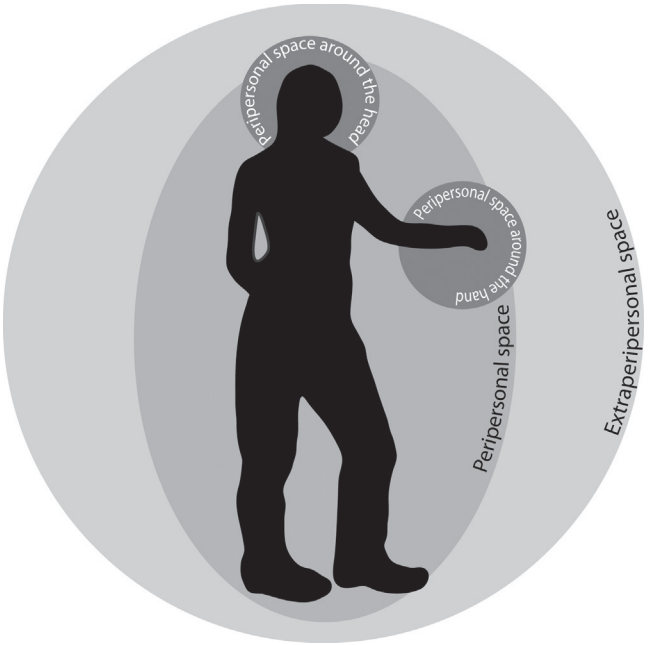

Fig. 4. Head and arm/hand peripersonal spaces have a privileged representation as compared to the rest of the body.

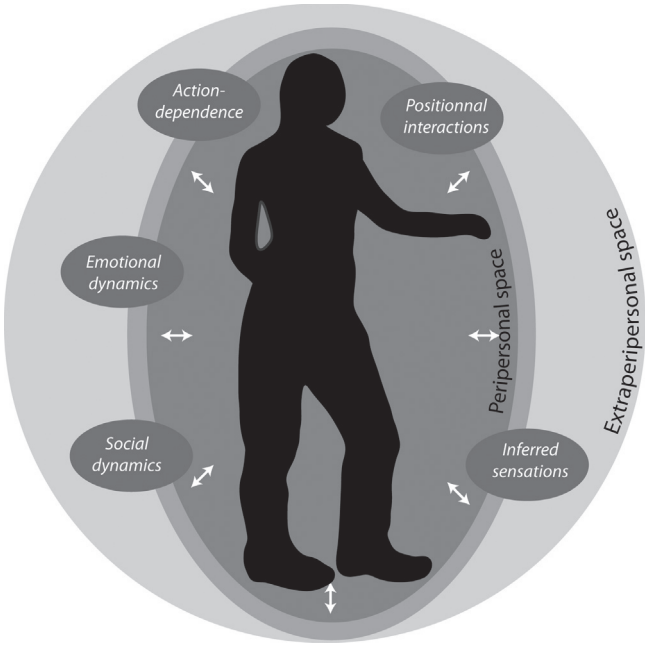

Fig. 5. The boundary between far and near space representations is plastic and dynamic, under the influence of a variety of endogenous and exogenous factors.

environment or its sub-elements and the subject's the body, while it does not encode the 3D structure of objects in the vicinity of the body (Durand et al., 2007). This contrasts with adjacent anterior intraparietal area AIP, whose neurons discharge during the fixation of graspable objects, during their grasping both in light and in dark (Sakata and Taira, 1994; Murata et al., 2000), as well as to the fine 3D structure of close by graspable objects (Durand et al., 2007). As a result, one can hypothesize that VIP's function is more about perceiving and locating objects in space than providing F4 with information about how to grasp them. In this context, electrical microstimulation studies provide insight about a possible functional role of this parieto-premotor VIP-F4 network. Specifically, the electrical microstimulation of area VIP produces eye blinking and squinting (this in spite of the fact that spontaneous eye blinks do not activate fundal IPS, Guipponi et al., 2014), ear folding back against the head and shoulder shrugging (Thier and Andersen, 1998), as well as lifting the upper lip in a face grimace, the retraction of the face from the contralateral side of space and the lifting of the contralateral arm and movement of the hand into lateral or upper lateral space (Cooke and Graziano, 2003; Graziano et al., 2005; Stepniewska et al., 2005), a movement repertoire that is also observed following air puffs delivered to the face (Cooke and Graziano, 2003; Graziano and Cooke, 2006). In F4, at sites with visual and tactile receptive fields encoding peripersonal space close to the head, a similar motor repertoire as that observed in VIP is also elicited by electrical microstimulations (Cooke and Graziano, 2004; Graziano et al., 2002; Graziano and Cooke, 2006). At sites with visual and tactile receptive fields encoding peripersonal space close to the arm or hand, fast withdrawal of the hand to a protective posture behind the back is elicited (Cooke and Graziano, 2004; Graziano et al., 2002; Graziano and Cooke, 2006). However, mirroring the distinct functional response properties of these two regions, distinct contributions of area VIP and area F4 to defense and avoidance seem to co-exist, as highlighted by the comparative electrical microstimulation study performed by Cooke and Graziano (2004), Graziano et al. (2002) and Graziano and Cooke (2006). While the above described motor repertoire could be elicited from the premotor cortex with thresholds as low as 20 μA, both in the awake and anesthetized monkey, in the parietal cortex, current intensities of 100 μA or more had to be used and the frequency and amplitude of this motor repertoire were greatly reduced by anesthesia. Another important difference needs to be highlighted. The electrical microstimulation of F4 systematically disrupts ongoing behavior (by the above described motor repertoire), but this ongoing behavior is abruptly resumed when the stimulation is interrupted. In VIP, the evoked defensive repertoire often diminishes over repeated electrical stimulation trials, indicating an adaptation to the stimulation. In addition, the complex movement pattern generated by the stimulation continues after the end of the stimulation (i.e. the monkey does not abruptly resumes the behavior it was performing prior to the stimulation), possibly indicating that the percept at the origin of the motor response is still active (Graziano and Cooke, 2006). Overall, these observations suggest a contribution of this VIP-F4 network to defense and obstacle avoidance behavior, the parietal pole of this network being more involved in the construction of a perception of the environment anchored to the head, and the premotor pole being more involved in the production of reflexive, rapid, complex defensive motor patterns aimed at protecting the body by producing defensive (e.g. closing of the eye lid, lifting the arm/hand in front of the head) or avoidance responses (moving the head away to the side, retrieving the arm and placing it behind the back). In other words, this network is proposed to sub-serve the representation and protection of near peripersonal space or safety margin around the body, with a specific emphasis on two vulnerable body parts, the head and the arm/hand unit (Fig. 5, Graziano and Cooke, 2006).

4.2. Looming stimuli and the dynamic intrusion into the peripersonal safety margin

When considering the concept of a safety margin, stable stimuli close to our body (e.g. a tree, a cup) do not have the same ecological significance as dynamic stimuli looming towards us. Indeed, looming stimuli are potentially more dangerous than other visual stimuli, including dynamic stimuli with no predicted impact to the body. Think in this respect of a predator or an aggressive conspecific jumping on us, or of a branch coming onto us at high speed. Such looming stimuli are known to trigger stereotyped defense responses (in monkeys: Schiff et al., 1962; in human infant: Ball and Tronick, 1971). Interestingly, threatening looming stimuli are perceived as

having a shorter time-to-impact latency as compared to non-threatening objects moving at the same objective speed (Vagnoni et al., 2012). In a recent study (Ben Hamed et al., 2013), we show that tactile sensitivity is enhanced at the predicted location and predicted time of impact of a looming visual stimulus to the face as compared to 1) baseline tactile sensitivity (average increase in $d'=0.44$, $n=10$, $p<0.01$ at corrected level), 2) the tactile sensitivity observed when the looming stimulus is temporally predictive but not spatially predictive (average increase in $d'=0.25$, $n=10$, $p<0.01$ at corrected level), and 3) the tactile sensitivity observed when the looming stimulus is spatially predictive but presented during the looming stimulus rather than at its expected time of impact (average increase in $d'=0.20$, $n=10$, $p<0.05$ at corrected level). Tactile perception is also enhanced as compared to baseline tactile sensitivity when the looming stimulus brushes past the face without however predicting an impact to the face (average increase in $d'=0.75$, $n=10$, $p<0.001$). This suggests a cross-modal processing of visual stimuli potentially impacting the face.

Interestingly, and in direct relation with these observations, the visual response occasionally observed in parietal tactile neurons (and more generally in bimodal visuo-tactile neurons) was initially interpreted as an "anticipatory activation", predictive of touch in the corresponding skin (Hyvärinen and Poranen, 1974). Amongst the several areas discussed above as hosting bimodal neurons, the selectivity of VIP and F4 neurons appears as optimally tuned for the detection of dynamic looming visual stimuli (Colby et al., 1993; Bremmer et al., 2002a, 2002b; Rizzolatti et al., 1981; Graziano et al., 1997), corroborating their possible role in the definition of a border-of-self safety zone. Accordingly, in a recent non-human primate fMRI experiment (Fig. 3, horizontal panels 3 and 4, Cléry et al., 2013, 2014), we present low luminosity looming stimuli predicting an impact to the face while monkeys fixated a central fixation point. These degraded visual looming stimuli were either presented on their own, or in conjunction with a very weak tactile stimulus (air puff), either in temporal coincidence with the looming visual stimuli (Fig. 3, horizontal panel 4) or in temporal offset, such that the visual stimuli are actually predicting the tactile stimuli (which are thus presented at the predicted time of impact of the looming stimulus to the face, Fig. 3, horizontal panel 3). This experiment is designed to identify the cortical sites that are maximally activated by the predictive bimodal stimuli. These robustly include striate and extrastriate visual cortical sites (not shown). Areas VIP (Fig. 3b3) and F4 (Fig. 3b3) are also robustly activated, bilaterally. Most importantly, these activations are systematically significantly higher when the looming stimulus is predictive of the tactile stimulus than when these two stimuli are presented simultaneously, a condition which hardly elicits any parietal (Fig. 3b4) or periarcuate activation (Fig. 3b4). Overall, these observations indicate that the peripersonal defense network described above is also involved in the prediction of intrusive impact prediction to the body. In addition, they strongly suggest that this parietal premotor VIP-F4 network most probably belongs to a larger functional network involving lower level visual areas.

4.3. The parieto-premotor VIP-F4 network and social cognition

Ishida et al. (2010) describe, in parietal area VIP, "body-matching neurons" that respond to visual stimuli presented near a specific body part of the monkey being recorded from (as classically described), but also to visual stimuli presented near the corresponding body part of the human experimenter. The response of the majority of these neurons depends on the position of the experimenter with respect to the monkey, though some of them are, to a certain extent, independent of this spatial relationship between the monkey and the observed experimenter. In humans, a shared representation for the space near oneself and near others has recently been described by Brozzoli et al. (2013). This suggests that, at minimum, the parietal node of the discussed parieto-premotor VIP-F4 network possibly contributes to the construction of both a representation of one own's body and of the body of others. This is to be contrasted with the description of the representation of others' actions in the parieto-premotor network for action described below.

In conclusion, as stated above, the peripersonal representation subserved by this parieto-premotor network, though serving the definition of a safety body margin contributing the definition of self (as a whole) with respect to the external world, over-represents two vulnerable body parts, namely the head and the arm/hand unit (Figs. 2 and 3). This network is tightly associated with defensive behavior, protecting the body margin from external aggression, and the prediction of intrusive impact to the body. Because of these specific properties, we predict that the peripersonal space representation subserved by this functional network dynamically adjusts to the general emotional and social context the subject is experiencing (see discussion below).

5. The parieto-premotor network for action

The second circuit is formed by parietal areas AIP and 7b and premotor area F5 (Fig. 2b). As will be detailed below, while areas 7b and F5 share sensory visual and tactile properties as well as motor hand-related properties subserving their central role in grasp planning and execution within a motor peripersonal space defined as the reachable space (see Sections 2.2 and 3), area AIP does not appear to contribute to peripersonal space representation per se (though it does represent 3D objects structure and thus possibly contributes to the definition of the motor affordances of objects; see Section 2.1). However, given the strong anatomical connections and otherwise functional homologies between these three cortical regions (Matelli and Luppino, 2001; Rizzolatti and Luppino, 2001), the contribution of areas F5 and 7b to grasping in peripersonal space cannot be discussed without also discussing the contribution of area AIP to this network.

5.1. Grasping

The second parieto-premotor network is formed by parietal areas 7b and AIP (not that this latter cortical region is not described to contain bimodal visuo-tactile neurons), and premotor area F5 (Fig. 2b, Rizzolatti and Luppino, 2001; Matelli and Luppino, 2001; Rizzolatti and Matelli, 2003). It is functionally specialized in the visuomotor transformation that subserves the grasping of objects in our environment, i.e. the online adjustment of the hand and finger configuration for a secured interaction with the objects. The neurons of area AIP can be classified into three different categories (see Sakata and Taira (1994) and Murata et al. (2000)). "Visual-dominant" neurons discharge during object fixation and when this object is grasped in light, but not in dark. "Visual-and-motor" neurons discharge during grasping both in light and in dark, but their response is higher when the grasped object is visible. These neurons also respond to the mere presentation of a graspable object. "Motor-dominant" neurons discharge during grasping whether in dark or in light but are not responsive to the presentation of an object. A specific coding for the 3D structure of objects is also described in this region (Durand et al., 2007). The reversible inactivation of this cortical region induces an inability for the monkey to correctly shape its hand and finger to grasp the presented object (Gallese et al., 1994). A high proportion of area 7b neurons respond not only to visual and tactile stimulations but also to motor activity (Hyvärinen, 1981; Hyvärinen and Poranen, 1974; Hyvärinen and Shelepin, 1979; Leinonen, 1980; Leinonen et al., 1979; Leinonen and Nyman, 1979; Robinson et al., 1978). These neurons respond for

simple actions (e.g. grasping a specific object) as well as to complex sequences of actions, though differently (e.g. grasp to bring to the mouth, Fogassi et al., 2005; Fogassi and Luppino, 2005). Last, as is the case for AIP neurons, 20% of area F5 neurons discharge in response to the visual presentation of 3D objects (Murata et al., 1997). The so-called canonical neurons are selectively activated by the vision of objects of a specific size, shape and orientation. Their visual specificity matches their motor specificity and their visual response is independent of whether an action is being planned or performed towards the object or not (Murata et al., 1997). Its inactivation leads to deficit similar to the one observed following AIP inactivations (Fogassi et al., 2001).

5.2. Objects, one's action and others' actions

The monkey ventral premotor visuomotor neurons of area F5 are classically subdivided into two categories of neurons. "Canonical" neurons, as described above, respond to visually presented objects and to actions generated towards these objects, both in dark and in light and are proposed to underlie visuomotor transformation for grasping (Murata et al., 1997; Raos et al., 2006). "Mirror" neurons respond during both the generation of an action and the observation of someone else performing the same action, and are proposed to play a role in action understanding (Gallese et al., 1996; Rizzolatti et al., 1996; Rizzolatti and Matelli, 2003; Rizzolatti and Fogassi, 2014). In a recent study, Bonini et al. (2014) show that neurons with canonical and mirror properties are often present at the same cortical sites. A subset of F5 neurons actually share both canonical and mirror properties (canonical-mirror neurons). In addition, the authors show that responses of canonical and canonical-mirror neurons to the presentation of graspable objects typically require the stimulus to be in peripersonal space. In other words, these neurons require the grasping action called for by the object to be feasible. In contrast, the action observation responses of mirror and canonical-mirror neurons are present irrespectively of whether the observed action is performed in the peripersonal or in the extrapersonal space. As a result, in this cortical region, space constrained responses to objects mostly rely on an action possibility rather than actual distance from the body. Interestingly, mirror-neurons can also be found in parietal area 7b (Fogassi et al., 2005; Fogassi and Luppino, 2005). These neurons, like the "canonical" 7b neurons, respond differentially to simple acts and to complex goal-directed sequences of acts specifying an action. Fogassi et al. suggest that these neurons not only code the observed act but also the intention of the agent when performing the whole sequence specifying the action. A further comparison between the properties of parietal 7b and premotor F5 mirror neurons suggests that the inferior parietal cortex plays an important role in the organization of natural ecological actions (Bonini et al., 2010). Because of these specific properties, we do not expect this functional network to be dynamically adjusts to the general emotional and social context the subject is experiencing. Rather, in addition to its dependence of its responses on whether an object is graspable, we predict a dynamical adjustment of these responses to the emotional and social nature of the object to be grasped (e.g. graspable object on fire, see discussion below).

6. Plastic AND dynamic peripersonal space representations

All throughout this review, we have considered peripersonal space as a static functional representation, determined by fixed body constraints such as the within reach space around the body or around the head. However, there is an ever growing body of evidence that peripersonal space should rather be considered as extremely dynamic and rapidly adjusting to both endogenous and exogenous factors (Fig. 5). Here, we distinguish two types of changes in peripersonal space representation. Plastic changes are defined as changes that occur following training or learning. In contrast, dynamic changes are defined as abrupt changes due to a correlated change in the environment or in the internal state of the individual. These two types of changes are expected to be mediated by different mechanisms (see below). Whenever monkey driven evidence is available, this will be discussed in priority (Section 6.1). In the absence of such experimental evidence, human data will be put forward, in order to stimulate future research on the neural bases of peripersonal space plasticity and dynamics in the non-human primate.

6.1. Action-dependence

Near space is not rigidly defined by the space at hand-reaching distance. Far space can indeed become included in near peripersonal space when subjects manipulate tools that allow them to act in a larger space around their body (Farnè and Làdavas, 2000; Berti and Frassinetti, 2000). This tool incorporation into the body schema and the correlated plastic expansion of peripersonal space representation cannot be solely based on the passive perceptual observation of the tool in the hand, but requires active repeated use of the tool to reach objects in far space (Farnè et al., 2005). This tool remapping of peripersonal space has been reviewed by several authors and is beyond the scope of the present work (Maravita et al., 2003; Maravita and Iriki, 2004; Làdavas and Serino, 2008; Cardinali et al., 2009; Makin et al., 2012; Brown and Goodale, 2013; Brozzoli et al., 2014; but see Holmes (2012)). We would just like to highlight here the fact that training, i.e., repeated action, appears to be important for tool remapping to take place, though this training does not need to be long in order to produce measurable effects on peripersonal space representation (Maravita et al., 2002; Sengül et al., 2012). Overall this suggests that tool remapping of peripersonal space relies on motor knowledge (Brown and Goodale, 2013). This is supported, amongst, other evidence, by the fact that peripersonal space representation dynamically adapts to the action the subject is actually performing (e.g. a reach versus a grasping movement, Brozzoli et al., 2010). In a set of monkey electrophysiological recording studies, Iriki et al. elegantly explore the neural bases of tool remapping of peripersonal space. In particular, they describe bimodal neurons, in the medial anterior intraparietal sulcus and in the post-central gyrus, whose visual receptive fields expand following tool use training so as to encompass the tool in addition to the hand or arm (Iriki et al., 1996; Maravita and Iriki, 2004). This was the case for both "distal" cells, whose tactile receptive field was on the skin of the hand, and "proximal" cells, whose tactile receptive field was on the skin of the shoulder. Importantly, these changes required active tool use. Using positron emission tomography (PET), Obayashi et al. (2001) further describe the activation, at the cortical level, of the pre-supplementary motor area and the premotor cortex at locations matching F4 and F5 areas discussed above. The increased corticocortical afferents to the intraparietal sulcus (Hihara et al., 2006) and the increased expression of neuronal plasticity markers in this cortical region (Ishibashi et al., 2002a, 2002b) following the learning of tool-use but not following its execution confirm that training on tool-use activates parietal neuronal plasticity mechanisms.

However, there is yet more to action-dependent plasticity of peripersonal space. For example, Lourenco and Longo (2009) show that changing the arm-related proprioceptive signals by wearing weights to the wrists results in a contraction of peripersonal space, indicating that peripersonal space does not exclusively rely on visuo-motor interactions, and supporting the idea of a functional link between peripersonal space representation and body schema (Cardinali et al., 2009). For example, Bassolino et al. (2010) show that an extension of peripersonal space can be achieved not only

by using a solid tools acting onto the far space environment, but also with a tool that acts onto far space without being physically connected to it (e.g. a mouse). This suggests that the driving information in tool-use remapping might actually be the perceptual resultant of the action onto far space rather than the action itself. In addition, the authors show that the subject's peripersonal space representation adjusts to whether the subjects are manipulating the mouse or not, suggesting that there is no such thing as a "near space" representation but rather, that it is dynamical in essence, constantly incorporating sensory, motor and higher-order elements (see below) in time.

6.2. Inferred sensations

In most daily life situations, visual stimuli are physically perceived and analyzed with respect to our self. However, some artificial situations lead us to infer the presence of a visual stimulus close to our body. For example, when facing a mirror, we see a visual image of our body projected somewhere in extrapersonal space. A visual stimulus seen through the mirror as close to our body will be referred to a real stimulus close to our actual body, though this stimulus is physically perceived in far space, and will be incorporated into our peripersonal space representation (Maravita et al., 2000; Holmes and Spence, 2006). To our knowledge, there is a unique experimental account of the putative neural bases of this mirror inferential effect. Iriki et al. (2001) show that the bimodal visuo-tactile neurons in the lateral anterior intraparietal cortex of the monkey respond both when a visual stimulus is presented within their visual receptive field close to the body, or when the animals viewed a video in which a visual stimulus is presented closed to their filmed body, at a location matching their visual receptive field. Another example is the case of body shadow. Several experiments suggest that the space round our body shadow is partially remapped as peripersonal space (Pavani and Castiello, 2004; Bonfiglioli et al., 2004; Galfano and Pavani, 2005). This ability to extend peripersonal space representation to other spaces referring to the body is proposed to serve defense and protective behaviors. Think of yourself drinking at a water pound, in the savanna, on the watch for any predator ready to jump on you. Both a change in the visual information from the water reflection and the body shadow limits are strong indicators of danger. However, the neural bases of such inferred peripersonal space are still scarce.

6.3. Positional interactions

Head and arm peripersonal spaces are often considered as independent spaces; however, recent evidence suggests that depending on the relative position of one with respect to the other, these peripersonal spaces can actually interact and merge. Sambo et al. (2012a) show that the hand blink reflex that is elicited by an electrical stimulation of the median nerve is dramatically increased when the hand is placed within the face peripersonal space. The authors suggest that this is due to a top down modulation exerted by the VIP-F4 parieto-motor network and having as effect to change the response thresholds of the medial nerve. Interestingly, the eye blink reflex that is elicited by an electrical stimulation of the trigeminal nerve is not affected by the proximity of the hand to the face, suggesting that the hand is being incorporated into the head peripersonal space and not the reverse. In addition, the hand blink reflex is highly dependent onto cognitive expectations and inferences. Indeed, it is enhanced only when participants expect to receive stimuli on the hand (placed close to the face, Sambo et al., 2012b). Last, this enhancement is abolished when a thin wooden screen is placed between the participants' face and their hand, creating a virtual separation between the face and hand peripersonal space representations. Again, the neural bases of such positional interaction in peripersonal spaces are scarce.

6.4. Social and emotional plasticity of peripersonal space

Last, several higher-order variables have been described to dynamically influence perceptual processes and the representation of peripersonal space. For example, Markman and Brendl (2005) demonstrate an interaction between word valence (positive words and negative words) and the representation of self, whereby subjects are faster at pulling a lever than at pushing it when presented with a positive word and faster at pushing than pulling when presented with a negative word. Likewise, positive objects induce an extension of the peripersonal space, such that they are perceived closer to the body than neutral or negative objects, as if they were included in the peripersonal space (Valls-Solé et al., 1997). As a result, the nature of the action one is performing is not only important in the definition of peripersonal space (Brozzoli et al., 2010), but also the emotional valence of the target as well as the emotional consequences of the actions. This is all the more marked in the context of social interactions (Teneggi et al., 2013). Indeed, Teneggi et al. (2013) describe that our peripersonal space is smaller when we are facing another individual standing in far space, as compared to when we are facing a mannequin placed at the same location. Importantly, the peripersonal boundary changes as a function of the social experience we are having with the individual facing us. Teneggi et al. show that, following an economic game, peripersonal space boundaries between our self and the other individual merge, but only if this person behaved cooperatively. Overall, this indicates a link between low-level sensorimotor processing shaping a core peripersonal space representation and high-level social and emotional cues dynamically adjusting this core representation. This type of dynamic adjustment of peripersonal space is proposed to serve defense and protective behaviors. Corroborating this putative function of peripersonal space dynamics induced by emotions, claustrophobic fear is positively correlated with a larger peripersonal space (Lourenco et al., 2011). These observations suggest that the enlarged peripersonal space might actually be at the origin of claustrophobia, anxiety to enclosed spaces and physically restrictive situations arising from the higher rate of objects and agents perceived as intruding into these subjects' peripersonal space.

7. Putative mechanisms subserving dynamic peripersonal space representations

7.1. Domain specific social and emotional dynamics in the processing of peripersonal space

As described in Section 6.1, action-dependent changes in peripersonal space representation is proposed to essentially involve the core 7b-AIP-F5 parieto-premotor network (and possibly other functionally coupled cortical and subcortical regions). A major property of this functional network is the dependence of its visual responses to the operational quality of the presented objects, i.e. to whether they are graspable or not. Emotional and social cues can alter the graspability of an object. For example, a graspable object on fire is no more graspable. Likewise, in the presence of a dominant conspecific, a graspable apple may become ungraspable for social peace motivations. As a result, we predict that the peripersonal space representation subserved by this functional network will dynamical adjust to the emotional and social nature of the object to be grasped. In contrast, we propose that the positional and inferential changes in peripersonal space representation described in Sections 6.2 and 6.3 essentially involve the core VIP-F4 parieto-premotor network, due to its central role in the definition of a protective margin of self. Likewise, we expect

this functional network to be involved in the dynamics in peripersonal space representations following changes in the emotional and social global context experienced by the subjects. This proposal does not exclude functional interactions between these two networks (and hence these two types of peripersonal spaces), as perception and action are not independent cortical functions (for a review, Rizzolatti and Matelli, 2003).

7.2. Plastic and dynamic

As stated in Section 6, plastic cortical changes are defined as changes taking place following training or learning. In contrast, dynamic changes are defined as abrupt changes in response to a change in the environment or in the internal state of the individual. Overall, peripersonal space appears to be not only plastic (Section 6.1), that is to say affected by training and repeated exposure to a given sensori-motor context, but also dynamic, that is capable of an instantaneous adjustment to the ongoing low-level (sensory and motor) and higher order (inferential, emotional, social) context (Sections 6.2, 6.3 and 6.4). Several groups have provided important insights on the neural basis of tool-induced plasticity in the non-human primate. However, in the face of the growing number of neuropsychological and psychological studies describing the dynamic properties of peripersonal space representations in humans, non-human primate studies describing its possible neural bases remain rare. Several studies have characterized the dynamic changes in the visual receptive fields of individual MT visual extrastriate (Womelsdorf et al., 2006, 2008; Anton-Erxleben et al., 2007) and parietal cortex (Ben Hamed et al., 1997, 2002) as a function of attention, demonstrating the highly dynamic context-dependent nature of the visual space representation. These attention-driven dynamic adjustments of how individual cells represent visual information are proposed to allow for an adjustment of spatial processing to the requirements of the ongoing behavior, corroborating the psychophysical evidence for an effect of attention on size and distance perception (Anton-Erxleben et al., 2007, 2010; Anton-Erxleben and Carrasco, 2013; Wardak et al., 2011). We propose that similar dynamic neuronal mechanisms underlie the overt dynamic changes in peripersonal space representation described above and result from the weighted integration, by local networks, of context-dependent incoming information (visual, tactile, proprioceptive, attention, emotional, social, cognitive, motor, etc.). Consequently, space representation dynamically is proposed to change as a function of the nature of processed information, while the unified space perception is proposed to be achieved via the fact that it arises from stable cortical networks. Like it has been described for attention (Buschman and Miller, 2007; Gregoriou et al., 2009, 2012), long-range top-down synchronization mechanisms in the functional networks highlighted above are expected to play a crucial role in the continuous adjustment of the core peripersonal space representation (as defined by low level cues) to the cognitive context. The peripersonal space dynamics induced by emotional and social situation are expected to involve long-range synchronization mechanisms between these core functional networks and such structures as the amygdala or the orbitofrontal cortex. Future experiments will allow to directly test this hypothesis.

Acknowledgments

O.G. was funded by the French Education Ministry. S.BH was funded by the French Agence Nationale de la Recherche (Grant #ANR-05-JCJC-0230-01).

References

Ackroyd, K., Riddoch, M.J., Humphreys, G.W., Nightingale, S., Townsend, S., 2002. Widening the sphere of influence: using a tool to extend extrapersonal visual space in a patient with severe neglect. Neurocase 8, 1–12.

Aimola, L., Schindler, I., Venneri, A., 2013. Task- and response related dissociations between neglect in near and far space: a morphometric case study. Behav. Neurol. 27, 245–257.

Akao, T., Kurkin, S.A., Fukushima, J., Fukushima, K., 2005. Visual and vergence eye movement-related responses of pursuit neurons in the caudal frontal eye fields to motion-in-depth stimuli. Exp. Brain Res. 164, 92–108.

Akbarian, S., Grüsser, O.J., Guldin, W.O., 1993. Corticofugal projections to the vestibular nuclei in squirrel monkeys: further evidence of multiple cortical vestibular fields. J. Comp. Neurol. 332, 89–104.

Akbarian, S., Grüsser, O.J., Guldin, W.O., 1994. Corticofugal connections between the cerebral cortex and brainstem vestibular nuclei in the macaque monkey. J. Comp. Neurol. 339, 421–437.

Alkan, Y., Biswal, B.B., Alvarez, T.L., 2011. Differentiation between vergence and saccadic functional activity within the human frontal eye fields and midbrain revealed through fMRI. PLoS One 6, e25866.

Alvarez, T.L., Alkan, Y., Gohel, S., Douglas Ward, B., Biswal, B.B., 2010. Functional anatomy of predictive vergence and saccade eye movements in humans: a functional MRI investigation. Vis. Res. 50, 2163–2175.

Anton-Erxleben, K., Abrams, J., Carrasco, M., 2010. Evaluating comparative and equality judgments in contrast perception: attention alters appearance. J. Vis. 10, 6.

Anton-Erxleben, K., Carrasco, M., 2013. Attentional enhancement of spatial resolution: linking behavioural and neurophysiological evidence. Nat. Rev. Neurosci. 14, 188–200.

Anton-Erxleben, K., Henrich, C., Treue, S., 2007. Attention changes perceived size of moving visual patterns. J. Vis. 7 (5), 1–9.

Avillac, M., Ben Hamed, S., Duhamel, J.-R., 2007. Multisensory integration in the ventral intraparietal area of the macaque monkey. J. Neurosci. 27, 1922–1932.

Avillac, M., Denève, S., Olivier, E., Pouget, A., Duhamel, J.-R., 2005. Reference frames for representing visual and tactile locations in parietal cortex. Nat. Neurosci. 8, 941–949.

Avillac, M., Olivier, E., Denève, S., Ben Hamed, S., Duhamel, J.R., 2004. Multisensory integration in multiple reference frames in the posterior parietal cortex. Cogn. Process. 5 (3), 159–166.

Ball, W., Tronick, E., 1971. Infant responses to impending collision: optical and real. Science 171, 818–820.

Bassolino, M., Serino, A., Ubaldi, S., Làdavas, E., 2010. Everyday use of the computer mouse extends peripersonal space representation. Neuropsychologia 48, 803–811.

Ben Hamed, S., Cléry, J., Guipponi, O., Wardak, C., 2013. Multisensory integration for looming visual. Société française des Neurosciences. Poster 156.

Ben Hamed, S., Duhamel, J.-R., Bremmer, F., Graf, W., 1997. Attentional modulation of visual receptive fields in the posterior parietal cortex of the behaving macaque. Experimental Brain Research Series, 25; pp. 371–384.

Ben Hamed, S., Duhamel, J.R., Bremmer, F., Graf, W., 2001. Representation of the visual field in the lateral intraparietal area of macaque monkeys: a quantitative receptive field analysis. Exp. Brain Res. 140, 127–144.

Ben Hamed, S., Duhamel, J.-R., Bremmer, F., Graf, W., 2002. Visual receptive field modulation in the lateral intraparietal area during attentive fixation and free gaze. Cereb. Cortex 12, 234–245.

Berti, A., Frassinetti, F., 2000. When far becomes near: remapping of space by tool use. J. Cogn. Neurosci. 12, 415–420.

Beschin, N., Robertson, I.H., 1997. Personal versus extrapersonal neglect: a group study of their dissociation using a reliable clinical test. Cortex 33, 379–384.

Bhattacharyya, R., Musallam, S., Andersen, R.A., 2009. Parietal reach region encodes reach depth using retinal disparity and vergence angle signals. J. Neurophysiol. 102, 805–816.

Bisiach, E., Perani, D., Vallar, G., Berti, A., 1986. Unilateral neglect: personal and extra-personal. Neuropsychologia 24, 759–767.

Bjoertomt, O., Cowey, A., Walsh, V., 2002. Spatial neglect in near and far space investigated by repetitive transcranial magnetic stimulation. Brain 125, 2012–2022.

Bjoertomt, O., Cowey, A., Walsh, V., 2009. Near space functioning of the human angular and supramarginal gyri. J. Neuropsychol. 3, 31–43.

Bonfiglioli, C., Pavani, F., Castiello, U., 2004. Differential effects of cast shadows on perception and action. Perception 33, 1291–1304.

Bonini, L., Maranesi, M., Livi, A., Fogassi, L., Rizzolatti, G., 2014. Space-dependent representation of objects and other's action in monkey ventral premotor grasping neurons. J. Neurosci. 34, 4108–4119.

Bonini, L., Rozzi, S., Serventi, F.U., Simone, L., Ferrari, P.F., Fogassi, L., 2010. Ventral premotor and inferior parietal cortices make distinct contribution to action organization and intention understanding. Cereb. Cortex 20, 1372–1385.

Bremmer, F., Duhamel, J.-R., Ben Hamed, S., Graf, W., 1997. The representation of movement in near extra-personal space in the macaque ventral intraparietal area (VIP). In: Thier, P., Karnath, H.-O. (Eds.), Parietal Lobe Contributions to Orientation in 3D Space, Experimental Brain Research Series, 25; pp. 619–630.

Bremmer, F., Duhamel, J.R., Ben Hamed, S., Graf, W., 2000. Stages of self-motion processing in primate posterior parietal cortex. Int. Rev. Neurobiol. 44, 173–198.

Bremmer, F., Duhamel, J.-R., Ben Hamed, S., Graf, W., 2002a. Heading encoding in the macaque ventral intraparietal area (VIP). Eur. J. Neurosci. 16, 1554–1568.

Bremmer, F., Graf, W., Ben Hamed, S., Duhamel, J.R., 1999. Eye position encoding in the macaque ventral intraparietal area (VIP). Neuroreport 10, 873–878.

Bremmer, F., Klam, F., Duhamel, J.-R., Ben Hamed, S., Graf, W., 2002b. Visual-vestibular interactive responses in the macaque ventral intraparietal area (VIP). Eur. J. Neurosci. 16, 1569–1586.

Bremmer, F., Schlack, A., Duhamel, J.R., Graf, W., Fink, G.R., 2001. Space coding in primate posterior parietal cortex. Neuroimage 14, S46–S51.

Bremmer, F., Schlack, A., Kaminiarz, A., Hoffmann, K.-P., 2013. Encoding of movement in near extrapersonal space in primate area VIP. Front. Behav. Neurosci. 7, 8.

Breveglieri, R., Hadjidimitrakis, K., Bosco, A., Sabatini, S.P., Galletti, C., Fattori, P., 2012. Eye position encoding in three-dimensional space: integration of version and vergence signals in the medial posterior parietal cortex. J. Neurosci. 32, 159–169.
Brown, L.E., Goodale, M.A., 2013. A brief review of the role of training in near-tool effects. Front. Psychol. 4, 576.
Brozzoli, C., Cardinali, L., Pavani, F., Farnè, A., 2010. Action-specific remapping of peripersonal space. Neuropsychologia 48, 796–802.
Brozzoli, C., Ehrsson, H.H., Farnè, A., 2014. Multisensory representation of the space near the hand: from perception to action and interindividual interactions. Neuroscientist 20, 122–135.
Brozzoli, C., Gentile, G., Bergouignan, L., Ehrsson, H.H., 2013. A shared representation of the space near oneself and others in the human premotor cortex. Curr. Biol. 23, 1764–1768.
Brozzoli, C., Makin, T.R., Cardinali, L., Holmes, N.P., Farnè, A., 2012. Peripersonal space: a multisensory interface for body–object interactions. In: Murray, M.M., Wallace, M.T. (Eds.), The Neural Bases of Multisensory Processes, Frontiers in Neuroscience. CRC Press, Boca Raton (FL).
Buschman, T.J., Miller, E.K., 2007. Top-down versus bottom-up control of attention in the prefrontal and posterior parietal cortices. Science 315, 1860–1862.
Cardinali, L., Brozzoli, C., Farnè, A., 2009. Peripersonal space and body schema: two labels for the same concept? Brain Topogr. 21, 252–260.
Chen, A., DeAngelis, G.C., Angelaki, D.E., 2011a. A comparison of vestibular spatiotemporal tuning in macaque parietoinsular vestibular cortex, ventral intraparietal area, and medial superior temporal area. J. Neurosci. 31, 3082–3094.
Chen, A., DeAngelis, G.C., Angelaki, D.E., 2011b. Representation of vestibular and visual cues to self-motion in ventral intraparietal cortex. J. Neurosci. 31, 12036–12052.
Chen, X., Deangelis, G.C., Angelaki, D.E., 2013. Diverse spatial reference frames of vestibular signals in parietal cortex. Neuron 80, 1310–1321.
Chen, X., DeAngelis, G.C., Angelaki, D.E., 2014. Eye-centered visual receptive fields in the ventral intraparietal area. J. Neurophysiol. 112, 353–361.
Cléry, J., Guipponi, O., Odouard, S., Wardak, C., Ben Hamed, S., 2014. Neural bases of impact prediction in the non-human primate. In: Proceedings of the 9th FENS Forum of Neuroscience. Poster D003.
Cléry, J., Guipponi, O., Wardak, C., Ben Hamed, S., 2013. Multisensory integration of dynamic stimuli in the non-human primate: a functional Magnetic Resonance Imaging (fMRI) study. Société française des Neurosciences. Poster 142.
Colby, C.L., Duhamel, J.R., Goldberg, M.E., 1993. Ventral intraparietal area of the macaque: anatomic location and visual response properties. J. Neurophysiol. 69, 902–914.
Cooke, D.F., Graziano, M.S.A., 2003. Defensive movements evoked by air puff in monkeys. J. Neurophysiol. 90, 3317–3329.
Cooke, D.F., Graziano, M.S.A., 2004. Sensorimotor integration in the precentral gyrus: polysensory neurons and defensive movements. J. Neurophysiol. 91, 1648–1660.
Coslett, H.B., Schwartz, M.F., Goldberg, G., Haas, D., Perkins, J., 1993. Multi-modal hemispatial deficits after left hemisphere stroke. A disorder of attention? Brain 116 (Pt 3), 527–554.
Cowey, A., Small, M., Ellis, S., 1994. Left visuo-spatial neglect can be worse in far than in near space. Neuropsychologia 32, 1059–1066.
Cowey, A., Small, M., Ellis, S., 1999. No abrupt change in visual hemineglect from near to far space. Neuropsychologia 37, 1–6.
Duhamel, J.R., Bremmer, F., Ben Hamed, S., Graf, W., 1997. Spatial invariance of visual receptive fields in parietal cortex neurons. Nature 389, 845–848.
Duhamel, J.-R., Colby, C.L., Goldberg, M.E., 1998. Ventral intraparietal area of the macaque: congruent visual and somatic response properties. J. Neurophysiol. 79, 126–136.
Durand, J.-B., Nelissen, K., Joly, O., Wardak, C., Todd, J.T., Norman, J.F., Janssen, P., Vanduffel, W., Orban, G.A., 2007. Anterior regions of monkey parietal cortex process visual 3D shape. Neuron 55, 493–505.
Durand, J.-B., Peeters, R., Norman, J.F., Todd, J.T., Orban, G.A., 2009. Parietal regions processing visual 3D shape extracted from disparity. Neuroimage 46, 1114–1126.
Farnè, A., Iriki, A., Làdavas, E., 2005. Shaping multisensory action–space with tools: evidence from patients with cross-modal extinction (Movement, Action and Consciousness: Toward a Physiology of Intentionality. A Special Issue in Honour of Marc Jeannerod). Neuropsychologia 43, 238–248.
Farnè, A., Làdavas, E., 2000. Dynamic size-change of hand peripersonal space following tool use. Neuroreport 11, 1645–1649.
Ferraina, S., Paré, M., Wurtz, R.H., 2000. Disparity sensitivity of frontal eye field neurons. J. Neurophysiol. 83, 625–629.
Fogassi, L., Ferrari, P.F., Gesierich, B., Rozzi, S., Chersi, F., Rizzolatti, G., 2005. Parietal lobe: from action organization to intention understanding. Science 308, 662–667.
Fogassi, L., Gallese, V., Buccino, G., Craighero, L., Fadiga, L., Rizzolatti, G., 2001. Cortical mechanism for the visual guidance of hand grasping movements in the monkey: a reversible inactivation study. Brain 124, 571–586.
Fogassi, L., Gallese, V., Fadiga, L., Luppino, G., Matelli, M., Rizzolatti, G., 1996. Coding of peripersonal space in inferior premotor cortex (area F4). J. Neurophysiol. 76, 141–157.
Fogassi, L., Luppino, G., 2005. Motor functions of the parietal lobe. Curr. Opin. Neurobiol. 15, 626–631.
Galfano, G., Pavani, F., 2005. Long-lasting capture of tactile attention by body shadows. Exp. Brain Res. 166, 518–527.
Gallese, V., Fadiga, L., Fogassi, L., Rizzolatti, G., 1996. Action recognition in the premotor cortex. Brain 119, 593–609.
Gallese, V., Murata, A., Kaseda, M., Niki, N., Sakata, H., 1994. Deficit of hand preshaping after muscimol injection in monkey parietal cortex. Neuroreport 5, 1525–1529.
Gamlin, P.D., Yoon, K., 2000. An area for vergence eye movement in primate frontal cortex. Nature 407, 1003–1007.
Genovesio, A., Ferraina, S., 2004. Integration of retinal disparity and fixation-distance related signals toward an egocentric coding of distance in the posterior parietal cortex of primates. J. Neurophysiol. 91, 2670–2684.
Gentilucci, M., Fogassi, L., Luppino, G., Matelli, M., Camarda, R., Rizzolatti, G., 1988. Functional organization of inferior area 6 in the macaque monkey. I. Somatotopy and the control of proximal movements. Exp. Brain Res. 71, 475–490.
Gentilucci, M., Scandolara, C., Pigarev, I.N., Rizzolatti, G., 1983. Visual responses in the postarcuate cortex (area 6) of the monkey that are independent of eye position. Exp. Brain Res. 50, 464–468.
Gnadt, J.W., Mays, L.E., 1995. Neurons in monkey parietal area LIP are tuned for eye-movement parameters in three-dimensional space. J. Neurophysiol. 73, 280–297.
Graziano, M.S.A., Aflalo, T.N.S., Cooke, D.F., 2005. Arm movements evoked by electrical stimulation in the motor cortex of monkeys. J. Neurophysiol. 94, 4209–4223.
Graziano, M.S.A., Cooke, D.F., 2006. Parieto-frontal interactions, personal space, and defensive behavior. Neuropsychologia 44, 2621–2635.
Graziano, M.S.A., Taylor, C.S.R., Moore, T., 2002. Complex movements evoked by microstimulation of precentral cortex. Neuron 34, 841–851.
Graziano, M.S., Hu, X.T., Gross, C.G., 1997. Visuospatial properties of ventral premotor cortex. J. Neurophysiol. 77, 2268–2292.
Graziano, M.S., Yap, G.S., Gross, C.G., 1994. Coding of visual space by premotor neurons. Science 266, 1054–1057.
Gregoriou, G.G., Gotts, S.J., Desimone, R., 2012. Cell-type-specific synchronization of neural activity in FEF with V4 during attention. Neuron 73, 581–594.
Gregoriou, G.G., Gotts, S.J., Zhou, H., Desimone, R., 2009. High-frequency, long-range coupling between prefrontal and visual cortex during attention. Science 324, 1207–1210.
Gross, C.G., Graziano, M.S.A., 1995. REVIEW: Multiple Representations of Space in the Brain. Neuroscientist 1, 43–50.
Guariglia, C., Antonucci, G., 1992. Personal and extrapersonal space: a case of neglect dissociation. Neuropsychologia 30, 1001–1009.
Guipponi, O., Odouard, S., Pinède, S., Wardak, C., Ben Hamed, S., 2014. fMRI cortical correlates of spontaneous eye blinks in the nonhuman primate. Cereb. Cortex, http://dx.doi.org/10.1093/cercor/bhu038.
Guipponi, O., Wardak, C., Ibarrola, D., Comte, J.-C., Sappey-Marinier, D., Pinède, S., Ben Hamed, S., 2013a. Multimodal convergence within the intraparietal sulcus of the macaque monkey. J. Neurosci. 33, 4128–4139.
Guipponi, O., Wardak, C., Odouard, S., Pinède, S., Ben Hamed, S., 2013b. Identification of the visuo-tactile convergence network: a functional magnetic imaging (fMRI) study in awake monkeys. Société française des Neurosciences. Poster 134.
Hadjidimitrakis, K., Breveglieri, R., Bosco, A., Fattori, P., 2012. Three-dimensional eye position signals shape both peripersonal space and arm movement activity in the medial posterior parietal cortex. Front. Integr. Neurosci. 6, 37.
Hadjidimitrakis, K., Breveglieri, R., Placenti, G., Bosco, A., Sabatini, S.P., Fattori, P., 2011. Fix your eyes in the space you could reach: neurons in the macaque medial parietal cortex prefer gaze positions in peripersonal space. PLoS One 6, e23335.
Halligan, P.W., Fink, G.R., Marshall, J.C., Vallar, G., 2003. Spatial cognition: evidence from visual neglect (Regul. Ed.). Trends Cogn. Sci. 7, 125–133.
Halligan, P.W., Marshall, J.C., 1991. Left neglect for near but not far space in man. Nature 350, 498–500.
Hepp-Reymond, M.C., Hüsler, E.J., Maier, M.A., Qi, H.X., 1994. Force-related neuronal activity in two regions of the primate ventral premotor cortex. Can. J. Physiol. Pharmacol. 72, 571–579.
Hihara, S., Notoya, T., Tanaka, M., Ichinose, S., Ojima, H., Obayashi, S., Fujii, N., Iriki, A., 2006. Extension of corticocortical afferents into the anterior bank of the intraparietal sulcus by tool-use training in adult monkeys. Neuropsychologia 44, 2636–2646.
Holmes, N.P., 2012. Does tool use extend peripersonal space? A review and re-analysis. Exp. Brain Res. 218, 273–282.
Holmes, N.P., Spence, C., 2006. Beyond the body schema: visual, prosthetic, and technological contributions to bodily perception and awareness. In: Knoblich, G., Thornton, I.M., Grosjean, M., Shiffrar, M. (Eds.), Human Body Perception from the Inside Out: Advances in Visual Cognition. Oxford University Press, New York, NY, US, pp. 15–64.
Hyvärinen, J., 1981. Regional distribution of functions in parietal association area 7 of the monkey. Brain Res. 206, 287–303.
Hyvärinen, J., Poranen, A., 1974. Function of the parietal associative area 7 as revealed from cellular discharges in alert monkeys. Brain 97, 673–692.
Hyvärinen, J., Shelepin, Y., 1979. Distribution of visual and somatic functions in the parietal associative area 7 of the monkey. Brain Res. 169, 561–564.
Iriki, A., Tanaka, M., Iwamura, Y., 1996. Coding of modified body schema during tool use by macaque postcentral neurones. Neuroreport 7, 2325–2330.
Iriki, A., Tanaka, M., Obayashi, S., Iwamura, Y., 2001. Self-images in the video monitor coded by monkey intraparietal neurons. Neurosci. Res. 40, 163–173.
Ishibashi, H., Hihara, S., Takahashi, M., Heike, T., Yokota, T., Iriki, A., 2002a. Tool-use learning selectively induces expression of brain-derived neurotrophic factor, its

receptor trkB, and neurotrophin 3 in the intraparietal multisensorycortex of monkeys. Brain Res. Cogn. Brain Res. 14, 3–9.
Ishibashi, H., Hihara, S., Takahashi, M., Heike, T., Yokota, T., Iriki, A., 2002b. Tool-use learning induces BDNF expression in a selective portion of monkey anterior parietal cortex. Brain Res. Mol. Brain Res. 102, 110–112.
Ishida, H., Nakajima, K., Inase, M., Murata, A., 2010. Shared mapping of own and others' bodies in visuotactile bimodal area of monkey parietal cortex. J. Cogn. Neurosci. 22, 83–96.
Jeannerod, M., Arbib, M.A., Rizzolatti, G., Sakata, H., 1995. Grasping objects: the cortical mechanisms of visuomotor transformation. Trends Neurosci. 18, 314–320.
Keller, I., Schindler, I., Kerkhoff, G., von Rosen, F., Golz, D., 2005. Visuospatial neglect in near and far space: dissociation between line bisection and letter cancellation. Neuropsychologia 43, 724–731.
Làdavas, E., Farnè, A., 2004. Visuo-tactile representation of near-the-body space. J. Physiol. 98, 161–170.
Làdavas, E., Serino, A., 2008. Action-dependent plasticity in peripersonal space representations. Cogn. Neuropsychol. 25, 1099–1113.
Leinonen, L., 1980. Functional properties of neurones in the posterior part of area 7 in awake monkey. Acta Physiol. Scand. 108, 301–308.
Leinonen, L., Hyvärinen, J., Nyman, G., Linnankoski, I., 1979. I. Functional properties of neurons in lateral part of associative area 7 in awake monkeys. Exp. Brain Res. 34, 299–320.
Leinonen, L., Nyman, G., 1979. II. Functional properties of cells in anterolateral part of area 7 associative face area of awake monkeys. Exp. Brain Res. 34, 321–333.
Lourenco, S.F., Longo, M.R., 2009. The plasticity of near space: evidence for contraction. Cognition 112, 451–456.
Lourenco, S.F., Longo, M.R., Pathman, T., 2011. Near space and its relation to claustrophobic fear. Cognition 119, 448–453.
Luppino, G., Ben Hamed, S., Gamberini, M., Matelli, M., Galletti, C., 2005. Occipital (V6) and parietal (V6A) areas in the anterior wall of the parieto-occipital sulcus of the macaque: a cytoarchitectonic study. Eur. J. Neurosci. 21, 3056–3076.
Luppino, G., Murata, A., Govoni, P., Matelli, M., 1999. Largely segregated parieto-frontal connections linking rostral intraparietal cortex (areas AIP and VIP) and the ventral premotor cortex (areas F5 and F4). Exp. Brain Res. 128, 181–187.
Makin, T.R., Holmes, N.P., Brozzoli, C., Farnè, A., 2012. Keeping the world at hand: rapid visuomotor processing for hand-object interactions. Exp. Brain Res. 219, 421–428.
Maravita, A., Clarke, K., Husain, M., Driver, J., 2002. Active tool use with the contralesional hand can reduce cross-modal extinction of touch on that hand. Neurocase 8, 411–416.
Maravita, A., Iriki, A., 2004. Tools for the body (schema) (Regul. Ed.). Trends Cogn. Sci. 8, 79–86.
Maravita, A., Spence, C., Clarke, K., Husain, M., Driver, J., 2000. Vision and touch through the looking glass in a case of crossmodal extinction. Neuroreport 11, 3521–3526.
Maravita, A., Spence, C., Driver, J., 2003. Multisensory integration and the body schema: close to hand and within reach. Curr. Biol. 13, R531–R539.
Markman, A.B., Brendl, C.M., 2005. Constraining theories of embodied cognition. Psychol. Sci. 16, 6–10.
Martinez-Trujillo, J.C., Medendorp, W.P., Wang, H., Crawford, J.D., 2004. Frames of reference for eye-head gaze commands in primate supplementary eye fields. Neuron 44, 1057–1066.
Matelli, M., Luppino, G., 2001. Parietofrontal circuits for action and space perception in the macaque monkey. Neuroimage 14, S27–S32.
Murata, A., Fadiga, L., Fogassi, L., Gallese, V., Raos, V., Rizzolatti, G., 1997. Object representation in the ventral premotor cortex (area F5) of the monkey. J. Neurophysiol. 78, 2226–2230.
Murata, A., Gallese, V., Luppino, G., Kaseda, M., Sakata, H., 2000. Selectivity for the shape, size, and orientation of objects for grasping in neurons of monkey parietal area AIP. J. Neurophysiol. 83, 2580–2601.
Obayashi, S., Suhara, T., Kawabe, K., Okauchi, T., Maeda, J., Akine, Y., Onoe, H., Iriki, A., 2001. Functional brain mapping of monkey tool use. Neuroimage 14, 853–861.
Olson, C.R., 2003. Brain representation of object-centered space in monkeys and humans. Annu. Rev. Neurosci. 26, 331–354.
Olson, C.R., Gettner, S.N., 1995. Object-centered direction selectivity in the macaque supplementary eye field. Science 269, 985–988.
Ortigue, S., Mégevand, P., Perren, F., Landis, T., Blanke, O., 2006. Double dissociation between representational personal and extrapersonal neglect. Neurology 66, 1414–1417.
Pavani, F., Castiello, U., 2004. Binding personal and extrapersonal space through body shadows. Nat. Neurosci. 7, 14–16.
Pitzalis, S., Di Russo, F., Spinelli, D., Zoccolotti, P., 2001. Influence of the radial and vertical dimensions on lateral neglect. Exp. Brain Res. 136, 281–294.
Pitzalis, S., Sereno, M.I., Committeri, G., Fattori, P., Galati, G., Tosoni, A., Galletti, C., 2013. The human homologue of macaque area V6A. Neuroimage 82, 517–530.
Pouget, A., Sejnowski, T.J., 1994. A neural model of the cortical representation of egocentric distance. Cereb. Cortex 4, 314–329.
Quinlan, D.J., Culham, J.C., 2007. fMRI reveals a preference for near viewing in the human parieto-occipital cortex. Neuroimage 36, 167–187.
Raos, V., Umiltá, M.-A., Murata, A., Fogassi, L., Gallese, V., 2006. Functional properties of grasping-related neurons in the ventral premotor area F5 of the macaque monkey. J. Neurophysiol. 95, 709–729.
Rizzolatti, G., Camarda, R., Fogassi, L., Gentilucci, M., Luppino, G., Matelli, M., 1988. Functional organization of inferior area 6 in the macaque monkey. II. Area F5 and the control of distal movements. Exp. Brain Res. 71, 491–507.
Rizzolatti, G., Cattaneo, L., Fabbri-Destro, M., Rozzi, S., 2014. Cortical mechanisms underlying the organization of goal-directed actions and mirror neuron-based action understanding. Physiol. Rev. 94, 655–706. http://dx.doi.org/10.1152/physrev.00009.2013.
Rizzolatti, G., Fadiga, L., Fogassi, L., Gallese, V., 1997. The space around us. Science 277, 190–191.
Rizzolatti, G., Fadiga, L., Gallese, V., Fogassi, L., 1996. Premotor cortex and the recognition of motor actions. Brain Res. Cogn. Brain Res. 3, 131–141.
Rizzolatti, G., Fogassi, L., 2014. The mirror mechanism: recent findings and perspectives. Philos. Trans. R. Soc. Lond. B Biol. Sci. 369, 20130420.
Rizzolatti, G., Fogassi, L., Gallese, V., 2002. Motor and cognitive functions of the ventral premotor cortex. Curr. Opin. Neurobiol. 12, 149–154.
Rizzolatti, G., Luppino, G., 2001. The cortical motor system. Neuron 31, 889–901.
Rizzolatti, G., Luppino, G., Matelli, M., 1998. The organization of the cortical motor system: new concepts. Electroencephalogr. Clin. Neurophysiol. 106, 283–296.
Rizzolatti, G., Matelli, M., 2003. Two different streams form the dorsal visual system: anatomy and functions. Exp. Brain Res. 153, 146–157.
Rizzolatti, G., Matelli, M., Pavesi, G., 1983. Deficits in attention and movement following the removal of postarcuate (area 6) and prearcuate (area 8) cortex in macaque monkeys. Brain 106, 655–673.
Rizzolatti, G., Scandolara, C., Matelli, M., Gentilucci, M., 1981. Afferent properties of periarcuate neurons in macaque monkeys. II. Visual responses. Behav. Brain Res. 2, 147–163.
Robinson, C.J., Burton, H., 1980. Somatotopographic organization in the second somatosensory area of *M. fascicularis*. J. Comp. Neurol. 192, 43–67.
Robinson, D.L., Goldberg, M.E., Stanton, G.B., 1978. Parietal association cortex in the primate: sensory mechanisms and behavioral modulations. J. Neurophysiol. 41, 910–932.
Romero, M.C., Pani, P., Janssen, P., 2014. Coding of shape features in the macaque anterior intraparietal area. J. Neurosci. 34, 4006–4021.
Romero, M.C., Van Dromme, I.C.L., Janssen, P., 2013. The role of binocular disparity in stereoscopic images of objects in the macaque anterior intraparietal area. PLoS One 8, e55340.
Sakata, H., Shibutani, H., Kawano, K., 1980. Spatial properties of visual fixation neurons in posterior parietal association cortex of the monkey. J. Neurophysiol. 43, 1654–1672.
Sakata, H., Taira, M., 1994. Parietal control of hand action. Curr. Opin. Neurobiol. 4, 847–856.
Sakata, H., Taira, M., Kusunoki, M., Murata, A., Tanaka, Y., Tsutsui, K., 1998. Neural coding of 3D features of objects for hand action in the parietal cortex of the monkey. Philos. Trans. R. Soc. Lond. B Biol. Sci. 353, 1363–1373.
Sambo, C.F., Liang, M., Cruccu, G., Iannetti, G.D., 2012a. Defensive peripersonal space: the blink reflex evoked by hand stimulation is increased when the hand is near the face. J. Neurophysiol. 107, 880–889.
Sambo, C.F., Forster, B., Williams, S.C., Iannetti, G.D., 2012b. To blink or not to blink: fine cognitive tuning of the defensive peripersonal space. J. Neurosci. 32, 12921–12927.
Schiff, W., Caviness, J.A., Gibson, J.J., 1962. Persistent fear responses in rhesus monkeys to the optical stimulus of "looming". Science 136, 982–983.
Sengül, A., van Elk, M., Rognini, G., Aspell, J.E., Bleuler, H., Blanke, O., 2012. Extending the body to virtual tools using a robotic surgical interface: evidence from the crossmodal congruency task. PLoS One 7, e49473.
Srivastava, S., Orban, G.A., Mazière, P.A.D., Janssen, P., 2009. A distinct representation of three-dimensional shape in macaque anterior intraparietal area: fast, metric, and coarse. J. Neurosci. 29, 10613–10626.
Stepniewska, I., Fang, P.-C., Kaas, J.H., 2005. Microstimulation reveals specialized subregions for different complex movements in posterior parietal cortex of prosimian galagos. Proc. Natl. Acad. Sci. USA 102, 4878–4883.
Teneggi, C., Canzoneri, E., di Pellegrino, G., Serino, A., 2013. Social modulation of peripersonal space boundaries. Curr. Biol. 23, 406–411.
Theys, T., Srivastava, S., van Loon, J., Goffin, J., Janssen, P., 2012. Selectivity for three-dimensional contours and surfaces in the anterior intraparietal area. J. Neurophysiol. 107, 995–1008.
Thier, P., Andersen, R.A., 1998. Electrical microstimulation distinguishes distinct saccade-related areas in the posterior parietal cortex. J. Neurophysiol. 80, 1713–1735.
Vagnoni, E., Lourenco, S.F., Longo, M.R., 2012. Threat modulates perception of looming visual stimuli. Curr. Biol. 22, R826–R827.
Valls-Solé, J., Valldeoriola, F., Tolosa, E., Marti, M.J., 1997. Distinctive abnormalities of facial reflexes in patients with progressive supranuclear palsy. Brain 120 (Pt 10), 1877–1883.
Verhoef, B.-E., Vogels, R., Janssen, P., 2010. Contribution of inferior temporal and posterior parietal activity to three-dimensional shape perception. Curr. Biol. 20, 909–913.
Vuilleumier, P., Valenza, N., Mayer, E., Reverdin, A., Landis, T., 1998. Near and far visual space in unilateral neglect. Ann. Neurol. 43, 406–410.
Wardak, C., Denève, S., Ben Hamed, S., 2011. Focused visual attention distorts distance perception away from the attentional locus. Neuropsychologia 49, 535–545.
Wardak, C., Ibos, G., Duhamel, J.-R., Olivier, E., 2006. Contribution of the monkey frontal eye field to covert visual attention. J. Neurosci. 26, 4228–4235.
Weiss, P.H., Marshall, J.C., Wunderlich, G., Tellmann, L., Halligan, P.W., Freund, H.J., Zilles, K., Fink, G.R., 2000. Neural consequences of acting in near versus far space: a physiological basis for clinical dissociations. Brain 123 (Pt 12), 2531–2541.

Weiss, P.H., Marshall, J.C., Zilles, K., Fink, G.R., 2003. Are action and perception in near and far space additive or interactive factors? Neuroimage 18, 837–846.
Womelsdorf, T., Anton-Erxleben, K., Pieper, F., Treue, S., 2006. Dynamic shifts of visual receptive fields in cortical area MT by spatial attention. Nat. Neurosci. 9, 1156–1160.
Womelsdorf, T., Anton-Erxleben, K., Treue, S., 2008. Receptive field shift and shrinkage in macaque middle temporal area through attentional gain modulation. J. Neurosci. 28, 8934–8944.
Yang, Y., Liu, S., Chowdhury, S.A., DeAngelis, G.C., Angelaki, D.E., 2011. Binocular disparity tuning and visual-vestibular congruency of multisensory neurons in macaque parietal cortex. J. Neurosci. 31, 17905–17916.

Axis I Discussion

The aim of this first axis of the thesis was to investigate the neural basis of impact prediction to the face and peripersonal space in non-human primates. The major question that we ask is: do the same regions contribute to multisensory convergence, to the prediction of the consequences of a looming visual stimulus onto tactile processing and to the construction of peripersonal space?

The perceptual and physiological binding of two sensory inputs into the representation of a unique external source is subjected to some degree of temporal tolerance, resulting in the description of a multisensory temporal binding window (for review, see Wallace and Stevenson, 2014), including when considering dynamic stimuli. Indeed, several studies demonstrate that the temporal coincidence (Sugita and Suzuki, 2003) and temporal correlation (Parise et al., 2012) between a looming visual stimulus and a sound maximize audiovisual integration. However, though this type of binding is relevant for an accurate description of the outside world, it remains inaccurate if the dynamic stimuli are predicting an interaction with the body. In Chapter 1, we show that in this context, the dynamic visual stimuli predict delayed heteromodal consequences onto the tactile sensory modality and that the human brain predictively anticipates these effects by enhancing tactile processing and tactile sensitivity at the predicted time and location of the impact (Chapter 1, Cléry et al., 2015a).

Some studies propose a general model for predictive neuronal processing that could be at the origin of the enhancement of tactile sensitivity during impact prediction. This model argues that phase resetting of ongoing neuronal oscillations by a given sensory input (looming visual), predictively prepares neurons to respond to a second sensory input (tactile) with a particular timing relationship with the first sensory input (Lakatos et al., 2005, 2007; Kayser et al., 2008;

van Atteveldt et al., 2014). What are the neural bases involved in these impact prediction mechanisms?

In Chapter 2 we sought to characterize the functional network involved in the prediction of touch to the body, with a non-human primate study using the same stimuli. We identified a core occipito-parieto-premotor functional network that is maximally activated when the looming visual stimuli spatially and temporally predict the tactile stimulus. We propose that these activation subserve the enhanced tactile sensitivity observed at the predicted location and time of impact on the face in our psychophysical study (Chapter 1, Cléry et al., 2015a). This enhancement corresponds to visuo-tactile integration processes and spatial and temporal prediction cues processes (Avillac et al., 2004, 2007; Beauchamp et al., 2004; Beauchamp, 2005b; Werner and Noppeney, 2011; Noppeney, 2012; Tyll et al., 2013).

With this paper, we would like to propose to further enrich this BCI framework (Körding et al., 2007; Shams and Beierholm, 2010; Wozny et al., 2010; Parise et al., 2012; Rohe and Noppeney, 2015a, 2015b, 2016) with an additional dimension beyond fusion and segregation, namely delayed consequences (prediction). While area VIP has been shown to perform multisensory source fusion (Avillac et al., 2004, 2007), we suggest that this area also performs multisensory prediction, possibly through a gamma-band synchronization mechanism (Maier et al., 2008; van Atteveldt et al., 2014).

Interestingly, the areas with maximal activations observed when the looming visual stimuli spatially and temporally predict the tactile stimulus, are those identified in a well-characterized visuo-tactile convergence network, namely, the post-arcuate premotor cortex (specifically premotor zone PMz, a subsector of area F4), intraparietal cortex (specifically the

ventral intraparietal area VIP) and striate and extrastriate visual areas (Guipponi et al., 2013, 2015). For the parieto-frontal network, in a context of multisensory prediction, the activations are more spread out and stronger than in a convergence context (Fig 3, Chapter 4). Therefore, this parieto-frontal network selectively involved in predicting impact to the face, highly overlaps with the visuo-tactile convergence network, indicating that several areas are activated by both visuo-tactile impact prediction and visual or tactile stimulations.

Besides, the parietal and the premotor components of this functional network have been involved in the representation of a defense peripersonal space (Graziano and Cooke, 2006; see for reviews, Cléry et al., 2015b) as well as in approaching behavior (Rizzolatti et al., 1997). In Chapter 3 and 4, we expand the description of this functional network and we show the activation of a dorsal parieto-frontal network including area F4 and VIP for near space encoding (Chapter 3) and more generally for peripersonal space representation (Chapter 4). Interestingly, these two regions have anatomical connections and functional homologies (Matelli and Luppino, 2001; Rizzolatti and Luppino, 2001; Cléry et al., 2015b), though the functional specificity of each of these regions and how they interact is still unclear.

This cortical network selectively involved in the processing of near space highly overlaps with the network predicting impact to the face and the visuo-tactile convergence network, indicating that several areas are activated by both visuo-tactile impact prediction, visual or tactile stimulations and by specific near space encoding. Therefore, these three mechanisms share a common parieto-frontal network (ventral intraparietal area / premotor area F4).

The peripersonal representation subserved by this parieto-premotor network, though serving to define a safety body margin contributing to the definition of the self (as a whole) with respect to the external world, has been shown to overrepresent two vulnerable body parts, namely the head and the arm/hand unit (Graziano and Cooke, 2006; Brozzoli et al., 2013, 2014; Chen et al., 2014; Cléry et al., 2015b). As a result, this network is tightly associated with a

defensive behavior, protecting the body margin from external aggression, and the prediction of intrusive impact to the body, including for the far space (remember that when the big cube is looming towards far space, we have the same pattern than when the small cube is looming towards near space, and thus we have the illusion of an approach into near space in spite of the fact that the stimulus is physically presented in far space). This possibly pertains to a more general mechanism that allows dynamical updating of the probability that surrounding elements from the environment, whether static or dynamic, whether corresponding to inanimate objects, potential predators or nearby conspecifics, are going to intrude into our comfort peripersonal space (Quesque et al., 2016)

We propose that this network does not only process the trajectory of the looming object with respect to the body, but also anticipates its consequences for the body and prepares protective actions in response to the looming stimulus.

Now that this parieto-frontal network is well identified by fMRI, future explorations will be to drive electrophysiological recording experiments in the same animals to unveil the precise neuronal computations underlying these three distinct mechanisms: visuo-tactile convergence, impact prediction to the face and near space encoding. In particular, it would be very interesting to explore how the same regions, local neuronal populations and single neurons, encode the multisensory stimuli according to the context. Indeed, in the VIP area, a multisensory integration at the neuron scale was demonstrated during the presentation of simultaneous visuo-tactile stimuli (Avillac et al., 2007). We show in fMRI that this region is particularly activated in a context of visual prediction of a tactile impact on the face. How are these different conditions encoded? Are the integration rules being Bayesian? Do these rules depend on the cognitive or sensory context imposed on animals? How are these priors implemented in the local neuronal computations? What are the dynamics of these rules?

A second exploration would be to study the boundaries of the peripersonal space and its dynamics as a function of high-level signals such as the social and non-social environment (Lourenco et al., 2011), or lower level signals such as, for example, by changing the proprioceptive information (Lourenco and Longo, 2009) or motor (e.g. Brozzoli et al., 2010). It is thus possible to 1) evaluate the position of this boundary by placing our stimulations at different distances from the animal, then 2) to measure the displacement of this boundary by manipulating social (presentation of conspecific images) and / or emotional contexts (presentation of appetitive or aversive images).

Lastly, we have shown that not only the same regions as a whole but also some well-identified voxels are activated by these three mechanisms (convergence, prediction and peripersonal space encoding). However, in fMRI, BOLD signal reflects the indirect activity of thousands of neurons for each voxel, so do the same neurons encode these three processes or is it rather a subpopulations of neurons that encodes each process separately within the same voxel? And what is the specific contribution of local field potentials (LFPs) input signals and spike output signals to the observed fMRI activations?

These different studies show that the brain, in general, and spatial representation, in particular, are highly plastic. Indeed, for example, the receptive fields can move and deform, an area can modify its responses according to the sensory and cognitive context of the moment, the operation of the network can adapt to the constraints of the environment, rules of information integration can change according to the context (Connor et al., 1996, 1997; Ben Hamed et al., 2002; Womelsdorf et al., 2006; Melcher and Colby, 2008; Anton-Erxleben et al., 2009; Hall and Colby, 2011; Liverence and Scholl, 2011; Wardak et al., 2011; Anton-Erxleben and Carrasco, 2013; Carrasco and Barbot, 2014; Zirnsak et al., 2014). How can this knowledge be used? Can this plasticity be induced to treat some pathologies, such as hemispatial neglect?

The next part of this thesis focuses on the study of visual plasticity and presents our preliminary results on the subject.

Specifically, I have developed a set of high-resolution MRI methods to assess functional (high-resolution visual mapping fMRI, rs-MRI), pharmacological (GABA spectroscopy imaging) and structural (anatomical MRI, DTI) imaging to define reference measures against which to evaluate the changes induced by plasticity at different times after its induction, through a longitudinal study performed in the same animals. This ongoing work is presented in the next axis of this thesis.

References

Anton-Erxleben K, Carrasco M (2013) Attentional enhancement of spatial resolution: linking behavioural and neurophysiological evidence. Nat Rev Neurosci 14:188–200.

Anton-Erxleben K, Stephan VM, Treue S (2009) Attention reshapes center-surround receptive field structure in macaque cortical area MT. Cereb Cortex 19:2466–2478.

Avillac M, Hamed SB, Duhamel J-R (2007) Multisensory Integration in the Ventral Intraparietal Area of the Macaque Monkey. J Neurosci 27:1922–1932.

Avillac M, Olivier E, Denève S, Ben Hamed S, Duhamel J-R (2004) Multisensory integration in multiple reference frames in the posterior parietal cortex. Cognitive Processing 5:159–166.

Beauchamp MS (2005) Statistical Criteria in fMRI Studies of Multisensory Integration. Neuroinformatics 3:93–113.

Beauchamp MS, Lee KE, Argall BD, Martin A (2004) Integration of Auditory and Visual Information about Objects in Superior Temporal Sulcus. Neuron 41:809–823.

Ben Hamed S, Duhamel J-R, Bremmer F, Graf W (2002) Visual receptive field modulation in the lateral intraparietal area during attentive fixation and free gaze. Cereb Cortex 12:234–245.

Brozzoli C, Cardinali L, Pavani F, Farnè A (2010) Action-specific remapping of peripersonal space. Neuropsychologia 48:796–802.

Brozzoli C, Ehrsson HH, Farnè A (2014) Multisensory representation of the space near the hand: from perception to action and interindividual interactions. Neuroscientist 20:122–135.

Brozzoli C, Gentile G, Bergouignan L, Ehrsson HH (2013) A Shared Representation of the Space Near Oneself and Others in the Human Premotor Cortex. Current Biology 23:1764–1768.

Carrasco M, Barbot A (2014) How Attention Affects Spatial Resolution. Cold Spring Harb Symp Quant Biol 79:149–160.

Chen X, Sanayei M, Thiele A (2014) Stimulus Roving and Flankers Affect Perceptual Learning of Contrast Discrimination in Macaca mulatta. PLoS ONE 9:e109604.

Cléry J, Guipponi O, Odouard S, Wardak C, Ben Hamed S (2015a) Impact prediction by looming visual stimuli enhances tactile detection. J Neurosci 35:4179–4189.

Cléry J, Guipponi O, Wardak C, Ben Hamed S (2015b) Neuronal bases of peripersonal and extrapersonal spaces, their plasticity and their dynamics: Knowns and unknowns. Neuropsychologia 70:313–326.

Connor CE, Gallant JL, Preddie DC, Van Essen DC (1996) Responses in area V4 depend on the spatial relationship between stimulus and attention. J Neurophysiol 75:1306–1308.

Connor CE, Preddie DC, Gallant JL, Van Essen DC (1997) Spatial attention effects in macaque area V4. J Neurosci 17:3201–3214.

Graziano MSA, Cooke DF (2006) Parieto-frontal interactions, personal space, and defensive behavior. Neuropsychologia 44:845–859.

Guipponi O, Cléry J, Odouard S, Wardak C, Ben Hamed S (2015) Whole brain mapping of visual and tactile convergence in the macaque monkey. NeuroImage 117:93–102.

Guipponi O, Wardak C, Ibarrola D, Comte J-C, Sappey-Marinier D, Pinède S, Hamed SB (2013) Multimodal Convergence within the Intraparietal Sulcus of the Macaque Monkey. J Neurosci 33:4128–4139.

Hall NJ, Colby CL (2011) Remapping for visual stability. Philos Trans R Soc Lond, B, Biol Sci 366:528–539.

Kayser C, Petkov CI, Logothetis NK (2008) Visual Modulation of Neurons in Auditory Cortex. Cereb Cortex 18:1560–1574.

Körding KP, Beierholm U, Ma WJ, Quartz S, Tenenbaum JB, Shams L (2007) Causal Inference in Multisensory Perception. PLoS ONE 2:e943.

Lakatos P, Chen C-M, O'Connell MN, Mills A, Schroeder CE (2007) Neuronal Oscillations and Multisensory Interaction in Primary Auditory Cortex. Neuron 53:279–292.

Lakatos P, Shah AS, Knuth KH, Ulbert I, Karmos G, Schroeder CE (2005) An Oscillatory Hierarchy Controlling Neuronal Excitability and Stimulus Processing in the Auditory Cortex. Journal of Neurophysiology 94:1904–1911.

Liverence BM, Scholl BJ (2011) Selective attention warps spatial representation: parallel but opposing effects on attended versus inhibited objects. Psychol Sci 22:1600–1608.

Lourenco SF, Longo MR (2009) The plasticity of near space: evidence for contraction. Cognition 112:451–456.

Lourenco SF, Longo MR, Pathman T (2011) Near space and its relation to claustrophobic fear. Cognition 119:448–453.

Maier JX, Chandrasekaran C, Ghazanfar AA (2008) Integration of bimodal looming signals through neuronal coherence in the temporal lobe. Curr Biol 18:963–968.

Matelli M, Luppino G (2001) Parietofrontal Circuits for Action and Space Perception in the Macaque Monkey. NeuroImage 14:S27–S32.

Melcher D, Colby CL (2008) Trans-saccadic perception. Trends Cogn Sci (Regul Ed) 12:466–473.

Noppeney U (2012) Characterization of Multisensory Integration with fMRI: Experimental Design, Statistical Analysis, and Interpretation. In: The Neural Bases of Multisensory Processes (Murray MM, Wallace MT, eds) Frontiers in Neuroscience. Boca Raton (FL): CRC Press/Taylor & Francis.

Parise CV, Spence C, Ernst MO (2012) When correlation implies causation in multisensory integration. Curr Biol 22:46–49.

Quesque F, Ruggiero G, Mouta S, Santos J, Iachini T, Coello Y (2016) Keeping you at arm's length: modifying peripersonal space influences interpersonal distance. Psychological Research:1–12.

Rizzolatti G, Fadiga L, Fogassi L, Gallese V (1997) The space around us. Science 277:190–191.

Rizzolatti G, Luppino G (2001) The Cortical Motor System. Neuron 31:889–901.

Rohe T, Noppeney U (2015a) Cortical Hierarchies Perform Bayesian Causal Inference in Multisensory Perception. PLoS Biol 13:e1002073.

Rohe T, Noppeney U (2015b) Sensory reliability shapes perceptual inference via two mechanisms. Journal of Vision 15:22.

Rohe T, Noppeney U (2016) Distinct Computational Principles Govern Multisensory Integration in Primary Sensory and Association Cortices. Curr Biol 26:509–514.

Shams L, Beierholm UR (2010) Causal inference in perception. Trends in Cognitive Sciences 14:425–432.

Tyll S, Bonath B, Schoenfeld MA, Heinze H-J, Ohl FW, Noesselt T (2013) Neural basis of multisensory looming signals. NeuroImage 65:13–22.

van Atteveldt N, Murray MM, Thut G, Schroeder CE (2014) Multisensory Integration: Flexible Use of General Operations. Neuron 81:1240–1253.

Wallace MT, Stevenson RA (2014) The construct of the multisensory temporal binding window and its dysregulation in developmental disabilities. Neuropsychologia 64C:105–123.

Wardak C, Denève S, Ben Hamed S (2011) Focused visual attention distorts distance perception away from the attentional locus. Neuropsychologia 49:535–545.

Werner S, Noppeney U (2011) The Contributions of Transient and Sustained Response Codes to Audiovisual Integration. Cereb Cortex 21:920–931.

Womelsdorf T, Anton-Erxleben K, Pieper F, Treue S (2006) Dynamic shifts of visual receptive fields in cortical area MT by spatial attention. Nat Neurosci 9:1156–1160.

Wozny DR, Beierholm UR, Shams L (2010) Probability matching as a computational strategy used in perception. PLoS Comput Biol 6.

Zirnsak M, Steinmetz NA, Noudoost B, Xu KZ, Moore T (2014) Visual space is compressed in prefrontal cortex before eye movements. Nature 507:504–507.

Axis II :

Plasticity of the adult visual representation

Introduction

Neuronal plasticity is an intrinsic property of the cerebral cortex that ensures the capability of the organism to adapt to environmental changes through a modification of neural circuitry and is the basis of fundamental processes, such as learning and memory, that are preserved during the entire lifespan (Pascual-Leone et al., 2005). It is at the core of early brain development and is finely organized by both gene expression and environmental influences. As development proceeds, this plasticity progressively reduces. In comparison, adult neuronal plasticity is very restricted.

1. Neuronal plasticity and *critical period*

During development, neuronal plasticity plays a crucial role in refining sensory cortical organization. Studies demonstrate that this mechanism is dependent on experience for visual, auditory and somatosensory systems and takes place within a specific temporal window called the *critical period* (Wiesel, 1982; Berardi et al., 2000; Pascual-Leone et al., 2005).

In research on the visual system, the most widely studied critical period is when monocular deprivation (MD) affects the ocular dominance of cortical neurons. It has been characterized in many species such as mice, rats, ferrets, cats, monkeys and humans (Huang et al., 1999; Fagiolini et al., 1994; Issa et al., 1999; Olson and Freeman, 1980; Harwerth et al., 1986; Banks et al., 1975, **Figure 8**). As shown by Figure 8, the critical period is only a defined portion of the life of the animal and it is devoted to the formation of neural connections. The length of this period will differ according to the animal species. Two main relationships will influence it. The first corresponds to the fact that the longer the life of the animal is, the longer the critical period will be. The second relationship concerns the complexity of the brain, so the more complex the brain, the longer the critical period (Berardi et al., 2000).

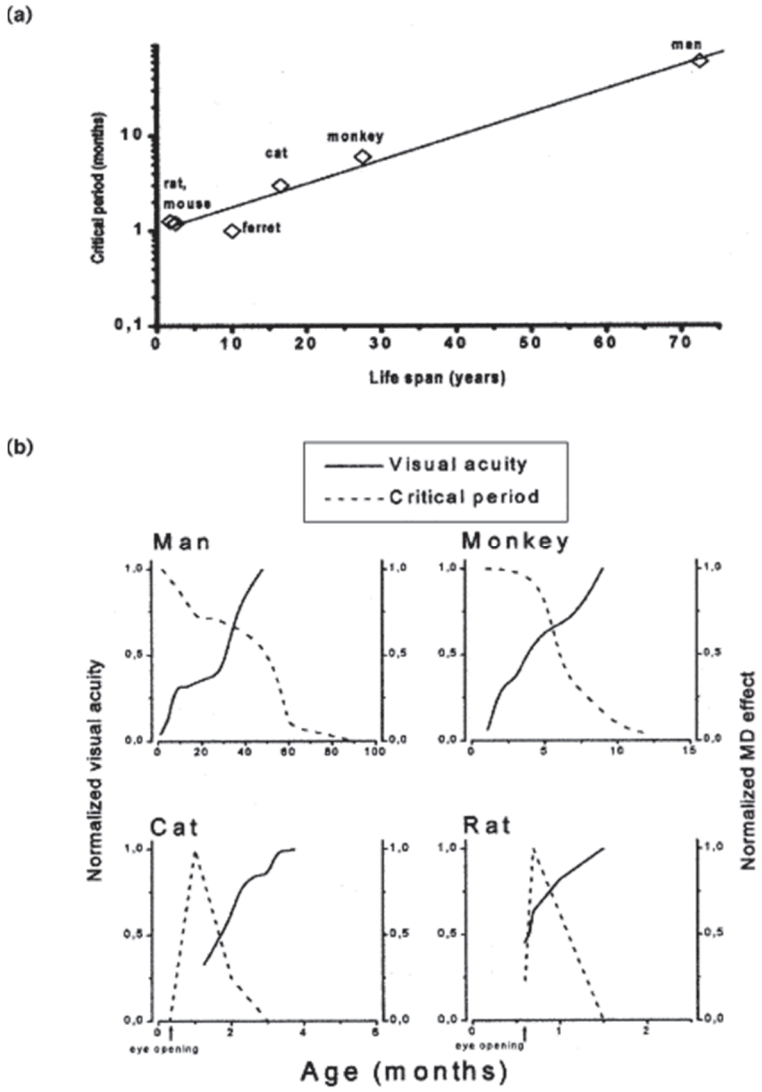

Figure 8: Critical period in Man, Monkey, Cat and Rat (from Berardi et al., 2000).

2. Some visual pathologies of the visual cortex

Abnormal visual experience during the critical period of development disrupts neuronal circuitry in the visual cortex leading to severe alterations in the visual representation. This is observed in several developmental pathologies such as amblyopia or congenital cataract. These pathologies bring a lot of difficulties in daily life.

a. Functional amblyopia

Amblyopia affects 2 to 5% of the human population (Carlton et al., 2008; Powell and Hatt, 2009). Amblyopia is a developmental disorder caused by physiological alterations in the visual cortex early in life resulting in eyesight deficiencies. Two main causes exist (Tailor et al., 2016): (i) a difference in the optical properties of the two eyes, reflected in a different spectacle prescription for the right and the left eye (anisometropia) and (ii) strabismus (misalignment of the visual axes). This pathology involves low- and high-level visual deficiencies: reduced visual acuity and contrast sensitivity, high levels of spatial uncertainty, spatial distortion and impaired reading abilities (for reviews, see Kiorpes, 2006; Levi, 2006). In the last century, it was generally believed that the visual deficiencies, and more particularly visual acuity, in amblyopia could be reversed if a treatment was used before the end of the critical period of brain development but not beyond this period and therefore adult amblyopia was thought to be irreversible. Over the last twenty years, studies both in rats and in humans have suggested that the mature amblyopic brain retains a substantial degree of plasticity (Li et al., 2011; Vedamurthy et al., 2015b).

b. Congenital and pediatric cataracts

Cataract is defined by an opacification of the normally transparent crystalline lens. This is common among the elderly but much rarer among younger people. However, congenital cataract (present at birth) and pediatric cataract (appearing between birth and the age of 16) do exist. This pathology results in a visual deprivation of the eye where cataract is present and induces severe amblyopia since the retina does not receive a clear image (Churchill and Graw, 2011; Rong et al., 2015). To treat this pathology, the main strategies applied are to remove the cataract and/or to implant an intraocular lens followed by optical corrections. The next step is to treat the severe amblyopia and therefore reinduce visual plasticity.

3. Neuronal plasticity in Adulthood

Neural plasticity is regularly induced, throughout the life, by structures such as the hippocampus which continuously generates cohorts of neurons (for review, see Gu et al., 2012). There is no critical period for these structures. Although adult neuronal plasticity used to be considered as extremely restricted compared to that observed during early brain development, growing evidence indicates that it can be drastically enhanced by specific manipulations (for reviews, Bavelier et al., 2010; Baroncelli et al., 2011). In particular, changes in the balance between excitation and inhibition (E/I) have been demonstrated to directly regulate the potential for plasticity within a given cortical network, **Figure 9** (very much like what takes place spontaneously in the visual cortex during early development, Di Cristo et al., 2007). These changes can be induced in different ways developed in the following points.

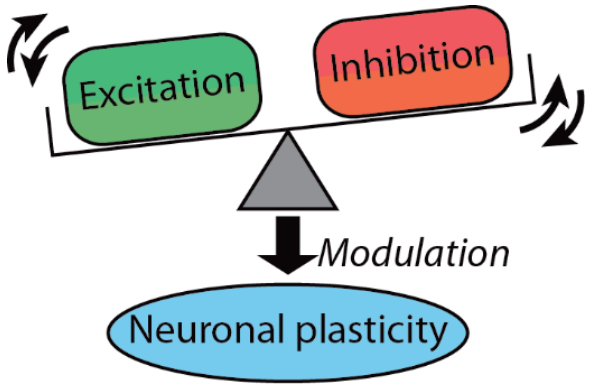

Figure 9 : Balance between excitation and inhibition modulate neuronal plasticity.

a. Local reduction of intracortical inhibition

Basal GABAergic inhibition is necessary to trigger the plasticity of ocular dominance and to modulate the onset and end of the critical period (Hensch et al., 1998; Fagiolini and Hensch, 2000). GABAergic inhibition also plays a crucial role in neuronal plasticity in adult animals: the balance between excitation and inhibition at the primary visual cortex V1, measured in the

resting-state, modulates the susceptibility of ocular dominance to deprivation (Pizzorusso et al., 2002; Harauzov et al., 2010; Heimel et al., 2011). Indeed, Harauzov et al. (2010) show that a local reduction in intra-cortical inhibition partially reactivates the plasticity of ocular dominance in response to monocular deprivation, in rats. Recently, Lunghi et al. (2015) have measured GABA concentration in adult human V1 using ultra-high-field 7T magnetic resonance spectroscopy before and after short-term monocular deprivation. Resting GABA concentration decreased in V1 after monocular deprivation, but was not affected in a control parietal area. They observed a high correlation between the decrease in GABA concentration in the visual cortex and the perceptual boost of the deprived eye induced by monocular deprivation and measured by binocular rivalry. Besides, after deprivation, GABA concentration measured during monocular stimulation correlated with the deprived eye dominance. Authors suggest that the reduction in resting GABAergic inhibition triggers homeostatic plasticity in adult human V1 after a brief period of abnormal visual experience. A study on mice (Davis et al., 2015), has successfully opened a new critical period by transplanting embryonic inhibitory neurons into the adult visual cortex of mice. This transplantation has allowed to reactivate visual cortical plasticity and to restore visual perception impairment after a deprivation during the juvenile critical period of the mouse.

These different studies confirm the key role of GABA in visual plasticity and the fact that the reduction of cortical inhibition can modulate this plasticity. To measure GABA concentration is thus a good way to evaluate neuronal plasticity.

b. Neuromodulations

Neuromodulations can induce changes in this balance between excitation and inhibition more in favor of excitation than of inhibition allowing neuronal plasticity restoration. Different types of neuromodulations exist and some examples for each are described below.

i. Cholinergic neuromodulations

Acetylcholine increases thalamocortical synaptic transmission compared to lateral intracortical connections (Giocomo and Hasselmo, 2007). Studies in animals (Kimura et al., 1999; Roberts et al., 2005) and in humans (Silver et al., 2008) have shown that acetylcholine regulates the spatial integration within the visual cortex, in particular by reducing the size and the diffusion of receptive fields excitation in the visual cortex and therefore playing on the excitation / inhibition balance. The knock-out mouse model for the *Lynx1* protein, a protein that is strongly present in adulthood and is directly bound to nicotinic acetylcholine receptors, reducing their sensitivity to the acetylcholine, spontaneously recovers its visual acuity after monocular deprivation (Morishita et al., 2010; Sadahiro et al., 2016). Cholinergic activation has thus made it possible to restore neuronal plasticity, notably by manipulating acetylcholine signaling allowing to promote remyelination and consequently the rewiring of old and new connections (Fields, 2015; for review, see Fields et al., 2017).

ii. Adrenergic neuromodulations

The central noradrenergic system is involved in novelty, stimulus salience, attentional processes as well as arousal, spatial and recognition memory. Noradrenaline (also called norepinephrine) is synthetized in the locus coeruleus and can modulate the activity of cortical GABAergic cells in the neocortex and hippocampus (Kawaguchi and Shindou, 1998). Kasamatsu (1982) has reported that an increase in the local availability of noradrenaline enhances neuronal plasticity, accelerating cortical recovery from the effects of prior monocular deprivation in cats. Indeed, it has been shown that the use of 6-hydroxydopamine (6-OHDA) destroying noradrenaline terminals suppresses visual plasticity in kitten and cortical recovery in cats after monocular deprivation but that an infusion of noradrenaline enhances this recovery (Kasamatsu, 1982, 1991; Gordon et al., 1988).

iii. Serotoninergic neuromodulations

The serotoninergic system appears early in the mammalian embryo playing a role in the developmental process and is widely distributed both in the body and in the central nervous system. Therefore, serotonin is involved in many aspects of the mammalian physiology (cardiovascular regulation, respiration, gastrointestinal system, thermoregulation, circadian rhythm) and brain functions (pain, appetite, aggression, sensorimotor activity, sexual behavior, mood, cognition, learning and memory; for review, see Sodhi and Sanders-Bush, 2004). This system is a key target to treat some diseases such as depression and to understand autism (Zafeiriou et al., 2009). Fluoxetine is a drug clinically used to treat depression. It is a selective serotonin reuptake inhibitor. Therefore, chronic administration of fluoxetine induces an increase of extracellular serotonin resulting in the restoration of neuronal plasticity in the adult visual system of the rat. Indeed, a reinstatement of ocular dominance plasticity as well as a promotion of visual function recovery in adult amblyopic animals, have been observed after a reduced cortical inhibition and increased expression of brain-derived neurotrophic factors in the visual cortex (Maya Vetencourt et al., 2008). Since this great new discovery, other studies using antidepressants have shown that they play a role in multiple neuroplasticity processes. These antidepressants are selective serotonin reuptake inhibitors, serotonin-norepinephrine reuptakes and multimodal-acting antidepressants (like vortioxetine), so they are all linked with serotoninergic neuromodulations (Castrén and Hen, 2013; Russo and Nestler, 2013; Pehrson et al., 2015). However, they do not use the same mechanisms. For example, in adult rats, vortioxetine regulates the expression of genes associated with plasticity in the frontal cortex, hippocampus, and amygdala but it also has similar effects in relation to fluoxetine (Waller et al., 2017). Clinical studies on serotoninergic modulation on neuroplasticity provide new interesting ways to reinduce plasticity in adulthood.

iv. Dopaminergic neuromodulations

Dopamine plays a major role in reward-motivated behavior and motor control. Some studies focus on Parkinson disease (PD), characterized by a loss of dopaminergic neurons in substantia negra resulting in a loss of dopamine in the dorsal lateral striatum. These studies have shown an exercise-induced increase in the dopamine D2 receptor expression, protein and binding in the striatum, and these changes influence and restore motor learning both in healthy and PD patients (Gilliam et al., 1984; MacRae et al., 1987; Foley and Fleshner, 2008; Fisher et al., 2013; for review, see Jakowec et al., 2016). Studies on rodents using a pharmacologically specific blockade of dopamine D2 receptors have shown that this receptor antagonism, in either the early or the late phases of motor skill learning, leads to impairment in glutamatergic-dependent synaptic potentiation in the striatum, and to alterations in motor learning but also in maintenance of learned motor behaviors (Yim et al., 2009; Beeler et al., 2010, 2012) and improvement of executive function including behavioral flexibility (Eddy et al., 2014).

c. Sensory intervention

In addition to potential pharmacological interventions, certain sensory interventions can induce plasticity through reduced input signals (He et al., 2006, 2007), increased input noises (Zhou et al., 2011) and environmental enrichment.

In amblyopic adult rats, the use of a complete visual deprivation through a complete darkness exposure for a period of 10 days promotes a significant recovery of vision once they are allowed to see binocularly (He et al., 2006, 2007). In amblyopic cats, the same period of darkness exposure improves gradually the visual acuity of the deprived (amblyopic) eye to normal levels in 1 week or less (Duffy and Mitchell, 2013; Mitchell et al., 2016). The same results are observed after a bilateral temporary retinal inactivation followed by a short period

of binocular visual experience promoting fast recovery of the visual acuity of the deprived eye to normal levels both in mice and kittens (Fong et al., 2016).

Zhou et al (2011) show a great capacity for naturally driving "negative" cortical changes, by exposing postcritical period juvenile or adult rats over a several-week-long period to moderate-level and continuous noise. In time, noise exposure reinstates critical period plasticity resulting in a plastic degradation of the selective representation of the detailed features of sound stimuli within the auditory system and cortex. Besides, a wide range of changes occurs in the cortex, most specifically in the auditory cortex which reacquires characteristics that apply for this cortical area in the critical period in a less mature (infantile) state. However, by returning animals to natural acoustic environments, these cortical changes are again reversed to reestablish a physically and functionally normal adult cortex.

Early on, by introducing environmental enrichment as an experimental protocol to investigate the influence of environment on the brain and behavior, has been shown that the intensity of environmental stimulation can induce brain changes ranging from the molecular to the anatomical and functional level (Rosenzweig, 1966; Rosenzweig and Bennett, 1969; for review, see Rosenkranz et al., 2014; van Praag et al., 2000). For example, environmental enrichment for animals corresponds to placing animals in large groups and to maintain them in widely stimulating environments where a variety of objects (e.g. toys, tunnels, nesting material and stairs) are present and change frequently. This combination of social and inanimate stimulations provides the optimal conditions for the animals to enhance exploration, cognitive activity, social interaction and physical exercise (Rosenzweig et al., 1978). Since then, other studies have shown that environmental enrichment accelerate the development of the visual system (e.g., visual acuity in rodents, Cancedda et al., 2004; Landi et al., 2007), and enhance visual-cortex plasticity in adulthood (for reviews, see Sale et al., 2009; Cooper and Mackey, 2016).

d. Repetitive behavioral manipulations

Other studies indicate that specific repetitive behavioral manipulations can also induce long-lasting plastic changes in vision such as perceptual learning and video game practice though the underlying neuronal bases of these observations remain to be uncovered (Levi, 2013).

i. Perceptual learning

Perceptual learning is a form of implicit memory, the unconscious acquisition of habits and skills with practice, involved improvement in sensory discrimination or detection by repeated exposure to sensory stimuli (Gilbert et al., 2009). Perceptual learning has been widely studied in the last and present centuries: part of these studies were interested in perceptual learning to treat amblyopia (Levi and Li, 2009a, 2009b). These studies show that practicing visual tasks can lead to dramatic and long-lasting improvements in the performance of these tasks by inducing permanent changes in both performance and neural processing in the visual cortex (Kiorpes, 2006; Levi, 2006). Using perceptual learning in amblyopic infants and adults forces them to use the amblyopic eye allowing to restore visual acuity in these patients. Perceptual learning operates via a reduction of internal neural noise and/or through a more efficient use of the stimulus information by retuning the weighting of the information (Li and Levi, 2004; Li et al., 2007, 2008).

ii. Video game practice

Playing action video games, for example *Halo*, *Call of Duty, World of Warcraft*, *Guild Wars* or *StarCraft*, requires rapid processing of sensory information and prompt action, forcing players to make decisions and execute responses at a far greater pace than is typical in everyday

life (Dye et al., 2009). Studies show that playing action video game benefits performance in an array of sensory, perceptual, and attentional tasks (Orosy-Fildes and Allan, 1989; Green and Bavelier, 2003, 2006; Castel et al., 2005; Feng et al., 2007; Li et al., 2016) but also improves a visuo-motor control (Li et al., 2016) that goes well beyond the specifics of game playing. However, the benefits are not the same if action video game training is practiced by healthy youngsters or older adults (for review, see Wang et al., 2016). Therefore, researchers have been interested in the use of these action video games for treating different pathologies such as amblyopia. Indeed, the action video game training can lead to the improvement of a wide range of fundamental functions, from low-level to high level, including visual acuity, positional acuity, spatial attention and stereopsis (Li et al., 2011; Vedamurthy et al., 2015a, 2015b, 2016; Guo et al., 2016). The recovery of these functions is faster than the one obtained with occlusion therapy in childhood amblyopia.

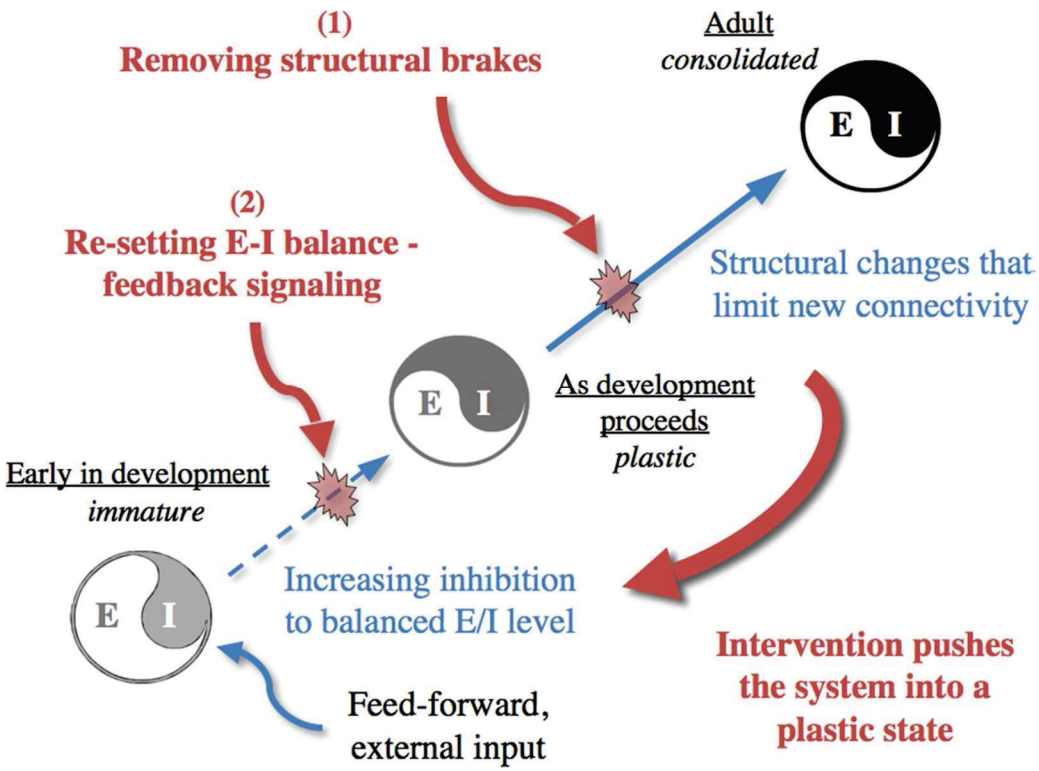

Figure 10: Evolving plastic capacity across the lifespan (blue arrows) suggests possible mechanisms for enhancing learning and recovery of functions in adulthood (red arrows). From Bavelier et al. 2010.

To summarize, the major effects of invasive, pharmacological or sensory interventions are to remove structural brakes (**Figure 10**, **(1)**) targeting perineuronal nets, myelin or epigenetic status; to reset the local balance between excitation and inhibition (E/I) to a juvenile state (**Figure 10**, **(2)**) by reducing inhibition and promoting excitation; to push the system into a plastic state. In this way, it is possible to observe a rewiring of plasticity and particularly of visual plasticity (Bavelier et al., 2010).

4. Visual representation: Scope of Axis II

a. Psychophysical evidence for dynamic spatio-temporal influences on visual representation.

A set of psychophysical studies demonstrates that the visual representation is continuously reshaped as a function of bottom-up influences (both driven by the external environment and intrinsic properties of the adult's visual system: Zénon et al., 2008, 2009a, 2009b) as well as top-down influences (driven by the subject's internal state and goals: Ibos et al., 2009; Wardak et al., 2011). This has the general effect of dynamically adjusting which part of the visual field is being processed with the highest resolution. For example, the space around the locus of attention is perceived as distorted and expanded up to 7-8° degrees away from this location (Wardak et al., 2011). These observations suggest that changes are taking place at several locations within the visual system dynamically affecting how neurons individually and collectively represent space. This is in sharp contrast with the notion of visual neurons reliably encoding a given well-defined portion of space, referred to as its receptive field.

b. Neurophysiological evidence for dynamic spatial and temporal influences on visual representation.

Studies on the neural substrates for these psychophysical observations demonstrate that parietal neurons represent the central visual field with a higher resolution during attentive fixation than during free gaze thanks to changes in the spatial position of their receptive fields (in LIP, Ben Hamed et al., 2002). When attention is focused away from the fixation point, the visual receptive fields of parietal neurons literally "move" in space with the final result of enhancing of the representation of the locus of attention and the space directly around it. The

same spatio-temporal visual representation dynamics can also be observed in prefrontal neurons suggesting that these dynamics is actually ubiquitous at all levels of the visual cortex, though the relative weight of external and internal influences varies at each processing stage (Ibos et al., 2013). In parallel with the demonstration that the receptive fields of individual visual neurons undergo a context and task dependent dynamics, my team additionally shows, using an online population decoding approach, that how visual information is encoded by the entire neuronal population also changes (Astrand et al., 2014, 2015). A classifier can be trained to predict the location of a visual stimulus from the instantaneous response of a prefrontal neuronal population (48 recording points) recorded while the monkey is performing a simple visual detection task in which the target can be presented at 4 possible locations. This decoder will only partially succeed in decoding these very same 4 locations from the prefrontal population response, if they are presented in a context in which the target can now be presented at 8 possible locations (including the 4 previous ones). This suggests drastic changes in the visual field representation and we propose that this short-term dynamic shares major characteristics with adult plasticity within the visual cortex at large.

c. Scope

While most of the visual cortex adult plasticity studies have targeted area V1, there is growing evidence that plasticity should be analyzed at the whole brain level (Gilbert and Li, 2012). In this perspective, the lateral intraparietal area (LIP) and the frontal eye field (FEF) appear to be crucial nodes in the visual system. Indeed, both are essential to conscious vision (Corbetta and Shulman, 2011; Boly et al., 2013). At the same time, there is now ample evidence that while FEF is at the source of the endogenous spatial signals that bias visual processing downstream so as to optimize performance (Wardak et al., 2006; Buschman and Miller, 2007; Ekstrom et al., 2008; Ibos et al., 2013), LIP prioritizes bottom-up information (Wardak et al.,

2004; Buschman and Miller, 2007; Ibos et al., 2013). As a result, we predict that while plasticity effects within the primary visual cortex are independent of how visual plasticity is induced, differences at other levels of visual processing will depend on how plasticity is triggered.

References

Astrand E, Enel P, Ibos G, Dominey PF, Baraduc P, Ben Hamed S (2014) Comparison of classifiers for decoding sensory and cognitive information from prefrontal neuronal populations. PLoS ONE 9:e86314.

Astrand E, Ibos G, Duhamel J-R, Ben Hamed S (2015) Differential dynamics of spatial attention, position, and color coding within the parietofrontal network. J Neurosci 35:3174–3189.

Banks MS, Aslin RN, Letson RD (1975) Sensitive period for the development of human binocular vision. Science 190:675–677.

Baroncelli L, Maffei L, Sale A (2011) New Perspectives in Amblyopia Therapy on Adults: A Critical Role for the Excitatory/Inhibitory Balance. Frontiers in Cellular Neuroscience 5.

Bavelier D, Levi DM, Li RW, Dan Y, Hensch TK (2010) Removing brakes on adult brain plasticity: from molecular to behavioral interventions. J Neurosci 30:14964–14971.

Beeler JA, Cao ZFH, Kheirbek MA, Ding Y, Koranda J, Murakami M, Kang UJ, Zhuang X (2010) Dopamine-dependent motor learning: insight into levodopa's long-duration response. Ann Neurol 67:639–647.

Beeler JA, Frank MJ, McDaid J, Alexander E, Turkson S, Bernardez Sarria MS, Bernandez MS, McGehee DS, Zhuang X (2012) A role for dopamine-mediated learning in the pathophysiology and treatment of Parkinson's disease. Cell Rep 2:1747–1761.

Ben Hamed S, Duhamel J-R, Bremmer F, Graf W (2002) Visual receptive field modulation in the lateral intraparietal area during attentive fixation and free gaze. Cereb Cortex 12:234–245.

Berardi N, Pizzorusso T, Maffei L (2000) Critical periods during sensory development. Curr Opin Neurobiol 10:138–145.

Boly M, Seth AK, Wilke M, Ingmundson P, Baars B, Laureys S, Edelman DB, Tsuchiya N (2013) Consciousness in humans and non-human animals: recent advances and future directions. Frontiers in Psychology 4. DOI: 10.3389/fpsyg.2013.00625

Buschman TJ, Miller EK (2007) Top-down versus bottom-up control of attention in the prefrontal and posterior parietal cortices. Science 315:1860–1862.

Cancedda L, Putignano E, Sale A, Viegi A, Berardi N, Maffei L (2004) Acceleration of Visual System Development by Environmental Enrichment. J Neurosci 24:4840–4848.

Carlton J, Karnon J, Czoski-Murray C, Smith KJ, Marr J (2008) The clinical effectiveness and cost-effectiveness of screening programmes for amblyopia and strabismus in children up to the age of 4-5 years: a systematic review and economic evaluation. Health Technol Assess 12:iii, xi-194.

Castel AD, Pratt J, Drummond E (2005) The effects of action video game experience on the time course of inhibition of return and the efficiency of visual search. Acta Psychologica 119:217–230.

Castrén E, Hen R (2013) Neuronal plasticity and antidepressant actions. Trends in Neurosciences 36:259–267.

Churchill A, Graw J (2011) Clinical and experimental advances in congenital and paediatric cataracts. Philosophical Transactions of the Royal Society B: Biological Sciences 366:1234.

Cooper EA, Mackey AP (2016) Sensory and cognitive plasticity: implications for academic interventions. Curr Opin Behav Sci 10:21–27.

Corbetta M, Shulman GL (2011) SPATIAL NEGLECT AND ATTENTION NETWORKS. Annu Rev Neurosci 34:569–599.

Davis MF, Figueroa Velez DX, Guevarra RP, Yang MC, Habeeb M, Carathedathu MC, Gandhi SP (2015) Inhibitory Neuron Transplantation into Adult Visual Cortex Creates a New Critical Period that Rescues Impaired Vision. Neuron 86:1055–1066.

Di Cristo G, Chattopadhyaya B, Kuhlman SJ, Fu Y, Bélanger M-C, Wu CZ, Rutishauser U, Maffei L, Huang ZJ (2007) Activity-dependent PSA expression regulates inhibitory maturation and onset of critical period plasticity. Nat Neurosci 10:1569–1577.

Duffy KR, Mitchell DE (2013) Darkness alters maturation of visual cortex and promotes fast recovery from monocular deprivation. Curr Biol 23:382–386.

Dye MWG, Green CS, Bavelier D (2009) Increasing Speed of Processing With Action Video Games. Current directions in psychological science 18:321.

Eddy MC, Stansfield KJ, Green JT (2014) Voluntary exercise improves performance of a discrimination task through effects on the striatal dopamine system. Learn Mem 21:334–337.

Ekstrom LB, Roelfsema PR, Arsenault JT, Bonmassar G, Vanduffel W (2008) Bottom-up dependent gating of frontal signals in early visual cortex. Science 321:414–417.

Fagiolini M, Hensch TK (2000) Inhibitory threshold for critical-period activation in primary visual cortex. Nature 404:183–186.

Fagiolini M, Pizzorusso T, Berardi N, Domenici L, Maffei L (1994) Functional postnatal development of the rat primary visual cortex and the role of visual experience: dark rearing and monocular deprivation. Vision Res 34:709–720.

Feng J, Spence I, Pratt J (2007) Playing an Action Video Game Reduces Gender Differences in Spatial Cognition. Psychological Science 18:850–855.

Fields RD (2015) A new mechanism of nervous system plasticity: activity-dependent myelination. Nat Rev Neurosci 16:756–767.

Fields RD, Dutta DJ, Belgrad J, Robnett M (2017) Cholinergic signaling in myelination. Glia. DOI: 10.1002/glia.23101.

Fisher BE, Li Q, Nacca A, Salem GJ, Song J, Yip J, Hui JS, Jakowec MW, Petzinger GM (2013) Treadmill exercise elevates striatal dopamine D2 receptor binding potential in patients with early Parkinson's disease. Neuroreport 24:509–514.

Foley TE, Fleshner M (2008) Neuroplasticity of dopamine circuits after exercise: implications for central fatigue. Neuromolecular Med 10:67–80.

Fong M, Mitchell DE, Duffy KR, Bear MF (2016) Rapid recovery from the effects of early monocular deprivation is enabled by temporary inactivation of the retinas. Proceedings of the National Academy of Sciences of the United States of America 113:14139.

Gilbert CD, Li W (2012) Adult visual cortical plasticity. Neuron 75:250–264.

Gilbert CD, Li W, Piech V (2009) Perceptual learning and adult cortical plasticity. The Journal of Physiology 587:2743–2751.

Gilliam PE, Spirduso WW, Martin TP, Walters TJ, Wilcox RE, Farrar RP (1984) The effects of exercise training on [3H]-spiperone binding in rat striatum. Pharmacol Biochem Behav 20:863–867.

Giocomo LM, Hasselmo ME (2007) Neuromodulation by glutamate and acetylcholine can change circuit dynamics by regulating the relative influence of afferent input and excitatory feedback. Mol Neurobiol 36:184–200.

Gordon B, Allen EE, Trombley PQ (1988) The role of norepinephrine in plasticity of visual cortex. Progress in Neurobiology 30:171–191.

Green CS, Bavelier D (2003) Action video game modifies visual selective attention. Nature 423:534–537.

Green CS, Bavelier D (2006) Enumeration versus multiple object tracking: the case of action video game players. Cognition 101:217–245.

Gu Y, Janoschka S, Ge S (2012) Neurogenesis and Hippocampal Plasticity in Adult Brain. In: Neurogenesis and Neural Plasticity (Belzung C, Wigmore P, eds), pp 31–48 Current Topics in Behavioral Neurosciences. Springer Berlin Heidelberg. ISBN: 978-3-642-36231-6 978-3-642-36232-3

Guo CX, Babu RJ, Black JM, Bobier WR, Lam CSY, Dai S, Gao TY, Hess RF, Jenkins M, Jiang Y, Kowal L, Parag V, South J, Staffieri SE, Walker N, Wadham A, Thompson B (2016) Binocular treatment of amblyopia using videogames (BRAVO): study protocol for a randomised controlled trial. Trials 17:504.

Harauzov A, Spolidoro M, DiCristo G, De Pasquale R, Cancedda L, Pizzorusso T, Viegi A, Berardi N, Maffei L (2010) Reducing intracortical inhibition in the adult visual cortex promotes ocular dominance plasticity. J Neurosci 30:361–371.

Harwerth RS, Smith EL, Duncan GC, Crawford ML, von Noorden GK (1986) Multiple sensitive periods in the development of the primate visual system. Science 232:235–238.

He H-Y, Hodos W, Quinlan EM (2006) Visual deprivation reactivates rapid ocular dominance plasticity in adult visual cortex. J Neurosci 26:2951–2955.

He H-Y, Ray B, Dennis K, Quinlan EM (2007) Experience-dependent recovery of vision following chronic deprivation amblyopia. Nat Neurosci 10:1134–1136.

Heimel JA, van Versendaal D, lle, Levelt CN (2011) The Role of GABAergic Inhibition in Ocular Dominance Plasticity. Neural Plasticity 2011:e391763.

Hensch TK, Fagiolini M, Mataga N, Stryker MP, Baekkeskov S, Kash SF (1998) Local GABA circuit control of experience-dependent plasticity in developing visual cortex. Science 282:1504–1508.

Huang ZJ, Kirkwood A, Pizzorusso T, Porciatti V, Morales B, Bear MF, Maffei L, Tonegawa S (1999) BDNF regulates the maturation of inhibition and the critical period of plasticity in mouse visual cortex. Cell 98:739–755.

Ibos G, Duhamel J-R, Ben Hamed S (2009) The spatial and temporal deployment of voluntary attention across the visual field. PLoS ONE 4:e6716.

Ibos G, Duhamel J-R, Hamed SB (2013) A Functional Hierarchy within the Parietofrontal Network in Stimulus Selection and Attention Control. J Neurosci 33:8359–8369.

Issa NP, Trachtenberg JT, Chapman B, Zahs KR, Stryker MP (1999) The critical period for ocular dominance plasticity in the Ferret's visual cortex. J Neurosci 19:6965–6978.

Jakowec MW, Wang Z, Holschneider D, Beeler J, Petzinger GM (2016) Engaging cognitive circuits to promote motor recovery in degenerative disorders. exercise as a learning modality. Journal of Human Kinetics 52:35.

Kasamatsu T (1982) Enhancement of neuronal plasticity by activating the norepinephrine system in the brain: a remedy for amblyopia. Hum Neurobiol 1:49–54.

Kasamatsu T (1991) Chapter 42 - Adrenergic regulation of visuocortical plasticity: a role of the locus coeruleus system. In: Progress in Brain Research (Pompeiano CDB and O), pp 599–616 Neurobiology of the Locus Coeruleus. Elsevier.

Kawaguchi Y, Shindou T (1998) Noradrenergic Excitation and Inhibition of GABAergic Cell Types in Rat Frontal Cortex. J Neurosci 18:6963–6976.

Kimura F, Fukuda M, Tsumoto T (1999) Acetylcholine suppresses the spread of excitation in the visual cortex revealed by optical recording: possible differential effect depending on the source of input. Eur J Neurosci 11:3597–3609.

Kiorpes L (2006) Visual Processing in Amblyopia: Animal Studies. Strabismus 14:3–10.

Landi S, Sale A, Berardi N, Viegi A, Maffei L, Cenni MC (2007) Retinal functional development is sensitive to environmental enrichment: a role for BDNF. FASEB J 21:130–139.

Levi DM (2006) Visual Processing in Amblyopia: Human Studies. Strabismus 14:11–19.

Levi DM (2013) Linking assumptions in amblyopia. Vis Neurosci 30:277–287.

Levi DM, Li RW (2009a) Improving the performance of the amblyopic visual system. Philos Trans R Soc Lond, B, Biol Sci 364:399–407.

Levi DM, Li RW (2009b) Perceptual learning as a potential treatment for amblyopia: A mini-review. Vision Research 49:2535–2549.

Li L, Chen R, Chen J (2016) Playing Action Video Games Improves Visuomotor Control. Psychol Sci 27:1092–1108.

Li RW, Klein SA, Levi DM (2008) Prolonged Perceptual Learning of Positional Acuity in Adult Amblyopia: Perceptual Template Retuning Dynamics. J Neurosci 28:14223–14229.

Li RW, Levi DM (2004) Characterizing the mechanisms of improvement for position discrimination in adult amblyopia. J Vis 4:476–487.

Li RW, Ngo C, Nguyen J, Levi DM (2011) Video-Game Play Induces Plasticity in the Visual System of Adults with Amblyopia. PLoS Biology 9. DOI: 10.1371/journal.pbio.1001135

Li RW, Provost A, Levi DM (2007) Extended Perceptual Learning Results in Substantial Recovery of Positional Acuity and Visual Acuity in Juvenile Amblyopia. Invest Ophthalmol Vis Sci 48:5046–5051.

Lunghi C, Emir UE, Morrone MC, Bridge H (2015) Short-Term Monocular Deprivation Alters GABA in the Adult Human Visual Cortex. Current Biology 25:1496–1501.

MacRae PG, Spirduso WW, Walters TJ, Farrar RP, Wilcox RE (1987) Endurance training effects on striatal D2 dopamine receptor binding and striatal dopamine metabolites in presenescent older rats. Psychopharmacology (Berl) 92:236–240.

Maya Vetencourt JF, Sale A, Viegi A, Baroncelli L, De Pasquale R, O'Leary OF, Castrén E, Maffei L (2008) The antidepressant fluoxetine restores plasticity in the adult visual cortex. Science 320:385–388.

Mitchell DE, MacNeill K, Crowder NA, Holman K, Duffy KR (2016) Recovery of visual functions in amblyopic animals following brief exposure to total darkness. The Journal of Physiology 594:149.

Morishita H, Miwa JM, Heintz N, Hensch TK (2010) Lynx1, a cholinergic brake, limits plasticity in adult visual cortex. Science 330:1238–1240.

Olson CR, Freeman RD (1980) Profile of the sensitive period for monocular deprivation in kittens. Exp Brain Res 39:17–21.

Orosy-Fildes C, Allan RW (1989) Psychology of Computer Use: XII. Videogame Play: Human Reaction Time to Visual Stimuli. Perceptual and Motor Skills 69:243–247.

Pascual-Leone A, Amedi A, Fregni F, Merabet LB (2005) The plastic human brain cortex. Annu Rev Neurosci 28:377–401.

Pehrson AL, Leiser SC, Gulinello M, Dale E, Li Y, Waller JA, Sanchez C (2015) Treatment of cognitive dysfunction in major depressive disorder—a review of the preclinical evidence for efficacy of selective serotonin reuptake inhibitors, serotonin–norepinephrine reuptake inhibitors and the multimodal-acting antidepressant vortioxetine. European Journal of Pharmacology 753:19–31.

Pizzorusso T, Medini P, Berardi N, Chierzi S, Fawcett JW, Maffei L (2002) Reactivation of ocular dominance plasticity in the adult visual cortex. Science 298:1248–1251.

Powell C, Hatt SR (2009) Vision screening for amblyopia in childhood. Cochrane Database Syst Rev:CD005020.

Roberts MJ, Zinke W, Guo K, Robertson R, McDonald JS, Thiele A (2005) Acetylcholine dynamically controls spatial integration in marmoset primary visual cortex. J Neurophysiol 93:2062–2072.

Rong X, Ji Y, Fang Y, Jiang Y, Lu Y (2015) Long-Term Visual Outcomes of Secondary Intraocular Lens Implantation in Children with Congenital Cataracts. PLoS ONE 10. DOI: 10.1371/journal.pone.0134864

Rosenkranz K, Seibel J, Kacar A, Rothwell J (2014) Sensorimotor Deprivation Induces Interdependent Changes in Excitability and Plasticity of the Human Hand Motor Cortex. J Neurosci 34:7375–7382.

Rosenzweig MR (1966) Environmental complexity, cerebral change, and behavior. American Psychologist 21:321–332.

Rosenzweig MR, Bennett EL (1969) Effects of differential environments on brain weights and enzyme activities in gerbils, rats, and mice. Dev Psychobiol 2:87–95.

Rosenzweig MR, Bennett EL, Hebert M, Morimoto H (1978) Social grouping cannot account for cerebral effects of enriched environments. Brain Research 153:563–576.

Russo SJ, Nestler EJ (2013) The brain reward circuitry in mood disorders. Nat Rev Neurosci 14:609–625.

Sadahiro M, Sajo M, Morishita H (2016) Nicotinic regulation of experience-dependent plasticity in visual cortex. Journal of Physiology-Paris 110:29–36.

Sale A, Berardi N, Maffei L (2009) Enrich the environment to empower the brain. Trends Neurosci 32:233–239.

Silver MA, Shenhav A, D'Esposito M (2008) Cholinergic Enhancement Reduces Spatial Spread of Visual Responses in Human Early Visual Cortex. Neuron 60:904–914.

Sodhi MSK, Sanders-Bush E (2004) Serotonin and brain development. In (Neurobiology B-IR), pp 111–174 Disorders of Synaptic Plasticity and Schizophrenia. Academic Press.

Tailor V, Bossi M, Greenwood JA, Dahlmann-Noor A (2016) Childhood amblyopia: current management and new trends. Br Med Bull 119:75–86.

van Praag H, Kempermann G, Gage FH (2000) Neural consequences of enviromental enrichment. Nat Rev Neurosci 1:191–198.

Vedamurthy I, Knill DC, Huang SJ, Yung A, Ding J, Kwon O-S, Bavelier D, Levi DM (2016) Recovering stereo vision by squashing virtual bugs in a virtual reality environment. Philos Trans R Soc Lond, B, Biol Sci 371.

Vedamurthy I, Nahum M, Bavelier D, Levi DM (2015a) Mechanisms of recovery of visual function in adult amblyopia through a tailored action video game. Sci Rep 5:8482.

Vedamurthy I, Nahum M, Huang SJ, Zheng F, Bayliss J, Bavelier D, Levi DM (2015b) A dichoptic custom-made action video game as a treatment for adult amblyopia. Vision Res 114:173–187.

Waller JA, Tamm JA, Abdourahman A, Pehrson AL, Li Y, Cajina M, Sánchez C (2017) Chronic vortioxetine treatment in rodents modulates gene expression of neurodevelopmental and plasticity markers. European Neuropsychopharmacology 27:192–203.

Wang P, Liu H-H, Zhu X-T, Meng T, Li H-J, Zuo X-N (2016) Action Video Game Training for Healthy Adults: A Meta-Analytic Study. Front Psychol 7:907.

Wardak C, Denève S, Ben Hamed S (2011) Focused visual attention distorts distance perception away from the attentional locus. Neuropsychologia 49:535–545.

Wardak C, Ibos G, Duhamel J-R, Olivier E (2006) Contribution of the monkey frontal eye field to covert visual attention. J Neurosci 26:4228–4235.

Wardak C, Olivier E, Duhamel J-R (2004) A deficit in covert attention after parietal cortex inactivation in the monkey. Neuron 42:501–508.

Wiesel TN (1982) Postnatal development of the visual cortex and the influence of environment. Nature 299:583–591.

Yim AJ, Andersen ML, Soeiro AC, Tufik S, Oliveira MGM (2009) Acute systemic blockade of D2 receptors does not accelerate the extinction of cocaine-associated place preference. Brain Research 1304:122–128.

Zafeiriou D., Ververi A, Vargiami E (2009) The Serotonergic System: Its Role in Pathogenesis and Early Developmental Treatment of Autism. Curr Neuropharmacol 7:150–157.

Zénon A, Hamed SB, Duhamel J-R, Olivier E (2008) Spatial and Temporal Dynamics of Attentional Guidance during Inefficient Visual Search. PLOS ONE 3:e2219.

Zénon A, Hamed SB, Duhamel J-R, Olivier E (2009a) Attentional guidance relies on a winner-take-all mechanism. Vision Research 49:1522–1531.

Zénon A, Hamed SB, Duhamel J-R, Olivier E (2009b) Visual search without attentional displacement. Journal of Vision 9:9–9.

Zhou X, Panizzutti R, Villers-Sidani É de, Madeira C, Merzenich MM (2011) Natural Restoration of Critical Period Plasticity in the Juvenile and Adult Primary Auditory Cortex. J Neurosci 31:5625–5634.

Axis II Objectives

The objective of this second axis is precisely to establish the link between studies on cerebral plasticity in humans and studies in animals focusing on the molecular and cellular mechanisms of adult plasticity. In this respect, non-human primate is a well-chosen experimental model, because it allows to combine and compare, within the same experiment and the same subject, invasive and non-invasive interventions. Moreover, the visual system of the non-human primate is close enough to the human visual system to facilitate the transfer of research results to human applications.

The aim is to be able to compare the cortical effects of visual plasticity in the adult brain when this plasticity is induced in different ways (either by sensory influences, cognitive influences or localized pharmacological influences).

We do not know exactly what changes will be induced by this visual plasticity, nor the magnitude of these effects. How can we measure neuronal plasticity?

The main objective of this second axis is to develop different methods and techniques of MRI acquisition in order to optimize the best observation of the effects of plasticity *in vivo*, in the non-human primate.

Chapter 5 :

Implementation of 3T MRI

The first step of this project was to adapt our different equipments and installations to the new 3Tesla MRI scanner (Siemens, Prisma) which will allow us to have a better spatial resolution than the 1.5Tesla MRI scanner used for previous studies (Axis 1, Chapter 2 and 3) and which is essential for observing fine plasticity changes.

1. Development of equipment and installations for 3T MRI acquisitions

a. Coils

With this new scanner, we also acquired an eight-channel phased-array coil (MRI Coil Laboratory, Laboratory for Neuro- and Psychophysiology, Katholieke Universiteit Leuven, Leuven, Belgium, see Kolster et al., 2014), specially dedicated to non-human primate acquisitions. This coil is made up of three components:

- A radial transmit coil which comes closest to the skull of the animal from above
- a four-channel phased-array receive coil for the animal's left hemisphere
- a four-channel phased-array receive coil for the animal's right hemisphere

All these elements allow us to be closer to the animal's brain in order to improve the spatial resolution, the signal-to-noise ratio and to cover the entire surface of the animal's brain as well as possible. Besides, with this system, the animals are able to watch a screen and perform behavioral tasks while being vigilant.

On the old 1.5T MRI scanner, we used a radial receive-only surface coil (10 cm diameter). Therefore, we have had to develop a new fixing system that was both rigid to minimize as much as possible the propagation of the vibrations induced by the scanner and flexible to adapt as

best as possible to the size of the head of the animal. We can now thus move the different elements of the antenna on the three spatial axes X, Y and Z (**Figure 11**).

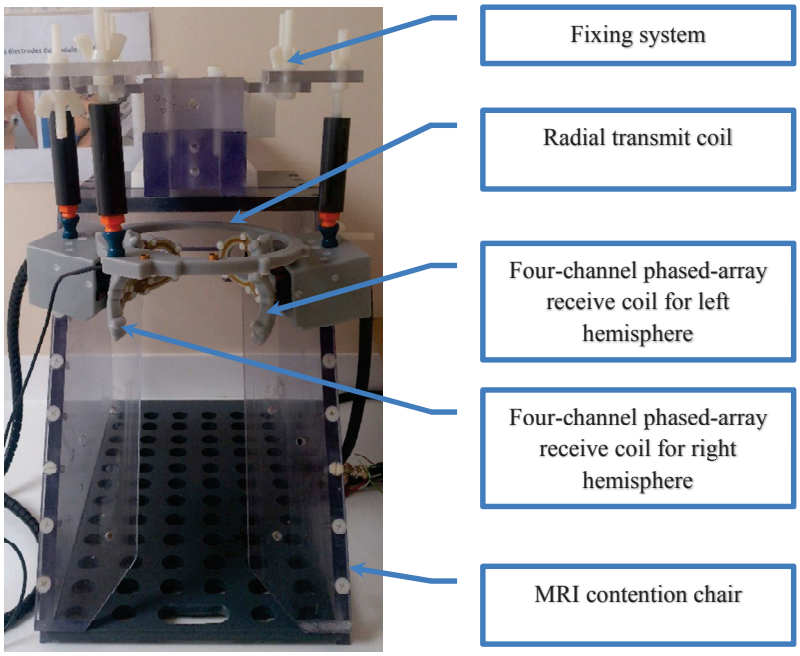

Figure 11 : Primate contention chair, MRI compatible ; with eight-channel phased-array receive coil and radial transmit coil system.

b. Screen

The tasks performed by the animals are played by a video projector projecting images on a home-made screen (**Figure 12**). Visual stimulations must be able to activate not only the center but also the periphery of the animal's visual field, so it is necessary to have a field of view as large as possible. For this, there are some limitations with the scanner due to its shape and size that we have to take into account. Indeed, the head of the animal must be at the center of the MRI bore, its visual field is therefore reduced by the size of the bore diameter (60 cm) and by the distance between the animal and the screen. We designed a semi-circular MRI-compatible screen that is located 40 cm from the tunnel edge, which corresponds to a distance of 60 cm between the eyes of the animal and the screen. As the size of the projected image is 32x32 cm, this allows us to have a field of view of about 15 degrees all around the screen center point.

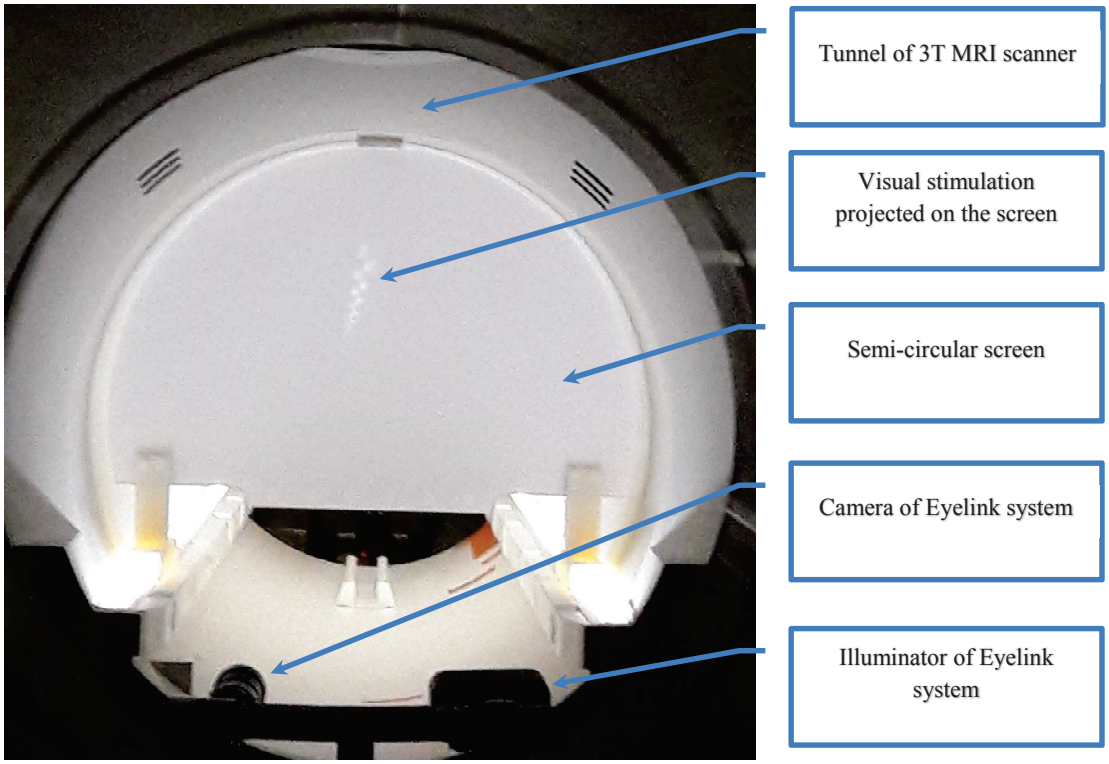

Figure 12: Visual stimulation projected onto the semi-circular screen inside the scanner.

c. Eyes signals recording

During MRI acquisitions, we record eyes signals (X, Y positions, pupil size) by means of a pupil-corneal reflection tracking system EyeLink at 1000Hz (SR-Research). It is composed of an infrared camera that can record the eyes signals in the dark, an illuminator that will maximize infrared rays for better signal and pupil contrast, as well as a specific recording software.

It was necessary to optimize the installation of the camera and the illuminator, since these two components cannot enter the tunnel because they would generate eddy currents which would create artefacts and distortions in the images acquired. It is therefore necessary to catch the eye of the animal despite the screen that is in the tunnel. The camera and illuminator are

installed at the edge of the tunnel (**Figure 12**); the animal's eye signal is recorded from below the screen (which is why the screen has a semi-circular shape).

d. MRI primate contention chair

The primate contention chair is the same as the one used for the MRI 1.5T acquisitions. It is built according to the model of Vanduffel et al. (2001, **Figure 13**). The animal is seated in sphinx position and its head is fixed by its MRI compatible implant to the contention chair.

The animal looks straight ahead, allowing it to see the screen where the visual stimulations are projected and to record the eyes signals. Two optical fibers, passed on either side of a vertical bar in front of the chair, serve for the manual response of the animal. Indeed, when the animal places its hand on the bar, it cuts off the light beam between the optical fibers indicating that the animal hold the bar (like a joystick). When the animal releases the bar, the optical beam between the fibers joins indicating that the animal has responded. Hydric rewards (water, syrup, fruit juice) are dispensed by a computer-controlled reward delivery system (Crist®) using a solenoid valve and a long plastic tube coming into the animal's mouth.

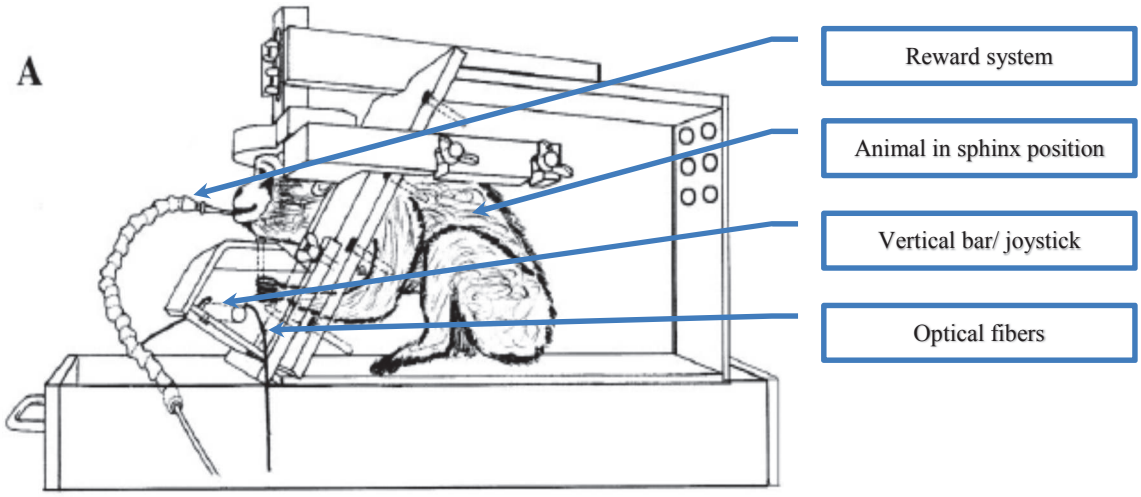

Figure 13 : MRI primate chair from Vanduffel (2001)

2. Development of MRI sequences

Nuclear magnetic resonance (MR) consists of studying changes in magnetization of the atomic nuclei (or spins) of a substance under the joint action of two magnetic fields: a *constant high magnetic field* (B_0) and a *rotating electromagnetic field* (B_1).

a. Functional Echo Planar Imaging sequence

The functional imaging we used is based on the magnetization of hemoglobin which is present in red blood cells. Hemoglobin can be either in an oxyhemoglobin form in cells oxygenated by the lungs or in a deoxyhemoglobin form in cells deoxygenated by tissue metabolism. While oxyhemoglobin is non-active in MR, deoxyhemoglobin is highly paramagnetic. Therefore, following the perturbation of the MR signal emitted by this molecule, it is possible to observe the cerebral activity. Indeed, the increasing activity in an area of the brain will lead to an influx of oxygenated blood which will drive the deoxygenated blood from this area, it is the BOLD signal (Blood Oxygenation level-dependent). This results in an excess of oxyhemoglobin in the venous capillaries of the activated area and, consequently, a relative decrease in the concentration of deoxyhemoglobin. This decrease in deoxyhemoglobin concentration results in a small increase in the signal in the activated territory on the T2*-weighted sequences (by elongation of the T2* of the blood in the capillaries, Kastler and Vetter, 2011).

To observe the blood flow modulations related to brain activity during our various cognitive tasks, we optimized a gradient-echo T2*-weighted Echo Planar Imaging (EPI) sequence. Images were taken as accelerated images in generalized autocalibrating partially parallel acquisition mode with foot-head acceleration direction and an acceleration factor (integrated parallel acquisition technique) of 2 (Grappa 2). The slices were acquired in cross-

section (from top to bottom), not interlaced (i.e. there is a 100 μm gap to avoid excitation on the sides).

Fourier transform space was in 6/8th, the bandwidth of 1190Hz and a flip angle of 90°. The field of view (FOV) of read-out was 105mm and that of phase was 95mm. The repetition time (TR) was 2000ms and the voxel resolution wass 1.25x1.25x1.25mm.

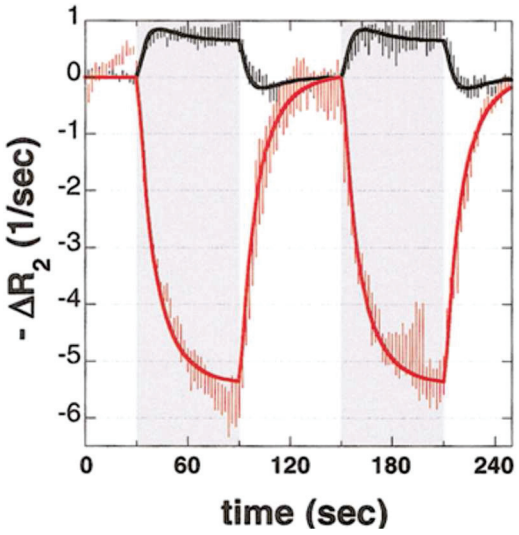

Figure 14: Relaxation rate changes for BOLD (black) and MION (red) contrast, together with the corresponding linear model fits, during two cycles of 60 s of stimulus (gray shaded intervals) followed by 60 s of baseline. At the end of the stimulus interval, MION relaxation rate changes were more than 7 times greater than BOLD changes. Peak MION signal change corresponds to a 25% increase in cerebral blood plasma volume (Leite et al., 2002).

Only two parameters in the sequence were likely to change depending on whether the animal had been previously injected with a contrast agent or not (Feraheme ®). The contrast agent composed of monocrystalline iron oxide nanoparticle (MION) was injected intravenously (IV) into the saphenous vein of the animal before certain functional acquisitions (e.g. fixation task). Using the contrast agent improved the contrast/noise ratio by ~3-fold (Vanduffel et al., 2001; Leite et al., 2002) and enhanced spatial selectivity of the MR signal changes (Zhao et al., 2005).

While brain activations produce an increase in MR signals in BOLD signal measurements, they lead to a decrease in MR signals in the presence of MION, essentially

corresponding to measurements of the blood brain volume. The hemodynamic signal is different depending on whether the BOLD signal or the MION signal is measured (the relaxation time R is longer in MION, **Figure 14**).

This is why it is important to change the Gradient Echo Time (TE) in the parameters of the functional sequence to be sure to measure brain activity (TE corresponds to the inverse of the relaxation time: TE = 1 / R, so a shorter TE is required when MION is present). The two parameters that change are therefore the TE and the number of slices acquired.

- Without MION: 31 cross-section slices with a TE of 30 ms.
- With MION: 38 cross-section slices with a TE of 18 ms.

The contrast between the gray matter and the white matter is more pronounced on the images acquired on the BOLD signal (**Figure 15**) than on the images acquired on the MION signal (**Figure 16**). However, on the latter, the convolutions are much clearer than on the images acquired in BOLD.

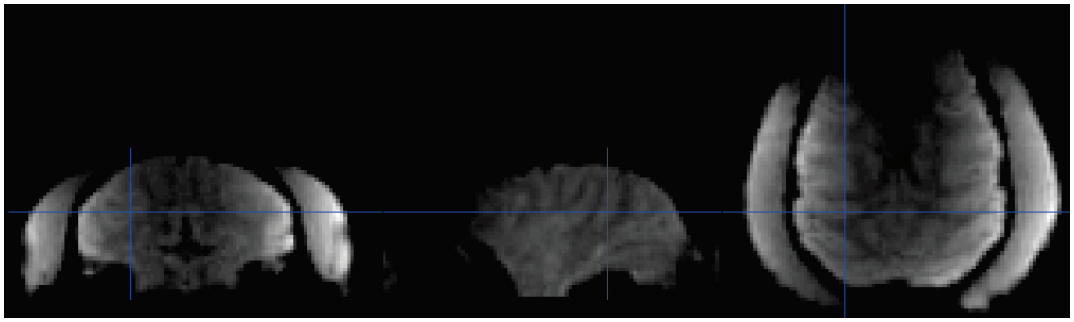

Figure 15: Example of raw functional images in BOLD signal (TE 30 ms)

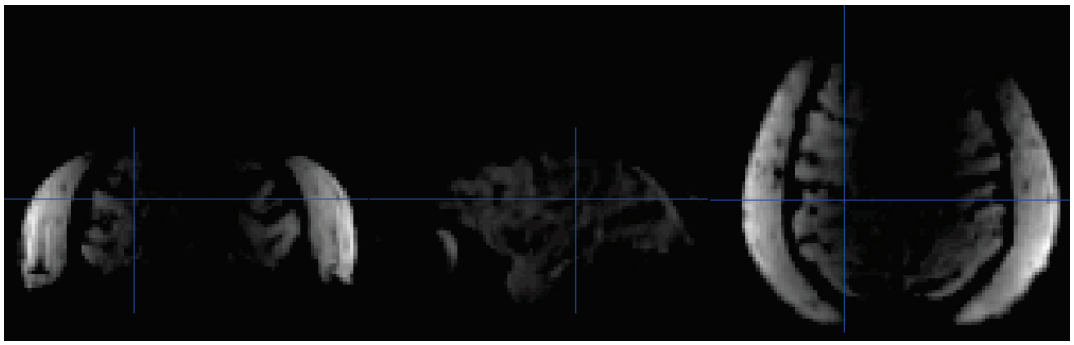

Figure 16: Example of raw functional images in MION signal (TE 18 ms)

b. Anatomical sequence

The anatomical images are acquired conventionally by T1-weighted imaging sequences (MPRAGE). This sequence provides a 3D image that shows the contrast between white matter (white), gray matter (gray) and cerebrospinal fluid (CSF) in black (**Figure 17**). Anatomical images are used for brain segmentation, surface extraction processing (fiducial, inflated and flattened maps, **Figure 18**), functional image registration and for projecting functional analysis results.

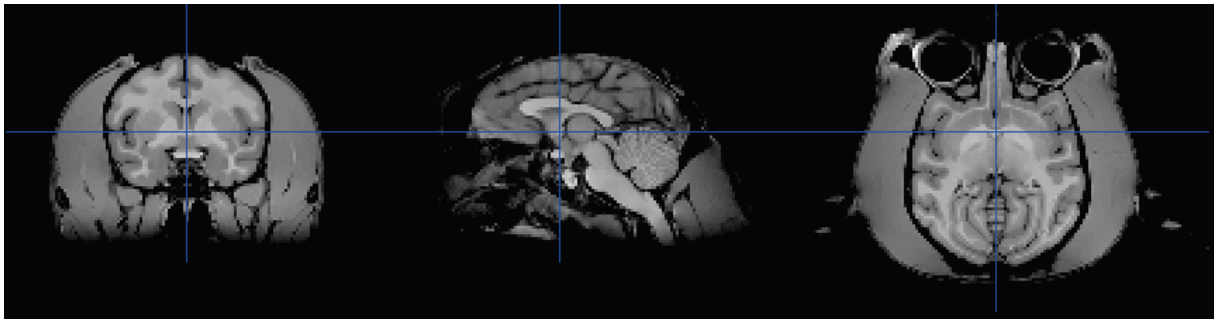

Figure 17: Example of anatomical images centered on anterior commissure (3D T1 MPRAGE)

For these acquisitions we used two L11 coils placed on each side of the skull of the anesthetized animal (intramuscular injection of zoletil, 10 mg / kg) and placed in a stereotactic apparatus. Our anatomical sequence is a 3D magnetization-prepared rapid gradient-echo (MPRAGE) with a spatial resolution of 0.5mm isotropic, a bandwidth of 130Hz, a TR of 3000ms, a TE of 5.38ms, an inversion time (TI) of 1100 ms, a flip angle of 8° and 192 slices acquired. Between three and four whole brain volumes are acquired in the same session averaged to improve the signal-to-noise ratio.

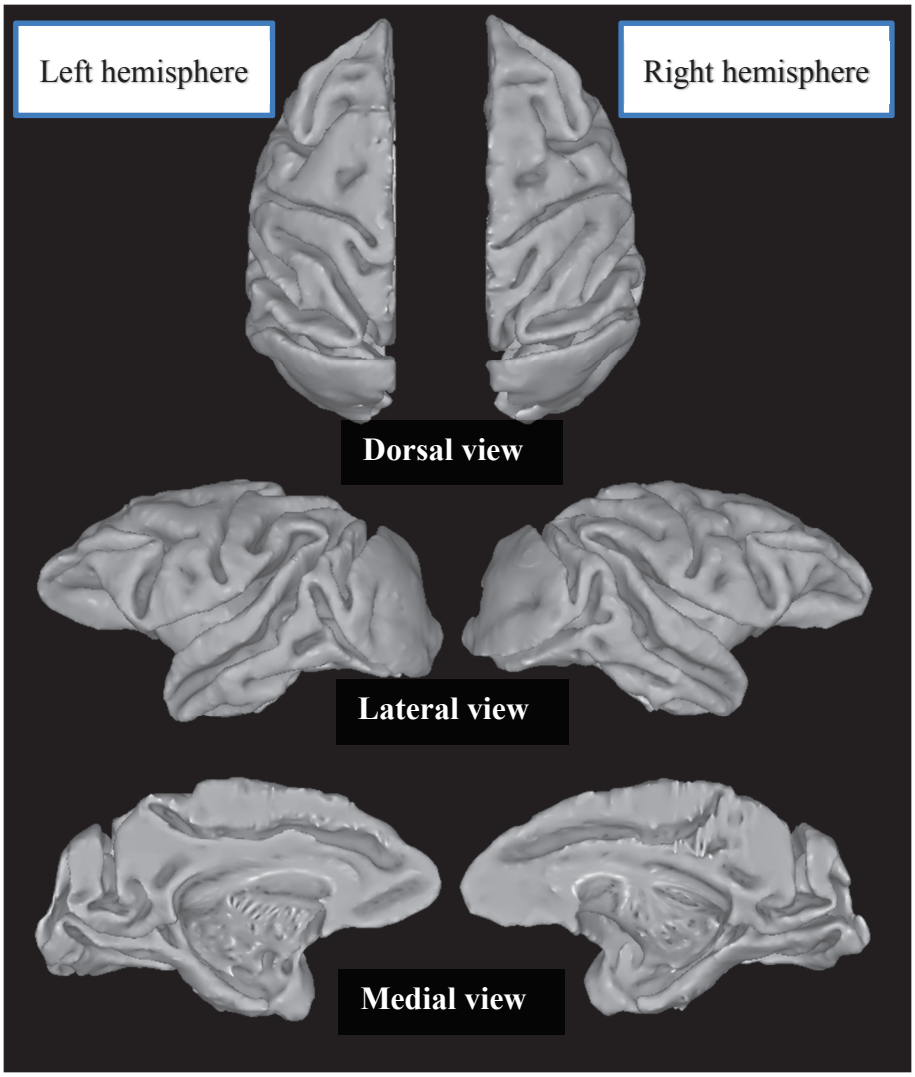

Figure 18: Fiducial map of anatomical surface in dorsal view, lateral view and medial view.

c. Diffusion Tensor Imaging sequence

Diffusion Tensor Imaging (DTI) is a unique non-invasive MRI-based technique that allows to visualize the position, orientation and anisotropy of the bundles of white matter brain and to analyze cerebral tissue microstructures *in vivo* by characterizing the diffusion properties of the water molecules at each point of the image. This technique allows to investigate white matter connections between different brain areas using a tractography technique and to generate biomarkers of white matter structure such as fractional anisotropy (FA) which measures its

directionality coherence (Pierpaoli et al., 1996; Basser et al., 2000; Garimella and Kraft, 2017; Warbrick et al., 2017). DTI is already used to study plasticity such as in studies on brain connectivity influenced by training (for review, see Moore et al., 2014); or in diseases (e.g. in Parkinson disease, for review, see Calabrese, 2016).

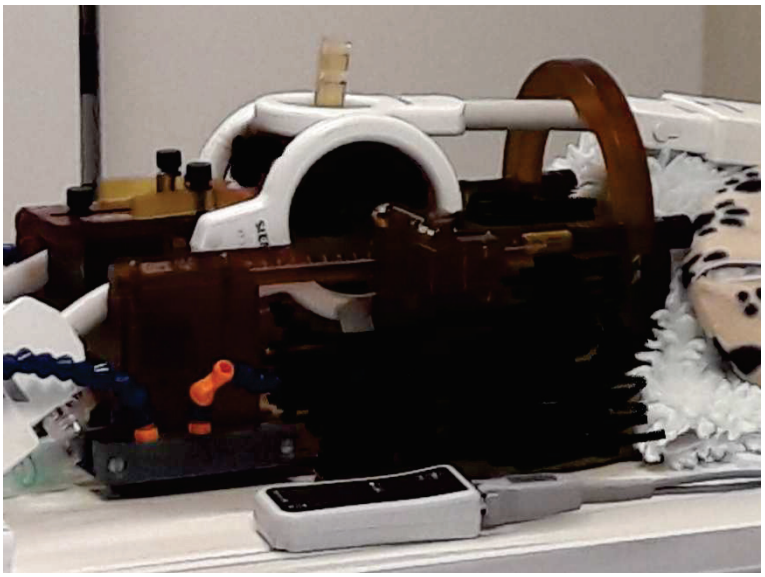

Figure 19: Setup for DTI acquisition with two L22 coils and one L7coil in anesthetized monkey.

This technique is very promising for the study of primate brains but remains limited due to its low sensitivity and spatial resolution and its vulnerability to motion and susceptibility artefacts. A recent study on postmortem rhesus macaque brain performing DTI on a 7 Tesla MRI scanner, provided new brain atlases with a very high resolution and better quality. However, the total acquisition time was of approximately 46 hours per specimen (Calabrese et al., 2015). The first step, here, was to perform DTI with high-resolution but in awake monkeys and so with a very much shorter acquisition time. For this, we used two L11 coils placed on each side of the skull of the anesthetized animal placed in a stereotactic frame (induced by intramuscular injection of ketamine, 10 mg / kg and followed by isoflurane 1-2%) and one L7 coil placed on the top of the head, around the headpost (**Figure 19**). Coils were combined with a custom pulse sequence based on a segmented 3-dimensional EPI sampling of Fourier space,

on a 3 Tesla MRI scanner with following parameters: diffusion weighted images (b-value of 1000s/mm^2), 30 directions diffusion gradient encoding with two B0, a spatial resolution of 0.5mm isotropic, an unprecedented voxel size of 0.125mm^3, a bandwidth of 776Hz, a TR of 750 ms, a TE of 71ms, 4 segments, a FOV of 105x125x56mm^3 and an acquisition time of 130 minutes (Tounekti et al., 2017).

Raw data has been reconstructed offline with Gadgetron software (http://gadgetron.github.io/). Magnetic susceptibility and eddy currents have been corrected. Fractional anisotropy maps were generated using FSL-DTIFIT (FMRIB software Library). The tractography was performed with the Euler method of DSI Studio (http://dsi-studio.labsolver.org). **Figure 20** shows an example of colored fractional anisotropy map and **Figure 21** shows an example of tractography maps. The obtained spatial resolution DTI maps are unprecedented in the awake monkey.

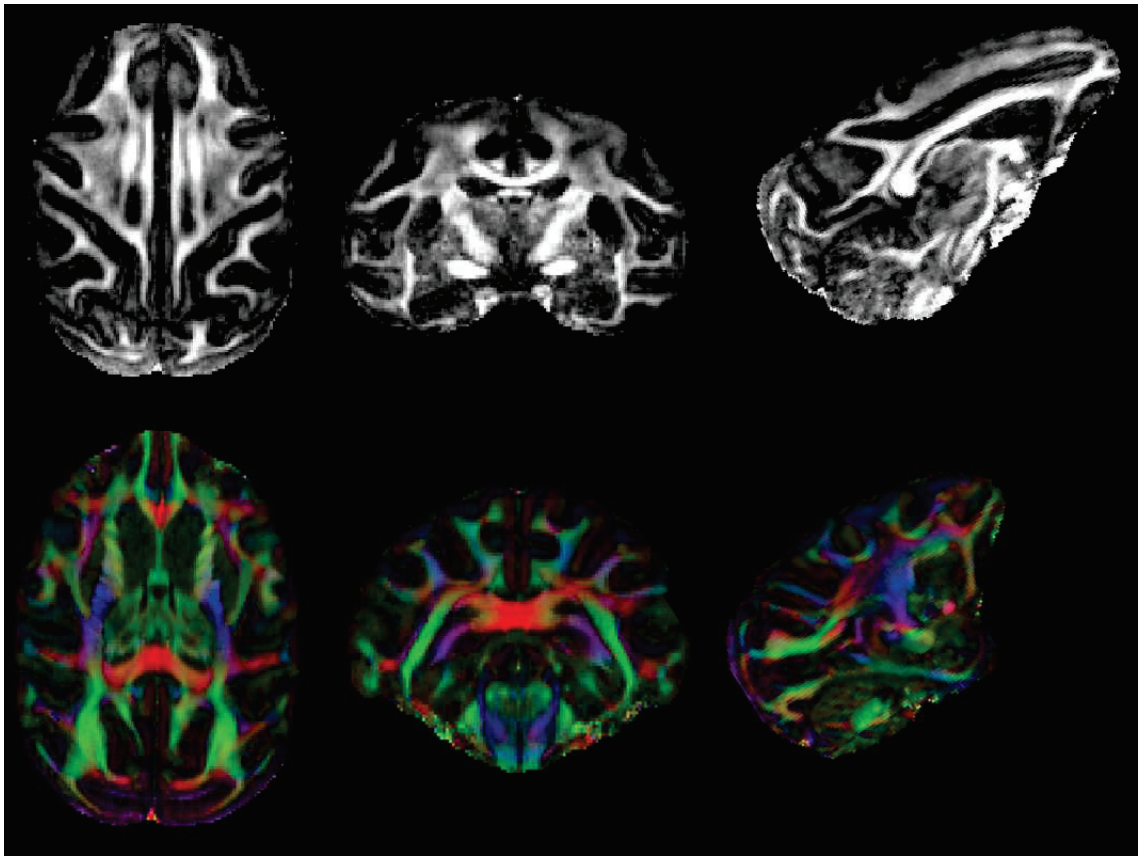

Figure 20: DTI acquisition in anesthetized macaque : uncolored (top) and colored (bottom) fractional anisotropy map.

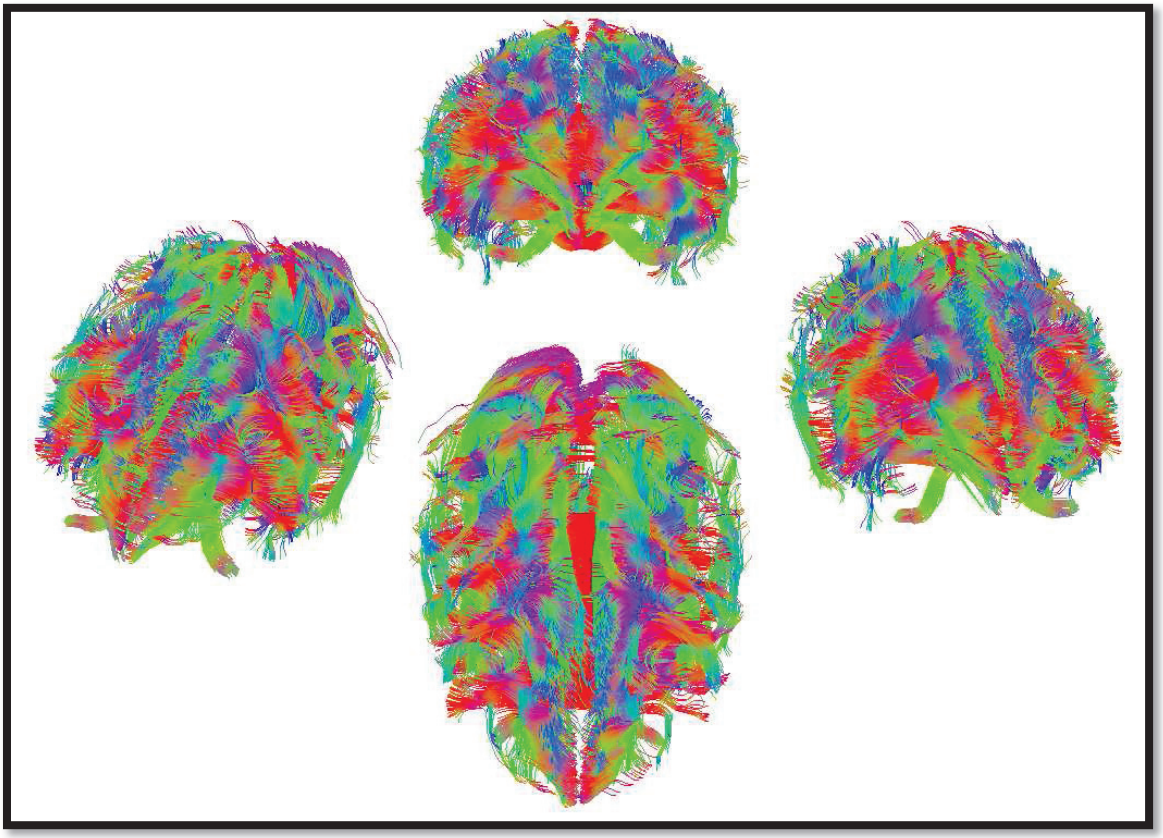

Figure 21: DTI acquisition in anesthetized macaque : different views of tractography maps

d. GABA spectroscopy sequence

Magnetic resonance spectroscopy (MRS) is the only non-invasive way to measure the local concentrations of GABA in the brain, *in vivo*. GABA detection is particularly challenging and requires special MRS techniques (Bogner et al., 2014). Indeed, the GABA concentration is low (around 1-2 mM) compared to the other metabolites dominating the MR spectrum and the spectral overlap of the main GABA peaks with peaks of other neurotransmitters which are present in much greater concentrations, in particular the creatine (Cr) peak at 3.0 ppm. (Novotny et al., 2003; Agarwal and Renshaw, 2012). However, this neurotransmitter seems to play a central role in rewiring plasticity (cf Axis II; Introduction; 3). Therefore, the measure of GABA concentration level and comparison of its different levels after plasticity induction could be a

very strong indicator of this plasticity induction and an indication about the neural changes playing a part in the balance between excitation and inhibition.

In humans, MRS are performed within a defined brain region of interest (ROI) with a box size of 30x30x30 mm and an acquisition time of 20 minutes. To define a smaller region is very complicated and results in a decrease in signal-to-noise ratio. However, since the brain of the macaque monkey is smaller than the human brain, we need to have a smaller ROI. We thus defined a ROI size of 15x8x10 mm in visual cortex and used four coils: two L11 coils placed on each side of the skull of the anesthetized animal, one L7 coil placed on the top of the head and one L4 coil placed just in the back of the skull.

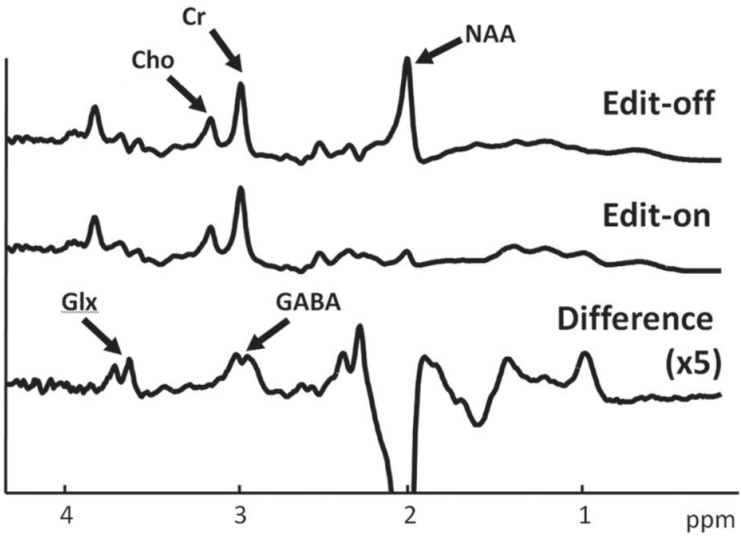

Figure 22: Average edit-ON, edit-OFF and edited spectra (difference between the edit-ON and edit-OFF data). The typical shapes of the Na-acetyl aspartate (NAA), Creatine (Cr), and choline (Cho) spectra can be clearly identified on the edit-off spectrum and the saturated NAA peak can be found on the edit-on spectrum. On the edited spectrum, an inverted NAA peak, Glx (glutamate and glutamine) peaks and GABA peak can be found at 2.02 ppm, 3.75 ppm and 3.0 ppm, respectively (from Tsai et al., 2016).

For our acquisition, after performing a classical MPRAGE (anatomical image) to define the ROI in the monkey brain, we used the MEGA-PRESS sequence (https://www.cmrr.umn.edu/spectro/) with the following parameters: a ROI size of 15x8x10 mm, a TR of 2000ms, a TE of 68ms, a bandwidth of 2000Hz, a number average of 640 (640 ON-OFF repetitions), 2048 points measured and an acquisition time of 50min. The editing pulse was applied to the GABA spins at 1.9ppm in order to selectively refocus the evolution of J-

coupling to the GABA spins at 3 ppm (for "ON"). The inversion pulse was applied at 7.5 ppm (which corresponds to 4.7ppm of water spins minus 1.9 ppm of the GABA spins plus 4.7ppm) for "OFF"). We made a manual shim for the acquisition to have a better water suppression.

We then used the most popular sequence: MEscher-GArwood (MEGA) difference editing with single-voxel Point RESolved Spectroscopy (PRESS) localization (Mescher et al., 1998; Mullins et al., 2014). Two spectra were acquired interleaved and subsequently subtracted: 1) an EDIT-ON spectrum with selective refocusing J-coupling evolution to the GABA spins at 3ppm, and 2) an EDIT-OFF spectrum without selective refocusing of the J-coupling evolution (Mescher et al., 1998; Mullins et al., 2014). The subtraction of the refocused ON spectrum from the non-refocused OFF spectrum removes the peaks that are not affected by the editing pulses and retains only those peaks that are affected by the editing pulses as shown by the example on Figure 22 (Tsai et al., 2016). A clear, though noisy GABA peak was obtained, validating our procedure to characterize changes in GABA following plastic changes in the adult monkey visual cortex.

e. Sequences to measure myelin index

Many white matter regions of the brain, such as the corpus callosum, contain a majority of unmyelinated axons in adulthood (Sturrock, 1980), making it conceivable that adult-born oligodendrocytes could engage in *de novo* myelination of previously naked axons suggesting a novel form of neural plasticity which has been termed "myelin plasticity" (for review, see Wang and Young, 2014). The late myelination of these axons would significantly alter their conduction speed, and thereby the functionality of the circuit. Activities ranging from motor task acquisition to cognitive training have been demonstrated to induce changes in white matter microstructure, which have been attributed to increased myelination (for review, see Fields,

2008; Richardson et al., 2011; Zatorre et al., 2012). This “myelin plasticity” might play a role in learning and memory and therefore changes in visual plasticity.

Some studies have suggested to measure cortical myelination in vivo with MRI (Clark et al., 1992; Barbier et al., 2002; Walters et al., 2003). Intracortical contrast related to myelin has been mapped in vivo (Sigalovsky et al., 2006; Bock et al., 2009, 2011, 2013; Geyer et al., 2011; Glasser and Essen, 2011; Barazany and Assaf, 2012; Cohen-Adad et al., 2012; Dick et al., 2012). Variations in signal intensities within the gray matter (i.e., myelin sensitivity) have been observed using quantitative T1 mapping (Sigalovsky et al., 2006; Geyer et al., 2011; Barazany and Assaf, 2012; Dick et al., 2012; Sereno et al., 2013), T1-weighted (Clark et al., 1992; Barbier et al., 2002; Walters et al., 2003; Clare and Bridge, 2005), T2-weighted (Yoshiura et al., 2000; Carmichael et al., 2006; Trampel et al., 2011), quantitative T2* (Fukunaga et al., 2010; Cohen-Adad et al., 2012; Cohen-Adad, 2014) and T2*-weighted images (Hinds et al., 2008; Zwanenburg et al., 2011; Sánchez-Panchuelo et al., 2012). Heavily myelinated areas have high signal intensities in T1-weighted images and low signal intensities in T2-weighted images. Glasser and Van Essen (2011) have developed a new method which corresponds to making the ratio between these two types of images (T1w/T2w). This ratio eliminates the bias of intensity of the image related to the magnetic resonance and improves the contrast of the noise for the myelin. We used this method to measure myelin index in our project.

We used a MPRAGE sequence to acquire T1w images with a spatial resolution of 0.5mm isotropic, a bandwidth of 250Hz, a TR of 3000ms, a TE of 3.62ms, an inversion time (TI) of 1100ms, a flip angle of 8° and 144 cross-sections acquired. The field of view (FOV) of read-out was 160mm and that of phase was 105mm.

We use a SPACE sequence to acquire T2w images with a spatial resolution of 0.5mm isotropic, a bandwidth of 710Hz, a TR of 3000ms, a TE of 366ms, a flip angle of 120° and 144

cross-sections acquired. The field of view (FOV) of read-out was 160mm and that of phase was 105mm.

All images were filtered with the Adaptive Optimized Nonlocal Means of Coupé and Manjon (2010). The T1w images were averaged and then the ratio was made. The image thus obtained is coregistered on the animal anatomical image by means of the JIP software (Mandeville et al., 2011) and projected on the anatomical image in Caret (van Essen et al., 2001). This allowed us to visualize and quantify the level of myelin on the cortex surface and thus be able to compare between each cycle of acquisitions and induction of plasticity the changes induced at the level of myelin.

References

Agarwal N, Renshaw PF (2012) Proton MR spectroscopy-detectable major neurotransmitters of the brain: biology and possible clinical applications. AJNR Am J Neuroradiol 33:595–602.

Barazany D, Assaf Y (2012) Visualization of cortical lamination patterns with magnetic resonance imaging. Cereb Cortex 22:2016–2023.

Barbier EL, Marrett S, Danek A, Vortmeyer A, van Gelderen P, Duyn J, Bandettini P, Grafman J, Koretsky AP (2002) Imaging cortical anatomy by high-resolution MR at 3.0T: detection of the stripe of Gennari in visual area 17. Magn Reson Med 48:735–738.

Basser PJ, Pajevic S, Pierpaoli C, Duda J, Aldroubi A (2000) In vivo fiber tractography using DT-MRI data. Magn Reson Med 44:625–632.

Bock NA, Hashim E, Janik R, Konyer NB, Weiss M, Stanisz GJ, Turner R, Geyer S (2013) Optimizing T1-weighted imaging of cortical myelin content at 3.0 T. Neuroimage 65:1–12.

Bock NA, Hashim E, Kocharyan A, Silva AC (2011) Visualizing myeloarchitecture with magnetic resonance imaging in primates. Ann N Y Acad Sci 1225 Suppl 1:E171-181.

Bock NA, Kocharyan A, Liu JV, Silva AC (2009) Visualizing the entire cortical myelination pattern in marmosets with magnetic resonance imaging. J Neurosci Methods 185:15–22.

Bogner W, Gagoski B, Hess AT, Bhat H, Tisdall MD, van der Kouwe AJW, Strasser B, Marjańska M, Trattnig S, Grant E, Rosen B, Andronesi OC (2014) 3D GABA imaging with real-time motion correction, shim update and reacquisition of adiabatic spiral MRSI. NeuroImage 103:290–302.

Calabrese E (2016) Diffusion Tractography in Deep Brain Stimulation Surgery: A Review. Front Neuroanat 10.

Calabrese E, Badea A, Coe CL, Lubach GR, Shi Y, Styner MA, Johnson GA (2015) A diffusion tensor MRI atlas of the postmortem rhesus macaque brain. Neuroimage 117:408–416.

Carmichael DW, Thomas DL, De Vita E, Fernández-Seara MA, Chhina N, Cooper M, Sunderland C, Randell C, Turner R, Ordidge RJ (2006) Improving whole brain structural MRI at 4.7 Tesla using 4 irregularly shaped receiver coils. Neuroimage 32:1176–1184.

Clare S, Bridge H (2005) Methodological issues relating to in vivo cortical myelography using MRI. Hum Brain Mapp 26:240–250.

Clark VP, Courchesne E, Grafe M (1992) In vivo myeloarchitectonic analysis of human striate and extrastriate cortex using magnetic resonance imaging. Cereb Cortex 2:417–424.

Cohen-Adad J (2014) What can we learn from T2* maps of the cortex? Neuroimage 93 Pt 2:189–200.

Cohen-Adad J, Polimeni JR, Helmer KG, Benner T, McNab JA, Wald LL, Rosen BR, Mainero C (2012) T_2* mapping and B_0 orientation-dependence at 7 T reveal cyto- and myeloarchitecture organization of the human cortex. Neuroimage 60:1006–1014.

Dick F, Tierney AT, Lutti A, Josephs O, Sereno MI, Weiskopf N (2012) In vivo functional and myeloarchitectonic mapping of human primary auditory areas. J Neurosci 32:16095–16105.

Fields RD (2008) White matter in learning, cognition and psychiatric disorders. Trends in Neurosciences 31:361–370.

Fukunaga M, Li T-Q, van Gelderen P, de Zwart JA, Shmueli K, Yao B, Lee J, Maric D, Aronova MA, Zhang G, Leapman RD, Schenck JF, Merkle H, Duyn JH (2010) Layer-specific variation of iron content in cerebral cortex as a source of MRI contrast. Proc Natl Acad Sci USA 107:3834–3839.

Garimella HT, Kraft RH (2017) A new computational approach for modeling diffusion tractography in the brain. Neural Regen Res 12:23–26.

Geyer S, Weiss M, Reimann K, Lohmann G, Turner R (2011) Microstructural Parcellation of the Human Cerebral Cortex - From Brodmann's Post-Mortem Map to in vivo Mapping with High-Field Magnetic Resonance Imaging. Front Hum Neurosci 5:19.

Glasser MF, Essen DCV (2011) Mapping Human Cortical Areas In Vivo Based on Myelin Content as Revealed by T1- and T2-Weighted MRI. J Neurosci 31:11597–11616.

Hinds O, Polimeni JR, Rajendran N, Balasubramanian M, Wald LL, Augustinack JC, Wiggins G, Rosas HD, Fischl B, Schwartz EL (2008) The intrinsic shape of human and macaque primary visual cortex. Cereb Cortex 18:2586–2595.

Kastler B, Vetter D (2011) Comprendre l'IRM, 7e édition. Elsevier Masson.

Kolster H, Janssens T, Orban GA, Vanduffel W (2014) The Retinotopic Organization of Macaque Occipitotemporal Cortex Anterior to V4 and Caudoventral to the Middle Temporal (MT) Cluster. J Neurosci 34:10168–10191.

Leite FP, Tsao D, Vanduffel W, Fize D, Sasaki Y, Wald LL, Dale AM, Kwong KK, Orban GA, Rosen BR, Tootell RBH, Mandeville JB (2002) Repeated fMRI Using Iron Oxide Contrast Agent in Awake, Behaving Macaques at 3 Tesla. NeuroImage 16:283–294.

Mandeville JB, Choi J-K, Jarraya B, Rosen BR, Jenkins BG, Vanduffel W (2011) fMRI of Cocaine Self-Administration in Macaques Reveals Functional Inhibition of Basal Ganglia. Neuropsychopharmacology 36:1187–1198.

Manjón J, Coupé P, Martí-Bonmatí L, Collins DL, Robles M (2010) Adaptive non-local means denoising of MR images with spatially varying noise levels. Journal of Magnetic Resonance Imaging 31:192–203.

Mescher M, Merkle H, Kirsch J, Garwood M, Gruetter R (1998) Simultaneous in vivo spectral editing and water suppression. NMR Biomed 11:266–272.

Moore E, Schaefer RS, Bastin ME, Roberts N, Overy K (2014) Can Musical Training Influence Brain Connectivity? Evidence from Diffusion Tensor MRI. Brain Sciences 4:405.

Mullins PG, McGonigle DJ, O'Gorman RL, Puts NAJ, Vidyasagar R, Evans CJ, Edden RAE (2014) Current practice in the use of MEGA-PRESS spectroscopy for the detection of GABA. NeuroImage 86:43–52.

Novotny EJ, Fulbright RK, Pearl PL, Gibson KM, Rothman DL (2003) Magnetic resonance spectroscopy of neurotransmitters in human brain. Ann Neurol 54:S25–S31.

Pierpaoli C, Jezzard P, Basser PJ, Barnett A, Di Chiro G (1996) Diffusion tensor MR imaging of the human brain. Radiology 201:637–648.

Richardson WD, Young KM, Tripathi RB, McKenzie I (2011) NG2-glia as Multipotent Neural Stem Cells: Fact or Fantasy? Neuron 70:661–673.

Sánchez-Panchuelo RM, Francis ST, Schluppeck D, Bowtell RW (2012) Correspondence of human visual areas identified using functional and anatomical MRI in vivo at 7 T. J Magn Reson Imaging 35:287–299.

Sereno MI, Lutti A, Weiskopf N, Dick F (2013) Mapping the human cortical surface by combining quantitative T(1) with retinotopy. Cereb Cortex 23:2261–2268.

Sigalovsky IS, Fischl B, Melcher JR (2006) Mapping an intrinsic MR property of gray matter in auditory cortex of living humans: a possible marker for primary cortex and hemispheric differences. Neuroimage 32:1524–1537.

Sturrock RR (1980) Myelination of the Mouse Corpus Callosum. Neuropathology and Applied Neurobiology 6:415–420.

Tounekti S, Troalen T, Bihan-Poudec Y, Cléry J, Lamberton F, Ben Hamed S, Hiba B (2017) High-resolution diffusion MRI of Macaque brain at 3T: 3D-EPI sampling of Fourier space.

Trampel R, Ott DVM, Turner R (2011) Do the congenitally blind have a stria of Gennari? First intracortical insights in vivo. Cereb Cortex 21:2075–2081.

Tsai S-Y, Fang C-H, Wu T-Y, Lin Y-R (2016) Effects of Frequency Drift on the Quantification of Gamma-Aminobutyric Acid Using MEGA-PRESS. Scientific Reports 6:24564.

van Essen DC, Drury HA, Dickson J, Harwell J, Hanlon D, Anderson CH (2001) An Integrated Software Suite for Surface-based Analyses of Cerebral Cortex. J Am Med Inform Assoc 8:443–459.

Vanduffel W, Fize D, Mandeville JB, Nelissen K, Van Hecke P, Rosen BR, Tootell RBH, Orban GA (2001) Visual Motion Processing Investigated Using Contrast Agent-Enhanced fMRI in Awake Behaving Monkeys. Neuron 32:565–577.

Walters NB, Egan GF, Kril JJ, Kean M, Waley P, Jenkinson M, Watson JDG (2003) In vivo identification of human cortical areas using high-resolution MRI: an approach to cerebral structure-function correlation. Proc Natl Acad Sci USA 100:2981–2986.

Wang S, Young KM (2014) White matter plasticity in adulthood. Neuroscience 276:148–160.

Warbrick T, Rosenberg J, Shah NJ (2017) The relationship between BOLD fMRI response and the underlying white matter as measured by fractional anisotropy (FA): A systematic review. Neuroimage.

Yoshiura T, Higano S, Rubio A, Shrier DA, Kwok WE, Iwanaga S, Numaguchi Y (2000) Heschl and superior temporal gyri: low signal intensity of the cortex on T2-weighted MR images of the normal brain. Radiology 214:217–221.

Zatorre RJ, Fields RD, Johansen-Berg H (2012) Plasticity in gray and white: neuroimaging changes in brain structure during learning. Nat Neurosci 15:528–536.

Zhao F, Wang P, Hendrich K, Kim S-G (2005) Spatial specificity of cerebral blood volume-weighted fMRI responses at columnar resolution. NeuroImage 27:416–424.

Zwanenburg JJM, Versluis MJ, Luijten PR, Petridou N (2011) Fast high resolution whole brain T2* weighted imaging using echo planar imaging at 7T. Neuroimage 56:1902–1907.

Chapter 6 :

Implementation of a semi-invasive animal model to study different ways of inducing plasticity and their consequences

1. Animals

a. Species

The rhesus macaque (macaca mulatta) is a dominant model for cognitive neuroscience since this species, among the different animal models that dominate the neurosciences, has the following characteristics: it is able to learn complex behavioral tasks used to study the human cognitive functions and shares strong anatomical and functional homologies with humans. This distinguishes it from rat and mouse models and makes it more suitable for the study of high-level cortical functions.

Because of its phylogenetic proximity to the human species, a large part of the fine observations made in this species (by targeted cell recordings or by anatomical studies) can be transposed directly into humans (whose study of cortical functions is dominated by fMRI). Our choice to work with macaques using fMRI, a discipline still emerging, is based on a desire to evaluate in more detail the conditions and limitations of the transposition of knowledge between NHP (non-human primates) and human cortical functions.

This project involves two rhesus macaques, two males of 8 and 9 kg, aged respectively 9 and 8.

b. Implantation of headpost

We performed surgery that aimed at implanting a headpost in the animals. This allowed us to fix the head of the animals during the scanning sessions, which is crucial for precise control of the oculomotor behavior and for the acquisition of MRI images.

Surgery involved cutting the skin and reaching the surface of the skull. Once this surface was thoroughly cleaned and aseptic, we installed histocompatible ceramic screws on the future

circumference of the headpost. These screws served as a grip to fix the skull to the acrylic dental cement which we then deposited. The headpost was placed at the top of the skull and secured to it by this same cement. A rest period of at least one month followed the laying of the headpost.

c. Training

Training the animal to come out of its cage to enter its restraint chair as well as to return into its cage from the chair was done by means of a restraining cane, a positive conditioning and reinforcement, and breaking down the different steps. The animal was first accustomed to the presence of the cane, then to be caned to its collar, to leave the cage with the cane and to enter the chair. All this was done step by step over several days or weeks to ensure that the animal was as calm and confident as possible.

The learning of the task of interest is carried out under conditions of water control in order to motivate the animals, so that the daily water requirements are covered by the experimental time and the associated rewards. Learning is composed of different stages. Each step acquired by the animal gives rise to the complexification of the task until the desired behavior is achieved. In this project, the animals learned to fix a central point on a screen either without any other stimulation or during the presentation of visual stimulations (passive or followed by a manual response). They were rewarded (hydric rewards: water, syrup or apple juice) to maintain this fixation as long as possible. Indeed, the reward delivery was scheduled to encourage long fixation without breaks (i.e. the interval between successive deliveries was decreased and their amount was increased, up to a fixed limit, as long as the eyes did not leave the tolerance window centered on the fixation spot), so as to be compatible with active fMRI designs.

d. MRI environment

Monkeys were trained in a mock scan environment resembling as much as possible the actual MRI scanner setup. For this, during training, the animals were habituated to the fixation of their headposts. MRI acquisitions being very noisy and occurring in the dark; the animals were also habituated to wear ear plugs and installed in a dark tunnel in sphinx position to better imitate the MRI scanner environment and reduce their nervosity during the actual acquisitions in the scanner.

e. Intravenous injection

For the acquisition of part of the cognitive tasks (retinotopic mapping and resting-state sessions), the animals received an intravenous injection of a contrast agent (Feraheme®). As this agent must be injected before the MRI acquisition session, it is done on awake animals. The animals were thus trained and used to this step of intravenous injection in order to remain as calm as possible and to minimize the stress induced by this manipulation.

2. Tasks for functional acquisition in awake monkeys

Several functional MRI acquisitions were performed in awake animals for each plasticity cycle. The sequences acquired are EPI sequences (cf Chapter 5, 2a).

a. Retinotopic mapping task

In lower visual areas (e.g., V1 through V5) the neurons are organized in an orderly fashion called topographic or retinotopic mapping, in the sense that they form a 2D representation of the visual image formed on the retina in such a way that neighboring regions of the image are represented by neighboring regions of the visual area. However, the retinotopic representation

in the cortical areas is distorted. The foveal area is represented by a relatively larger area in V1 than the peripheral areas (for review, see Wandell and Winawer, 2011). Functional MRI is a powerful tool for investigating the retinotopic organization of the macaque visual cortex in individual subjects (Brewer et al., 2002; Vanduffel et al., 2002; Fize et al., 2003; Kolster et al., 2009, 2014; Patel et al., 2010; Arcaro et al., 2011; Janssens et al., 2014). Retinotopic mapping makes it possible to measure a map of visual receptive fields whose size can be modified (widened and narrowed) following the induction of plasticity (d'Almeida et al., 2013; Chang et al., 2015; Striem-Amit et al., 2015).

For this, the animal must fix a central point throughout the sequence. It is rewarded to maintain this fixation as long as possible. During this time, visual stimulations are played. Functional time series (runs) to measure polar angle and eccentricity in which the visual stimuli are played respectively by a rotating wedge and by an expanding ring are alternated. Within a run the visual stimulation cycle is repeated 2 times.

- *Rotating wedge:*

It corresponds to a black and white checkerboard in the shape of a wedge that flickers at 3.33Hz. This wedge rotates around the central fixation point in a counterclockwise direction and is composed of two segments in the azimuthal direction and 20 segments radially (**Figure 23a**). There are 30 positions and thus 6° between two adjacent segments in the azimuthal direction. The radial sizes of the segments were adjusted according to a log(r) law to approximate the human cortical magnification factor. All positions are not played within the same run because it would be too long for the animal. Therefore, there are two different runs, one run for the first fifteen positions and one for the last fifteen. 139 whole brain volumes are acquired during a run, for a total time of 278 seconds per run.

➢ *Expanding ring:*

It corresponds to a black and white checkerboard in the shape of a ring which flickers at 3.33Hz. This ring is expanding and reducing around the central fixation point (**Figure 23b**). This concentric ring is composed of 60 squares in the azimuthal direction. There are 19 annuli. The radial sizes of the segments were adjusted according to a log(r) law to approximate the human cortical magnification factor. 177 whole brain volumes are acquired during a run, for a total time of 354 seconds per run.

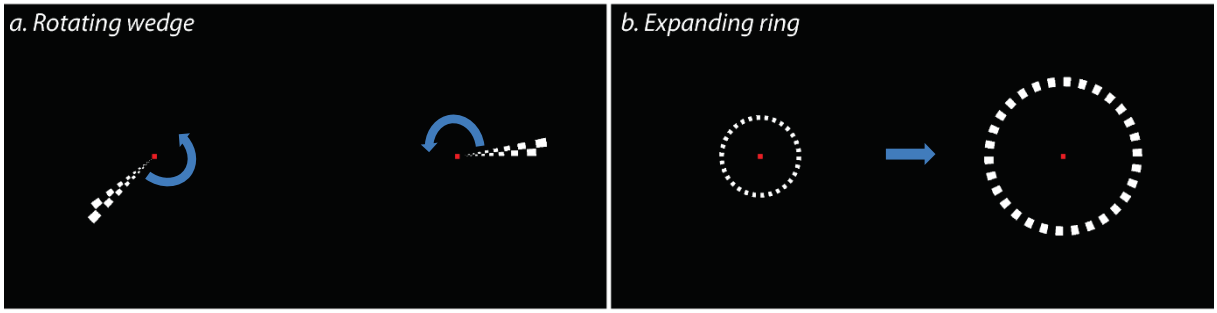

Figure 23: Retinotopic mapping task: a. Rotating wedge, b. Expanding ring

For retinotopic mapping tasks, the monkeys were required to fixate the central point throughout the run despite the visual stimulations played (wedges or annuli). They were rewarded for maintaining this fixation as long as possible.

b. Classical peripheral visual detection task

The peripheral detection task allows us to obtain a behavioral measurement because it is an active task, contrary to retinotopic mapping which is a passive task. 176 whole brain volumes are acquired during a run, corresponding to an average of 40 correct trials per task.

During this task, the monkeys were required to fixate a central point throughout the run. In this task, monkeys were rewarded when they correctly detected a target that appeared randomly in the four quadrants (with no other visual stimulations, black background). The monkeys were required to respond by raising its hand from the bar after target appearance.

c. Resting-state

Functional acquisition during resting-state gives an overview of brain activations in the absence of environmental stimulations (visual, tactile, reward) and allows to analyze the functional connectivity of different brain networks in order to see how they evolve following the plasticity induction. This type of run is acquired at the beginning of the session to avoid all activations linked to the active tasks and not to the resting-state. Accordingly, the animal is inside the scanner but is not solicited (it is in the dark, it does not receive any reward). 181 whole brain volumes are acquired during a run (around 6 minutes, van Dijk et al., 2010).

3. Tasks for plasticity induction

As seen in introduction, plasticity can be induced in the visual cortex of adult monkeys in different ways (sensory training, cognitive training, pharmacological injection…). The visual field is divided into four distinct visual quadrants. One of the visual quadrants is the target of the induction of plasticity. For each new cycle, the selected visual quadrant is different from the previous cycle. This makes it possible to compare each visual quadrants with the others, within the same cycle of plasticity induction and to see the effect of it, but also between each cycle in order to see the effects of the different plasticity. In the present thesis, I will describe only the sensory training method used to induce plasticity within the visual cortex of our adult monkeys.

a. Bottom-up influences through sensory training

Bottom-up influences are both driven by the external environment and intrinsic properties of the adult's visual system (Zénon et al., 2008, 2009a, 2009b). To study the plasticity involved in these influences, we will induce plasticity via sensory training. This reinforcement will be

achieved by over-stimulation of one of the quadrants of the visual field. We will expect these manipulations to increase the spatial resolution of the visual map at the level of the visual quadrant defined.

To do this, we created two tasks: a simple fixation task and a detection task.

i. Simple fixation task

The monkeys will be required to fixate a central point throughout the run. They will be rewarded for maintaining this fixation as long as possible. Visual stimulations will correspond to clouds of white dots on a black background. The position of dots will be randomized but biased by the greater quantity of dots in the test quadrant (40 times of dots, **Figure 24a**).

ii. Detection task in the presence of salient distractors

The monkeys will be required to fixate a central point throughout the run. Visual stimulations and background will be the same as in the simple fixation task. In this task, monkeys will be rewarded when they will correctly detect a target that will appear randomly in the four quadrants (manual response by peripheral visual detection, **Figure 24b**).

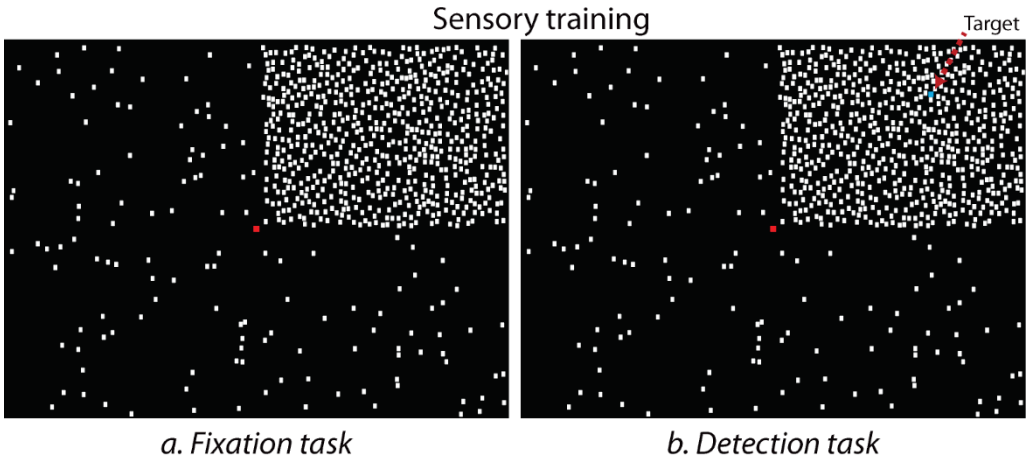

Figure 24: Task to induce plasticity by sensory training : a. Passive fixation task, b. Active peripheral visual detection task.

Monkeys will be train to perform these two tasks for at least two months.

4. Acquisition sessions content

Different types of imaging data were and will be acquired before and after each plasticity induction in 3T scanner. The first step of this project, after the development of sequences and monkeys training of classical tasks, were to acquire the cycle T0 which corresponds to the period before plasticity induction. For this first cycle, we acquired in several sessions in an anesthetized animal:

- Anatomical imaging
- DTI imaging
- GABA spectroscopy imaging
- T1w and T2w for myelin index

For functional imaging data, awake animals performed the resting-state task, the retinotopic mapping task and classical detection task during two weeks to have a great number of runs (for all type of tasks, we kept only the runs in which monkeys had their gaze within the tolerance window more than 85% of the time).

After this first cycle, monkeys will be train during two months to perform the two tasks described above (Axis II, Chapter 6, 3a.) to observe bottom-up influences on plasticity induced by this sensory training. The second cycle T1 of MRI acquisitions corresponds to the period after the first plasticity induction. As in cycle T0, the same types of imaging data will be acquired during sessions with anesthetized animal. During MRI awake sessions, animals will perform the resting-state task and the retinotopic mapping task as in cycle T0. They will also perform the simple fixation task and the detection task in the presence of salient distractors.

We will report the observed plastic changes occurring throughout the visual cortex through different measures:

1) Behavioral indicators of persistent functional changes in visual processing, reflecting the onset of plasticity as well as the stabilization of its effects. Using detection tasks allows us to probe visual contrast sensitivity as a function of the spatial location (classical detection task, at T0) and bottom-up visual integration processes (detection task in the presence of salient distractors, at T1).

2) By analyzing how these manipulations progressively alter the temporal pattern of information flow between lower and higher visual cortical regions

3) By comparing the high-resolution fMRI mapping of their retinotopic organization between the different cycles of plasticity induction to assess changes in term of receptive field (size, overlap…)

4) By quantifying whole-brain changes in functional resting-state connectivity (as in Babapoor-Farrokhran et al., 2013).

5) By comparing the myelin index reflecting myelin changes induced by plasticity (increase of myelin density, new myelinated areas…)

6) By assessing changes in water diffusion and water revealing new connections and reorganization of connections.

7) By quantifying the GABA concentration to evaluate if this plasticity induces a reduction of GABA concentration and plays a role in the balance between excitation and inhibition.

References

Arcaro MJ, Pinsk MA, Li X, Kastner S (2011) Visuotopic Organization of Macaque Posterior Parietal Cortex: A Functional Magnetic Resonance Imaging Study. J Neurosci 31:2064–2078.

Babapoor-Farrokhran S, Hutchison RM, Gati JS, Menon RS, Everling S (2013) Functional connectivity patterns of medial and lateral macaque frontal eye fields reveal distinct visuomotor networks. J Neurophysiol 109:2560–2570.

Brewer AA, Press WA, Logothetis NK, Wandell BA (2002) Visual Areas in Macaque Cortex Measured Using Functional Magnetic Resonance Imaging. J Neurosci 22:10416–10426.

Chang L-H, Yotsumoto Y, Salat DH, Andersen GJ, Watanabe T, Sasaki Y (2015) Reduction in the retinotopic early visual cortex with normal aging and magnitude of perceptual learning. Neurobiol Aging 36:315–322.

d'Almeida OC, Mateus C, Reis A, Grazina MM, Castelo-Branco M (2013) Long term cortical plasticity in visual retinotopic areas in humans with silent retinal ganglion cell loss. Neuroimage 81:222–230.

Fize D, Vanduffel W, Nelissen K, Denys K, d'Hotel CC, Faugeras O, Orban GA (2003) The Retinotopic Organization of Primate Dorsal V4 and Surrounding Areas: A Functional Magnetic Resonance Imaging Study in Awake Monkeys. J Neurosci 23:7395–7406.

Janssens T, Zhu Q, Popivanov ID, Vanduffel W (2014) Probabilistic and Single-Subject Retinotopic Maps Reveal the Topographic Organization of Face Patches in the Macaque Cortex. J Neurosci 34:10156–10167.

Kolster H, Janssens T, Orban GA, Vanduffel W (2014) The Retinotopic Organization of Macaque Occipitotemporal Cortex Anterior to V4 and Caudoventral to the Middle Temporal (MT) Cluster. J Neurosci 34:10168–10191.

Kolster H, Mandeville JB, Arsenault JT, Ekstrom LB, Wald LL, Vanduffel W (2009) Visual Field Map Clusters in Macaque Extrastriate Visual Cortex. J Neurosci 29:7031–7039.

Patel GH, Shulman GL, Baker JT, Akbudak E, Snyder AZ, Snyder LH, Corbetta M (2010) Topographic organization of macaque area LIP. PNAS 107:4728–4733.

Striem-Amit E, Ovadia-Caro S, Caramazza A, Margulies DS, Villringer A, Amedi A (2015) Functional connectivity of visual cortex in the blind follows retinotopic organization principles. Brain 138:1679–1695.

van Dijk KRA, Hedden T, Venkataraman A, Evans KC, Lazar SW, Buckner RL (2010) Intrinsic Functional Connectivity As a Tool For Human Connectomics: Theory, Properties, and Optimization. Journal of Neurophysiology 103:297–321.

Vanduffel W, Fize D, Peuskens H, Denys K, Sunaert S, Todd JT, Orban GA (2002) Extracting 3D from Motion: Differences in Human and Monkey Intraparietal Cortex. Science 298:413–415.

Wandell BA, Winawer J (2011) Imaging retinotopic maps in the human brain. Vision research 51:718.

Zénon A, Hamed SB, Duhamel J-R, Olivier E (2008) Spatial and Temporal Dynamics of Attentional Guidance during Inefficient Visual Search. PLOS ONE 3:e2219.

Zénon A, Hamed SB, Duhamel J-R, Olivier E (2009a) Attentional guidance relies on a winner-take-all mechanism. Vision Research 49:1522–1531.

Zénon A, Hamed SB, Duhamel J-R, Olivier E (2009b) Visual search without attentional displacement. Journal of Vision 9:9–9.

Chapter 7 :

Visual cortical representation (T0) before plasticity induction in the adult non-human primate

I will present here the first results obtained for this projects, namely, imaging and behavioral data acquired for the T0 cycle. All these data will serve as a baseline for the future acquisitions allowing to compare and observe the changes induced by the different types of plasticity induction.

1. Behavioral data

Detection tasks allowed us to extract behavioral data. We extracted the number of "Hits", "Correct rejection", "Miss", "False alarm" and "Late" but also reaction times.

- **Reaction times (RT)**: it corresponds to the time between the appearance of the target and monkey's response. The monkey had to respond with a RT between 150 and 1000ms to be rewarded.
- **Hits**: In this trial, the monkey did respond correctly after the appearance of the target and he was rewarded. It means that he released the bar with its hand after perceiving the target.
- **Correct rejection**: In this trial, there was no target. The monkey did not release its hand of the bar but fixated correctly the fixation point therefore he was rewarded.
- **Miss**: In this trial, the monkey did not release the bar after the target appeared and thus did not receive any reward.
- **False alarm**: In this trial, the monkey released the bar although there was no target or it had not yet appeared (RT < 150ms). It was considered as an anticipation. The animal did not receive any reward.

- **Late**: In this trial, the monkey released the bar after target appeared but too late to be rewarded. It means that the time between the appearance of the target and the monkey's response was too long (RT > 1000ms).

Performances

This first detection task is relatively easy for monkeys. As shown by **Figure 25**, monkey 1 (M1) performed a lot of correct trials (93.8% with 75.04% of Hits and 18.76% of Correct rejection %) and few mistakes (6.21% with 0.44% of Miss; 5.75% of False alarm and 0% of Late). Monkey 2 (M2) performed also a lot of correct trials (74.09% with 57.93% of Hits and 16.16% of Correct rejection) but he made more mistakes (25.9% with 5.92% of Miss; 19.98% of False alarm and 0% of Late). The two monkeys did not have exactly the same behavior. For almost 20% of trials, M2 had more false alarms and therefore more anticipation than M1.

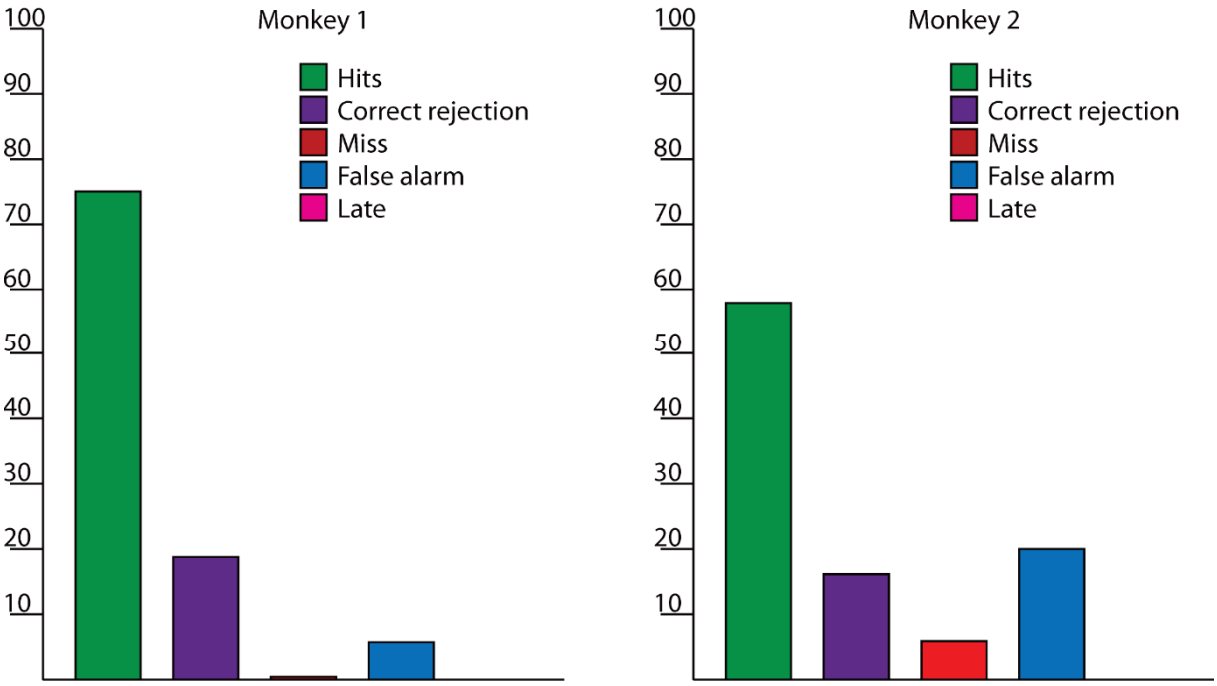

Figure 25: Global performance of monkey 1 and monkey 2 during detection tasks.

Data were also separated and analyzed by visual quadrants. In this case, we considered only trials in which a target appeared (there is no correct rejection because this parameter is only for no target apparition). For M1 (**Figure 26**), we have the same proportion of responses

for each quadrant (~99% of Hits). Therefore, this animal has no bias for one of the quadrants. If we compare the number of false alarms between the global performance and the analysis by visual quadrants, we observe very few false alarms (only 1 false alarm) for trials with a target suggesting that the greatest number of false alarms in the global performance (65 false alarms) were performed during trials without a target. It means that the animal released the bar when he only needed to fixate.

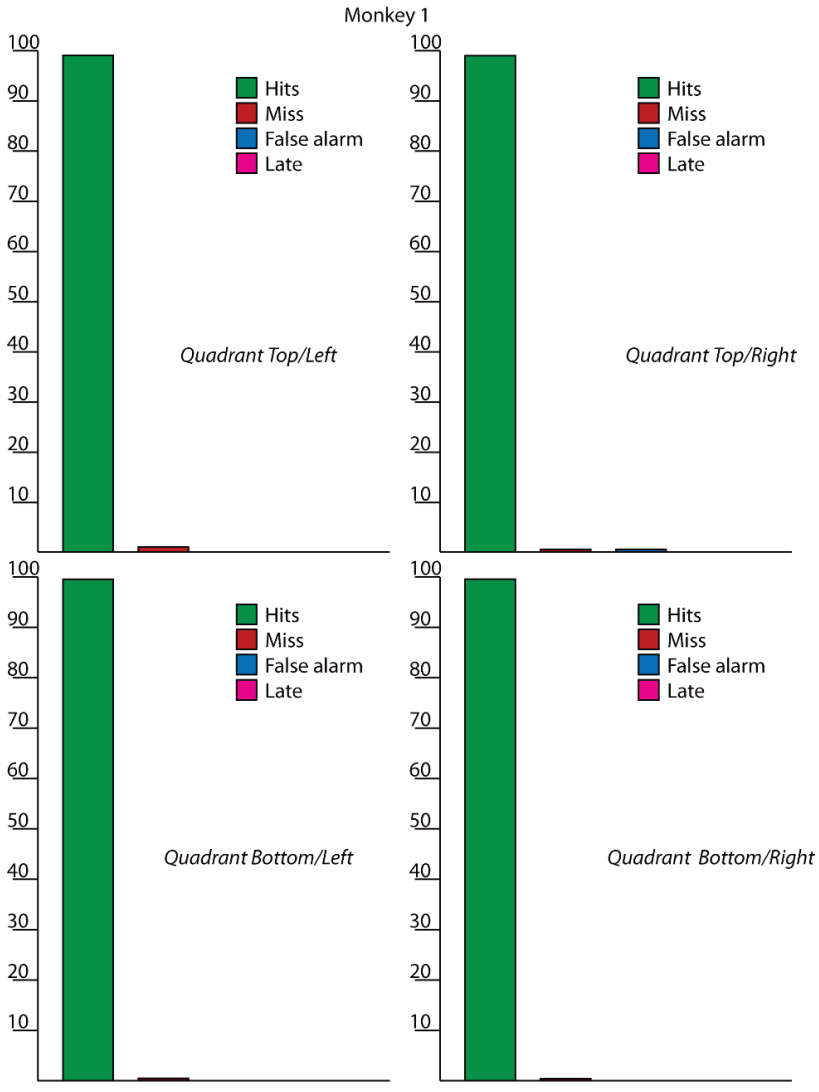

Figure 26: Performance divided into visual quadrants for monkey 1.

For M2 (**Figure 27**), we also have the same proportion of responses for each quadrant (~90% of Hits). Therefore, this animal has no bias for one of the quadrants. If we compare the number of false alarms between the global performance and the analysis by visual quadrants,

we observe very few false alarms (only 7 false alarms) for trials with a target suggesting, as with M1, that the greatest number of false alarms in the global performance (199 false alarms) were performed during trials without a target. On the contrary, the animal M2 performed some miss responses (59 miss) but it is not dependent on any visual quadrant.

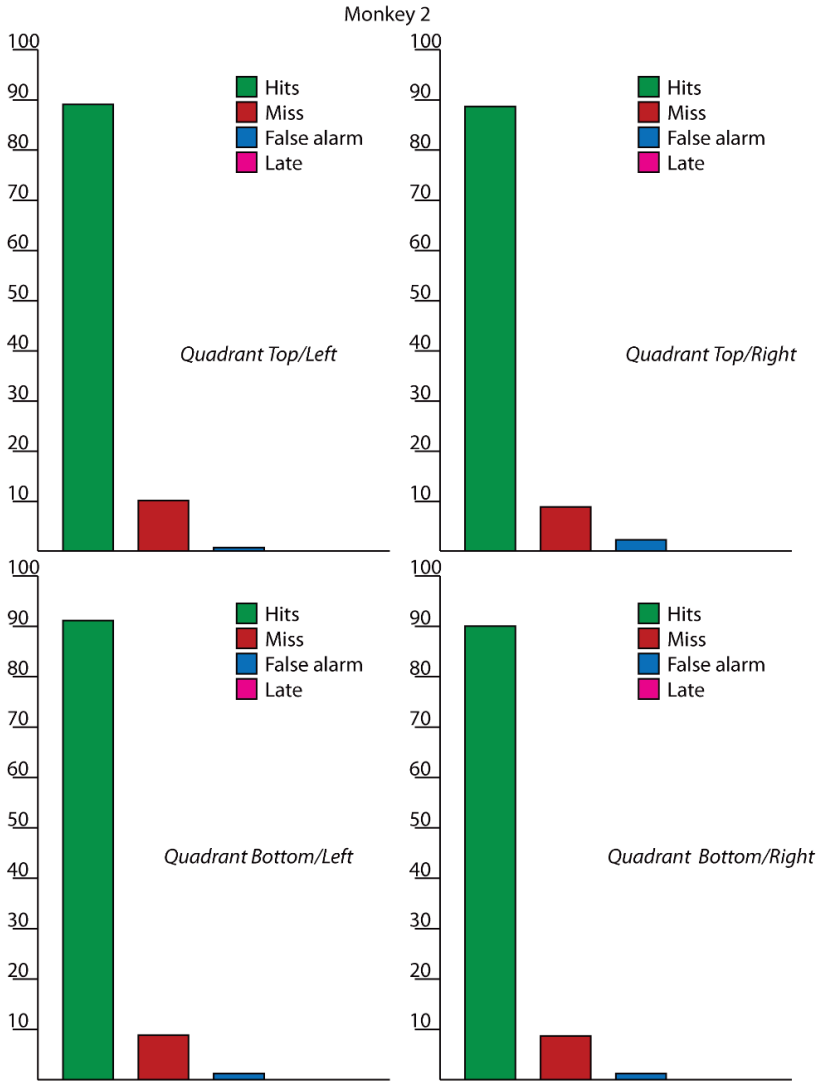

Figure 27: Performance divided into visual quadrants for monkey 2.

These first results show that neither of the two monkeys has any bias for a particular visual quadrant. When we will induce plasticity we expect to see changes in the proportion of responses between the over-stimulated quadrant and the other three.

Reaction times

First, we analyzed reaction times in a global way (**Figure 28**). The mean of RT for monkey 1 is 336 ms (standard deviation, STD: 26 ms) and for monkey 2, it is 322 ms (STD: 29 ms). Monkey 2 is faster than monkey 1 (Fisher test: $7.5\ 10^{-66}$; two-tailed paired-ttest: $4.5\ 10^{-8}$).

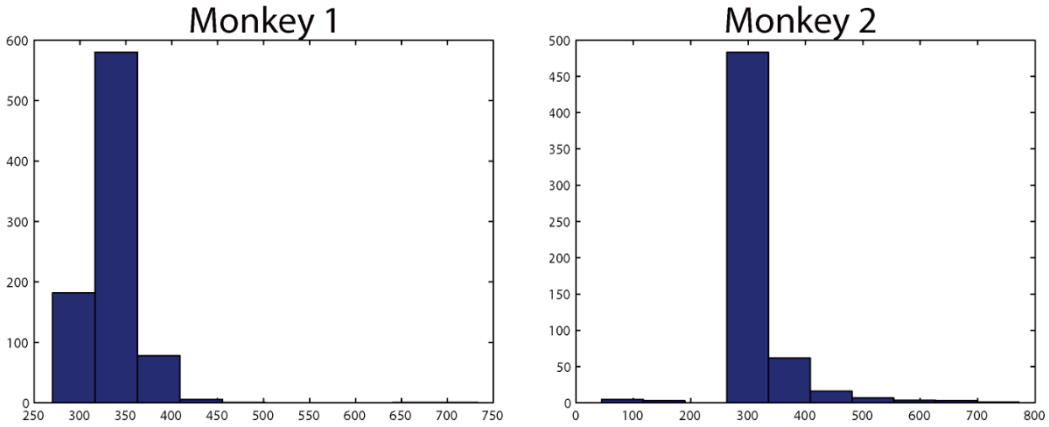

Figure 28: Reactions times distribution for monkey 1 and monkey 2.

Secondly, we analyzed reaction times separately by visual quadrants (**Figure 29** and **Figure 30**)

Monkey 1 has a mean RT of 340 ms for the top/left quadrant, 346 ms for the top/right quadrant, 332 ms for the bottom/left quadrant and 325 ms for the bottom/right quadrant (**Figure 29**). Reaction times between these four quadrants are significantly different (anova, $2.4\ 10^{-13}$). RTs for bottom quadrants are significantly shorter than RTs for top quadrants (two-tailed paired-ttest: $2.3\ 10^{-12}$).

Monkey 2 has a mean RT of 323 ms for the top/left quadrant, 329 ms for the top/right quadrant, 318 ms for the bottom/left quadrant and 317 ms for the bottom/right quadrant (**Figure 30**). Reaction times between these four quadrants are not significantly different (anova, 0.26). However, we can note that RTs for bottom quadrants tend to be shorter than RTs for top quadrants (Fisher test: 0.03; two-tailed paired-ttest: 0.06).

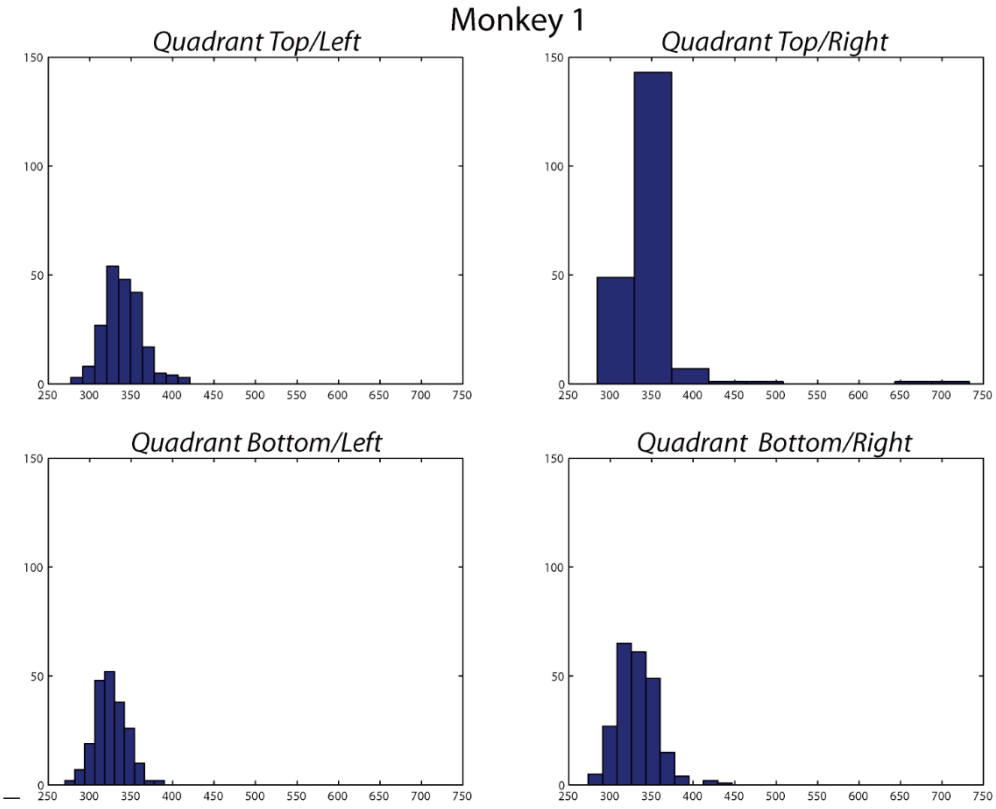

Figure 29: Reaction times distribution divided into visual quadrant for monkey 1

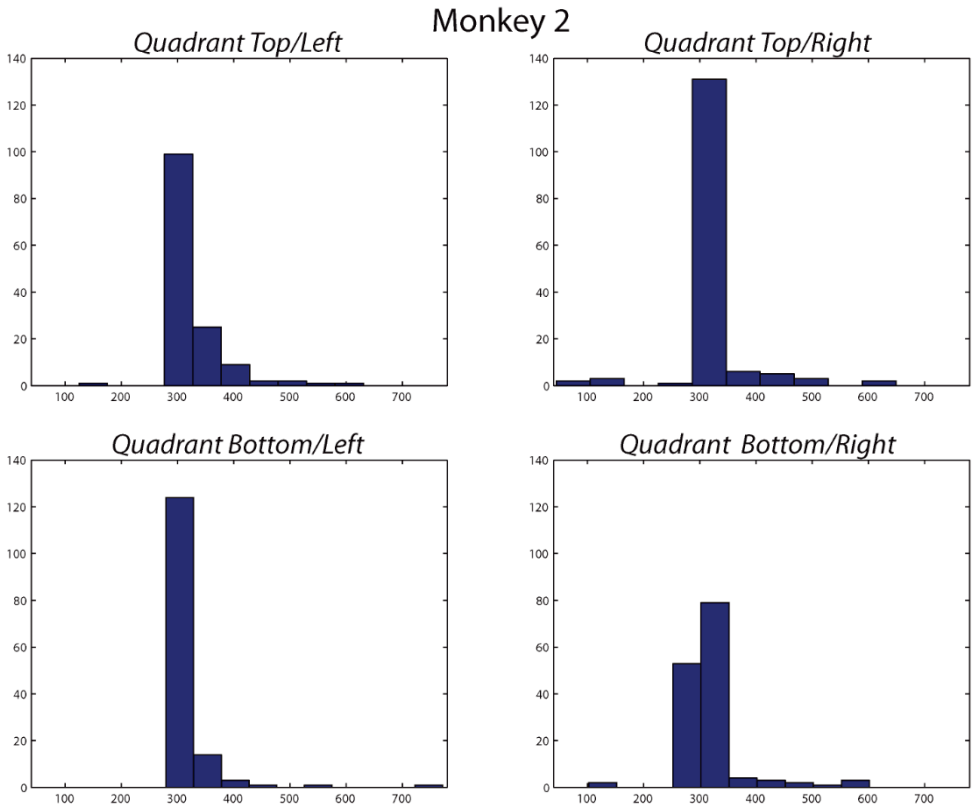

Figure 30: Reaction times distribution divided into visual quadrant for monkey 2.

These second results show that both monkeys have different RTs between the different quadrants and in particular, bottom quadrants have shorter RTs than top quadrants.

When we will induce plasticity we expect to see changes in RTs on the over-stimulated quadrant compared to the other three, between before and after plasticity induction. In other words, this T0 characterization will serve as reference.

2. Retinotopic mapping

Today, only monkey 1 performed functional imaging sessions with a contrast agent injection. We used phase-encoded mapping method and calculated a fast Fourier transform of the observed time series to generate the different retinotopic maps (based on methods using by Sereno et al., 1995; Alvarez et al., 2015).

Figure 31 and **Figure 32** show the retinotopic maps respectively, for polar-angle and for eccentricity, in the left and right hemispheres of monkey 1. We can see that the ventral portions of V1, V2, V3 and V4 contain maps of the upper visual field while the lower visual field quadrants are represented in the dorsal portions of the areas. Visual stimulations are mapped in the contralateral hemifield. It means that for the task "wedge 1" in which stimulations are essentially played in the right visual field, they are mapped by the left hemisphere while for the task "wedge 2" in which stimulations are essentially played in the left visual field, they are mapped by the right hemisphere (**Figure 31)**. This is more visible with the task "annuli", we can see the different annuli mapped on the visual cortex with the shape of these annuli. Besides, this task shows that the central visual field is mapped by the central part of visual areas and this mapping is expanded when the annuli is expanded (**Figure 32**). Overall, we reproduce using this high-resolution retinotopic mapping approach what is already described in the literature in terms of topographical organization of areas V1 to V4. This topography will serve as a reference T0 for the subsequent post-plasticity mappings.

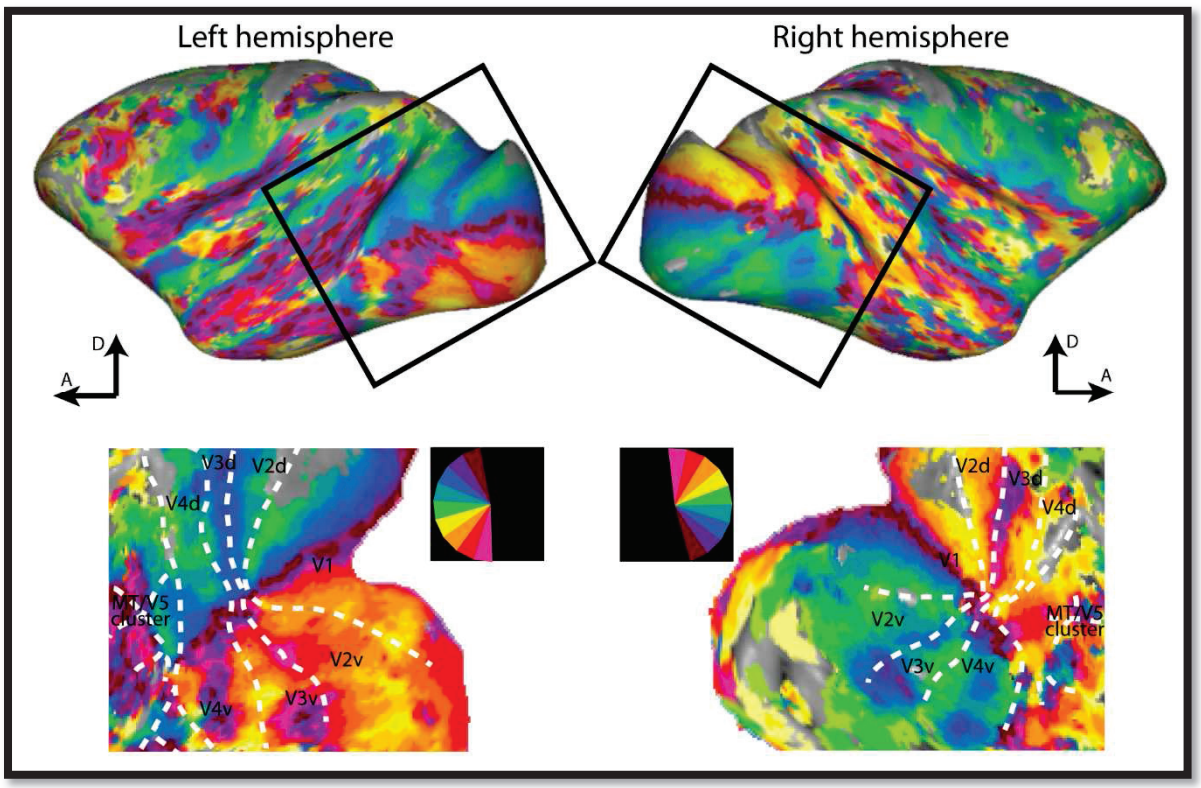

Figure 31: Retinotopic maps for polar-angle in the left (by Wedge1 task) and right hemispheres (by Wedge 2 task) represented on inflated (top panel) and flattened maps (lower panel). The color code is indicated in the figure. Dashed white lines delineate the different visual areas, based on the F99 monkey template brain in Caret.

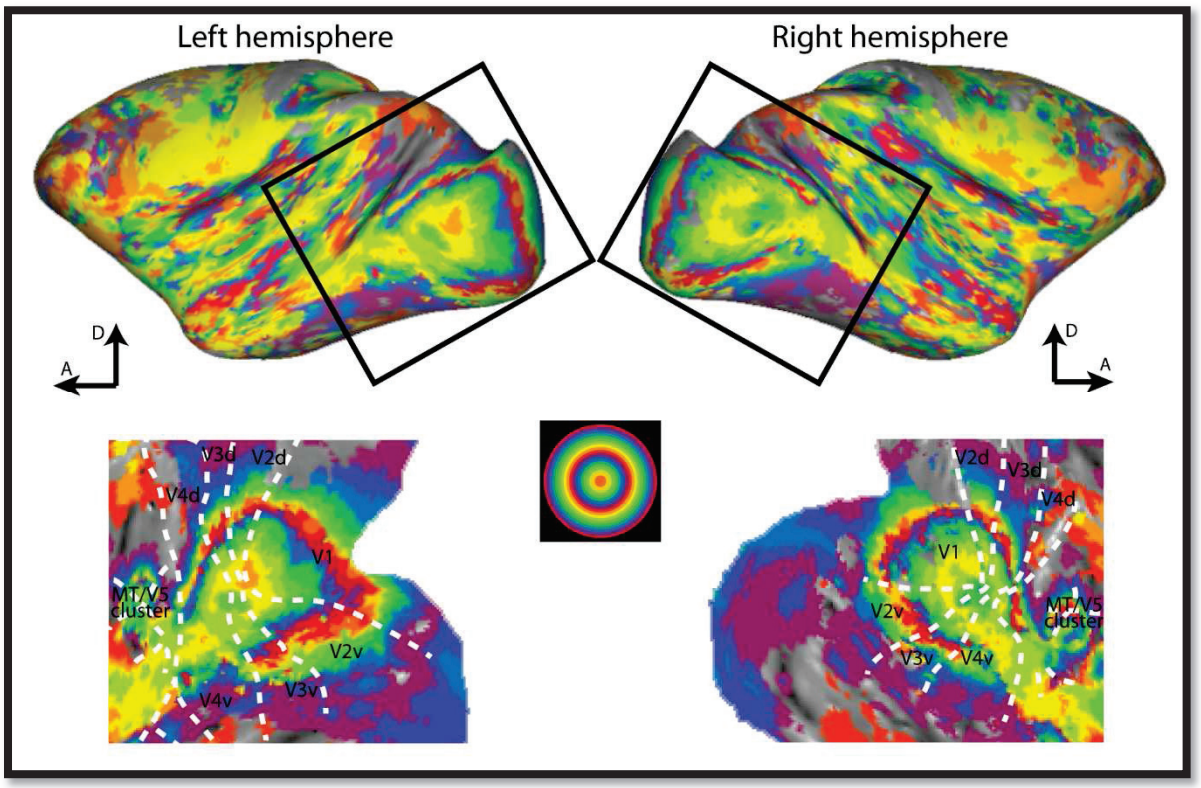

Figure 32: Retinotopic maps for eccentricity in the left and right hemispheres (by Annuli task) represented on inflated (top panel) and flattened maps (lower panel). The color code is indicated in the figure. Dashed white lines delineate the different visual areas, based on the F99 monkey template brain in Caret.

3. Resting-State analyses

Today, only monkey 1 performed functional imaging sessions with a contrast agent injection. We performed different resting-state analyses with the software CONN (http://www.nitrc.org/projects/conn/).

ROI to ROI analysis

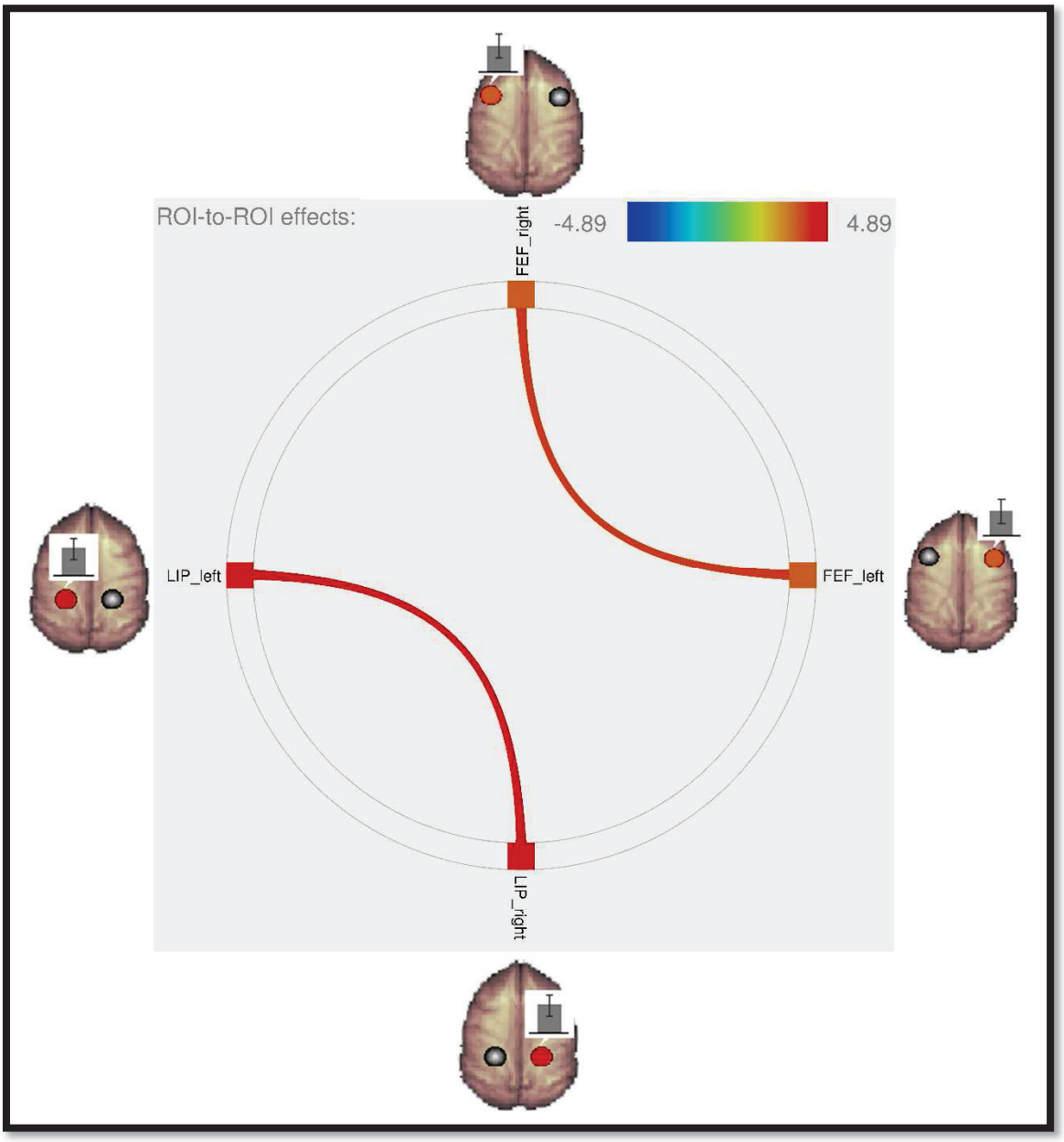

Figure 33: Strong correlations between left and right FEF, and between left and right LIP.

We built regions of interest (ROI) using MarsBar toolbox (Brett et al., 2002) based on anatomical images of the animal and monkey brain atlases made available on http://scalablebrainatlas.incf.org (essentially Paxinos et al., 2000; Calabrese et al., 2015). ROIs defined for FEF regions are built by a box with widths in XYZ (mm) of 2x3x2 centered at [-17.8; 5.6; 14] mm from the anterior commissure for left FEF and at [16.2; 6.6; 14] mm for right FEF. ROIs defined for LIP regions are built by a box with widths in XYZ (mm) of 2x5x2 centered at [-11.8; -17.4; 15] mm from the anterior commissure for left LIP and at [11.2; -17.4; 15] mm for right LIP. We also performed the probabilistic independent component analysis approach (ICA) to identify different resting-state networks bilaterally

ROI to ROI analysis in monkey 1 (**Figure 33**) show that the left and right FEFs are strongly positively correlated (FDR-corrected pvalue: 0.020, two-side inference) and the left and right LIPs are also strongly positively correlated (FDR-corrected pvalue: 0.0048, two-side inference).

Seed to Voxel analysis

Seed to voxel analysis searches which voxels of brain are correlated (positively or negatively) with the defined ROI (the same ROIs as above).

The left and right FEFs seed connectivity maps show that both FEFs are strongly functionally connected together (**Figure 34)**. We observed a lot of positive connectivities between FEF and visual areas (V1, V2, V4) in both hemispheres and for both seeds. FEF are also positively connected with secondary somatosensory area II (SII), primary somatosensory areas 3a and 2, with temporal areas (middle temporal area MT, medial superior temporal area MST, temporoparietal associated area TPO) and more importantly with parietal areas (ventral

and lateral intraparietal areas; VIP and LIP respectively). We also observed negative connectivities between FEF and premotor areas (F2, F4, F5), primary somatosensory areas (areas 1 and 3b), orbitofrontal area 45A, parietals areas 7 and 7op. The left and right FEFs seed connectivity maps are fairly symmetrical. However, the left FEF seems to have a stronger connectivity than the right FEF.

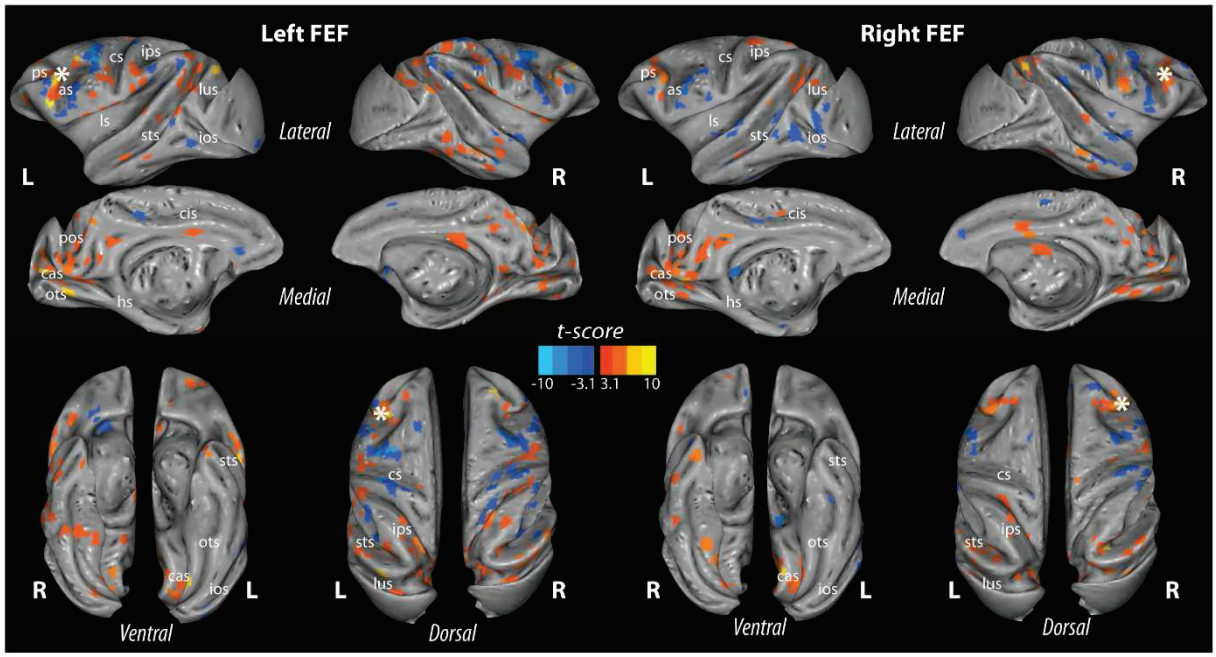

Figure 34: Left FEF (left) and right FEF (right) seed connectivity maps projected onto the inflated anatomy of monkey 1 (t-score > 3.1 set at cluster significance of P < 0.001, uncorrected). ***The connectivity maps are shown on lateral, medial, ventral, and dorsal views. Asterisks show the location of the seed region. pos, parieto-occipital sulcus; cas, calcarine sulcus; cs, central sulcus; hs, hippocampal sulcus; cis, cingulate sulcus; sts, superior temporal sulcus; ios, inferior occipital sulcus; lus, lunate sulcus; ots, occipitotemporal sulcus; ps, principal sulcus; L, left; R, right.***

The left and right LIPs seed connectivity maps show that both LIPs are strongly functionally connected together (**Figure 35**). We observed lot of positive connectivities between LIP and visual areas (V1, V2, V3a, V4) in both hemispheres and for both seeds. LIP are also positively connected with premotor area F4, primary somatosensory area 1, with other parietal regions (VIP and medial intraparietal area MIP), with temporal areas (MT, MST and TPO) and more importantly with both FEFs. The left and right LIPs seed connectivity maps are fairly symmetrical. We observe very few negative connectivities.

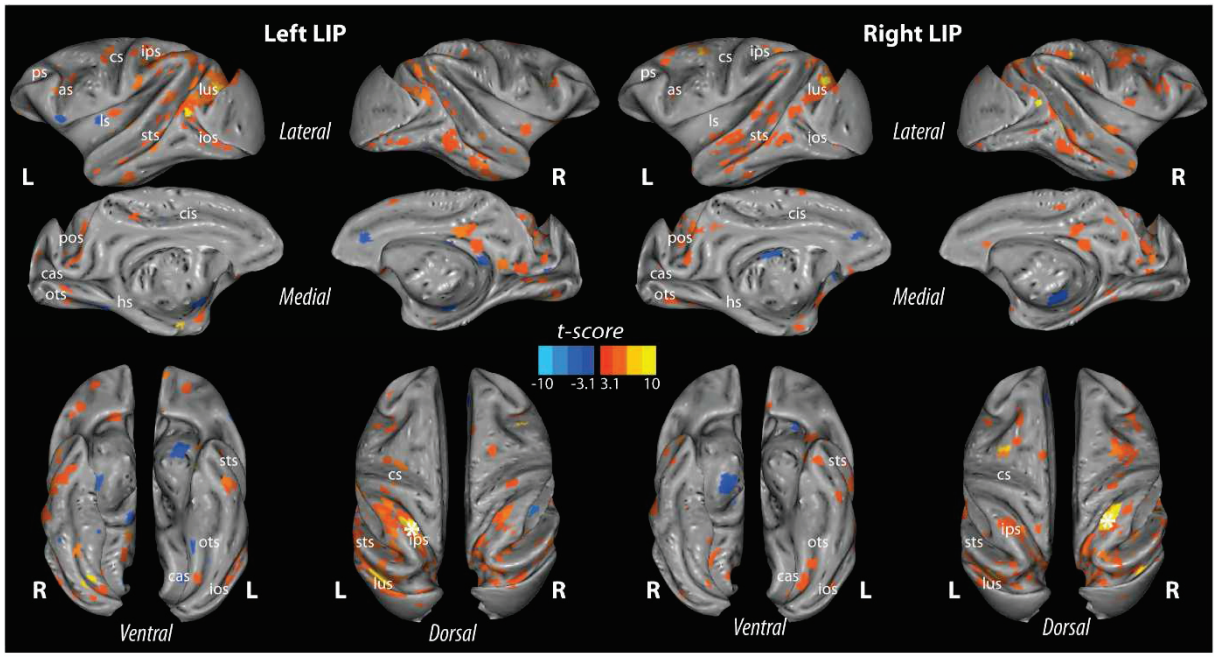

Figure 35: Left LIP (left) and right LIP (right) seed connectivity maps projected onto the inflated anatomy of monkey 1 (t-score > 3.1 set at cluster significance of P < 0.001, uncorrected). ***The connectivity maps are shown on lateral, medial, ventral, and dorsal views. Asterisks show the location of the seed region. pos, parieto-occipital sulcus; cas, calcarine sulcus; cs, central sulcus; hs, hippocampal sulcus; cis, cingulate sulcus; sts, superior temporal sulcus; ios, inferior occipital sulcus; lus, lunate sulcus; ots, occipitotemporal sulcus; ps, principal sulcus; L, left; R, right***

This analysis shows that FEF, LIP and visual areas (our target functional regions) are strongly connected, we expect to observe changes in this connectivity (e.g. reinforcement of the connectivity strength) after plasticity induction.

ICA analysis

Using the ICA approach, we identified in monkey 1 nine resting-state networks bilaterally (somatomotor, somatosensory, foveal visual, peripheral visual, central visual, superior temporal sulcus, executive, auditif and fronto-parietal networks) comparable to those previously described in both anesthetized and awake monkeys (Moeller et al., 2009; Hutchison et al., 2011).

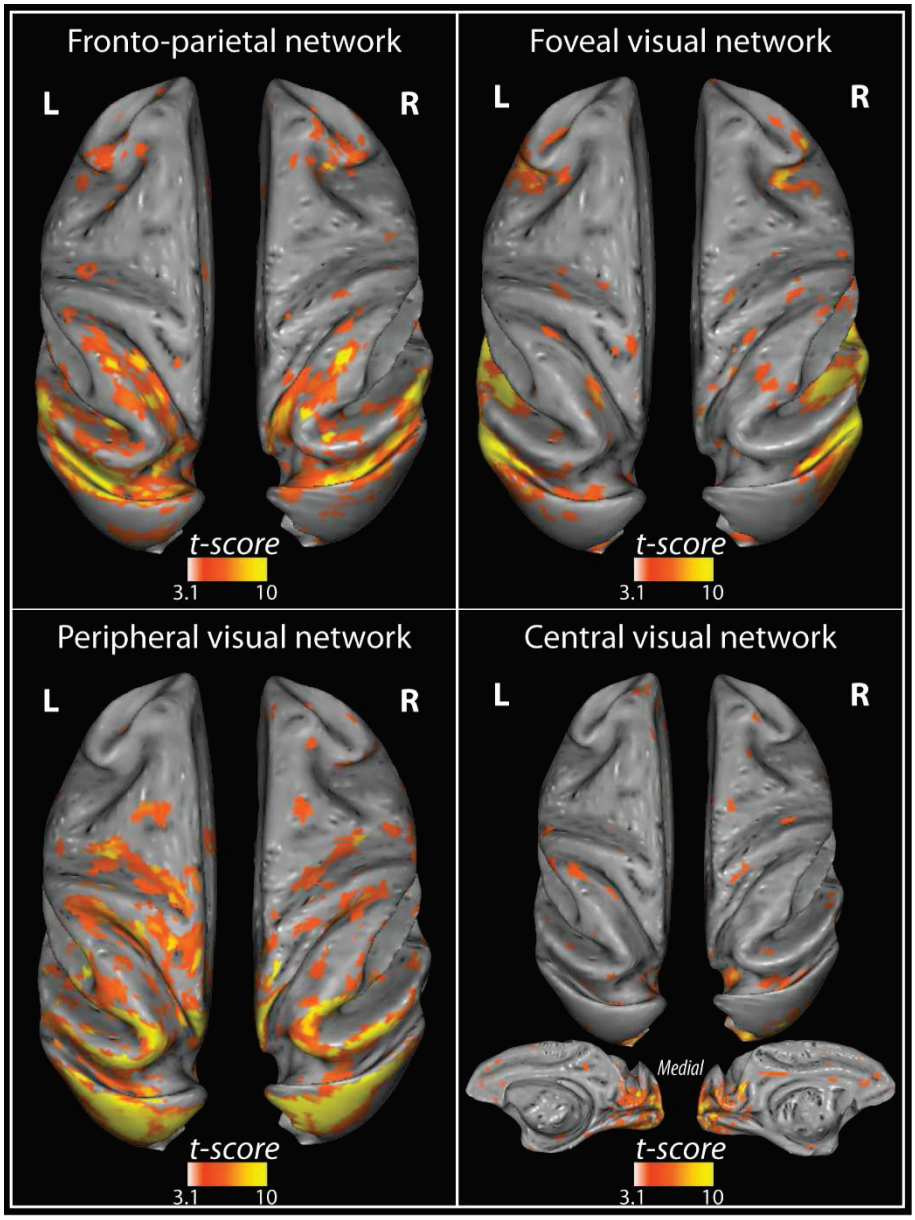

Figure 36: Illustration of the four most interesting cortical networks for our project, identified by the ICA in monkey 1 and projected onto the inflated anatomy of monkey 1, in dorsal view (t-score > 3.1 set at cluster significance of P < 0.001, uncorrected).

We are most interested in the four following networks: parieto-frontal, peripheral visual, central visual and foveal visual (**Figure 36**). Indeed, these four networks involve visuals areas, LIP or FEF and we expect to see changes between these networks before and after plasticity induction.

4. Diffusion tensor imaging data

Colored fractional anisotropy maps

By means of DTI imaging, we obtained the fractional anisotropy maps (FA) for both monkeys (**Figure 37**). It is an index for the amount of diffusion asymmetry within a voxel. The colors assigned to voxels are based on a combination of anisotropy and direction. The orientation of the principal eigenvector controls hue and anisotropy controls brightness (for more details, see review Minati and Weglarz, 2007), as in:

$$\text{Red}=|e_{1,x}| \cdot FA$$
$$\text{Green}=|e_{1,y}| \cdot FA$$
$$\text{Blue}=|e_{1,z}| \cdot FA$$

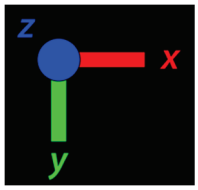

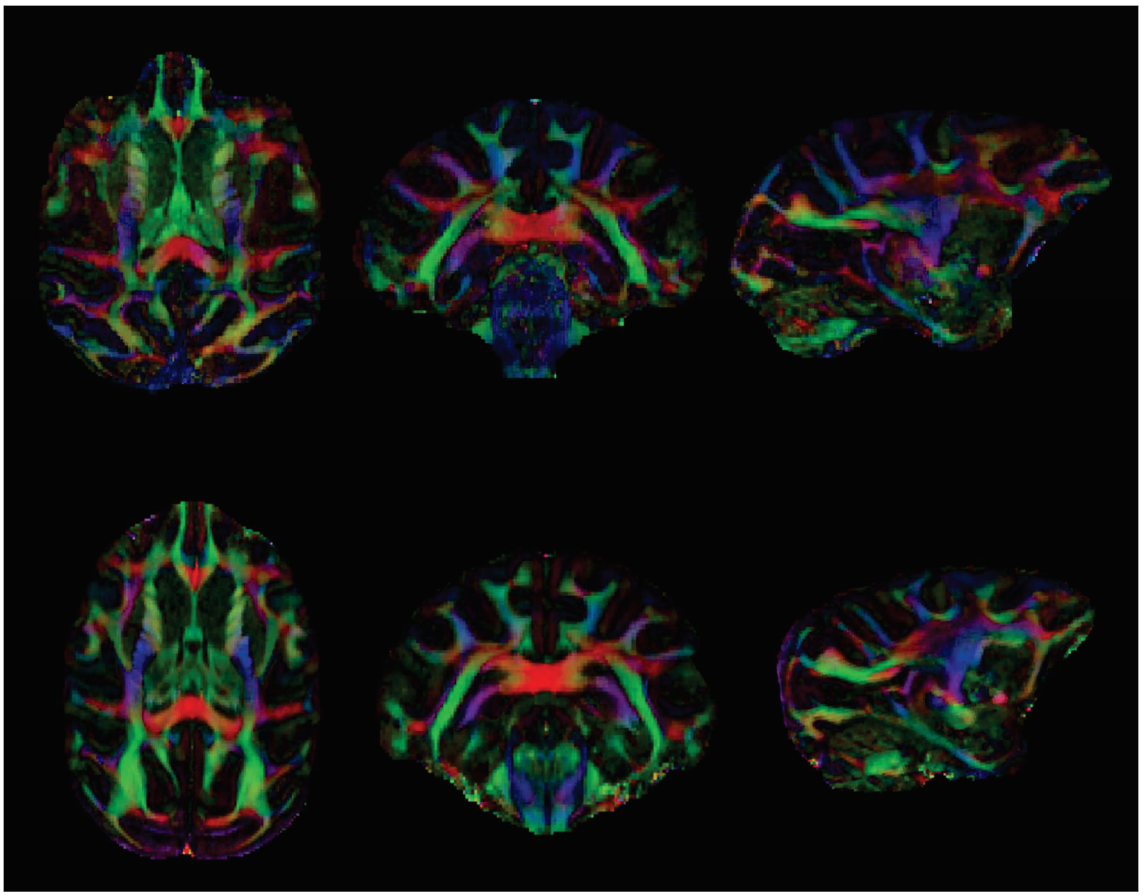

Figure 37: Colored fractional anisotropy map for monkey 1 (top) and monkey 2 (bottom).

The denser an axonal bundle is, the more membranes and myelin hinder and restrict diffusion transversally, rendering diffusion more anisotropic: as a consequence, diffusion anisotropy is considered as a rough index of axonal density. Insofar as denser bundles are assumed to imply stronger anatomical connectivity, anisotropy may be considered as an indicator of connection strength (Basser, 1995; Minati et al., 2008; Basser and Pierpaoli, 2011).

Tractography maps

By means of DTI imaging, we also obtained tractography maps for both monkeys (**Figure 38**) which correspond to the fiber trajectories in and out of the region selected (whole brain, part of brain, voxels…).

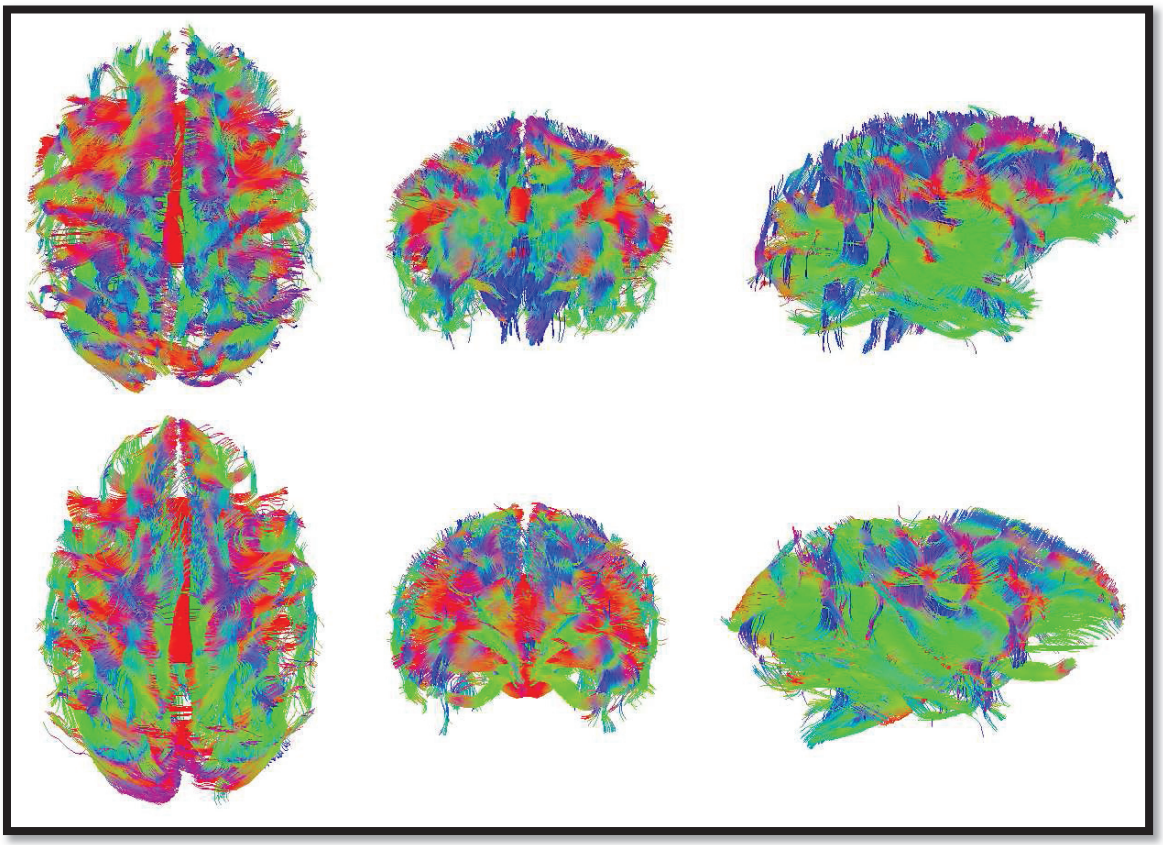

Figure 38: Tractography maps for monkey 1 (top) and monkey 2 (bottom).

We can see that in both monkeys we have fibers in all directions (x, y and z). For example, a complex structure in the brain is the corpus callosum. In this structure, part of the fibers are essentially in red color and so in X axis (left to right or right to left direction) allowing for the connections between the two hemispheres. A large part of this corpus is in green color, so in Y axis (posterior to anterior or from anterior to posterior direction) allowing for the connections from the frontal to the occipital lobe and conversely. And finally some fibers are in blue color, so in Z axis allowing for the connections between top and bottom regions. We expect plasticity changes to reflect onto FA index measures, but it is however unclear whether changes will also be quantifiable onto the tractography reconstructions. This remains to be explored.

5. Myelin index

In anesthetized monkeys, we performed acquisitions of T1w and T2w images. Following the Glasser and Van Essen method (2011), we calculated the ratio T1w/T2w and we projected the results onto the inflated surface of each monkey by means of Caret (**Figure 39**). This ratio eliminates the bias of intensity of the image related to the magnetic resonance and improves the contrast of the noise for the myelin. The myelin maps were displayed at quarter and 96th percentiles for the hemisphere as a whole, with saturation above (red) and below (black) these values.

For each monkey, the visual cortex (including V1) and motor areas are highly myelinated, parietal (including LIP), temporal and central gyri are also strongly myelinated whereas the medial part of the brain appears to be low myelinated. The fundus of sulci is less myelinated. For both animals, the right hemisphere seems to be more myelinated than the left hemisphere.

However, we do not have the same pattern of myelination for both animals. We observe stronger and more spread out myelination for M2 compared to M1. For example, FEF areas are clearly heavily myelinated in M2 whereas only a small portion of FEF is myelinated in M1. Whether this inter-individual change will correlate with differences in plasticity onset and amplitude will be of outmost interest.

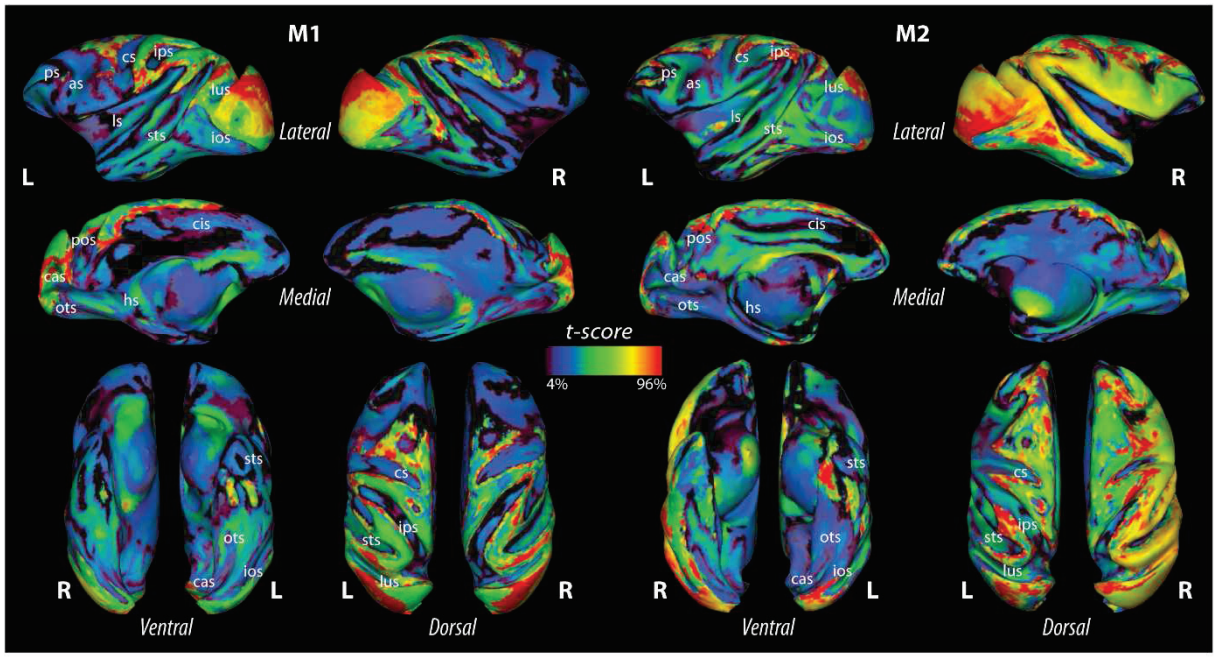

Figure 39: Myelin maps projected onto the inflated surface of monkey 1 (M1) and monkey 2 (M2). ***The myelin maps are shown on lateral, medial, ventral, and dorsal views. pos, parieto-occipital sulcus; cas, calcarine sulcus; cs, central sulcus; hs, hippocampal sulcus; cis, cingulate sulcus; sts, superior temporal sulcus; ios, inferior occipital sulcus; lus, lunate sulcus; ots, occipitotemporal sulcus; ps, principal sulcus; L, left; R, right. The scale is T1w/T2w = 4% (black) to 96 % (red).***

6. GABA spectroscopy

These are the first results obtained with the MEGA-PRESS sequence. MRS GABA spectroscopy was performed within a region of interest defined on the left visual cortex and centered at [-13.3; 62.9; -19.3] position. The size of this region was 15x8x10mm (**Figure 40**). The MRS acquisition lasted 50 minutes and used the four coils. The images were analyzed and preprocessed by means of FID-A (Simpson et al., 2017) and GANETT softwares (Edden et al., 2014).

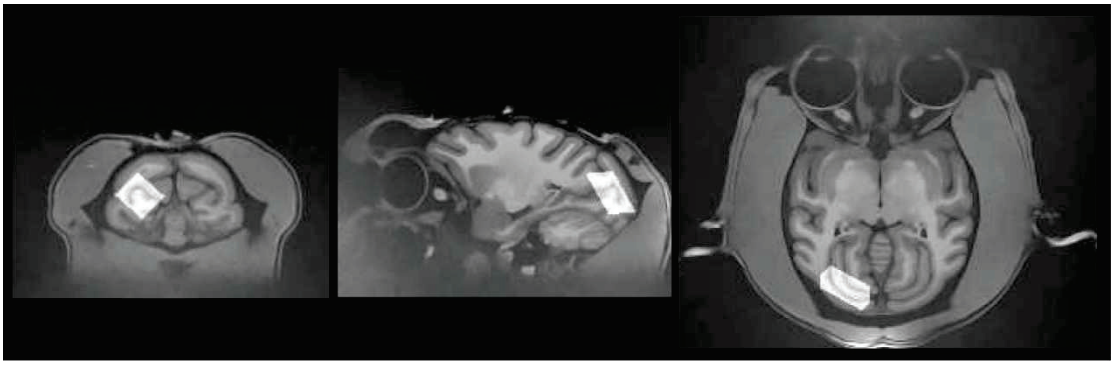

Figure 40: Coronal, sagittal and transversal views of the defined region of interest in left visual cortex, in monkey 2.

Spectra of different coils were phase-aligned that is to say they were aligned with respect to the orientation of the coils relative to the ROI defined and then, coils were combined (**Figure 41**).

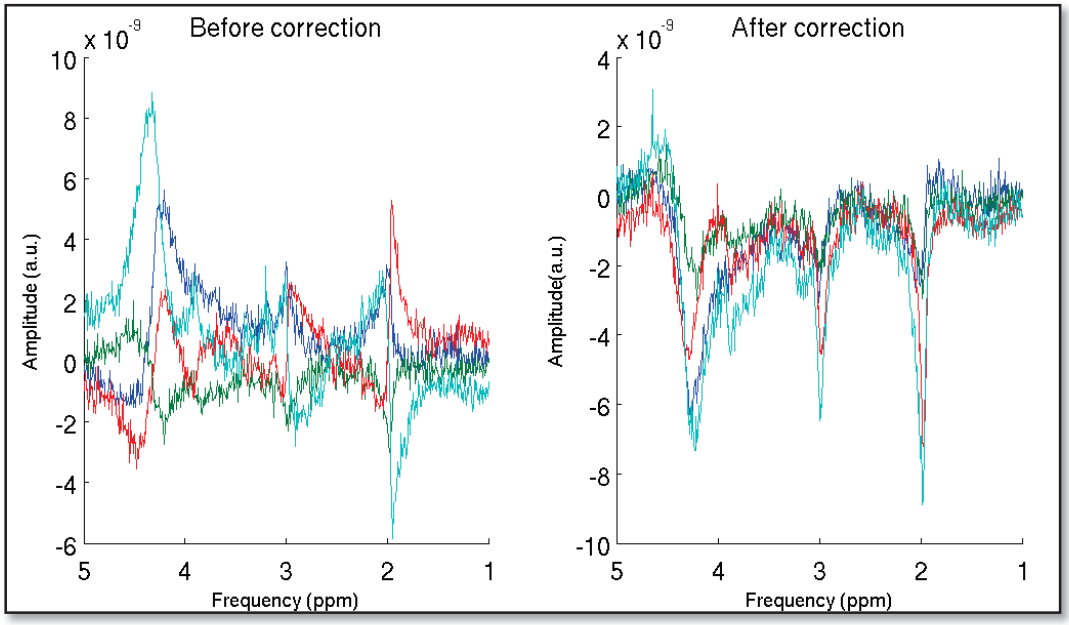

Figure 41: Results of multi-coils combination.

Then, we removed motion-corrupted averages: averages were calculated for all spectra and if points were three times different from the standard deviation, they were removed with their pairs (ON-OFF pairs). As our animal is anesthetized, few points are removed (**Figure 42**). **Figure 43** shows the results of removal of bad averages shown in Figure 42 but focuses on between 3.12 and 2.72ppm of spectra (around the creatine peak) according to each repetition

over time, which means over each ON-OFF repetitions. We see more colored maps around 3ppm which corresponds to the creatine peak and suggests the presence of GABA peak.

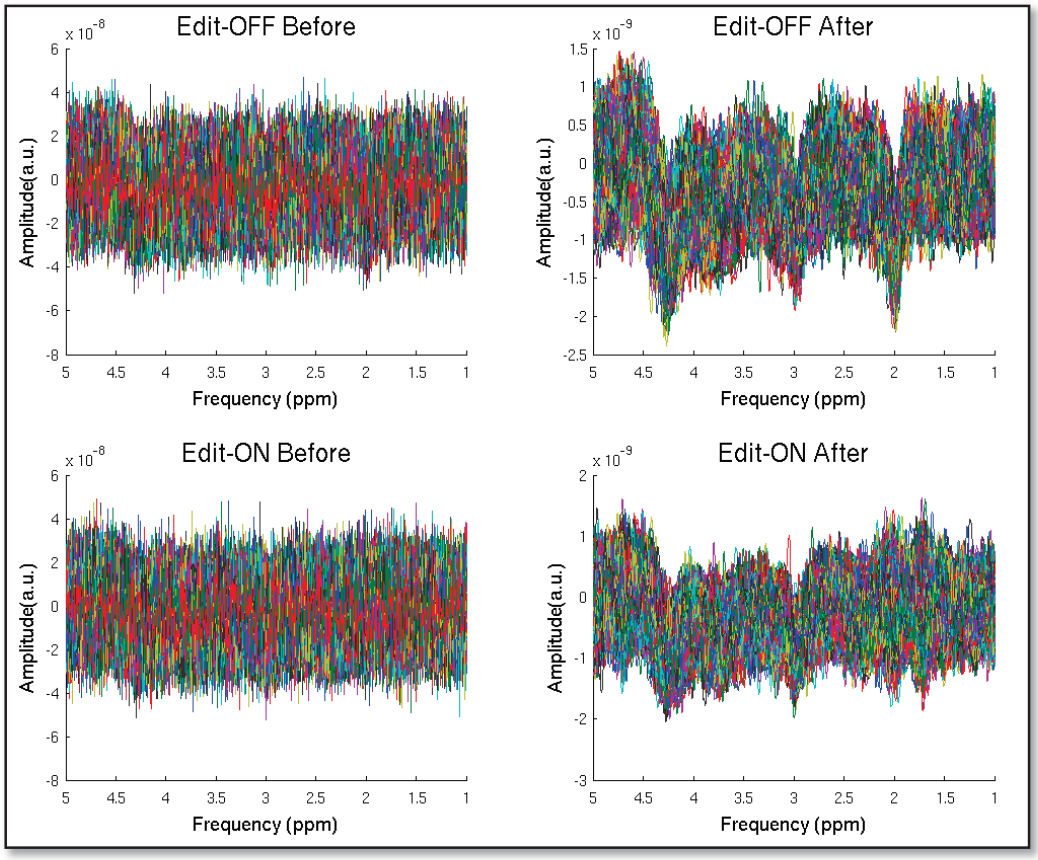

Figure 42 : Results of removal of bad averages

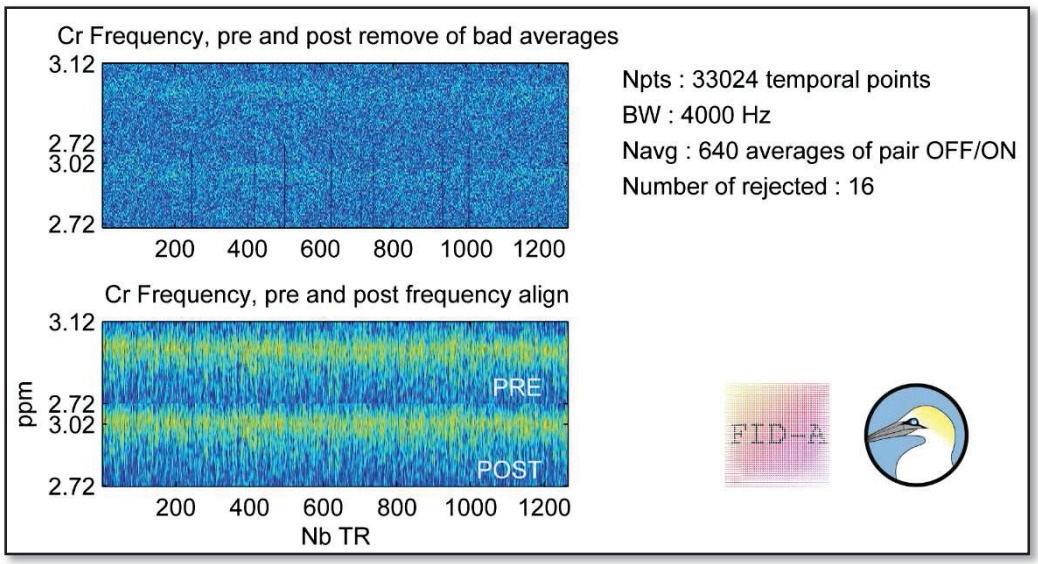

Figure 43: Results of removal of bad averages focusing on creatine peak (between 3.12 and 2.72 ppm, top panel) and results of frequency alignment of spectra on the creatine peaks (bottom panel).

Spectra were filtered at 3 Hz. During the next steps, spectra were frequency aligned with respect to peak position of creatine (at 3.02 ppm, **Figure 43**) on the spectrum and a zero-order phase correction was applied to maximize this peak of creatine and optimized the differential between ON and OFF spectra.

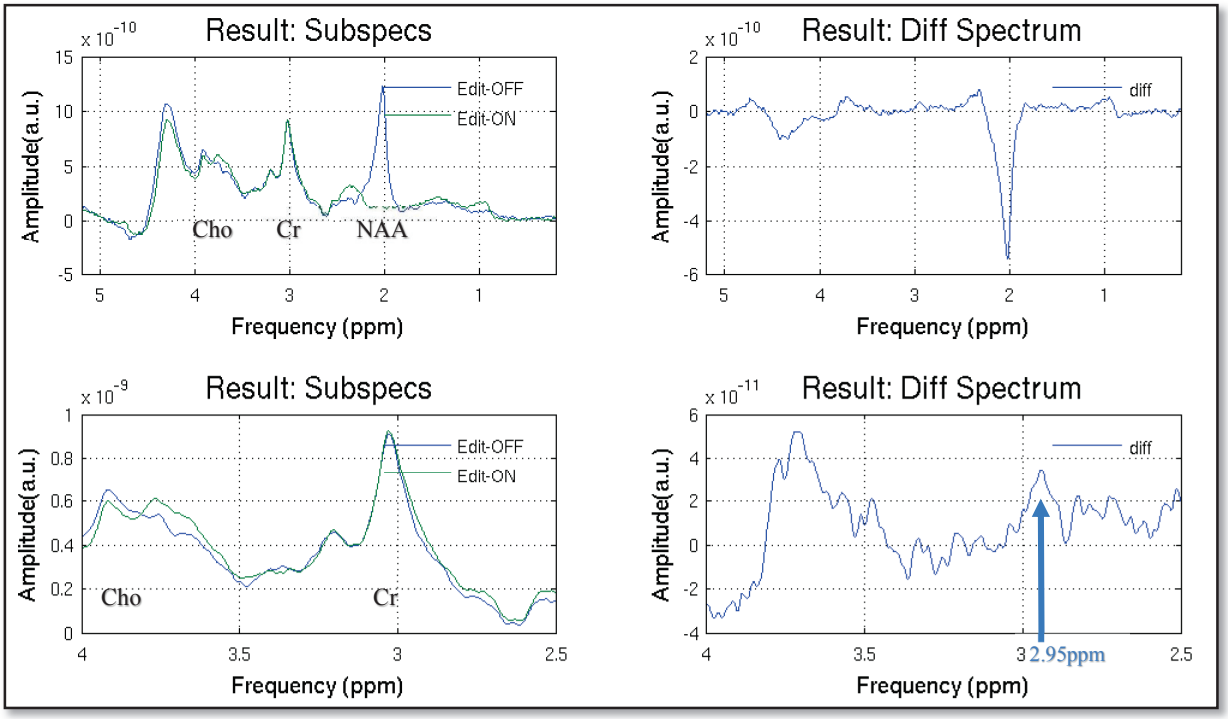

Figure 44: Results of the subspectra subtraction of ON-OFF spectrum (top panel) and focus of this differential spectrum display between 2.5 and 4 ppm (bottom panel). ***Na-acetyl aspartate (NAA), Creatine (Cr) and Choline (Cho).***

Figure 44 shows that, although there is a lot of noise in spectra, the different peaks of Na-acetyl aspartate (NAA), Creatine (Cr) and Choline (Cho) at 2.02, 3.02 and 3.75 ppm, respectively. We have a large peak around 2.95 ppm which could correspond to the GABA peak.

By means of Gannett, the GABA spectrum was fitted by a Gaussian model to quantify the relative GABA concentration (relative to water quantity) by calculating the integral area under the GABA peak (**Figure 45**). We found 15.552 i.u. (institutional units).

It is unclear whether this identified GABA peak has a high enough signal-to-noise ratio (SNR) to detect the subtle expected GABA changes following plasticity onset. Our second acquisition phase will allow us to address this point experimentally.

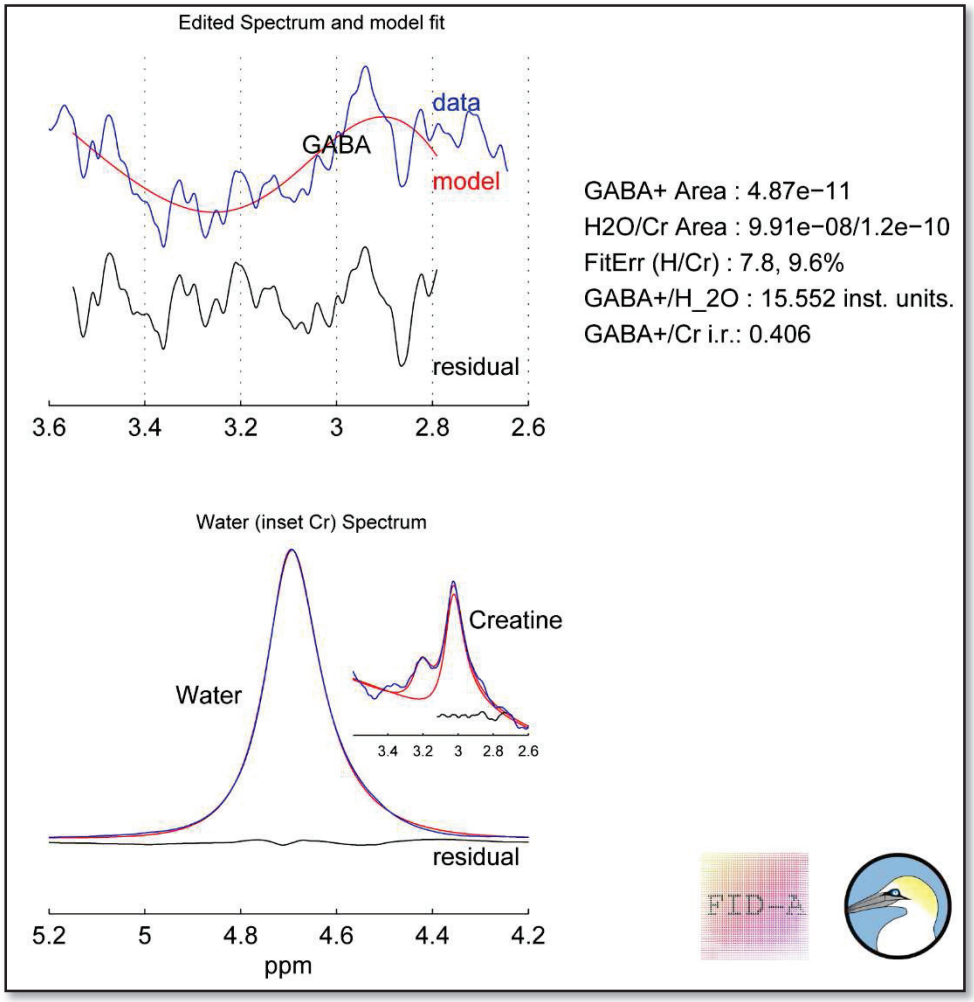

Figure 45: Gannett outputs with Gaussian fit onto GABA spectrum and estimation of GABA concentration (top panel) and water spectrum (bottom model).

In conclusion, all tools are ready and all analyses characterizing T0 pre-plasticity anatomical functional and connectivity data have been performed for Monkey M1 and are ongoing for Monkey M2, thus setting the reference lines for pursuing the project. I will continue supervising this project in the coming months and transferring my expertise to the students who will take it over.

References

Alvarez I, De Haas BA, Clark CA, Rees G, Schwarzkopf DS (2015) Comparing different stimulus configurations for population receptive field mapping in human fMRI. Front Hum Neurosci 9:96.

Basser PJ (1995) Inferring microstructural features and the physiological state of tissues from diffusion-weighted images. NMR Biomed 8:333–344.

Basser PJ, Pierpaoli C (2011) Microstructural and physiological features of tissues elucidated by quantitative-diffusion-tensor MRI. 1996. J Magn Reson 213:560–570.

Brett M, Anton J-L, Valabregue R, Poline J-B (2002) Region of interest analysis using the MarsBar toolbox for SPM 99. Presented at the 8th International Conference on Functional Mapping of the Human Brain (June 2–6, 2002, Sendai, Japan), 16:S497.

Calabrese E, Badea A, Coe CL, Lubach GR, Shi Y, Styner MA, Johnson GA (2015) A diffusion tensor MRI atlas of the postmortem rhesus macaque brain. Neuroimage 117:408–416.

Edden RAE, Puts NAJ, Harris AD, Barker PB, Evans CJ (2014) Gannet: A Batch-Processing Tool for the Quantitative Analysis of Gamma-Aminobutyric Acid–Edited MR Spectroscopy Spectra. Journal of magnetic resonance imaging : JMRI 40:1445.

Glasser MF, Essen DCV (2011) Mapping Human Cortical Areas In Vivo Based on Myelin Content as Revealed by T1- and T2-Weighted MRI. J Neurosci 31:11597–11616.

Hutchison RM, Leung LS, Mirsattari SM, Gati JS, Menon RS, Everling S (2011) Resting-state networks in the macaque at 7 T. NeuroImage 56:1546–1555.

Minati L, Banasik T, Brzezinski J, Mandelli ML, Bizzi A, Bruzzone MG, Konopka M, Jasinski A (2008) Elevating tensor rank increases anisotropy in brain areas associated with intra-voxel orientational heterogeneity (IVOH): a generalised DTI (GDTI) study. NMR Biomed 21:2–14.

Minati L, Weglarz WP (2007) Physical foundations, models, and methods of diffusion magnetic resonance imaging of the brain: A review. Concepts in Magnetic Resonance Part A: Bridging Education and Research 30:278–307.

Moeller S, Nallasamy N, Tsao DY, Freiwald WA (2009) Functional connectivity of the macaque brain across stimulus and arousal states. J Neurosci 29:5897–5909.

Paxinos G, Huang X-F, Toga A (2000) The Rhesus Monkey Brain in Stereotaxic Coordinates. Faculty of Health and Behavioural Sciences - Papers (Archive) Available at: http://ro.uow.edu.au/hbspapers/3613.

Sereno MI, Dale AM, Reppas JB, Kwong KK, Belliveau JW, Brady TJ, Rosen BR, Tootell RB (1995) Borders of multiple visual areas in humans revealed by functional magnetic resonance imaging. Science 268:889–893.

Simpson R, Devenyi GA, Jezzard P, Hennessy TJ, Near J (2017) Advanced processing and simulation of MRS data using the FID appliance (FID-A)—An open source, MATLAB-based toolkit. Magn Reson Med 77:23–33.

Axis II Discussion

The different results presented in Chapter 7 remain preliminary and further in-depth analyses will be necessary. However, these first results are promising for our project to measure and observe neural changes after plasticity induction. We will discuss these different first results below.

Behavioral data

Behavioral data extracted in runs of detection tasks show that most importantly, at T0, so before plasticity induction, we have no bias in any of the two monkeys for any visual quadrant in term of responses proportion (correct, miss, false alarm…). We expect that after performing the task for plasticity induction using bottom-up influences (cf Methodology, 3.a), monkeys will be better in the visual over-stimulated quadrant because their attention will be biased toward this quadrant. This could induce more incorrect responses: more miss trials or incorrect responses for the other three quadrants but also more false alarms for the over-stimulated quadrant.

Reaction times analyses show that in both monkeys we have differences of RTs between the different visual quadrants. The fact that RTs are different between the four quadrants is not problematic because we will compare RTs within the same visual quadrant following each plasticity cycle (to see if RTs are shorter or longer after plasticity induction). We expect to have shorter RTs in the over-stimulated quadrant between before and after plasticity induction thanks to an enhancement of visual processing in this quadrant.

More interestingly, at T0, we observe that bottom visual quadrants have shorter RTs than top quadrants suggesting a vertical asymmetry in the visual function. This has been previously described in numerous studies using a variety of paradigms and methodologies (Danckert and

Goodale, 2001; Maehara et al., 2004; Chen et al., 2005; Khan and Lawrence, 2005; Liu et al., 2006; Qu et al., 2006; Carlsen et al., 2007) and showing a greater functionality of the inferior visual field (Sample et al., 1997; Levine and McAnany, 2005). Some studies that have directly examined latency differences between superior and inferior visual fields, suggest that the inferior visual field has a shorter latency in terms of motor reaction times, for example for discriminating a range of stimuli, including those that differ in contrast, hue, and motion (Payne, 1967; Maehara et al., 2004; Levine and McAnany, 2005; Qu et al., 2006; Fortenbaugh et al., 2015).

Whatever the distinctions that contribute to these field differences, they may be seen to make some ecological sense (Previc, 1990). The lower visual field is where the hands (or paws) work at fine tasks like separating seeds and peels from fruit, or capturing small prey (Previc, 1990; Levine and McAnany, 2005).

Retinotopic mapping

In our retinotopic mapping analyses, we found a functional topography of the visual cortex close to those found by recent retinotopic mapping studies (Kolster et al., 2009, 2014; Arcaro et al., 2011; Janssens et al., 2014). Indeed, the polar-angle maps reveal the retinotopic organization of V1-V4 in agreement with earlier-cell (Daniel and Whitteridge, 1961; Essen and Zeki, 1978; Gattass and Gross, 1981; Gattass et al., 1981, 1988, 1997, 2005; Van Essen et al., 1984; Felleman and Van Essen, 1991) and fMRI studies (Vanduffel et al., 2001; Brewer et al., 2002; Fize et al., 2003; Kolster et al., 2009, 2014). It means that V1/V2 and V3/V4 boundaries correspond to a vertical meridian and the V2/V3 and rostral V4 boundaries correspond to a horizontal meridian (Kolster et al., 2009). Besides, the upper quadrant is represented ventrally and the lower quadrant dorsally in areas V1, V2, V3 and V4. The eccentricity maps confirm that the central representations of V1-V4 refer to the central visual field.

Further analyses may be carried out in our retinotopic mapping data such as population receptive field (pRFs) estimates. This new method computes a model of the population receptive field from responses to a wide range of stimuli and estimates the visual field map as well as other neuronal population properties, such as receptive field size and laterality. The visual field maps obtained with the pRF method are more accurate than those obtained using conventional visual field mapping, and allow to draw with high precision the visual field maps to the center of the foveal representation. This method is being increasingly used to studies cortical topographies and their changes with age, diseases or plasticity, both in humans and in the non-human primate (Dumoulin and Wandell, 2008; Kolster et al., 2009, 2010, 2014; Harvey and Dumoulin, 2011; Brewer and Barton, 2014; Schwarzkopf et al., 2014; Alvarez et al., 2015; Thomas et al., 2015; van Dijk et al., 2016; Anderson et al., 2017).

Resting-State analyses

Our resting-state results are coherent with what we can find in literature, in particular in recent papers on functional connectivity patterns of frontal eye fields (Hutchison et al., 2012, 2015; Babapoor-Farrokhran et al., 2013). However, we found some differences. Indeed, we performed resting-state analyses for intra-subject and in an awake monkey. Some studies showed that anesthetics agents can modulate resting-state networks. Recently Hutchison et al. (2014) showed that assessing dynamic functional connectivity patterns revealed that the functional repertoire of brain states is related to anesthesia depth and most strikingly, that the number of state transitions linearly decreases with increased isoflurane dosage. Taken together, the results indicate dose-specific spatial and temporal alterations of functional connectivity that occur beyond the typically defined endpoint of consciousness.

We have tested three different approaches to analyze resting-state data. For the rest of the project, we will use only seed-to-voxel and ICA approaches. Indeed, the ROI-to-ROI analysis is too stringent because this tests connectivity only between the voxels of ROI defined. Consequently, the exact location of the ROI and its size play an important role for the connectivity tested. Seed-to-voxel analysis allows to know how the ROIs defined are connected with the whole brain and thus allows to more easily see changes in this connectivity patterns. For example, we have seen that FEF areas are connected with LIP areas but not for the entire LIP areas. The question that we can ask here is, can we observe stronger connectivity between these areas and/or more extended and/or new points connected to these areas, after plasticity induction?

The ICA approach gives us a more global view of brain connectivity showing the different independent networks identified. With this approach we will compare the different plasticity induction cycles and see how these networks can evolve with plasticity (network more extended? Stronger? Reinforced?)?

Diffusion tensor imaging data

Recently, a team has performed DTI of the postmortem rhesus macaque brain on a 7Tesla with a very high-resolution (150x150x150µm) and the best quality. However, the total acquisition time was approximately of 46 hours per specimen (Calabrese et al., 2015). Here, we succeeded in performing DTI with high-resolution (500x500x100µm) but in awake monkeys and this with very much shorter acquisition time. Our acquisition lasted 130 minutes (Tounekti et al., 2017). To our knowledge we are the first team to achieve this feat. This is very promising for the study of DTI *in vivo*, with high-resolution.

With DTI data, we will want to perform seed connectivity. It means we will define a ROI (in FEF, LIP and V1) and search how fibers enter and exit these areas and more interestingly if they are directly connected through these fibers (no intermediaries). This approach will allow us to see how plasticity induction interferes in this structural connectivity (Saur et al., 2008; Gold et al., 2010; Purcell et al., 2011; Bennett and Rypma, 2013). This work is still in progress.

Myelin index

To create myelin maps of our two monkeys, we calculated the ratio of T1w/T1W. We then projected these results on Caret. These results are preliminary data. Indeed, we want to perform the entire method of Glasser and Van Essen (2011). They used the software FreeSurfer (http://surfer.nmr.mgh.harvard.edu/) which is more frequently used for humans (Caret is more frequently used for monkeys). FreeSurfer segmentation generates different files including ribbon.mgz file which corresponds to the cortical (gray matter) ribbon of the brain. Its means voxels with voxels centers located between the white and pial surfaces. This allows to see myelination more precisely not only in surface view (fiducial, inflated…) but also in sagittal, cortical and transversal views and to see areal boundaries for some cortical areas (Glasser and Essen, 2011; Glasser et al., 2014). Performing FreeSurfer segmentation in monkeys is a more involving and complicated process than for human cortical reconstruction. We are currently working on this step of development.

Glasser et al. (2014) have reviewed some *in vivo* mapping studies both in humans and in non-human primates. They reported that primary sensory or motor areas are heavily myelinated whereas associations areas are less myelinated (Sereno et al., 1995; Glasser and Essen, 2011; Power et al., 2011; Yeo et al., 2011). They suggested, on the one hand, that these heavily myelinated regions may need to be more static and hardwired to perform their lower-order

sensory and motor functions. On the other hand, lightly myelinated areas, which have largely higher-order cognitive functions, may have greater synaptic plasticity and thus require more adaptable, dynamic, and plastic circuitry than heavily myelinated ones.

Interestingly, by comparing the myelin maps of humans, chimpanzee and macaques, they reported that humans have more lightly than heavily myelinated regions, whereas they reported the reverse trend in the non-human primate. This suggests that the human brain is more plastic and dynamic which may allow for higher cognitive abilities such as language. Further studies on this topic will be necessary to test this hypothesis.

The first step of plasticity induction uses bottom-up influences; we expect to see changes in myelination patterns between visual, frontal and parietal areas. If the above hypothesis is correct, we can predict two possibilities: our V1-LIP-FEF network will have a reduction of myelination to allow dynamic and plastic changes with the addition of new connections or suppression of others; or our V1-LIP-FEF network will have a stronger heavy myelination to reinforce the olds connections and consolidate this strength network.

The fact that humans have a brain potentially more plastic than non-human primates is promising. Indeed, if we succeed in reinducing plasticity with our tasks and see changes in the macaque brain, we can expect to see the same changes or stronger changes in humans and thus treat some pathologies such as amblyopia in the adult brain.

Spectroscopy GABA

Magnetic resonance spectroscopy (MRS) is the only non-invasive way to measure the local concentrations of GABA in the brain, *in vivo*. GABA detection is particularly challenging and requires special MRS techniques. Performing MRS on monkeys is very challenging due to the smaller size of their brain compared to the human brain. In spite of this difficulty, we tried to perform this on anesthetized monkeys with a really small ROI size (15x8x10 mm).

Unfortunately, we had too much noise in our signal (after spectrum subtraction) due to a signal-to-noise ratio too weak. Therefore, we were not able to clearly identify the GABA spectrum and confirm that the GABA concentration level estimation within V1 visual area was correct. Despite the noise, it seemed possible to identify a GABA peak which was not centered at 3 ppm but shifted toward 2.95 ppm.

Because we performed spectroscopy on an anesthetized animal, we skipped the step of the alignment of frequency averages. We also skipped the step of removing points before and after echo as we assumed that the magnetic field of B0 is stable. Because we have a lot of noise in our spectra (as shown in Figure 42), the peak of creatine is difficult to discriminate and this could result in a wrong frequency shift for phase-correction for centering spectra onto the creatine peak and lead to a GABA peak more in 2.95 ppm than in 3.02 ppm. However, in a study performed in adults with a region of interest defined in visual cortex (Yoon et al., 2010), this GABA peak shift is also observed. Further analyses and setup optimization to reduce the noise in our signal are necessary. We are currently searching for different solutions to solve this problem. One of them is to try to perform a longer acquisition. Another solution is to test with our eight-channel phased-array coil.

A very interesting way to perform GABA spectroscopy is to use MRS imaging. This approach uses a 3D MEGA-editing MRS imaging sequence (Bogner et al., 2014). This sequence is characterized by real-time motion correction, dynamic shim updates and selective reacquisition of adiabatic spiral to eliminate subtraction artifacts due to scanner instabilities and subject motion. The localization is made by Adiabatic Selective Refocusing (LASER) to improve the localization accuracy and signal-to-noise ratio. This aspect is very important for us to improve our signal-to-noise ratio in our really small ROI compare to the MEGA-PRESS sequence. Besides, this sequence is insensitive to the effects of B1, which means insensitive to

the excitation quality and refocalisation. Lastly, this sequence has a K-space encoding via a weighted stack of spirals which provides 3D metabolic mapping with flexible scan times.

Along with the improvement of our current GABA spectroscopy method with the MEGA-PRESS sequence and the search for an appropriate and optimal environment (time, coils, position, ROI size…), we are trying to obtain the MEGA-LASER sequence and adapt it to our 3T Siemens Prisma scanner.

References

Alvarez I, De Haas BA, Clark CA, Rees G, Schwarzkopf DS (2015) Comparing different stimulus configurations for population receptive field mapping in human fMRI. Front Hum Neurosci 9:96.

Anderson EJ, Tibber MS, Schwarzkopf DS, Shergill SS, Fernandez-Egea E, Rees G, Dakin SC (2017) Visual Population Receptive Fields in People with Schizophrenia Have Reduced Inhibitory Surrounds. J Neurosci 37:1546–1556.

Arcaro MJ, Pinsk MA, Li X, Kastner S (2011) Visuotopic Organization of Macaque Posterior Parietal Cortex: A Functional Magnetic Resonance Imaging Study. J Neurosci 31:2064–2078.

Babapoor-Farrokhran S, Hutchison RM, Gati JS, Menon RS, Everling S (2013) Functional connectivity patterns of medial and lateral macaque frontal eye fields reveal distinct visuomotor networks. J Neurophysiol 109:2560–2570.

Bennett IJ, Rypma B (2013) Advances in Functional Neuroanatomy: A Review of Combined DTI and fMRI Studies in Healthy Younger and Older Adults. Neurosci Biobehav Rev 37:1201–1210.

Bogner W, Gagoski B, Hess AT, Bhat H, Tisdall MD, van der Kouwe AJW, Strasser B, Marjańska M, Trattnig S, Grant E, Rosen B, Andronesi OC (2014) 3D GABA imaging with real-time motion correction, shim update and reacquisition of adiabatic spiral MRSI. NeuroImage 103:290–302.

Brewer AA, Barton B (2014) Visual cortex in aging and Alzheimer's disease: changes in visual field maps and population receptive fields. Front Psychol 5:74.

Brewer AA, Press WA, Logothetis NK, Wandell BA (2002) Visual Areas in Macaque Cortex Measured Using Functional Magnetic Resonance Imaging. J Neurosci 22:10416–10426.

Calabrese E, Badea A, Coe CL, Lubach GR, Shi Y, Styner MA, Johnson GA (2015) A diffusion tensor MRI atlas of the postmortem rhesus macaque brain. Neuroimage 117:408–416.

Carlsen AN, Maslovat D, Chua R, Franks IM (2007) Perceptual processing time differences owing to visual field asymmetries. Neuroreport 18:1067–1070.

Chen Y, Wyatt HJ, Swanson WH (2005) Pupillary evaluation of retinal asymmetry: development and initial testing of a technique. Vision Res 45:2549–2563.

Danckert J, Goodale MA (2001) Superior performance for visually guided pointing in the lower visual field. Exp Brain Res 137:303–308.

Daniel PM, Whitteridge D (1961) The representation of the visual field on the cerebral cortex in monkeys. J Physiol (Lond) 159:203–221.

Dumoulin SO, Wandell BA (2008) Population receptive field estimates in human visual cortex. NeuroImage 39:647–660.

Essen DC, Zeki SM (1978) The topographic organization of rhesus monkey prestriate cortex. J Physiol (Lond) 277:193–226.

Felleman DJ, Van Essen DC (1991) Distributed hierarchical processing in the primate cerebral cortex. Cereb Cortex 1:1–47.

Fize D, Vanduffel W, Nelissen K, Denys K, d'Hotel CC, Faugeras O, Orban GA (2003) The Retinotopic Organization of Primate Dorsal V4 and Surrounding Areas: A Functional Magnetic Resonance Imaging Study in Awake Monkeys. J Neurosci 23:7395–7406.

Fortenbaugh FC, Silver MA, Robertson LC (2015) Individual differences in visual field shape modulate the effects of attention on the lower visual field advantage in crowding. J Vis 15.

Gattass R, Gross CG (1981) Visual topography of striate projection zone (MT) in posterior superior temporal sulcus of the macaque. J Neurophysiol 46:621–638.

Gattass R, Gross CG, Sandell JH (1981) Visual topography of V2 in the macaque. J Comp Neurol 201:519–539.

Gattass R, Nascimento-Silva S, Soares JG., Lima B, Jansen AK, Diogo ACM, Farias MF, Botelho MM Eliã P, Mariani OS, Azzi J, Fiorani M (2005) Cortical visual areas in monkeys: location, topography, connections, columns, plasticity and cortical dynamics. Philos Trans R Soc Lond B Biol Sci 360:709–731.

Gattass R, Sousa AP, Gross CG (1988) Visuotopic organization and extent of V3 and V4 of the macaque. J Neurosci 8:1831–1845.

Gattass R, Sousa AP, Mishkin M, Ungerleider LG (1997) Cortical projections of area V2 in the macaque. Cereb Cortex 7:110–129.

Glasser MF, Essen DCV (2011) Mapping Human Cortical Areas In Vivo Based on Myelin Content as Revealed by T1- and T2-Weighted MRI. J Neurosci 31:11597–11616.

Glasser MF, Goyal MS, Preuss TM, Raichle ME, Van Essen DC (2014) Trends and properties of human cerebral cortex: Correlations with cortical myelin content. NeuroImage 93, Part 2:165–175.

Gold BT, Powell DK, Xuan L, Jicha GA, Smith CD (2010) Age-related slowing of task switching is associated with decreased integrity of frontoparietal white matter. Neurobiol Aging 31:512–522.

Harvey BM, Dumoulin SO (2011) The Relationship between Cortical Magnification Factor and Population Receptive Field Size in Human Visual Cortex: Constancies in Cortical Architecture. J Neurosci 31:13604–13612.

Hutchison RM, Culham JC, Flanagan JR, Everling S, Gallivan JP (2015) Functional subdivisions of medial parieto-occipital cortex in humans and nonhuman primates using resting-state fMRI. NeuroImage 116:10–29.

Hutchison RM, Gallivan JP, Culham JC, Gati JS, Menon RS, Everling S (2012) Functional connectivity of the frontal eye fields in humans and macaque monkeys investigated with resting-state fMRI. Journal of Neurophysiology 107:2463–2474.

Hutchison RM, Hutchison M, Manning KY, Menon RS, Everling S (2014) Isoflurane induces dose-dependent alterations in the cortical connectivity profiles and dynamic properties of the brain's functional architecture. Hum Brain Mapp 35:5754–5775.

Janssens T, Zhu Q, Popivanov ID, Vanduffel W (2014) Probabilistic and Single-Subject Retinotopic Maps Reveal the Topographic Organization of Face Patches in the Macaque Cortex. J Neurosci 34:10156–10167.

Khan MA, Lawrence GP (2005) Differences in visuomotor control between the upper and lower visual fields. Exp Brain Res 164:395–398.

Kolster H, Janssens T, Orban GA, Vanduffel W (2014) The Retinotopic Organization of Macaque Occipitotemporal Cortex Anterior to V4 and Caudoventral to the Middle Temporal (MT) Cluster. J Neurosci 34:10168–10191.

Kolster H, Mandeville JB, Arsenault JT, Ekstrom LB, Wald LL, Vanduffel W (2009) Visual Field Map Clusters in Macaque Extrastriate Visual Cortex. J Neurosci 29:7031–7039.

Kolster H, Peeters R, Orban GA (2010) The Retinotopic Organization of the Human Middle Temporal Area MT/V5 and Its Cortical Neighbors. J Neurosci 30:9801–9820.

Levine MW, McAnany JJ (2005) The relative capabilities of the upper and lower visual hemifields. Vision Research 45:2820–2830.

Liu T, Heeger DJ, Carrasco M (2006) Neural correlates of the visual vertical meridian asymmetry. J Vis 6:1294–1306.

Maehara G, Okubo M, Michimata C (2004) Effects of background color on detecting spot stimuli in the upper and lower visual fields. Brain Cogn 55:558–563.

Payne WH (1967) Visual reaction times on a circle about the fovea. Science 155:481–482.

Power JD, Cohen AL, Nelson SM, Wig GS, Barnes KA, Church JA, Vogel AC, Laumann TO, Miezin FM, Schlaggar BL, Petersen SE (2011) Functional Network Organization of the Human Brain. Neuron 72:665–678.

Previc FH (1990) Functional specialization in the lower and upper visual fields in humans: Its ecological origins and neurophysiological implications. Behavioral and Brain Sciences 13:519–542.

Purcell JJ, Turkeltaub PE, Eden GF, Rapp B (2011) Examining the central and peripheral processes of written word production through meta-analysis. Front Psychol 2:239.

Qu Z, Song Y, Ding Y (2006) Asymmetry between the upper and lower visual fields: An event-related potential study. CHINESE SCI BULL 51:536–541.

Sample PA, Irak I, Martinez GA, Yamagishi N (1997) Asymmetries in the normal short-wavelength visual field: implications for short-wavelength automated perimetry. Am J Ophthalmol 124:46–52.

Saur D, Kreher BW, Schnell S, Kümmerer D, Kellmeyer P, Vry M-S, Umarova R, Musso M, Glauche V, Abel S, Huber W, Rijntjes M, Hennig J, Weiller C (2008) Ventral and dorsal pathways for language. Proc Natl Acad Sci USA 105:18035–18040.

Schwarzkopf DS, Anderson EJ, de Haas B, White SJ, Rees G (2014) Larger extrastriate population receptive fields in autism spectrum disorders. J Neurosci 34:2713–2724.

Sereno MI, Dale AM, Reppas JB, Kwong KK, Belliveau JW, Brady TJ, Rosen BR, Tootell RB (1995) Borders of multiple visual areas in humans revealed by functional magnetic resonance imaging. Science 268:889–893.

Thomas JM, Huber E, Stecker GC, Boynton GM, Saenz M, Fine I (2015) Population receptive field estimates of human auditory cortex. NeuroImage 105:428–439.

Tounekti S, Troalen T, Bihan-Poudec Y, Cléry J, Lamberton F, Ben Hamed S, Hiba B (2017) High-resolution diffusion MRI of Macaque brain at 3T: 3D-EPI sampling of Fourier space.

van Dijk JA, de Haas B, Moutsiana C, Schwarzkopf DS (2016) Intersession reliability of population receptive field estimates. NeuroImage 143:293–303.

Van Essen DC, Newsome WT, Maunsell JH (1984) The visual field representation in striate cortex of the macaque monkey: asymmetries, anisotropies, and individual variability. Vision Res 24:429–448.

Vanduffel W, Fize D, Mandeville JB, Nelissen K, Van Hecke P, Rosen BR, Tootell RBH, Orban GA (2001) Visual Motion Processing Investigated Using Contrast Agent-Enhanced fMRI in Awake Behaving Monkeys. Neuron 32:565–577.

Yeo BTT, Krienen FM, Sepulcre J, Sabuncu MR, Lashkari D, Hollinshead M, Roffman JL, Smoller JW, Zöllei L, Polimeni JR, Fischl B, Liu H, Buckner RL (2011) The organization of the human cerebral cortex estimated by intrinsic functional connectivity. Journal of Neurophysiology 106:1125–1165.

Yoon JH, Maddock RJ, Rokem A, Silver MA, Minzenberg MJ, Ragland JD, Carter CS (2010) Gamma-Aminobutyric Acid Concentration is Reduced in Visual Cortex in Schizophrenia and Correlates with Orientation-Specific Surround Suppression. J Neurosci 30:3777–3781.

Conclusions and perspectives

The aim of the present thesis was to investigate the neural bases of space representation in the awake non-human primate using functional magnetic resonance imaging.

In the first axis, we have shown that, in humans, dynamic looming visual stimuli enhance tactile sensitivity at the predicted location and time of impact on the face (Cléry et al., 2015a, Chapter 1). A similar study, performed in awake monkeys and in fMRI, confirms that this type of stimuli leads to maximal cortical brain activations. Importantly, we highlight the involvement of a parieto-frontal network which seems to subserve the tactile enhancement observed when studying humans (Chapter 2). This parieto-frontal network is essentially composed of the intraparietal area VIP and the premotor area F4 which have already been described as encoding multisensory convergence processing (Guipponi et al., 2015).

The identification of the neural bases that encode near and far space shows that the parieto-frontal network identified in multisensory convergence and integration processing also participates to the peripersonal space encoding (Chapter 3 and 4). A network involved in at least three different processing shows its important contribution in space representation mechanisms.

Some studies (for reviews, see Cléry et al., 2015b; de Vignemont and Iannetti, 2015, Introduction Part II) have assessed that the peripersonal space is dynamic and plastic and therefore the "virtual" boundary between this space and the extrapersonal space can be shrinked or expanded according to emotional, social or actions components. However, the majority of these studies explore these aspects at the behavioral level. In the present thesis, we contribute to the definition of the neural bases encoding near and far space in a neutral environment. A direct perspective of this first axis is to use fMRI to identify the changes in cortical activations when we stimulate the peripersonal space with objects that have a positive or negative value but also with social or anti-social stimuli. This will allow us to investigate how the parieto-frontal network is activated by the context.

Most importantly, the two fMRI studies of Axis I can lead us to perform others experiments with the same experimental design, in the same animal, and using a single cell recording technique. The site recording will be at the exact location of the activated areas identified in impact prediction and peripersonal space encoding thanks to fMRI, in particular about the parieto-frontal network. How are patterns activity at whole brain (and population) level correlated and reflected at neuronal level? More precisely, are the same neurons involved in the three processes of multisensory convergence, impact prediction and peripersonal space encoding or rather are there sub-populations of neurons involved in each process separately in the same voxel?

In the second axis, we develop numerous challenging technics and methods that will allow us to observe neural changes after plasticity induction. Some of these methods need to be more refined and further analyzed but they show themselves to be really promising for the study of plasticity in the non-human primate.

The next step will be to induce plasticity to confirm that our methods are correct. The first plasticity will be induced by means of bottom-up influences through sensory training (cf Axis II; Methodology; Chapter 6; 3). These manipulations are expected to increase the spatial resolution of the visual map in the visual quadrant over-stimulated, all the more when the stimulations are coupled with a visuomotor response. The second plasticity will be induced by means of top-down cognitive influences through prior reinforcement. For example, the priors the monkeys have about space can be manipulated by systematically reinforcing a goal-oriented behavior in a defined quadrant either with a higher reward or a higher probability of target appearance than in the other location. In this case of plasticity induction, we will expect to observe a locale increase in the spatial resolution of the visual map.

Another type of plasticity induction, which explains, in part, why we work with monkey for our plasticity project, is pharmacological neuromodulation. We have seen in the introduction of Axis II that numerous neuromodulators can lead to plasticity. The one that we are interested in more particularly is the GABA which plays a central role in the balance between excitation and inhibition. An interesting method is to locally inject bicuculline GABA antagonist (Wardak et al., 2006) in the visual cortex and therefore to reduce GABAergic inhibition in this area. We expect that to lead to more excitation than inhibition in the balance E/I and to induce plasticity in the visual cortex. The combination of pharmacological neuromodulation, sensory and cognitive influences may enable us to potentiate and maximize the plasticity power and neural changes.

We hope that this project, in addition to providing a long-missing integrative view of plasticity in the adult visual cortex, will provide new directions of investigation to treat abnormal visual experience due to eye misalignment in early childhood (amblyopia, congenital cataract) or visual deficits due to acute cortical lesions (following head traumas or cerebrovascular accidents) leading to such conditions as anopsia or neglect, thus addressing major issues in the physiopathology of the visual cortex.

Future interesting perspectives, linking the two axes of the present thesis, would be to study whether the parieto-frontal network (VIP-F4) involved in multisensory convergence, impact prediction and peripersonal space (Guipponi et al., 2013, 2015, Cléry et al., 2015a, 2015b, Chapter 2 and 3) can be modulated using the same strategies of plasticity induction, i.e. sensory modulation, cognitive modulation and pharmacological modulation but with tasks designed directly to imply these three mechanisms and allowing to reinforce them. Besides, couldn't current remediation treatments of some pathologies, such as hemispatial neglect, due

to lesions or impairments in the areas involved in these mechanisms, be treated by means of plasticity induction tasks and a better understanding of adult plasticity mechanisms?

Can the network involved in visual representation such as the attentional parieto-frontal network involving LIP and FEF (Ben Hamed et al., 2002; Wardak et al., 2002, 2004, 2006; Ibos et al., 2013; Astrand et al., 2015, 2016) have an impact on the peripersonal space after plasticity induction? Or more precisely, do the different tasks we will use to induce plasticity have only a local effect, a more spread out effect or a global effect on the brain?

However, even though we applied fMRI to the non-human primate to bridge the gap between the two major sources of knowledge, namely monkey electrophysiology and human neuroimaging techniques, some research projects on both monkeys and humans need to be conducted to confirm our results and compare the difference between humans and non-human primates.

The two axes of the present thesis open numerous new ways of research investigations.

References

Astrand E, Ibos G, Duhamel J-R, Ben Hamed S (2015) Differential dynamics of spatial attention, position, and color coding within the parietofrontal network. J Neurosci 35:3174–3189.

Astrand E, Wardak C, Baraduc P, Ben Hamed S (2016) Direct Two-Dimensional Access to the Spatial Location of Covert Attention in Macaque Prefrontal Cortex. Current Biology 26:1699–1704.

Ben Hamed S, Duhamel J-R, Bremmer F, Graf W (2002) Visual receptive field modulation in the lateral intraparietal area during attentive fixation and free gaze. Cereb Cortex 12:234–245.

Cléry J, Guipponi O, Odouard S, Wardak C, Ben Hamed S (2015a) Impact prediction by looming visual stimuli enhances tactile detection. J Neurosci 35:4179–4189.

Cléry J, Guipponi O, Wardak C, Ben Hamed S (2015b) Neuronal bases of peripersonal and extrapersonal spaces, their plasticity and their dynamics: Knowns and unknowns. Neuropsychologia 70:313–326.

de Vignemont F, Iannetti GD (2015) How many peripersonal spaces? Neuropsychologia 70:327–334.

Guipponi O, Cléry J, Odouard S, Wardak C, Ben Hamed S (2015) Whole brain mapping of visual and tactile convergence in the macaque monkey. NeuroImage 117:93–102.

Guipponi O, Wardak C, Ibarrola D, Comte J-C, Sappey-Marinier D, Pinède S, Hamed SB (2013) Multimodal Convergence within the Intraparietal Sulcus of the Macaque Monkey. J Neurosci 33:4128–4139.

Ibos G, Duhamel J-R, Hamed SB (2013) A Functional Hierarchy within the Parietofrontal Network in Stimulus Selection and Attention Control. J Neurosci 33:8359–8369.

Wardak C, Ibos G, Duhamel J-R, Olivier E (2006) Contribution of the monkey frontal eye field to covert visual attention. J Neurosci 26:4228–4235.

Wardak C, Olivier E, Duhamel J-R (2002) Saccadic target selection deficits after lateral intraparietal area inactivation in monkeys. J Neurosci 22:9877–9884.

Wardak C, Olivier E, Duhamel J-R (2004) A deficit in covert attention after parietal cortex inactivation in the monkey. Neuron 42:501–508.

Appendices

Appendix 1

Whole brain mapping of visual and tactile convergence in the macaque monkey.

Published in “ NeuroImage”, en mai 2015 • 117 (2015) 93–102

NeuroImage 117 (2015) 93–102

Contents lists available at ScienceDirect

NeuroImage

journal homepage: www.elsevier.com/locate/ynimg

Whole brain mapping of visual and tactile convergence in the macaque monkey

Olivier Guipponi, Justine Cléry, Soline Odouard, Claire Wardak, Suliann Ben Hamed *

Centre de Neuroscience Cognitive, CNRS UMR 5229, Université Claude Bernard Lyon I, 67 Bd Pinel, 69675 Bron cedex, France

ARTICLE INFO

Article history:
Received 17 March 2015
Accepted 8 May 2015
Available online 16 May 2015

Keywords:
Multisensory
Monkey fMRI
Functional connectivity
Context dependent
Macaque

ABSTRACT

The proposal that sensory processing is achieved in segregated anatomical pathways has been profoundly revisited following the description of cross-modal anatomical connections both at higher and at lower processing levels. However, an understanding of the cortical extent of these long range cross-modal functional influences has been missing. Here, we use functional magnetic resonance imaging (fMRI) to map, in the non-human primate brain, the cortical regions which are activated by both visual and tactile stimulations. We describe an unprecedented pattern of functional visuo-tactile convergence, encompassing both low-level visual and somatosensory areas and multiple higher-order associative areas. We also show that the profile of this convergence depends on the physical properties of the mapping stimuli, indicating that visuo-tactile convergence is most probably even more prevailing than what we actually describe. Overall, these observations substantiate the view that the brain is massively multisensory.

Introduction

Advances in neurosciences in the last decades have repeatedly challenged our views on the organization of cortical sensory processing. Early anatomical (Kuypers et al., 1965) and lesion studies (Massopust et al., 1965) led to the description of segregated anatomical pathways, each processing a specific sensory modality. In 1991, Felleman and Van Essen (1991) refined this view, proposing a massively parallel, hierarchical processing organization of the visual system, in which the initial sensory stages are performed by low level unimodal sensory areas, while later processing stages are performed by multisensory higher-order associative regions, such as the temporal cortex (Barraclough et al., 2005; Beauchamp et al., 2004) or the parietal cortex (Avillac et al., 2005; Duhamel et al., 1998; Guipponi et al., 2013; Schlack et al., 2005; Sereno and Huang, 2006). The subsequent description of heteromodal connection in early sensory processing areas (e.g. auditory projections onto visual cortex or vice-versa: Falchier et al., 2002; Rockland and Ojima, 2003; Cappe and Barone, 2005; somatosensory projections onto auditory cortex or vice-versa: Cappe and Barone, 2005; Budinger et al., 2006; de la Mothe et al., 2006; Smiley et al., 2007; visual projections onto somatosensory cortex: Wallace et al., 2004) further nuanced this view, suggesting that multisensory processing takes place at earlier processing stages than commonly admitted. The contribution of these heteromodal projections to the modulation of the response of early sensory neurons is confirmed both by single cell recording studies (Iurilli et al., 2012; Schroeder and Foxe, 2005; Vasconcelos et al., 2011) and functional neuroimaging studies (Amedi et al., 2001; Macaluso et al., 2000; Sathian et al., 1997). On the basis of the growing evidence for pervasive multisensory influences at all levels of cortical processing, Ghazanfar and Schroeder (2006) question, in a recent review, whether multisensory processing could actually be an essential property of neocortex.

Here, functional magnetic resonance imaging (fMRI) in the non-human primate allows us to capture the spatial pattern of visuo-tactile cortical convergence, the extent of which has been overlooked by previous studies, both in low-level visual and somatosensory areas and in multiple higher-order associative areas. In particular, we show that the profile of this visuo-tactile convergence is functionally shaped by the physical properties of the stimuli used for the sensory mapping.

Material and methods

Ethical statement

All procedures were in compliance with the guidelines of the European Community on animal care (European Community Council, Directive No. 86–609, November 24, 1986). All the protocols used in this experiment were approved by the animal care committee (Department of Veterinary Services, Health & Protection of Animals, permit number 69 029 0401) and the Biology Department of the University Claude Bernard Lyon 1. The animals' welfare and the steps taken to ameliorate suffering were in accordance with the recommendations of the Weatherall report, "The use of non-human primates in research". The study involved two rhesus monkeys (*Macaca mulatta*, a male, 7 kg, age

* Corresponding author at: Centre de Neuroscience Cognitive, CNRS UMR 5229, Université Claude Bernard Lyon I, 67 Bd Pinel, 69675 Bron cedex, France.
E-mail address: benhamed@isc.cnrs.fr (S. Ben Hamed).

http://dx.doi.org/10.1016/j.neuroimage.2015.05.022
1053-8119/

7 and a female, 5 kg, age 5), as accepted in non-human primate fMRI studies. The animals were housed in twin cages (2 m^2 by 2 m height in total). The twin cages could be separated in two individual cages or connected to form a unique housing for a pair of monkeys thus offering the monkeys a socially enriched environment. This last configuration was the norm. Twin cages communicated with a larger play cage ($4 \times 1.5 \times 2$ m^3) to which the monkeys were granted access on days on which they were not involved in experiments. Light was switched on and off at fixed hours (on: 7.30 a.m and off: 8 p.m), all year round. Monkeys had free access to food pellets. They were also given fresh fruits and nuts. During week days, monkeys had access to water during the training sessions. Additional water and fruits were given in order to achieve a minimum of 30–40 ml/kg of daily water intake. Animals had free access to water starting from Friday late afternoon to Sunday night. All cages were enriched with mirrors, hanging ropes, balls and foraging baskets. No procedure that might cause discomfort or pain was undertaken without adequate analgesia or anesthesia. The specific surgical procedures are detailed below. The general health status of the animals was monitored every day by competent and authorized personal. In agreement with the 3R 'reduction' recommendation, the two animals involved in the present study were enrolled later in another experiment.

Subjects and materials

Two rhesus monkeys (female M1, male M2, 5–7 years old, 5–7 kg) participated in the study. The animals were implanted with a custom-made PEI plastic MRI compatible headset covered by dental acrylic. The anesthesia during surgery was induced by Zoletil (Tiletamine-Zolazepam, Virbac, 15 mg/kg) and followed by Isoflurane (Belamont, 1–2%). Post-surgery analgesia was ensured thanks to Temgesic (buprenorphine, 0.3 mg/ml, 0.01 mg/kg). During recovery, proper analgesic and a full antibiotic coverage was provided (long action Terramycin, one injection during the surgery and one 5 days later, 0.1 ml/kg, i.m.). The surgical procedures conformed to the European and National Institutes of Health guidelines for the care and use of laboratory animals.

During the scanning sessions, monkeys sat in a sphinx position in a plastic monkey chair positioned within a horizontal magnet (1.5-T MR scanner Sonata; Siemens, Erlangen, Germany) facing a translucent screen placed 90 cm from the eyes. Their head was restrained and equipped with MRI-compatible headphones customized for monkeys (MR Confon GmbH, Magdeburg, Germany). A radial receive-only surface coil (10-cm diameter) was positioned above the head. Eye position was monitored at 120 Hz during scanning using a pupil-corneal reflection tracking system (Iscan®, Cambridge, MA). Monkeys were rewarded with liquid dispensed by a computer-controlled reward delivery system (Crist®) thanks to a plastic tube coming to their mouth. The task, all the behavioral parameters as well as the sensory stimulations were controlled by two computers running with Matlab® and Presentation®. The fixation point the monkeys were instructed to fixate, as well as the visual stimuli, were projected onto a screen with a Canon XEED SX60 projector. Tactile stimulations were delivered through Teflon tubing and 6 articulated plastic arms connected to istant air pressure electro-valves. Monkeys were trained in a mock scan environment approaching to the best the actual MRI scanner setup.

Task and stimuli

The animals were trained to maintain fixation on a red central spot ($0.24° \times 0.24°$) while stimulations (visual or tactile) were delivered. The monkeys were rewarded for staying within a $2° \times 2°$ tolerance window centered on the fixation spot. The reward delivery was scheduled to encourage long fixation without breaks (i.e. the interval between successive deliveries was decreased and their amount was increased, up to a fixed limit, as long as the eyes did not leave the window). The two sensory modalities were tested in independent interleaved runs (see below for the organization of the runs). Stimulation strength was maximized in order to saturate the evoked neuronal response and induce an unambiguously strong percept for all types of stimuli.

Visual stimulations

Large field ($32° \times 32°$) visual stimulations consisted of white bars ($3.2° \times 24.3°$, horizontal, vertical, or 45° oblique) or white random dots on a black background (Fig. 1A). Three conditions were tested in blocks of 10 pulses (TR = 2.08 s): 1) *coherent movement*, with bars moving in one of the 8 cardinal directions or expanding or contracting random dots pattern (with 5 possible optic flow origins: center, upper left (−8°, 8°), upper right, lower left and lower right); each coherent movement sequence lasted 850 ms and 24 such sequences were pseudo-randomly presented in a given coherent movement block; 2) *scrambled movement*, in which the different frames of a given coherent movement sequence were randomly reorganized; 3) *static*, in which individual frames randomly picked from the coherent movement visual stimuli sequences, were presented for 250 ms. As a result, within a given block, 850 ms portions of the different stimuli (bars/dots/directions/origins) of the same category (coherent/scrambled/static) were pseudo-randomly interleaved. The movement related activations were reported for the parietal cortex in a previous paper (Guipponi et al., 2013). In the present paper, we focus on the static stimulations, so that in all analyses, the visual stimulation vs. fixation contrast corresponds to static visual stimuli compared to the fixation, except in the analysis presented in Figs. 4 and 5.

Tactile stimulations

They consisted of air puffs delivered to three different locations on the left and the right of the animals' body (Fig. 1B): 1) *center* of the face, close to the nose and the mouth; 2) *periphery* of the face, above the eyebrows; 3) *shoulders* (cf. Guipponi et al. (2013)). The intensity of the stimulations ranged from 0.5 bars (center/periphery) and 1 bar (shoulders), to adjust for the larger distance between the extremity of the stimulation tubes and the skin, as well as for the difference in hair density. The inter-stimulus interval for air-puff presentation was random (mean of 1210 ms, s.d. of 148 ms). Though the air-puff delivery system produced a weak noise at air-puff production, the entire system was placed outside the MRI room and the noise could thus not reach the

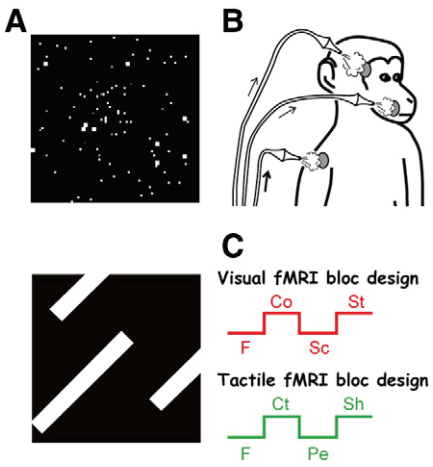

Fig. 1. Stimulation fMRI protocol. A. Two examples of whole field visual stimuli: optic flows and large-field bars. These stimuli were assembled to evoke either static, coherent movement or scrambled dynamic visual stimulation. B. Tactile stimulations: air-puffs were delivered to the center of the face, the periphery of the face, or the shoulders, simultaneously on the left and right sides of the monkeys. C. fMRI block design. Visual runs consisted of a pseudorandom association of fixation blocks (F), coherent visual movement blocks (Co), scrambled visual movement blocks (Sc) and static visual stimulation blocks (St). Tactile runs consisted of a pseudorandom association of fixation blocks (F), center of the face tactile stimulations (Ct), periphery of the face tactile stimulations (Pe) and shoulder tactile stimulations (Sh).

monkeys. On the monkeys' side, the air puffs did not produce any notable noise. In any case, the monkeys were surrounded by the noise of the MRI scanner and their ears were covered with MRI-compatible headphones thus isolating them from their auditory environment.

Scanning

Before each scanning session, a contrast agent, monocrystalline iron oxide nanoparticle (Sinerem, Guerbet or Feraheme, AMAG, Vanduffel et al., 2001), was injected into the animal's femoral/saphenous vein (4–10 mg/kg) in order to increase the signal–noise ratio and the spatial resolution. For the sake of clarity, the polarity of the contrast agent MR signal changes, which are negative for increased blood volumes, was inverted. We acquired gradient-echo echoplanar (EPI) images covering the whole brain (1.5 T; repetition time (TR) 2.08 s; echo time (TE) 27 ms; 32 sagittal slices; 2 × 2 × 2-mm voxels). Functional time series (runs) were organized as follows (Fig. 1C): a 10-volume block of pure fixation (baseline) was followed by a 10-volume block of stimulation category 1, a 10-volume block of stimulation category 2, and a 10-volume block of stimulation category 3; this sequence was played four times, resulting in a 160-volume run. The blocks for the 3 categories were presented in 6 counterbalanced possible orders. A *retinotopy* localizer was run independently in the two monkeys using exactly the stimulations of Fize et al. (2003). This localizer was used to localize the central and peripheral representations of visual areas within each hemisphere, in both animals. During each scanning session, the runs of different modalities and different orders were pseudo-randomly intermixed. A total of 40 (34) runs was acquired for visual stimulations in M1 (/M2), 36 (40) runs for tactile stimulations. Fifty-seven (45) runs were obtained for the retinotopy localizer in independent sessions for M1 (/M2).

Analysis

A total of 23 (25) runs were selected for the visual stimulation condition, 21 (32) for the tactile stimulation condition and 20 (24) for the retinotopy localizer, based on the quality of the monkeys fixation throughout each run (>85% within the tolerance window). Time series were analyzed using SPM8 (Wellcome Department of Cognitive Neurology, London, United Kingdom). For spatial preprocessing, functional volumes were first realigned and rigidly coregistered with the anatomy of each individual monkey (T1-weighted MPRAGE 3D 0.6 × 0.6 × 0.6 mm or 0.5 × 0.5 × 0.5 mm voxel acquired at 1.5 T) in stereotactic space. The JIP program (Mandeville et al., 2011) was used to perform a non-rigid coregistration (warping) of a mean functional image onto the individual anatomies. The same procedure was used to coregister the functional images of monkey M1 onto the anatomy of monkey M2 (i.e., realignment followed by a rigid and then a non-rigid coregistration).

Fixed effect individual analyses were performed for each sensory modality in each monkey, with a level of significance set at $p < 0.05$ corrected for multiple comparisons ((FWE, $t > 4.89$) and $p < 0.001$ uncorrected ($t > 3.1$) (see Table 1)). We also performed conjunction analyses (statistical levels set at $p < 0.05$ at corrected level and $p < 0.001$ at uncorrected level). In all analyses, realignment parameters, as well as eye movement traces, were included as covariates of no interest to remove eye movement and brain motion artifacts. When coordinates are provided, they are expressed with respect to the anterior commissure. As the results were consistent in the two animals for all the discussed cortical regions (i.e. activations observed in at least 3 out of 4 hemispheres), we present a group analysis in order to simplify the presentation of the results. Fixed effect group analyses were performed for each sensory modality and for conjunction analyses with a level of significance set at $p < 0.001$ ($t > 3.1$) and projected onto the anatomy of monkey M2. Results are displayed on M2 flattened maps obtained with Caret ((van Essen et al., 2001); http://www.nitrc.org/projects/caret/).

We performed regions of interest (ROIs) analyses using MarsBar toolbox (Brett et al., 2002), based on the individual conjunction analyses results. The ROIs were defined using the activations obtained at corrected level (FWE, $t > 4.89$) or at uncorrected level (t-scores > 3.1) when the activations failed to reach the corrected level. When the activations obtained at corrected level were too large and included several areas, we defined a geometric cubic ROI (2 × 2 × 2 mm) centered on the local maximum t-score. For each ROI, each run and each contrast of interest, we extracted the percent of signal change (PSC) using SPM8 and the MarsBar toolbox. The significance of these PSCs across all runs was assessed using a paired t-test, in Matlab™ (The MathWorks Inc., Natick, MA, USA). P-values are not corrected for multiple comparisons. The majority of the described effects in Fig. 3 are highly significant ($p < 0.001$) and would survive a Bonferroni correction for $n = 2$ (test for visual and for tactile PSC significance). The fact that most of the reported effects are described in the two hemispheres of both monkeys strongly indicates that our statistical descriptions do not correspond to false positive assessments. In addition, areas where statistical significance was reached for only one animal or less than three hemispheres are discussed with caution.

Assigning the activations to a specific cortical area was performed on each individual monkey brain using the monkey brain atlases made available on http://scalablebrainatlas.incf.org. These atlases allow mapping specific anatomical coronal sections with several cytoarchitetonic parcellation studies. We used the Lewis and Van Essen (2000) and the Paxinos Rhesus Monkey (1999) parcellations. For some areas, we additionally referred to more recent works (e.g. Petrides et al., 2005; or Belmalih et al., 2009). We further checked that the group activations faithfully reflected, in their localization and their assignment, the individual activations identified in each monkey.

Potential covariates

In all analyses, realignment parameters, as well as eye movement traces, were included as covariates of no interest to remove eye movement and brain motion artifacts. However, some of the stimulations might have induced a specific behavioral pattern biasing our analysis, not fully accounted for by the above regressors. While we cannot completely rule out this possibility, our experimental set-up allows to minimize its impact. Monkeys worked head-restrained (to maintain the brain at the optimal position within the scanner, to minimize movement artifacts on the fMRI signal and to allow for a precise monitoring of their eye movements). *Uncertainty about tactile stimulation location.* As a result of the head restraint, the tactile stimulations to the center were stable in a given session. When drinking the liquid reward, small lip movements occurred. These movements thus correlated with reward timing and were on average equally distributed over the different sensory runs and the different conditions within each run (we checked that the monkeys had equal performance among the different conditions within a given run). The center of the face air-puffs were placed on the cheeks on each side of the monkey's nose at a location that was not affected by the lip movements. Peripheral body stimulation air-puffs were directed to the shoulders, at a location that was not affected by possible arm movements by the monkey. This was possible because the monkey chair tightly fit the monkey's width. *Air-puffs.* Air-puffs are often considered as aversive stimuli evoking a wide variety of emotional overt behavioral reactions such as eye movements, blinks or facial mimics. In our study, the intensity of the air-puffs was adjusted such that the tactile stimulations were well above detection threshold, yet not evoking any overt behavior in the monkey. As a result, at the beginning of the training period, monkeys were curious about this novel stimulus and did have typical blink and eye exploration patterns. This interrupted the reward schedule as the fixation criterion was violated. The monkeys quickly habituated to the stimuli and reverted to the expected fixation behavior. The fact that these air-puffs did not evoke eye movements is documented in the supplementary

Table 1
Summary of the visuo-tactile conjunction activations, for the individual ROIs identified in the left and right hemispheres of monkeys M1 and M2.

	M1/left hemisphere					M1/right hemisphere				
	Coordinates			Size	T–value	V and T	Coordinates			Size	T–value	V and T
Visual areas												
V1v	[−15 ; −36 ; −3]			11	6.07	V>T	[6 ; −37 ; −5]			64	4.55	V>T
V1d	[−8 ; −41 ; 6]			1	5.49	V>T	[8 ; −41 ; 5]			5	4.05	V>T
V2v	[−9 ; −36 ; −7]			71	6.5	V>T	[6 ; −41 ; −8]			10	4.17	V>T
V2d	[−5 ; −30 ; 0]			96	9.85	V>T	[3 ; −30 ; 1]			155	9.43	V>T
V3/V3a	[−9 ; −30 ; 7]			*	5.24	V>T	[5 ; −30 ; 4]			*	5.14	V>T
V4	[−12 ; −35 ; 9]			2	4.9	V>T	[23 −30 2]			6	6.01	V>T
Temporal areas												
MST	[−11 ; −23 ; 2]			39	7.28	V>T	[10 ; −22 ; 4]			22	6.36	V>T
FST							[12 ; −16 ; −2]			1	3.13	V>T
Parietal areas												
PIP	[−10 ; −27 ; 5]			26	6.19	V>T	[7 ; −26 ; 2]			26	3.61	V>T
VIPposterior	[−10 ; −22 ; 8]			31	6.61	V>T	[9 ; −22 ; 9]			11	7.12	V>T
VIPanterior	[−14 ; −16 ; 9]			2	5.93	V=T	[13 ; −15 ; 11]			3	3.48	T>V
7b	[−24 ; −18 ; 8]			1	5.27	V>T						
7op	[−23 ; −20 ; 9]			2	3.79	V=T	[16 ; −22 ; 11]			1	3.68	V>T
Medial areas												
24c–d	[−8 ; 8 ; 16]			1	2.77	V>T	[4 ; 8 ; 18]			1	2.69	V=T
PreSMA												
Somatosensory cortex												
SII/PV												
SII	[−17 ; −3 ; 8]			*	1.67	T>V	[18 ; −3 ; 6]			*	1.86	T>V
3a							[15 ; −4 ; 12]			8	3.99	T>V
2							[21 ; −11 ; 13]			1	3.16	T>V
Pi	[−18 ; 0 ; −4]			7	1.97	V=T	[15 ; 2 ; −5]			1	1.66	T>V
Ig												
Premotor areas												
F5a	[−20 ; 6 ; 10]			4	5,79	T>V	[17 ; 4 ; 11]			3	5.65	V>T
F4/F5p	[−20 ; −3 ; 13]			1	3.15	T>V	[15 ; −4 ; 12]			8	3.99	T>V
Prefrontal areas												
9/46v	[−17 ; 14 ; 12]			*	5.46	T>V	[14 ; 13 ; 12]			48	6.82	V>T
GrF/ProM	[−20 ; 10 ; 6]			2	5.38	V=T	[17 ; 9 ; 8]			11	7.39	V>T
44	[−16 ; 3 ; 8]			1	5.17	V>T	[11 ; 1 ; 9]			2	5.47	V>T
Orbitofrontal areas												
11	[−18 ; 16 ; 10]			41	7.47	V=T	[13 ; 16 ; 8]			*	6.25	T>V
13	[−13 ; 15 ; 7]			*	6.19	V>T	[10 ; 16 ; 8]			*	5.5	T>V

	M2/left hemisphere					M2/right hemisphere				
	Coordinates			Size	T–value	V and T	Coordinates			Size	T–value	V and T
Visual areas												
V1v	[−11 ; −36 ; −1]			*	4.72	V>T	[14 ; −30 ; −1]			*	4.66	V>T
V1d	[−6 ; −40 ; 2]			2	4.91	V>T	[8 ; −41 ; 1]			6	5.59	V>T
V2v	[−6 ; −33 ; −6]			6	5.3	V>T	[5 ; −33 ; −4]			1	5.14	V>T
V2d	[−6 ; −36 ; 0]			55	6.04	V>T	[6 ; −38 ; 0]			24	6.72	V>T
V3/V3a	[−15 ; −31 ; 8]			*	2.58	V>T	[15 ; −31 ; 8]			*	3.42	V>T
V4	[−17 ; −30 ; 8]			42	4.55	V>T	[16 ; −30 ; 9]			13	4.28	V>T
Temporal areas												
MST	[−12 ; −20 ; 2]			4	2,84	V>T	[15 ; −22 ; 6]			1	2,89	V>T
FST												
Parietal areas												
PIP	[−10 ; −27 ; 1]			*	3.79	V>T	[10 ; −27 ; 1]			*	3.16	V>T
VIPposterior	[−10 ; −17 ; 9]			10	6.65	V>T	[10 ; −17 ; 9]			11	6.64	V>T
VIPanterior												
7b												
7op	[−16 ; −19 ; 11]			5	4.22	V>T	[17 ; −18 ; 11]			9	4.62	T>V
Medial areas												
24c–d	[−2 ; 9 ; 13]			3	4.93	V>T	[5 ; 9 ; 12]			*	4.03	V=T
PreSMA	[−3 ; 5 ; 18]			2	3.87	V=T	[3 ; 3 ; 18]			5	3.64	V=T
Somatosensory cortex												
SII/PV	[−27 ; −7 ; 4]			4	3.54	T>V						
SII	[−17 ; −5 ; 8]			1	3.11	T>V	[16 ; −2 ; 4]			*	3.13	T>V
3a												
2	[−15 ; −12 ; 16]			12	3.87	T>V	[15 ; −14 ; 16]			11	3.85	T>V
Pi	[−17 ; −1 ; −4]			5	3.78	T>V	[18 ; −5 ; −2]			*	4.01	T>V
Ig	[−16 ; −11 ; 2]			8	3.62	V>T	[18 ; −5 ; 2]			51	4.55	T>V
Premotor areas												
F5a												
F4/F5p	[−17 ; −4 ; 14]			2	2.75	V>T	[18 ; −1 ; 13]			1	3.18	T>V
Prefrontal areas												
9/46v	[−15 ; 13 ; 10]			42	7.55	V>T	[14 ; 13 ; 11]			47	6.82	V>T
GrF/ProM	[−20 ; 8 ; 3]			9	5.63	V>T	[19 ; 8 ; 4]			34	7.64	V>T
44	[−15 ; 1 ; 8]			3	5.16	V>T	[15 ; 4 ; 7]			36	8.66	V>T
Orbitofrontal areas												
11	[−14 ; 12 ; 9]			*	4.92	V>T	[11 ; 14 ; 9]			*	4.85	V>T
13	[−11 ; 10 ; 7]			*	4.76	T>V	[7 ; 10 ; 4]			*	4.66	T>V

*: ROI created by an 8 mm3 sphere. In gray, the ROIs identified on the group but not on the single subject at uncorrected level. The table describes the anatomical localization of each ROI with respect to the anterior commissure, its size, the associated maximum t-score and whether a significant difference is observed between the tactile and visual PSCs with respect to fixation.

information. Confirming this, the monkeys' fixation performance didn't vary between the tactile and visual runs (One-way ANOVA, M1, $p = 0.98$, M2, $p = 0.23$). A finer analysis of fixation performance as a function of the stimulation blocs in each type of runs is provided in the supplementary information. The potential eye movement or blink confound are further explored below. Air-puffs are also often suspected to activate the auditory system. In the present study, the air-puff delivery system was placed outside the MRI scanner room and the monkeys were wearing headphones to protect their hearing from the high intensity sound produced by the scanner. By placing a microphone inside the headphones, we confirm that no air-puff triggered sound could be recorded, whether in the absence or presence of a weak MRI scanner noise (see supplementary material). We also show that none of the tactile contrasts of interest produced an activation similar to that obtained for pure auditory stimulations (see supplementary material), in the core auditory region, on the inferior lateral bank of the lateral sulcus. *Eye movements*. Monkeys were required to maintain their gaze on a small fixation point, within a tolerance window of $2° \times 2°$. This was controlled online and was used to motivate the animal to maximize fixation rates (as fixation disruptions, such as saccades or drifts, affected the reward schedule). Eye traces were also analyzed offline for the selection of the runs to include in the analysis (good fixation for 85% of the run duration, with no major fixation interruptions). A statistical analysis (already mentioned above) indicates that the monkeys' performance was not significantly different across the visual or tactile (One-way ANOVA, M1, $p = 0.75$, M2, $p = 0.65$). This suggests that the overall oculomotor behavior was constant across types of runs. Importantly, the frontal eye fields (FEF, Bruce and Goldberg, 1985) and the lateral intraparietal area (LIP, Barash et al., 1991; Ben Hamed et al., 2001, 2002), two key cortical oculomotor regions that are activated by eye movements including microsaccades, are not identified in our successive analyses, while their activity can be shown to correlate with the eye movements regressor of our fMRI design (data not shown). *Eye blinks*. Last, air-puffs to the face might have evoked eye blinks inducing some degree of variability in the point of impact of the air-puffs, but most importantly might have led to a confound between eye blink activations and face tactile activations. In a recent study (Guipponi et al., 2014), we identified the cortical network activated by eye blinks. Several regions highlighted by this analysis, such as medial parietal area MIP and the lateral most portion of precentral area ProM, are not reported in the present study. This greatly minimizes blinks as potential confound. *Reward schedule*. The reward schedule was the same between tactile and visual runs, and was directly related to the fixation performance of the animals. Since performance was similar in both types of runs, reward schedule was also similar.

Results

Monkeys were exposed, in independent time series, to visual (Fig. 2, upper panel, red scale, static visual stimulations versus fixation contrast) or tactile (Fig. 2, upper panel, green scale, center of the face tactile stimulations versus fixation contrast) stimulations, while fixating a central point. In the following, we specifically focus on the visuo-tactile conjunction network, i.e. on the functional network that is activated both by visual and tactile stimulations.

Unimodal visual and tactile cortical networks

In order to identify the inter-individual visuo-tactile convergence invariants between the two monkeys, we performed a group analysis allowing to identify the cortical regions that are robustly activated in both monkeys (Fig. 2). Static visual stimulations massively activated the occipital striate and extrastriate areas, the temporal cortex (superior temporal sulcus), the parietal cortex (inferior and medial parietal convexity and the lateral and posterior parts of the intraparietal sulcus), the prefrontal cortex (principal and arcuate sulci) and the inferior orbitofrontal cortex (Fig. 2, upper panel, red scale). Center of the face tactile stimulations strongly activated primary (central sulcus) and secondary (lateral sulcus) somatosensory cortices, the cingulate cortex, the parietal cortex (anterior superior and inferior parietal convexities, anterior intraparietal sulcus), the prefrontal cortex (ventro-lateral prefrontal cortex and premotor cortex) and the inferior orbitofrontal cortex (Fig. 2, upper panel, green scale).

Visuo-tactile convergence network

Fig. 2 (lower panel, purple scale) represents the visuo-tactile conjunction statistical maps identifying the cortical regions responding both to static visual stimuli and center of the face tactile stimuli. This analysis reveals parietal activations including posterior intraparietal area PIP, ventral intraparietal area VIP, area 7b and parietal opercular area 7op; prefrontal activations in area 46v/9, precentral area F4/F5, area 44 at the fundus of the inferior branch of the arcuate sulcus and prefrontal area GrF or ProM (GrF, Petrides et al., 2005; ProM, Belmalih et al., 2009); cingulate activations in area 24c-d; insular activations in area Pi and in a region anterior to SII/PV in the upper bank of the lateral sulcus, which we call SII*; and orbitofrontal activations in areas 11 and 13. Interestingly, both visual and tactile stimulations also activated, bilaterally, visual striate and extrastriate areas (V1, V2, V3, V3A), medial superior temporal area MST, as well as somatosensory area 2. This analysis allows to identify strong multisensory convergence invariants between the two monkeys.

In order to analyze the visual and tactile response patterns in these convergence regions, at the same time as also gain an insight on inter-individual differences in multisensory convergence, we additionally performed an individual visuo-tactile conjunction analysis (as above, but on each individual monkey). These maps are remarkably similar to the group map presented in Fig. 2 (data not shown; to some exceptions described in Table 1 and below). For each monkey, regions of interest (ROIs) were then extracted from the individual monkey conjunction analysis, and assigned to a given cortical area based on their location on the individual's own brain (see methods, Table 1).

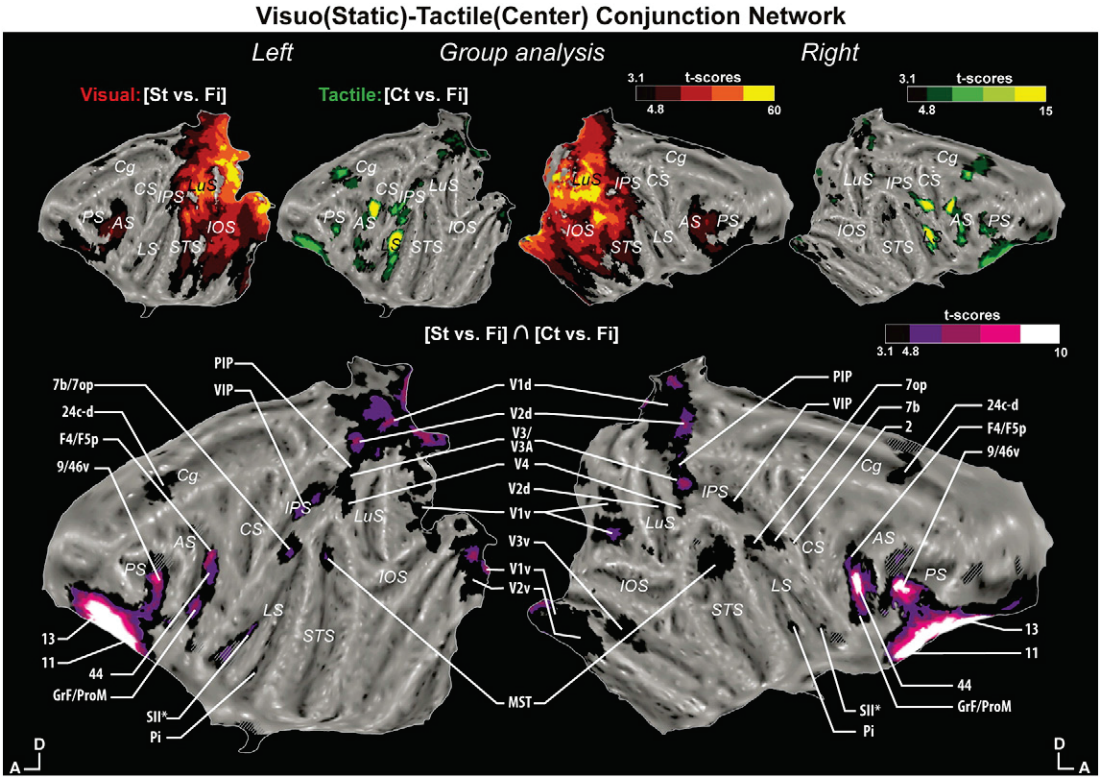

Fig. 2. Visual, tactile modalities and their convergence network. Activations are presented on the flattened representation of the cortex obtained with Caret. The upper part of the figure shows the unimodal activations: (1) static visual stimulations versus fixation contrast (black regions correspond to t scores >= 3.1, $p < 0.001$ uncorrected level, and t scores >4.8, $p < 0.05$, FWE-corrected level; the regions significant at corrected level, $p < 0.05$ FWE, are associated with the red color scale); and (2) tactile center of the face stimulations versus fixation contrast (idem but with a green color scale). The lower part of the figure provides whole-brain flat maps of the visuo-tactile conjunction analysis (idem but with a purple color scale). The contrasts used for the conjunction are the unimodal visual and tactile contrasts described above. A, Anterior; D, Dorsal; MST: medial superior temporal area; Pi: parainsular cortex; PIP: posterior intraparietal area; SII*: secondary somatosensory cortex, anteriorly; VIP: ventral intraparietal area; V1v: visual area V1, ventral part; V1c: visual area V1, central part; V1d: visual area V1, dorsal part; V2v: visual area V2, ventral part; V2d: visual area V2, dorsal part; V3: visual area V3; V3A: visual area V3A; 2: somatosensory area 2; F4/F5: activation overlapping with areas F4 and F5p; 7b: somatosensory area 7b; 7op: opercular area 7; 44: area 44; GrF/ProM: area GrF or ProM; 11: orbitofrontal area 11; 13: orbitofrontal area 13; 24c-d: cingulate area 24c-d; 9/46v: area 9/46v. Cortical sulci: AS, arcuate sulcus; Cg, cingulate sulcus; CS, central sulcus; IOS, inferior occipital sulcus; IPS, intraparietal sulcus; LS, lateral (Sylvian) sulcus; LuS, lunate sulcus; PS, principal sulcus; STS, superior temporal sulcus.

Focusing on the inter-individual invariants, Fig. 3 represents the percentage signal change (PSC) with respect to the fixation baseline, measured during each of the reference visual (red bars) and the tactile (green bars) stimulation blocs, for the ROIs that are also identified on the group analysis presented in Fig. 2. By definition, all these ROIs have significant PSCs with respect to the fixation baseline, both during the reference visual stimulation blocs and the reference tactile stimulation blocs (Fig. 3, with few exceptions discussed below). As expected, all visual striate and extrastriate areas have significantly higher visual than tactile PSCs. In contrast, somatosensory area 2, in the precentral cortex, has significantly higher tactile than visual PSCs. In the parietal convergence areas, visual responses dominated, to the exception of the right and left anterior VIP and the left 7op areas identified in monkey M1. This also tended to be the case in the cingulate convergence regions though, this was significantly so in only two hemispheres out of four. In the frontal and prefrontal cortex, areas 11, 44, Grf/ProM and 9/46v have, overall, stronger visual than tactile PSCs, while areas 13 and F4/F5 have stronger tactile than visual PSCs. SII* and Pi can be identified on the group conjunction analysis but not on the individual conjunction analysis of monkey M1. We thus defined ROIs on the group and probed the corresponding PSCs in monkey M1. In both hemispheres, visual PSCs were positive. However they failed to reach significance. We predict that more complex textured stimuli associated with specific tactile exploration behavior can lead to stronger visual activations of this region. Unpublished data from our own group indeed indicates that 3D objects placed close to the monkeys' face do activate this cortical region, bilaterally in these same two monkeys. MST and 24c-d can also be identified on the group conjunction analysis but not on the individual conjunction analysis of M2 and M1 respectively. Both the visual and tactile PSCs within the ROIs defined on the group conjunction analyses for these two regions are statistically different from zero.

A certain degree of inter-individual variability can also be observed across monkeys. Specifically, monkey M1 has two bilateral visuo-tactile convergence regions in the fundus of the intra-parietal sulcus, which we here call VIP anterior and VIP posterior (VIP, for ventral intraparietal area, Guipponi et al., 2013; please note that this is in no way the suggestion of a new nomenclature; rather it is a label that allows us to describe the functional properties at these two distinct fundal IPS cortical sites identified in monkey M1), as well as a bilateral prefrontal visuo-tactile convergence in F5a. This monkey additionally has unilateral visuo-tactile convergence regions, in the fundus of temporal sulcus (area FST), in parietal area 7b and in precentral somatosensory area 3a. Monkey M2 has a bilateral visuo-tactile convergence in the preSMA, and in insular area Ig. This monkey additionally has a unilateral visuo-tactile convergence region, in somatosensory area SII/PV.

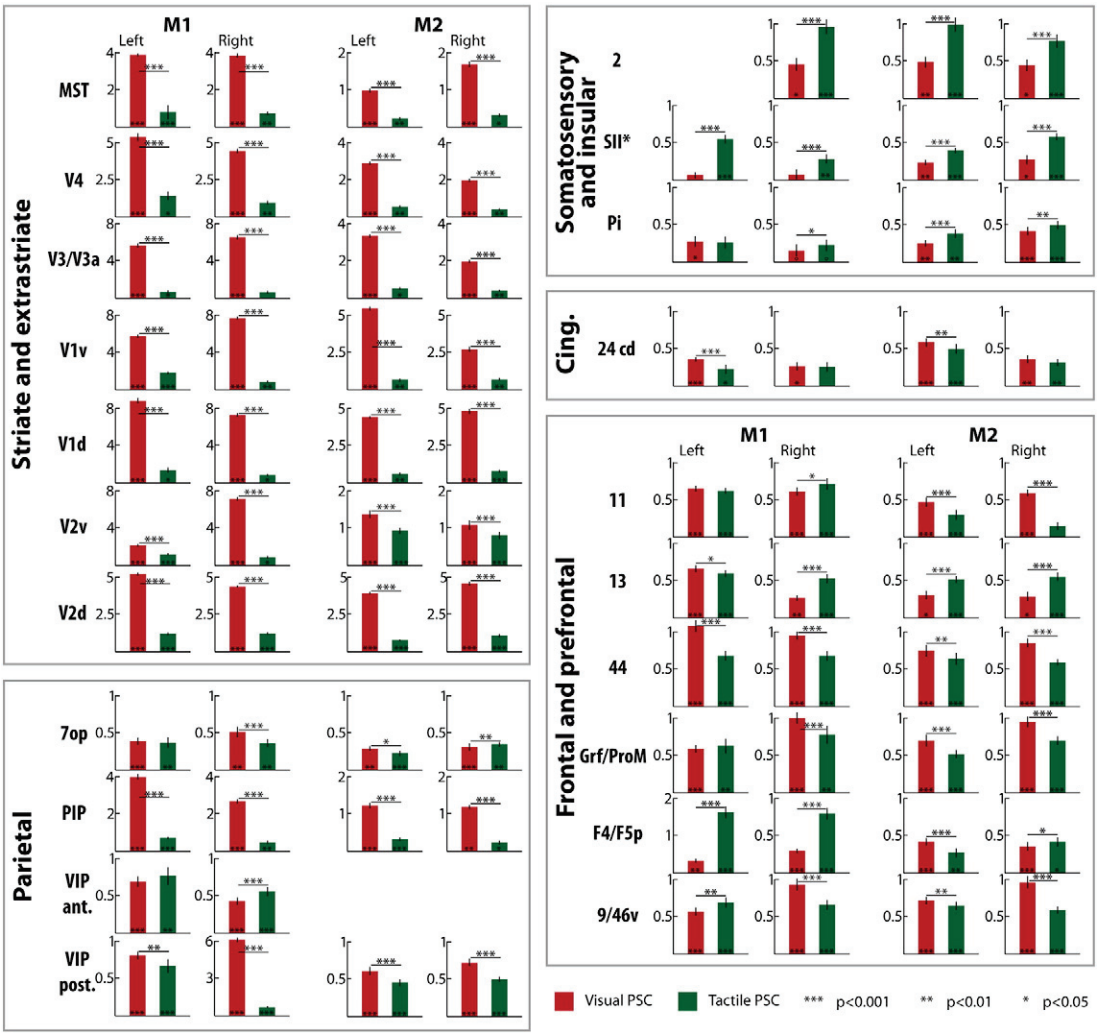

Fig. 3. Percentage signal change (PSC) with respect to the fixation baseline, for the static visual stimulation blocks (visual runs, red) and the tactile to the center of the face stimulation blocks (tactile runs, green), for each of the regions of interest (ROIs) presented in Fig. 2, as identified from the individual conjunction analysis maps of monkeys M1 (left most columns) and M2 (right most columns), for the left (left) and right (right) hemispheres. The significance of each PSC is indicated (° < 0.07; * < 0.05; ** < 0.01; *** < 0.001), as well as the significance of the difference between the visual and tactile PSCs.

Visuo-tactile convergence depends on the location of the tactile stimulation on the body

Fig. 4 reproduces the above described visuo-tactile convergence network for tactile stimulations to the center of the face (light green, 2467 significant voxels in all), together with the visuo-tactile convergence networks defined by periphery of the face (middle scale green, 1329 significant voxels in all) and shoulders (dark green, 259 significant voxels in all) tactile stimulations. Center of the face tactile stimulations globally activate a larger visuo-tactile convergence network, only partially overlapping the visuo-tactile convergence networks defined by the periphery of the face (overlap of 410 significant voxels, 16.6% of Center of the face visuo-tactile convergence) and shoulder tactile stimulations (overlap of 65 significant voxels, 2.6% of Center of the face visuo-tactile convergence). In particular, while some convergence regions were activated by the three types of tactile stimulations, other regions were activated by only one or two types of tactile stimulations (see supplementary information for more detailed quantifications). Importantly, within the occipital, posterior parietal and temporal visual cortex, visuo-tactile convergence spared the central most visual representation (within the central 1.5°, Fig. 4, white shaded cortex, as defined using standard retinotopic localizers, Fize et al., 2003) and prevailed in regions representing the peripheral visual field (Fig. 4, dark gray shading; a further close comparison with Fize et al., 2003, suggests maximum convergence beyond the central 5 to 7°). This preferential visuo-tactile convergence in the cortical regions representing peripheral vision was present whether the convergence was defined using center of the face (peripheral visual field: 1065 voxels (43.1% of a total of 2467 voxels); central visual field: 101 voxels (4.1% of a total of 2467 voxels)), periphery of the face (peripheral visual field: 447 voxels (33.6% of a total of 1329 voxels); central visual field: 118 voxels (8.9% of a total of 1329 voxels)), or shoulder tactile stimulations (peripheral visual field: 81 voxels (31.2% of a total of 259 voxels); central visual field: 24 voxels (9.3% of a total of 259 voxels), see supplementary information).

Visuo-tactile convergence depends on the type of visual stimulation used

Fig. 5 reproduces the visuo-tactile convergence network presented in Fig. 2 for static visual stimulations (yellow, 2467 significant voxels in all), together with the visuo-tactile convergence networks defined by coherent movement visual stimulations (orange, 2374 significant voxels in all) and scrambled visual stimulations (dark red, 1898 significant voxels in all). Static visual stimulations reveal the largest visuo-tactile convergence cortical network, embedding most of the visuo-tactile convergence activations revealed by the coherent (overlap of 2181 significant voxels, 88.4% of static visuo-tactile convergence) or scrambled (overlap of 1860 significant voxels, 75.4% of static visuo-tactile convergence, see supplementary information for more detailed quantifications) visual stimulation modalities. However, it is interesting to note that some cortical regions such as the anterior cingulate cortex and the lateral sulcus activations are not activated by scrambled visual stimuli.

Discussion

We describe an extended network of visuo-tactile convergence, involving both early sensory processing and higher level associative cortical areas, the precise configuration of which depends upon the sensory stimulation being investigated. In the following, we discuss the functional and physiological implications of these observations.

Multisensory convergence at early sensory processing stages

We describe widespread somatosensory functional influences onto the striate and extrastriate cortex, capturing the spatial extent of the synaptic consequences of these somatosensory projections onto the visual cortex (Goense and Logothetis, 2008; Logothetis et al., 2001; Logothetis and Pfeuffer, 2004; Magri et al., 2012). These are not expected to necessarily be at the origin of tactile spikes in the visual cortex, but rather of the modulation of visual responses by tactile stimuli (often interpreted as attention-related effects: Sathian et al. (1997); Macaluso et al. (2000); Amedi et al. (2001)).

These influences are remarkably widespread, covering almost 50% of the visual cortex dedicated to the representation of the peripheral visual field. Surprisingly, there are very few accounts of direct anatomical projections from low level somatosensory cortices onto the visual cortex. Cappe and Barone (2005); Cappe et al. (2009) describe, in the marmoset, direct projections from visual area MTc onto somatosensory areas 1 and 3a, but no reverse projections. Clavagnier et al. (2004) describe projections from the multisensory superior temporal polysensory area STP onto V1, possibly at the origin of both auditory and somatosensory inputs on this area. However, STP is unlikely at the source of the entire visuo-tactile convergence we describe in the visual cortex as visuo-tactile convergence within STP does not represent the center of the face (Fig. 4). Privileged anatomical connections between somatosensory area 2 and the somatosensory complex SII/PV on the one hand and visual areas V1, V2, V3A and MST might have been missed, in the absence of functional indications allowing to precisely target tracer injections at

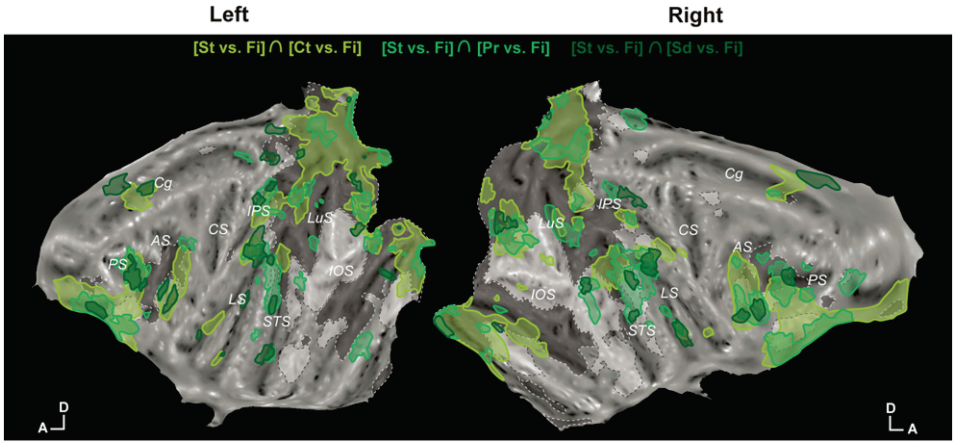

Fig. 4. Visuo-tactile activations for the center of the face, periphery of the face, and shoulders presented on whole-brain flat maps at $p < 0.001$ uncorrected level. For every conjunction analyses, the visual component is the static visual stimulations versus fixation contrast. The center of the face (light green), periphery of the face (middle scale green), and shoulder (dark green) components of the conjunction correspond, respectively, to the center of the face versus fixation, periphery of the face versus fixation, and shoulder versus fixation contrasts. The hyphenated white (delimiting dark background) and black (delimiting white background) lines represent respectively the center and the peripheral retinotopic representations. For other conventions, see Fig. 2.

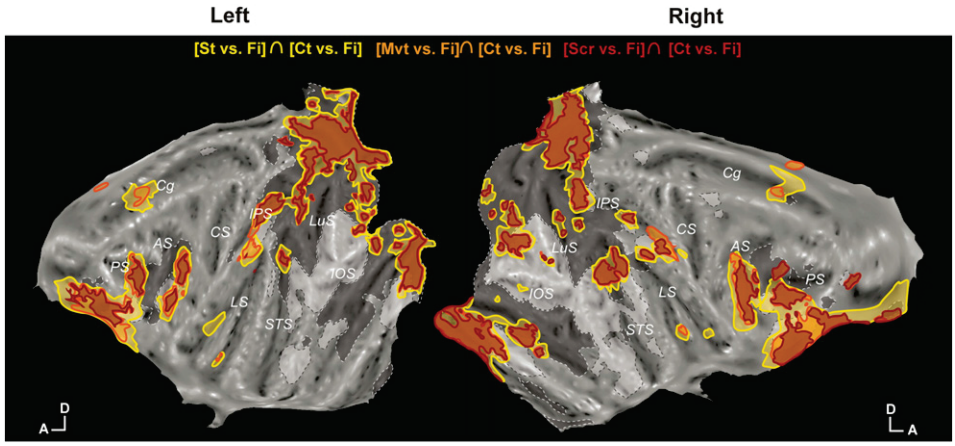

Fig. 5. Visuo-tactile activations for the static visual stimulations, the movement visual stimulations and the scrambled visual stimulations presented on whole-brain flat maps at $p < 0.001$ uncorrected level. For every conjunction analyses, the tactile component is the center of the face versus fixation contrast. The static visual stimulation (yellow), movement visual stimulation (orange), and scrambled visual stimulation (dark red) components of the conjunction correspond, respectively, to the static visual stimulations versus fixation, movement visual stimulations versus fixation, and scrambled visual stimulations versus fixation contrasts. The hyphenated white (delimiting dark background) and black (delimiting white background) lines represent respectively the center and the peripheral retinotopic representations. For other conventions, see Fig. 2.

relevant sites. For example, though quite large, the anatomical tracer injections used in the recent studies by Markov et al. (2011, 2013, 2014) to describe the large-scale regularities in macaque cortical networks, rarely encompass the entire anatomically defined area. Alternatively, a sub-cortical route could also mediate the functional connectivity we describe here (Liang et al., 2013). High resolution fMRI allowing a functional mapping of the thalamus and a quantification of effective thalamocortical connectivity, coupled with tracer injections targeted to selected functional visuo-tactile convergence ROIs could be used to directly address this question.

Interestingly, visuo-tactile convergence within the visual cortex is localized in the peripheral visual field representation, similar to what is described for the auditory projections (Falchier et al., 2002; Rockland and Ojima, 2003) and putative proprioceptive projections (e.g. in relation with blinks, Guipponi et al., 2014), onto areas V1 and V2. The functional significance of this bias for the periphery of the visual field is unclear. Multisensory integration enhances perception when sensory inputs are uncertain, the combination of the several incoming sensory information allowing to disambiguate this uncertainty (Alais and Burr, 2004; Ernst and Banks, 2002). When a given sensory modality provides enough information about the environment, the benefit of multisensory integration decreases both as measured behaviorally (Alais and Burr, 2004; Ernst and Banks, 2002) and at the neuronal level (Beauchamp, 2005; Fetsch et al., 2013; Helbig et al., 2012). This principle could be at the origin of the progressive evolutionary selection of heteromodal projections specifically onto cortical regions representing the periphery of the visual field.

This visuo-tactile convergence provides the neural substrates for the modulation of visual cortex by tactile stimulation (Amedi et al., 2001; Macaluso et al., 2000; Sathian et al., 1997). Importantly, disrupting the visual cortex alters in turn tactile discrimination (Zangaladze et al., 1999). Concordantly, visuo-tactile convergence is also observed on the upper bank of the lateral sulcus (possibly within the SII/PV complex) as well as in area 2. Its spatial extent is much smaller than what is observed in the visual cortex. This could reflect a major functional difference between vision and somatosensation. Alternatively, visuo-tactile convergence within the somatosensory pathway might be specific of more complex visual stimuli than those used in the present study, such as small 3D objects and textured stimuli potentially evoking tactile experience.

Multisensory convergence in higher-order associative cortical regions

We confirm multisensory convergence in several higher order cortical regions: the posterior parietal cortex (Hikosaka et al., 1988; Duhamel et al., 1998; Bremmer et al., 1999, 2000, 2002a,b; Avillac et al., 2004, 2005, 2007; Schlack et al., 2005; Rozzi et al., 2008; Guipponi et al., 2013), the anterior parietal cortex (Hikosaka et al., 1988; Huang et al., 2012), the superior temporal sulcus (Barraclough et al., 2005; Beauchamp et al., 2004; Bruce et al., 1981; Hikosaka et al., 1988) including medial superior temporal area MST as described in humans (Beauchamp et al., 2007), the posterior arcuate prefrontal cortex (Graziano et al., 1994, 1997; Graziano and Gandhi, 2000; Graziano and Cooke, 2006; Fogassi et al., 1996), the insular and peri-insular cortex (Augustine, 1996), the cingulate cortex (Laurienti et al., 2003) as well as the inferior orbitofrontal cortex (Rolls, 2004; Rolls and Baylis, 1994). Several of these higher-order associative cortical regions have been described to be the site of multisensory visuo-tactile integration, a process through which the response of individual neurons to a bimodal sensory input differs from the sum of their responses to each unimodal stimulus presented on their own. This is for example the case for the ventral intraparietal area within the parietal cortex (Duhamel et al., 1997; Avillac et al., 2004, 2007) and the prefrontal polysensory zone in the posterior arcuate prefrontal cortex (Cooke and Graziano, 2004), two cortical regions that are suggested to subserve a peripersonal defense space (Graziano et al., 2002; Graziano and Cooke, 2006; Cléry et al., 2014) and the prediction of impact to the face (Cléry et al., 2014, 2015). As is the case for these two cortical regions, each of the visuo-tactile convergence regions highlighted by the present work could contribute to a distinct functional aspect of the incoming visuo-tactile information (e.g. location, identity, texture, emotional valence, Werner and Noppeney, 2010). Remarkably, overall, a large portion of the cortex is involved in this process.

Multisensory convergence as a general property of the neocortex

We show that the visuo-tactile convergence patterns vary within these several cortical regions as a function of the specific stimulation type. Multisensory convergence within the visual cortex is largest for tactile stimuli directed to the center of the face, but this bias is less marked for the rest of the cortex. In the orbitofrontal cortex convergence patterns are co-localized for all tactile stimulation types. Elsewhere, the overlap ranges from partial (inferior precentral gyrus, ventral premotor cortex) to weak (superior temporal cortex, parietal cortex, cingulate cortex), potentially suggesting a topographical organization of these convergence maps. In particular, and consistent with the recent description of a higher-level visuo-tactile homunculus within the parietal cortex (Huang et al., 2012), we show a parietal visuo-tactile-center-of-the-face activation in the fundus and medial bank of the

intraparietal sulcus. Medial to it and posteriorly, we describe a parietal visuo-tactile-shoulder activation. A study investigating visuo-tactile convergence using topographically more distant tactile stimuli (e.g. center of the face, arm and foot) would allow to precisely test for parietal as well as temporal and cingulate visuo-tactile homunculi.

Likewise, the visuo-tactile convergence patterns also varied within these several cortical regions as a function of the characteristics of the visual stimulations. Static visual stimulations evoked the largest visuo-tactile convergence. In lower order visual areas, coherent movement and scrambled movement stimulations led to the same patterns of visuo-tactile convergence, while in higher order areas, coherent visual movement evoked larger convergence patterns. Some regions, such as the anterior cingulate cortex and the insula showed visuo-tactile convergence only for static or coherent movement visual stimuli.

Varying the nature of visual stimulus (e.g. small moving object, large field visual stimuli, 3D objects, textured objects), tactile stimuli (e.g. painful, hot or cold, mechanical, textured) as well as the behavioral requirements (e.g. no task as here, detection, discrimination), is expected to reveal new visuo-tactile convergence patterns. For example, Vasconcelos et al. (2011) show that, during a free tactile exploration task, the visual neurons of rats carry comparable amount of information about the identity of objects as somatosensory neurons but not during a tactile discrimination task. At the neuronal level, phase resetting mechanisms could be at the origin of such a dynamic (see van Atteveldt et al. (2014) for a review). We thus propose that multisensory convergence is a general (Schroeder and Foxe, 2005), context-dependent, dynamical property of the neocortex, subserving 'amodal' perception and decision-making processes, that is, processes that are not determined by unique sensory channels.

Cortical sulci

AS, arcuate sulcus; CgS, cingulate sulcus; CeS; central sulcus; IOS, inferior occipital sulcus; IPS, intraparietal sulcus; LaS, lateral (Sylvian) sulcus; LuS, lunate sulcus; OTS, occipital temporal sulcus; POS, parieto-occipital sulcus; PS, principal sulcus; STS, superior temporal sulcus.

Acknowledgments

We thank S. Maurin for the technical support and J.L. Charieau and F. Hérant for the animal care. This work was supported by Agence Nationale de la Recherche (ANR-05-JCJC-0230-01).

Appendix A. Supplementary data

Supplementary data to this article can be found online at http://dx.doi.org/10.1016/j.neuroimage.2015.05.022.

References

Alais, D., Burr, D., 2004. The ventriloquist effect results from near-optimal bimodal integration. Curr. Biol. 14, 257–262. http://dx.doi.org/10.1016/j.cub.2004.01.029.
Amedi, A., Malach, R., Hendler, T., Peled, S., Zohary, E., 2001. Visuo-haptic object-related activation in the ventral visual pathway. Nat. Neurosci. 4, 324–330. http://dx.doi.org/10.1038/85201.
Augustine, J.R., 1996. Circuitry and functional aspects of the insular lobe in primates including humans. Brain Res. Brain Res. Rev. 22, 229–244.
Avillac, M., Olivier, E., Denève, S., Ben Hamed, S., Duhamel, J.-R., 2004. Multisensory integration in multiple reference frames in the posterior parietal cortex. Cogn. Process. 5, 159–166. http://dx.doi.org/10.1007/s10339-004-0021-3.
Avillac, M., Denève, S., Olivier, E., Pouget, A., Duhamel, J.-R., 2005. Reference frames for representing visual and tactile locations in parietal cortex. Nat. Neurosci. 8, 941–949. http://dx.doi.org/10.1038/nn1480.
Avillac, M., Ben Hamed, S., Duhamel, J.-R., 2007. Multisensory integration in the ventral intraparietal area of the macaque monkey. J. Neurosci. Off. J. Soc. Neurosci. 27, 1922–1932. http://dx.doi.org/10.1523/JNEUROSCI.2646-06.2007.
Barash, S., Bracewell, R.M., Fogassi, L., Gnadt, J.W., Andersen, R.A., 1991. Saccade-related activity in the lateral intraparietal area. II. Spatial properties. J. Neurophysiol. 66, 1109–1124.
Barraclough, N.E., Xiao, D., Baker, C.I., Oram, M.W., Perrett, D.I., 2005. Integration of visual and auditory information by superior temporal sulcus neurons responsive to the sight of actions. J. Cogn. Neurosci. 17, 377–391. http://dx.doi.org/10.1162/0898929053279586.
Beauchamp, M.S., 2005. See me, hear me, touch me: multisensory integration in lateral occipital-temporal cortex. Curr. Opin. Neurobiol. 15, 145–153. http://dx.doi.org/10.1016/j.conb.2005.03.011.
Beauchamp, M.S., Lee, K.E., Argall, B.D., Martin, A., 2004. Integration of auditory and visual information about objects in superior temporal sulcus. Neuron 41, 809–823. http://dx.doi.org/10.1016/S0896-6273(04)00070-4.
Beauchamp, M.S., Yasar, N.E., Kishan, N., Ro, T., 2007. Human MST but not MT responds to tactile stimulation. J. Neurosci. Off. J. Soc. Neurosci. 27, 8261–8267. http://dx.doi.org/10.1523/JNEUROSCI.0754-07.2007.
Belmalih, A., Borra, E., Contini, M., Gerbella, M., Rozzi, S., Luppino, G., 2009. Multimodal architectonic subdivision of the rostral part (area F5) of the macaque ventral premotor cortex. J. Comp. Neurol. 512, 183–217. http://dx.doi.org/10.1002/cne.21892.
Ben Hamed, S., Duhamel, J.R., Bremmer, F., Graf, W., 2001. Representation of the visual field in the lateral intraparietal area of macaque monkeys: a quantitative receptive field analysis. Exp. Brain Res. 140, 127–144.
Ben Hamed, S., Duhamel, J.-R., Bremmer, F., Graf, W., 2002. Visual receptive field modulation in the lateral intraparietal area during attentive fixation and free gaze. Cereb. Cortex 1991 (12), 234–245.
Bremmer, F., Graf, W., Ben Hamed, S., Duhamel, J.R., 1999. Eye position encoding in the macaque ventral intraparietal area (VIP). Neuroreport 10, 873–878.
Bremmer, F., Duhamel, J.R., Ben Hamed, S., Graf, W., 2000. Stages of self-motion processing in primate posterior parietal cortex. Int. Rev. Neurobiol. 44, 173–198.
Bremmer, F., Duhamel, J.-R., Ben Hamed, S., Graf, W., 2002a. Heading encoding in the macaque ventral intraparietal area (VIP). Eur. J. Neurosci. 16, 1554–1568.
Bremmer, F., Klam, F., Duhamel, J.-R., Ben Hamed, S., Graf, W., 2002b. Visual–vestibular interactive responses in the macaque ventral intraparietal area (VIP). Eur. J. Neurosci. 16, 1569–1586.
Brett, M., Anton, J.-L., Valabregue, R., Poline, J.-B., 2002. Region of interest analysis using the MarsBar toolbox for SPM 99. Present. 8th Int. Conf. Funct. Mapp. Hum. Brain June 2–6 2002 Sendai Jpn 16, p. S497.
Bruce, C.J., Goldberg, M.E., 1985. Primate frontal eye fields. I. Single neurons discharging before saccades. J. Neurophysiol. 53, 603–635.
Bruce, C., Desimone, R., Gross, C.G., 1981. Visual properties of neurons in a polysensory area in superior temporal sulcus of the macaque. J. Neurophysiol. 46, 369–384.
Budinger, E., Heil, P., Hess, A., Scheich, H., 2006. Multisensory processing via early cortical stages: connections of the primary auditory cortical field with other sensory systems. Neuroscience 143, 1065–1083. http://dx.doi.org/10.1016/j.neuroscience.2006.08.035.
Cappe, C., Barone, P., 2005. Heteromodal connections supporting multisensory integration at low levels of cortical processing in the monkey. Eur. J. Neurosci. 22, 2886–2902. http://dx.doi.org/10.1111/j.1460-9568.2005.04462.x.
Cappe, C., Rouiller, E.M., Barone, P., 2009. Multisensory anatomical pathways. Hear. Res. 258, 28–36. http://dx.doi.org/10.1016/j.heares.2009.04.017.
Clavagnier, S., Falchier, A., Kennedy, H., 2004. Long-distance feedback projections to area V1: implications for multisensory integration, spatial awareness, and visual consciousness. Cogn. Affect. Behav. Neurosci. 4, 117–126.
Cléry, J., Guipponi, O., Wardak, C., Ben Hamed, S., 2014. Neuronal bases of peripersonal and extrapersonal spaces, their plasticity and their dynamics: knowns and unknowns. Neuropsychologia http://dx.doi.org/10.1016/j.neuropsychologia.2014.10.022.
Cléry, J., Guipponi, O., Odouard, S., Wardak, C., Ben Hamed, S., 2015. Impact prediction by looming visual stimuli enhances tactile detection. J. Neurosci. 35, 4179–4189. http://dx.doi.org/10.1523/JNEUROSCI.3031-14.2015.
Cooke, D.F., Graziano, M.S.A., 2004. Sensorimotor integration in the precentral gyrus: polysensory neurons and defensive movements. J. Neurophysiol. 91, 1648–1660. http://dx.doi.org/10.1152/jn.00955.2003.
De la Mothe, L.A., Blumell, S., Kajikawa, Y., Hackett, T.A., 2006. Cortical connections of the auditory cortex in marmoset monkeys: core and medial belt regions. J. Comp. Neurol. 496, 27–71. http://dx.doi.org/10.1002/cne.20923.
Duhamel, J.R., Bremmer, F., Ben Hamed, S., Graf, W., 1997. Spatial invariance of visual receptive fields in parietal cortex neurons. Nature 389, 845–848.
Duhamel, J.-R., Colby, C.L., Goldberg, M.E., 1998. Ventral intraparietal area of the macaque: congruent visual and somatic response properties. J. Neurophysiol. 79, 126–136.
Ernst, M.O., Banks, M.S., 2002. Humans integrate visual and haptic information in a statistically optimal fashion. Nature 415, 429–433. http://dx.doi.org/10.1038/415429a.
Falchier, A., Clavagnier, S., Barone, P., Kennedy, H., 2002. Anatomical evidence of multimodal integration in primate striate cortex. J. Neurosci. Off. J. Soc. Neurosci. 22, 5749–5759 (doi:20026562).
Felleman, D.J., Van Essen, D.C., 1991. Distributed hierarchical processing in the primate cerebral cortex. Cereb. Cortex 1991 (1), 1–47.
Fetsch, C.R., DeAngelis, G.C., Angelaki, D.E., 2013. Bridging the gap between theories of sensory cue integration and the physiology of multisensory neurons. Nat. Rev. Neurosci. 14, 429–442. http://dx.doi.org/10.1038/nrn3503.
Fize, D., Vanduffel, W., Nelissen, K., Denys, K., d' Hotel, C.C., Faugeras, O., Orban, G.A., 2003. The retinotopic organization of primate dorsal V4 and surrounding areas: a functional magnetic resonance imaging study in awake monkeys. J. Neurosci. 23, 7395–7406.
Fogassi, L., Gallese, V., Fadiga, L., Luppino, G., Matelli, M., Rizzolatti, G., 1996. Coding of peripersonal space in inferior premotor cortex (area F4). J. Neurophysiol. 76, 141–157.
Ghazanfar, A.A., Schroeder, C.E., 2006. Is neocortex essentially multisensory? Trends Cogn. Sci. 10, 278–285. http://dx.doi.org/10.1016/j.tics.2006.04.008.
Goense, J.B.M., Logothetis, N.K., 2008. Neurophysiology of the BOLD fMRI signal in awake monkeys. Curr. Biol. 18, 631–640. http://dx.doi.org/10.1016/j.cub.2008.03.054.

Graziano, M.S.A., Cooke, D.F., 2006. Parieto-frontal interactions, personal space, and defensive behavior. Neuropsychologia 44, 2621–2635.
Graziano, M.S., Gandhi, S., 2000. Location of the polysensory zone in the precentral gyrus of anesthetized monkeys. Exp. Brain Res. 135, 259–266.
Graziano, M.S., Yap, G.S., Gross, C.G., 1994. Coding of visual space by premotor neurons. Science 266, 1054–1057.
Graziano, M.S., Hu, X.T., Gross, C.G., 1997. Visuospatial properties of ventral premotor cortex. J. Neurophysiol. 77, 2268–2292.
Graziano, M.S.A., Taylor, C.S.R., Moore, T., 2002. Complex movements evoked by microstimulation of precentral cortex. Neuron 34, 841–851.
Guipponi, O., Wardak, C., Ibarrola, D., Comte, J.-C., Sappey-Marinier, D., Pinède, S., Ben Hamed, S., 2013. Multimodal convergence within the intraparietal sulcus of the macaque monkey. J. Neurosci. 33, 4128–4139. http://dx.doi.org/10.1523/JNEUROSCI.1421-12.2013.
Guipponi, O., Odouard, S., Pinède, S., Wardak, C., Ben Hamed, S., 2014. fMRI cortical correlates of spontaneous eye blinks in the nonhuman primate. Cereb. Cortex http://dx.doi.org/10.1093/cercor/bhu038.
Helbig, H.B., Ernst, M.O., Ricciardi, E., Pietrini, P., Thielscher, A., Mayer, K.M., Schultz, J., Noppeney, U., 2012. The neural mechanisms of reliability weighted integration of shape information from vision and touch. NeuroImage 60, 1063–1072. http://dx.doi.org/10.1016/j.neuroimage.2011.09.072.
Hikosaka, K., Iwai, E., Saito, H., Tanaka, K., 1988. Polysensory properties of neurons in the anterior bank of the caudal superior temporal sulcus of the macaque monkey. J. Neurophysiol. 60, 1615–1637.
Huang, R.-S., Chen, C., Tran, A.T., Holstein, K.L., Sereno, M.I., 2012. Mapping multisensory parietal face and body areas in humans. Proc. Natl. Acad. Sci. U. S. A. 109, 18114–18119. http://dx.doi.org/10.1073/pnas.1207946109.
Iurilli, G., Ghezzi, D., Olcese, U., Lassi, G., Nazzaro, C., Tonini, R., Tucci, V., Benfenati, F., Medini, P., 2012. Sound-driven synaptic inhibition in primary visual cortex. Neuron 73, 814–828. http://dx.doi.org/10.1016/j.neuron.2011.12.026.
Kuypers, H.G., Szwarcbart, M.K., Mishkin, M.M., Rosvold, H.E., 1965. Occipitotemporal corticocortical connections in the rhesus monkey. Exp. Neurol. 11, 245–262.
Laurienti, P.J., Wallace, M.T., Maldjian, J.A., Susi, C.M., Stein, B.E., Burdette, J.H., 2003. Cross-modal sensory processing in the anterior cingulate and medial prefrontal cortices. Hum. Brain Mapp. 19, 213–223. http://dx.doi.org/10.1002/hbm.10112.
Lewis, J.W., Van Essen, D.C., 2000. Corticocortical connections of visual, sensorimotor, and multimodal processing areas in the parietal lobe of the macaque monkey. J. Comp. Neurol. 428, 112–137. http://dx.doi.org/10.1002/1096-9861(20001204)428:1<112::AID-CNE8>3.0.CO;2-9.
Liang, M., Mouraux, A., Iannetti, G.D., 2013. Bypassing primary sensory cortices—a direct thalamocortical pathway for transmitting salient sensory information. Cereb. Cortex 1991 (23), 1–11. http://dx.doi.org/10.1093/cercor/bhr363.
Logothetis, N.K., Pfeuffer, J., 2004. On the nature of the BOLD fMRI contrast mechanism. Magn. Reson. Imaging 22, 1517–1531. http://dx.doi.org/10.1016/j.mri.2004.10.018.
Logothetis, N.K., Pauls, J., Augath, M., Trinath, T., Oeltermann, A., 2001. Neurophysiological investigation of the basis of the fMRI signal. Nature 412, 150–157. http://dx.doi.org/10.1038/35084005.
Macaluso, E., Frith, C.D., Driver, J., 2000. Modulation of human visual cortex by crossmodal spatial attention. Science 289, 1206–1208.
Magri, C., Schridde, U., Murayama, Y., Panzeri, S., Logothetis, N.K., 2012. The amplitude and timing of the BOLD signal reflects the relationship between local field potential power at different frequencies. J. Neurosci. Off. J. Soc. Neurosci. 32, 1395–1407. http://dx.doi.org/10.1523/JNEUROSCI.3985-11.2012.
Mandeville, J.B., Choi, J.-K., Jarraya, B., Rosen, B.R., Jenkins, B.G., Vanduffel, W., 2011. fMRI of cocaine self-administration in macaques reveals functional inhibition of basal ganglia. Neuropsychopharmacology 36, 1187–1198. http://dx.doi.org/10.1038/npp.2011.1.
Markov, N.T., Misery, P., Falchier, A., Lamy, C., Vezoli, J., Quilodran, R., Gariel, M.A., Giroud, P., Ercsey-Ravasz, M., Pilaz, L.J., Huissoud, C., Barone, P., Dehay, C., Toroczkai, Z., Van Essen, D.C., Kennedy, H., Knoblauch, K., 2011. Weight consistency specifies regularities of macaque cortical networks. Cereb. Cortex 1991 (21), 1254–1272. http://dx.doi.org/10.1093/cercor/bhq201.
Markov, N.T., Ercsey-Ravasz, M., Lamy, C., Ribeiro Gomes, A.R., Magrou, L., Misery, P., Giroud, P., Barone, P., Dehay, C., Toroczkai, Z., Knoblauch, K., Van Essen, D.C., Kennedy, H., 2013. The role of long-range connections on the specificity of the macaque interareal cortical network. Proc. Natl. Acad. Sci. U. S. A. 110, 5187–5192. http://dx.doi.org/10.1073/pnas.1218972110.
Markov, N.T., Ercsey-Ravasz, M.M., Ribeiro Gomes, A.R., Lamy, C., Magrou, L., Vezoli, J., Misery, P., Falchier, A., Quilodran, R., Gariel, M.A., Sallet, J., Gamanut, R., Huissoud, C., Clavagnier, S., Giroud, P., Sappey-Marinier, D., Barone, P., Dehay, C., Toroczkai, Z., Knoblauch, K., Van Essen, D.C., Kennedy, H., 2014. A weighted and directed interareal connectivity matrix for macaque cerebral cortex. Cereb. Cortex 1991 (24), 17–36. http://dx.doi.org/10.1093/cercor/bhs270.
Massopust, L.C., Barnes, H.W., Verdura, J., 1965. Auditory frequency discrimination in cortically ablated monkeys. J. Aud. Res. 5, 85–93.
Paxinos, G., Huang, X.-F., Toga, A.W., 1999. The Rhesus monkey brain in stereotaxic coordinates.
Petrides, M., Cadoret, G., Mackey, S., 2005. Orofacial somatomotor responses in the macaque monkey homologue of Broca's area. Nature 435, 1235–1238. http://dx.doi.org/10.1038/nature03628.
Rockland, K.S., Ojima, H., 2003. Multisensory convergence in calcarine visual areas in macaque monkey. Int. J. Psychophysiol. Off. J. Int. Organ. Psychophysiol. 50, 19–26.
Rolls, E.T., 2004. Convergence of sensory systems in the orbitofrontal cortex in primates and brain design for emotion. Anat. Rec. A: Discov. Mol. Cell. Evol. Biol. 281, 1212–1225. http://dx.doi.org/10.1002/ar.a.20126.
Rolls, E.T., Baylis, L.L., 1994. Gustatory, olfactory, and visual convergence within the primate orbitofrontal cortex. J. Neurosci. Off. J. Soc. Neurosci. 14, 5437–5452.
Rozzi, S., Ferrari, P.F., Bonini, L., Rizzolatti, G., Fogassi, L., 2008. Functional organization of inferior parietal lobule convexity in the macaque monkey: electrophysiological characterization of motor, sensory and mirror responses and their correlation with cytoarchitectonic areas. Eur. J. Neurosci. 28, 1569–1588. http://dx.doi.org/10.1111/j.1460-9568.2008.06395.x.
Sathian, K., Zangaladze, A., Hoffman, J.M., Grafton, S.T., 1997. Feeling with the mind's eye. Neuroreport 8, 3877–3881.
Schlack, A., Sterbing-D'Angelo, S.J., Hartung, K., Hoffmann, K.-P., Bremmer, F., 2005. Multisensory space representations in the macaque ventral intraparietal area. J. Neurosci. Off. J. Soc. Neurosci. 25, 4616–4625. http://dx.doi.org/10.1523/JNEUROSCI.0455-05.2005.
Schroeder, C.E., Foxe, J., 2005. Multisensory contributions to low-level, "unisensory" processing. Curr. Opin. Neurobiol. 15, 454–458. http://dx.doi.org/10.1016/j.conb.2005.06.008.
Sereno, M.I., Huang, R.-S., 2006. A human parietal face area contains aligned head-centered visual and tactile maps. Nat. Neurosci. 9, 1337–1343. http://dx.doi.org/10.1038/nn1777.
Smiley, J.F., Hackett, T.A., Ulbert, I., Karmas, G., Lakatos, P., Javitt, D.C., Schroeder, C.E., 2007. Multisensory convergence in auditory cortex, I. Cortical connections of the caudal superior temporal plane in macaque monkeys. J. Comp. Neurol. 502, 894–923. http://dx.doi.org/10.1002/cne.21325.
Van Atteveldt, N., Murray, M.M., Thut, G., Schroeder, C.E., 2014. Multisensory integration: flexible use of general operations. Neuron 81, 1240–1253. http://dx.doi.org/10.1016/j.neuron.2014.02.044.
Van Essen, D.C., Drury, H.A., Dickson, J., Harwell, J., Hanlon, D., Anderson, C.H., 2001. An integrated software suite for surface-based analyses of cerebral cortex. J. Am. Med. Inform. Assoc. 8, 443–459. http://dx.doi.org/10.1136/jamia.2001.0080443.
Vanduffel, W., Fize, D., Mandeville, J.B., Nelissen, K., Van Hecke, P., Rosen, B.R., Tootell, R.B., Orban, G.A., 2001. Visual motion processing investigated using contrast agent-enhanced fMRI in awake behaving monkeys. Neuron 32, 565–577.
Vasconcelos, N., Pantoja, J., Belchior, H., Caixeta, F.V., Faber, J., Freire, M.A.M., Cota, V.R., Anibal de Macedo, E., Laplagne, D.A., Gomes, H.M., Ribeiro, S., 2011. Cross-modal responses in the primary visual cortex encode complex objects and correlate with tactile discrimination. Proc. Natl. Acad. Sci. U. S. A. 108, 15408–15413. http://dx.doi.org/10.1073/pnas.1102780108.
Wallace, M.T., Ramachandran, R., Stein, B.E., 2004. A revised view of sensory cortical parcellation. Proc. Natl. Acad. Sci. U. S. A. 101, 2167–2172. http://dx.doi.org/10.1073/pnas.0305697101.
Werner, S., Noppeney, U., 2010. Distinct functional contributions of primary sensory and association areas to audiovisual integration in object categorization. J. Neurosci. Off. J. Soc. Neurosci. 30, 2662–2675. http://dx.doi.org/10.1523/JNEUROSCI.5091-09.2010.
Zangaladze, A., Epstein, C.M., Grafton, S.T., Sathian, K., 1999. Involvement of visual cortex in tactile discrimination of orientation. Nature 401, 587–590. http://dx.doi.org/10.1038/44139.

Appendix 2

Somatosensory, reward, and eye fields organization within the monkey rostral cingulate motor area.

Article in preparation

Somatosensory, reward, and eye fields organization within the monkey cingulate motor areas.

Justine Cléry[1], Céline Amiez[2], Olivier Guiponni[1], Claire Wardak[1], Emmanuel Procyk[2*] and Suliann Ben Hamed[1*]

1. Centre de Neuroscience Cognitive, UMR 5229, CNRS, Université Claude Bernard Lyon1, Bron, France
2. INSERM U846, Stem Cell and Brain Research Institute, UMR S-846, Université Claude Bernard Lyon1, Bron, France

* Authors have equally contributed to this work

Corresponding authors: Suliann Ben Hamed, suliann.benhamed@isc.cnrs.fr, Centre de Neuroscience Cognitive, UMR 5229, 67 bd Pinel, 69675 Bron cedex, France; Emmanuel Procyk, Emmanuel.procyk@inserm.fr

Abstract

Several premotor areas have been identified within the cingulate cortex of human and non-human primates. However, the function of these areas is yet to be uncovered. Recent brain imaging work (fMRI) in humans revealed a topographic anatomo-functional overlap between the processing of feedback during exploratory behaviors and the corresponding body fields in the rostral cingulate motor area (RCZa), suggesting an embodied representation of feedback. In particular, a face field in RCZa processes juice feedback. The embodied principle could be extended such that unexpected or relevant information obtained through the eye or the face might be processed by the corresponding fields in cingulate motor areas. Here we combined fMRI data from multiple experiments to verify whether this would also apply to cingulate functional anatomy in monkeys. We show that activations for juice reward, eye movement, eye blink, and tactile stimulation on the face overlap over two subfields within the cingulate sulcus likely corresponding to the rostral and caudal cingulate motor areas (CMAr and CMAc). This suggest that in monkeys as in humans, behaviorally relevant information is processed through multiple cingulate body/effector maps.

Keywords: Reward, eye movements, feedback, embodied cognition, cingulate cortex

Introduction

Neurophysiological and anatomical studies in animals and neuroimaging studies in humans have identified several subdivisions in the medial wall of the frontal lobe (Neubert et al. 2015; Picard and Strick 1996). One intriguing outcome of these studies is that multiple cognitive, motor, and - or limbic functions are ascribed to the same territories in particular in and around the cingulate sulcus, the so-called midcingulate cortex (Vogt 2009). The issue of identifying functional areas in the midcingulate cortex (MCC) is complicated by the existence of multiple cingulate motor areas (CMAs). In this region, up to 3 CMAs have been described in both humans and monkeys (Shima and Tanji 1998; Dum and Strick 1991; Picard and Strick 1996; Morecraft and Tanji 2009; Amiez and Petrides 2014; Procyk et al. 2014). The rostral cingulate motor area (RCZa in humans, CMAr in monkeys) contains a somatomotor map, defined in particular for the lower limb, the upper limb, and the face. Also, the same area receives input from the spinothalamic pathway involved in pain processing (Misra and Coombes 2015; Dum et al. 2009). This suggests a role of RCZa/CMAr in some kind of motor or sensorimotor control. However, the same region has also been associated with various motivational and cognitive functions like conflict monitoring, feedback monitoring, value-based control of action, and foraging (Procyk et al. 2000; Amiez et al. 2005, 2006; Botvinick 2007; Quilodran et al. 2008; Alexander and Brown 2011; Shackman et al. 2011; Rushworth et al. 2012; Shenhav et al. 2013; Khamassi et al. 2015). This multiplicity of functions suggests either unresolved separation of functional contributions, or integration and convergence of functions.

In more posterior parts of the cingulate sulcus face, arm, and leg fields have been observed but their contribution to behaviour is much less understood (Cadoret and Smith 1997; Crutcher et al. 2004; Wang et al. 2004; Morecraft and Tanji 2009). Only one face field is observed, whereas arm and leg fields might be present in several maps (RCZp and CCZ in humans, and CMAc subdivided in CMAv & d in monkeys). In monkeys, the connectivity of CMAc suggests stronger links to motor control, and the connection with the primary face area (in M1) might be less prominent than for CMAr (Morecraft and Tanji 2009). Its contribution to activations during various fMRI experiments in humans is unclear as

population averaging often prevents clear anatomo-functional identification. Finally, the correspondences between RCZp and CCZ in humans and CMAc or CMAd and CMAv in monkeys are still unclear.

Based on a re-evaluation of the data from the literature, we recently provided support for a principle of embodied feedback in the rostral cingulate motor area (Procyk et al. 2014). In this hypothesis, feedback relevant for adaptation is processed by the body map corresponding to the feedback domain. For instance, juice reward outcomes, particularly used in monkey experiments, would be processed by the face representation in RCZa/CMAr. Our previous work in humans reported a second more caudal activation in MCC (in RCZp) for juice feedback although quite inconsistently across subjects, and rostral to the more caudal CCZ area (Amiez et al. 2013). The feedback embodied hypothesis is strongly supported by human imaging experiments, and a meta-analysis of monkey data suggests the same principle applies in non-human primates (Procyk et al. 2014). However direct evidence in monkeys is lacking. Such evidence would be crucial to validate a hypothesis that clarifies the passionate debates on cingulate functions. In summary, evidence from human experiments strongly suggests that feedback during exploration is processed by somatomotor maps in RCZa and maybe also in RCZp. Confirmations of embodied feedback processing in monkeys' CMAs, and of the respective contributions of rostral and caudal CMAs are necessary to better understand the anatomo-functional organization of MCC.

In this context, we tested with functional magnetic resonance imaging (fMRI) in behaving macaques the relative position of peak activations for reward, eye movements, blink and tactile stimulations on the face and shoulder. We tested whether reward-related activation would anatomically overlap with eye-related (saccade and blink) and other face-related activations, an overlap that would support the embodied feedback hypothesis. We show this overlap in single subject analyses as well as the existence of functional overlaps in two apparent face fields in separate CMAs.

Material and Methods

Subjects and materials

All procedures were in compliance with the guidelines of the European Community on animal care (European Community Council, Directive 2010/63/UE). All the protocols used in this experiment were approved by the local animal care committee (agreement # C2EA42-12-10-0401-002). The animals' welfare and the steps taken to ameliorate suffering were in accordance with the recommendations of the Weatherall report, "The use of non-human primates in research".

Two rhesus monkeys (female M1, male M2, 5-7 years old, 5-7 kg) participated to the study. The animals were implanted with a plastic MRI compatible headset covered by dental acrylic. The anesthesia during surgery was induced by Zoletil (Tiletamine-Zolazepam, Virbac, 5 mg/kg) and followed by Isoflurane (Belamont, 1-2%). Post-surgery analgesia was ensured with Temgesic (buprenorphine, 0.3 mg/ml, 0.01 mg/kg). During recovery, proper analgesic and antibiotic coverage were provided. The surgical procedures conformed to European, and National Institutes of Health guidelines for the care and use of laboratory animals.

During the scanning sessions, monkeys sat in a sphinx position in a plastic monkey chair positioned within a horizontal magnet (1.5-T MR scanner Sonata; Siemens, Erlangen, Germany) facing a translucent screen placed 90 cm from the eyes. Their head was restrained and equipped with MRI-compatible headphones customized for monkeys (MR Confon GmbH, Magdeburg, Germany). A radial receive-only surface coil (10-cm diameter) was positioned above the head. Eye position was monitored at 120 Hz during scanning using a pupil-corneal reflection tracking system (Iscan®, Cambridge, MA). Monkeys were rewarded with liquid dispensed by a computer-controlled reward delivery system (Crist®) with a plastic tube coming to their mouth. The task, all the behavioral parameters as well as the sensory stimulations were monitored by two computers running with Matlab®7.10 and Presentation®16.3. Visual stimulations were projected onto the screen with a Canon XEED SX60 projector. Auditory stimulations were dispensed with a MR Confon GmbH system (Magdeburg, Germany). Tactile stimulations were delivered through Teflon tubing and 6 articulated plastic arms

connected to distant air pressure electro-valves. Monkeys were trained in a mock scan environment similar to the best the actual MRI scanner setup.

Task and stimuli

The animals were trained to maintain fixation on a red central spot (0.24°x0.24°) while stimulations (visual or tactile) were delivered. The monkeys were rewarded for staying within a 2°x2° tolerance window centered on the fixation spot. The reward delivery was scheduled to encourage long fixation without breaks (*i.e.* the interval between successive deliveries was decreased and their amount was increased, up to a fixed limit, as long as the eyes did not leave the window). The different modalities were tested in independent interleaved runs (see below for the organization of the runs).

Visual stimulations. Large field (32°x32°) visual stimulations consisted in white bars (3.2°x24.3°, horizontal, vertical, or 45° oblique) or white random dots on a black background. Three conditions were tested in blocks of 10 pulses (TR = 2.08 sec): *coherent movement*, *scrambled movement*, and *static* visual stimuli (details are provided in Guipponi et al. 2013).

Auditory stimulations.

In both monkeys, we used *coherent movement*, scrambled and static auditory stimuli. *Scrambled stimulations* were obtained by cutting the movement sounds in 100 or 300 ms segments and randomly mixing them. *Static stimulations* consisted of auditory stimuli evoking a stable stimulus in space (cf. Guipponi et al. 2013).

Tactile stimulations.

They consisted in air puffs delivered to 2 different locations on the left and the right of the animals' body: (1) *center of the face*, close to the nose and the mouth; (2) *shoulders* (cf. Guipponi et al. 2013).

Functional time series (runs) were organized as follows: a 10-volume block of pure fixation (baseline) was followed by a 10-volume block of category 1 stimulus type, a 10-volume block of category 2 stimulus type; this sequence was played 4 times. The blocks for the 2 categories were presented in 6 counterbalanced possible orders. A retinotopy localizer was run independently in the 2 monkeys using exactly the stimulations of Fize et al. (2003). This localizer is used to localize the central

and peripheral representations of visual areas within each hemisphere, in both animals. These localizer runs are also used to identify eye movement related activations (see below).

Scanning

Before each scanning session, a contrast agent, monocrystalline iron oxide nanoparticle (Sinerem, Guerbet or Feraheme, AMAG), was injected into the animal's femoral/saphenous vein (4-10 mg/kg). Brain activations produce decreased signals using contrast agent whereas produce increased MR signals in BOLD measurements. For the sake of clarity, the polarity of the contrast agent MR signal changes, which corresponds essentially to a cerebral blood volume (CBV) measurement, was inverted (Vanduffel et al. 2001; Leite et al. 2002; Zhao et al. 2005). We acquired gradient-echo echoplanar (EPI) images covering the whole brain (1.5 T; repetition time (TR) 2.08 s; echo time (TE) 27 ms; 32 sagittal slices; 2x2x2-mm voxels). During each scanning session, the runs of different modalities and different orders were pseudorandomly intermixed. A total of 40 (34) runs was acquired for visual stimulations in M1 (/M2), 36 (40) runs for tactile stimulations, 37 (42) runs for complex auditory stimulations. Fifty-seven (45) runs were obtained for the retinotopy localizer were obtained in independent sessions for M1 (/M2).

Analysis

The analyzed runs were selected based on the quality of the monkeys' fixation (>85% within the tolerance window): a total of 23 (25) runs was selected for visual stimulations in M1 (/M2), 20(32) for tactile stimulations, 26(32) for complex auditory stimulations and 20 (24) for the retinotopy localizer. Time series were analyzed and spatial preprocessing is performed using SPM8 (Wellcome Department of Cognitive Neurology, London, United Kingdom). For spatial preprocessing, functional volumes were first realigned and rigidly coregistered with the anatomy of each individual monkey (T1-weighted MPRAGE 3D 0.6x0.6x0.6 mm or 0.5x0.5x0.5 mm voxel acquired at 1.5T) in stereotactic space. The JIP program (Mandeville et al. 2011) was used to perform a nonrigid coregistration (warping) of a mean functional image onto the individual anatomies.

For tactile to the center of the face or to the shoulders, fixed effect individual analyses were performed for each sensory modality in each monkey using a GLM, with a level of significance set at $p<0.001$ uncorrected level.

The reward analyses were performed on auditory runs only, so as to observe relatively pure reward-related activations and avoid influences from the strong activations induced by visual stimulations (auditory activations are very weak compared to visual). The timing of the reward event is extracted from log presentation of each auditory runs and a GLM analysis is performed.

For each run and each animal for tactile and auditory runs, we extracted the timings of the blink events and performed, using a GLM, conjunction analyses between tactile and auditory stimuli (see Guipponi et al. 2014).

In all analyses, realignment parameters, as well as eye movement traces, were included as covariates of no interest to remove eye movements and brain motion artifacts. The eye movement traces correspond to breaks of fixation. In order to identify the eye movement related activations, we analyzed these eye movement traces in runs obtained for the retinotopy localizer. Results are displayed on coronal sections from each individual anatomy or on individual fiducial maps obtained with Caret (van Essen et al. 2001; http://www.nitrc.org/projects/caret/).

Spatial fMRI precision and single individual analyses

The present study is a meta-analysis of fMRI data that were collected on a 1.5T scanner, with a voxel size of 2x2x2mm. The functional volumes further underwent a spatial processing, including a non-rigid coregistration (warping) of the mean functional image onto the individual anatomies. This spatial filtering is obviously limiting and does not allow for a fine-grained spatial resolution. However, two arguments support the validity of the reported observations. First, though the functional activation of one voxel corresponds to the activity of thousands of neurons and thus does not allow identification of specific types of neurons, our results are, as described in the discussion, strikingly coherent with previous electrophysiological studies (Morecraft et al. 1996, 2007; Tokuno et al. 1997; Wang et al. 2015). Second, this study relies on data collected in two monkeys, each monkey performing

all the different tasks, in independent functional blocks, over several days. As a result, each monkey serves as its own control. This actually allows powerful cross-correlation and statistical-parametric mapping techniques (Menon and Kim 1999). We describe major activation trends along the cingulate sulcus across the four hemispheres of the two animals. In particular, a clustered organization of the several activation peaks, including activation peaks defined on independent functional runs, is described in all hemispheres, some of which fall on precisely the same coronal sections. This indicates that the spatial resolution of our fMRI acquisitions was not limiting in this respect. We do not however attempt to make any more specific claims on the functional organization of the different activations within each cluster. Higher field neuroimaging would be needed to properly address this question.

Results

Two monkeys sat in the scanner, in sphinx position, and received juice reward for fixating a fixation spot. Tactile (air puff) stimulations on center of the face and on the shoulder, eye movements, reward delivery events and eye blinks were used as regressors to evaluate the contribution of each of these events to signal variation in the cingulate sulcus, and then test the degree of anatomical overlap of the corresponding activations. Figure 1 represents the activations observed for each condition (schematically represented in figure 1B), and for the right and left hemisphere of each monkey, with a special focus on the cingulate sulcus represented either on coronal sections (Figure 1C, central columns, Y position in mm relative to the genu of the arcuate -ArcGen) and on fiducial 3D close up (Figure 1C, left and right columns, location of the coronal section represented by a plane and position of the genu of the arcuate sulcus represented by an arrow). Figure 1A represents the position of the close ups of figure 1C on the fiducial reconstruction of each hemisphere of each monkey. All reported activations are present in at least three hemispheres out of four and can thus be considered as representative of the functional organization of the cingulate sulcus.

Reward-related activations. As expected we observed reward-related activations in both hemispheres of both monkeys, at symmetric locations centered in the dorsal bank of the cingulate

sulcus (Figure 1C1). This fits with many previous accounts of outcome-related neural activity in monkeys (Wallis and Kennerley 2010; see Procyk et al. 2014 for a meta-analysis).

Eye movement-related and blink-related activations. Several anatomical studies suggest links between the frontal eye fields located in the anterior bank of the arcuate sulcus, eye lid muscle innervation and rostral cingulate motor area (CMAr), most probably with the face field of CMAr (Wang et al. 2004; Luppino et al. 2003; Gong et al. 2005; see Procyk et al. 2014). In the present data, activations correlating with eye movements were observed in both hemispheres of monkey M1 within the cingulate sulcus. In monkey M2, eye movement-related activations were present only in the right hemisphere at uncorrected level (Figure 1C2). Blink-related activations were found in the dorsal bank of the cingulate sulcus in the two monkeys, and bilaterally in monkey M1 (Figure 1C3).

Tactile-related activations. Tactile stimulations to the center of the face activated several regions of the medial wall, including within the cingulate sulcus. These activations were found in both hemispheres and in both monkeys (Figure 1C4). Activations during tactile stimulations to the shoulders were also observed within the cingulate sulcus peaking at levels just anterior to the genu of the arcuate (ArcGen) (Figure 1C5).

Location and overlap of these different cingulate activations. As represented in figure 1C, an activation for each task was observed in the cingulate sulcus at levels anterior to the ArcGen in at least one hemisphere of each monkey. This level is a landmark often used as a reference to study frontal lobe anatomy in macaques, and the face field in CMAr has been proposed to lie anterior to this landmark (Procyk et al. 2014). This is further confirmed when focusing this time on the overlap between the different activations described above (figure 2A). Indeed, this representation reveals a region of strong functional overlap anterior to the rostro-caudal level of the ArcGen, most probably coinciding with CMAr, as well as a second region of strong functional overlap posterior to the rostro-caudal level of the ArcGen, most probably coinciding with CMAc (caudal cingulate motor area).

While the limits of clusters with significant voxels describe regions that are activated by the events of interest, they do not allow to describe anatomo-functional heterogeneities within these activated

regions (e.g. multiple activation peaks). We thus also extracted all the local maximal peaks within the activations of interest as obtained by SPM for each condition in cingulate sulcus and we projected them on the fiducial brain reconstruction using *caret*. Confirming the above observation that maximal functional overlap was present both anterior and posterior the ArcGen, we can see that, in both monkeys, activation peaks cluster at two different locations: anterior to ArcGen (average position: +5.9 mm) and one posterior to this landmark, at an average of -2.4 mm. Importantly, all of reward-related, eye-movement related, blink-related and face tactile-related peaks are also found within this most posterior cluster, thus functionally mirroring the anterior cluster. The peaks related to eye movements were however more robust in the rostral region, and present posteriorly in the sulcus only in one hemisphere of one monkey (monkey M1; Fig. 2B).

Discussion

Our results show the convergence of activations related to face sensory (somatosensory, sensory consequences of spontaneous blinks) and motor (reward, eye movements, spontaneous blink) processes in two distinct loci within the cingulate sulcus (Figure 3). These data provide important information on the anatomo-functional organization of the cingulate sulcus. Indeed, the location of these two convergence loci with respect to the genu of the arcuate sulcus match the location of rostral and caudal CMAs, as defined by anatomic and electrophysiological studies, and thus confirm the existence of a dedicated face field within each of these two CMAs. In addition, these data confirm the relationship between reward processing and the face field within CMAr. Importantly they also suggest that this embodied reward-signal processing also concerns the posterior face field associated with CMAc. These issues are discussed below.

Monkey CMAr and CMAc face fields

Although CMAr is often discussed in relation to its well-known arm and hand representations, a face/eye field has also been described using experimental anatomical tract tracing and microstimulations (Mitz and Godschalk 1989; Morecraft et al. 1996, 2007, Figure 3; Tokuno et al. 1997).

Another region representing the face is also identified in a more caudal cingulate motor area (CMAv, Morecraft et al. 1996, 2007, Figure 3; Tokuno et al. 1997). Each of these two face representations are anterior to an arm representation and project selectively to the face representation of M1 and also directly to the facial nucleus (Morecraft et al. 2001). In addition, a [^{14}C]-2-Déoxyglucose functional imaging study suggests that the anterior cingulate sulcus region has denser connections to extraocular motoneurons, and is more widely activated for saccades, than the posterior region (Moschovakis et al. 2004). This result is in line with our findings showing more robust peaks related to eye movements in the anterior region.

Using single subject fMRI and by tracking activity variations correlating with face and eye related events, we demonstrate two clusters within the cingulate sulcus. We propose that the first cluster corresponds to the face field of CMAr. Located at an average of 5.9 mm anterior to the ArcGen this matches the location of the eye/face area estimated through meta-analysis (Procyk et al. 2014, Figure 3). The second posterior cluster of face related activations, located on average 2.4mm posterior to ArcGen, is proposed to correspond to the second face/eye field that was observed in several neuroanatomical studies (Morecraft et al. 1996; Luppino et al. 2003; Wang et al. 2004; Morecraft et al. 2007, Figure 3). In these studies, a small region connected to the eye fields of the frontal cortex or to the primary face area in M1, is described in the ventral bank of the cingulate sulcus, at levels posterior to the ArcGen. This field has been associated to the CMAc (caudal) or to the ventral subdivision, CMAv, depending on authors (Tokuno et al. 1997; Morecraft and Tanji 2009). Note that in humans, 3 cingulate motor areas have been observed and shown to be aligned on the rostro-caudal axis in and around the cingulate sulcus (Picard and Strick 1996, Figure 3; Amiez and Petrides 2014). Of these, only the 2 most rostral regions contain face fields, RCZa and RCZp. We propose that our current work using fMRI in monkeys is actually revealing the monkey face fields homologue to those found in RCZa and RCZp in humans. This functional homology is in agreement with the high similarity in the functional and large scale connectivity fingerprints in the human and monkey cortical medial wall that has recently been described (Neubert et al. 2015).

Integrated sensorimotor functions of the CMA face fields

The frontal eye fields (FEF) project to the anterior cingulate cortex in two foci (Wang et al. 2004) matching in their location the activations reported in the present work. In addition, Mitz and Godschalk (1989) show that eye movements can be evoked from area CMAr with intracortical microstimulations. In turn, CMAr area projects to F7-SEF (the supplementary eye field). It is thus at the core of a prefrontal oculomotor network and appears to be involved in several high order aspects of motor control (Shima et al. 1991; Shima and Tanji 1998; Procyk et al. 2000; Koyama et al. 2001; Schall et al. 2002).

Likewise, we show here that activations in both CMAr and CMAc regions relate to somatomotor functions in identical simple stimulation conditions. Shima and Tanji (1991) have found that although both CMAc and CMAr single units responded to self-paced and signal triggered arm movements, CMAr was characterized by more units being active long before the production of self-paced movements. CMAr might be involved in more complex behavioral aspects, such as adaptive action selection based on reward (Shima and Tanji 1998; Tanji et al. 2002), and CMAc might be more related to motor functions. This dissociation most probably also applies to the somatosensory processing taking place in these two regions. More experiments are needed to dissociate potential functional differences between the face fields of these two cingulate premotor areas.

Embodied feedback processing and CMAr and CMAc face/eye fields

Another major outcome of our study is the confirmation of the anatomo-functional overlap, within the cingulate sulcus, of reward-related activations and activations related to the eyes and face (eye movements, blinks, air puff to the face). These data thus provide supplementary evidence for embodiment of feedback in the cingulate cortex as discussed in particular regarding the rostral CMA (RCZa) (Amiez et al. 2013; Procyk et al. 2014). The hypothesis is that the somatomotor information that is relevant for behavioral adaptation (feedback) is processed within the corresponding cingulate body representation. For instance, we have shown in humans that juice feedback provided during learning, but not during repetition, induces activation within the RCZa face representation (Amiez et al. 2013). In contrast, activations in the face region of M1 do not vary between learning and repetition.

We actually propose that each of these CMA face fields further contain precise subfields for oculomotor, upper face, tongue/mouth, and lower face, matching the body map. In our current fMRI approach activations, the different activations of interest overlap, most probably due to a limited spatial resolution as compared to the expected resolution of a finer grained description of these two CMA face fields. This remains to be tested.

This embodied feedback processing framework can actually be extended further. A recent meta-analysis of neurophysiological and neuroanatomical data in monkeys suggests that CMAr reward/outcome related activity, which has been repeatedly observed during cognitive tasks, was actually observed in the face field of CMAr (Procyk et al. 2014). In this context, reward serves as a strong feedback to reinforce learning. In the same line, during experimental cognitive tasks, monkeys have to gather information through multiple channels (saccades, juice, arm movements), this information continuously updating the monkey about the ongoing task. This embodied feedback processing framework predicts that an eye field within CMAr contributes to behavioral adaptation in a way very similar to what has been proposed for reward signals. Breaks of fixation requirements for instance, usually induce trial abortion and absence of reward. We have shown that subsets of CMAr neurons, in the same region where reward related activity was found, selectively encoded negative feedback at break of fixation (Amiez et al. 2005; Quilodran et al. 2008). Likewise, blinks leading to break fixation errors, can be followed by adaptive increased control to avoid ulterior misses (Stoll et al. 2015). Here we show that blinks and eye movements as well as tactile stimulation on the face, evoke co-localized activations in CMAr. The exact functional role of the eye/face field is unknown. Yet, anatomy shows that the amygdala projections to the cingulate motor field preferentially innervate the face representation of CMAr and that, in turn, this CMAr region innervates all nuclear subdivision of the facial nucleus of the pontine tegmentum (Morecraft et al. 2001, 2007). Supporting a functional role of these amygdala-cingulate cortex projections, a study in humans (Fish et al. 1993), reported that the stimulation of the amygdala induces eye closure, blinking and changes in facial expressions. The CMAr face field might thus contribute to control face-related reactions and/or to gather information from

the eye/face domain that could serve, for instance, adaptation in social contexts (Mosher et al. 2014; Gothard 2014).

Acknowledgements

J.C. was funded by the Fondation pour la Recherche Médicale. S.BH was funded by the French Agence nationale de la recherche (Grant #ANR-05-JCJC-0230-01). We would like to thank J.-L. Charieau and F. Hérant for animal care.

References

Alexander WH, Brown JW. 2011. Medial prefrontal cortex as an action-outcome predictor. Nat Neurosci. 14:1338–1344.

Amiez C, Joseph J-P, Procyk E. 2005. Anterior cingulate error-related activity is modulated by predicted reward. Eur J Neurosci. 21:3447–3452.

Amiez C, Joseph JP, Procyk E. 2006. Reward encoding in the monkey anterior cingulate cortex. Cereb Cortex N Y N 1991. 16:1040–1055.

Amiez C, Neveu R, Warrot D, Petrides M, Knoblauch K, Procyk E. 2013. The Location of Feedback-Related Activity in the Midcingulate Cortex Is Predicted by Local Morphology. J Neurosci. 33:2217–2228.

Amiez C, Petrides M. 2014. Neuroimaging Evidence of the Anatomo-Functional Organization of the Human Cingulate Motor Areas. Cereb Cortex. 24:563–578.

Botvinick MM. 2007. Conflict monitoring and decision making: reconciling two perspectives on anterior cingulate function. Cogn Affect Behav Neurosci. 7:356–366.

Cadoret G, Smith AM. 1997. Comparison of the neuronal activity in the SMA and the ventral cingulate cortex during prehension in the monkey. J Neurophysiol. 77:153–166.

Crutcher MD, Russo GS, Ye S, Backus DA. 2004. Target-, limb-, and context-dependent neural activity in the cingulate and supplementary motor areas of the monkey. Exp Brain Res. 158:278–288.

Dum RP, Levinthal DJ, Strick PL. 2009. The Spinothalamic System Targets Motor and Sensory Areas in the Cerebral Cortex of Monkeys. J Neurosci. 29:14223–14235.

Dum RP, Strick PL. 1991. The origin of corticospinal projections from the premotor areas in the frontal lobe. J Neurosci Off J Soc Neurosci. 11:667–689.

Fish DR, Gloor P, Quesney FL, Olivier A. 1993. Clinical responses to electrical brain stimulation of the temporal and frontal lobes in patients with epilepsy. Pathophysiological implications. Brain J Neurol. 116 (Pt 2):397–414.

Fize D, Vanduffel W, Nelissen K, Denys K, d'Hotel CC, Faugeras O, Orban GA. 2003. The Retinotopic Organization of Primate Dorsal V4 and Surrounding Areas: A Functional Magnetic Resonance Imaging Study in Awake Monkeys. J Neurosci. 23:7395–7406.

Gong S, DeCuypere M, Zhao Y, LeDoux MS. 2005. Cerebral cortical control of orbicularis oculi motoneurons. Brain Res. 1047:177–193.
Gothard KM. 2014. The amygdalo-motor pathways and the control of facial expressions. Front Neurosci. 8:43.
Guipponi O, Odouard S, Pinède S, Wardak C, Hamed SB. 2014. fMRI Cortical Correlates of Spontaneous Eye Blinks in the Nonhuman Primate. Cereb Cortex. bhu038.
Guipponi O, Wardak C, Ibarrola D, Comte J-C, Sappey-Marinier D, Pinède S, Hamed SB. 2013. Multimodal Convergence within the Intraparietal Sulcus of the Macaque Monkey. J Neurosci. 33:4128–4139.
Khamassi M, Quilodran R, Enel P, Dominey PF, Procyk E. 2015. Behavioral Regulation and the Modulation of Information Coding in the Lateral Prefrontal and Cingulate Cortex. Cereb Cortex. 25:3197–3218.
Koyama T, Kato K, Tanaka YZ, Mikami A. 2001. Anterior cingulate activity during pain-avoidance and reward tasks in monkeys. Neurosci Res. 39:421–430.
Leite FP, Tsao D, Vanduffel W, Fize D, Sasaki Y, Wald LL, Dale AM, Kwong KK, Orban GA, Rosen BR, Tootell RBH, Mandeville JB. 2002. Repeated fMRI Using Iron Oxide Contrast Agent in Awake, Behaving Macaques at 3 Tesla. NeuroImage. 16:283–294.
Luppino G, Rozzi S, Calzavara R, Matelli M. 2003. Prefrontal and agranular cingulate projections to the dorsal premotor areas F2 and F7 in the macaque monkey. Eur J Neurosci. 17:559–578.
Mandeville JB, Choi J-K, Jarraya B, Rosen BR, Jenkins BG, Vanduffel W. 2011. fMRI of Cocaine Self-Administration in Macaques Reveals Functional Inhibition of Basal Ganglia. Neuropsychopharmacology. 36:1187–1198.
Menon RS, Kim S-G. 1999. Spatial and temporal limits in cognitive neuroimaging with fMRI. Trends Cogn Sci. 3:207–216.
Misra G, Coombes SA. 2015. Neuroimaging Evidence of Motor Control and Pain Processing in the Human Midcingulate Cortex. Cereb Cortex. 25:1906–1919.
Mitz AR, Godschalk M. 1989. Eye-movement representation in the frontal lobe of rhesus monkeys. Neurosci Lett. 106:157–162.
Morecraft RJ, Louie JL, Herrick JL, Stilwell-Morecraft KS. 2001. Cortical innervation of the facial nucleus in the non-human primate: a new interpretation of the effects of stroke and related subtotal brain trauma on the muscles of facial expression. Brain J Neurol. 124:176–208.
Morecraft RJ, McNeal DW, Stilwell-Morecraft KS, Gedney M, Ge J, Schroeder CM, van Hoesen GW. 2007. Amygdala interconnections with the cingulate motor cortex in the rhesus monkey. J Comp Neurol. 500:134–165.
Morecraft RJ, Schroeder CM, Keifer J. 1996. Organization of face representation in the cingulate cortex of the rhesus monkey. Neuroreport. 7:1343–1348.
Morecraft RJ, Tanji J. 2009. Cingulofrontal interactions and the cingulate motor areas. Cingulate Neurobiol Dis Oxf Univ Press UK. 113–144.
Moschovakis AK, Gregoriou GG, Ugolini G, Doldan M, Graf W, Guldin W, Hadjidimitrakis K, Savaki HE. 2004. Oculomotor areas of the primate frontal lobes: a transneuronal transfer of rabies virus and [14C]-2-deoxyglucose functional imaging study. J Neurosci Off J Soc Neurosci. 24:5726–5740.
Mosher CP, Zimmerman PE, Gothard KM. 2014. Neurons in the monkey amygdala detect eye contact during naturalistic social interactions. Curr Biol CB. 24:2459–2464.
Neubert F-X, Mars RB, Sallet J, Rushworth MFS. 2015. Connectivity reveals relationship of brain areas for reward-guided learning and decision making in human and monkey frontal cortex. Proc Natl Acad Sci U S A. 112:E2695–E2704.

Picard N, Strick PL. 1996. Motor Areas of the Medial Wall: A Review of Their Location and Functional Activation. Cereb Cortex. 6:342–353.
Procyk E, Tanaka YL, Joseph JP. 2000. Anterior cingulate activity during routine and non-routine sequential behaviors in macaques. Nat Neurosci. 3:502–508.
Procyk E, Wilson CRE, Stoll FM, Faraut MCM, Petrides M, Amiez C. 2014. Midcingulate Motor Map and Feedback Detection: Converging Data from Humans and Monkeys. Cereb Cortex. bhu213.
Quilodran R, Rothé M, Procyk E. 2008. Behavioral shifts and action valuation in the anterior cingulate cortex. Neuron. 57:314–325.
Rushworth MF, Kolling N, Sallet J, Mars RB. 2012. Valuation and decision-making in frontal cortex: one or many serial or parallel systems? Curr Opin Neurobiol, Decision making. 22:946–955.
Schall JD, Stuphorn V, Brown JW. 2002. Monitoring and control of action by the frontal lobes. Neuron. 36:309–322.
Shackman AJ, Salomons TV, Slagter HA, Fox AS, Winter JJ, Davidson RJ. 2011. The integration of negative affect, pain and cognitive control in the cingulate cortex. Nat Rev Neurosci. 12:154–167.
Shenhav A, Botvinick MM, Cohen JD. 2013. The Expected Value of Control: An Integrative Theory of Anterior Cingulate Cortex Function. Neuron. 79:217–240.
Shima K, Aya K, Mushiake H, Inase M, Aizawa H, Tanji J. 1991. Two movement-related foci in the primate cingulate cortex observed in signal-triggered and self-paced forelimb movements. J Neurophysiol. 65:188–202.
Shima K, Tanji J. 1998. Role for cingulate motor area cells in voluntary movement selection based on reward. Science. 282:1335–1338.
Stoll FM, Wilson CRE, Faraut MCM, Vezoli J, Knoblauch K, Procyk E. 2015. The Effects of Cognitive Control and Time on Frontal Beta Oscillations. Cereb Cortex N Y N 1991.
Tanji J, Shima K, Matsuzaka Y. 2002. Reward-based planning of motor selection in the rostral cingulate motor area. Adv Exp Med Biol. 508:417–423.
Tokuno H, Takada M, Nambu A, Inase M. 1997. Reevaluation of ipsilateral corticocortical inputs to the orofacial region of the primary motor cortex in the macaque monkey. J Comp Neurol. 389:34–48.
van Essen DC, Drury HA, Dickson J, Harwell J, Hanlon D, Anderson CH. 2001. An Integrated Software Suite for Surface-based Analyses of Cerebral Cortex. J Am Med Inform Assoc. 8:443–459.
Vanduffel W, Fize D, Mandeville JB, Nelissen K, Van Hecke P, Rosen BR, Tootell RBH, Orban GA. 2001. Visual Motion Processing Investigated Using Contrast Agent-Enhanced fMRI in Awake Behaving Monkeys. Neuron. 32:565–577.
Vogt B. 2009. Cingulate Neurobiology and Disease. OUP Oxford.
Wallis JD, Kennerley SW. 2010. Heterogeneous reward signals in prefrontal cortex. Curr Opin Neurobiol. 20:191–198.
Wang L, Mruczek REB, Arcaro MJ, Kastner S. 2015. Probabilistic Maps of Visual Topography in Human Cortex. Cereb Cortex. 25:3911–3931.
Wang Y, Matsuzaka Y, Shima K, Tanji J. 2004. Cingulate cortical cells projecting to monkey frontal eye field and primary motor cortex. Neuroreport. 15:1559–1563.
Zhao F, Wang P, Hendrich K, Kim S-G. 2005. Spatial specificity of cerebral blood volume-weighted fMRI responses at columnar resolution. NeuroImage. 27:416–424.

Figures and legends

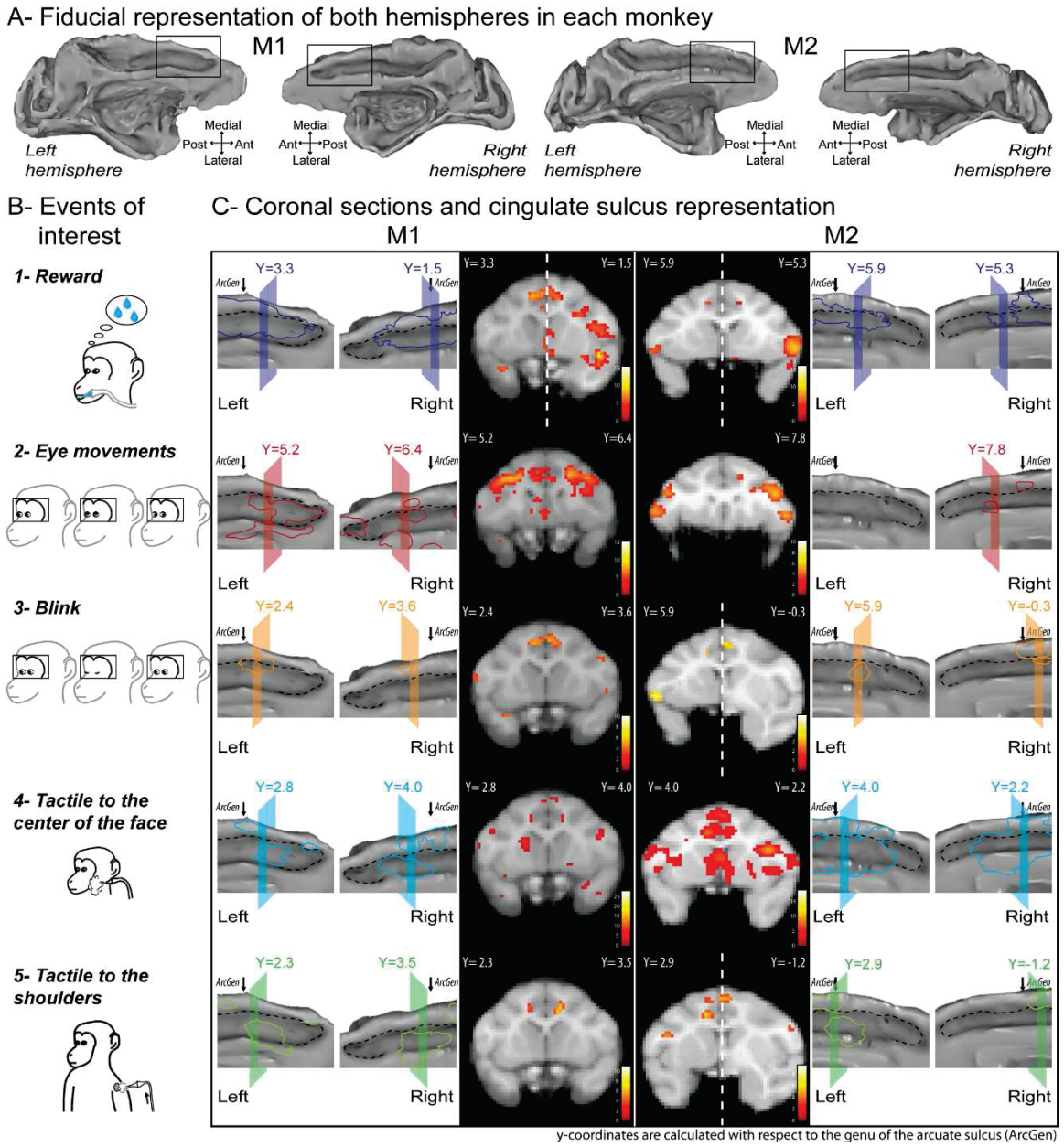

Figure 1. (A) 3D fiducial representation of the cortex, obtained with Caret (left and right hemispheres of each monkey). The dark inset corresponds to the peri-cingulate region represented in (C). The limits of the cingulate sulcus are depicted in dashed lines. (B) Schematic representation of events of interest: 1) Reward (dark blue in figure 1C); 2) Eye movements (red in figure 1C); 3) Spontaneous blinks (orange in figure 1C); 4) Tactile stimulations to the center of the monkey's face (light blue in figure 1C); 5) Tactile stimulations to the monkeys' shoulders (light green in figure 1C). (C) Spatial extent of fMRI cingulate cortex activations in each monkey, for the different events of interest, presented on a close

up of the fiducial representation of the cingulate region (dark insets on the whole brain 3D maps presented in figure 1A) and on selected coronal sections taken at the level of the coronal planes represented on the close up fiducial. The y-coordinates are calculated with respect to the genu of the arcuate sulcus (ArcGen). For all studies, coronal sections show activations at uncorrected level ($p<0.001$). This is also the case for the fiducial activation maps, except for study 3, for monkey M1 (FWE-corrected level, $p<0.05$, uncorrected-level activations encompassing the whole extend of the region of interest).

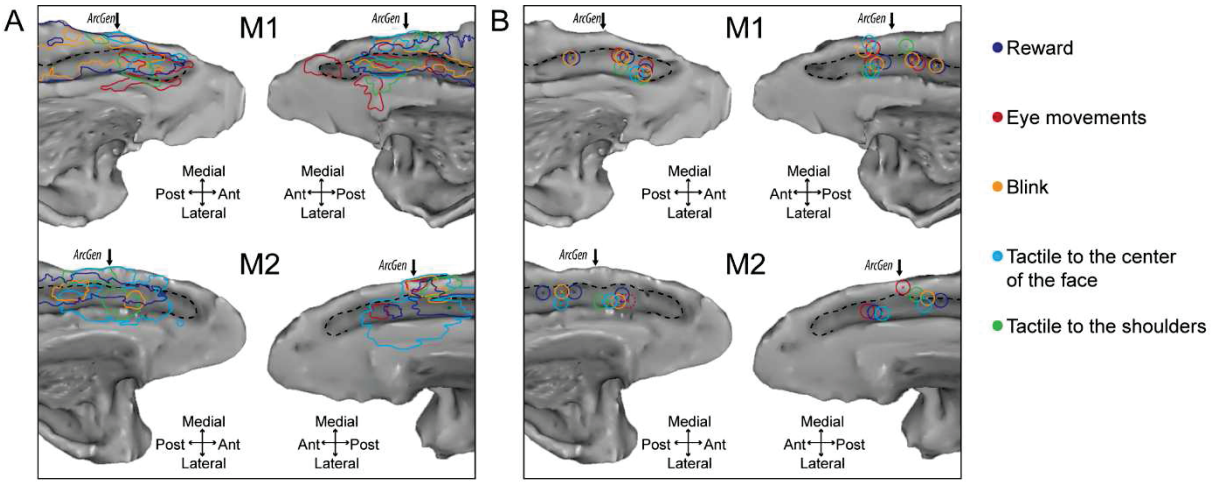

Figure 2. (A) Overlap of the contours of the cingulate cortical activations identified in figure 1, projected onto the fiducial representation of the left and right cingulate cortex, for each monkey, at uncorrected level ($p<0.001$). (B) Local peaks identified in each functional activation with respect to the genu of the arcuate sulcus (ArcGen).

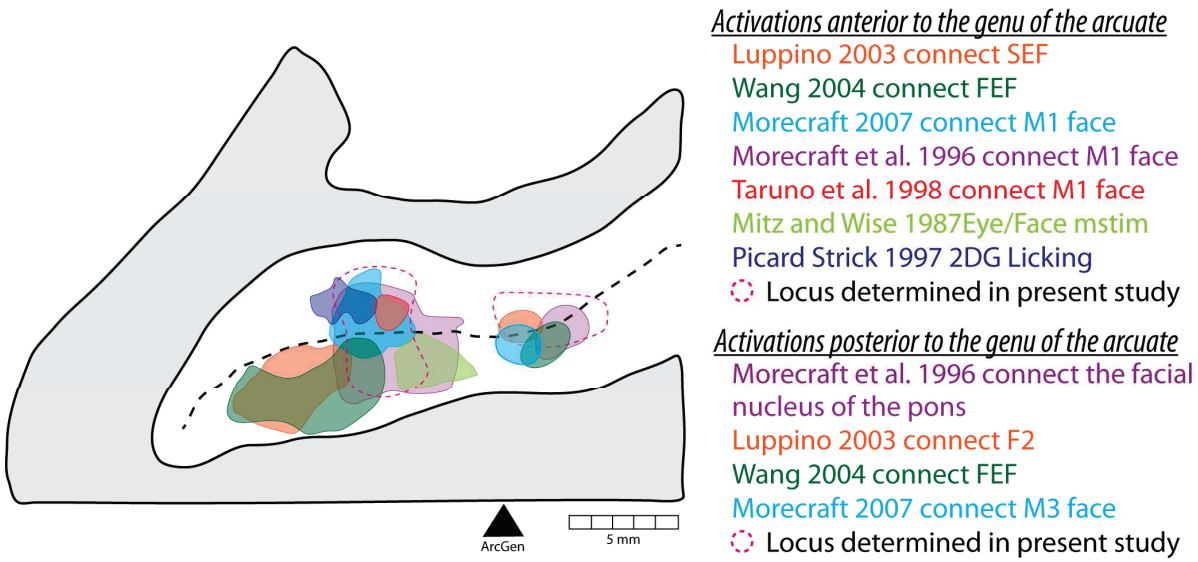

Figure 3. Two loci are represented in cingulate cortex. Activations anterior and/or posterior to the genu of the arcuate are observed in different neuroanatomical studies and overlap with the two loci found in this present study.

Appendix 3

Noradrenaline differentially affects attention-related evidence accumulation and decision thresholds

Article in preparation

Noradrenaline differentially affects attention-related evidence accumulation and decision thresholds

Froesel M[1*], Reynaud AJ[2*], Guedj C[2], Ben Hadj Hassen S[1], Cléry J[1], Meunier M[2], Ben Hamed S[1*], Hadj-Bouziane F[2*]

[1] Institut des Sciences Cognitives Marc Jeannerod, UMR5229, CNRS-Université Claude Bernard Lyon I, 67 Boulevard Pinel, 69675 Bron, France

[2] ImpAct Team, Institut National de la Santé et de la Recherche Médicale, U1028, Centre National de la Recherche Scientifique, UMR5292, Lyon Neuroscience Research Center Lyon, France ; Université de Lyon, France.

* co-first or co-last authors

Corresponding authors: Suliann Ben Hamed, benhamed@isc.cnrs.fr

Fadila Hadj-Bouziane, fadila.hadj-bouziane@inserm.fr

Keywords: attention, reaction time, atomoxetine, macaque monkey, LATER model.

Abstract

Attention is a central cognitive function that plays an essential role in the perceptual analysis of our environment and in the production of appropriate behavioral responses. It has been proposed to operate along three different subsystems: the alert system, the orientation system, and the executive control system (Posner and Petersen, 1990). The contribution of the locus cœruleus-noradrenaline (NA) system to each of these attentional subsystems is still controversial (Aston-Jones and Cohen, 2005). The present study analyses whether NA modulates evidence accumulation and response decision thresholds selectively as a function of the attentional sub-process.

Seven monkeys had to saccade to 10° targets as fast as possible either during a simple target detection task or during a cued target detection task (Fan et al., 2002). In this latter task, 80 % of the trials were valid cue trials. The remaining 20% trials were either no-cue trials, invalid cue trials or neutral cue trials. In addition, a distractor could appear at the same time as the target, in 66% of the trials, either in the same or in the opposite hemifield. Monkeys either received a saline injection or Atomoxetine (ATX), or an inhibitor of NA-reuptake, enhancing its transmission. Reaction times (RT) distributions were compared using the LATER model to quantify whether the observed changes induced by the attentional condition or the pharmacological neuromodulation were better modeled by a change in evidence accumulation or in decision threshold (Noorani and Carpenter, 2016).

Overall, the modulation of attention orientation (comparing valid vs. invalid RT distributions) by ATX was mediated by a change in the decision threshold. This was also the case for distractor interference (comparing distractor vs. no distractor RT distributions) and alert (comparing no cue vs. neutral cue RT distributions, 3/7 monkeys). In contrast, the modulation of executive control by ATX was mediated by a change in evidence accumulation between the simple RT task and the no-cue trials of the cued task. These results suggest that

NA influences different facets of the attention function and that these effects might rely on different neuronal processes.

References

Aston-Jones G, Cohen JD (2005) An integrative theory of locus coeruleus-norepinephrine function: Adaptive Gain and Optimal Performance. Annual Review of Neuroscience 28:403–450.

Fan J, McCandliss BD, Sommer T, Raz A, Posner MI (2002) Testing the efficiency and independence of attentional networks. J Cogn Neurosci 14:340–347.

Noorani I, Carpenter RHS (2016) The LATER model of reaction time and decision. Neurosci Biobehav Rev 64:229–251.

Posner MI, Petersen SE (1990) The attention system of the human brain. Annu Rev Neurosci 13:25–42.

331.12

Noradrenaline differentially affects attention-related evidence accumulation and decision thresholds

Froesel M[1], Reynaud AJ[2], Guedj C[2], Ben Hadj Hassen S[1], Cléry J[1], Meunier M[2], Ben Hamed S[1], Hadj-Bouziane F[2],

[1]Institut des Sciences Cognitives Marc Jeannerod, CNRS UMR 5229, BRON, France; [2]ImpAct Team, INSERM, U1028, CNRS UMR5292, BRON, France

Introduction

Attention is a central cognitive function that plays an essential role in the perceptual analysis of our environment and in the production of appropriate behavioral responses. It has been proposed to operate along three different subsystems: the **alert system**, the **orientation system**, and the **executive control system** (Posner and Peterson, 1990). The contribution of the locus cœruleus-noradrenaline (NA) system to each of these attentional subsystems is still controversial (Aston-Jones and Cohen, 2005). The present study analyzes whether NA modulates evidence accumulation and response decision thresholds selectively as a function of the attentional sub-process.

Methods

Seven rhesus monkeys performed alternatively two tasks: **simple detection task** (pur condition) and **cued detection task**: mixed task (4 cue conditions + 3 distractor conditions). They had to saccade to the target (10° eccentricity).

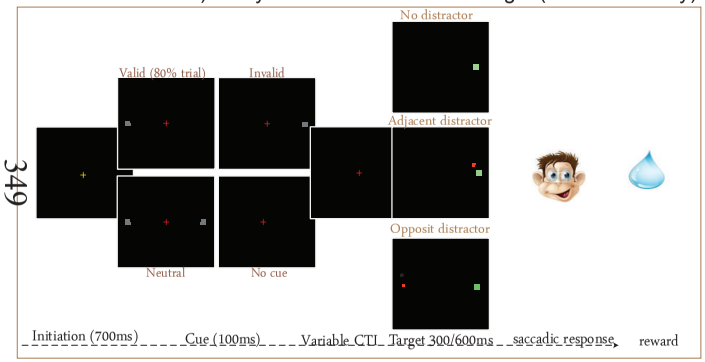

Drug administration: Intramusclar injections were done 30 min before each session, either with one of 4-5 different doses of Atomoxetine (ATX), a NA reuptake inhibitor at 0.1/0.5/1/1.5 mg/kg or with saline (NaCl) as control.
Variable: Reaction time (RT): time between the appearance of the target and the saccadic response.

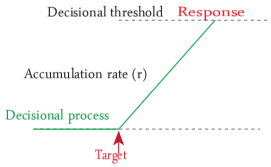

LATER model: RT is the result of a decisional process which strats with the target (T), rises with an accumulation rate (r) and ends at the decisional threshold (θ) with a response.

Strategies :
Change of the accumulation rate (shift of the line [1])
Change of the decisional threshold (swivel of the ligne [2])

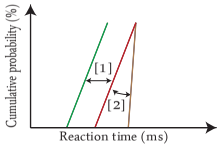

Data analysis: Log likelihood ratio tests were performed for each subject to determine whether a particular strategy was used between the different trial types (Noorani and Carpenter, 2016). To evaluate the effect of ATX in RT distribution we performed non parametric paired test on the group of subject.

Excecutive control

Comparison pur/no cue conditions:

Distribution in two components: Early and main

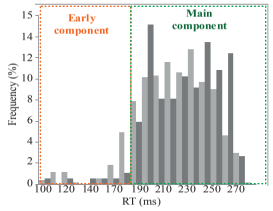

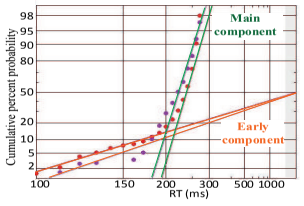

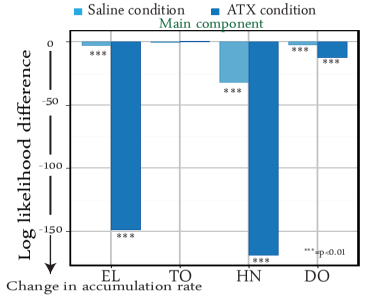

Main component
RTs in the pur condition are faster than in the no cue condition, it is driven by a change of the accumulation rate.
ATX enhaces this effect

Early component
There is more early saccades in pur than in no cue condition
No effect of ATX on this component

Conclusion: The strategy linked to excecutive control is a change of accumulation rate: adaptation of the context content. ATX enhances this strategy on the main component but has no effect on the early component: ATX targets the superior areas of the cortex.

Orientation

Comparison valid/invalid conditions

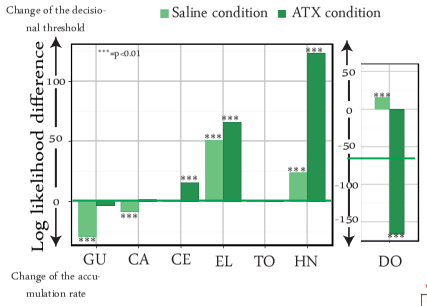

RTs are faster in valid than in invalid condition (orientation effect). This is driven by a change of the decisional threshold.

ATX enhances the strategy of the change a effect of decisional threshold (p=0.028)

The change of RTs following the administration of ATX on the orientation effect is driven by RTs of the valid condition. This change is the result of the faster accumulation rate in presence of the molecule.

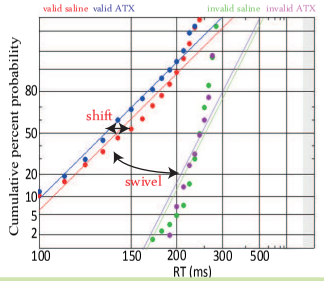

Conclusion: Orienting effect is due to a faster decision threshold in valid than in invalid condition. ATX improves this strategy by optimising the accumulation rate in valid condition. It helps to take into account the context (80% of valid cues) to improve the use of this cue.

Alerting effect

Comparison no cue/neutral conditions

RTs in neutral condition are faster than in no cue condition.

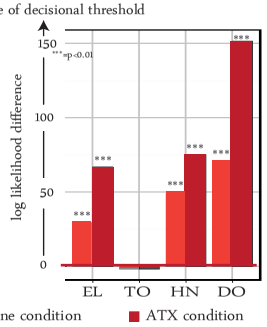

ATX conforts the primary strategy of changing the decision threshold in function of the neutral cue presence (p=0.04)

Conclusion: The decision threshold is lower in the presence of neutral cue than in its absence. The cue is used.
ATX increases the certainty of this strategy.

Distractors effect

Comparison opposit/no distractor conditions

The opposit distractor slows down the RTs by changing the decisional threshold

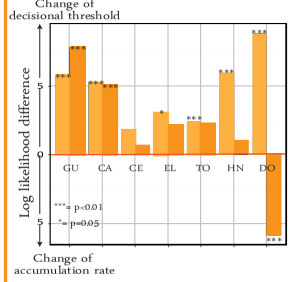

The decisional threshold is slower in presense of the opposit distractor.

With ATX this strategy is less prononced (p=0.02).

Comparison adjacent/no distractor conditions

The adjacent distractor has either a beneficial effect with a faster rate of accumulation or a negative effect with a later decision threshold.

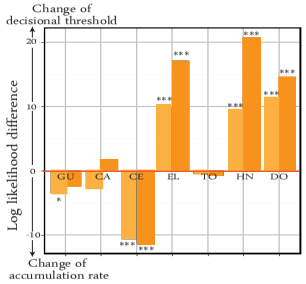

In both case, ATX increases the certainty of the strategy (p=0.03 and p=0.06)

Saline condition ATX condition

Conclusion: The opposit distractor disrupts the response to the target. ATX decreases the strategy used to treat this distractor: better filtration. The adjacent distractor is either beneficial or negative depending on the strategy used to treat it. ATX increases the certainty of these strategies.The filtration is less effective and the disruption more pronounced.

Aston-Jones G, Cohen JD (2005) An integrative theory of locus coeruleus-norepinephrine function: Adaptive Gain and Optimal Performance. Annual Review of Neuroscience 28:403–450.
Noorani I, Carpenter RHS (2016) The LATER model of reaction time and decision. Neurosci Biobehav Rev 64:229–251.
Posner MI, Petersen SE (1990) The attention system of the human brain. Annu Rev Neurosci 13:25–42.

mathilda.froesel@isc.cnrs.fr
Neural Bases of Spatial Cognition and Action
Institut des Sciences Cognitives Marc Jeannerod, 67 boulevard Pinel, 69500 BRON

Appendix 4

In-vivo High-Resolution DTI of Macaque Monkey Brain at 3T.

Article in preparation

In-vivo High-Resolution DTI of Macaque Monkey Brain at 3T.

Tounekti S.[1,2], Troalen T.[2], Bihan-Poudec Y.[1], Clery J.[1], Froesel M.[1], Lamberton F[3], Ben Hamed S.[1], Hiba B.[1,4]

[1]Institut des Sciences Cognitives Marc Jeannerod, CNRS UMR 5229, Université Claude Bernard Lyon I, France

[2]Siemens Healthcare SAS, Saint-Denis, France,

[3]Cermep, Lyon, France

[4]INCIA CNRS, UMR 5287, Université de Bordeaux, France

Corresponding authors: Bassem Hiba, bhiba@isc.cnrs.fr

Keywords: Diffusion Tensor Imaging, macaque monkey, in vivo, high resolution, tractography.

Abstract

Introduction:

Diffusion Tensor Imaging (DTI) is a unique non-invasive technique that allows to analyze the microstructure of *in vivo* brain tissues by characterizing the diffusion properties of water molecules. This technique is very promising for the study of the non-human primate brain but remains limited by its low sensitivity, spatial-resolution, vulnerability to motion and susceptibility artefacts. Here, we propose the three surface coils combined with a custom sequence pulse based on a segmented 3D Echo-Planner Imaging (EPI) sampling of Fourier space. The purpose of this study is to demonstrate the feasibility of acquiring high resolution DTI data on anesthetized monkeys in a 3 Tesla MR scanner.

Materials and methods:

An in vivo MRI study was performed on a 3 Tesla Siemens Prisma MRI scanner (Erlangen, Germany) with a maximum gradient amplitude of 80 mT/m. The radiofrequency transmission was performed using a full body coil, then three surface coils were used for signal reception. Four healthy adult Rhesus macaques were involved in this study. The monkeys were anesthetized by intramuscular injection of ketamine (10 mg / kg). Then, they are intubated and placed in a sphinx position in a custom-build MRI compatible stereotaxic frame (*Kopf Instruments*). During the acquisition, the anesthesia was maintained by isoflurane 1.5% (*Aestiva MRI GE Healthcare*). Their physiological functions were monitored continuously (*Expression MR200, InVivo*) through the acquisition time.

A segmented 3D-EPI readout module was implemented and combined with the standard monopolar diffusion preparation scheme (Stejskal and Tanner, 1965) to collect the diffusion weighted volume dataset. The scan parameters were as follows: Repetition-Time/Echo-Time: 750/71 ms; Matrix size: 210×248 mm^2; Field of view: 105×125×56 mm^3; spatial isotropic resolution of 0.5mm; slice number: 112. Thirty diffusion encoding directions were acquired

with b-value of 1000 s/mm2. Two additional volumes were collected with a b-value of 0 s/mm^2. Another volume was acquired with reversed phase encoding direction. The total scan duration was about 130 min. Diffusion tensor maps were computed using FMRIB Software Library (http://fsl.fmrib.ox.ac.uk/fsl/fslwiki/).

Results:

The segmented 3D-EPI sequence pulse allows to perform in vivo DTI for the non-human primate brain at an isotropic spatial resolution of up to 0.5 mm (0.125mm^3 cubic voxel size). Therefore, it leads to a significant increase in the sensitivity of the diffusion-weighted images at this resolution.

Discussion and conclusion

In this work, a diffusion-weighted 3D-EPI pulse sequence was implemented and used with a segmented sampling of Fourier space in order to minimize susceptibility and motion artifacts in DTI data. To our knowledge, the highest spatial resolution obtained for in vivo DTI macaque brain was 0.7 mm. This resolution was achieved with a 2D EPI sequence associated with an 8-channel phased array coil implanted on the skull of the animal for a total acquisition time of 3 hours (Janssens et al., 2012). The 3D-EPI sequence pulse is an alternative approach to perform in vivo DTI for non-human primate brain at submillimeter spatial resolution with an improved signal-to-noise ratio (SNR). However, this approach requires a long acquisition time which should be, in the future, reduced by using the parallel imaging techniques.

References

Janssens T, Keil B, Farivar R, McNab JA, Polimeni JR, Gerits A, Arsenault JT, Wald LL, Vanduffel W (2012) An implanted 8-channel array coil for high-resolution macaque MRI at 3T. Neuroimage 62:1529–1536.

Stejskal EO, Tanner JE (1965) Spin Diffusion Measurements: Spin Echoes in the Presence of a Time-Dependent Field Gradient. The Journal of Chemical Physics 42:288–292.

In-vivo High-Resolution DTI of Macaque Monkey Brain at 3T

Tounekti Slimane[1,2], Troalen Thomas[2], Bihan-Poudec Yann [1], Clery Justine[1], Froesel M[1], Lamberton Franck[3], Ben Hamed Suliann[1], Hiba Bassem[1,4]

[1]Centre de Neuroscience Cognitive, CNRS UMR 5229,BRON, [2]Siemens Healthcare SAS, Saint-Denis,
[3]Cermep, Lyon, [4]INCIA CNRS, UMR 5287, Université de Bordeaux, France

Introduction :

Diffusion Tensor Imaging (DTI) is a unique non-invasive technique that allows to analyze microstructures of in vivo brain tissues. However, due to its low spatial resolution and low produced SNR, it requires a specific methodology for its application in non-human primate. We implemented and optimized a diffusion MRI pulse sequence based on segmented 3D-EPI sampling of Fourier space. The aim of this study is to demonstrate the feasibility of acquiring high resolution DTI data in anesthetized macaque monkeys on a clinical 3 Tesla MRI scanner.

Materials & methods :

Acquisitions were performed on a 3 Tesla Siemens Prisma MRI scanner (Erlangen, Germany). Three surface coils were used for signal reception. Data were acquired on four healthy adult Rhesus macaques. The macaques were placed in a sphinx position in a custom-build MRI-compatible stereotaxic frame throughout the MRI acquisition. The subjects were intubated and maintained under gaseous anesthesia (1.5% Isoflurane). Their physiological functions were continuously monitored during the acquisition (respiration, CO2, ECG).

The 3D-EPI readout module based on a segmented sampling of Fourier space was developed and implemented to acquire data (Figure 1).

The diffusion scan parameters were: TR/TE= 750/71ms; 4 segments; bandwidth= 776 Hz; FOV= 105x125x56 mm³; spatial isotropic resolution of 0.5mm; the diffusion-weighted images were acquired for 30 directions (b-value = 1000 s/mm²), as well as two B0 images. Scan acquisitions lasted 130 min. Raw data were reconstructed offline via Gadgetron software. The effects of magnetic susceptibility and eddy currents have been corrected using FSL Top-up and Eddy functions. FSL DTIFIT was used to calculate the diffusion tensor. The tractography was performed with the Euler method of DSI Studio.

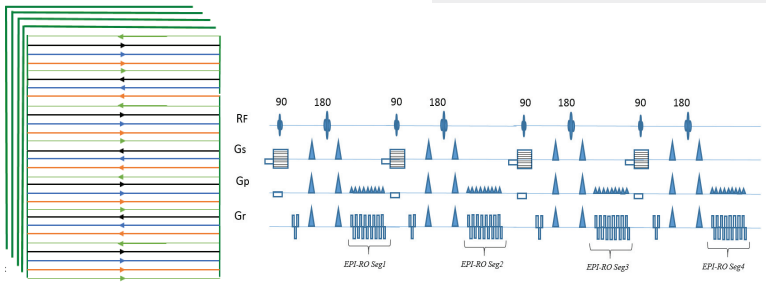

Fig.1 : Diagram of the diffusion-weighted 3D-EPI pulse sequence based on a segmented sampling of Fourier space.

	RSB (B = 0 s/mm²)	RSB (B = 1000 s/mm²)
CSF	76,26	9,61
WM	60,75	38,6
GM	63,43	34,2

Tab.1 : Mean values of SNR measured in cerebrospinal fluid (CSF), white matter (WM) and grey matter (GM).

Results :

The segmented EPI-3D pulse sequence significantly increases the sensitivity of the acquisition and allows to obtain diffusion-weighted images in high isotropic spatial resolution and with a high SNR (table 1).
Figure 2 shows the colored Fraction anisotropy maps obtained on the macaque. At the spatial isotropic resolution of 0.5 mm, the DTI data in this study appear to be sufficient to analyze the microstructures of brain tissues and to accurately tract the white matter (Figure 3) and the whole brain (Figure 4).

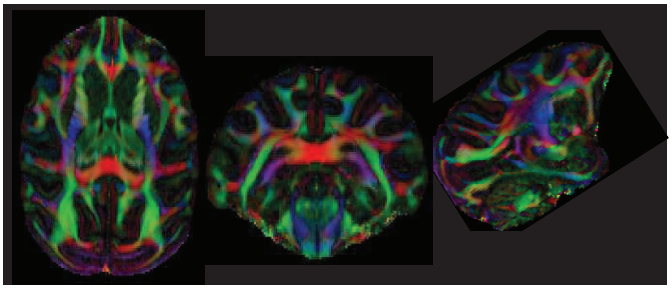

Fig.2 : Fractional anisotropy colored map (axial, coronal and sagittal view) acquired in anesthetized macaques at 3T with isotropic spatial resolution of 0.5 mm.

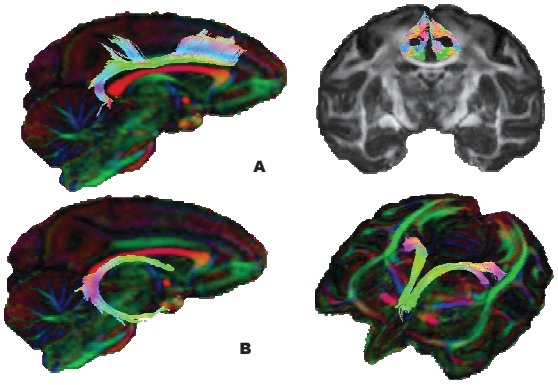

Fig.3 : Fornix (A) and Cingulum (B) tractographies displayed on FA maps.

Discussion:

3D spatial encoding of the data allows to have diffusion-weighted images with a high SNR which makes it possible to push the isotropic spatial resolution to 0.5 mm. The segmentation of the 3D EPI sampling of Fourier space and the application data corrections conduce to obtain images exempt of artefacts.
The implementation of an acceleration technique (parallel imaging, multislabs) allows to reduce the acquisition time and consequently to increase the number of diffusion encoding directions or the number of b-values.

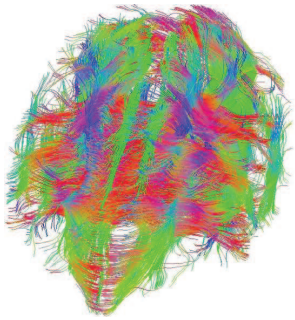

Fig.4 : Whole Brain tractography.

Conclusion :

Thanks to the proposed acquisition method, DTI data with 0.5 mm isotropic spatial resolution were acquired for the first time *in vivo* on non-human primate brain. This methodology offers a powerful tool for the non-invasive analysis of brain tissues.
Methodological developments are in progress to reduce the total acquisition time.

List of illustrations